

# University of Wollongong - Research Online

## Thesis Collection

Title: 3-hydroxykynurenine in the human lens

Author: Anastasia Korlimbinis

Year: 2006

Repository DOI:

### Copyright Warning

You may print or download ONE copy of this document for the purpose of your own research or study. The University does not authorise you to copy, communicate or otherwise make available electronically to any other person any copyright material contained on this site.

You are reminded of the following: This work is copyright. Apart from any use permitted under the Copyright Act 1968, no part of this work may be reproduced by any process, nor may any other exclusive right be exercised, without the permission of the author. Copyright owners are entitled to take legal action against persons who infringe their copyright. A reproduction of material that is protected by copyright may be a copyright infringement. A court may impose penalties and award damages in relation to offences and infringements relating to copyright material.

Higher penalties may apply, and higher damages may be awarded, for offences and infringements involving the conversion of material into digital or electronic form.

**Unless otherwise indicated, the views expressed in this thesis are those of the author and do not necessarily represent the views of the University of Wollongong.**

Research Online is the open access repository for the University of Wollongong. For further information contact the UOW Library: [research-pubs@uow.edu.au](mailto:research-pubs@uow.edu.au)

*University of Wollongong Thesis Collections*

*University of Wollongong Thesis Collection*

---

*University of Wollongong*

*Year 2006*

---

## 3-hydroxykynurenine in the human lens

Anastasia Korlimbinis  
University of Wollongong

Korlimbinis, Anastasia, 3-hydroxykynurenine in the human lens, PhD thesis, School of Chemistry, University of Wollongong, 2006. <http://ro.uow.edu.au/theses/488>

This paper is posted at Research Online.

<http://ro.uow.edu.au/theses/488>

## **NOTE**

This online version of the thesis may have different page formatting and pagination from the paper copy held in the University of Wollongong Library.

## **UNIVERSITY OF WOLLONGONG**

### **COPYRIGHT WARNING**

You may print or download ONE copy of this document for the purpose of your own research or study. The University does not authorise you to copy, communicate or otherwise make available electronically to any other person any copyright material contained on this site. You are reminded of the following:

Copyright owners are entitled to take legal action against persons who infringe their copyright. A reproduction of material that is protected by copyright may be a copyright infringement. A court may impose penalties and award damages in relation to offences and infringements relating to copyright material. Higher penalties may apply, and higher damages may be awarded, for offences and infringements involving the conversion of material into digital or electronic form.

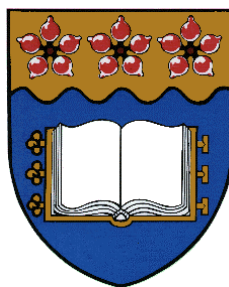
# **3-Hydroxykynurenine in the Human Lens**

A thesis submitted in partial fulfillment of the  
requirements for the award of the degree

**Doctor of Philosophy**

From

University of Wollongong



by

**Anastasia Korlimbinis BMedChem(Hons)**

Department of Chemistry

February 2006

## **Certification**

I, Anastasia Korlimbinis, declare that this thesis, submitted in partial fulfillment of the requirements for the award of Doctor of Philosophy, in the Department of Chemistry, University of Wollongong, is wholly my own work unless otherwise referenced or acknowledged. The document has not been submitted for qualifications at any other academic institution.

Anastasia Korlimbinis

February 2006

## **Acknowledgements**

*I would like to thank my supervisor Professor Roger Truscott, for allowing me the opportunity to undertake a PhD. I would also like to thank him for his excellent advice, expertise, encouragement and patience throughout the project.*

*I would like to thank the NMR staff, Dr Wilford Lie and Ms Sandra Chapman, for their assistance with the NMR spectrometers.*

*I would like to thank Dr Jen Burgess, Mr Larry Hick, Dr Andrew Aquilina and Dr Peter Hains for their assistance with the mass spectrometers.*

*I am forever grateful to Dr Nicole Parker, for her assistance at the beginning of the project, and I want to thank her for her friendship and all the laughs during the last 4 years.*

*I would like to thank Dr Nicole Parker for providing Kyn adducts in Chapter 3, Dr Peter Hains for providing the data for P6 in Chapter 5, Dr Peter Hains for reading Chapters 2, 3, 4 and 5, Dr Andrew Aquilina for providing the database on peptides with UV filter modifications, Professor John Rayner from the School of Mathematics and Applied Statistics, for his assistance with the statistical analysis in Chapter 3, Jasminka Mizdrak for providing the 3OHKynG, and Michael Friedrich for providing pure  $\alpha$ -crystallin.*

*I thank past and present members of the cataract lab for an enjoyable experience.*

*Finally I would like to thank my family, Mum, Dad, Katerina and Christina, who have always supported every decision I have ever made, and this thesis would not have been possible without their support, encouragement and patience – thank you.*

## **Publications**

Sections of the work described in this thesis have been reported in the following publications:

**Korlimbinis, A.**, Hains, P.G., Truscott, R.J.W. & Aquilina, J.A. 3-Hydroxykynurenine Oxidizes  $\alpha$ -Crystallin: Potential Role in Cataractogenesis. *Biochemistry* **2006**, *45*, 1852-1860

**Korlimbinis, A.** & Truscott, R.J.W. Identification of 3-Hydroxykynurenine Bound to Proteins in the Human Lens. A Possible Role in Age-Related Nuclear Cataract. *Biochemistry* **2006**, *45*, 1950-1960

## **Table of Contents**

|   |            |
|---|------------|
| <b>Certification .....</b>  | <b>ii</b>  |
| <b>Acknowledgements.....</b>  | <b>iii</b> |
| <b>Publications.....</b>  | <b>iv</b>  |
| <b>Abbreviations .....</b>  | <b>ix</b>  |
| <b>List of Figures.....</b>   | <b>xi</b>  |
| <b>List of Schemes .....</b>  | <b>xix</b> |
| <b>List of Tables .....</b>   | <b>xx</b>  |
| <b>Abstract.....</b>  | <b>xxi</b> |
| <b>Chapter 1 .....</b>  | <b>1</b>   |
| <b>Introduction .....</b>   | <b>1</b>   |
| <b>1.1 General Introduction .....</b>   | <b>1</b>   |
| <b>1.2 The Human Eye.....</b>   | <b>2</b>   |
| <b>1.3 The Lens.....</b>  | <b>3</b>   |
| <b>1.4 Components of the Lens .....</b>   | <b>5</b>   |
| 1.4.1 Proteins in the Lens .....  | 7          |
| 1.4.2 Antioxidants .....  | 8          |
| 1.4.3 UV Filters.....   | 9          |
| <b>1.5 Aging of the Human Lens.....</b>   | <b>12</b>  |
| <b>1.6 Cataract.....</b>  | <b>18</b>  |
| <b>1.7 Age-Related Nuclear (ARN) Cataract.....</b>  | <b>20</b>  |
| <b>1.8 3OHKyn .....</b>   | <b>23</b>  |
| <b>1.9 Aims of the Project.....</b>   | <b>26</b>  |
| <b>Chapter 2 .....</b>  | <b>27</b>  |
| <b>Synthesis and Characterisation of 3OHKyn Amino Acid Adducts.....</b>                                       | <b>27</b>  |
| <b>2.1 Introduction .....</b>   | <b>27</b>  |
| <b>2.2 Materials and Methods.....</b>   | <b>29</b>  |
| 2.2.1 Materials.....  | 29         |
| 2.2.2 Synthesis and Purification of 3OHKyn Modified Amino Acids .....   | 29         |
| 2.2.3 High Performance Liquid Chromatography (HPLC) for Purification of the<br>3OHKyn Amino Acid Adducts..... | 30         |
| 2.2.4 Formation of the 3OHKyn Amino Acid Adducts at pH 7.2 .....  | 31         |



|   |               |
|---|---------------|
| 2.2.5 Acid Hydrolysis of 3OHKyn Amino Acid Adducts .....  | 31            |
| 2.2.6 Stability of 3OHKyn Amino Acid Adducts at pH 4.0 .....  | 31            |
| 2.2.7 Stability of 3OHKyn Amino Acid Adducts at pH 7.2 .....  | 31            |
| 2.2.8 Incubation of 3OHKyn-Cys in the Presence of Excess N- $\alpha$ - <i>t</i> -Boc-His and N- $\alpha$ - <i>t</i> -Boc-Lys..... | 32            |
| 2.2.9 HPLC for Acid Hydrolysis and Stability Studies .....  | 32            |
| 2.2.10 Mass Spectrometry.....   | 32            |
| 2.2.11 Tandem Mass Spectrometry (MS/MS) .....   | 33            |
| 2.2.12 High Resolution Mass Spectrometry .....  | 33            |
| 2.2.13 NMR Spectroscopy .....   | 33            |
| 2.2.14 Fluorescence and UV-visible Spectroscopy.....  | 34            |
| <b>2.3 Results .....</b>  | <b>35</b>     |
| 2.3.1 Synthesis of the 3OHKyn Amino Acid Adducts .....  | 35            |
| 2.3.2 Formation of the 3OHKyn Amino Acid Adducts at pH 7.2 .....  | 40            |
| 2.3.3 Mass Spectrometric Characterisation of the 3OHKyn Amino Acid Adducts.....   | 42            |
| 2.3.4 NMR Characterisation of 3OHKyn Amino Acid Adducts .....   | 50            |
| 2.3.5 UV-visible and Fluorescence Characterisation of the 3OHKyn Amino Acid Adducts .....   | 52            |
| 2.3.6 Stability of 3OHKyn Amino Acid Adducts.....   | 60            |
| 2.3.7 Acid Hydrolysis of 3OHKyn Amino Acid Adducts .....  | 66            |
| 2.3.8 Incubation of 3OHKyn-Cys in the Presence of Excess N- $\alpha$ - <i>t</i> -Boc-His and N- $\alpha$ - <i>t</i> -Boc-Lys..... | 67            |
| <b>2.4 Discussion.....</b>  | <b>75</b>     |
| <br><b>Chapter 3 .....</b>  | <br><b>83</b> |
| <b>Lens Proteins Modified with 3OHKyn.....</b>  | <b>83</b>     |
| <b>3.1 Introduction .....</b>   | <b>83</b>     |
| <b>3.2 Materials and Methods.....</b>   | <b>85</b>     |
| 3.2.1 Materials.....  | 85            |
| 3.2.2 Preparation of Calf Lens Protein (CLP) <sup>196</sup> .....   | 85            |
| 3.2.3 Incubation of CLP with 3OHKyn at pH 7.2 for 48 Hours <sup>103</sup> .....   | 85            |
| 3.2.4 Incubation of CLP with 3OHKyn at pH 9.5 .....   | 86            |
| 3.2.5 Acid Hydrolysis of CLP and CLP Modified with 3OHKyn.....  | 86            |
| 3.2.6 Preparation of Human Lens Protein.....  | 86            |
| 3.2.7 Acid Hydrolysis of Human Lens Protein .....   | 86            |
| 3.2.8 HPLC .....  | 86            |
| 3.2.9 Quantification of Protein-Bound 3OHKyn .....  | 87            |
| 3.2.10 Incubation of CLP with 3OHKyn at pH 7.2 for 24 Days.....   | 88            |
| 3.2.11 Measurement of Protein Sulfhydryl (PSH) Levels in 3OHKyn-Modified Protein .....  | 88            |
| 3.2.12 Incubation of $\alpha$ -Crystallin with 3OHKyn at pH 7.2 for 48 Hours.....   | 88            |
| 3.2.13 HPLC to Purify Modified $\alpha$ -Crystallin.....  | 88            |
| 3.2.14 Trypsin Digestion.....   | 89            |
| 3.2.15 HPLC of Trypsin Digests.....   | 89            |
| 3.2.16 Measurement of Oxygen Levels .....   | 89            |
| 3.2.17 Hydrogen Peroxide (H <sub>2</sub> O <sub>2</sub> ) Assay.....  | 89            |

|  |            |
|--|------------|
| 3.2.18 Sodium Dodecyl Sulphate Polyacrylamide Gel Electrophoresis (SDS-PAGE).....    | 89         |
| 3.2.19 Mass Spectrometry.....  | 90         |
| 3.2.20 Tandem Mass Spectrometry (MS/MS) .....  | 90         |
| 3.2.21 Fluorescence and UV-visible Spectroscopy.....                                 | 90         |
| 3.2.22 Statistical Analysis .....  | 90         |
| <b>3.3 Results .....</b>   | <b>91</b>  |
| 3.3.1 CLP Modified with 3OHKyn.....  | 91         |
| 3.3.2 Fluorescence and UV-visible Spectroscopy of CLP Modified with 3OHKyn .....     | 93         |
| 3.3.3 Acid Hydrolysis of Lens Protein.....   | 96         |
| 3.3.4 Acid Hydrolysis of Human Lens Proteins .....                                   | 98         |
| 3.3.5 Determination of 3OHKyn Bound to Proteins.....                                 | 101        |
| 3.3.6 CLP Modified with 3OHKyn for 24 Days.....                                      | 136        |
| 3.3.7 Identification of CLP Peptides Modified with 3OHKyn .....                      | 139        |
| 3.3.8 Bovine $\alpha$ -Crystallin Modified with 3OHKyn.....                          | 148        |
| 3.3.9 Tryptic Digestion of Modified $\alpha$ A-Crystallin.....                       | 154        |
| 3.3.10 Acid Hydrolysis of Modified $\alpha$ A-Crystallin.....                        | 160        |
| 3.3.11 Tryptic Digestion of Modified $\alpha$ B-Crystallin.....                      | 161        |
| <b>3.4 Discussion.....</b>   | <b>168</b> |
| <b>Chapter 4 .....</b>   | <b>178</b> |
| <b>Does 3OHKyn Crosslink Lens Proteins? .....</b>                                    | <b>178</b> |
| 4.1 Introduction .....   | 178        |
| 4.2 Materials and Methods.....   | 180        |
| 4.2.1 Materials.....   | 180        |
| 4.2.2 Incubations with 3OHKyn- <i>t</i> -Boc-His and 3OHKyn- <i>t</i> -Boc-Lys ..... | 180        |
| 4.2.3 Incubation of CLP Modified by 3OHKyn at pH 7.2.....                            | 181        |
| 4.2.4 SDS-PAGE.....  | 182        |
| 4.2.5 HPLC .....   | 182        |
| 4.2.6 Mass Spectrometry.....   | 182        |
| 4.2.7 Tandem Mass Spectrometry (MS/MS) .....   | 182        |
| 4.2.8 Fluorescence and UV-visible Spectroscopy .....                                 | 182        |
| 4.2.9 NMR Spectroscopy .....   | 182        |
| <b>4.3 Results .....</b>   | <b>183</b> |
| 4.3.1 Incubations with the 3OHKyn- <i>t</i> -Boc-His Adduct.....                     | 183        |
| 4.3.2 Incubations with the 3OHKyn- <i>t</i> -Boc-Lys Adduct .....                    | 201        |
| 4.3.3 Incubation of 3OHKyn-Modified CLP (pH 7.2) .....                               | 210        |
| 4.3.4 Incubation of 3OHKyn-Modified CLP (pH 9.5) .....                               | 221        |
| <b>4.4 Discussion.....</b>   | <b>233</b> |
| <b>Chapter 5 .....</b>   | <b>239</b> |
| <b>Isolation of Novel Compounds from Human Cataract Lenses .....</b>                 | <b>239</b> |
| 5.1 Introduction .....   | 239        |
| 5.2 Materials and Methods.....   | 242        |
| 5.2.1 Materials.....   | 242        |

|   |                |
|---|----------------|
| 5.2.2 Preparation of Cataract Lens Protein .....              | 242            |
| 5.2.3 Hydrolysis of Cataract Lens Protein .....               | 242            |
| 5.2.4 First Stage of HPLC Purification .....                  | 242            |
| 5.2.5 Second Stage of HPLC Purification.....                  | 243            |
| 5.2.5.1 HPLC Gradient for P1.....                             | 243            |
| 5.2.5.2 HPLC Gradient for P2, P3, P4 and P5 .....             | 243            |
| 5.2.5.3 HPLC Gradient for P6 (second HPLC purification) ..... | 243            |
| 5.2.5.4 HPLC Gradient for P6 (third HPLC purification) .....  | 244            |
| 5.2.6 Mass Spectrometry .....                                 | 244            |
| 5.2.7 Tandem Mass Spectrometry (MS/MS) .....                  | 244            |
| 5.2.8 High Resolution Mass Spectrometry .....                 | 244            |
| 5.2.9 NMR Spectroscopy .....                                  | 244            |
| 5.2.10 UV-visible Spectroscopy .....                          | 244            |
| <b>5.3 Results .....</b>                                      | <b>245</b>     |
| 5.3.1 Analysis of P1 .....                                    | 245            |
| 5.3.2 Analysis of P2 .....                                    | 250            |
| 5.3.3 Analysis of P3 .....                                    | 255            |
| 5.3.4 Analysis of P4 .....                                    | 259            |
| 5.3.5 Analysis of P5 .....                                    | 268            |
| 5.3.6 Analysis of P6 .....                                    | 272            |
| <b>5.4 Discussion.....</b>                                    | <b>274</b>     |
| <br><b>Chapter 6 .....</b>                                    | <br><b>280</b> |
| <br><b>Conclusions and Future Directions .....</b>            | <br><b>280</b> |
| <br><b>References .....</b>                                   | <br><b>283</b> |
| <br><b>Appendix 1 .....</b>                                   | <br><b>296</b> |

## **Abbreviations**

|                               |  |
|-------------------------------|--|
| ACN                           | acetonitrile   |
| AGE                           | advanced glycation end   |
| AHBDG                         | 4-(2-amino-3-hydroxyphenyl)-4-oxobutanoic acid <i>O</i> - $\beta$ -D-diglucoside |
| AHBG                          | 4-(2-amino-3-hydroxyphenyl)-4-oxobutanoic acid <i>O</i> - $\beta$ -D-glucoside   |
| ARN                           | age-related nuclear  |
| Boc                           | butyloxycarbonyl   |
| CLP                           | calf lens protein  |
| Cys                           | cysteine   |
| Da                            | dalton   |
| DCI                           | deuterium chloride   |
| D <sub>2</sub> O              | deuterium oxide  |
| DTND                          | 5,5'-dithio-bis(2-nitrobenzoic acid)   |
| DTT                           | dithiothreitol   |
| EDTA                          | ethylenediaminetetraacetic acid  |
| Em                            | emission   |
| ESI-MS                        | electrospray ionisation mass spectrometry  |
| Ex                            | excitation   |
| Guanidine HCl                 | guanidine hydrochloride  |
| GSH                           | glutathione (reduced)  |
| His                           | histidine  |
| H <sub>2</sub> O <sub>2</sub> | hydrogen peroxide  |
| HRP                           | horseradish peroxidase   |
| Kyn                           | kynurenine   |
| Kyn-GSH                       | kynurenine-glutathione   |
| Lys                           | lysine   |
| Met                           | methionine   |
| M <sub>ox</sub>               | methionine sulfoxide   |
| MS/MS                         | tandem mass spectrometry   |
| Msr                           | methionine sulfoxide reductase   |

|                                 |  |
|---------------------------------|--|
| MW                              | molecular weight   |
| NanoESI-MS                      | nanoelectrospray ionisation mass spectrometry              |
| Na <sub>2</sub> CO <sub>3</sub> | sodium carbonate   |
| NaHCO <sub>3</sub>              | sodium bicarbonate   |
| NaN <sub>3</sub>                | sodium azide   |
| NMR                             | nuclear magnetic resonance                                 |
| 3OHKyn                          | 3-hydroxykynurenine  |
| 3OHKyn-GSH                      | 3-hydroxykynurenine-glutathione                            |
| 3OHKynG                         | 3-hydroxykynurenine <i>O</i> -β-D-glucoside                |
| 3OHKynG-GSH                     | 3-hydroxykynurenine <i>O</i> -β-D-glucoside-glutathione    |
| OPD                             | <i>o</i> -phenylenediamine                                 |
| PDA                             | photodiode array   |
| PMSF                            | phenylmethylsulfonyl fluoride                              |
| PSH                             | protein sulfhydryl   |
| PTM                             | post-translational modification                            |
| RP-HPLC                         | reversed phase high performance liquid chromatography      |
| SDS-PAGE                        | sodium dodecyl sulphate polyacrylamide gel electrophoresis |
| SH                              | sulfhydryl   |
| TFA                             | trifluoroacetic acid                                       |
| Tris-HCl                        | tris(hydroxymethyl)aminomethane hydrochloride              |
| Trp                             | tryptophan   |
| W <sub>ox</sub>                 | oxidised tryptophan  |

## List of Figures

|  |    |
|--|----|
| <b>Figure 1.1</b> Schematic diagram of the cross section of the human eye. <sup>10</sup>   | 2  |
| <b>Figure 1.2</b> Cross-section of the human lens (adapted from J. Harding). <sup>14</sup>   | 4  |
| <b>Figure 1.3</b> Structure of GSH.  | 9  |
| <b>Figure 1.4</b> Structures of the AGE products found in human lenses. <sup>105,106,130,131</sup>   | 16 |
| <b>Figure 1.5</b> The Pirie classification of nuclear cataracts <sup>161</sup> using slit lamp photographs. <sup>164</sup><br>The colour of the nucleus increases with increasing severity of nuclear cataract.  | 20 |
| <b>Figure 1.6</b> Structures of non-disulfide bond crosslink compounds identified in cataract lens proteins.   | 22 |
| <b>Figure 1.7</b> Structure of Phenoxazone.  | 24 |
| <b>Figure 2.1</b> Structures of the 3OHKyn amino acid adducts.   | 28 |
| <b>Figure 2.2</b> HPLC trace of 3OHKyn and L-Cys. 3OHKyn was incubated with L-Cys at pH 9.5, 37°C for 48 hours (UV detection monitored at 360 nm). The peak at 15.6 min is unreacted 3OHKyn, and the peak at 18.9 min is the 3OHKyn amino acid adduct, 3OHKyn-Cys.   | 37 |
| <b>Figure 2.3</b> HPLC trace of 3OHKyn and N- $\alpha$ - <i>t</i> -Boc-L-His. 3OHKyn was incubated with N- $\alpha$ - <i>t</i> -Boc-L-His at pH 9.5, 37°C for 48 hours (UV detection monitored at 360 nm). The peak at 14.8 min is unreacted 3OHKyn, the peak at 18.3 min contained N- $\alpha$ - <i>t</i> -Boc-L-His, the peak at 19.8 min is unknown. The peak at 22.6 min is 3OHKyn-yellow, the peak at 25.0 min is xanthommatin, and the peak at 26.2 min is the 3OHKyn amino acid adduct, 3OHKyn- <i>t</i> -Boc-His.    | 38 |
| <b>Figure 2.4</b> HPLC trace of 3OHKyn and N- $\alpha$ - <i>t</i> -Boc-L-Lys. 3OHKyn was incubated with N- $\alpha$ - <i>t</i> -Boc-L-Lys at pH 9.5 and 37°C for 48 hours (UV detection monitored at 360 nm). The peak at 14.8 min is unreacted 3OHKyn, the peak at 18.7 min contained N- $\alpha$ - <i>t</i> -Boc-L-Lys, the peak at 20.1 min is unknown. The peak at 22.5 min is 3OHKyn-yellow, the peak at 25.0 min is xanthommatin, and the peak at 26.8 min is the 3OHKyn amino acid adduct, 3OHKyn- <i>t</i> -Boc-Lys. | 39 |
| <b>Figure 2.5</b> Formation of 3OHKyn amino acid adducts over a 5 day incubation. 3OHKyn was incubated with a 25-fold molar excess of N- $\alpha$ - <i>t</i> -Boc-L-His, N- $\alpha$ - <i>t</i> -Boc-L-Lys, or Cys at pH 7.2, 37°C.  | 41 |
| <b>Figure 2.6</b> MS/MS spectrum of the protonated molecular ion of 3OHKyn-Cys <i>m/z</i> 329.   | 44 |
| <b>Figure 2.7</b> MS/MS spectrum of the protonated molecular ion of 3OHKyn- <i>t</i> -Boc-His <i>m/z</i> 463.  | 46 |
| <b>Figure 2.8</b> MS/MS spectrum of the protonated molecular ion of 3OHKyn- <i>t</i> -Boc-Lys <i>m/z</i> 454.  | 48 |
| <b>Figure 2.9</b> UV-visible spectra of 3OHKyn-Cys at various pH values; A, pH 2.1; B, pH 5.5; C, pH 7.2; D, pH 9.5.   | 54 |
| <b>Figure 2.10</b> 3-D Fluorescence spectra of 3OHKyn-Cys at various pH values; A, pH 2.1; B, pH 5.5; C, pH 7.2; D, pH 9.5.  | 55 |
| <b>Figure 2.11</b> UV-visible spectra of 3OHKyn- <i>t</i> -Boc-His at various pH values; A, pH 2.1; B, pH 5.5; C, pH 7.2; D, pH 9.5.   | 56 |
| <b>Figure 2.12</b> 3-D Fluorescence spectra of 3OHKyn- <i>t</i> -Boc-His at various pH values; A, pH 2.1; B, pH 5.5; C, pH 7.2; D, pH 9.5.   | 57 |
| <b>Figure 2.13</b> UV-visible spectra of 3OHKyn- <i>t</i> -Boc-Lys at various pH values; A, pH 2.1; B, pH 5.5; C, pH 7.2; D, pH 9.5.   | 58 |

|  |    |
|--|----|
| <b>Figure 2.14</b> 3-D Fluorescence spectra of 3OHKyn- <i>t</i> -Boc-Lys at various pH values; <i>A</i> , pH 2.1; <i>B</i> , pH 5.5; <i>C</i> , pH 7.2; <i>D</i> , pH 9.5.....   | 59 |
| <b>Figure 2.15</b> Stability of the 3OHKyn amino acid adducts and 3OHKyn at pH 7.2 in the absence (■) and presence (◆) of oxygen. <i>A</i> , 3OHKyn; <i>B</i> , 3OHKyn-Cys; <i>C</i> , 3OHKyn- <i>t</i> -Boc-His; <i>D</i> , 3OHKyn- <i>t</i> -Boc-Lys.....  | 63 |
| <b>Figure 2.16</b> Stability of the 3OHKyn amino acid adducts and 3OHKyn at pH 4.0 in the absence (■) and presence (◆) of oxygen. <i>A</i> , 3OHKyn; <i>B</i> , 3OHKyn-Cys; <i>C</i> , 3OHKyn- <i>t</i> -Boc-His; <i>D</i> , 3OHKyn- <i>t</i> -Boc-Lys.....  | 64 |
| <b>Figure 2.17</b> Formation of breakdown products from stability study of 3OHKyn amino acid adducts at pH 7.2 in the absence of oxygen. <i>A</i> , 3OHKyn-Cys; <i>B</i> , 3OHKyn- <i>t</i> -Boc-His; <i>C</i> , 3OHKyn- <i>t</i> -Boc-Lys. ....   | 65 |
| <b>Figure 2.18</b> 3OHKyn-Cys was incubated with excess N- $\alpha$ - <i>t</i> -Boc-His and N- $\alpha$ - <i>t</i> -Boc-Lys at pH 7.2 for a total of 48 hours. Shown is the 48 hour time sample (aliquot). The peak at 28.4 min is unreacted 3OHKyn-Cys. The peak at 30.6 min contained unreacted N- $\alpha$ - <i>t</i> -Boc-His, and the peak at 32.4 min contained unreacted N- $\alpha$ - <i>t</i> -Boc-Lys. The peak at 33.5 min is 3OHKyn-yellow, the peak at 35.1 min is 3OHKyn- <i>t</i> -Boc-His and the peak at 36.0 min is 3OHKyn- <i>t</i> -Boc-Lys. The peak at 39.5 min is unknown (U39.5). .... | 69 |
| <b>Figure 2.19</b> The rate of loss of 3OHKyn-Cys in relation to the rate of formation of 3OHKyn-yellow, 3OHKyn- <i>t</i> -Boc-His, 3OHKyn- <i>t</i> -Boc-Lys and unknown compound eluting at 39.5 min (U39.5) on the HPLC chromatogram (Figure 2.18). ....  | 70 |
| <b>Figure 2.20</b> Mass spectra of U39.5. <i>A</i> , ESI mass spectrum; <i>B</i> , MS/MS spectrum of <i>m/z</i> 664 ion.....   | 71 |
| <b>Figure 2.21</b> Proposed structures of molecular ion <i>m/z</i> 664, and fragment ions <i>m/z</i> 608, 564 and 409. ....  | 72 |
| <b>Figure 2.22</b> Mass spectra of aliquot from autoxidation of 3OHKyn at pH 7.2. <i>A</i> , ESI mass spectrum of aliquot after 3 hours of incubation; <i>B</i> , MS/MS spectrum of ion <i>m/z</i> 409. ....   | 73 |
| <b>Figure 2.23</b> UV-visible spectrum of U39.5.....   | 74 |
| <b>Figure 2.24</b> Structures of the common fragment ions for all three 3OHKyn amino acid adducts. ....  | 76 |
| <b>Figure 3.1</b> Photograph of the CLP modified with 3OHKyn at pH 7.2 on the left; and CLP modified with 3OHKyn at pH 9.5 on the right. CLP was incubated with 3OHKyn at 37°C for 48 hours. As can be seen the protein modified at pH 7.2 was pink and the protein modified at pH 9.5 was brown. ....   | 91 |
| <b>Figure 3.2</b> SDS-PAGE of proteins. Lane 1: Marker; Lane 2: CLP; Lane 3: CLP modified with 3OHKyn at pH 7.2; Lane 4: CLP modified with 3OHKyn at pH 9.5. <i>A</i> , Non-reducing conditions; <i>B</i> , Reducing conditions.....   | 92 |
| <b>Figure 3.3</b> CLP modified with 3OHKyn at pH 7.2 for 48 hours. <i>A</i> , UV-visible spectrum, (protein concentration: 10 mg/mL in 6 M guanidine HCl); <i>B</i> , 3-D fluorescence spectrum, (protein concentration: 2 mg/mL in 6 M guanidine HCl). ....   | 94 |
| <b>Figure 3.4</b> CLP modified with 3OHKyn at pH 9.5 for 48 hours. <i>A</i> , UV-visible spectrum, (protein concentration: 1 mg/mL in 6 M guanidine HCl); <i>B</i> , 3-D fluorescence spectrum, (protein concentration: 2 mg/mL in 6 M guanidine HCl). ....  | 95 |
| <b>Figure 3.5</b> HPLC chromatograms of acid hydrolysed lens protein samples. <i>A</i> , CLP; <i>B</i> , CLP modified by 3OHKyn at pH 7.2 for 48 hours; <i>C</i> , CLP modified by 3OHKyn at pH 9.5 for 48 hours. ....   | 97 |

|   |     |
|---|-----|
| <b>Figure 3.6</b> HPLC chromatograms of human lens sample (76 year old male) hydrolysed with HCl and antioxidants. <i>A</i> , Lens sample spiked with 3OHKyn amino acid adducts prior to hydrolysis, in order to observe the elution time of the standards; <i>B</i> , Hydrolysed human lens sample (unspiked). ..... | 99  |
| <b>Figure 3.7</b> MS/MS spectra of 3OHKyn-Cys. <i>A</i> , Authentic 3OHKyn-Cys; <i>B</i> , HPLC peak isolated from an aged human lens (76 year old male); <i>m/z</i> 329 is the molecular ion. ....   | 100 |
| <b>Figure 3.8</b> Synthesis of standard 3OHKyn-GSH. <i>A</i> , HPLC chromatogram; <i>B</i> , MS/MS spectrum of ion <i>m/z</i> 515. ....   | 103 |
| <b>Figure 3.9</b> Incubation of 3OHKyn-Cys with excess GSH at pH 9.5. Recovery of 3OHKyn-Cys and the yield of 3OHKyn-GSH.....   | 104 |
| <b>Figure 3.10</b> Incubation of 3OHKyn- <i>t</i> -Boc-His with excess GSH at pH 9.5. Recovery of 3OHKyn- <i>t</i> -Boc-His and the yield of 3OHKyn-GSH. ....   | 105 |
| <b>Figure 3.11</b> Incubation of 3OHKyn- <i>t</i> -Boc-Lys with excess GSH at pH 9.5. Recovery of 3OHKyn- <i>t</i> -Boc-Lys and the yield of 3OHKyn-GSH.....  | 105 |
| <b>Figure 3.12</b> Incubation of Kyn-Cys with excess GSH at pH 9.5. Recovery of Kyn-Cys and the yield of Kyn-GSH. ....  | 106 |
| <b>Figure 3.13</b> Incubation of Kyn- <i>t</i> -Boc-His with excess GSH at pH 9.5. Recovery of Kyn- <i>t</i> -Boc-His and yield of Kyn-GSH. ....  | 107 |
| <b>Figure 3.14</b> Incubation of Kyn- <i>t</i> -Boc-Lys and excess GSH at pH 9.5. Recovery of Kyn- <i>t</i> -Boc-Lys and yield of Kyn-GSH. ....   | 108 |
| <b>Figure 3.15</b> Yield of 3OHKyn-GSH from CLP that had been modified with 3OHKyn. Modified protein was incubated with excess GSH at pH 9.5 for 4 hours. <i>A</i> , HPLC chromatogram of filtrate; <i>B</i> , MS/MS spectrum of ion <i>m/z</i> 515 in the 30 min peak (Figure 3.15A).....                            | 109 |
| <b>Figure 3.16</b> HPLC chromatogram of the ethanol extract from a human normal lens cortex (81 years old).....   | 111 |
| <b>Figure 3.17</b> HPLC chromatograms of human lens protein incubated with excess GSH at pH 9.5 for 4 hours. <i>A</i> , Normal 79 year old nucleus; <i>B</i> , Normal 79 year old cortex. ....  | 113 |
| <b>Figure 3.18</b> MS/MS spectra of the three kynurenine derived UV filter GSH adducts isolated from a normal human lens nucleus. <i>A</i> , Molecular ion <i>m/z</i> 677; <i>B</i> , Molecular ion <i>m/z</i> 499; <i>C</i> , Molecular ion <i>m/z</i> 515.....  | 114 |
| <b>Figure 3.19</b> Protein – bound 3OHKyn. The concentration of 3OHKyn bound to the nuclear proteins of normal human lenses as a function of age. ....  | 115 |
| <b>Figure 3.20</b> Free 3OHKyn. The concentration of free 3OHKyn in the nucleus. <i>A</i> , Normal lenses; <i>B</i> , Dark cataract lenses; <i>C</i> , Light cataract lenses. ....  | 117 |
| <b>Figure 3.21</b> Free 3OHKyn. The concentration of free 3OHKyn in the cortex. <i>A</i> , Normal lenses; <i>B</i> , Dark cataract lenses; <i>C</i> , Light cataract lenses.....  | 118 |
| <b>Figure 3.22</b> Plot of the concentration of free 3OHKyn in the nucleus versus the concentration of bound 3OHKyn in the nucleus of normal aged lenses.....   | 119 |
| <b>Figure 3.23</b> Protein – bound 3OHKynG. The concentration of bound 3OHKynG in the nucleus. <i>A</i> , Normal lenses; <i>B</i> , Dark cataract lenses; <i>C</i> , Light cataract lenses.....   | 121 |
| <b>Figure 3.24</b> Protein – bound 3OHKynG. The concentration of bound 3OHKynG in the cortex. <i>A</i> , Normal lenses; <i>B</i> , Dark cataract lenses; <i>C</i> , Light cataract lenses.....  | 122 |
| <b>Figure 3.25</b> Free 3OHKynG. The concentration of free 3OHKynG in the nucleus. <i>A</i> , Normal lenses; <i>B</i> , Dark cataract lenses; <i>C</i> , Light cataract lenses. ....  | 124 |



|  |     |
|--|-----|
| <b>Figure 3.26</b> Free 3OHKynG. The concentration of free 3OHKynG in the cortex. <i>A</i> , Normal lenses; <i>B</i> , Dark cataract lenses; <i>C</i> , Light cataract lenses. ....  | 125 |
| <b>Figure 3.27</b> Plot of the concentration of free vs bound 3OHKynG. <i>A</i> , Nucleus; <i>i</i> , Normal lenses; <i>ii</i> , Dark cataract; <i>iii</i> , Light cataract lenses; <i>B</i> , Cortex; <i>i</i> , Normal lenses; <i>ii</i> , Dark cataract; <i>iii</i> , Light cataract lenses. ....   | 127 |
| <b>Figure 3.28</b> Protein – bound Kyn. The concentration of bound Kyn in the nucleus. <i>A</i> , Normal lenses; <i>B</i> , Dark cataract lenses; <i>C</i> , Light cataract lenses. ....   | 129 |
| <b>Figure 3.29</b> Protein – bound Kyn. The concentration of bound Kyn in the cortex. <i>A</i> , Normal lenses; <i>B</i> , Dark cataract lenses; <i>C</i> , Light cataract lenses. ....  | 130 |
| <b>Figure 3.30</b> Free Kyn. The concentration of free Kyn in the nucleus. <i>A</i> , Normal lenses; <i>B</i> , Dark cataract lenses; <i>C</i> , Light cataract lenses. ....   | 132 |
| <b>Figure 3.31</b> Free Kyn. The concentration of free Kyn in the cortex. <i>A</i> , Normal lenses; <i>B</i> , Dark cataract lenses; <i>C</i> , Light cataract lenses. ....  | 133 |
| <b>Figure 3.32</b> Plot of the concentration of free vs bound Kyn. <i>A</i> , Nucleus; <i>i</i> , Normal lenses; <i>ii</i> , Dark cataract; <i>iii</i> , Light cataract lenses; <i>B</i> , Cortex; <i>i</i> , Normal lenses; <i>ii</i> , Dark cataract; <i>iii</i> , Light cataract lenses. ....   | 135 |
| <b>Figure 3.33</b> Photograph of CLP modified with 3OHKyn at pH 7.2 under low oxygen. Aliquots were taken at 0, 3, 6, 9, 12, 15, 18, 21 and 24 days. ....  | 137 |
| <b>Figure 3.34</b> Formation of 3OHKyn amino acid adducts in CLP over time. CLP was incubated with 3OHKyn at 37 <sup>0</sup> C for a total of 24 days. ....  | 138 |
| <b>Figure 3.35</b> The content of PSH in CLP modified with 3OHKyn at 37 <sup>0</sup> C for 24 days. ....   | 138 |
| <b>Figure 3.36</b> HPLC chromatograms following trypsin digestion of CLP modified with 3OHKyn for 12 days. Arrowed peaks were collected for mass spectral analysis. <i>A</i> , UV trace; <i>B</i> , Fluorescence trace. ....   | 139 |
| <b>Figure 3.37</b> ESI mass spectrum of the peak eluting at 45.1 min in Figure 3.36. ....  | 140 |
| <b>Figure 3.38</b> ESI mass spectrum of the peak eluting at 50.5 min (Figure 3.36). ....   | 143 |
| <b>Figure 3.39</b> MS/MS spectrum of ion (M+3H) <sup>3+</sup> <i>m/z</i> 398.3. The sequence confirms that the peptide is $\alpha$ B T6-7 (DRFSVNLDVK). ....   | 145 |
| <b>Figure 3.40</b> MS/MS spectrum of ion (M+2H) <sup>2+</sup> <i>m/z</i> 519.4. The sequence confirms that the peptide is $\alpha$ A T3 (TLGPFYPSR). ....  | 146 |
| <b>Figure 3.41</b> MS/MS spectrum of ion (M+2H) <sup>2+</sup> <i>m/z</i> 594.4. The sequence confirms that the peptide is $\beta$ B1 T14 (WDTWSSSYR). ....   | 146 |
| <b>Figure 3.42</b> $\alpha$ -Crystallin was modified with 3OHKyn at 37 <sup>0</sup> C for 48 hours. <i>A</i> , HPLC chromatogram of the initial aliquot of the reaction mixture at time zero; <i>B</i> , HPLC chromatogram of the reaction mixture after incubation for 48 hours. ....   | 150 |
| <b>Figure 3.43</b> Transformed mass spectra. <i>A</i> , Native bovine $\alpha$ B-crystallin; <i>B</i> , Modified bovine $\alpha$ B-crystallin. ....  | 151 |
| <b>Figure 3.44</b> Transformed mass spectra. <i>A</i> , Native bovine $\alpha$ A-crystallin; <i>B</i> , Modified bovine $\alpha$ A-crystallin. ....  | 152 |
| <b>Figure 3.45</b> Photograph of modified $\alpha$ -crystallins. Bovine $\alpha$ -crystallin was incubated with 3OHKyn at 37 <sup>0</sup> C for 48 hours under low oxygen tension. Native $\alpha$ -crystallin is white in colour. As shown, the modified $\alpha$ A- and $\alpha$ B-crystallins are pink in colour, and were purified by HPLC. .... | 153 |
| <b>Figure 3.46</b> HPLC chromatogram of tryptic digest products of $\alpha$ A-crystallin following modification with 3OHKyn. Arrow indicates the peak that contained a peptide with an oxidised amino acid residue. ....   | 155 |

|  |     |
|--|-----|
| <b>Figure 3.47</b> MS/MS spectrum of an oxidised $\alpha$ A-crystallin peptide, residues 1-11, showing oxidation at Met1. The sequence for this peptide is shown above the spectrum. ....  | 156 |
| <b>Figure 3.48</b> nanoESI-MS spectrum of tryptically digested 3OHKyn-modified $\alpha$ A-crystallin. ....   | 158 |
| <b>Figure 3.49</b> MS/MS spectrum of an oxidised $\alpha$ A-crystallin peptide, residues 120-145, showing oxidation at Met138. ....  | 159 |
| <b>Figure 3.50</b> HPLC chromatogram of acid hydrolysed 3OHKyn-modified $\alpha$ A-crystallin. ....  | 160 |
| <b>Figure 3.51</b> HPLC chromatogram of tryptic digest products of $\alpha$ B-crystallin after modification with 3OHKyn. Arrows indicate peaks that contained peptides with oxidatively modified amino acid residues. ....   | 162 |
| <b>Figure 3.52</b> MS/MS spectrum of an oxidised $\alpha$ B-crystallin peptide, residues 1-11, showing oxidation at Met1. ....   | 163 |
| <b>Figure 3.53</b> MS/MS spectrum of an oxidised $\alpha$ B-crystallin peptide, residues 1-11, showing oxidation at Met1 and Trp9. ....  | 164 |
| <b>Figure 3.54</b> MS/MS spectrum of an oxidised $\alpha$ B-crystallin peptide, residues 57-69, showing oxidation at Met68. ....   | 166 |
| <b>Figure 3.55</b> MS/MS spectrum of an oxidised $\alpha$ B-crystallin peptide, residues 57-69, showing oxidation at Met68 and Trp60. ....   | 167 |
| <b>Figure 4.1</b> HPLC separation of 3OHKyn- <i>t</i> -Boc-His incubated at pH 7.2. X is 3OHKyn- <i>t</i> -Boc-His. Peak 3 is an impurity stable to oxidation. A, Initial reaction mixture; B, Reaction mixture after 12 days of incubation. Arrowed peaks were collected for mass spectrometry. Absorbance monitored at 360 nm; C, Absorbance monitored at 440 nm. ....                 | 185 |
| <b>Figure 4.2</b> ESI mass spectra of peaks eluting from HPLC chromatogram in Figure 4.1B. ....  | 186 |
| <b>Figure 4.3</b> Rate of formation of unknown products in peaks 1, 2, 3, 4, and 5 from Figure 4.1B. The inset shows the rate of loss of 3OHKyn- <i>t</i> -Boc-His, in relation to the formation of products. Peak 3 is an impurity from the synthesis of 3OHKyn- <i>t</i> -Boc-His, which is stable to oxidation. ....  | 187 |
| <b>Figure 4.4</b> HPLC of the acid digest of 3OHKyn- <i>t</i> -Boc-His following incubation for 12 days. HPLC chromatograms of, A, Absorbance monitored at 360 nm. Peaks 1, 2, 3, and 4 were collected for mass spectral analysis. B, Absorbance monitored at 440 nm. ....   | 189 |
| <b>Figure 4.5</b> ESI mass spectra of peaks eluting from the HPLC chromatogram in Figure 4.4A. ....  | 190 |
| <b>Figure 4.6</b> Incubation of 3OHKyn- <i>t</i> -Boc-His with a 20-fold molar excess of N- $\alpha$ - <i>t</i> -Boc-His for 12 days. HPLC chromatograms of, A, Initial reaction mixture; B, Reaction mixture after 12 days of incubation. Peak 1 eluted at 32.5 min, peak 2 at 33.5 min, peak 3 at 34.9 min, peak 4 at 39.7 min and peak 5 at 40.6 min (identical to Figure 4.1B). .... | 192 |
| <b>Figure 4.7</b> HPLC of the acid digest of 3OHKyn- <i>t</i> -Boc-His with a 20-fold molar excess of N- $\alpha$ - <i>t</i> -Boc-His following incubation for 12 days. HPLC chromatograms of, A, Absorbance monitored at 360 nm. Peak 1 eluted at 25.0 min, peak 2 at 28.6 min,   |     |

|  |     |
|--|-----|
| peak 3 at 32.5 min and peak 4 at 34.7 min. <i>B</i> , Absorbance monitored at 440 nm.  | 193 |
| <b>Figure 4.8</b> Incubation of 3OHKyn- <i>t</i> -Boc-His with a 20-fold molar excess of N- $\alpha$ - <i>t</i> -Boc-Lys for 12 days. HPLC chromatograms of, <i>A</i> , Initial reaction mixture; <i>B</i> , Reaction mixture after 12 days of incubation. Peak 1 eluted at 32.3 min, peak 2 at 33.2 min, peak 3 at 34.5 min, peak 4 at 39.9 min and peak 5 at 40.3 min (~identical to Figure 4.1B). | 195 |
| <b>Figure 4.9</b> HPLC of the acid digest of 3OHKyn- <i>t</i> -Boc-His with a 20-fold molar excess of N- $\alpha$ - <i>t</i> -Boc-Lys following incubation for 12 days. HPLC chromatograms of, <i>A</i> , Absorbance monitored at 360 nm. Peak 1 eluted at 25.3 min, peak 2 at 28.7 min, peak 3 at 32.5 min and peak 4 at 34.6 min. <i>B</i> , Absorbance monitored at 440 nm.                       | 196 |
| <b>Figure 4.10</b> MS/MS spectrum of the molecular ion <i>m/z</i> 550, eluting as a doublet in the hydrolysed HPLC profiles, involving 3OHKyn- <i>t</i> -Boc-His incubations.  | 197 |
| <b>Figure 4.11</b> HPLC chromatogram of peak 2 (Figures 4.1B, 4.6B and 4.8B) following deprotection with acid.   | 198 |
| <b>Figure 4.12</b> UV-visible spectra. <i>A</i> , Peak 2 (Figures 4.1B, 4.6B and 4.8B) ( <i>m/z</i> 650); <i>B</i> , Peak 2' (Figures 4.4A, 4.7A and 4.9A) ( <i>m/z</i> 550).  | 199 |
| <b>Figure 4.13</b> Proton NMR spectrum of peak 2' (Figures 4.4A, 4.7A and 4.9A) ( <i>m/z</i> 550).   | 200 |
| <b>Figure 4.14</b> Incubation of 3OHKyn- <i>t</i> -Boc-Lys at pH 7.2. HPLC chromatograms, <i>A</i> , Initial reaction mixture; <i>B</i> , Reaction mixture after 12 days of incubation.  | 202 |
| <b>Figure 4.15</b> HPLC of the acid digest of 3OHKyn- <i>t</i> -Boc-Lys following incubation for 12 days. HPLC chromatograms of, <i>A</i> , Absorbance monitored at 360 nm; <i>B</i> , Absorbance monitored at 440 nm.   | 203 |
| <b>Figure 4.16</b> Incubation of 3OHKyn- <i>t</i> -Boc-Lys with a 20-fold molar excess of N- $\alpha$ - <i>t</i> -Boc-His for 12 days. HPLC chromatograms of, <i>A</i> , Initial reaction mixture; <i>B</i> , Reaction mixture after 12 days of incubation.  | 205 |
| <b>Figure 4.17</b> HPLC of the acid digest of 3OHKyn- <i>t</i> -Boc-Lys with a 20-fold molar excess of N- $\alpha$ - <i>t</i> -Boc-His following incubation for 12 days. HPLC chromatograms of, <i>A</i> , Absorbance monitored at 360 nm. <i>B</i> , Absorbance monitored at 440 nm.  | 206 |
| <b>Figure 4.18</b> Incubation of 3OHKyn- <i>t</i> -Boc-Lys with a 20-fold molar excess of N- $\alpha$ - <i>t</i> -Boc-Lys for 12 days. HPLC chromatograms of, <i>A</i> , Initial reaction mixture; <i>B</i> , Reaction mixture after 12 days of incubation.  | 208 |
| <b>Figure 4.19</b> HPLC of the acid digest of 3OHKyn- <i>t</i> -Boc-Lys with a 20-fold molar excess of N- $\alpha$ - <i>t</i> -Boc-Lys following incubation for 12 days. HPLC chromatograms of, <i>A</i> , Absorbance monitored at 360 nm. <i>B</i> , Absorbance monitored at 440 nm.  | 209 |
| <b>Figure 4.20</b> SDS-PAGE of proteins from incubation of 3OHKyn modified CLP. Lane 1: Marker; Lane 2: Aliquot time = 0 days; Lane 3: Aliquot time = 3 days; Lane 4: Aliquot time = 6 days; Lane 5: Aliquot time = 9 days; Lane 6: Aliquot time = 12 days; Lane 7: Aliquot time = 15 days. <i>A</i> , Non-reducing conditions; <i>B</i> , Reducing conditions.                                      | 211 |
| <b>Figure 4.21</b> 3-D Fluorescence spectra of aliquots from the protein mixture. <i>A</i> , Initial aliquot; <i>B</i> , Aliquot after 15 days of incubation.  | 212 |
| <b>Figure 4.22</b> HPLC chromatogram of the filtrate from the protein aliquot after 1 day of incubation at pH 7.2.   | 213 |
| <b>Figure 4.23</b> ESI mass spectra of the peaks eluting in Figure 4.22. <i>A</i> , Peak 1 eluting at 30 min; <i>B</i> , Peak 2 eluting at 32.4 min; <i>C</i> , Peak 3 eluting at 33.7 min.  | 214 |

|   |     |
|---|-----|
| <b>Figure 4.24</b> HPLC chromatograms of acid hydrolysed proteins. <i>A</i> , Initial aliquot; <i>B</i> , Aliquot after 15 days of incubation. Arrowed peaks were collected for mass spectrometry.....  | 217 |
| <b>Figure 4.25</b> ESI mass spectra of peaks eluting in Figure 4.24B. <i>A</i> , Peak 2; <i>B</i> , Peak 3; <i>C</i> , Peak 4; <i>D</i> , Peak 5; <i>E</i> , Peak 6; <i>F</i> , Peak 7.....   | 218 |
| <b>Figure 4.26</b> ESI mass spectra of peaks eluting in Figure 4.24B. <i>A</i> , Peak 8; <i>B</i> , Peak 9; <i>C</i> , Peak 10; <i>D</i> , Peak 11; <i>E</i> , Peak 12; <i>F</i> , Peak 13.....   | 219 |
| <b>Figure 4.27</b> Concentration of 3OHKyn-Cys and 3OHKyn-His in protein samples during incubation of CLP originally modified by 3OHKyn at pH 7.2.....  | 220 |
| <b>Figure 4.28</b> SDS-PAGE of proteins from incubation of 3OHKyn modified CLP. Lane 1: Marker; Lane 2: Aliquot time = 0 days; Lane 3: Aliquot time = 1 days; Lane 4: Aliquot time = 2 days; Lane 5: Aliquot time = 3 days; Lane 6: Aliquot time = 4 days; Lane 7: Aliquot time = 6 days; Lane 8: Aliquot time = 8 days; Lane 9: Aliquot time = 10 days. <i>A</i> , Non-reducing conditions; <i>B</i> , Reducing conditions. .... | 222 |
| <b>Figure 4.29</b> 3-D Fluorescence spectra of the aliquots from the protein mixture. <i>A</i> , Initial aliquot; <i>B</i> , Aliquot after 10 days of incubation. ....  | 223 |
| <b>Figure 4.30</b> HPLC chromatogram of the filtrate from the protein aliquot after 1 day of incubation. ....   | 224 |
| <b>Figure 4.31</b> ESI mass spectra of the peaks eluting in Figure 4.30. <i>A</i> , Peak 1 eluting at 27 min; <i>B</i> , Peak 2 eluting at 28.3 min; <i>C</i> , Peak 3 eluting at 29.4 min; <i>D</i> , Peak 4 eluting at 29.8 min; <i>E</i> , Peak 5 eluting at 31.9 min; <i>F</i> , Peak 6 eluting at 40.5 min. ....   | 226 |
| <b>Figure 4.32</b> HPLC chromatograms of acid hydrolysed proteins. <i>A</i> , Initial aliquot; <i>B</i> , Aliquot after 10 days of incubation. Arrowed peaks were collected for mass spectrometry.....  | 229 |
| <b>Figure 4.33</b> ESI mass spectra of peaks eluting in Figure 4.32B. <i>A</i> , Peak 2; <i>B</i> , Peak 3; <i>C</i> , Peak 4; <i>D</i> , Peak 5. ....  | 230 |
| <b>Figure 4.34</b> ESI mass spectra of peaks eluting in Figure 4.32B. <i>A</i> , Peak 6; <i>B</i> , Peak 7; <i>C</i> , Peak 8; <i>D</i> , Peak 9. ....  | 231 |
| <b>Figure 4.35</b> Concentration of 3OHKyn-Cys, 3OHKyn-His and 3OHKyn-Lys in protein samples during incubation of CLP originally modified by 3OHKyn at pH 9.5. ...  | 232 |
| <b>Figure 4.36</b> Possible structures of the unknown compound formed from the 3OHKyn- <i>t</i> -Boc-His incubations, whereby the imidazole ring is linked twice.....   | 235 |
| <b>Figure 5.1</b> HPLC chromatograms of acid hydrolysed lens protein samples (~ 1 mg hydrolysed protein was injected in each case). <i>A</i> , CLP; <i>B</i> , Normal human lens nuclear protein, from a 76 year old lens; <i>C</i> , Pooled human cataract lens nuclear protein. The HPLC profiles of all human cataract lens protein hydrolysed were consistent.....  | 241 |
| <b>Figure 5.2</b> HPLC chromatogram of P1 after a second purification stage using a Phenomenex Synergi Fusion column, and 0.1% (v/v) formic acid HPLC buffers. ....   | 245 |
| <b>Figure 5.3</b> UV-visible spectrum of the peak eluting at 14.7 min in Figure 5.2. ....   | 246 |
| <b>Figure 5.4</b> ESI mass spectrum of the peak eluting at 14.7 min in Figure 5.2. ....   | 247 |
| <b>Figure 5.5</b> MS/MS spectra. MS/MS of ions that were present in the ESI mass spectrum (Figure 5.4). <i>A</i> , <i>m/z</i> 658; <i>B</i> , <i>m/z</i> 505; <i>C</i> , <i>m/z</i> 419; <i>D</i> , <i>m/z</i> 331; <i>E</i> , <i>m/z</i> 270; <i>F</i> , <i>m/z</i> 166.....   | 249 |

|  |     |
|--|-----|
| <b>Figure 5.6</b> HPLC chromatogram of P2 after a second purification stage using a Phenomenex Synergi Fusion column, and 0.1% (v/v) formic acid HPLC buffers. ....  | 250 |
| <b>Figure 5.7</b> UV-visible spectrum of the peak eluting at 27.8 min in Figure 5.6. ....  | 251 |
| <b>Figure 5.8</b> ESI mass spectrum of the sharp peak eluting at 27.8 min in Figure 5.6.....   | 252 |
| <b>Figure 5.9</b> MS/MS spectra. MS/MS of ions that were present in the ESI mass spectrum (Figure 5.8). <i>A</i> , <i>m/z</i> 806; <i>B</i> , <i>m/z</i> 713; <i>C</i> , <i>m/z</i> 615; <i>D</i> , <i>m/z</i> 508; <i>E</i> , <i>m/z</i> 420. ....  | 254 |
| <b>Figure 5.10</b> HPLC chromatogram of P3 after a second purification stage. The single peak eluting at 26.6 min was collected for analysis by UV-visible and mass spectrometry.....  | 255 |
| <b>Figure 5.11</b> UV-visible spectrum of the peak eluting at 26.6 min in Figure 5.10. ....  | 256 |
| <b>Figure 5.12</b> ESI mass spectrum of the peak eluting at 26.6 min in Figure 5.10. ....  | 257 |
| <b>Figure 5.13</b> MS/MS spectra. MS/MS of ions that were present in the ESI mass spectrum (Figure 5.12). <i>A</i> , <i>m/z</i> 665; <i>B</i> , <i>m/z</i> 641; <i>C</i> , <i>m/z</i> 279. ....  | 258 |
| <b>Figure 5.14</b> HPLC chromatogram of P4 after a second purification stage. The single peak eluting at 31.1 min was collected for analysis by UV-visible and mass spectrometry.....  | 259 |
| <b>Figure 5.15</b> UV-visible spectrum of the peak eluting at 31.1 min in Figure 5.14. ....  | 260 |
| <b>Figure 5.16</b> ESI mass spectrum of the peak eluting at 31.1 min in Figure 5.14. ....  | 261 |
| <b>Figure 5.17</b> MS/MS spectra. MS/MS of ions that were present in the ESI mass spectrum (Figure 5.16). <i>A</i> , <i>m/z</i> 790; <i>B</i> , <i>m/z</i> 670; <i>C</i> , <i>m/z</i> 404; <i>D</i> , <i>m/z</i> 387; <i>E</i> , <i>m/z</i> 353; <i>F</i> , <i>m/z</i> 284; <i>G</i> , <i>m/z</i> 192. ....        | 264 |
| <b>Figure 5.18</b> Proton NMR spectrum of the peak eluting at 31.1 min in Figure 5.14. ...   | 266 |
| <b>Figure 5.19</b> gCOSY spectrum of the peak eluting at 31.1 min in Figure 5.14. <i>A</i> , Entire gCOSY spectrum; <i>B</i> , Aromatic region of the gCOSY spectrum. ....   | 267 |
| <b>Figure 5.20</b> HPLC chromatogram of P5 after a second purification stage. The single peak eluting at 34.5 min was collected for analysis by UV-visible and mass spectrometry.....  | 268 |
| <b>Figure 5.21</b> UV-visible spectrum of the peak eluting at 34.5 min in Figure 5.20. ....  | 269 |
| <b>Figure 5.22</b> ESI mass spectrum of the peak eluting at 34.5 min in Figure 5.20. ....  | 270 |
| <b>Figure 5.23</b> MS/MS spectra. MS/MS of ions that were present in the ESI mass spectrum (Figure 5.22). <i>A</i> , <i>m/z</i> 993; <i>B</i> , <i>m/z</i> 790; <i>C</i> , <i>m/z</i> 697; <i>D</i> , <i>m/z</i> 607.....  | 271 |
| <b>Figure 5.24</b> Purification of P6. <i>A</i> , HPLC chromatogram of second purification (see Section 5.2.5.3 for details); <i>B</i> , HPLC chromatogram of third purification (see Section 5.2.5.4 for details); <i>C</i> , ESI mass spectrum of the peaks eluting as a doublet at 28 min in Figure 5.24B. .... | 273 |

## **List of Schemes**

|  |     |
|--|-----|
| <b>Scheme 1.1</b> Tryptophan metabolism: The Kynurenine pathway. Glu refers to glucose (β-linked), and GSH refers to glutathione.....  | 11  |
| <b>Scheme 1.2</b> Formation of protein UV filter adducts.....  | 13  |
| <b>Scheme 1.3</b> Deamidation of <i>A</i> , Glutamine; <i>B</i> , Asparagine.....  | 14  |
| <b>Scheme 1.4</b> Mechanism of formation of H <sub>2</sub> O <sub>2</sub> , via 3OHKyn autoxidation. <sup>181</sup> .....  | 23  |
| <b>Scheme 1.5</b> Formation of pigments in arthropods from oxidation of 3OHKyn. <sup>184</sup> .....   | 25  |
| <b>Scheme 2.1</b> Synthesis of 3OHKyn amino acid adducts. 3OHKyn is deaminated at pH 9.5, and the intermediate compound is susceptible to nucleophilic attack via a Michael addition. Amino acid side chains of Cys, His or Lys were covalently attached to the 3OHKyn amino acid side chain. .... | 35  |
| <b>Scheme 2.2</b> Mechanism for the formation of breakdown products of 3OHKyn-Cys at pH 7.2.....   | 79  |
| <b>Scheme 2.3</b> Mechanism of formation of U39.5, <i>m/z</i> 664. ....  | 81  |
| <b>Scheme 3.1</b> Decomposition of UV filter amino acid adducts, and formation of UV filter GSH adducts. 3OHKyn or Kyn amino acid adducts together with excess GSH were incubated at pH 9.5 for 4 hours.....   | 102 |
| <b>Scheme 4.1</b> Possible scheme for formation of 3OHKyn amino acid crosslinks. ....  | 179 |
| <b>Scheme 4.2</b> Route of formation of xanthurenic acid from autoxidation of protein-bound 3OHKyn. ....   | 236 |

## **List of Tables**

|   |     |
|---|-----|
| <b>Table 1.1</b> Major components of the human lens. <sup>9,16-19</sup> .....   | 6   |
| <b>Table 2.1</b> Proposed structures of the major fragment ions of 3OHKyn-Cys observed in the MS/MS spectrum. ....  | 45  |
| <b>Table 2.2</b> Proposed structures of the major fragment ions of 3OHKyn- <i>t</i> -Boc-His observed in the MS/MS spectrum. ....   | 47  |
| <b>Table 2.3</b> Proposed structures of the major fragment ions of 3OHKyn- <i>t</i> -Boc-Lys observed in the MS/MS spectrum. ....   | 49  |
| <b>Table 2.4</b> Summary of the <sup>1</sup> H and <sup>13</sup> C NMR spectral assignments for the 3OHKyn amino acid adducts. The atom numbering adopted is shown below. ....                          | 51  |
| <b>Table 2.5</b> Recovery of 3OHKyn amino acid adducts after acid hydrolysis for 24 hours at 110 <sup>0</sup> C in the presence of antioxidants. ....   | 66  |
| <b>Table 2.6</b> Summary of the 3-D fluorescence intensities for each 3OHKyn amino acid adduct. ....  | 78  |
| <b>Table 3.1</b> Lists all of the doubly charged ions (M+2H) <sup>2+</sup> in the ESI mass spectrum (Figure 3.37) detected in the peak eluting at 45.1 min on the HPLC chromatogram (Figure 3.36). .... | 141 |
| <b>Table 3.2</b> Lists all of the triply charged ions (M+3H) <sup>3+</sup> in the ESI mass spectrum (Figure 3.37) detected in the peak eluting at 45.1 min on the HPLC chromatogram (Figure 3.36). .... | 142 |
| <b>Table 3.3</b> Lists all of the charged ions in the ESI mass spectrum (Figure 3.38) for the peak eluting at 50.5 min on the HPLC chromatogram (Figure 3.36). ....                                     | 144 |
| <b>Table 4.1</b> Combination of incubations undertaken with the 3OHKyn amino acid adducts. ....   | 181 |
| <b>Table 4.2</b> List of the 3-D fluorescence intensities for each aliquot from the incubation. ....  | 212 |
| <b>Table 4.3</b> List of the 3-D fluorescence intensities for each aliquot from the incubation. ....  | 223 |
| <b>Table 4.4</b> Expected molecular ions of the 3OHKyn crosslink compounds. ....  | 233 |
| <b>Table 5.1</b> List of characteristic ions, and absorbance maxima for each of the 3OHKyn and Kyn amino acid adducts. <sup>103</sup> .....   | 239 |
| <b>Table 5.2</b> Summary of the ions and fragment ions identified in the peaks, P1, P2, P3, P4, P5 and P6, which were isolated and purified from hydrolysed human cataract lens proteins. ....          | 278 |
| <b>Table 5.3</b> List of modifications in human cataract lens proteins. <sup>104-107,130,212</sup> .....  | 279 |

## **Abstract**

The human lens contains three kynurenine UV filters, 3-hydroxykynurenine *O*- $\beta$ -D-glucoside (3OHKynG), kynurenine (Kyn) and 3-hydroxykynurenine (3OHKyn), and it absorbs UV light in the 300-400 nm region due to their presence. UV filters may also prevent UV-induced photodamage to the retina and lens. After middle age, the UV filters, 3OHKynG and Kyn become bound progressively to proteins in the centre of our lenses. This feature is, in part, responsible for normal age-dependant human lens colouration.

To provide proof that 3OHKyn is bound to normal human lenses, model studies were undertaken. Cysteine (Cys), histidine (His) and lysine (Lys) residues in lens proteins had been previously shown to bind to UV filters *in vivo*, therefore adducts of these amino acids and 3OHKyn were synthesised and characterised by mass spectrometry, fluorescence, UV-visible and NMR spectroscopy in Chapter 2. The stability properties of each of the 3OHKyn amino acid adducts were also determined, with incubations performed at pH 4.0 and pH 7.2. 3OHKyn-*t*-Boc-His was identified as the most stable of the three adducts. 3OHKyn-*t*-Boc-Lys and 3OHKyn-Cys both decomposed at pH 7.2 forming numerous oxidation products. The stability of each adduct to acid hydrolysis was also examined.

In Chapter 3, calf lens protein was incubated with 3OHKyn, and acid hydrolysis showed that Cys was the primary site of modification when the incubation was undertaken at pH 7.2. However, when the incubation was undertaken at a higher pH (for example, pH 9.5), 3OHKyn readily modified Cys, His and Lys residues. Previously acid hydrolysis of human lens protein had identified Kyn attachment to the proteins. However, acid hydrolysis was not an appropriate method for detecting 3OHKyn attached to human lens proteins because 3OHKynG is also bound to human lens proteins. Therefore, a new assay was developed, and it was found that 3OHKyn does indeed bind to human lens proteins in an age-dependant manner. The assay also provides data for 3OHKynG and Kyn attachment to human lens proteins.



In Chapter 3,  $\alpha$ -crystallin was also incubated with 3OHKyn under low oxygen tension, and the findings from this study showed that 3OHKyn modified the Cys residue in  $\alpha$ A-crystallin. In addition, oxidation of methionine and tryptophan was observed. Age-related nuclear cataract is associated with colouration, insolubilisation and extensive oxidation of Cys and methionine residues. It appears that 3OHKyn in the lens may promote the oxidation and modifications of proteins, and may contribute to oxidative stress in the human lens.

In Chapter 4, the aim was to examine if 3OHKyn could act as a crosslinker of cataract lens proteins. 3OHKyn is known to readily oxidise and yield highly reactive species. It was therefore proposed that 3OHKyn bound to lens proteins could promote crosslinking, insolubilisation and colouration of lens proteins following formation of oxidised species. 3OHKyn amino acid adducts were incubated with excess amino acids, and the resulting products examined. These compounds may be analogous to those that would form in a cataract lens. In addition, 3OHKyn-modified protein was incubated and the products were examined by SDS-PAGE, fluorescence spectroscopy and mass spectrometry. Results showed that 3OHKyn, under the conditions used, does not crosslink lens protein. Proof of the hypothesis that 3OHKyn crosslinks proteins in the lens requires the isolation of characteristic chemical markers from cataract lens proteins that contain the modified 3OHKyn molecules.

In Chapter 5, the aim was to isolate novel compounds from the hydrolysates of human cataract lens proteins and to determine their chemical properties.

Overall this thesis provides evidence that 3OHKyn plays a role in the post-translational modification of normal human lens proteins, and it also provides preliminary data on the role of 3OHKyn in human cataract.

## **Chapter 1**

### **Introduction**

#### **1.1 General Introduction**

Blindness affects many people worldwide. Currently it is estimated that 37 million people in the world are blind, and a further 124 million people suffer from vision impairment. Of these, only 75% can be treated for their blindness.<sup>1</sup> Vision 2020 reports that a further 1 to 2 million people a year go blind.<sup>1</sup> Unfortunately, a large proportion (90%) of the blind live in poor or under developed countries where resources are not readily available. For example, Africa has 6.8 million blind people, and the South East Asian region and the Western Pacific Region have at least 11.6 million blind people.<sup>1</sup>

Numerous diseases affect vision, including glaucoma, retinopathy, macula degeneration and cataract. Each of these diseases requires further medical research to understand their etiology, and to assist future generations with the development of more cost effective cures and treatments.

Cataract is the most common cause of blindness worldwide.<sup>2,3</sup> An enormous amount of research has been undertaken on this disease, but there are still many unanswered questions. Cataract is defined as the opacification or cloudiness of the lens.<sup>4</sup> Age-related nuclear (ARN) cataract is the most common type of cataract,<sup>5</sup> and is responsible for 48% of world blindness.<sup>6</sup> Today, the aging population is increasing and therefore the prevalence of cataract will continue to increase in the coming decades.<sup>7</sup>

This thesis will look at one UV filter, 3OHKyn, and examine its role in the human lens. The work presented in this thesis will add to our understanding of the changes that occur during nuclear cataract formation.

## **1.2 The Human Eye**

The eye is spherical, enclosed by three layers and filled with fluid. The outermost layers of the eye include the sclera and the cornea, followed by the choroid, ciliary body and iris, and the innermost layer of the eye is the retina (Figure 1.1).<sup>8</sup> The human adult eye is approximately 24 mm in diameter.<sup>9</sup> The sclera is dense, white and an opaque coating of the eye and is not directly involved in the visual process. The cornea is a transparent tissue located anterior to the globe of the eye, and is covered by a thin tear film (~7-8  $\mu\text{m}$ ). Posterior to the cornea is the aqueous humor, which is secreted by the ciliary epithelium. Posterior to the aqueous humor is a transparent tissue, the lens, whose primary function is to focus and filter images onto the retina. The lens is suspended in place by zonular ligaments. The vitreous humor is a gel substance that occupies approximately 90% of the total volume of the eye, and provides structural support for the adjacent ocular tissues. Finally, detection of light occurs at the retina. Light first passes through the tear film followed by the cornea, aqueous humor, the lens, the vitreous humor and finally the light is absorbed by the photoreceptors on the retina, where an electrical signal is produced and that signal is transmitted through the ganglion cell layer to the brain.<sup>8,9</sup>

**Figure 1.1** Schematic diagram of the cross section of the human eye.<sup>10</sup>

### 1.3 The Lens

The lens has a high concentration of protein and a unique arrangement of fibre cells, which together provide the high refractive index essential for focusing images onto the retina.<sup>9,11,12</sup> It is a transparent tissue surrounded by an elastic collagenous capsule that allows small molecules into and out of the lens from the surrounding structures, for example, nutrients from the aqueous humor.<sup>13,14</sup> The parts of the lens include the nucleus, cortex, epithelial cells, lens fiber cells and sutures (Figure 1.2).

The lens of an embryo consists only of the nucleus, and throughout life the lens continuously grows and develops. The epithelial cells have a high metabolic rate, and are located on the anterior surface underlying the capsule. These cells undergo mitosis at the equator and differentiate into elongated fibre cells. New fibre cells are laid down as concentric layers on previously formed embryonic fibres.<sup>9</sup> The fibre cells occupy the remaining lens, and metabolic activity occurs in this region of the lens *i.e.* the cortex.<sup>15</sup> Development of the fibre cells results in the accumulation of soluble crystallins, water channel membranes, lipids and numerous other components that insert into the fibre cell plasma membrane.<sup>9</sup>

As fibre cells mature they elongate and extend from the anterior surface of the lens and curve around to the back of the lens to meet in a region referred to as lens sutures<sup>14</sup> (Figure 1.2), and, there is a concomitant loss of the nuclei and other intracellular organelles such as the mitochondria, Golgi bodies and rough and smooth endoplasmic reticulum.<sup>9</sup> The lens nucleus contains the oldest cells and there is no protein turnover, since fibre cells do not contain DNA and RNA. Protein synthesis only occurs in the epithelium and the developing fibre cells of the lens. Amino acids are transported into the lens via the aqueous humor.<sup>9,14</sup>

**Figure 1.2** Cross-section of the human lens (adapted from J. Harding).<sup>14</sup>

## 1.4 Components of the Lens

### *Summary*

The lens contains many chemical compounds. Table 1.1 lists the major components of the human lens. The lens contains amino acids of varying quantity, and many low molecular compounds including two antioxidants; glutathione and ascorbic acid. UV filters are also located in the lens and are low molecular weight compounds. In recent years the levels of 4-(2-amino-3-hydroxyphenyl)-4-oxobutanoic acid *O*- $\beta$ -D-glucoside (AHBG), 4-(2-amino-3-hydroxyphenyl)-4-oxobutanoic acid *O*-diglucoside (AHBDG), 3-hydroxykynurenine (3OHKyn), 3-hydroxykynurenine *O*- $\beta$ -D-glucoside (3OHKynG), and kynurenine, (Kyn) have been quantified. In addition, oxygen has also been identified as a component of the human lens. Proteins, antioxidants and UV filters will be discussed in greater detail in the following section.

**Table 1.1** Major components of the human lens.<sup>9,16-19</sup>

### 1.4.1 Proteins in the Lens

Proteins in the lens comprise approximately 38% of the wet mass.<sup>20</sup> The protein concentration in the centre of the human lens is approximately 450 mg/mL.<sup>21</sup> Crystallins are the major soluble proteins in the mammalian lens and make up over 90% of the lens proteins. The remaining 10% of the lens proteins are comprised of membrane and cytoskeleton proteins.<sup>4</sup> There is little or no protein turnover in the lens therefore the proteins are long-lived.<sup>22</sup> Crystallins are structural proteins responsible for the refractive properties and stability of the lens.<sup>11,23-26</sup> There are many classes of crystallins based on oligomeric size. Bovine and human lens proteins contain three classes of crystallins, the  $\alpha$ -,  $\beta$ - and  $\gamma$ -crystallins. Other classes of crystallins, for example, the  $\delta$ -crystallins are found in birds and reptiles<sup>27</sup>, and  $\zeta$ -crystallins are found in guinea pigs.<sup>28</sup>

#### *$\alpha$ -Crystallin*

$\alpha$ -Crystallin is a polydisperse, multimeric protein with a molecular weight distribution ranging from 300 kDa to over 1000 kDa.<sup>29</sup> It has two subunits,  $\alpha$ A and  $\alpha$ B, each with a monomeric mass of approximately 20 kDa. The amino acid sequence homology between  $\alpha$ A- and  $\alpha$ B-crystallin is approximately 60%.<sup>25</sup>  $\alpha$ -Crystallin is a structural protein. It also functions as a molecular chaperone in the lens, by regulating protein folding during synthesis and protecting the lens proteins against misfolding and aggregation.<sup>22,30-33</sup>  $\alpha$ A- and  $\alpha$ B-crystallin are continuously synthesised during lens development,<sup>34-37</sup> and are found in the lens epithelial cells, but their synthesis is up regulated upon differentiation to the lens fibre cells.<sup>38,39</sup>  $\alpha$ A-Crystallin is primarily found in the lens tissue, however  $\alpha$ B-crystallin is ubiquitous, and is also found in non-lenticular tissues.<sup>40-42</sup> Increased amounts of  $\alpha$ B-crystallin have been associated with various neurological diseases, for example, Alexander's disease,<sup>43</sup> Creutzfeldt-Jakob disease,<sup>44,45</sup> Alzheimer's disease<sup>46</sup> and Parkinson's disease.<sup>44</sup>

#### *$\beta$ - and $\gamma$ -Crystallin*

The  $\beta$ - and  $\gamma$ -crystallins are structural proteins in the lens.  $\beta$ -Crystallins are oligomers and  $\gamma$ -crystallins are monomers, both built up out of four Greek key motifs organised into two domains.<sup>47</sup> The  $\beta$ -crystallins have acidic ( $\beta$ A1 (23 kDa),  $\beta$ A2 (21 kDa),  $\beta$ A3



(25 kDa) and  $\beta$ A4 (22 kDa)) and basic ( $\beta$ B1 (27 kDa),  $\beta$ B2 (23 kDa) and  $\beta$ B3 (24 kDa)) polypeptides.<sup>48-50</sup> The  $\beta$ -crystallin genes are fibre cell specific, however the acidic  $\beta$ -crystallin genes have a wider expression pattern and their protein products are found in both the nucleus and the cortex of the lens.<sup>36,37</sup>

There are seven  $\gamma$ -crystallin genes in the mammalian genome. Six of the  $\gamma$ -crystallin genes ( $\gamma$ A,  $\gamma$ B,  $\gamma$ C,  $\gamma$ D,  $\gamma$ E,  $\gamma$ F) are closely linked in a repeated gene cluster and are similar in sequence, each with a mass of approximately 20 kDa. The seventh gene,  $\gamma$ S-crystallin, is located on another chromosome and is more diverse in sequence.<sup>51</sup> The  $\gamma$ -crystallins are also fibre cell specific, and are the last crystallins to be synthesised during fibre cell differentiation, being preceded by the  $\alpha$ - and then the  $\beta$ -crystallins.<sup>38,39,52</sup>  $\gamma$ -Crystallins are not found in the immature fibre cells in the cortical region. The  $\gamma$ A-F-crystallin genes are expressed in early lens development and their products are mainly found in the lens nuclear region.<sup>37,39</sup>

#### 1.4.2 Antioxidants

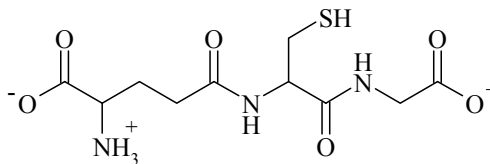
The lens, like many other tissues and cells in the body, is susceptible to oxidative damage. It is permeable and small molecules like hydrogen peroxide ( $\text{H}_2\text{O}_2$ ), which is found in the aqueous humor, will diffuse into the lens and oxidise amino acid residues in proteins. Recently it has been shown that oxygen is present in the lens.<sup>53,54</sup> The lens requires antioxidants to offer protection, however with age, the level of antioxidants decreases.<sup>19,55</sup> The two antioxidants present in the lens include, ascorbic acid and reduced glutathione (GSH).

##### *Ascorbic Acid*

Ascorbic acid is present at high levels in the lens<sup>56</sup> and can function as an antioxidant. However, ascorbic acid displays prooxidant properties and in the presence of metal ions, free radical and other active oxygen species such as  $\text{H}_2\text{O}_2$  are formed.<sup>57</sup> Ascorbic acid also induces the formation of non-disulfide bond crosslinks and insolubilisation of the lens proteins.<sup>58-62</sup>

### GSH

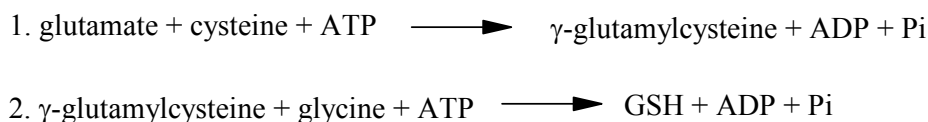
GSH is a tripeptide,  $\gamma$ -glutamyl-cysteinyl-glycine, containing a thiol group (Figure 1.3).<sup>63,64</sup>



GSH

**Figure 1.3** Structure of GSH.

GSH is found in millimolar levels in the lens.<sup>65</sup> The levels are highest in the epithelium<sup>66</sup> and are higher in the cortex than in the nucleus.<sup>67</sup> GSH is synthesised in the cortex<sup>68,69</sup> sequentially in two steps from L-glutamate, L-cysteine and glycine, according to the following reactions:



The first reaction is catalysed by  $\gamma$ -glutamylcysteine synthetase and the second reaction is catalysed by glutathione synthetase.<sup>70,71</sup> The functions of GSH in the lens include:<sup>9,18,72</sup>

- Maintaining protein sulfhydryl groups in a reduced form, and preventing the formation of high molecular weight aggregates;
- Detoxifying  $\text{H}_2\text{O}_2$ ;
- Amino acid transportation as a  $\gamma$ -glutamyl donor to the  $\alpha$ -amino groups of acceptor amino acids such as cysteine or glutamine;
- Ion transportation, especially  $\text{Na}^+$  and  $\text{K}^+$ , by protecting the sulfhydryl groups of  $\text{Na}^+, \text{K}^+$ -ATPase from oxidation.

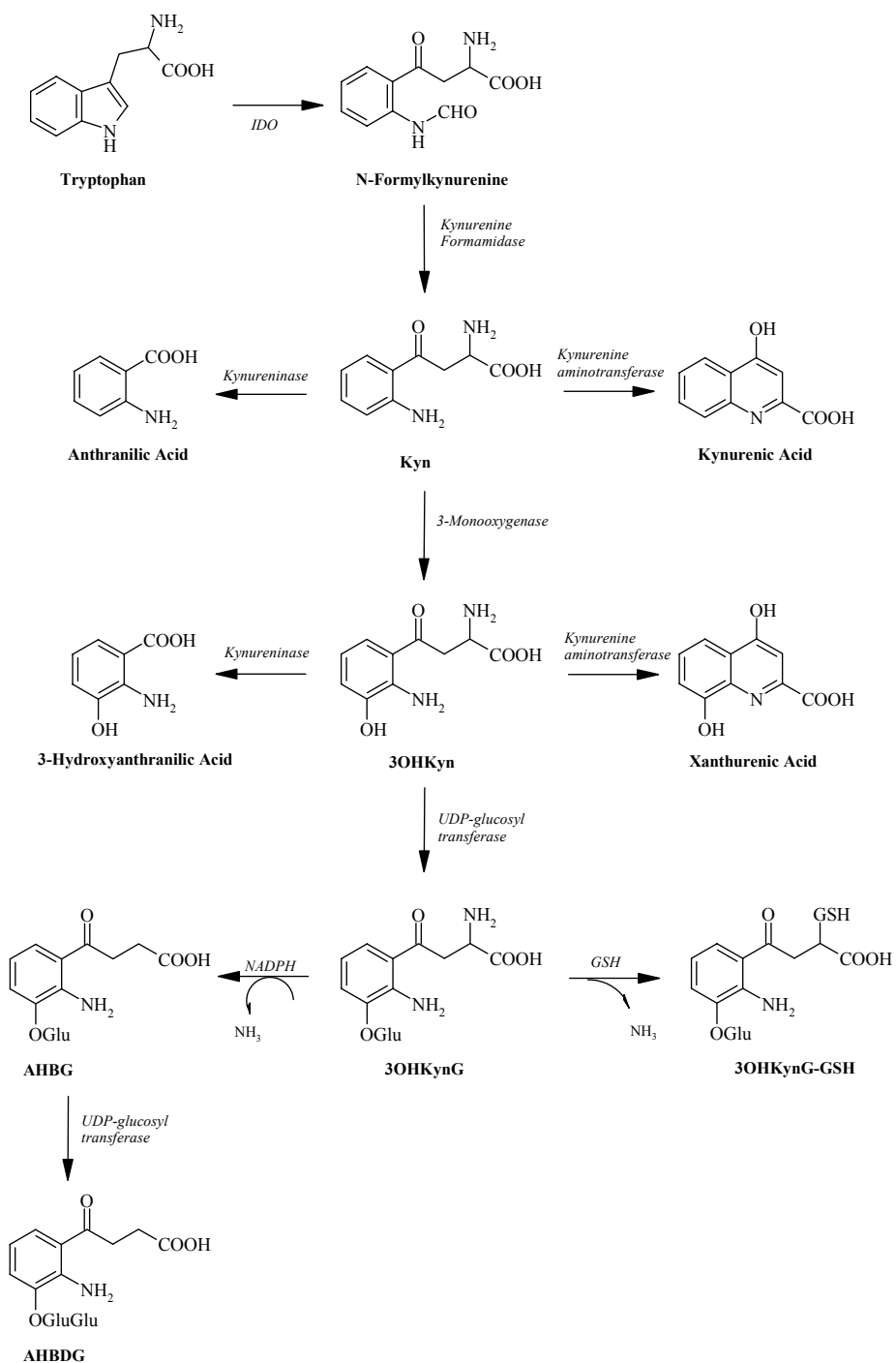
#### 1.4.3 UV Filters

Low molecular weight fluorescent compounds called UV filters are also present in the human lens. Primate UV filters are synthesised from the metabolism of tryptophan

(Trp), and absorb UV light in the 300-400 nm region on the UV spectrum. UV filters have a peak absorption centred between 360 and 370 nm.<sup>73</sup> These compounds prevent UV-induced photodamage to the retina<sup>74</sup> and aid in visual acuity.<sup>73</sup> The most abundant UV filter in the lens is 3OHKynG,<sup>75</sup> followed by Kyn and 3OHKyn.<sup>20,73,76-79</sup> More recently, AHBDG,<sup>80</sup> AHBG,<sup>81</sup> and the glutathione adduct of 3OHKynG<sup>82</sup> have also been identified as fluorescent UV filter compounds in aged human lenses.

The UV filters are synthesised in the lens cortex. The first step of the Kyn pathway involves oxidative cleavage of the indole ring of Trp by the enzyme indoleamino 2,3-dioxygenase (IDO) to form *N*-formylkynurenine.<sup>83</sup> Kynurenine formamidase catalyses the formation of Kyn, 3-monooxygenase catalyses the formation of 3OHKyn, glycosylation via UDP-glucosyl transferase yields 3OHKynG, deamination followed by Michael addition of GSH yields 3OHKyn-GSH, or deamination followed by reduction of the alkene yields AHBG, and further glycosylation via UDP-glucosyl transferase yields AHBDG (see Scheme 1.1).<sup>73,84,85</sup>

The kynurenine pathway also occurs in other tissues, and Scheme 1.1 only shows some of the products of Trp metabolism. Interaction of Kyn and 3OHKyn with kynurenine aminotransferase yields kynurenic acid and xanthurenic acid respectively. Hydrolysis of Kyn and 3OHKyn with kynureninase yields anthranilic acid and 3-hydroxyanthranilic acid respectively, but they are not found in the lens. Xanthurenic acid was thought to be present in normal human lenses,<sup>86</sup> however a later study showed that it was absent.<sup>87</sup>



**Scheme 1.1** Tryptophan metabolism: The Kynurenine pathway. Glu refers to glucose ( $\beta$ -linked), and GSH refers to glutathione.

## 1.5 Aging of the Human Lens

There are a number of structural and biochemical changes that occur in the human lens with age. It is unclear if the changes listed below are risk factors for the development of age-related cataract.

### *Barrier*

A barrier to the diffusion of small molecules<sup>88</sup> including water,<sup>89</sup> into the lens nucleus begins at middle age. The barrier is located between the nucleus and cortex interface, however the biochemical basis of the barrier is unknown. As a result of the barrier, unstable compounds such as the kynurenines spend long periods of time in the centre of the lens and have more time to chemically react in this region. A barrier to the diffusion of GSH into the nucleus predisposes the lens center to oxidation.<sup>90,91</sup>

### *Antioxidants*

The concentration of antioxidants in the lens decreases with age. The concentration of GSH in young human lens nucleus is ~4.5 mM and this decreases to ~1 mM with age. In the cortex, the concentration of GSH in the young lens is ~6 mM and this decreases to ~3 mM with age.<sup>19,55</sup> The barrier may contribute to the decrease in GSH concentration with age. In addition, there is an increase in the levels of 3OHKynG-GSH with age, and this compound forms when deaminated 3OHKynG binds covalently via a Michael addition to GSH.<sup>19,82</sup> GSH is an antioxidant, and it has an important role in protecting the lens from modifications. Once the level of GSH decreases, the lens crystallins then become prone to post-translational modifications.

### *Colouration and Fluorescence*

A young human lens is colourless to a very pale yellow colour. With age the lens increases in colour and fluorescence.<sup>92-95</sup> In older lenses, absorption of light extends to approximately 500 nm.<sup>95,96</sup> Insoluble proteins in the lens nucleus appear to be responsible for the increase in non-tryptophan fluorescence, which is observed, with increasing age. A green fluorophore with maximum wavelength at Ex 440 nm/Em 520 nm, and a blue fluorophore with maximum wavelength at Ex 340 nm/Em 400 nm are observed.<sup>97,98</sup> The attachment of kynurenines and glycation products to the lens

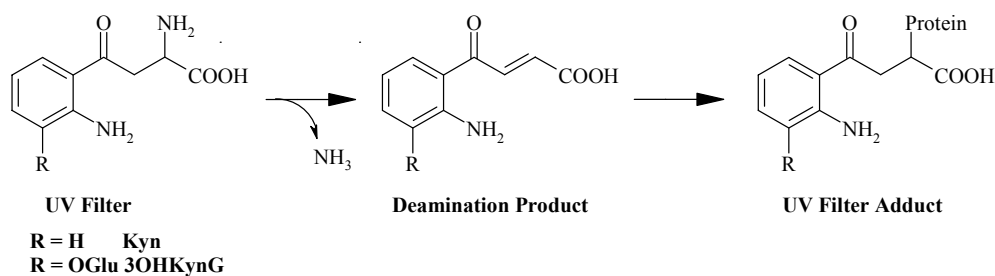
crystallins appear to be, at least in part, responsible for the age-dependent yellowing of the human lens.<sup>76,99-107</sup>

### ***Presbyopia***

Presbyopia is the loss of ability to focus properly on close objects or fine print. The ciliary muscle, (the muscle that surrounds the lens) expands and contracts, changing the curvature of the lens to accommodate for near and distant vision.<sup>10</sup> Presbyopia begins at approximately age 45 and gradually worsens over the coming decades. It begins when the aging lens thickens and becomes more rigid,<sup>108</sup> therefore the ciliary muscle is less efficient at changing the lens shape for near and distant focus.<sup>10</sup>

### ***UV Filters***

In the cortex and the nucleus, the concentration of free UV filters, 3OHKynG, Kyn and 3OHKyn, decreases with age at a rate of 12% per decade, from age 20 to 80 years old.<sup>19</sup> The UV filters, 3OHKynG, Kyn and 3OHKyn have been shown to be unstable at physiological pH, and deamination of the UV filters results in the formation of a reactive deamination product<sup>109</sup> (Scheme 1.2). The deamination product has been shown to undergo condensation reactions with reduced GSH in the lens,<sup>82</sup> and the nucleophilic amino acids of lens crystallins<sup>110-112</sup> (Scheme 1.2). Hood, *et al.* and Vazquez, *et al.* showed that 3OHKynG and Kyn are both bound to the human nuclear lens proteins, and that the amount bound increases with age.<sup>101,103</sup> The lens barrier<sup>90</sup> seems to be responsible for this phenomenon, since UV filters reside in the nucleus for longer periods of time, and there is a greater extent of deamination, which results in more UV filters bound to the highly nucleophilic amino acid residues on the crystallin proteins.



**Scheme 1.2** Formation of protein UV filter adducts.

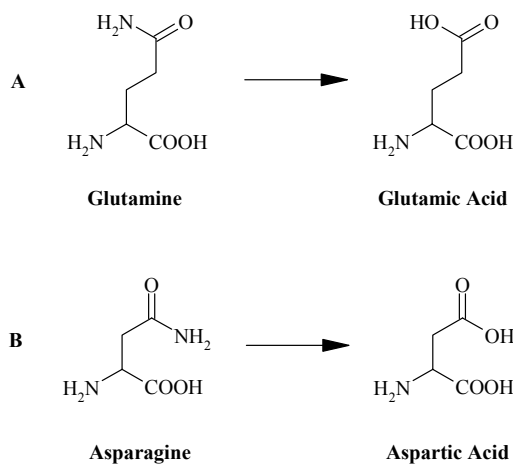
**Post-Translational Modifications (PTMs) of the Crystallins**

The crystallin proteins of the aging human lens undergo numerous PTMs. Most modifications increase with age. The modifications include, deamidation, glycosylation, phosphorylation, racemisation, and truncation, and will be discussed below.

**Deamidation**

Over time glutamine and asparagine residues undergo hydrolysis of a side chain amide to form glutamic acid and aspartic acid respectively (Scheme 1.3), and the molecular weight increases by 1 Da. Deamidation results in a more polar carboxylate anion, which may encourage ionic interactions that lead to conformational changes in the crystallins which could result in the formation of disulphide bonds within the cysteinyl crystallins although this is controversial.<sup>91</sup>

Deamidation has been identified in human aged  $\gamma$ S-crystallin, at glutamine-92 and 170. Asparagine-24, 49, 118, 124 and 137 and glutamine-26, 47, 54, 66 and 67 are sites of deamidation in human aged  $\gamma$ D-crystallin, and asparagine-24 and 137, and glutamine-26, 66, 67, 142 and 148 are deamidation sites in  $\gamma$ C-crystallin.<sup>113</sup> Deamidation has also been observed at asparagine-146 in human aged  $\alpha$ B-crystallin,<sup>114</sup> glutamine-50 in human  $\alpha$ A-crystallin,<sup>115</sup> and asparagine-101 in the high molecular weight aggregate of  $\alpha$ A-crystallin.<sup>116</sup>



**Scheme 1.3** Deamidation of *A*, Glutamine; *B*, Asparagine.

### *Glycosylation*

Nonenzymatic glycation of proteins via the Maillard reaction occurs by condensation of a sugar (e.g. glucose) molecule with protein amino groups (e.g. Lys) to form covalent adducts. This results in the colouration, fluorescence, crosslinking and sometimes insolubilisation of the protein.<sup>117-122</sup> Advanced glycation end (AGE) products form during the later stages of the Maillard reaction, and accumulate in long-lived proteins, like the lens crystallins,<sup>104,122,123</sup> but the exact mechanism of their formation is unknown. Dicarbonyls, glyoxal and methylglyoxal are often intermediates in the Maillard reaction.<sup>124</sup> Examples of AGE products identified in human lenses includes, pentosidine,<sup>104</sup> glyoxal-lysine dimer (GOLD) and methylglyoxal-lysine dimer (MOLD),<sup>125,126</sup> *N*<sup>ε</sup>-(carboxymethyl)lysine (CML),<sup>127</sup> *N*<sup>ε</sup>-(1-(1-carboxy)ethyl)lysine (CEL),<sup>128</sup> and Vesperlysine A.<sup>129</sup> Methylglyoxal-derived hydroimidazolone AGE products have been recently discovered. They consist of three isomers but only two can be quantified in the lens since the third is highly unstable. The two isomers include *N*<sub>δ</sub>-(5-hydro-5-methyl-4-imidazol-2-yl)-ornithine (MG-H1) and 2-amino-5-(2-amino-5-hydro-5-methyl-4-imidazol-1-yl)pentanoic acid (MG-H2).<sup>130</sup> 2-Ammonio-6-(3-oxidopyridinium-1-yl)hexanoate (OP-Lysine) is also a newly identified AGE product in cataract and aged lens proteins.<sup>106</sup> The structures of the AGE products are shown in Figure 1.4.



**Figure 1.4** Structures of the AGE products found in human lenses.<sup>105,106,130,131</sup>

#### *Phosphorylation*

Aged  $\alpha$ -crystallin proteins are subject to phosphorylation of serine residues. In  $\alpha$ B-crystallin serine-45<sup>132</sup> and 59<sup>133</sup> have both been identified as sites of phosphorylation.

#### *Racemisation*

In aged crystallin proteins from the human lens nucleus, aspartic acid undergoes racemisation. L-Aspartic acid residues are converted to D-Aspartic acid. D-Aspartic acid accumulates at a rate of 0.14% per year in the nuclear lens proteins.<sup>134</sup> D-Aspartic acid has been identified in high molecular weight aggregates and water-insoluble protein.<sup>135</sup> More specifically, D isomers have been identified at aspartic acid-58, 151,<sup>136</sup> 105 and 106<sup>137</sup> in  $\alpha$ A-crystallin, and aspartic acid-36 and 62 in  $\alpha$ B-crystallin.<sup>138</sup>

*Truncation*

Human aged crystallins undergo cleavages of the N- and the C-terminal polypeptides. Cleavages have been identified in  $\alpha$ -,  $\beta$ - and  $\gamma$ -crystallins.<sup>36,50,139-142</sup>

***Result of PTMs***

Possibly as a result of these many PTMs, crystallins become progressively denatured over time and form large aggregates in the lens.

*Insolubilisation and Superaggregation*

During normal aging there is an increase in the high molecular weight protein fraction and a conversion from water-soluble to a water-insoluble protein fraction. These changes do not compromise lens transparency. With age old lens proteins unfold and denature and these become prone to aggregation.<sup>29,143,144</sup> After age 40 water-soluble  $\alpha$ -crystallin completely disappears from the human lens nucleus.<sup>33,145</sup>

## **1.6 Cataract**

Cataract is the opacification of the lens.<sup>4</sup> Aging and the accompanying changes to the chemical composition of the lens components are the most likely reasons for cataract. Cataract can be classified by age of onset (e.g. congenital, juvenile or age-related), or by the location of opacity within the lens (e.g. cortical or nuclear).

### ***Symptoms of Cataract***

Typically age-related cataract develops slowly and initially affects vision only slightly. As opacification increases, vision becomes blurred, cloudy or dim. There is an increase in glare from bright lights and the sun. Vision may become more nearsighted, night vision may worsen and many colours will appear less vivid.<sup>10</sup>

### ***Risk Factors***

Aging is by far the major risk factor of cataract.<sup>146,147</sup> Other risk factors include diabetes, alcohol, smoking, diet, steroid use, UV light, heatstroke, hypertension and poverty.<sup>2,146,148-154</sup>

### ***Treating Cataract***

Currently there are no efficacious means available to prevent the formation of cataract. People suffering from cataract are treated with surgery. Previously surgeons used extracapsular (lens contents) or intracapsular (lens and capsule) surgery to treat cataract. Both procedures require large incisions to be made under the upper eyelid, and recovery takes many weeks. Today ultrasound phacoemulsification is the most common technique used by ophthalmologists. The technique involves a small incision, and an ultrasonic probe of high frequency sound waves is inserted, and used to break up the cataractous lens. It is then removed through a tiny needlelike tube. An artificial intraocular lens is then implanted. Patients generally recover well from this procedure.<sup>10</sup> Some surgeons choose to treat the opacities in the lens with an erbium:YAG laser (wavelength 2940 nm). The laser is inserted through a very small incision (0.8 mm compared to 2.5 mm for phacoemulsification), however one study showed that patients with highly dense nuclear opacities treated with laser, experienced increases in intraocular pressure, irreversible corneal edema and posterior capsule

rupture, compared to patients treated with ultrasound phacoemulsification,<sup>155</sup> whereas others report satisfactory outcomes from laser treatment.<sup>156</sup>

However, more research is needed to improve the current techniques in order to achieve greater efficacy and safety. A drug for prevention or therapy would be ideal since many patients suffering cataract are aged, surgical procedures can be traumatic for many elderly and the procedure is costly.

### 1.7 Age-Related Nuclear (ARN) Cataract

ARN cataract is the most common form of cataract, in which the proteins become coloured, oxidised, insoluble and crosslinked.<sup>14,157-160</sup> Pirie devised a classification system for ARN cataract. Type I cataract is cortical cataract, and Types II to V are nuclear cataracts in increasing order of severity (Figure 1.5). A normal lens nucleus is yellow, whereas a Type V cataract nucleus is brown/black.<sup>161</sup> Cortical cataract appears to be a result of an ionic imbalance.<sup>162</sup> Nuclear cataract lenses have a very low concentration of GSH in the centre of the lens.<sup>163</sup> This may be due to an increase in the barrier with cataract.

**Figure 1.5** The Pirie classification of nuclear cataracts<sup>161</sup> using slit lamp photographs.<sup>164</sup> The colour of the nucleus increases with increasing severity of nuclear cataract.

#### *Oxidation*

During ARN cataract formation, oxidation of amino acids takes place. Approximately 90% of the Cys are oxidised to form disulfide bonds, and 45% of the methionines form methionine sulfoxide, in advanced nuclear cataract.<sup>159</sup> Hydroxyl radical oxidation of lens proteins is known to be associated with ARN cataract. Hydroxylation of protein-bound amino acids, such as, DOPA, *o*- and *m*-tyrosine, 3-hydroxyvaline, 5-hydroxyleucine and dityrosine, have all been observed.<sup>165</sup>

#### *Insolubilisation*

Proteins are usually solubilised in 8 M urea, however with the onset of ARN cataract, there is a major increase in a urea-insoluble fraction. This fraction can only be solubilised in the presence of a reducing agent such as, 2-mercaptoethanol or dithiothreitol.<sup>158</sup>

### ***Crosslinking***

Crosslinking is a characteristic feature of ARN cataract. Since the 1970s many crosslinked compounds have been identified in cataractous lens proteins. In 1972, Buckingham was first to document crosslinking in lens proteins.<sup>166</sup> Crosslinking refers to both disulfide bond and non-disulfide bond linkages. Buckingham demonstrated non-disulfide bond crosslinking in cataractous lens proteins. Normal and cataractous lens nuclear proteins were reduced and examined by gel filtration, showing the presence of high molecular weight proteins in the cataractous lens proteins.<sup>166</sup>

In 1973, Harding reduced and carboxymethylated human normal lens nuclear proteins, and Type II cataract lens nuclear proteins,<sup>161</sup> and reported that approximately 5% of the protein in the cataract lenses was composed of high molecular weight aggregates, as a result of protein-disulfide bond linkages, rather than protein-GSH bonds. However, disulfide bonds were not identified in normal lens nuclear and cortical proteins.<sup>167</sup>

Histidinoalanine (Figure 1.6) is an amino acid crosslink compound first identified in connective tissue,<sup>168</sup> and later identified in human lens nuclear proteins.<sup>169</sup> This compound is thought to be formed by the reaction between a histidine and a serine or a cysteine residue in close proximity.<sup>170</sup> Histidinoalanine has been quantified in normal human nuclear proteins, and similar levels were also identified in Type I and II nuclear cataract proteins. However the level of histidinoalanine in Type III and IV nuclear cataract proteins is seven and sixtyseven times higher than the normal human nuclear proteins, respectively.<sup>169</sup> Connective tissue, like lens tissue contains long-lived proteins. The level of histidinoalanine increases with age in connective tissue, and results in hardening of this tissue.<sup>168,171</sup> It is unclear if histidinoalanine is responsible for the hardening of the lens tissue.

Bessemers, *et al.* identified Lanthionine (Figure 1.6), a symmetric thioether formed by oxidative degradation of cystine, in human cataractous lenses.<sup>172</sup> Pentosidine (Figure 1.4), a non-disulfide bond crosslink product involving arginine and lysine linked in an imidazo (4,5,6) pyridinium ring formed by a 5-carbon sugar, has been identified in

human brunescent (high levels of pigmentation) cataract lens proteins.<sup>104</sup> Vesperlysine A (Figure 1.6), a lysine crosslink of the Maillard reaction, has been identified in normal and diabetic human aged lens proteins, and is identical to LM-1 (Figure 1.6).<sup>105</sup> Cheng, *et al.* isolated 1-(5-amino-5-carboxypentyl)-4-(5-amino-5-carboxypentylamino)-3-hydroxy-2,3-dihydropyridinium (the authors abbreviated the name to, lysine-lysine pyridinium (K2P)) (Figure 1.6) from one hundred and fifty normal human lenses and three hundred and fifty Type I and II human cataract lenses. Quantitation in various lenses showed that the level of K2P was higher in cataract lens proteins.<sup>107</sup> OP-Lysine, MG-H1 and MG-H2 (Figure 1.4) are all AGE products, and non-disulfide bond crosslinks in cataract lens proteins.<sup>106,130</sup> The majority of non-disulfide crosslinks so far identified are linked via a Lys residue. The pKa value of Lys, His and Cys,<sup>103</sup> suggest that the Lys residues in proteins are the least ionized at the neutral pH and should react at a slower rate.<sup>173</sup>

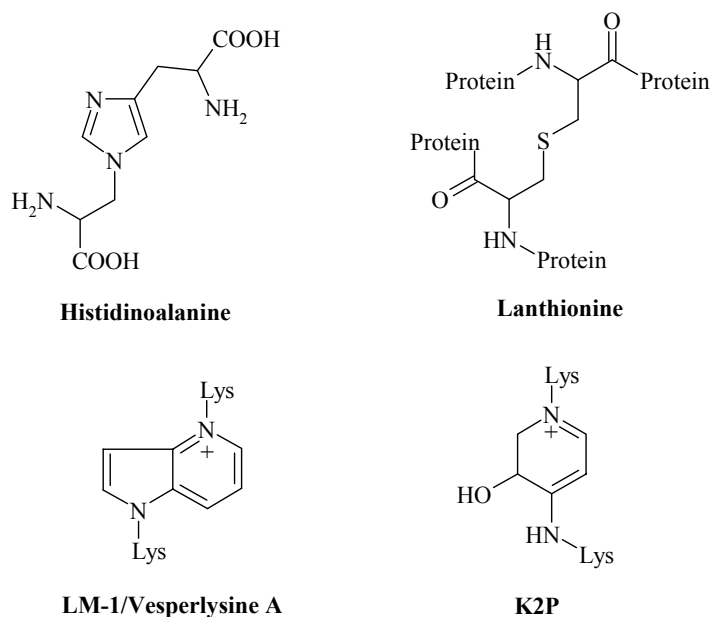


**Figure 1.6** Structures of non-disulfide bond crosslink compounds identified in cataract lens proteins.

### 1.8 3OHKyn

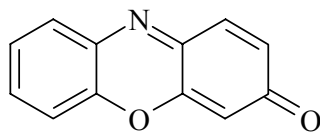
3OHKyn is an *o*-aminophenol. It is a UV filter in the lens,<sup>19</sup> however it is also found in other parts of the body, for example, the brain, where increased levels of 3OHKyn have been implicated in a number of disease states, such as, Huntington's disease and Parkinson's disease.<sup>174-176</sup> In neuronal cell cultures, 3OHKyn is cytotoxic at concentrations as low as 1  $\mu$ M, causing oxidative stress through the formation of  $H_2O_2$ .<sup>177,178</sup> 3OHKyn also effectively chelates iron (III) and copper (II).<sup>179</sup> Oxidation of 3OHKyn is still observed even in Chelex treated phosphate buffers (phosphate buffers contain trace levels of copper and iron).<sup>180</sup>

Autoxidation of 3OHKyn results in the production of  $H_2O_2$ . The mechanism of formation of  $H_2O_2$  via 3OHKyn autoxidation is shown in Scheme 1.4. It is believed that  $H_2O_2$  is generated from reduction of oxygen by the phenoxide anion of 3OHKyn to generate  $O_2^-$ , and its dismutation to yield approximately 1 mole of  $H_2O_2$  per mole of 3OHKyn.<sup>181</sup> The  $pK_a$  of the phenoxyl group of 3OHKyn is 9.6.<sup>182</sup> Thus a small fraction of 3OHKyn in the phenoxide state at neutral pH may be sufficient to allow autoxidation to proceed.<sup>181</sup>

**Scheme 1.4** Mechanism of formation of  $H_2O_2$ , via 3OHKyn autoxidation.<sup>181</sup>



Ommochromes are natural pigments responsible for the colouration of eyes as well as certain other parts of the insect body. They are found primarily among arthropods. These pigments were first identified by Becker, and the name “ommochrome” was assigned as a result of their location *i.e.* in the ommatidies of the insect eye.<sup>183</sup> Ommochromes are acidic pigments, insoluble in neutral solvents, however soluble in buffered solutions of pH 6. Ommochromes were initially divided into two groups; *Ommatins*, which exhibit a characteristic change in colour when oxidised or reduced; and *Ommins*, which are stable under alkali conditions and have molecular weights of approximately 650 Da.<sup>183</sup> Further investigations by Butenandt, *et al.* showed that the ommatins consisted of three pigments; xanthommatin, a yellow phenoxazone (Figure 1.7) pigment; rhodommatin, a red pigment; and ommin D, a red pigment.<sup>184</sup>



**Phenoxazone**

**Figure 1.7** Structure of Phenoxazone.

Ommochromes are products of the metabolism of tryptophan. There are numerous pigments formed, since the final steps of the synthesis can diverge in such a way that a variety of pigments are produced. Xanthommatin is formed through the oxidative condensation of two molecules of 3OHKyn. The quinoline ring is formed by elimination of one mole of ammonia (Scheme 1.5). The synthesis of xanthommatin is in accordance with the general scheme for the synthesis of phenoxazones from *o*-aminophenols.<sup>184</sup> Phenoxazones exhibit a UV absorbance at 440 nm. Xanthommatin is reduced easily into dihydroxanthommatin by the uptake of two hydrogen atoms, and is reoxidised readily upon standing in air into xanthommatin, which is more stable. Ommatin D (Scheme 1.5) is stable towards oxidation, and is the sulphate ester of dihydroxanthommatin, that can be formed through a hydrolytic reaction. Rhodommatin (Scheme 1.5) is a derivative of dihydroxanthommatin and contains a glucose molecule, however the mechanism of its formation is unknown.<sup>184</sup>

Vazquez, *et al.* characterised major oxidations products from autoxidation of 3OHKyn under physiological conditions. The major autoxidation products were identified as xanthommatin, DHQCA and hydroxyxanthommatin.<sup>181</sup> Incubation of 3OHKyn with lens proteins, under oxidative conditions, results in tanned products that resemble cataractous material.<sup>100,185,186</sup>

**Scheme 1.5** Formation of pigments in arthropods from oxidation of 3OHKyn.<sup>184</sup>

### **1.9 Aims of the Project**

The aim of this study is to understand some of the roles of the UV filter 3OHKyn in the human lens. Based on previous studies it is known that UV filters, such as Kyn and 3OHKynG bind to lens protein in an age-dependant manner. But unlike Kyn and 3OHKynG, 3OHKyn is very unstable to oxidation and thus it is expected that 3OHKyn could play a role in the formation of ARN cataract, if it too were bound to proteins in the human lens.

Specific aims of this study are to:

- Synthesise the three 3OHKyn amino acid adducts expected in normal lenses, and characterise each adduct using mass spectrometry, NMR spectroscopy and UV-visible and 3-D fluorescence spectroscopy. In addition, to determine the stability properties of each adduct.
- Determine if 3OHKyn is attached to human lens proteins.
- Examine the potential role of 3OHKyn as a crosslinker of lens proteins.
- Identify novel compounds in the hydrolysates of human cataractous lens proteins.

## Chapter 2

### Synthesis and Characterisation of 3OHKyn Amino Acid Adducts

#### 2.1 Introduction

Human lenses become more fluorescent with age<sup>93</sup> due to PTM of the structural proteins. Although a number of compounds have been reported as adducts to human lens proteins,<sup>104-107</sup> it is not known which of these is primarily responsible for the increased fluorescence.

At neutral pH, UV filters undergo deamination of the amino acid side chain to produce intermediate compounds that are susceptible to nucleophilic attack via Michael addition.<sup>109</sup> Amino acid residues such as Cys, His, and Lys are known to be the most reactive with UV filters.<sup>110,111,187</sup> 3OHKynG and Kyn, become covalently attached to proteins in the human lens in an age-dependent manner.<sup>101,103</sup> At the same time, the level of free UV filters in the lens decreases.<sup>19</sup> This is especially true after the lens barrier forms at middle age,<sup>88-90</sup> when UV filters reside for longer time periods within the nuclear region of the lens and are able to deaminate to a greater extent.

3OHKyn differs in one very important regard from the other Kyn UV filters, in that, the aromatic portion of 3OHKyn can readily oxidise.<sup>181,184,188</sup> In model systems, numerous dimeric and other coloured products result from oxidation of 3OHKyn under physiological conditions.<sup>181,184</sup> If such processes also occur after 3OHKyn has become linked to proteins, coloured, insoluble and crosslinked proteins could result. It has been proposed that this could be a contributing factor in the development of human ARN cataract,<sup>100,185,186,189,190</sup> but proof has been lacking largely because of the problems associated with analysing the low levels of such a readily oxidised molecule.

As a first step in testing this theory, adducts (Figure 2.1) between 3OHKyn and the nucleophilic amino acids, Cys, His and Lys, were prepared and characterised by mass spectrometry, NMR spectroscopy, UV-visible and 3-D fluorescence spectroscopy. The

stability of each adduct at pH 4.0 and 7.2 was examined, and the stability of each adduct to acid hydrolysis was also examined.

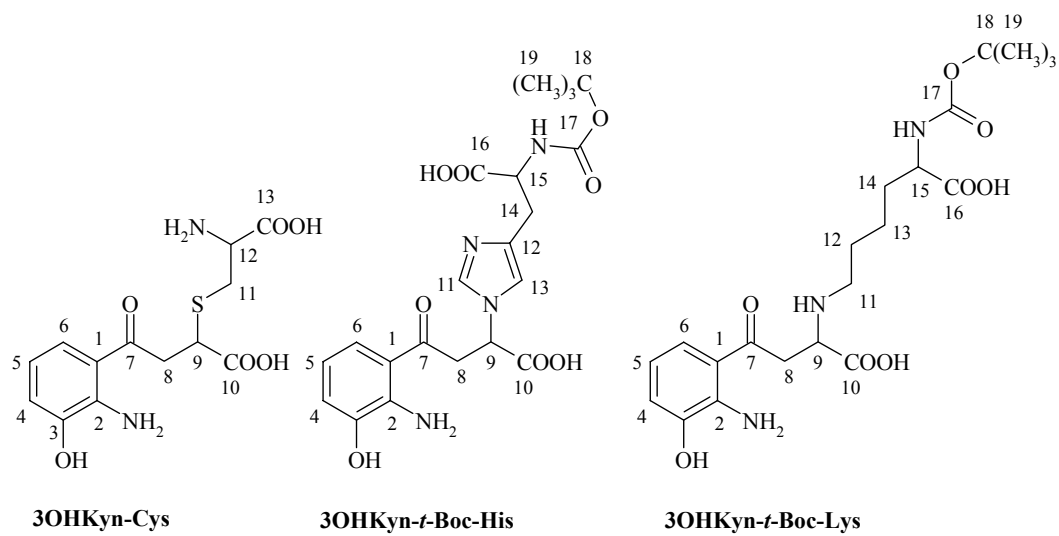


**Figure 2.1** Structures of the 3OHKyn amino acid adducts.

## 2.2 Materials and Methods

### 2.2.1 Materials

All organic solvents and acids were HPLC grade (Ajax, Auburn, NSW, Australia). Milli-Q<sup>®</sup> water (purified to 18.2 MΩ/cm<sup>2</sup>) was used in the preparation of all solutions. The amino acids (N- $\alpha$ -*t*-Boc-L-His, N- $\alpha$ -*t*-Boc-L-Lys and L-Cys), formic acid, hydrochloric acid (HCl) (6 M, sequencing grade), 3OHKyn, phenol, thioglycolic acid and trifluoroacetic acid (TFA) were obtained from Sigma-Aldrich Chemical Co. (St. Louis, MO, U.S.A.).

### 2.2.2 Synthesis and Purification of 3OHKyn Modified Amino Acids

3OHKyn (50 mg) was dissolved in 50 mM Na<sub>2</sub>CO<sub>3</sub>/NaHCO<sub>3</sub> buffer, pH 9.5 (30 mL). The amino acids (N- $\alpha$ -*t*-Boc-L-His, N- $\alpha$ -*t*-Boc-L-Lys and L-Cys) were added in 10-fold molar excess. The pH was readjusted to 9.5 with 0.1 M NaOH if required, and then the resulting solution was bubbled with argon, sealed, wrapped in foil and incubated at 37<sup>0</sup>C for 48 hours.<sup>103</sup> After adjusting the pH to between 4 and 5 with glacial acetic acid, the resulting mixture was separated by semi-preparative or analytical HPLC. The yield, NMR, MS/MS data, and high resolution mass spectra are given below.

#### *N*- $\alpha$ -*tert*-Butoxycarbonyl-L-lysyl-3-hydroxy-DL-kynurenine (3OHKyn-*t*-Boc-Lys):

11.3 mg, 11%. Found: MH<sup>+</sup>, 454.2264. Calculated for C<sub>21</sub>H<sub>32</sub>N<sub>3</sub>O<sub>8</sub>: MH<sup>+</sup>, 454.2189; ESI-MS/MS of *m/z* 454 (MH<sup>+</sup>), 354 (100%), 247 (7%), 208 (10%), 203 (96%), 152 (24%), 147 (28%), 128 (12%).

$\delta$ H 7.54 (1H, d, *J* 8.0, H-6), 7.16 (1H, d, *J* 7.0, H-4), 6.96 (1H, t, *J* 8.0, 8.0, H-5), 4.20 (1H, m, H-9), 4.12 (1H, m, H-15), 3.82 (2H, m, CH<sub>2</sub>-8), 3.19 (2H, m, CH<sub>2</sub>-11), 1.89 (1H, m, CH<sub>2</sub>-14), 1.81 (2H, m, CH<sub>2</sub>-12), 1.75 (1H, m, CH<sub>2</sub>-14), 1.51 (2H, m, CH<sub>2</sub>-13), 1.29 (9H, s, 3xCH<sub>3</sub>);

$\delta$ C 200.2 (CO-7), 172.8 (CO-10), 146.5 (C-3), 134.1 (C-2), 122.8 (C-6), 120.2 (C-4), 120.1 (C-5), 81.8 (C-18), 57.3 (C-9), 53.7 (C-15), 47.1 (C-11), 38.6 (C-8), 30.1 (C-14), 27.7 (C-19), 25.0 (C-12), 22.3 (C-13).

#### *N*- $\alpha$ -*tert*-Butoxycarbonyl-L-histidyl-3-hydroxy-DL-kynurenine (3OHKyn-*t*-Boc-His):

8.6 mg, 9%. Found: MH<sup>+</sup>, 463.1771. Calculated for C<sub>21</sub>H<sub>27</sub>N<sub>4</sub>O<sub>8</sub>: MH<sup>+</sup>, 463.1829;

ESI-MS/MS of  $m/z$  463 ( $MH^+$ ), 407 (52%), 363 (100%), 317 (15%), 209 (10%), 208 (12%), 156 (52%), 110 (5%).

$\delta H$  8.75 (1H, s, H-11), 7.42 (1H, d,  $J$  8.0, H-6), 7.34 (1H, s, H-13), 7.03 (1H, d,  $J$  8.0, H-4), 6.90 (1H, t,  $J$  7.5, 8.0, H-5), 5.47 (1H, m, H-9), 4.30 (1H, m, H-15), 3.92 (2H, m,  $CH_2$ -8), 3.17 (1H, dd,  $J$  15.5, 15.5,  $CH_2$ -14), 2.97 (1H, m,  $CH_2$ -14), 1.93 (9H, s,  $3 \times CH_3$ );

$\delta C$  199.1 (CO-7), 172.4 (CO-10), 147.0 (C-3), 135.6 (C-11), 135.3 (C-2), 129.7 (C-12), 122.6 (C-6), 122.0 (C-5), 120.7 (C-4), 119.9 (C-13), 119.2 (C-1), 81.8 (C-18), 59.1 (C-9), 52.8 (C-15), 41.9 (C-8), 27.5 (C-19), 26.8 (C-14), 26.8 (C-14).

**L-Cysteiny-3-hydroxykynurenine (3OHKyn-Cys):** 12.4 mg, 17%. Found:  $MH^+$ , 329.0789. Calculated for  $C_{13}H_{17}N_2O_6S$ :  $MH^+$ , 329.0807; ESI-MS/MS of  $m/z$  329 ( $MH^+$ ), 311 (30%), 240 (10%), 208 (60%), 202 (100%), 190 (65%), 162 (80%), 122 (5%), 110 (12%).

$\delta H$  7.69 (1H, d,  $J$  7.5, H-6), 7.43 (1H, t,  $J$  8.0, 8.5, H-5), 7.32 (1H, d,  $J$  8.5, H-4), 4.35 (1H, m, H-12), 3.97 (1H, m, H-9), 3.77 (1H, m,  $CH_2$ -8), 3.66 (1H, d,  $J$  4.5,  $CH_2$ -8), 3.43 (1H, d,  $J$  4.5,  $CH_2$ -11), 3.33 (1H, d,  $J$  5.0,  $CH_2$ -11);

$\delta C$  200.5 (CO-7), 175.9 (CO-10), 170.8 (CO-13), 150.4 (C-3), 128.3 (C-5), 127.3 (C-1), 122.2 (C-6), 121.5 (C-4), 118.6 (C-2), 52.1 (C-12), 41.7 (C-9), 40.9 (C-8), 31.6 (C-11), 31.3 (C-11).

### 2.2.3 High Performance Liquid Chromatography (HPLC) for Purification of the 3OHKyn Amino Acid Adducts

Reversed phase high performance liquid chromatography (RP-HPLC) was performed on an ICI HPLC system (ICI Instruments, Australia). For analytical scale separation of the 3OHKyn amino acid adducts, a Phenomenex column (Jupiter C18, 300 Å, 5  $\mu m$ , 4.6 x 250 mm) was used with the following mobile phase conditions: solvent A (aqueous 0.05% (v/v) TFA) for 5 minutes followed by a linear gradient of 0-50% solvent B (80% (v/v) acetonitrile/ $H_2O$ , 0.05% (v/v) TFA) over 20 minutes, followed by a linear gradient of 50-100% B over 15 minutes and re-equilibration in the aqueous phase for 15 minutes. The flow rate was 1 mL/min. Semi-preparative separations were performed using the

same conditions as those for the analytical separations except that a Hypersil® (BDS C18, 5  $\mu$ m, 10 x 250 mm) column was used at a flow rate of 3 mL/min.

#### **2.2.4 Formation of the 3OHKyn Amino Acid Adducts at pH 7.2**

3OHKyn (1.12 mg) and either N- $\alpha$ -*t*-Boc-L-His, N- $\alpha$ -*t*-Boc-L-Lys or Cys (25-fold molar excess) were dissolved in 0.1 M phosphate buffer, pH 7.2 (5 mL), and chloroform (20  $\mu$ l) was added to inhibit bacterial growth. The pH was readjusted to 7.2 with 4 M NaOH if required, and the resulting solution was bubbled with argon, sealed, wrapped in foil and incubated at 37<sup>0</sup>C for 5 days. Aliquots were taken daily and examined by analytical HPLC in order to determine the yield of the adducts. pH remained constant during the entire incubation.

#### **2.2.5 Acid Hydrolysis of 3OHKyn Amino Acid Adducts**

Each 3OHKyn amino acid adduct (~0.5 mg) was hydrolysed in an evacuated hydrolysis tube with 6 M HCl (1 mL), thioglycolic acid (5% v/v), and phenol (1% w/v) for 24 hours at 110<sup>0</sup>C.<sup>165</sup> Following hydrolysis, the mixture was freeze dried, dissolved in 0.1% (v/v) TFA and purified by HPLC.

#### **2.2.6 Stability of 3OHKyn Amino Acid Adducts at pH 4.0**

3OHKyn amino acid adducts (0.2 mg) were dissolved in 0.1 M sodium acetate/acetic acid buffer, pH 4.0 (3 mL), and the resulting solutions were bubbled with either argon or oxygen before being sealed, wrapped in foil, and incubated for 48 hours at 37<sup>0</sup>C. Aliquots were taken every 12 hours and examined by HPLC in order to determine the recovery of the adducts.

#### **2.2.7 Stability of 3OHKyn Amino Acid Adducts at pH 7.2**

3OHKyn amino acid adducts (0.2 mg) were dissolved in 0.1 M phosphate buffer, pH 7.2 (3 mL), and chloroform (20  $\mu$ L) was added to inhibit bacterial growth. The pH was adjusted to 7.2 with 4 M NaOH if required. The resulting solutions were bubbled with either argon or oxygen before being sealed, wrapped in foil, and incubated for 120 hours at 37<sup>0</sup>C. Aliquots were taken every 24 hours and examined by HPLC.



### 2.2.8 Incubation of 3OHKyn-Cys in the Presence of Excess N- $\alpha$ -*t*-Boc-His and N- $\alpha$ -*t*-Boc-Lys

3OHKyn-Cys (2 mg) was dissolved in 0.1 M phosphate buffer, pH 7.2 (4 mL) with a 20-fold molar excess of N- $\alpha$ -*t*-Boc-His, and a 20-fold molar excess of N- $\alpha$ -*t*-Boc-Lys. Chloroform (20  $\mu$ L) was added to inhibit bacterial growth, and the pH was adjusted to 7.2 with 4 M NaOH if required. The solution was bubbled with argon, sealed wrapped in foil and incubated for 48 hours at 37<sup>0</sup>C. Aliquots were taken every 12 hours and examined by HPLC.

### 2.2.9 HPLC for Acid Hydrolysis and Stability Studies

RP-HPLC was performed on a Shimadzu SCL-10A VP system controller, with an LC-10AT VP pump, SIL-10AD VP auto injector with a 500  $\mu$ L loop, and a SPD-M10AVP diode array detector. Analytical scale separations, were performed on a Phenomenex column (Jupiter C18, 300 Å, 5 $\mu$ m, 4.6 x 250 mm). The following gradient was used: solvent A (aqueous 0.1% (v/v) TFA) for 5 minutes followed by linear gradient of 0-50% solvent B (80% (v/v) acetonitrile/H<sub>2</sub>O, 0.1% (v/v) TFA) over 20 minutes followed by a linear gradient of 50-100% B over 15 minutes and re-equilibration in the aqueous phase for 15 minutes. The flow rate was 0.5 mL/min.

### 2.2.10 Mass Spectrometry

Electrospray ionisation mass spectrometry (ESI-MS) was performed on a Quadrupole Time-of-Flight Q-TOF2 hybrid mass spectrometer (Micromass, Manchester, UK) in positive ion mode. Samples were dissolved in 50% (v/v) aqueous acetonitrile, 0.2% (v/v) formic acid and injected into a Rheodyne injector with a 10  $\mu$ L loop. Nitrogen was used as both the bath and nebulizing gas. The capillary voltage was 2.8 kV and the cone voltage ranged from 20 eV to 40 eV. The mass spectrometer was calibrated with (Glu<sup>1</sup>)-Fibrinopeptide B (0.5 pmol/ $\mu$ L). Typically 10-20 scans were summed to obtain representative spectra. Spectra were acquired with an integration time of 2.4 seconds and a 0.1 second delay.

Nanoelectrospray ionisation mass spectrometry (nanoESI-MS) was performed on a Quadrupole Time-of-Flight Q-TOF2 hybrid mass spectrometer (Micromass,

Manchester, UK) in positive ion mode. Samples were dissolved in 5-10  $\mu\text{L}$  of solvent (50% (v/v) aqueous acetonitrile, 0.2% (v/v) formic acid) and 2  $\mu\text{L}$  loaded into medium NanoES spray capillaries (ES380, Proxeon Biosystems, Denmark), using a 10  $\mu\text{L}$  syringe (SGE, Australia). The capillary voltage was 0.8 kV.

#### 2.2.11 Tandem Mass Spectrometry (MS/MS)

Tandem mass spectrometry (MS/MS) spectra were acquired using the same conditions as above. The collision energy ranged from 20 eV to 30 eV.

#### 2.2.12 High Resolution Mass Spectrometry

High resolution mass spectra were acquired on the Q-TOF2 mass spectrometer. Samples were dissolved in 50% (v/v) aqueous acetonitrile, 0.2% (v/v) formic acid. The molecular ions were calibrated against a lock mass arising from a co-injection of a solution of polyethylene glycol in 50% (v/v) aqueous acetonitrile with 1% (v/v) ammonia.

#### 2.2.13 NMR Spectroscopy

One-dimensional (1-D) and two-dimensional (2-D)  $^1\text{H}$  and  $^{13}\text{C}$  NMR spectra were recorded on a Varian Mercury 500 Fourier Transform spectrometer. The spectrometer operated at 500 MHz for  $^1\text{H}$  NMR and 125 MHz for  $^{13}\text{C}$  NMR respectively. For each compound the following 2-D experiments were performed:  $^1\text{H}$ - $^1\text{H}$  correlation spectroscopy (gCOSY), and  $^1\text{H}$ - $^{13}\text{C}$  heteronuclear spectroscopy (gHMBC and gHSQC). All experiments were run in  $\text{D}_2\text{O}$  (1 mL) to which deuterium chloride (DCI) (1  $\mu\text{L}$ ) was added to enhance stability. The  $^1\text{H}$  and  $^{13}\text{C}$  NMR data are reported as chemical shifts ( $\delta$ ) in parts per million (ppm). Samples were referenced to HOD at 4.81 ppm and in the case of carbon, acetonitrile was added and referenced at 117 ppm. Coupling constants are given in Hz. The integrated intensity, multiplicity and general assignment of each resonance are described in parentheses. The abbreviations used to describe the multiplicity are as follows: d: doublet, dd: doublet of doublets, m: multiplet, s: singlet, and t: triplet.

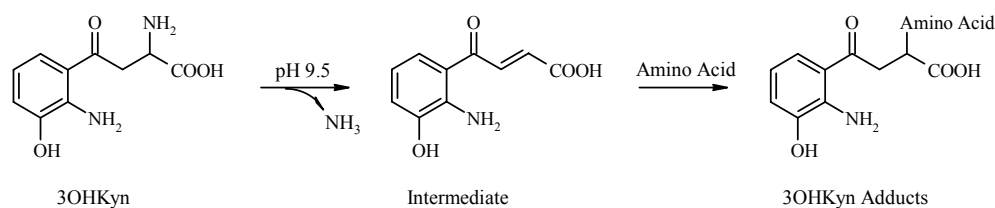
#### **2.2.14 Fluorescence and UV-visible Spectroscopy**

Fluorescence spectra were obtained on a Hitachi F-4500 fluorescence spectrometer (Tokyo, Japan) in three-dimensional (3-D) scan mode. Slit widths were routinely 10 nm for excitation and 5 nm for emission, the scan speed was 12 000 nm/min, the sampling interval was 10 nm. UV-visible absorbance spectra were recorded on a Varian CARY 500 Scan UV-Vis-NIR spectrophotometer (Palo Alto, CA, USA).

## 2.3 Results

### 2.3.1 Synthesis of the 3OHKyn Amino Acid Adducts

The 3OHKyn amino acid adducts were synthesised by incubation of N- $\alpha$ -*t*-Boc protected His and Lys (to prevent modification of the  $\alpha$ -amino group) and free Cys with 3OHKyn at pH 9.5 for 48 hours. Under these high pH conditions, side chains of Kyn derivatives deaminate more readily than at neutral pH.<sup>109</sup> At a pH above neutral pH UV filters undergo deamination to form reactive intermediates (see Scheme 2.1).<sup>109</sup> These deaminated compounds are then highly susceptible to nucleophilic attack via a Michael addition. In the lens, the side chain of amino acid residues, Cys, His and Lys and GSH, are examples of nucleophiles that are known to covalently attach to Kyn and 3OHKynG.<sup>82,103</sup> The aim was to synthesise the corresponding Cys, His and Lys adducts of 3OHKyn (Scheme 2.1).



**Scheme 2.1** Synthesis of 3OHKyn amino acid adducts. 3OHKyn is deaminated at pH 9.5, and the intermediate compound is susceptible to nucleophilic attack via a Michael addition. Amino acid side chains of Cys, His or Lys were covalently attached to the 3OHKyn amino acid side chain.

Initially the reaction mixtures were yellow, but after 48 hours of incubation each solution had turned brown in colour. The crude sample mixtures were purified by RP-HPLC (the conditions are described in Section 2.2.3). The products were monitored at 360 nm. A yield of 17% was recorded for the pure 3OHKyn-Cys adduct, 9% for 3OHKyn-*t*-Boc-His, and 11% for the 3OHKyn-*t*-Boc-Lys adduct. Low yields were presumably obtained for each adduct since 3OHKyn readily oxidises under basic conditions with the formation of numerous products.<sup>181,184</sup>

The HPLC chromatogram (Figure 2.2) for the purification of 3OHKyn-Cys exhibited 2 peaks, eluting at 15.6 min and 18.9 min. Each peak was initially examined by mass spectrometry. The mass spectrum for the first peak eluting at 15.6 min had an abundant molecular ion at  $m/z$  225, consistent with unreacted 3OHKyn. The mass spectrum of the peak at 18.9 min had a molecular ion at  $m/z$  329 (theoretical molecular ion of 3OHKyn-Cys). This product was freeze dried to produce a yellow powder that was further characterised by MS/MS, NMR, UV-visible and 3-D fluorescence spectroscopy.

The HPLC chromatogram for the purification of 3OHKyn-*t*-Boc-His is shown in Figure 2.3. Six major peaks eluted at 14.8, 18.3, 19.8, 22.6, 25.0, and 26.2 min. Each peak was initially examined by mass spectrometry. The peak at 14.8 min was confirmed as unreacted 3OHKyn. The peak at 18.3 min contained unreacted N- $\alpha$ -*t*-Boc-L-His with an  $m/z$  256. The peak at 19.8 min could not be identified. The peak at 22.6 min was identified as 3OHKyn-yellow (an intramolecular cyclisation product of 3OHKyn<sup>191</sup>)  $m/z$  208 by mass spectrometry. The peak at 25.0 min was identified as xanthommatin (an oxidation product of 3OHKyn<sup>181,184</sup>). Finally the peak at 26.2 min had a molecular ion at  $m/z$  463 (theoretical molecular ion of 3OHKyn-*t*-Boc-His). This product was further characterised by MS/MS, NMR, UV-visible and 3-D fluorescence spectroscopy.

The HPLC chromatogram for the purification of 3OHKyn-*t*-Boc-Lys is shown in Figure 2.4. Six major peaks eluted at 14.8, 18.7, 20.1, 22.5, 25.0, and 26.8 min. Each peak was initially examined by mass spectrometry. The peak at 14.8 min was identified as unreacted 3OHKyn. The peak at 18.7 min contained unreacted N- $\alpha$ -*t*-Boc-L-Lys with a molecular ion at  $m/z$  247. The peak at 20.1 min could not be identified, the peak at 22.5 min was identified as 3OHKyn-yellow. The peak at 25.0 min was identified as xanthommatin. Finally the peak at 26.8 min had a molecular ion at  $m/z$  454 (theoretical molecular ion of 3OHKyn-*t*-Boc-Lys). This product was also further characterised by MS/MS, NMR, UV-visible and 3-D fluorescence spectroscopy.

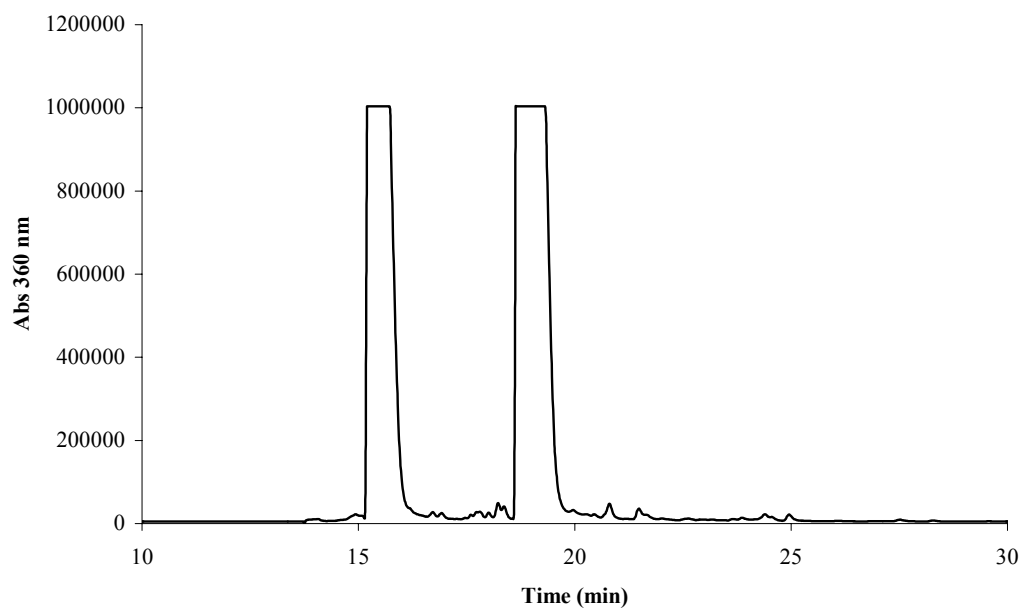


**Figure 2.2** HPLC trace of 3OHKyn and L-Cys. 3OHKyn was incubated with L-Cys at pH 9.5, 37<sup>0</sup>C for 48 hours (UV detection monitored at 360 nm). The peak at 15.6 min is unreacted 3OHKyn, and the peak at 18.9 min is the 3OHKyn amino acid adduct, 3OHKyn-Cys.

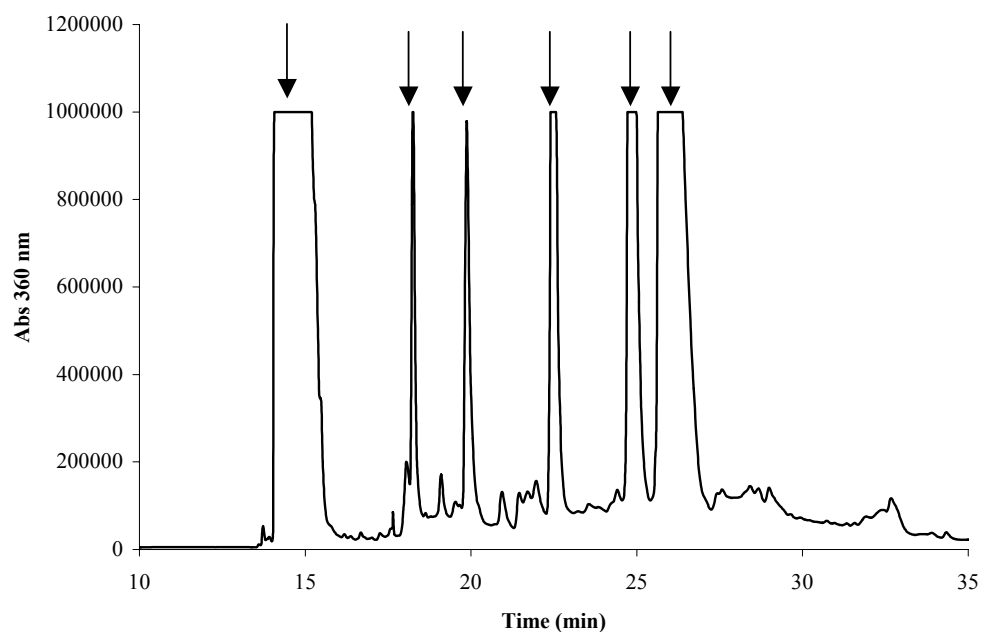


**Figure 2.3** HPLC trace of 3OHKyn and N- $\alpha$ -*t*-Boc-L-His. 3OHKyn was incubated with N- $\alpha$ -*t*-Boc-L-His at pH 9.5, 37<sup>0</sup>C for 48 hours (UV detection monitored at 360 nm). The peak at 14.8 min is unreacted 3OHKyn, the peak at 18.3 min contained N- $\alpha$ -*t*-Boc-L-His, the peak at 19.8 min is unknown. The peak at 22.6 min is 3OHKyn-yellow, the peak at 25.0 min is xanthommatin, and the peak at 26.2 min is the 3OHKyn amino acid adduct, 3OHKyn-*t*-Boc-His.

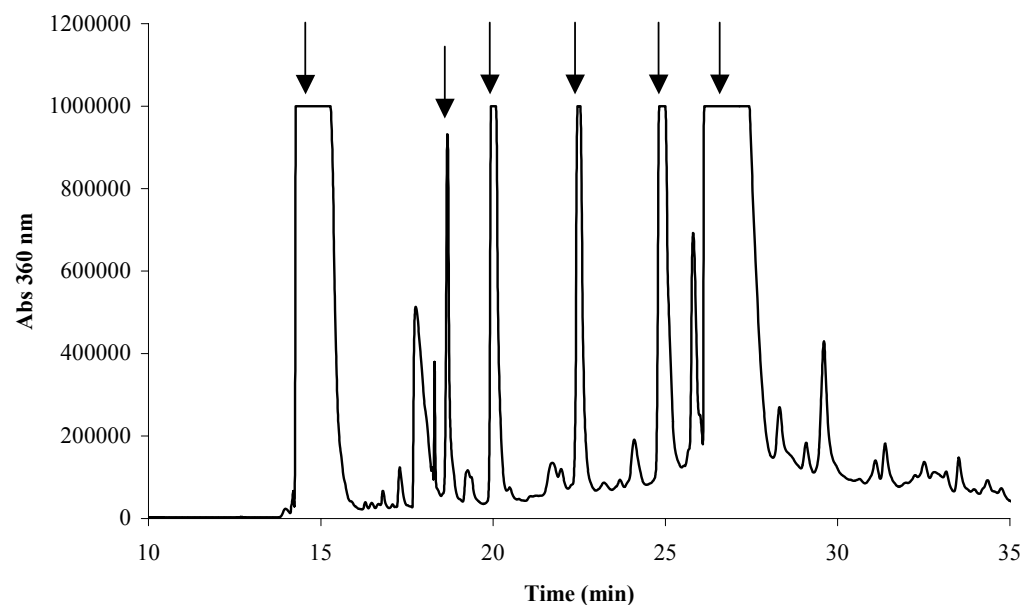


**Figure 2.4** HPLC trace of 3OHKyn and N- $\alpha$ -*t*-Boc-L-Lys. 3OHKyn was incubated with N- $\alpha$ -*t*-Boc-L-Lys at pH 9.5 and 37<sup>0</sup>C for 48 hours (UV detection monitored at 360 nm). The peak at 14.8 min is unreacted 3OHKyn, the peak at 18.7 min contained N- $\alpha$ -*t*-Boc-L-Lys, the peak at 20.1 min is unknown. The peak at 22.5 min is 3OHKyn-yellow, the peak at 25.0 min is xanthommatin, and the peak at 26.8 min is the 3OHKyn amino acid adduct, 3OHKyn-*t*-Boc-Lys.



### 2.3.2 Formation of the 3OHKyn Amino Acid Adducts at pH 7.2

The rate of deamination of UV filter side chains increases as the pH increases. 3OHKyn is an *o*-aminophenol compound and is known to be unstable under basic conditions. The 3OHKyn amino acid adducts were synthesised at pH 9.5 based on previous studies<sup>103</sup> to encourage deamination, but to understand the reactivity at physiological pH, the relative formation of these adducts at pH 7.2 was also examined. 3OHKyn was incubated with N- $\alpha$ -*t*-Boc-L-His, N- $\alpha$ -*t*-Boc-L-Lys and Cys separately at pH 7.2 and 37<sup>0</sup>C, for 5 days. Figure 2.5 shows the relative rate of formation of the 3OHKyn amino acid adducts over a 5-day incubation.

The initial amount of the adducts formed after 1 day of incubation was 3OHKyn-*t*-Boc-His, greater than 3OHKyn-Cys and greater than 3OHKyn-*t*-Boc-Lys. The 3OHKyn-Cys adduct curve showed that the yield decreased after 3 days of incubation. After 2 days of incubation, a yield of 12% was observed for 3OHKyn-Cys but on day 3, the yield of 3OHKyn-Cys had dropped to 4%, and this continued to drop to 2% by day 5.

The 3OHKyn-*t*-Boc-His adduct plateaued after 1 day. On day 1 the yield of this adduct was 8%, on day 2 this increased to 9%. Then the amount slowly decreased over the next three days. On day 5 a yield of 6% of pure 3OHKyn-*t*-Boc-His was recovered.

The 3OHKyn-*t*-Boc-Lys adduct curve showed that the yield decreased after 4 days. After one day of incubation, 4% of pure 3OHKyn-*t*-Boc-Lys was produced. The amount of this adduct increased to 7% on day 3, and then dropped to 3% by day 5.

This study shows that the relative amounts of adduct at 1 day of incubation are a result of adduct formation, whereas the amounts of adduct at the end of the 5 day incubation are a result of both adduct formation and stability.

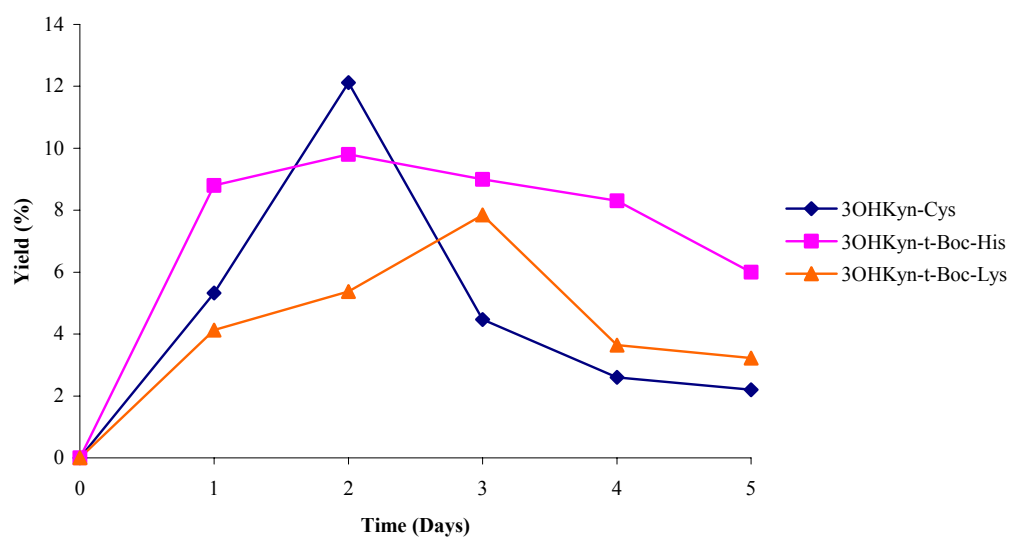


**Figure 2.5** Formation of 3OHKyn amino acid adducts over a 5 day incubation. 3OHKyn was incubated with a 25-fold molar excess of N- $\alpha$ -*t*-Boc-L-His, N- $\alpha$ -*t*-Boc-L-Lys, or Cys at pH 7.2, 37<sup>0</sup>C.

### 2.3.3 Mass Spectrometric Characterisation of the 3OHKyn Amino Acid Adducts

The structures of the 3OHKyn amino acid adducts were investigated initially by mass spectrometry, since NMR characterisation was difficult due to the low yields produced. MS/MS was found to be an important tool for characterising these adducts structurally. ESI mass spectra were initially acquired for each of the adducts. The theoretical molecular ions for each of the adducts (3OHKyn-Cys,  $m/z$  329; 3OHKyn-*t*-Boc-His,  $m/z$  463 and 3OHKyn-*t*-Boc-Lys,  $m/z$  454) were present in the ESI mass spectra (spectra not shown). MS/MS of the molecular ions were performed to confirm the structures.

MS/MS of ion at  $m/z$  329 (3OHKyn-Cys) is shown in Figure 2.6, and resulted in fragment ions at  $m/z$  311, 240, 208, 202, 190, 162, 122 and 110. The proposed structures for these major fragment ions are shown in Table 2.1, and these are comparable to the structures of the fragment ions of Kyn-Cys<sup>192</sup> whereby 3OHKyn-Cys has the addition of an oxygen atom. A loss of water from the molecular ion generated the fragment ion at  $m/z$  311.

MS/MS of ion  $m/z$  463 (3OHKyn-*t*-Boc-His) is shown in Figure 2.7, and resulted in fragment ions  $m/z$  407, 363, 317, 211, 208, 190, 162, 156, 136 and 110. The proposed structures for these major fragment ions are shown in Table 2.2, and the structures are comparable to the structures of the fragment ions of Kyn-*t*-Boc-His.<sup>192</sup> A loss of the *t*-Boc group generated the product ion  $m/z$  363.

MS/MS of ion  $m/z$  454 (3OHKyn-*t*-Boc-Lys) is shown in Figure 2.8, and resulted in fragment ions  $m/z$  398, 354, 247, 208, 203, 152, 147 and 128. The proposed structures for these major fragment ions are shown in Table 2.3, and the structures are comparable to the structures of the fragment ions of Kyn-*t*-Boc-Lys.<sup>192</sup> A loss of the *t*-Boc group generated the product ion  $m/z$  354.

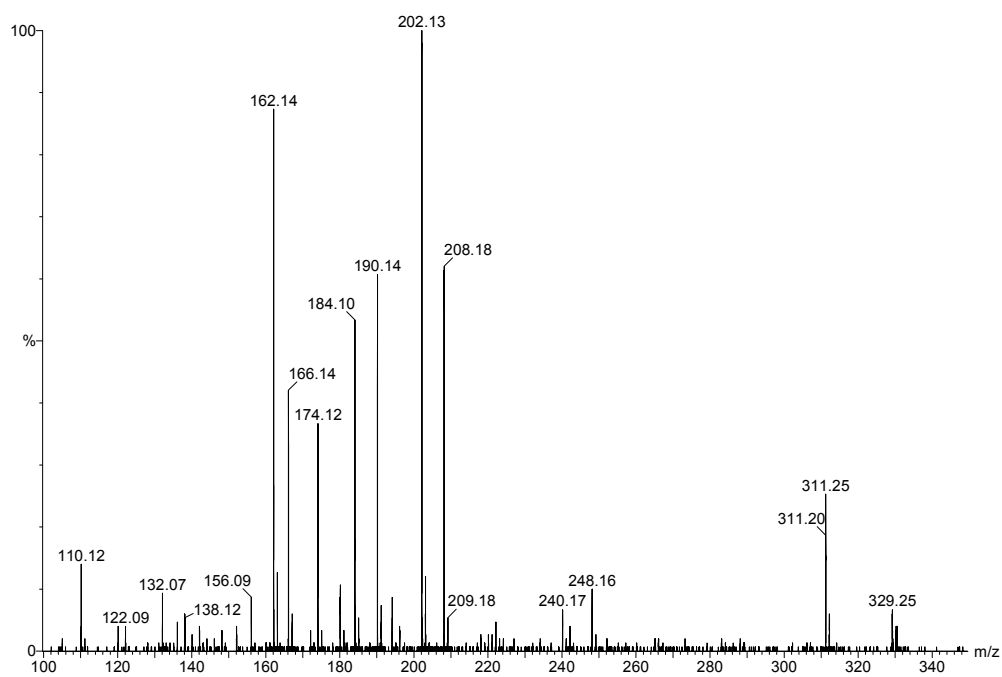
A fragment ion present in all adducts was  $m/z$  208 and this corresponds to 3-hydroxykynurenine yellow (3OHKyn-yellow)<sup>192</sup> (Tables 2.1, 2.2 and 2.3), a known intramolecular cyclisation product of 3OHKyn at neutral pH.<sup>191</sup> Two other fragment ions present in all three MS/MS spectra were  $m/z$  162 and  $m/z$  110. Therefore these

three ions ( $m/z$  208, 162 and 110) are ‘characteristic’ fragment ions for all three 3OHKyn amino acid adducts.

Fragment ions  $m/z$  122, 147 and 156 were present in 3OHKyn-Cys (Figure 2.6), 3OHKyn-*t*-Boc-Lys (Figure 2.8) and 3OHKyn-*t*-Boc-His (Figure 2.7) respectively, corresponding to the molecular masses of the amino acid residues Cys, Lys and His respectively.

MS/MS confirmed that the amino acids were attached to the 3OHKyn amino acid side chain. 3OHKyn-Cys had a fragment ion  $m/z$  202 (Table 2.1), which was derived from  $\alpha$ -cleavage at the carbonyl (C-7) on the 3OHKyn side chain (see Figure 2.1 for the numbering of the atoms). This fragment ion shows that the Cys has attached through C-9 on the 3OHKyn amino acid side chain. 3OHKyn-*t*-Boc-Lys had a fragment ion  $m/z$  203 (Table 2.3), which was derived from cleavage at C-9 and C-17 (minus the *t*-Boc) (Figure 2.1). Similarly this fragment ion shows that the Lys has attached through C-9 on the 3OHKyn amino acid side chain. These two ions were abundant ions in the MS/MS spectra, and could be used as markers for identifying these two adducts *in vivo*.

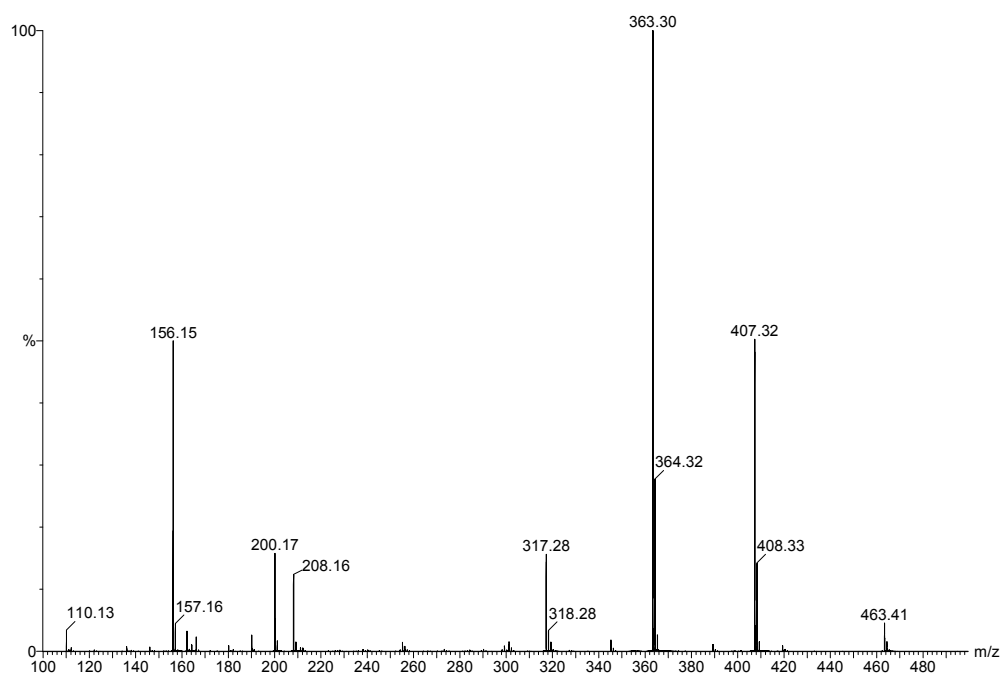
High resolution mass spectrometric data were also obtained for the molecular ions of each of the three adducts to confirm the elemental compositions: 3OHKyn-Cys 329.0789 (calculated for  $C_{13}H_{17}N_2O_6S$ , 329.0807), 3OHKyn-*t*-Boc-His 463.1771 (calculated for  $C_{21}H_{27}N_4O_8$ , 463.1829), and 3OHKyn-*t*-Boc-Lys 454.2264 (calculated for  $C_{21}H_{32}N_3O_8$ , 454.2189). To further confirm the structure of the 3OHKyn amino acid adducts NMR spectroscopy was undertaken.



**Figure 2.6** MS/MS spectrum of the protonated molecular ion of 3OHKyn-Cys  $m/z$  329.

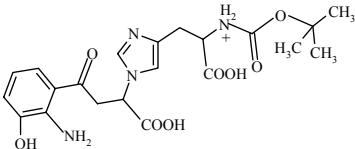
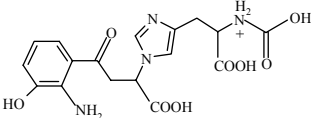
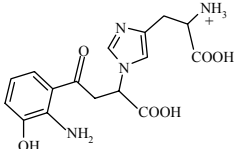
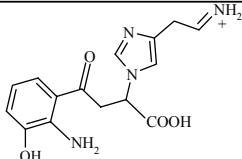
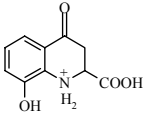
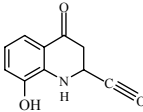
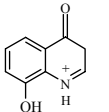
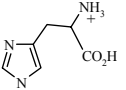
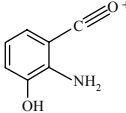
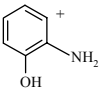
**Table 2.1** Proposed structures of the major fragment ions of 3OHKyn-Cys observed in the MS/MS spectrum.

| Observed Ion ( $m/z$ ) | Proposed Structure |
|------------------------|--------------------|
| 329                    |                    |
| 311                    |                    |
| 240                    |                    |
| 208                    |                    |
| 202                    |                    |
| 190                    |                    |
| 162                    |                    |
| 152                    |                    |
| 136                    |                    |
| 122                    |                    |
| 110                    |                    |



**Figure 2.7** MS/MS spectrum of the protonated molecular ion of 3OHKyn-*t*-Boc-His  $m/z$  463.

**Table 2.2** Proposed structures of the major fragment ions of 3OHKyn-*t*-Boc-His observed in the MS/MS spectrum.

| Observed Ion ( <i>m/z</i> ) | Proposed Structure   |
|-----------------------------|--|
| 463                         |    |
| 407                         |    |
| 363                         |    |
| 317                         |   |
| 208                         |  |
| 190                         |  |
| 162                         |  |
| 156                         |  |
| 136                         |  |
| 110                         |  |



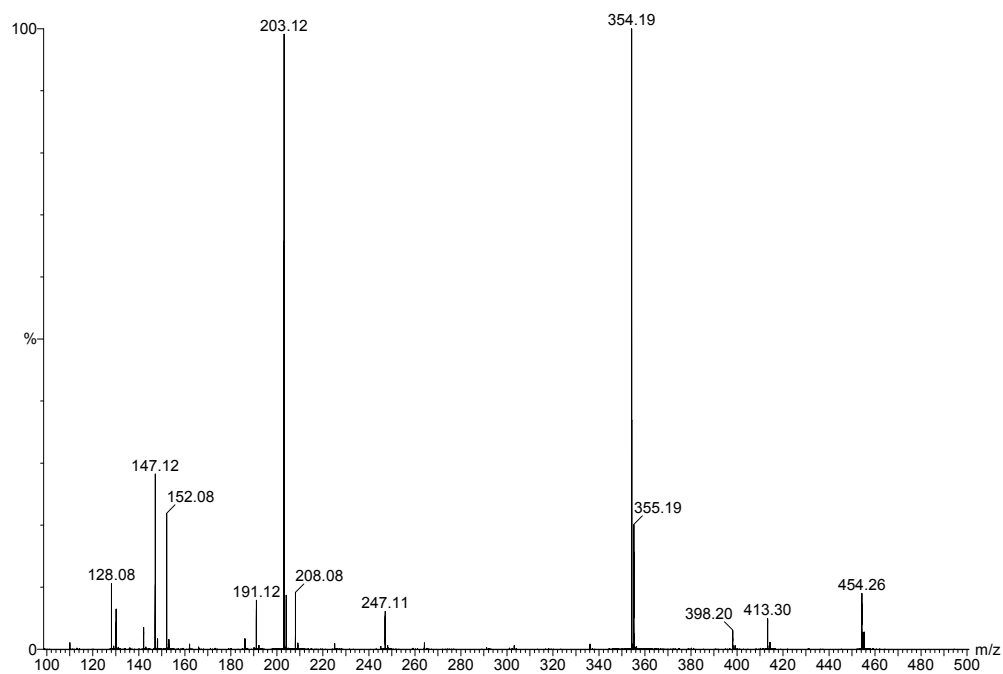


**Figure 2.8** MS/MS spectrum of the protonated molecular ion of 3OHKyn-*t*-Boc-Lys  $m/z$  454.

**Table 2.3** Proposed structures of the major fragment ions of 3OHKyn-*t*-Boc-Lys observed in the MS/MS spectrum.

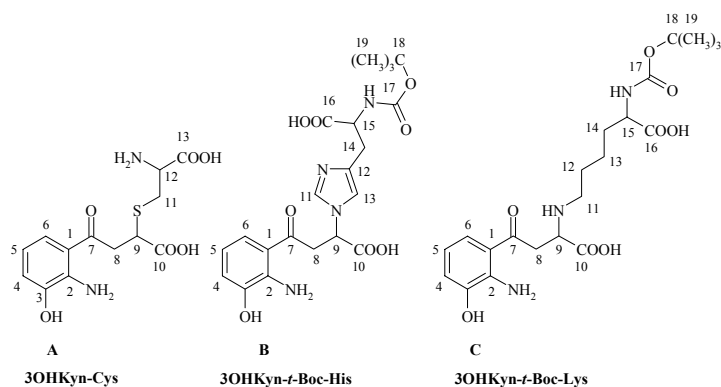
| Observed Ion ( $m/z$ ) | Proposed Structure |
|------------------------|--------------------|
| 454                    |                    |
| 398                    |                    |
| 354                    |                    |
| 247                    |                    |
| 208                    |                    |
| 203                    |                    |
| 162                    |                    |
| 152                    |                    |
| 147                    |                    |
| 128                    |                    |
| 110                    |                    |

### 2.3.4 NMR Characterisation of 3OHKyn Amino Acid Adducts

NMR studies were undertaken to characterise the 3OHKyn amino acid adducts. 1-D and 2-D spectra were acquired for each adduct. Samples were dissolved in acidified D<sub>2</sub>O, to stabilise each adduct, since *o*-aminophenols readily oxidise at neutral pH.<sup>184</sup> The adducts were not separated into individual diastereoisomers since the resolution by HPLC was inadequate. The chemical shifts for the <sup>1</sup>H and <sup>13</sup>C NMR spectra are listed in Table 2.4. The chemical shifts of the protons and carbons for each 3OHKyn amino acid adduct was similar to the chemical shifts reported for the Kyn amino acid adducts.<sup>103</sup> In addition, the chemical shifts for 3OHKyn-*t*-Boc-Lys were similar to those reported by Staniszewska, *et al.* who synthesised an antigen using 3OHKyn and *N*- $\alpha$ -acetyl-Lys, for immunohistochemical studies.<sup>193</sup> All protons could be assigned from the <sup>1</sup>H NMR spectra (Table 2.4). 2-D NMR experiments (gCOSY, gHSQC and gHMBC) were acquired to demonstrate the proton coupling and to characterise the carbon atoms. The chemical shifts for CH-9 and CH<sub>2</sub>-8 were deshielded<sup>103</sup> with reference to 3OHKyn since highly nucleophilic amino acid residues are attached at C-9. gHMBC experiments confirmed that each amino acid was covalently attached to the 3OHKyn amino acid side chain at C-9. Since the adducts were not very soluble, and there was a limited amount of sample available, the quaternary carbons could not be resolved, and therefore structural characterisation of the 3OHKyn amino acid adducts by NMR could not be successfully completed. However the NMR experiments undertaken did confirm that the amino acids were attached at C-9 on the 3OHKyn amino acid side chain as predicted.

**Table 2.4** Summary of the  $^1\text{H}$  and  $^{13}\text{C}$  NMR spectral assignments for the 3OHKyn amino acid adducts. The atom numbering adopted is shown below.

| Adducts: A, 3OHKyn-Cys; B, 3OHKyn- <i>t</i> -Boc-His; C, 3OHKyn- <i>t</i> -Boc-Lys |            |            |            |                              |            |            |          |  |  |
|--|------------|------------|------------|------------------------------|------------|------------|----------|--|--|
| $^1\text{H}$ NMR<br>(ppm)  | Adducts    |            |            | $^{13}\text{C}$ NMR<br>(ppm) | Adducts    |            |          |  |  |
|  | A          | B          | C          |                              | A          | B          | C        |  |  |
| H-4  | 7.32       | 7.03       | 7.16       | C-1                          | 127.3      | 119.2      | <i>a</i> |  |  |
| H-5  | 7.43       | 6.90       | 6.96       | C-2                          | 118.6      | 135.3      | 134.1    |  |  |
| H-6  | 7.69       | 7.42       | 7.54       | C-3                          | 150.4      | 147.0      | 146.5    |  |  |
| H-8  | 3.77, 3.66 | 3.92       | 3.82       | C-4                          | 121.5      | 120.7      | 120.2    |  |  |
| H-9  | 3.97       | 5.47       | 4.20       | C-5                          | 128.3      | 122.0      | 120.1    |  |  |
| H-11   | 3.43, 3.33 | 8.75       | 3.19       | C-6                          | 122.2      | 122.6      | 122.8    |  |  |
| H-12   | 4.35       |            | 1.81       | C-7                          | 200.5      | 199.1      | 200.2    |  |  |
| H-13   |            | 7.34       | 1.51       | C-8                          | 40.9       | 41.9       | 38.6     |  |  |
| H-14   |            | 3.17, 2.97 | 1.89, 1.75 | C-9                          | 41.7       | 59.1       | 57.3     |  |  |
| H-15   |            | 4.3        | 4.12       | C-10                         | 175.9      | 172.4      | 172.8    |  |  |
| H-19   |            | 1.93       | 1.29       | C-11                         | 31.6, 31.3 | 135.6      | 47.1     |  |  |
|  |            |            |            | C-12                         | 52.1       | 192.7      | 25.0     |  |  |
|  |            |            |            | C-13                         | 170.8      | 119.9      | 22.3     |  |  |
|  |            |            |            | C-14                         |            | 26.8, 26.8 | 30.1     |  |  |
|  |            |            |            | C-15                         |            | 52.8       | 53.7     |  |  |
|  |            |            |            | C-16                         |            | <i>a</i>   | <i>a</i> |  |  |
|  |            |            |            | C-17                         |            | <i>a</i>   | <i>a</i> |  |  |
|  |            |            |            | C-18                         |            | 81.8       | 81.8     |  |  |
|  |            |            |            | C-19                         |            | 27.5       | 27.7     |  |  |

<sup>a</sup> Carbons were not visible due to poor resolution

### 2.3.5 UV-visible and Fluorescence Characterisation of the 3OHKyn Amino Acid Adducts

UV-visible spectra were obtained for each adduct at various pH values, to examine the absorbance of each adduct, and to gain information on their relative stability. The UV-visible spectra for the three adducts and 3OHKyn (data not shown) were found to be essentially identical under the various conditions. The solutions used in this study include, 0.1% (v/v) TFA pH 2.1, 6 M guanidine HCl pH 5.5, 0.1 M phosphate buffer pH 7.2, and sodium carbonate/bicarbonate buffer pH 9.5. Figure 2.9 shows the UV-visible spectra for 3OHKyn-Cys at various pH values. As can be seen, broad peaks were observed with wavelength maxima centred at 374 nm and 267 nm (Figure 2.9A, B and C) under acidic and neutral conditions. However at a higher pH (pH 9.5) (Figure 2.9D) there were no visible peaks of absorbance, indicating the compound had been structurally modified under these conditions. Similarly, the UV-visible spectra for 3OHKyn-*t*-Boc-His (Figure 2.11) exhibited broad peaks with wavelength maxima centred at 375 nm and 270 nm (Figure 2.11A, B and C) at acidic and neutral pH. At pH 9.5 (Figure 2.11D) there was again no visible absorbance. The UV-visible spectra for 3OHKyn-*t*-Boc-Lys are shown in Figure 2.13. Broad peaks with wavelength maxima centred at 367 nm and 266 nm were observed (Figure 2.13A, B and C) under acidic and neutral conditions, and there was no absorbance observed at pH 9.5 (Figure 2.13D).

3-D Fluorescence spectra showed that each adduct was fluorescent, but at different excitation (Ex) and emission (Em) wavelengths. 3OHKyn-Cys exhibited maximal fluorescence intensities at Ex 350 nm/Em 520 nm and Ex 420 nm/Em 520 nm at pH 2.1, Ex 340 nm/Em 510 nm and Ex 430 nm/Em 510 nm at pH 5.5, and Ex 330 nm/Em 510 nm and Ex 400 nm/Em 520 nm at pH 7.2 (Figure 2.10A, B and C). The 3-D fluorescence spectrum was significantly different at pH 9.5 with only one contour at Ex 360 nm/Em 520 nm (Figure 2.10D).

3OHKyn-*t*-Boc-His exhibited maximal fluorescence intensities at Ex 370 nm/Em 520 nm at pH 2.1, Ex 350 nm/Em 520 nm at pH 5.5, and Ex 430 nm/Em 530 nm at pH 7.2 (Figure 2.12A, B and C). At pH 9.5, the exhibited maximal fluorescence intensity was Ex 340 nm/Em 510 nm (Figure 2.12D). 3OHKyn-*t*-Boc-Lys was also fluorescent, and

exhibited maximal fluorescence intensities at Ex 420 nm/Em 520 nm at pH 2.1, Ex 350 nm/Em 520 nm and Ex 410 nm/Em 520 nm at pH 5.5, and Ex 360 nm/Em 520 nm at pH 7.2 (Figure 2.14A, B and C). At pH 9.5, the exhibited maximal fluorescence intensity was Ex 330 nm/Em 510 nm (Figure 2.14D).

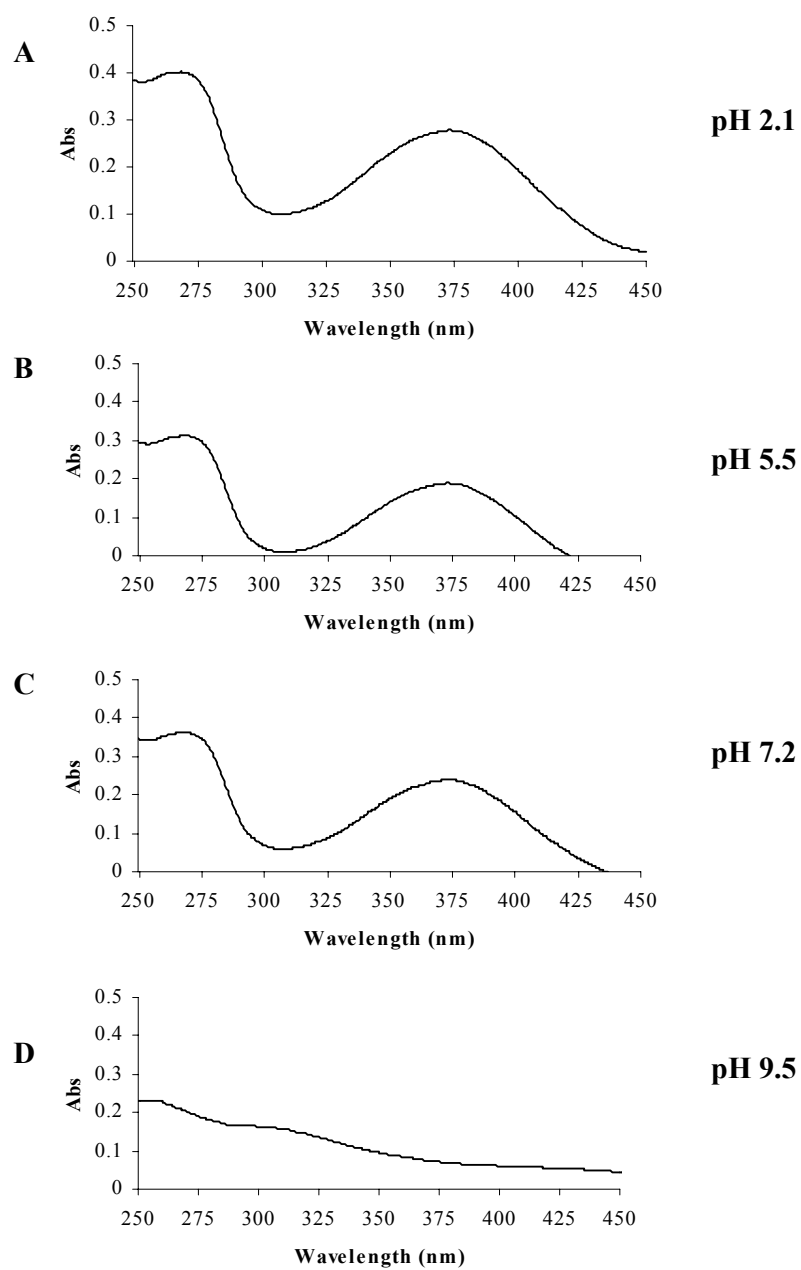


**Figure 2.9** UV-visible spectra of 3OHKyn-Cys at various pH values; *A*, pH 2.1; *B*, pH 5.5; *C*, pH 7.2; *D*, pH 9.5.

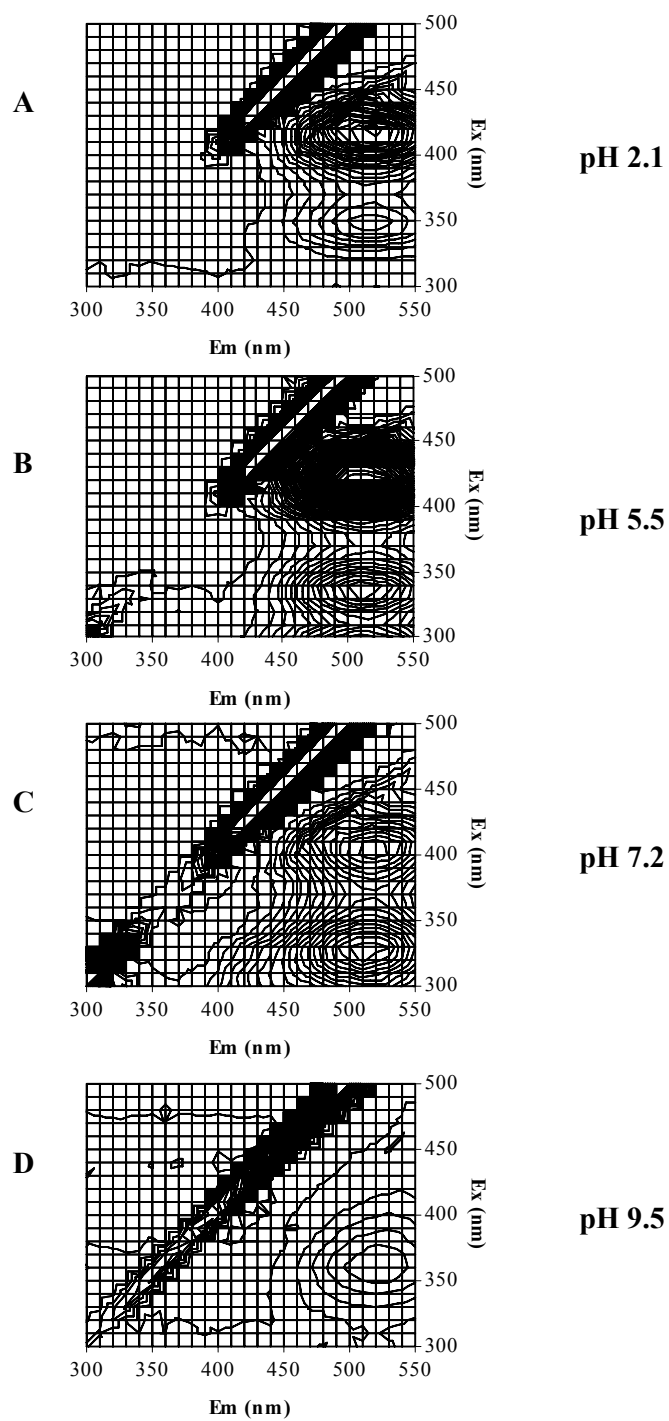


**Figure 2.10** 3-D Fluorescence spectra of 3OHKyn-Cys at various pH values; *A*, pH 2.1; *B*, pH 5.5; *C*, pH 7.2; *D*, pH 9.5.



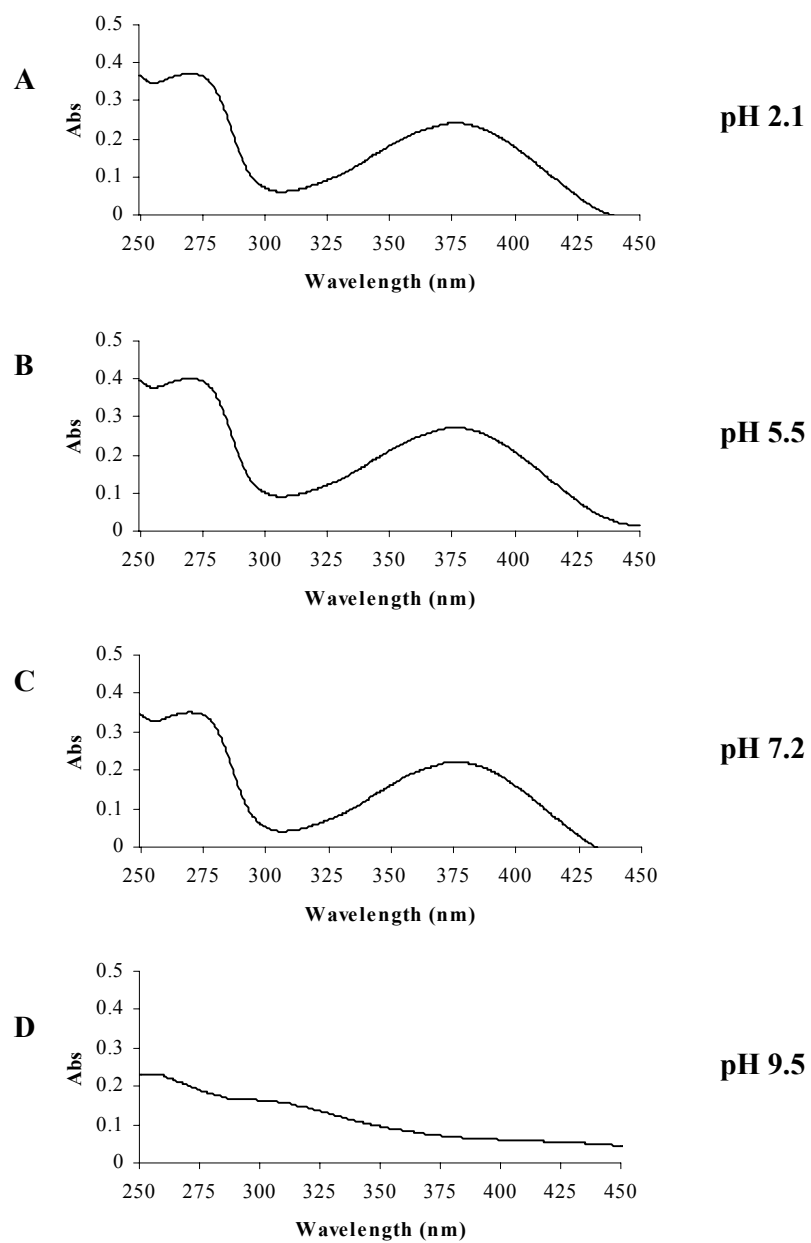


**Figure 2.11** UV-visible spectra of 3OHKyn-*t*-Boc-His at various pH values; *A*, pH 2.1; *B*, pH 5.5; *C*, pH 7.2; *D*, pH 9.5.

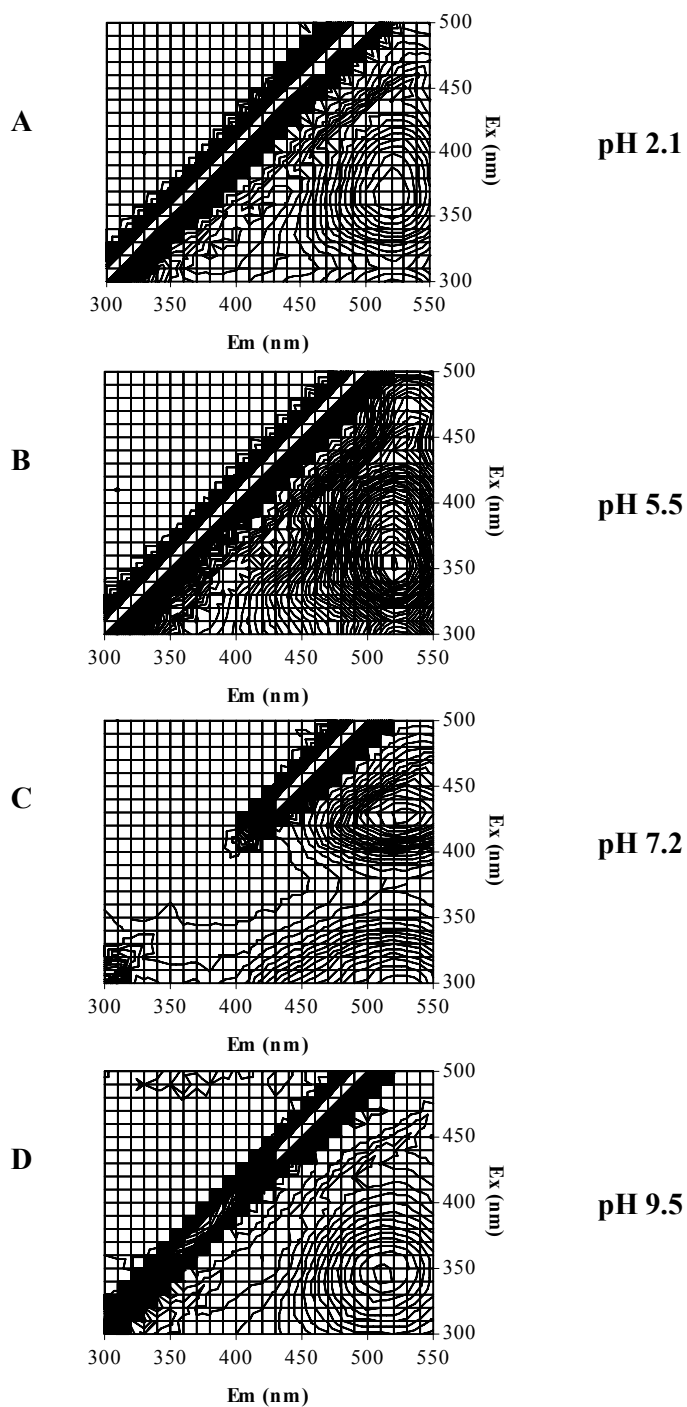


**Figure 2.12** 3-D Fluorescence spectra of 3OHKyn-*t*-Boc-His at various pH values; *A*, pH 2.1; *B*, pH 5.5; *C*, pH 7.2; *D*, pH 9.5.

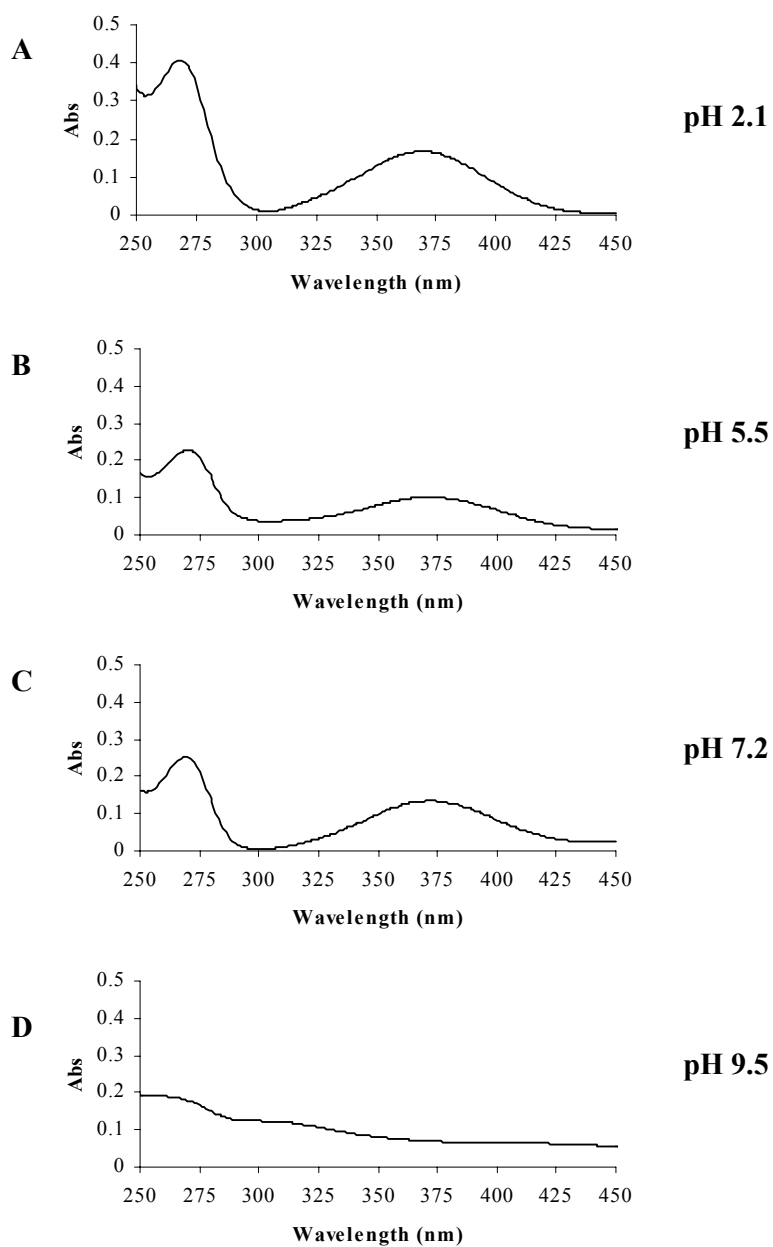


**Figure 2.13** UV-visible spectra of 3OHKyn-*t*-Boc-Lys at various pH values; *A*, pH 2.1; *B*, pH 5.5; *C*, pH 7.2; *D*, pH 9.5.

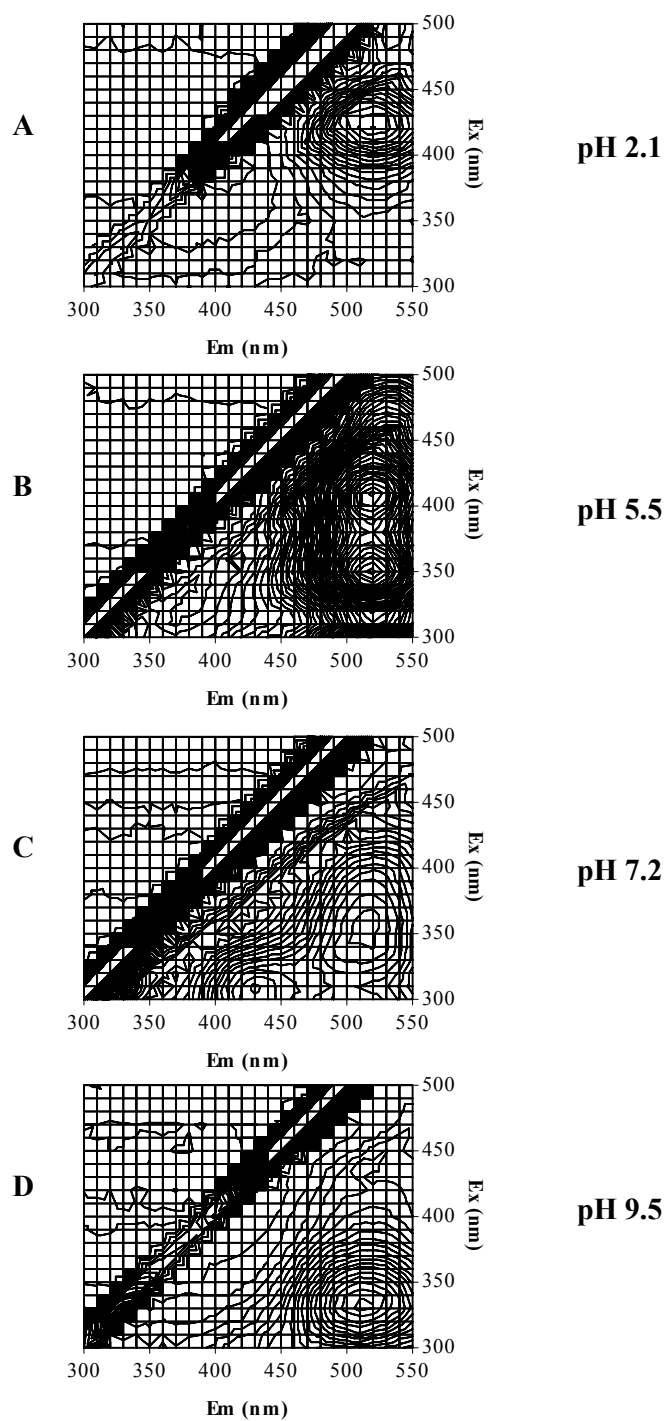


**Figure 2.14** 3-D Fluorescence spectra of 3OHKyn-*t*-Boc-Lys at various pH values; *A*, pH 2.1; *B*, pH 5.5; *C*, pH 7.2; *D*, pH 9.5.

### 2.3.6 Stability of 3OHKyn Amino Acid Adducts

3OHKyn is known to autoxidise readily at neutral pH with the production of H<sub>2</sub>O<sub>2</sub> and numerous other products.<sup>181,184</sup> It was of interest to discover if the 3OHKyn amino acid adducts were also unstable under physiological conditions.

Stability experiments were performed at pH 7.2 both in the presence, and in the absence, of oxygen. The results are shown in Figure 2.15. In the absence of oxygen, only 15% of 3OHKyn (Figure 2.15A) remained after 5 days of incubation and these results are comparable to those obtained by Taylor, *et al.* whose incubations were done in 25 mM carbonate buffer (pH 7.0).<sup>109</sup> 3OHKyn-Cys and 3OHKyn-*t*-Boc-Lys (Figure 2.15B and D) adducts were found to be less stable than 3OHKyn, resulting in yields of 3% and 7% respectively after 5 days. By contrast, under the same conditions, the His adduct (Figure 2.15C) was recovered in 51% yield.

In the presence of oxygen, the adducts were markedly less stable. There was, for example, no 3OHKyn recovered after 96 hours at pH 7.2 (Figure 2.15A), and no detectable peak for the Cys adduct after only 24 hours of incubation (Figure 2.15B). No trace of the Lys adduct was observed after 48 hours of incubation (Figure 2.15D). Again the His adduct was most stable but even this adduct showed a recovery of 11% after 120 hours (Figure 2.15C).

These data illustrate that all of the 3OHKyn amino acid adducts are unstable under physiological conditions and that this instability is exacerbated by exposure to oxygen. The Cys and Lys adducts are, more labile, and more readily oxidised, than 3OHKyn itself.

One objective of the current study was to develop a method for detecting 3OHKyn if it is attached to proteins. Because of their instabilities, and susceptibility to oxidation, coupled with the fact that they are likely to be present in low levels, isolation of 3OHKyn adducts presents a technical challenge.

On the basis of the studies with 3OHKyn at neutral pH detailed above, and previous investigations, which showed that high pH promoted autoxidation,<sup>181</sup> we investigated the use of acidic pH to see if this would lead to stabilising the adducts. If 3OHKyn adducts, were found to be stabilised under such acidic conditions, these could then be used for their isolation from modified proteins. Stability studies were therefore performed on each of the adducts at pH 4.0 for 48 hours since this time would be required by for example, enzymatic digestion. As described for the incubations at neutral pH, two sets of experiments were performed; one in the absence of oxygen, and one in the presence of oxygen. The results are shown in Figure 2.16 and illustrate a marked effect of acidic pH on adduct stability. In the absence of oxygen 3OHKyn was recovered in 90% yield (Figure 2.16A) after 48 hours; whereas the Cys and Lys (Figure 2.16B and D) adducts showed a 70% recovery, and 3OHKyn-*t*-Boc-His (Figure 2.16C) was detected in 53% recovery after this time. In the presence of oxygen the recoveries of all of the compounds were diminished. That of 3OHKyn dropped to 76%, and the Cys, His and Lys adducts were recovered in yields of 20%, 11% and 36% respectively. On the basis of these data (Figures 2.15 and 2.16), in order to maximise recoveries of 3OHKyn-containing amino acids, acidic pH is required and efforts would need to be taken to exclude oxygen during sample isolation. The only exception may be 3OHKyn-His which displayed reasonable stability at pH 7.2 and pH 4.0 both in the presence and absence of oxygen.

The 3OHKyn amino acid adducts are unstable at pH 7.2. The formation of the unknown breakdown products was exacerbated in the presence of oxygen. Figure 2.17 shows the rate of formation of the unknown breakdown products that formed at pH 7.2 in the absence of oxygen for each of the adducts. The majority of the unknown breakdown compounds could not be structurally identified from the mass spectral data alone. There were seven breakdown products formed from the instability of 3OHKyn-Cys that eluted at 27.3, 28.3, 29.9, 31.2, 32.9, 33.4 and 35.7 min on the HPLC chromatogram (chromatogram not shown), and the levels of these unknown peaks have been graphed in Figure 2.17A over the 5 day incubation period.

There were four breakdown products formed from the instability of 3OHKyn-*t*-Boc-His that eluted at 30.8, 31.8, 38.1 and 39.0 min on the HPLC chromatogram (chromatogram not shown). The levels of these unknown peaks have been graphed in Figure 2.17B. There were three breakdown products formed from the instability of 3OHKyn-*t*-Boc-Lys that eluted at 30.7, 33.1 and 38.1 min on the HPLC chromatogram (chromatogram not shown). The levels of these unknown peaks have been graphed (Figure 2.17C). Figure 2.17 shows that over the 5-day period the quantity of these unknown breakdown products continuously increases as the level of the 3OHKyn amino acid adduct decreases, due to the instability of these adducts at pH 7.2.

The product eluting at 27.3 min in Figure 2.17A, 30.8 min in Figure 2.17B and 30.7 min in Figure 2.17C was identified as xanthurenic acid, a breakdown product of 3OHKyn, by MS/MS. Although the compound eluted at different times in each HPLC chromatogram, co-elution with standard xanthurenic acid confirmed the compound as one of the breakdown products. The remaining breakdown products could not be identified from the mass spectral data, however the breakdown product eluting at 39.0 min in Figure 2.17B showed a prominent ion  $m/z$  664, and the proposed structure of this compound has been derived in Section 2.3.8.

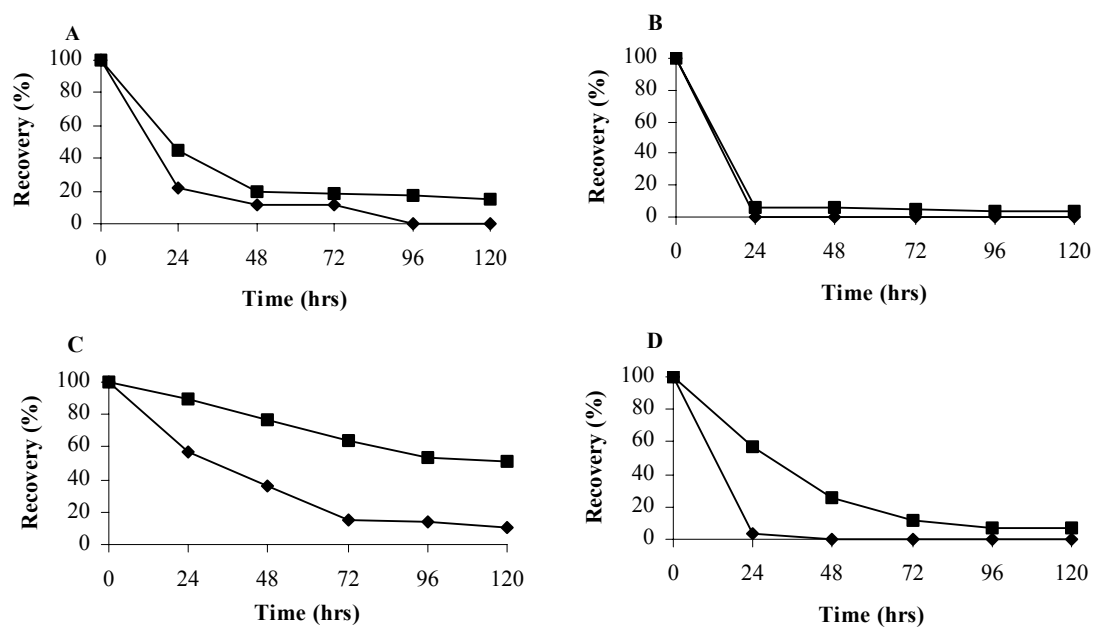


**Figure 2.15** Stability of the 3OHKyn amino acid adducts and 3OHKyn at pH 7.2 in the absence (■) and presence (◆) of oxygen. *A*, 3OHKyn; *B*, 3OHKyn-Cys; *C*, 3OHKyn-*t*-Boc-His; *D*, 3OHKyn-*t*-Boc-Lys.



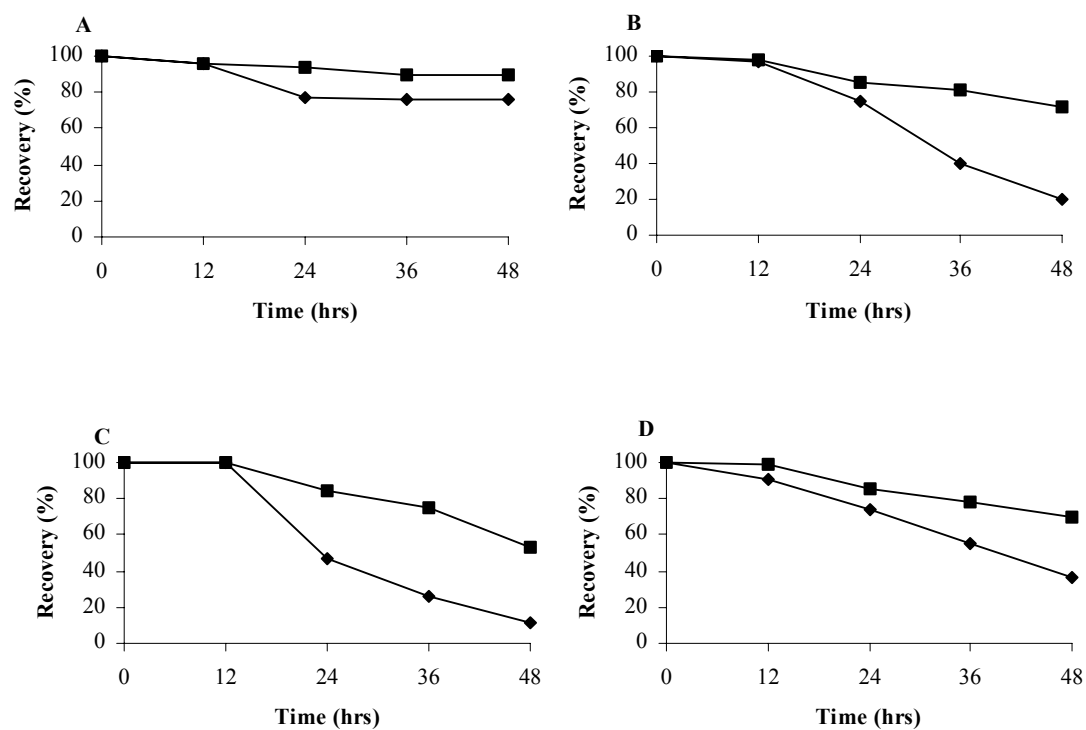


**Figure 2.16** Stability of the 3OHKyn amino acid adducts and 3OHKyn at pH 4.0 in the absence (■) and presence (◆) of oxygen. *A*, 3OHKyn; *B*, 3OHKyn-Cys; *C*, 3OHKyn-*t*-Boc-His; *D*, 3OHKyn-*t*-Boc-Lys.

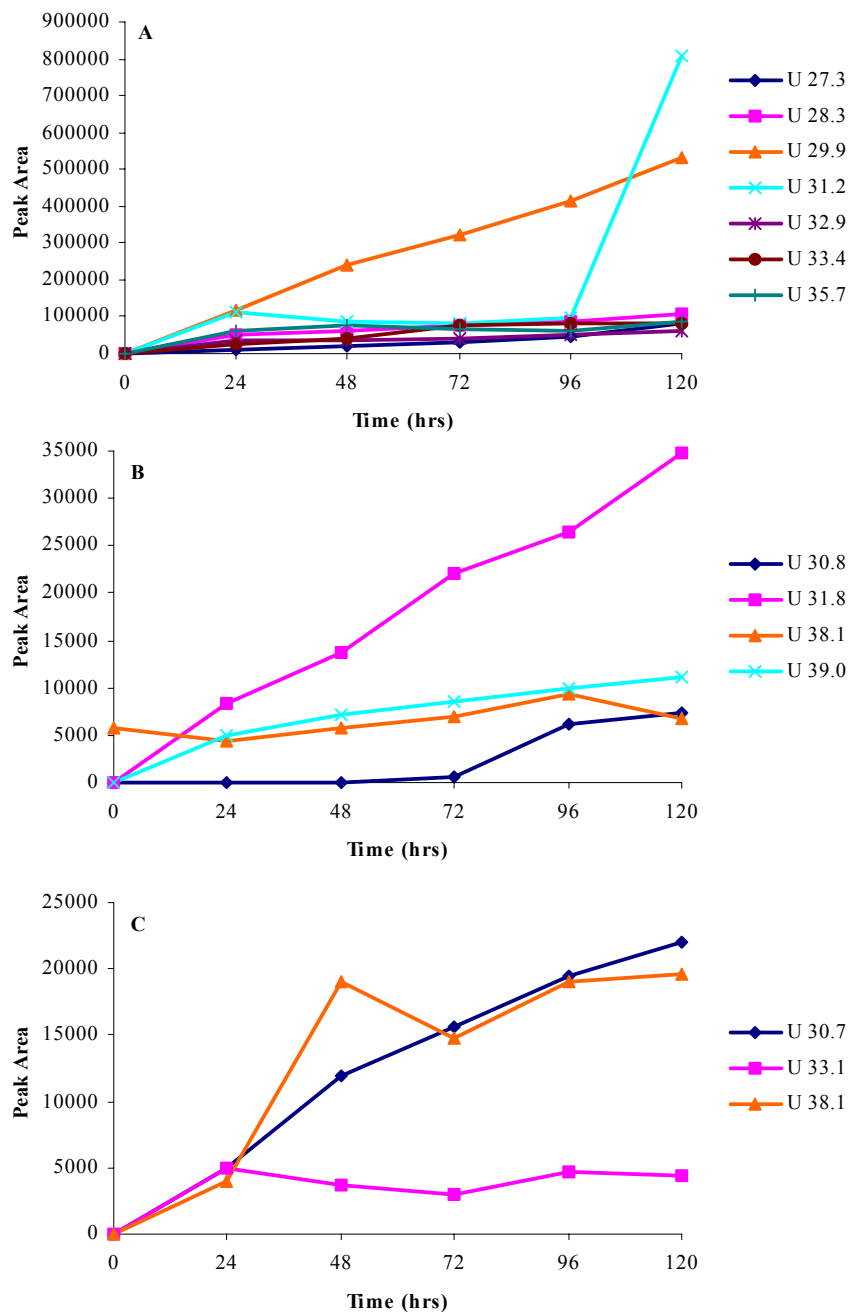


**Figure 2.17** Formation of breakdown products from stability study of 3OHKyn amino acid adducts at pH 7.2 in the absence of oxygen. *A*, 3OHKyn-Cys; *B*, 3OHKyn-*t*-Boc-His; *C*, 3OHKyn-*t*-Boc-Lys.

### 2.3.7 Acid Hydrolysis of 3OHKyn Amino Acid Adducts

The stability of each adduct under conditions used for the hydrolysis of proteins was determined by hydrolysing with 6 M HCl in the presence of antioxidants,<sup>165</sup> since low yields were recovered initially for each adduct in the absence of such antioxidants (3OHKyn-Cys 17%, 3OHKyn-His, 20% and 3OHKyn-Lys, 24%). If antioxidants were added the recoveries were markedly improved; 3OHKyn-Cys, 87%; 3OHKyn-His, 78% and 3OHKyn-Lys, 95% (Table 2.5). Under the same conditions, the recovery of 3OHKyn was 58%. The HPLC profiles (not shown) showed the presence of other minor compounds in addition to the major adduct peak, but these minor peaks were not examined further.

**Table 2.5** Recovery of 3OHKyn amino acid adducts after acid hydrolysis for 24 hours at 110<sup>0</sup>C in the presence of antioxidants.

| Adduct     | Recovery (%) |
|------------|--------------|
| 3OHKyn     | 58%          |
| 3OHKyn-Cys | 87%          |
| 3OHKyn-His | 78%          |
| 3OHKyn-Lys | 95%          |

### 2.3.8 Incubation of 3OHKyn-Cys in the Presence of Excess N- $\alpha$ -*t*-Boc-His and N- $\alpha$ -*t*-Boc-Lys

This experiment was undertaken to further examine the reactivity of the UV filter compounds. The aim was to see if the 3OHKyn attached to Cys could cleave and form deaminated 3OHKyn, and covalently attach to either N- $\alpha$ -*t*-Boc-His or N- $\alpha$ -*t*-Boc-Lys. Synthetic 3OHKyn-Cys was incubated with excess N- $\alpha$ -*t*-Boc-His and N- $\alpha$ -*t*-Boc-Lys in phosphate buffer at pH 7.2 for 48 hours. Aliquots were taken at 12 hourly intervals and analysed by HPLC. Figure 2.18 is the HPLC chromatogram for the aliquot at 48 hours of incubation. There were seven major peaks eluting, and mass spectrometry was utilised to analyse these compounds. In Figure 2.18 a doublet peak eluted at 28.4 min. MS/MS confirmed that this peak was 3OHKyn-Cys. Mass spectrometry of the second peak eluting at 30.6 min showed that the molecular ion was  $m/z$  256. MS/MS of this ion confirmed that the compound contained unreacted N- $\alpha$ -*t*-Boc-His. MS/MS confirmed that the peak at 32.4 min contained unreacted N- $\alpha$ -*t*-Boc-Lys with a molecular ion of  $m/z$  247. The peak eluting at 33.5 min was confirmed by mass spectrometry to be 3OHKyn-yellow (an intramolecular cyclisation product of 3OHKyn at neutral pH).<sup>191</sup> The large peak eluting at 35.1 min had a molecular ion of  $m/z$  463, MS/MS confirmed that the compound was 3OHKyn-*t*-Boc-His. The peak at 36.0 min was confirmed as 3OHKyn-*t*-Boc-Lys. The peak that eluted at 39.5 min could not be identified, but had a relatively abundant ion at  $m/z$  664 in the ESI mass spectrum.

In Figure 2.19, the 3OHKyn amino acid adducts as well as 3OHKyn-yellow and the unknown compound were quantified over the 48 hour incubation period. After 12 hours of incubation, the amount of 3OHKyn-Cys had decreased to 0.47 mM, and 3OHKyn-*t*-Boc-His, 3OHKyn-*t*-Boc-Lys and 3OHKyn-yellow had formed at concentrations of 0.25, 0.13 and 0.36 mM, respectively. The level of 3OHKyn-Cys continued to decrease to 0.11 mM at 48 hours of incubation, whereas 3OHKyn-*t*-Boc-His continued to increase to 0.48 mM, and 3OHKyn-*t*-Boc-Lys increased to 0.19 mM. The maximum amount of 3OHKyn-yellow was formed at 12 hours of incubation, following that, the amount of 3OHKyn-yellow decreased to 0.19 mM at 48 hours of incubation. The unknown compound that eluted at 39.5 min (U39.5), detected after 24 hours of incubation, continued to form over the following 24 hours.

The unknown compound eluting at 39.5 min (U39.5) in the HPLC chromatogram had an apparent molecular ion at  $m/z$  664 in the ESI mass spectrum (Figure 2.20A). MS/MS of this molecular ion yielded spectrum Figure 2.20B. The major fragment ions are  $m/z$  608 (loss of 56 Da),  $m/z$  564 (further loss of 44 Da) and  $m/z$  409 (further loss of 155 Da). Figure 2.21 shows the proposed structures for these ions. Molecular ion  $m/z$  664 appears to be due to a phenoxazone compound made up from 3OHKyn-*t*-Boc-His attached to an oxidised 3OHKyn molecule. The fragment ion  $m/z$  564 is a loss of 100 Da from the molecular ion  $m/z$  664, and is typical of the loss of a *t*-Boc group. A further loss of 155 Da is indicative of a loss of His yielding  $m/z$  409.

Theoretically this compound could form from autoxidation of 3OHKyn alone. In order to prove that  $m/z$  409 could be derived from autoxidation of 3OHKyn, 3OHKyn was incubated in phosphate buffer at pH 7.2 and 37°C for several days, and aliquots were taken and monitored by mass spectrometry for the formation of ion at  $m/z$  409. A  $m/z$  409 ion was identified after 3 hours of incubation, and the ESI mass spectrum is shown in Figure 2.22A. The  $m/z$  409 ion could not be detected after 2 days of incubation, indicating that it is unstable. The MS/MS spectrum of ion  $m/z$  409 is shown in Figure 2.22B and a common fragment ion also seen in Figure 2.20B is  $m/z$  391, loss of water.

The chemical name of U39.5 is, 1,3,4,5-tetrahydro-11-(2-(*N*- $\alpha$ -*tert*-butyloxycarbonyl-histidyl)-(4-hydroxy-1,4-dioxo-butanyl)-1,5-dioxo-2H-pyrido(3,2-*a*)phenoxazine-3-carboxylic acid, and to further confirm the proposed structure of this compound, high resolution mass spectrometric data was obtained for the molecular ion 664.2438 (calculated for C<sub>31</sub>H<sub>30</sub>N<sub>5</sub>O<sub>12</sub>, 664.2496).

In addition, the UV-visible spectrum (Figure 2.23) further confirmed that U39.5 contains a phenoxazone moiety since a broad peak with a maximum absorbance centred at 437 nm is shown. Phenoxazones exhibit a broad UV-visible peak centred at 440 nm.<sup>184</sup>

To confirm the structure of U39.5, more material would need to be collected for NMR.

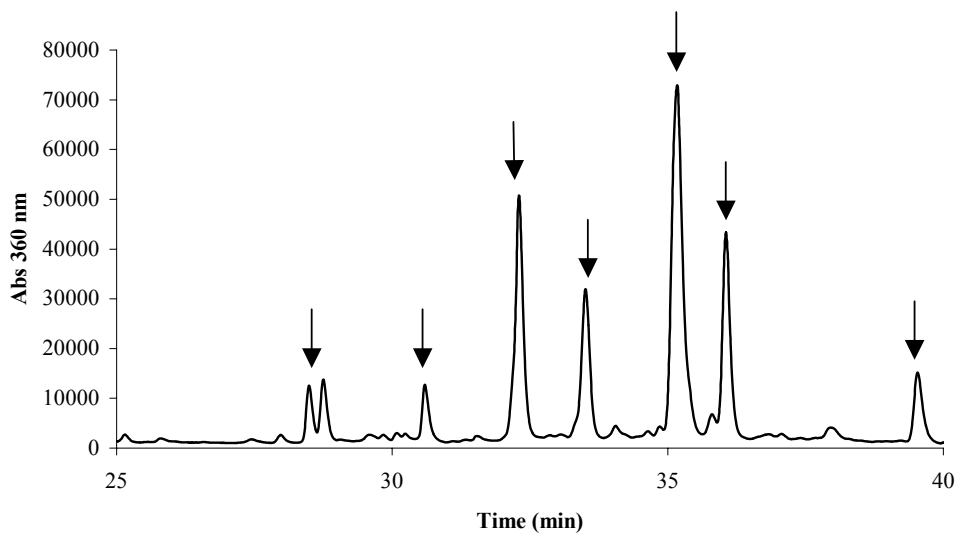


**Figure 2.18** 3OHKyn-Cys was incubated with excess N- $\alpha$ -*t*-Boc-His and N- $\alpha$ -*t*-Boc-Lys at pH 7.2 for a total of 48 hours. Shown is the 48 hour time sample (aliquot). The peak at 28.4 min is unreacted 3OHKyn-Cys. The peak at 30.6 min contained unreacted N- $\alpha$ -*t*-Boc-His, and the peak at 32.4 min contained unreacted N- $\alpha$ -*t*-Boc-Lys. The peak at 33.5 min is 3OHKyn-yellow, the peak at 35.1 min is 3OHKyn-*t*-Boc-His and the peak at 36.0 min is 3OHKyn-*t*-Boc-Lys. The peak at 39.5 min is unknown (U39.5).

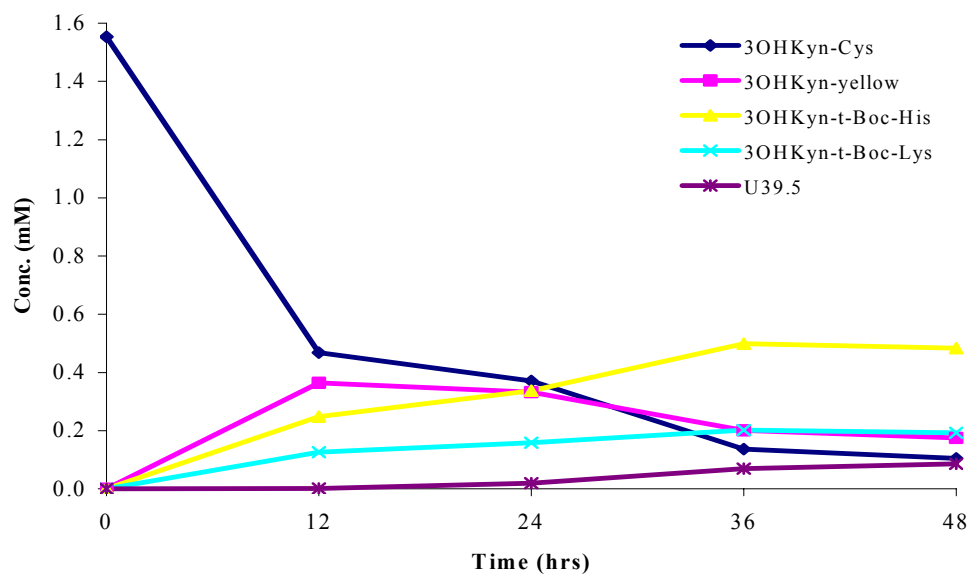


**Figure 2.19** The rate of loss of 3OHKyn-Cys in relation to the rate of formation of 3OHKyn-yellow, 3OHKyn-*t*-Boc-His, 3OHKyn-*t*-Boc-Lys and unknown compound eluting at 39.5 min (U39.5) on the HPLC chromatogram (Figure 2.18).

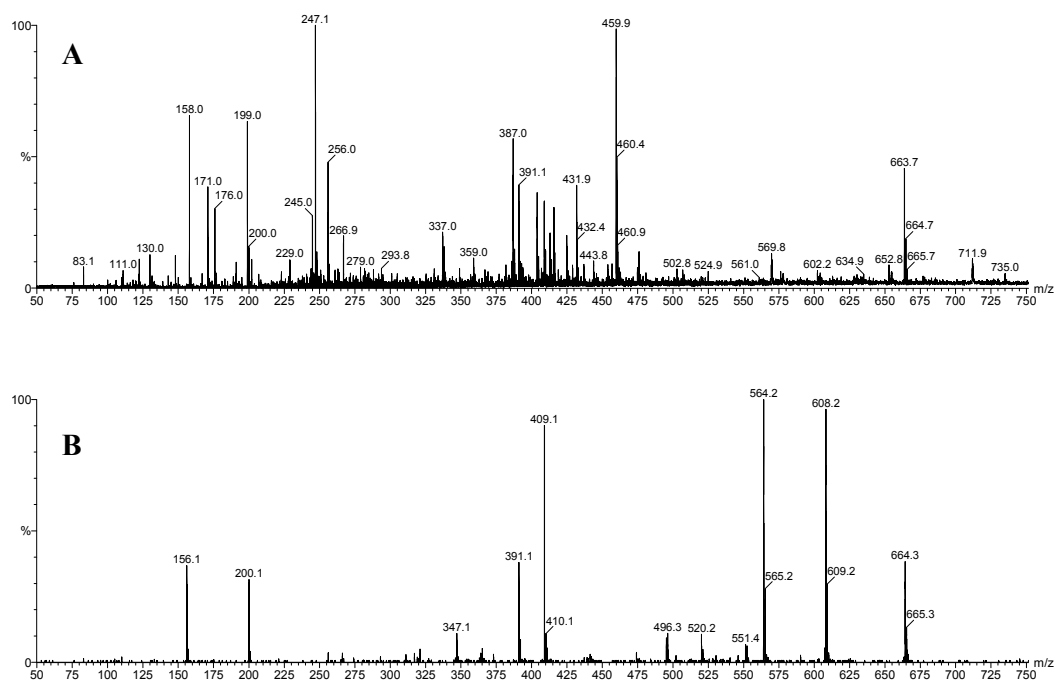


**Figure 2.20** Mass spectra of U39.5. *A*, ESI mass spectrum; *B*, MS/MS spectrum of  $m/z$  664 ion.



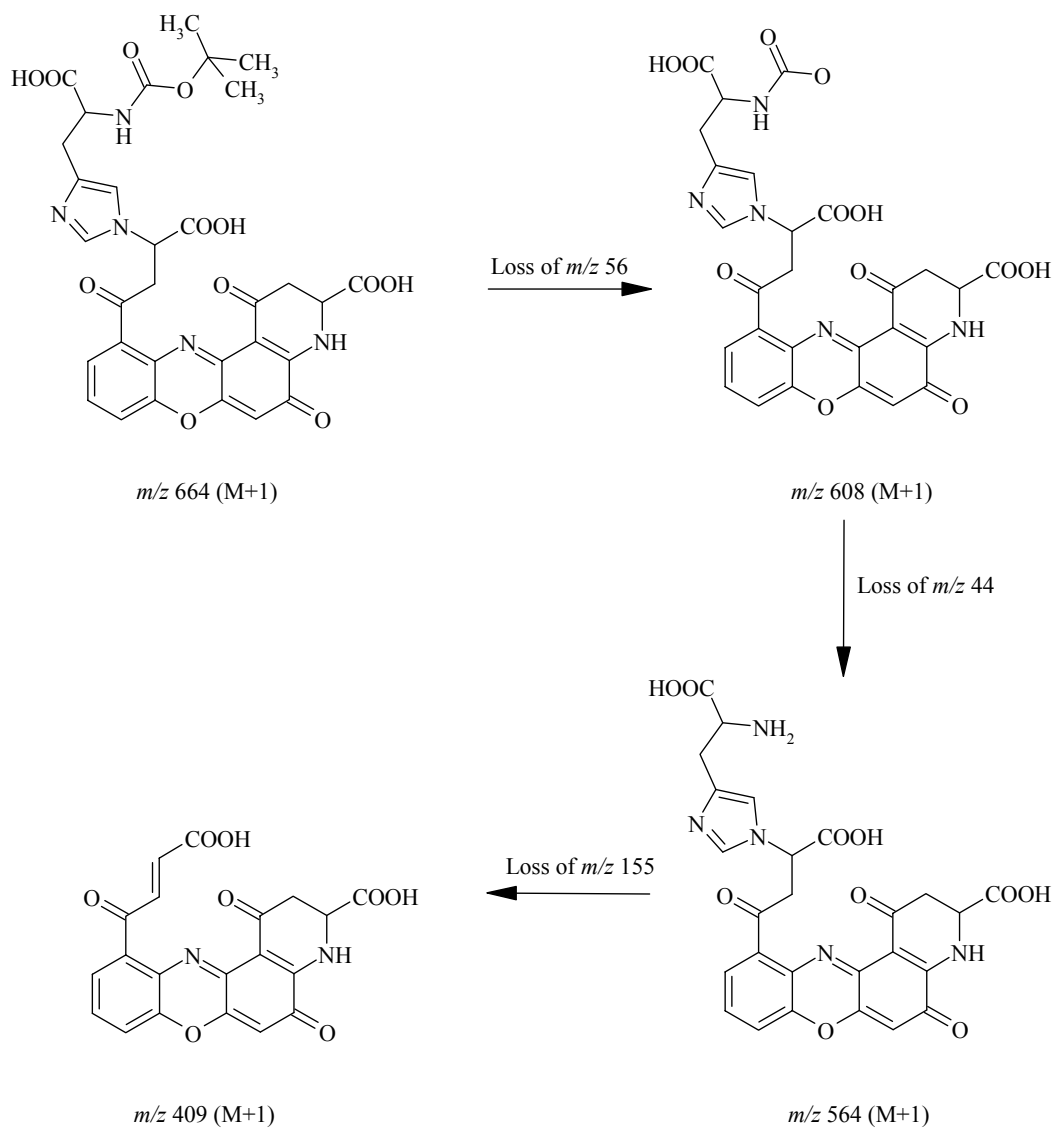


**Figure 2.21** Proposed structures of molecular ion  $m/z$  664, and fragment ions  $m/z$  608, 564 and 409.

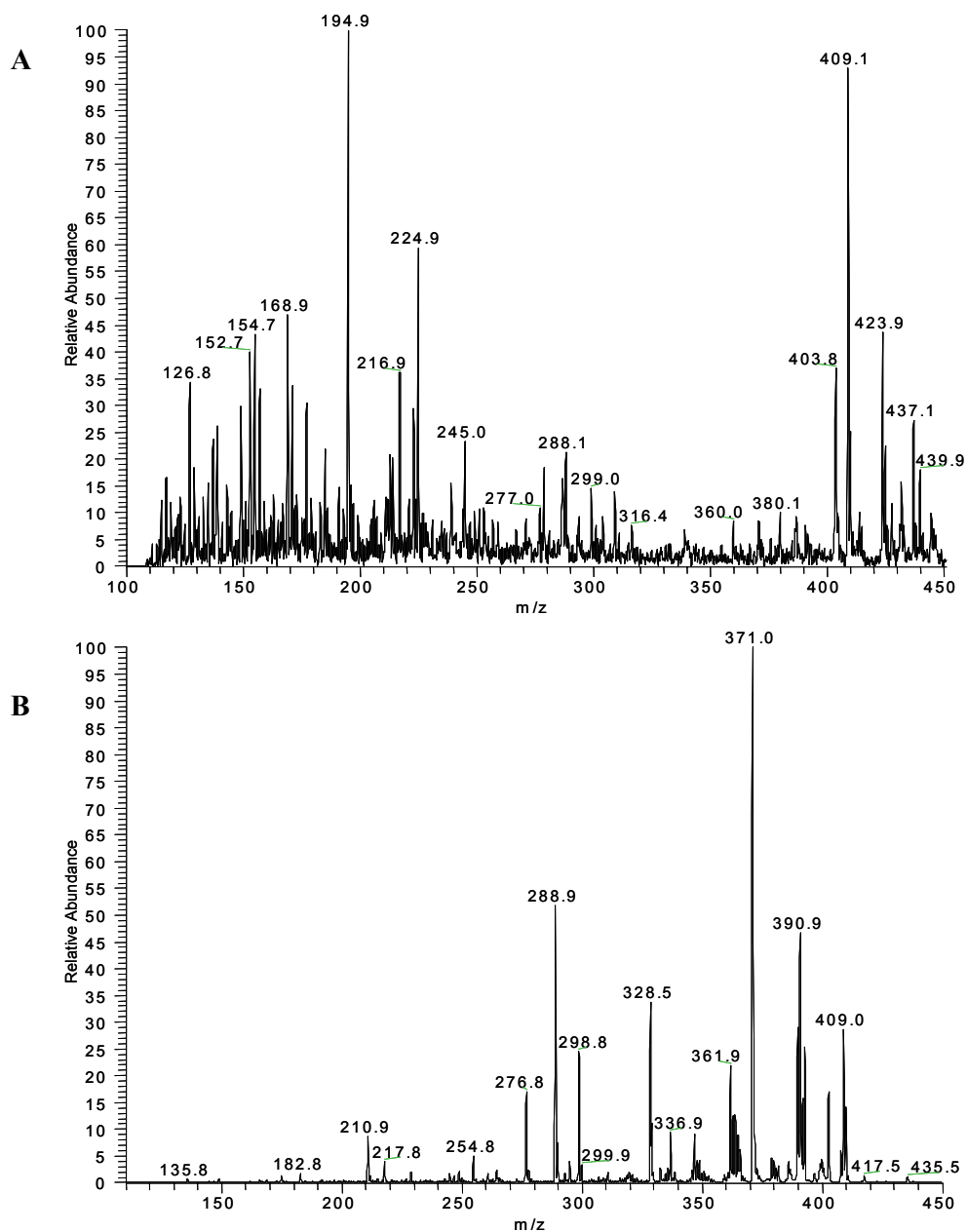


**Figure 2.22** Mass spectra of aliquot from autoxidation of 3OHKyn at pH 7.2. *A*, ESI mass spectrum of aliquot after 3 hours of incubation; *B*, MS/MS spectrum of ion  $m/z$  409.

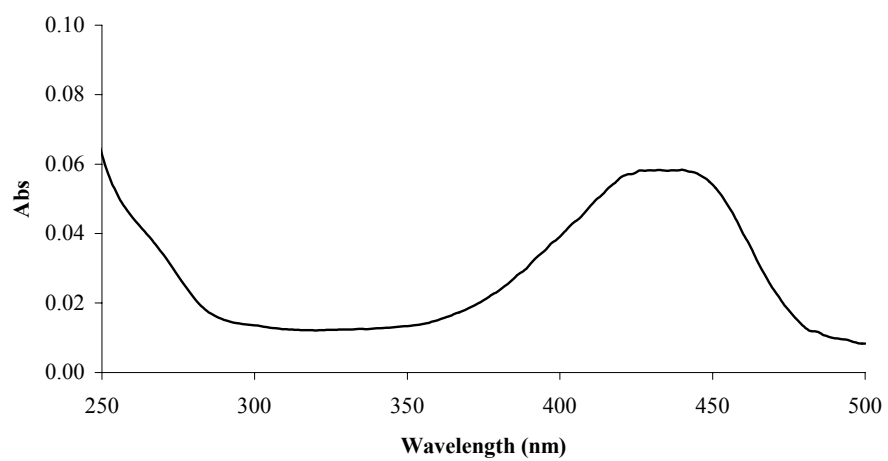


**Figure 2.23** UV-visible spectrum of U39.5.

## 2.4 Discussion

It is known that the human lens UV filter compounds, 3OHKynG and Kyn, attach covalently to lens proteins, particularly after middle age.<sup>101,103</sup> This is, at least in part, responsible for the age-dependent yellowing of the human lens. In the case of Kyn, attachment is via Cys, His and Lys residues.<sup>103,110-112</sup> The covalent attachment of these compounds arises because of the spontaneous deamination of the UV filters at pH 7 (Scheme 2.1).<sup>109</sup> The current study examined 3OHKyn, which is the third kynurenine UV filter compound known to be present in the lens. It deaminates more rapidly than the other two UV filters.<sup>109</sup> Unlike 3OHKynG and Kyn, 3OHKyn is an *o*-aminophenol, and is therefore likely to be much less stable at neutral pH, particularly under oxidative conditions.<sup>181,184</sup> In order to investigate the properties of such compounds, the 3OHKyn amino acid adducts of Cys, His and Lys were synthesised and characterised, by NMR spectroscopy, mass spectrometry, UV-visible and 3-D fluorescence spectroscopy. The stability of each 3OHKyn amino acid adduct at pH 4.0 and 7.2 was also examined. In addition, the stability towards acid hydrolysis was also examined.

The 3OHKyn amino acid adducts were synthesised using the method of Vazquez, *et al.* for Kyn amino acid adducts.<sup>103</sup> The reaction was undertaken at a high pH (*i.e.* pH 9.5) since it increases the rate of deamination of the UV filter amino acid side chain. However, unlike Kyn, 3OHKyn is unstable under basic conditions,<sup>181,184</sup> and therefore, the yields for the reaction were low in comparison. The yields for the 3OHKyn adducts were 17% for 3OHKyn-Cys, 9% for 3OHKyn-*t*-Boc-His, and 11% for the 3OHKyn-*t*-Boc-Lys adduct, compared to 49% for Kyn-Cys, 30% for Kyn-*t*-Boc-His, and 56% for the Kyn-*t*-Boc-Lys.<sup>103</sup> Characterisation of the 3OHKyn amino acid adducts by NMR spectroscopy was difficult since low yields were obtained, and the adducts were rather insoluble. The chemical shifts for the <sup>1</sup>H and <sup>13</sup>C of each 3OHKyn amino acid was similar to the chemical shifts reported for the Kyn amino acid adducts.<sup>103</sup> In addition, the chemical shifts for 3OHKyn-*t*-Boc-Lys were similar to those reported by Staniszewska, *et al.*<sup>193</sup> who have synthesised an antigen using 3OHKyn and *N*- $\alpha$ -acetyl Lys, for immunohistochemical studies. The carbons and hydrogens could all be assigned except for the quarternary carbons, which could not be resolved. The gHMBC

experiments confirmed that in each case, attachment of the amino acid was through C-9 of the UV filter amino acid side chain.

Mass spectrometry was also important for confirming the structure of each 3OHKyn amino acid adduct, and it could be used for later investigations. MS/MS of the molecular ions yielded fragment ions that were comparable to the fragment ions of the Kyn amino acid adducts, since, the difference between them should be 16 Da (the mass of an oxygen atom) higher for 3OHKyn (if the fragments contain the aromatic ring).

MS/MS analysis of all three 3OHKyn amino acid adducts showed that although all three adducts contain the 3OHKyn aromatic moiety, there are only three common fragment ions present in the MS/MS of each adduct. The fragment ion  $m/z$  208, (Figure 2.24) corresponds to 3OHKyn-yellow, an intramolecular cyclisation product of 3OHKyn at neutral pH.<sup>191</sup> In addition, the fragment ions  $m/z$  162 and 110 (Figure 2.24) are also common fragment ions for all three 3OHKyn amino acid adducts. It is unknown why these three fragment ions are the only common ions amongst all three adducts. However, the collision energy used during MS/MS, together with the stability of each adduct may be responsible for this outcome. Other fragment ions that contain the 3OHKyn aromatic moiety, include,  $m/z$  190 and 136, which was observed for 3OHKyn-Cys and 3OHKyn-*t*-Boc-His adducts, and  $m/z$  152, which was observed for the 3OHKyn-Cys and 3OHKyn-*t*-Boc-Lys adducts (Tables 2.1, 2.2 and 2.3).

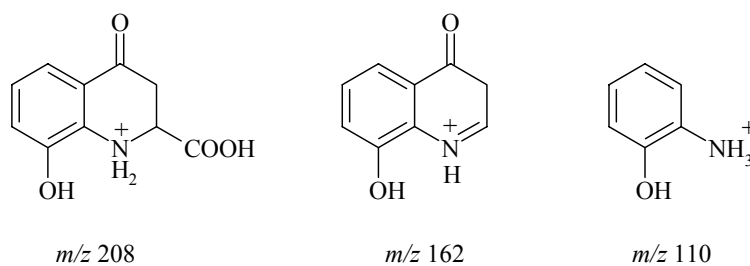


**Figure 2.24** Structures of the common fragment ions for all three 3OHKyn amino acid adducts.

In the MS/MS spectra of 3OHKyn-*t*-Boc-Lys and 3OHKyn-Cys there were two abundant fragment ions at  $m/z$  203 and 202 respectively, which further confirm the proposed structures of the 3OHKyn amino acid adducts. These ions are a portion of the amino acid covalently attached to a portion of 3OHKyn at C-9 (Table 2.1 and 2.3). These ions are also characteristic for Kyn-Lys and Kyn-Cys.<sup>103</sup> Therefore, these two ions may be used as markers for detecting UV filter attachment in protein digests.

Since 3OHKynG and Kyn covalently attach to human lens protein after middle age,<sup>101,103</sup> it was assumed that 3OHKyn should also attach. However, the level of free 3OHKyn in the lens is considerably less than 3OHKynG and Kyn.<sup>19</sup> The average amount of 3OHKynG in 20 year old human lenses is approximately 400 nmol/gram of protein, compared to 15 nmol of 3OHKyn per gram of protein, and these concentrations decrease at a rate of ~12% per decade.<sup>19</sup> Characterising the fragment ions of the 3OHKyn adducts (Table 2.1, 2.2 and 2.3) is important, since these will act as ‘markers’ for identifying these adducts in lens proteins, where it is expected that these levels will be very low.

The UV-visible spectra for each adduct was essentially identical at pH 2.1, 5.5 and 7.2. 3OHKyn-Cys, 3OHKyn-*t*-Boc-His and 3OHKyn-*t*-Boc-Lys all exhibited broad peaks centred at 374, 375 and 367 nm respectively, on the UV-visible spectra. These absorbances are comparable to the UV-visible absorbance of lens UV filters, which are centred at 365 nm.<sup>73</sup> Each of the 3OHKyn amino acid adducts was yellow and therefore they may contribute to age-related lens colouration.<sup>93</sup> The 3OHKyn adducts did not exhibit a broad peak at any wavelength between 250 and 450 nm, at pH 9.5. Once each adduct was added to the sodium carbonate/bicarbonate buffer, pH 9.5, the solution rapidly turned a dark yellow/orange colour. The colour of the solutions when the 3OHKyn adducts were added to TFA, guanidine HCl and phosphate buffer, were all a pale yellow colour by comparison. The darker coloured solution that resulted at pH 9.5, indicates that the 3OHKyn amino acid adducts had begun to oxidise possibly to phenoxazones, but the spectra did not contain the typical broad peak centred at 440 nm, typical for phenoxazones.<sup>184</sup>

The 3-D fluorescence data for each 3OHKyn amino acid adduct has been summarised in Table 2.6. Two fluorophores with Ex 440 nm/Em 520 nm and Ex 340 nm/Em 400 nm increase in intensity with aging of the lens.<sup>97,98</sup> All of the 3OHKyn amino acid adducts fluoresced, and the observed fluorescence excitation/emission wavelengths are similar to those in human lenses.

**Table 2.6** Summary of the 3-D fluorescence intensities for each 3OHKyn amino acid adduct.

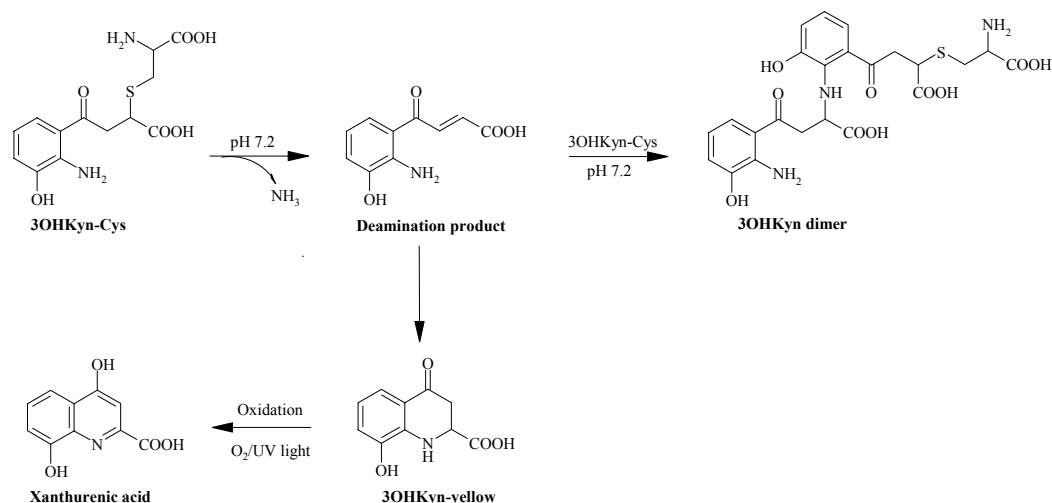
| 3OHKyn Adduct             | Ex (nm)/Em (nm)    |                    |                    |         |
|---------------------------|--------------------|--------------------|--------------------|---------|
|                           | pH 2.1             | pH 5.5             | pH 7.2             | pH 9.5  |
| 3OHKyn-Cys                | 350/520<br>420/520 | 340/510<br>430/510 | 330/510<br>400/520 | 360/520 |
| 3OHKyn- <i>t</i> -Boc-His | 370/520            | 350/520            | 430/530            | 340/510 |
| 3OHKyn- <i>t</i> -Boc-Lys | 420/520            | 350/520<br>410/520 | 360/520            | 330/510 |

Stability studies were performed at pH 7.2 and 4.0 under non-oxidative conditions to determine the properties of each 3OHKyn amino acid adduct. At pH 7.2, 3OHKyn-*t*-Boc-His was the most stable adduct. Decomposition of all adducts was accelerated in the presence of oxygen. 3OHKyn-*t*-Boc-Lys and 3OHKyn-Cys were both unstable at pH 7.2. Under oxidative conditions, the Lys and Cys adducts could not be recovered after 48 and 24 hours of incubation respectively. Under non-oxidative conditions, minimum amounts of 3OHKyn-Cys and 3OHKyn-*t*-Boc-Lys could be recovered after 5 days of incubation (Figure 2.15).

At pH 4.0, the stability of each adduct improved. Under non-oxidative conditions, the Cys and Lys adducts were recovered in ~70% yield and His adduct recovered in ~50% yield, after 48 hours (Figure 2.16). Therefore, acidic conditions can be used, for example, for protease digestion of 3OHKyn-modified proteins, in order to isolate modified peptides that can be characterised by MS/MS. EDTA was not added to any of

the reaction mixtures and metals such as  $\text{Cu}^{2+}$  and  $\text{Fe}^{2+}$  may play a role in the autoxidation of the adducts. This was not investigated.

A number of additional peaks were identified in the HPLC chromatograms (chromatograms not shown) of each adduct following incubation at pH 7.2 (stability studies). The isolated peaks were examined by mass spectrometry, but only one compound could be identified. Xanthurenic acid was the only compound identified as a breakdown product of all three adducts at pH 7.2. Xanthurenic acid forms from oxidation of 3OHKyn-yellow<sup>86,109,191</sup> (Scheme 2.2). Other breakdown products expected from the autoxidation of 3OHKyn amino acid adducts at pH 7.2 include, deaminated 3OHKyn and 3OHKyn-yellow. For example, 3OHKyn cleaves from the 3OHKyn-Cys adduct and results in the deaminated compound. 3OHKyn-yellow forms from cyclisation of the deaminated compound (Scheme 2.2). Since the ions for deaminated 3OHKyn and 3OHKyn-yellow could not be detected in the mass spectra of any of the isolated peaks from the HPLC chromatogram, this indicates that these two compounds are both unstable. Another compound, which has been identified in Kyn stability studies, is Kyn dimer.<sup>194</sup> At neutral pH, Kyn deaminates and is susceptible to nucleophilic attack by the *ortho* amino group of unreacted Kyn, producing Kyn dimer. Analysis of all the peaks from each 3OHKyn stability study failed to show the presence of a 3OHKyn dimer. An example of a 3OHKyn dimer is shown in Scheme 2.2.



**Scheme 2.2** Mechanism for the formation of breakdown products of 3OHKyn-Cys at pH 7.2.



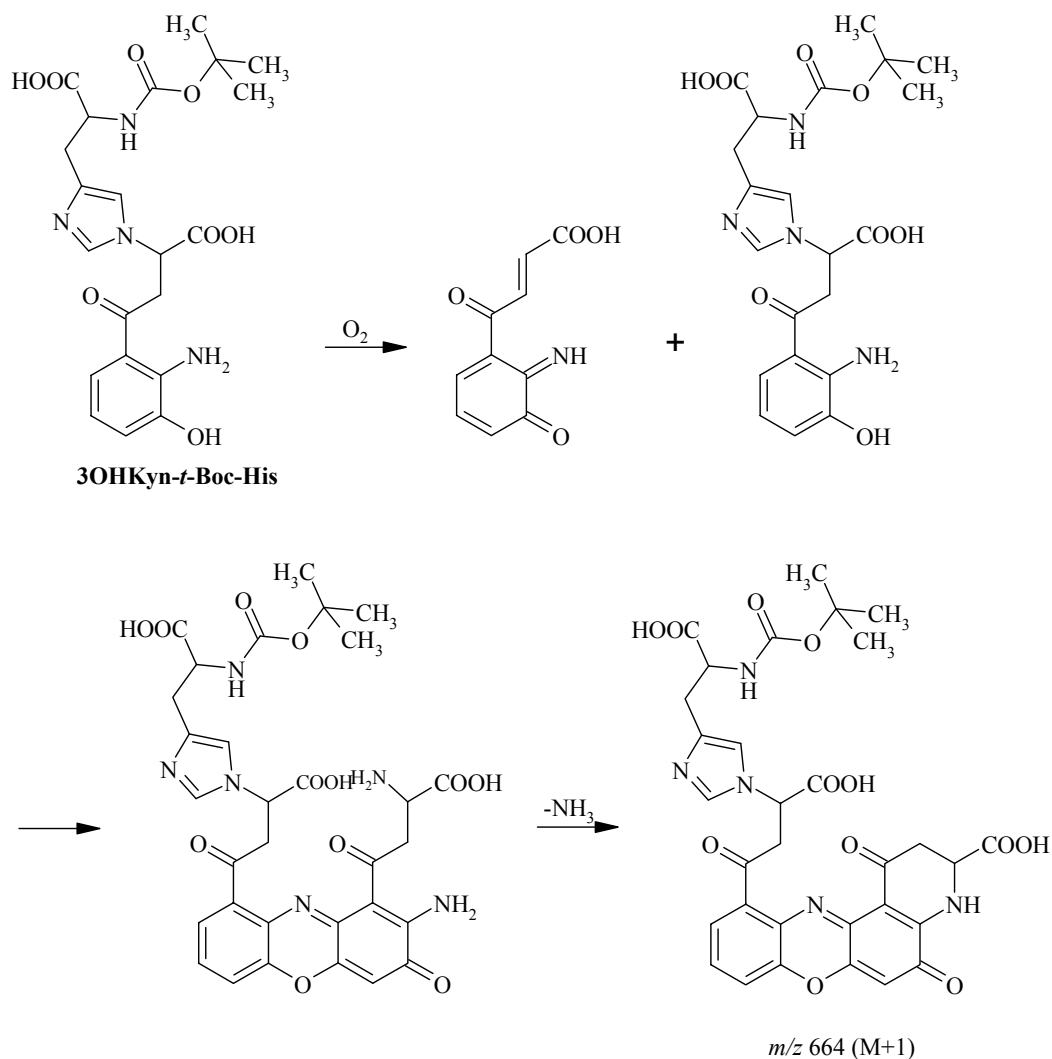
The stability of the 3OHKyn adducts was also determined under conditions used for acid hydrolysis of proteins. Acid hydrolysis was the technique used to identify Kyn adducts in lens proteins.<sup>103</sup> The addition of antioxidants in this procedure increased the recovery of each of the adducts. The protocol (thioglycolic acid 5% (v/v) and phenol 1% (w/v)) was adopted from a paper by Fu, *et al.* where these compounds were used as a reductant and antioxidant respectively to optimise the recovery of DOPA from lens samples.<sup>165</sup> The recovery of the 3OHKyn amino acid adducts from acid hydrolysis with antioxidants was approximately 4-fold higher than without thioglycolic acid and phenol. Although the 3OHKyn adducts are recoverable from acid hydrolysis, these compounds are unstable in comparison to the Kyn adducts. The recovery of Kyn adducts from acid hydrolysis without antioxidants is 96% for Kyn-Cys and Kyn-Lys and 99% for Kyn-His.<sup>103</sup>

Incubation of 3OHKyn-Cys, together with excess N- $\alpha$ -*t*-Boc-His and N- $\alpha$ -*t*-Boc-Lys, at pH 7.2, showed that deaminated 3OHKyn formed from 3OHKyn-Cys, and readily transferred to either N- $\alpha$ -*t*-Boc-His or N- $\alpha$ -*t*-Boc-Lys, forming 3OHKyn-*t*-Boc-His and 3OHKyn-*t*-Boc-Lys. This experiment further demonstrated the intrinsic instability of the 3OHKyn amino acid adducts, and it also suggests how 3OHKyn may react *in vivo*.

The HPLC chromatogram (Figure 2.18) showed that a new product had also formed with a molecular ion at  $m/z$  664. This ion was also observed as a breakdown product of 3OHKyn-*t*-Boc-His at pH 7.2. Since this ion was observed reproducibly, it was of interest to try to characterise this compound. A proposed structure of this compound is shown in Figure 2.21. Oxidation of 3OHKyn yields a phenoxazone.<sup>184</sup> The MS/MS spectrum of this unknown compound, which was originally referred to as U39.5, showed a prominent loss of 100 Da, indicative of the loss of a *t*-Boc group. A further loss of 155 Da was indicative of a loss of a His. The proposed structure of the resulting fragment ion,  $m/z$  409, consisted of a phenoxazone moiety with a deaminated 3OHKyn amino acid side chain. To confirm that the ion  $m/z$  409 was derived from autoxidation of 3OHKyn, 3OHKyn was incubated at pH 7.2, and this ion was present in the reaction mixture. Finally, the UV-visible spectrum of U39.5 exhibited a broad peak with a maximum absorbance centred at 437 nm. An absorbance centred at 440 nm on the UV-

visible spectrum is characteristic of phenoxazones.<sup>184</sup> The data supports the proposed structure of U39.5.

The chemical name of U39.5 is 1,3,4,5-tetrahydro-11-(2-(*N*- $\alpha$ -*tert*-butyloxycarbonyl-histidyl)-(4-hydroxy-1,4-dioxo-butanyl)-1,5-dioxo-2H-pyrido(3,2-*a*)phenoxazine-3-carboxylic acid, and the mechanism of formation of this compound (Scheme 2.3) is similar to the formation of xanthommatin.<sup>184</sup>



**Scheme 2.3** Mechanism of formation of U39.5,  $m/z$  664.

In conclusion, three 3OHKyn amino acid adducts were synthesised and characterised. The characterisation of the fragment ions is important in future work, where these ions could be used as markers in protein digests. Additionally, a new oxidation product of 3OHKyn-*t*-Boc-His has been identified.

## Chapter 3

### Lens Proteins Modified with 3OHKyn

#### 3.1 Introduction

The function of the lens is to transmit, filter and focus light upon the retina.<sup>9</sup> The high refractive index of the lens is due to the high concentration of structural proteins:  $\alpha$ ,  $\beta$  and  $\gamma$  crystallins.<sup>9</sup> In addition to transmitting most visible wavelengths, the human lens absorbs UV light in the 300-400 nm region due at least in part to the presence of several tryptophan-derived UV filter compounds.<sup>73,75</sup> These compounds prevent UV-induced photodamage to the retina.<sup>74</sup>

In Chapter 2, the 3OHKyn amino acid adducts were synthesised and characterised. In this Chapter, the reactivity of 3OHKyn with calf lens protein (CLP) is examined. If 3OHKyn can bind to CLP, then it is expected that 3OHKyn may be bound to proteins from older normal human lenses, and further, that these modified proteins may retain the *o*-aminophenol moieties, in a state that could be oxidised, if conditions in the lens become oxidative, such as, ARN cataract.

Previous model studies have shown that CLP modified by Kyn at pH 7.2, results in modification at Cys residues. Proteins modified by Kyn at higher pH results in modifications at Cys, His and Lys residues.<sup>103</sup> Kyn amino acid adducts have been identified in normal aged lens nuclear proteins, and in human cataract lens proteins. The levels identified in cataract lenses were lower than those in normal lenses.<sup>195</sup>

In previous model studies in which 3OHKyn was incubated with proteins, oxidative conditions were employed to mimic the environment known to occur in the nucleus of the ARN cataract lens.<sup>100,185,186</sup> By contrast, in normal lenses there is little or no evidence of significant protein oxidation.<sup>91</sup>

Using the data obtained from the stability studies of the synthetic 3OHKyn amino acid adducts, a novel assay was developed that allowed quantification of the levels of

3OHKyn, Kyn and 3OHKynG attached to proteins from both normal and cataract lenses.

## 3.2 Materials and Methods

### 3.2.1 Materials

All organic solvents and acids were HPLC grade (Ajax, Auburn, NSW, Australia). Milli-Q<sup>®</sup> water (purified to 18.2 M $\Omega$ /cm<sup>2</sup>) was used in the preparation of all solutions. Formic acid, HCl (6 M, sequencing grade), 3OHKyn, thioglycolic acid, phenol, TFA, ethylenediaminetetraacetic acid (EDTA), phenylmethylsulfonyl fluoride (PMSF), 1,4-dithiothreitol (DTT), sodium azide (NaN<sub>3</sub>), guanidine hydrochloride (guanidine HCl), reduced glutathione (GSH), tris(hydroxymethyl)aminomethanehydrochloride (Tris-HCl), 5,5'-dithio-bis(2-nitrobenzoic acid) (DTNB), horseradish peroxidase (HRP), *o*-phenylenediamine (OPD) and dialysis tubing (MW cut off 20,000) were obtained from Sigma-Aldrich Chemical Co. (St. Louis, MO, U.S.A.). Pre-weighed Trypsin was purchased from Promega. Vivaspin (6 mL) protein concentrators (MW cut off 10,000 Da) were purchased from Vivascience.

### 3.2.2 Preparation of Calf Lens Protein (CLP)<sup>196</sup>

Fresh calf eyes (from animals less than 2 years old) were obtained from Wollondilly Abattoirs Pty Ltd (Picton, Australia). The lenses were removed from each eye, and the capsule was removed from each lens and stored at 4<sup>0</sup>C until used. A 50 mM Tris-HCl buffer pH 7.2 containing 5 mM EDTA, 1 mM PMSF, 1 mM DTT and 0.04% NaN<sub>3</sub> was used for the extraction. Each lens was homogenised with the buffer (2 mL per lens). Soluble protein remaining after centrifugation (15000 g, 5<sup>0</sup>C, 30 min) was dialysed against water and freeze dried.

### 3.2.3 Incubation of CLP with 3OHKyn at pH 7.2 for 48 Hours<sup>103</sup>

CLP (50 mg) and 3OHKyn (10 mg) were added to 0.1 M phosphate buffer, pH 7.2 (10 mL) containing chloroform (10  $\mu$ L). The solution was thoroughly bubbled with argon (5 mins), sealed, wrapped in foil and incubated at 37<sup>0</sup>C for 48 hours. At the end of the incubation, ethanol was added to give a final concentration of 80% (v/v) ethanol, and then centrifuged (8000 g, 10<sup>0</sup>C, 20 min). To ensure the removal of all non-covalently bound material, the insoluble protein was dissolved in 6 M guanidine HCl (10 mL), and dialysed overnight against 0.1 M sodium acetate/acetic acid buffer, pH 4.0, and the protein was freeze dried.

### **3.2.4 Incubation of CLP with 3OHKyn at pH 9.5**

CLP (50 mg) and 3OHKyn (10 mg) were added to 50 mM Na<sub>2</sub>CO<sub>3</sub>/NaHCO<sub>3</sub> buffer, pH 9.5 (10 mL). The solution was bubbled with argon, sealed, wrapped in foil and incubated at 37<sup>0</sup>C for 48 hours. The protein was extracted using the same conditions as at pH 7.2 (Section 3.2.3).

### **3.2.5 Acid Hydrolysis of CLP and CLP Modified with 3OHKyn**

CLP (10 mg), CLP modified with 3OHKyn at pH 7.2 (10 mg) or at pH 9.5 (10 mg) were hydrolysed in an evacuated hydrolysis tube with HCl (1 mL), thioglycolic acid (5% v/v) and phenol (1% w/v) for 24 hours at 110<sup>0</sup>C. The samples were freeze dried and dissolved in 0.1% (v/v) aqueous TFA and purified by HPLC.

### **3.2.6 Preparation of Human Lens Protein**

Human lenses were obtained from The NSW Lions Eye Bank (Sydney, Australia). Nuclei were obtained using a cork borer (5 mm), and the ends were removed (1 mm), remaining nuclei were homogenised in 500 µL of 6 M guanidine HCl, and dialysed overnight against a 0.1 M sodium acetate/acetic acid buffer, pH 4.0. The protein was freeze dried.

### **3.2.7 Acid Hydrolysis of Human Lens Protein**

Human lens protein was hydrolysed with HCl, thioglycolic acid and phenol as in Section 3.2.5. Half of the lens protein was spiked before hydrolysis with 3OHKyn amino acid adducts, and the remaining protein was hydrolysed without spiking. The samples were freeze dried and dissolved in 0.1% (v/v) aqueous TFA and purified by HPLC.

### **3.2.8 HPLC**

See Section 2.2.9 for details.

### 3.2.9 Quantification of Protein-Bound 3OHKyn

3OHKyn was removed from the proteins by incubation at basic pH. The deaminated 3OHKyn that was released was trapped using excess GSH that both added to the conjugated ketone and prevented autoxidation.

(a) Model Studies: Protein modified with 3OHKyn at pH 7.2 (that had previously been dialysed to remove non-covalently bound material) (50 mg) was dissolved in 6 M guanidine HCl (0.6 mL) containing reduced GSH (500 mg) and 2.4 mL of 50 mM  $\text{Na}_2\text{CO}_3/\text{NaHCO}_3$  buffer, pH 9.5 added. The pH was readjusted to 9.5 with 6 M NaOH, and the resulting solution was bubbled with argon, sealed, wrapped in foil and incubated at 37°C for 4 hours. After adjusting the pH to less than 5 with acetic acid the solution was ultra-filtered (6000 g, 4°C, 60 min) in a Vivaspin concentrator (MW cut off 10,000 Da) to separate the non-covalently bound material (filtrate) from the protein. The filtrate was examined by HPLC using the 0.1% (v/v) TFA buffer system.

(b) Human lenses: Human lens nuclei and cortices (22 normal lenses, from The NSW Lions Eye Bank (Sydney, Australia), age range 17 to 83 and 20 cataractous lenses, age range 55 to 101 were obtained from K.T. Sheth Eye Hospital, Rajkot, Gujarat, India) were extracted with 100% (v/v) (300 µL) ethanol and then with 80% (v/v) (300 µL) ethanol and centrifuged (8000 g, 10°C, 20 min). The ethanol supernatants were dried down and resuspended in 0.1% (v/v) TFA and analysed by HPLC for levels of free UV filters. To ensure the removal of all non-covalently bound material, the insoluble protein remaining after ethanol extraction was dissolved in 6 M guanidine HCl (2 mL), and dialysed overnight against 0.1 M sodium acetate/acetic acid buffer, pH 4.0. The protein was then freeze dried. The human lens proteins and reduced GSH (100 mg) were dissolved in 6 M guanidine HCl (0.4 mL) and 50 mM  $\text{Na}_2\text{CO}_3/\text{NaHCO}_3$  buffer, pH 9.5 (1.1 mL) added. The pH was readjusted to 9.5 with 6 M NaOH, and the resulting solution was bubbled with argon, sealed, wrapped in foil and incubated for 4 hours at 37°C. After adjusting the pH to less than 5 with acetic acid the solution was ultra-filtered (6000 g, 4°C, 60 min) in a Vivaspin concentrator (MW cut off 10,000 Da) to separate the non-covalently bound material from the protein. The filtrate was examined for levels of bound UV filters by HPLC using the 0.1% (v/v) TFA buffer system.



### **3.2.10 Incubation of CLP with 3OHKyn at pH 7.2 for 24 Days**

CLP (200 mg) and 3OHKyn (40 mg) were dissolved in 0.1M phosphate buffer, pH 7.2 (40 mL). Chloroform (40  $\mu$ L) was added to inhibit bacterial growth. The solution was bubbled with argon, sealed and wrapped in foil and incubated at 37<sup>0</sup>C for 24 days. Aliquots were taken every 3 days and ultra-filtered through a Vivaspin concentrator (MW cut off 10,000 Da) with Milli Q water (6,000 g, 4<sup>0</sup>C). The protein was freeze dried.

### **3.2.11 Measurement of Protein Sulfhydryl (PSH) Levels in 3OHKyn-Modified Protein**

CLP or CLP modified by 3OHKyn (2 mg) were added 0.2 M ammonium bicarbonate/8 M urea (125  $\mu$ L), 0.5 % (w/v) SDS (1975  $\mu$ L), 0.2 M Tris HCl pH 8.2 (375  $\mu$ L) and read at 412 nm. 0.01 M DTNB (25  $\mu$ L) (made up in methanol) was then added and the solutions were left to stand for 30 min in the dark then read again at 412 nm. A standard curve of L-Cys was used to quantify the amount of PSH in the protein samples.

### **3.2.12 Incubation of $\alpha$ -Crystallin with 3OHKyn at pH 7.2 for 48 Hours**

Bovine  $\alpha$ -crystallin (20 mg) and 3OHKyn (4 mg) were dissolved in 0.1 M phosphate buffer, pH 7.2 (4 mL), and chloroform (20  $\mu$ L) was added to inhibit bacterial growth. The solution was thoroughly bubbled with argon (5 min), sealed, wrapped in foil and incubated at 37<sup>0</sup>C for 48 hours. An aliquot was taken at time zero for mass spectral analysis. The remaining mixture after 48 hours of incubation was dissolved in aqueous 1% (v/v) formic acid, purified by HPLC and the modified protein was freeze dried.

### **3.2.13 HPLC to Purify Modified $\alpha$ -Crystallin**

RP-HPLC was performed on a Shimadzu SCL-10A VP system controller. For analytical scale separations, a Phenomenex column (Jupiter 5u C18 300 Å 250 x 4.60 mm) was used with the following mobile phase conditions: solvent A (aqueous 1% (v/v) formic acid) and solvent B (80% (v/v) ACN/H<sub>2</sub>O, 1% (v/v) formic acid) using a linear gradient for 40 min 0-100% B followed by a re-equilibration in the aqueous phase for 15 min. The flow rate was 1 mL/min. Absorbance was monitored at 280 nm.

### 3.2.14 Trypsin Digestion

Trypsin (20 µg) was added to CLP modified with 3OHKyn for 12 days (1 mg), unmodified αA (1 mg), unmodified αB (1 mg), 3OHKyn-modified αA (1 mg) or 3OHKyn-modified αB-crystallin (0.5 mg) in 50 mM ammonium bicarbonate solution, pH 8.0 (1 mL). The solutions were bubbled with argon sealed, wrapped in foil and incubated at 37°C for 3 hours. The mixtures were then purified by HPLC.

### 3.2.15 HPLC of Trypsin Digests

HPLC was performed on the same system and column as Section 3.2.13. The following mobile phase conditions were used: solvent A (aqueous 0.1% (v/v) TFA) for 5 min followed by a linear gradient of 0-50% solvent B (80% (v/v) ACN/H<sub>2</sub>O, 0.1% (v/v) TFA) over 50 min followed by a linear gradient of 50-100% B over 15 min and re-equilibration in the aqueous phase for 15 min. The flow rate was 0.5 mL/min. Absorbance was monitored at 229 nm

### 3.2.16 Measurement of Oxygen Levels

Oxygen levels were measured using a Strathkelvin (Glasgow, UK) oxygen electrode in a 1 mL cell at 37°C, connected to a Strathkelvin 781 oxygen meter with electrode output coupled to a MacLab (ADI Instruments, Sydney, Australia).

### 3.2.17 Hydrogen Peroxide (H<sub>2</sub>O<sub>2</sub>) Assay

A HRP/OPD assay was used to measure the H<sub>2</sub>O<sub>2</sub> concentration. Reaction mixture (10 µL), Milli-Q H<sub>2</sub>O (10 µL), 0.2 M phosphate buffer, pH 5.8 containing HRP (50 µL), and OPD (5 mg/mL) (100 µL), were added to a micro-titre plate, mixed and allowed to react for 5 min at room temperature, and quenched with 1 M HCl (30 µL). The absorbance was measured at 490 nm and the concentration of H<sub>2</sub>O<sub>2</sub> was calculated by reference to a standard curve.

### 3.2.18 Sodium Dodecyl Sulphate Polyacrylamide Gel Electrophoresis (SDS-PAGE)

An 8% (w/v) polyacrylamide resolving gel and an 8% (w/v) stacking gel were used to separate proteins. Gels were electrophoresed in a Bio-Rad MiniProtean III apparatus with a Bio-Rad 1000/500 power supply. To a 10 µL aliquot of sample (containing 30 µg

of protein), 10  $\mu$ L of 2x sample buffer was added. Sample buffer contained Tris buffer (0.25 M, pH 6.8), glycerol (10% v/v), SDS (10% w/v) and bromophenol blue for colour. An SDS-PAGE running buffer (Tris Base (1.9 g/L), Glycine (9 g/L) SDS (0.6 g/L)) was used to immerse the gels, which were run at 200 V for 1 hour. Gels were then washed with water and stained with SimplyBlue™ SafeStain (Invitrogen) for 1 hour and destained overnight in 20% (w/v) sodium chloride. Gels were imaged using a Canon CanoScan 9950F image scanner.

### **3.2.19 Mass Spectrometry**

See Section 2.2.10 for details.

### **3.2.20 Tandem Mass Spectrometry (MS/MS)**

See Section 2.2.11 for details.

### **3.2.21 Fluorescence and UV-visible Spectroscopy**

See Section 2.2.14 for details.

### **3.2.22 Statistical Analysis**

A one-way ANOVA test was performed using JMP 5.1 software. Comparisons were made between the data points for the normal lenses and the Dark and Light cataract lenses.

### 3.3 Results

#### 3.3.1 CLP Modified with 3OHKyn

The UV filters 3OHKynG and Kyn are known to modify lens proteins at Cys, His and Lys residues.<sup>101,103</sup> Since the corresponding 3OHKyn amino acid adducts had been synthesised and characterised, the aim was to modify CLP with 3OHKyn, and identify the sites of modification on the protein. CLP was modified with 3OHKyn at pH 7.2 and at pH 9.5 (see Figure 3.1 for the colour of the modified protein at each pH). The higher pH promotes deamination of 3OHKyn and increases the reactivity of the nucleophilic side chain, therefore higher yields of adducts are expected under these conditions.<sup>109</sup>



**Figure 3.1** Photograph of the CLP modified with 3OHKyn at pH 7.2 on the left; and CLP modified with 3OHKyn at pH 9.5 on the right. CLP was incubated with 3OHKyn at 37°C for 48 hours. As can be seen the protein modified at pH 7.2 was pink and the protein modified at pH 9.5 was brown.

Each of the modified proteins were run on an SDS gel to further determine their properties. Gels are shown in Figure 3.2. The gel in Figure 3.2A was run under non-reducing conditions, and the gel in Figure 3.2B was run under reducing conditions. CLP was run as a comparison (Figure 3.2A and 3.2B Lane 2). CLP contains  $\alpha$ ,  $\beta$ , and  $\gamma$  crystallins. The CLP exhibited various bands at 20 and 25 KDa on the gels (Figure 3.2A and B Lane 2). Proteins modified by 3OHKyn at pH 7.2 and 9.5 also exhibited the same bands (Lanes 3 and 4 respectively). The modified proteins in Figure 3.2A also exhibited a minor band between markers 37 and 50 KDa. The loading buffer was not a reducing buffer (*i.e.* DTT was not added to reduce disulphide bond linkage). Since CLP also contained a band between markers 37 and 50 kDa, it demonstrates that the disulfide bond linkage is derived from the original CLP. The addition of reducing conditions resulted in disappearance of these bands (Figure 3.2B).

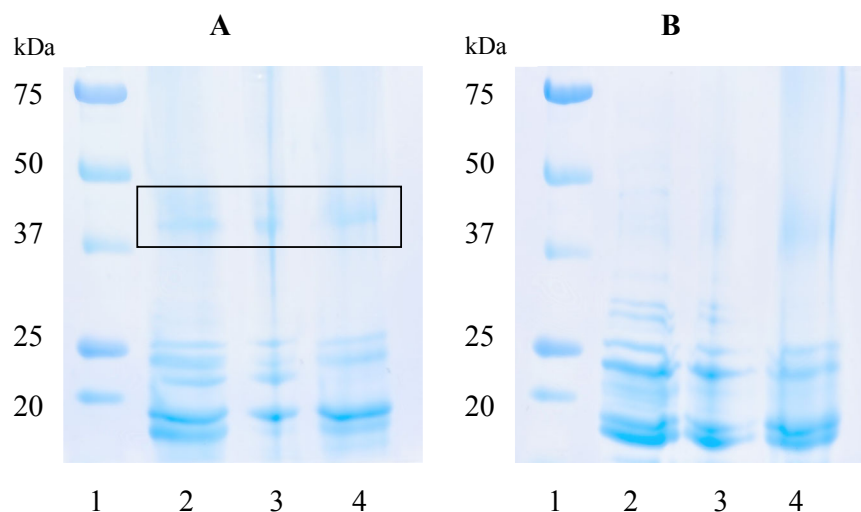


**Figure 3.2** SDS-PAGE of proteins. Lane 1: Marker; Lane 2: CLP; Lane 3: CLP modified with 3OHKyn at pH 7.2; Lane 4: CLP modified with 3OHKyn at pH 9.5. *A*, Non-reducing conditions; *B*, Reducing conditions.

### 3.3.2 Fluorescence and UV-visible Spectroscopy of CLP Modified with 3OHKyn

The CLP modified with 3OHKyn at pH 7.2 and 9.5 was characterised by 3-D fluorescence and UV-visible spectroscopy. The spectra for CLP modified with 3OHKyn at pH 7.2 are shown in Figure 3.3. A broad peak was observed in the UV-visible spectrum with a wavelength maximum centred at 370 nm (Figure 3.3A), and the maximal fluorescence intensity was observed at Ex 370 nm/Em 490 nm.

The spectra for CLP modified with 3OHKyn at pH 9.5 are shown in Figure 3.4. The UV-visible spectrum exhibited a broad peak with a wavelength maximum centred at 369 nm (Figure 3.4A), and maximal fluorescence intensity was observed at Ex 360 nm/Em 485 nm. The protein concentration for the UV-visible spectroscopy was 10 mg/mL in 6 M guanidine HCl for protein modified at pH 7.2, and 1 mg/mL in 6 M guanidine HCl for protein modified at pH 9.5. The protein concentration for the 3-D fluorescence was 2 mg/mL in 6 M guanidine HCl. The pH of 6 M guanidine HCl is ~5.5. The proteins could not be dissolved in 8 M urea, or in phosphate buffer, therefore, UV-visible and 3-D fluorescence data could not be obtained for these modified proteins at any other pH.

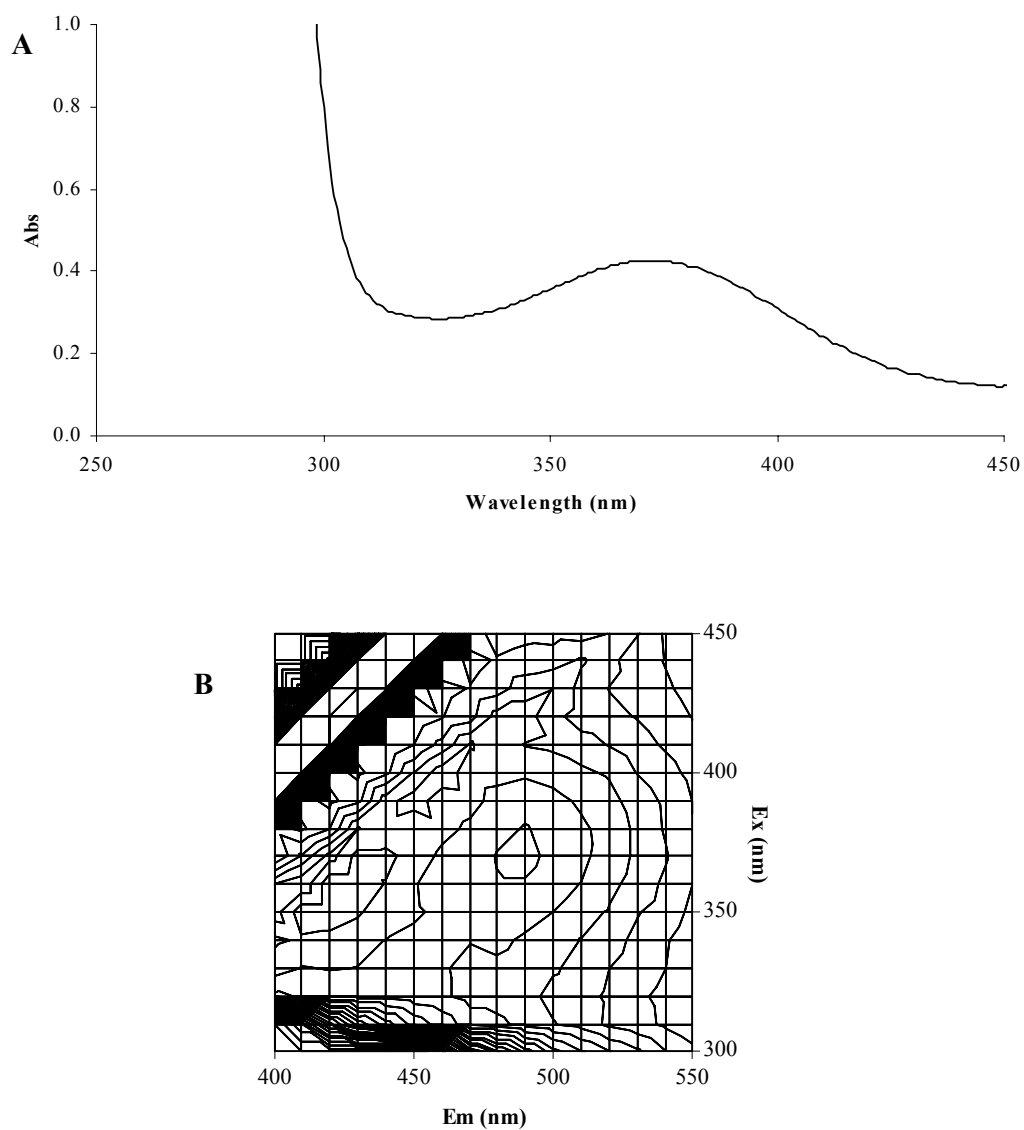


**Figure 3.3** CLP modified with 3OHKyn at pH 7.2 for 48 hours. *A*, UV-visible spectrum, (protein concentration: 10 mg/mL in 6 M guanidine HCl); *B*, 3-D fluorescence spectrum, (protein concentration: 2 mg/mL in 6 M guanidine HCl).

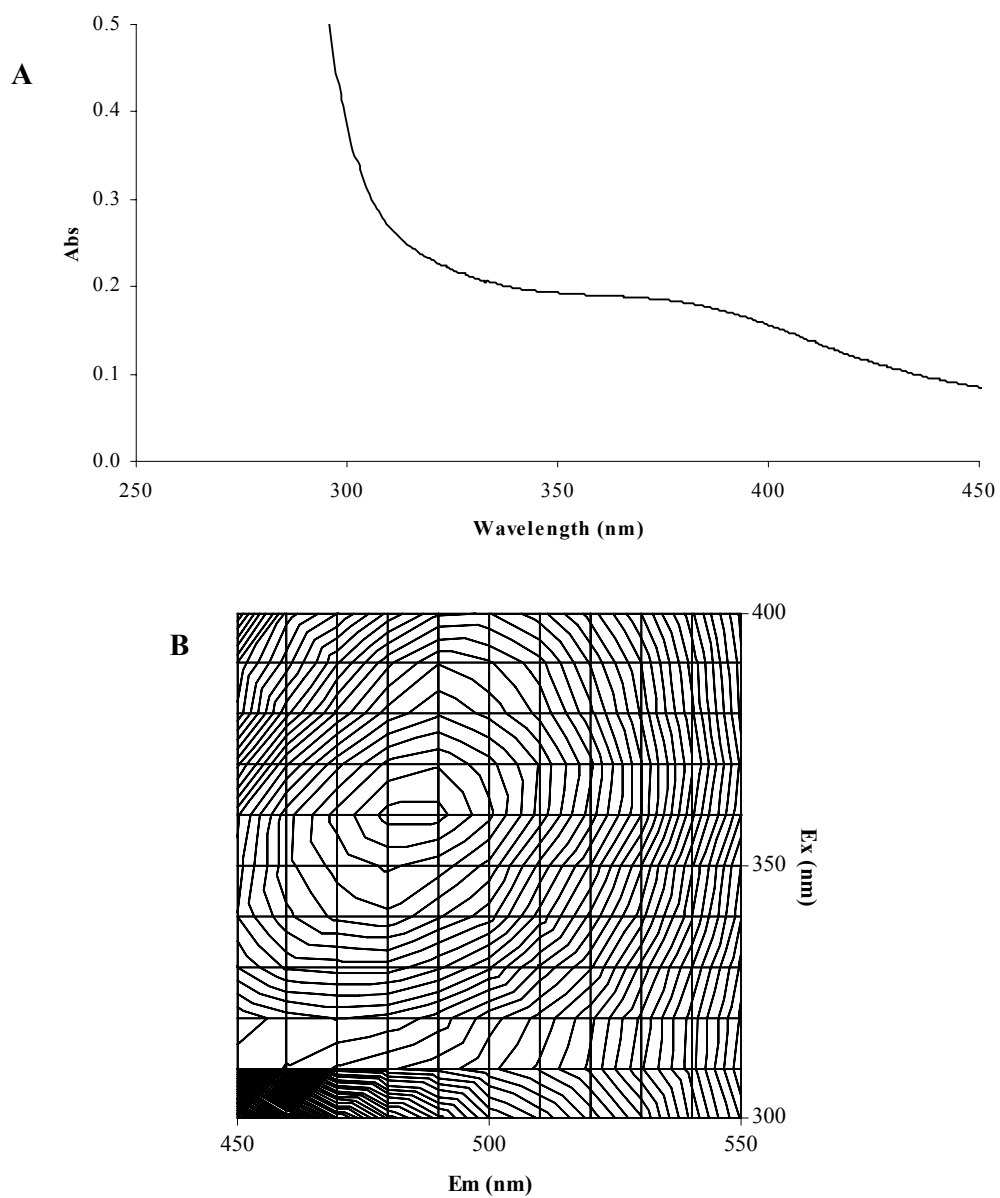


**Figure 3.4** CLP modified with 3OHKyn at pH 9.5 for 48 hours. *A*, UV-visible spectrum, (protein concentration: 1 mg/mL in 6 M guanidine HCl); *B*, 3-D fluorescence spectrum, (protein concentration: 2 mg/mL in 6 M guanidine HCl).



### 3.3.3 Acid Hydrolysis of Lens Protein

Previously acid hydrolysis (without antioxidants) of CLP modified with Kyn has demonstrated Kyn attachment at Cys, His and Lys residues on the protein.<sup>103</sup> As noted previously, the higher pH promotes deamination of 3OHKyn, and reactivity of the nucleophilic side chains so that higher yields of adducts are expected under these conditions. Proteins modified with 3OHKyn were hydrolysed with acid and antioxidants, and hydrolysates separated by RP-HPLC. The chromatograms are shown in Figure 3.5B and 3.5C. Unmodified CLP was hydrolysed for comparison (Figure 3.5A). The HPLC profile of protein modified at pH 7.2 (Figure 3.5B) showed a doublet at 28.7 min when monitored at 360 nm. This pair was at the same retention time as synthetic 3OHKyn-Cys, which also elutes as a doublet peak. MS/MS of the prominent ion  $m/z$  329 which was present in the sample peak corresponding to the mass of 3OHKyn-Cys, fragmented to give  $m/z$  311, 240, 208, 202, 190, 162, 152, 136, 122 and 110 which are all characteristic ions of 3OHKyn-Cys. No characteristic ions of the His and Lys adducts could be found at the retention times of the corresponding standards.

The HPLC chromatogram of the hydrolysate of CLP modified at pH 9.5 (Figure 3.5C), also showed a double peak eluting at 28.7 min. Using the same conditions as described for the pH 7.2 incubation, MS/MS confirmed that this doublet was 3OHKyn-Cys. Peaks that eluted earlier were also collected and analysed by MS/MS. The peak at 26.0 min displayed an ion at  $m/z$  363, which corresponds to the mass of 3OHKyn-His. MS/MS of this molecular ion yielded fragments at  $m/z$  317, 208, 190, 162, 156, 136 and 110 which are characteristic fragments of authentic 3OHKyn-His. The peak at 25.3 min contained as the major component, a compound with a molecular ion of  $m/z$  of 354 corresponding to the mass of 3OHKyn-Lys. MS/MS analysis of  $m/z$  354 resulted in major fragment ions,  $m/z$  247, 208, 203, 162, 152, 147, 128 and 110, all of which are characteristic of 3OHKyn-Lys.

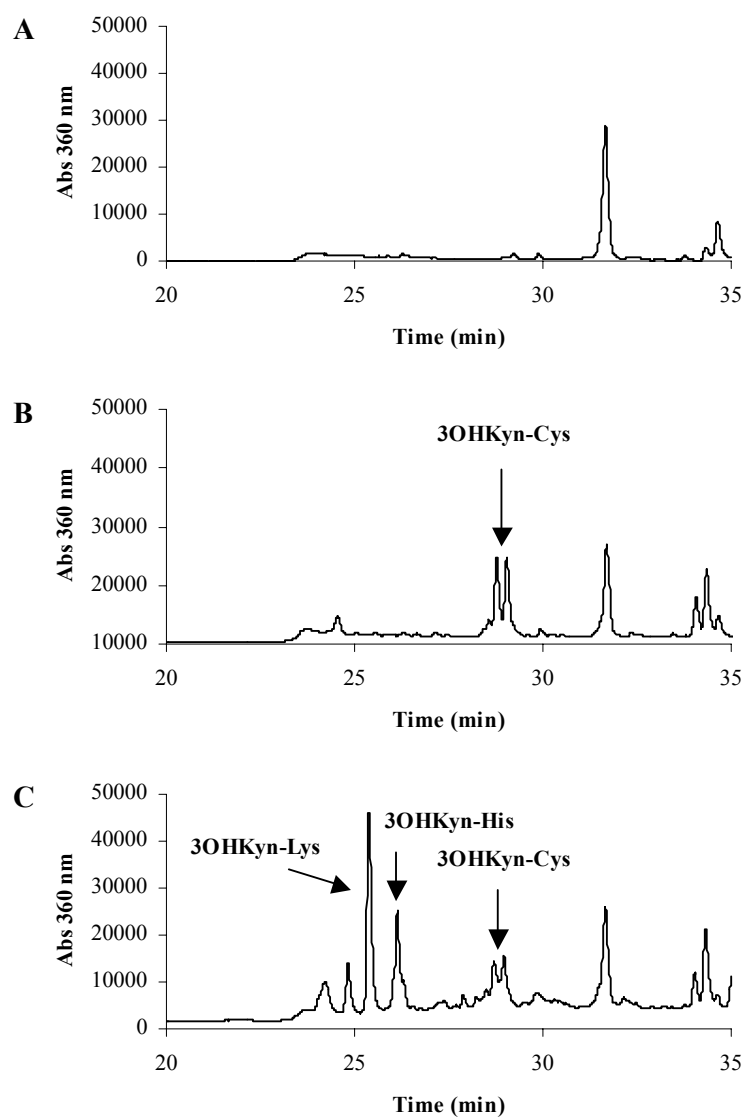


**Figure 3.5** HPLC chromatograms of acid hydrolysed lens protein samples. *A*, CLP; *B*, CLP modified by 3OHKyn at pH 7.2 for 48 hours; *C*, CLP modified by 3OHKyn at pH 9.5 for 48 hours.

### 3.3.4 Acid Hydrolysis of Human Lens Proteins

Since the *in vitro* study confirmed that 3OHKyn can bind to lens proteins under conditions thought to be similar to those present in the normal human lens, and that modified amino acids can be recovered from acid digests of the proteins, we examined proteins isolated from an aged (76 year old male) normal human lens to determine if 3OHKyn amino acid adducts could be detected. Figure 3.6 shows the HPLC chromatograms of the hydrolysed human lens protein. Once the protein from the nucleus was extracted with ethanol and freeze dried, half the protein was spiked with the 3OHKyn amino acid adducts prior to hydrolysis with antioxidants (Figure 3.6A), in order to identify where the 3OHKyn adducts elute in the protein matrix. Standard 3OHKyn-Lys eluted at 23.5 min, 3OHKyn-His eluted at 23.8 min and 3OHKyn-Cys eluted as a doublet at 26.7 min. The remaining half of the protein was hydrolysed as per normal (Figure 3.6B). A small doublet was observed using detection at 360 nm (26.9 min) (Figure 3.6B). MS/MS confirmed that the doublet in the human sample was indeed 3OHKyn-Cys, since fragmentation of the ion at  $m/z$  329 yielded the same product fragment ions as authentic 3OHKyn-Cys (Figure 3.7). Quantitation using the standard curve for 3OHKyn-Cys, showed that this peak corresponded to 2.14 nmole 3OHKyn-Cys/mg protein. 3OHKyn-Cys was also detected in two other human lens digests at similar levels (59 and 68 years old, 2.59 nmole/mg protein and 2.67 nmole/mg protein respectively, spectra not shown). The peaks where 3OHKyn-His and Lys standards eluted were also collected however these adducts could not be detected.

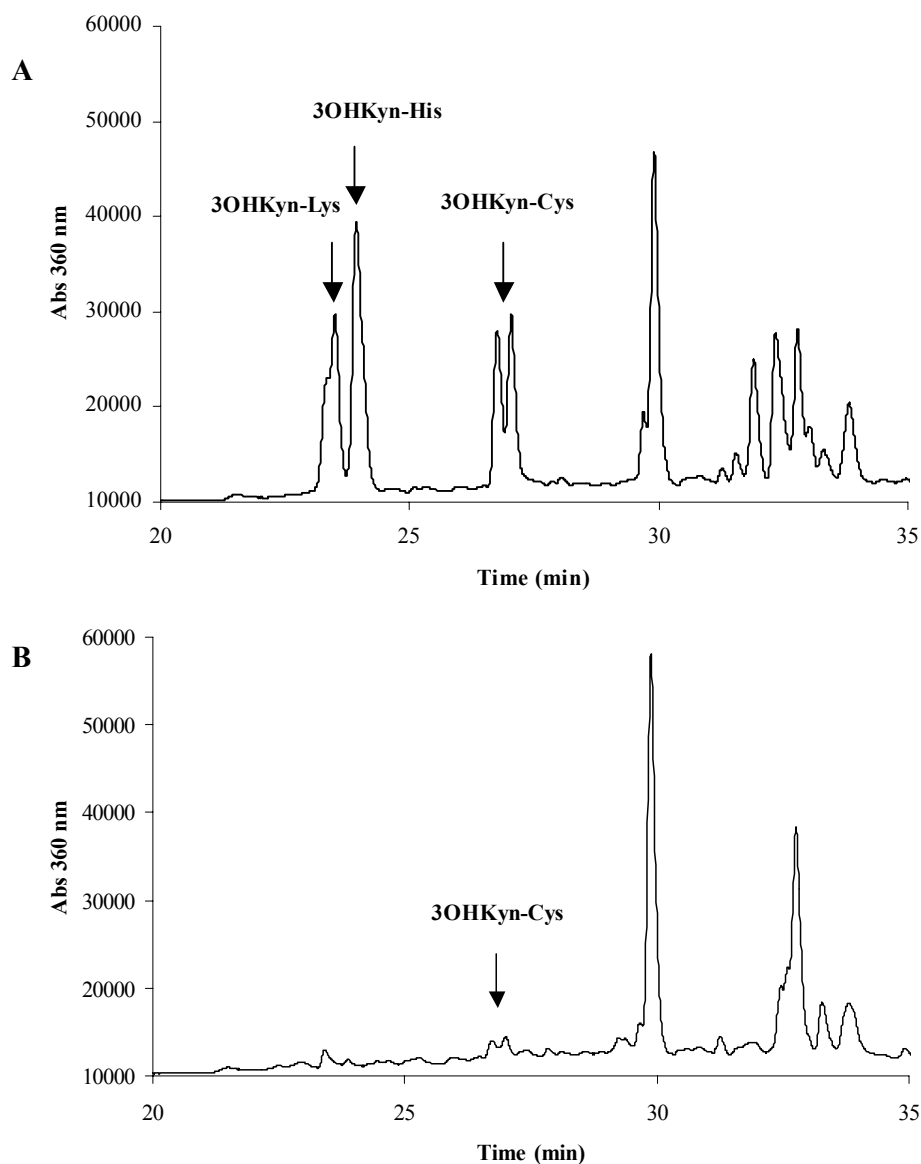


**Figure 3.6** HPLC chromatograms of human lens sample (76 year old male) hydrolysed with HCl and antioxidants. *A*, Lens sample spiked with 3OHKyn amino acid adducts prior to hydrolysis, in order to observe the elution time of the standards; *B*, Hydrolysed human lens sample (unspiked).

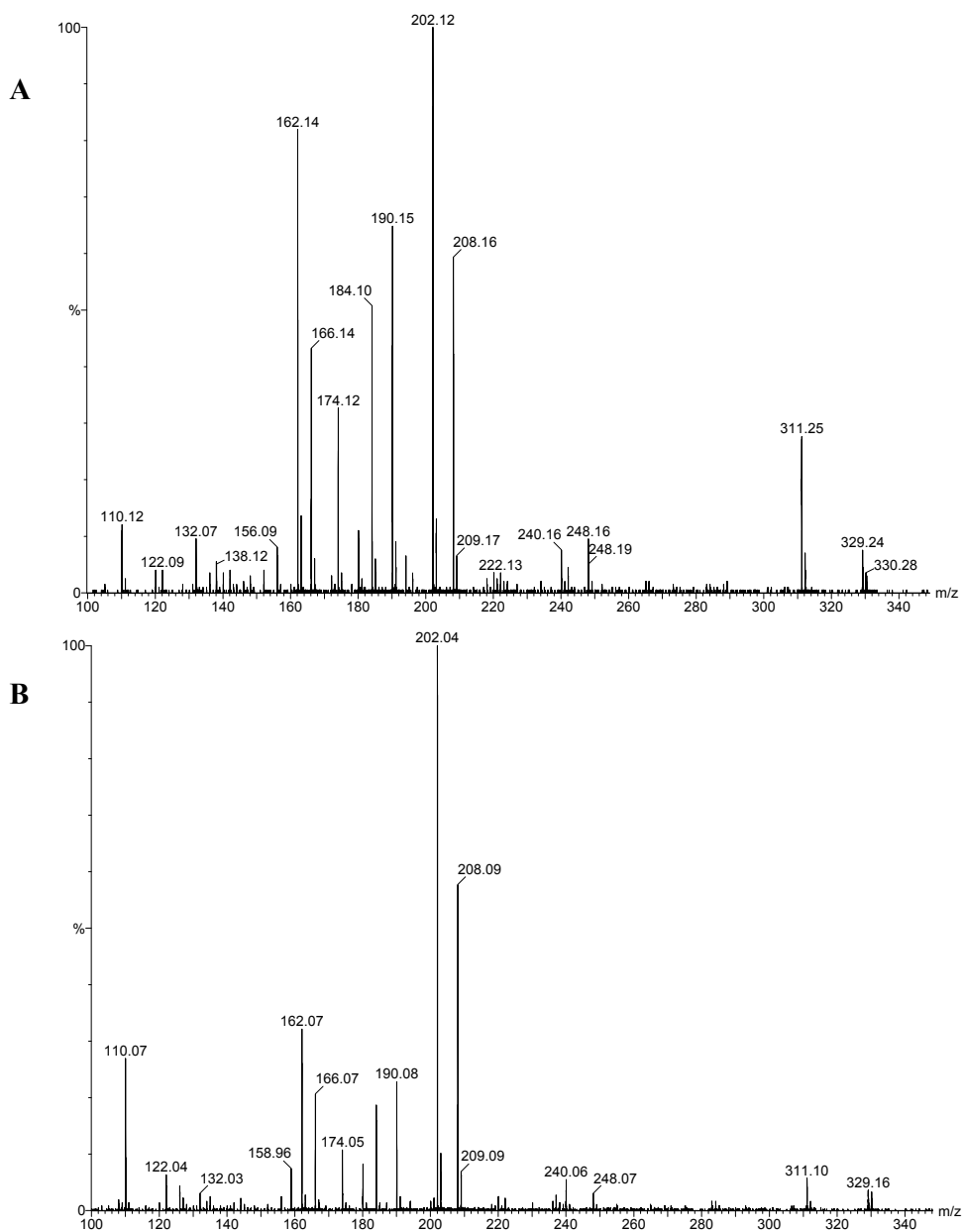


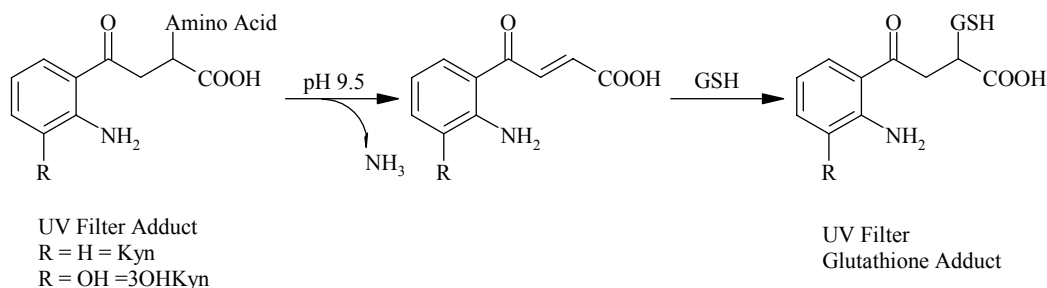
**Figure 3.7** MS/MS spectra of 3OHKyn-Cys. *A*, Authentic 3OHKyn-Cys; *B*, HPLC peak isolated from an aged human lens (76 year old male); *m/z* 329 is the molecular ion.

### 3.3.5 Determination of 3OHKyn Bound to Proteins

Acid hydrolysis is not an appropriate method to determine protein-bound 3OHKyn in lens proteins, since acid hydrolysis of 3OHKynG also yields 3OHKyn. In previous research, it had been shown that GSH binds covalently to the deamination product that results from exposure of 3OHKynG to base. This novel fluorescent diastereoisomeric adduct is found in the human lens.<sup>82</sup>

This study was undertaken to examine whether simple exposure of the Cys, His or Lys adducts of 3OHKyn, or CLP modified by 3OHKyn, to base could lead to the release of the corresponding deamination product (see Scheme 3.1), since it is known that exposure to neutral or basic conditions promotes decomposition of the 3OHKyn amino acid adducts. Basic conditions (pH 9.5) were used to speed the decomposition reaction and under such conditions the released unsaturated ketone is highly susceptible to both oxidation and further reactions. Therefore, GSH was added to prevent oxidation, and to rapidly trap the deamination compound.

Model studies with the UV filter adducts were undertaken. 3OHKyn-Cys, 3OHKyn-*t*-Boc-His, 3OHKyn-*t*-Boc-Lys, Kyn-Cys, Kyn-*t*-Boc-His and Kyn-*t*-Boc-Lys were each incubated with excess GSH at pH 9.5 at 37<sup>0</sup>C, over various incubation times to determine the optimal incubation time for release of deaminated UV filters. At a high pH (*i.e.* 9.5) UV filter adducts are cleaved and it was anticipated that in the presence of a thiol functional group (*i.e.* GSH), the UV filter would form a glutathione adduct (*i.e.* 3OHKyn-GSH or Kyn-GSH) (see Scheme 3.1).



**Scheme 3.1** Decomposition of UV filter amino acid adducts, and formation of UV filter GSH adducts. 3OHKyn or Kyn amino acid adducts together with excess GSH were incubated at pH 9.5 for 4 hours.

To confirm that the 3OHKyn-GSH adduct was indeed formed, a standard of 3OHKyn-GSH was synthesised from 3OHKyn and excess GSH at pH 9.5<sup>197</sup> and purified by HPLC. The HPLC profile is shown in Figure 3.8A. Peaks were collected and identified by mass spectrometry. The peak eluting at 24 min was identified as unreacted 3OHKyn by MS/MS. The doublet peak eluting at 30 min was identified as 3OHKyn-GSH. A doublet peak was expected since GSH is a pure enantiomer with 2 stereogenic carbons, and when GSH covalently binds to 3OHKyn, another stereogenic carbon is created. The molecular ion for 3OHKyn-GSH is  $m/z$  515. This ion was present in the ESI mass spectrum (not shown), and the MS/MS spectrum of this ion is shown in Figure 3.8B. The characteristic fragment ions of 3OHKyn-GSH are  $m/z$  386, corresponding to a loss of glutamate,  $m/z$  368 to a further loss of water, and the ion  $m/z$  308, to the molecular ion of GSH. Ions  $m/z$  208, 190, 162, and 110 are characteristic fragment ions of 3OHKyn.<sup>197</sup>

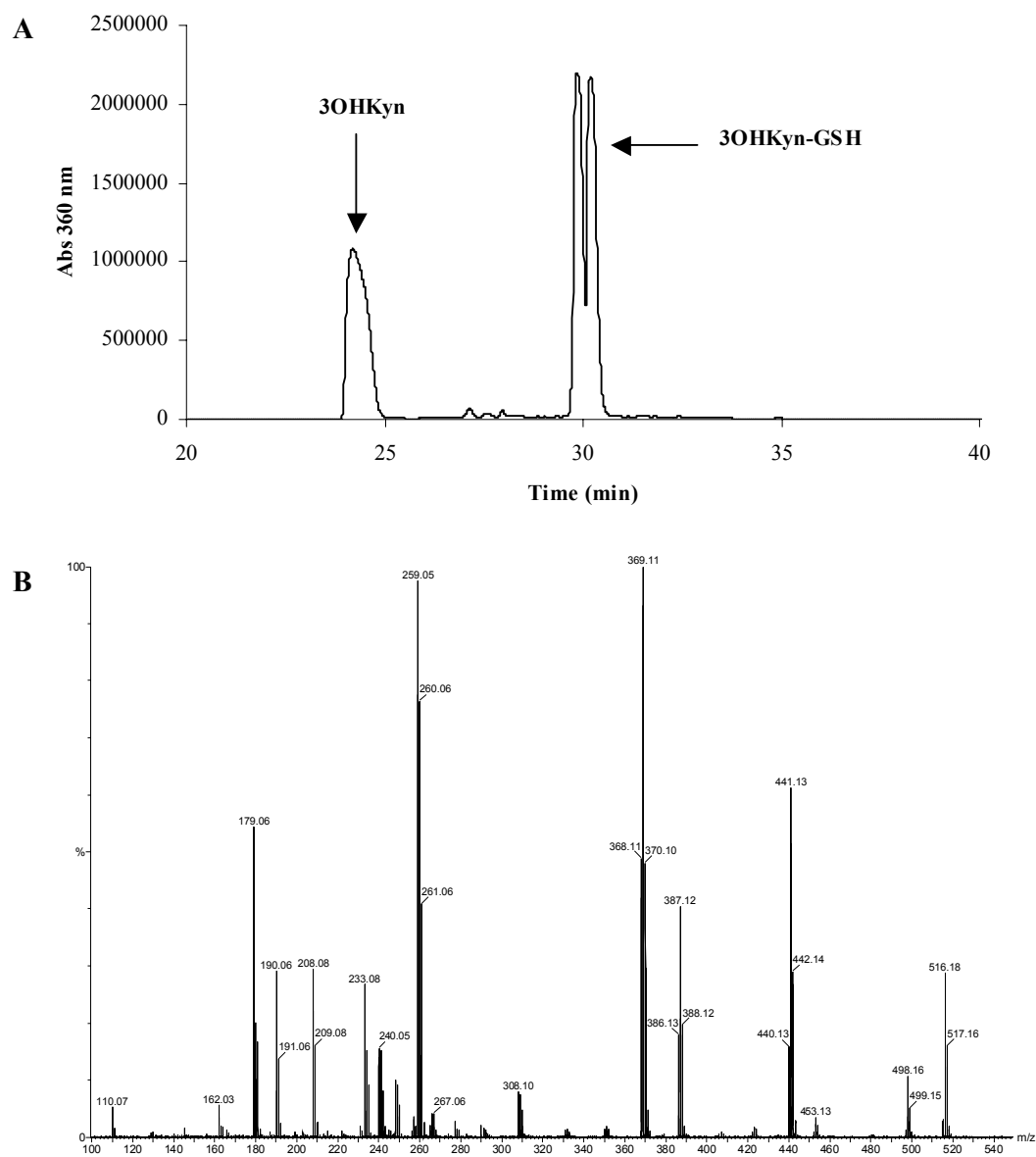


**Figure 3.8** Synthesis of standard 3OHKyn-GSH. *A*, HPLC chromatogram; *B*, MS/MS spectrum of ion  $m/z$  515.



To determine the yield of the GSH UV filter adducts, model studies were undertaken with each of the UV filter adducts, over various incubation times to determine optimal conditions.

Each 3OHKyn amino acid adduct was incubated with excess GSH and the recovery of the starting material, and the yield of newly formed GSH adduct are shown in the following figures. Peaks were collected from the HPLC and examined by mass spectrometry. 3OHKyn-Cys was incubated with excess GSH for 4 hours and aliquots were taken at 2 hour intervals, the yields are shown in Figure 3.9. After 2 hours of incubation, there was 10% recovery of 3OHKyn-Cys and 67% yield of 3OHKyn-GSH. After 4 hours of incubation there was a 7% recovery of 3OHKyn-Cys and 61% yield of 3OHKyn-GSH.

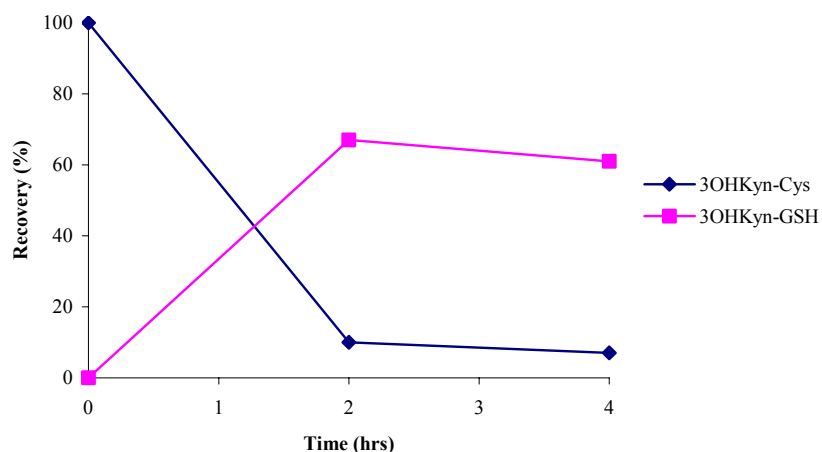


**Figure 3.9** Incubation of 3OHKyn-Cys with excess GSH at pH 9.5. Recovery of 3OHKyn-Cys and the yield of 3OHKyn-GSH.

3OHKyn-*t*-Boc-His was incubated with excess GSH for 48 hours at pH 9.5, and aliquots were taken at 0, 2, 4, 8, 24 and 48 hours. The yields are shown in Figure 3.10. After 2, 4, 8, 24 and 48 hours of incubation, there was 93, 89, 85, 81 and 79% recovery of 3OHKyn-*t*-Boc-His respectively, and the yield of 3OHKyn-GSH at 2, 4, 8, 24 and 48 hours was 0.5, 0.5, 1.6, 5 and 9.4% respectively.

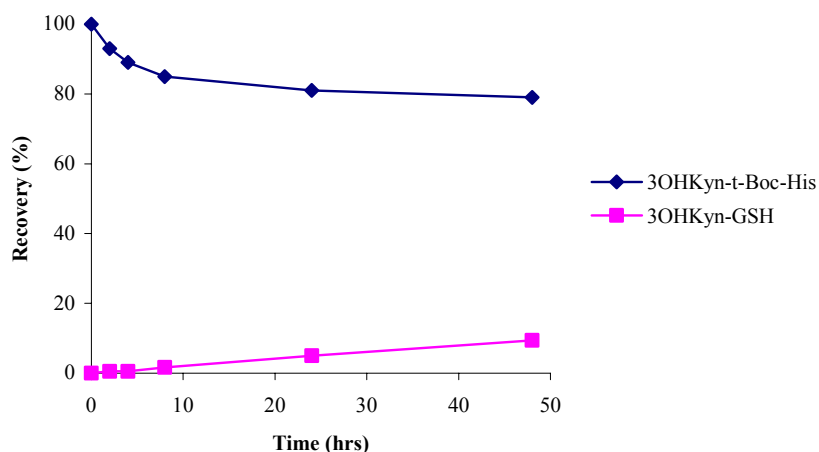


**Figure 3.10** Incubation of 3OHKyn-*t*-Boc-His with excess GSH at pH 9.5. Recovery of 3OHKyn-*t*-Boc-His and the yield of 3OHKyn-GSH.

3OHKyn-*t*-Boc-Lys was incubated with excess GSH for 48 hours and aliquots were taken at 0, 2, 4, 8, 24 and 48 hours. The recoveries are shown in Figure 3.11. After 2, 4, 8, 24 and 48 hours of incubation, there was 46, 22, 11, 0 and 0% recovery of 3OHKyn-*t*-Boc-Lys respectively and the yield of 3OHKyn-GSH at 2, 4, 8, 24 and 48 hours was 48, 73, 78, 75 and 69% respectively.

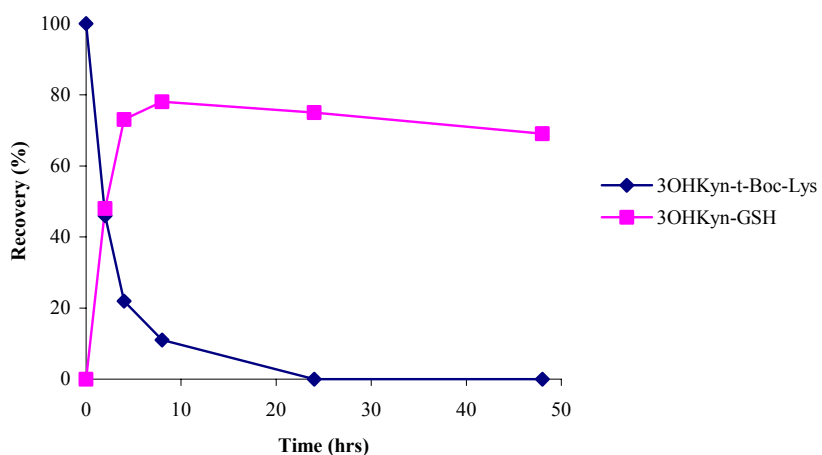


**Figure 3.11** Incubation of 3OHKyn-*t*-Boc-Lys with excess GSH at pH 9.5. Recovery of 3OHKyn-*t*-Boc-Lys and the yield of 3OHKyn-GSH.

The incubations of Kyn amino acid adducts and excess GSH at pH 9.5 were also undertaken for comparison. The molecular ion of Kyn-GSH is  $m/z$  499. The fragment ions include  $m/z$  370, corresponding to a loss of glutamate, the ion at  $m/z$  352 to a further loss of water, and the ion  $m/z$  308 is the molecular ion of GSH. Ions  $m/z$  192, 174 and 146 are characteristic fragment ions of Kyn.<sup>197</sup>

Kyn-Cys and excess GSH were incubated for 4 hours. Results are shown in Figure 3.12. After 2 hours of incubation, there was 25% recovery of Kyn-Cys and 55% yield of Kyn-GSH. After 4 hours of incubation there was a 17% recovery of Kyn-Cys and 59% yield of Kyn-GSH.

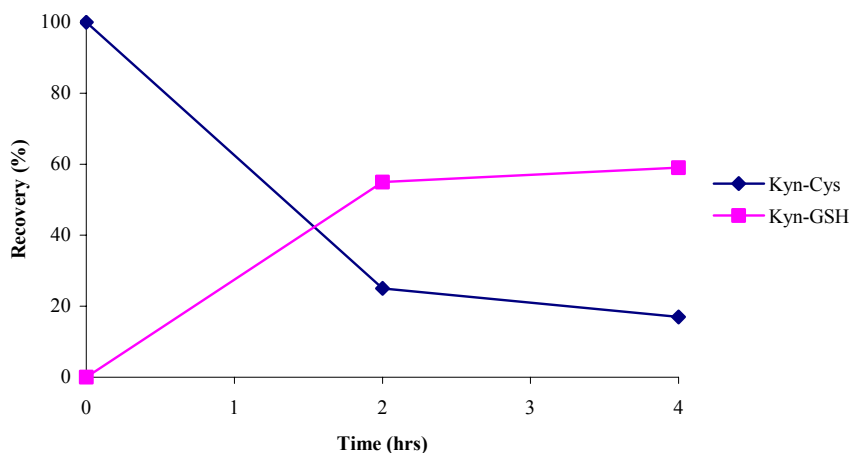


**Figure 3.12** Incubation of Kyn-Cys with excess GSH at pH 9.5. Recovery of Kyn-Cys and the yield of Kyn-GSH.

Kyn-*t*-Boc-His together with excess GSH were incubated for 4 hours and aliquots were taken every 2 hours. The recovery is shown in Figure 3.13. After 2 hours of incubation, there was 88% recovery of Kyn-*t*-Boc-His and 2% yield of Kyn-GSH. After 4 hours of incubation there was an 83% recovery of Kyn-*t*-Boc-His and 3% yield of Kyn-GSH.

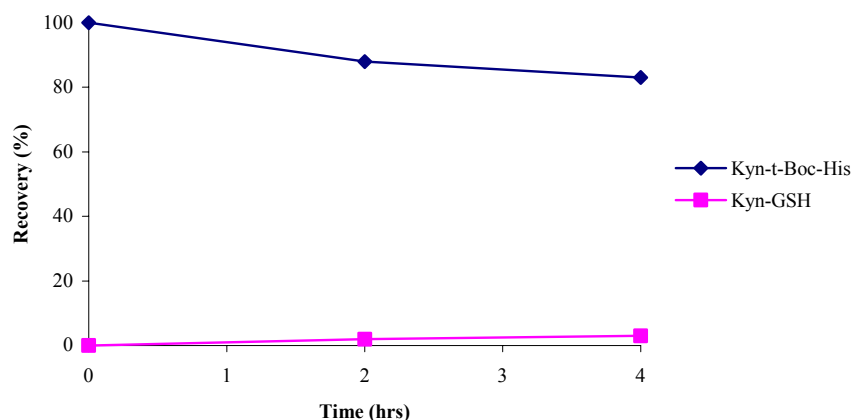


**Figure 3.13** Incubation of Kyn-*t*-Boc-His with excess GSH at pH 9.5. Recovery of Kyn-*t*-Boc-His and yield of Kyn-GSH.

Kyn-*t*-Boc-Lys was incubated with excess GSH for 4 hours and aliquots were taken every 2 hours. The recovery is shown in Figure 3.14. After 2 hours of incubation, there was 7% recovery of Kyn-*t*-Boc-Lys and 76% yield of Kyn-GSH. After 4 hours of incubation there was a 2% recovery of Kyn-*t*-Boc-Lys and 80% yield of Kyn-GSH.

This method of incubating UV filter adducts for 4 hours at a high pH in the presence of GSH would be a useful method for detecting 3OHKyn or Kyn or possibly 3OHKynG bound to Lys and Cys residues on lens protein but not His residues.

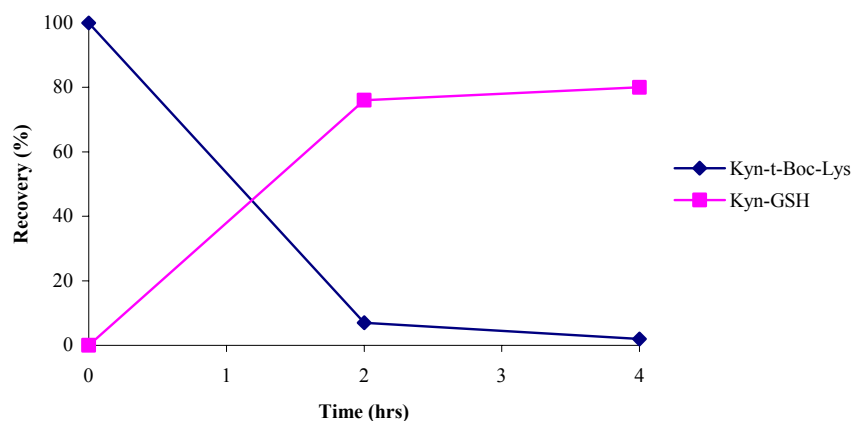


**Figure 3.14** Incubation of Kyn-*t*-Boc-Lys and excess GSH at pH 9.5. Recovery of Kyn-*t*-Boc-Lys and yield of Kyn-GSH.

An experiment to determine the yield recovery of GSH adducts using the same methodology was applied to purified CLP that had been modified with 3OHKyn at pH 7.2 (where Cys is the only modified amino acid on this protein), that did not contain non-covalently bound material. The protein was incubated with excess GSH at pH 9.5 for 4 hours. The solution was ultra-filtered to separate the cleaved compounds from the remaining protein. The HPLC chromatogram of the filtrate (Figure 3.15A) showed a doublet eluting at 30 min. The ESI mass spectrum of this peak (spectrum not shown) showed an abundant ion at  $m/z$  515. MS/MS analysis of this ion (Figure 3.15B) confirmed that it was 3OHKyn-GSH, since the spectrum was identical to that of authentic 3OHKyn-GSH (Figure 3.8B). Quantification of the filtrate showed that there was a 67% yield of 3OHKyn-GSH adduct, since the amount of 3OHKyn-Cys was known from prior acid hydrolysis of the protein.

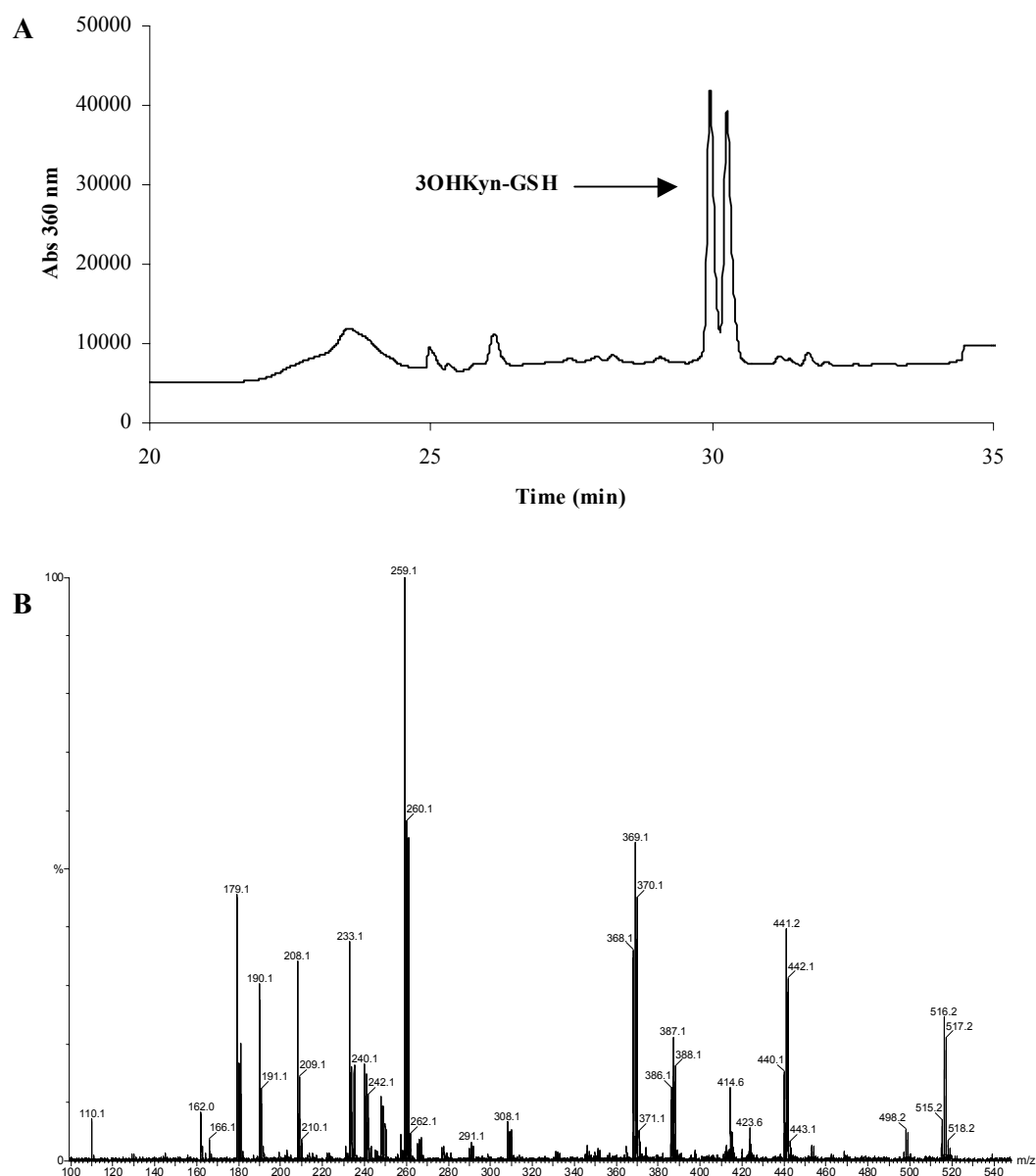


**Figure 3.15** Yield of 3OHKyn-GSH from CLP that had been modified with 3OHKyn. Modified protein was incubated with excess GSH at pH 9.5 for 4 hours. *A*, HPLC chromatogram of filtrate; *B*, MS/MS spectrum of ion  $m/z$  515 in the 30 min peak (Figure 3.15A).

As mentioned previously the primary aim of this study was to determine if 3OHKyn is bound to human lens protein. Twenty-two normal and twenty cataract human lenses were examined. The model studies with the UV filter adducts and the modified protein all showed that incubation of adducts with excess GSH at pH 9.5 results in the release of the UV filter as a UV filter GSH adduct.

The normal human lenses ranged from 17 to 83 years of age, and the human cataract lenses were divided into Dark or Light (Light, Type I/II, and Dark, Type III/IV Pirie classification<sup>161</sup>) coloured nuclei. The ten Dark lenses were 60 to 101 years old and the ten Light cataract lenses ranged in age from 55 to 85. The nuclei and cortices were each examined separately for levels of bound UV filters. Each nucleus and cortex was extracted with ethanol and the extracts from the cataract lenses and the extracts from five normal lenses were analysed for levels of free UV filters. The free UV filters were quantified and a comparison was made with the levels of bound UV filters in the lenses. Following ethanol extraction, the insoluble protein of each nucleus and cortex was dialysed with 6 M guanidine HCl to ensure the removal of any non-covalently bound material. The protein was freeze dried. Excess solid GSH, and a minimum amount of 6 M guanidine HCl, were added to ensure the protein was completely dissolved, the carbonate buffer was then added, the pH adjusted to 9.5, and incubated for 4 hours (see Section 3.2.9 for further details).

#### *Free UV Filters*

The HPLC chromatographic pattern of the ethanol extracts for the normal and cataract lenses were essentially identical. Figure 3.16 is the HPLC chromatogram of an ethanol extract of a human normal cortex age 81 years old. 3OHKyn eluted at 24.3 min, 3OHKynG eluted at 25 min, Kyn eluted at 25.9 min, 3OHKynG-GSH eluted at 28.3 min and AHBG eluted at 30 min. An unknown compound eluted at 28.6 min. The HPLC chromatogram is comparable to the HPLC chromatogram by Bova, *et al.*<sup>19</sup>

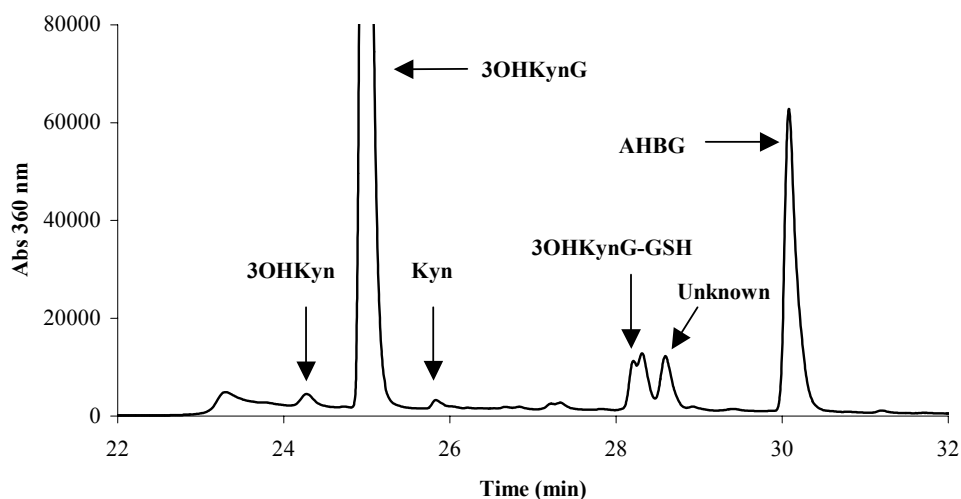


**Figure 3.16** HPLC chromatogram of the ethanol extract from a human normal lens cortex (81 years old).

#### *Protein - Bound UV Filters*

After the human lens protein was incubated at pH 9.5, it was ultra-filtered, and the filtrate was examined for UV filters. The HPLC chromatograms of the nucleus and cortex of normal and cataractous lens filtrates were similar in pattern. Figure 3.17A is the HPLC chromatogram of a normal 79 year old nuclear filtrate, and Figure 3.17B is the HPLC profile of the normal 79 year old cortex filtrate. The HPLC chromatogram in Figure 3.17A shows three doublets eluting at 28.5 min, 29.6 min and 33 min, and the HPLC chromatogram in Figure 3.17B shows two doublets eluting at 28.5 min and 33 min. The large peak at 28.5 min contained a component with a major ion in the ESI spectrum at  $m/z$  677 (spectrum not shown). MS/MS (Figure 3.18A) of this ion revealed major fragment ions at  $m/z$  515, 386, 368, 208, 190, 162 and 110. This compound was therefore identified as 3OHKynG-GSH.<sup>82</sup>

The doublet peak at 33 min was smaller, and the major ion in the ESI spectrum was  $m/z$  499. MS/MS (Figure 3.18B) of this ion showed that the major fragment ions were  $m/z$  370, 352, 308, 192, 174 and 146. This compound was identified as Kyn-GSH, since the



MS/MS and the HPLC elution times were identical to those of Kyn-GSH, synthesised by incubation of Kyn and GSH under basic pH conditions.<sup>197</sup>

The doublet at 29.6 min in Figure 3.17A was the smallest, and it eluted at the same time as synthetic 3OHKyn-GSH. MS/MS analysis (Figure 3.18C) of the  $m/z$  515 ion showed fragment ions at  $m/z$  386, 368, 208, 190, 162 and 110, as expected for 3OHKyn-GSH. The peak at ~29.6 min in Figure 3.17B was extremely small and very broad. This product eluted at relatively the same retention time as 3OHKyn-GSH, therefore this peak was collected and examined by mass spectrometry. The ion  $m/z$  515 was only present at 2% abundance in the ESI spectrum (spectrum not shown) *i.e.* this ion was on the baseline of the spectrum. MS/MS of this ion (spectrum not shown) exhibited very few fragment ions of 3OHKyn-GSH, and they were also in very low abundance. Therefore this product could not conclusively be confirmed as 3OHKyn-GSH.

Since 3OHKynG was present in much higher concentrations than 3OHKyn, it was important to demonstrate that the 3OHKyn was not derived via the hydrolysis of the glucoside during the incubation period. 3OHKynG was incubated with GSH under the same conditions used for the lens proteins. After 4 hours at pH 9.5, a large doublet peak corresponding to 3OHKynG-GSH was observed, but there were no detectable peaks in the region where 3OHKyn-GSH eluted (HPLC spectrum not shown). This region was collected for analysis by mass spectrometry, but no ions at  $m/z$  515, corresponding to 3OHKyn-GSH, was detected. The absence of hydrolysis is consistent with the stability of glucosides to base.

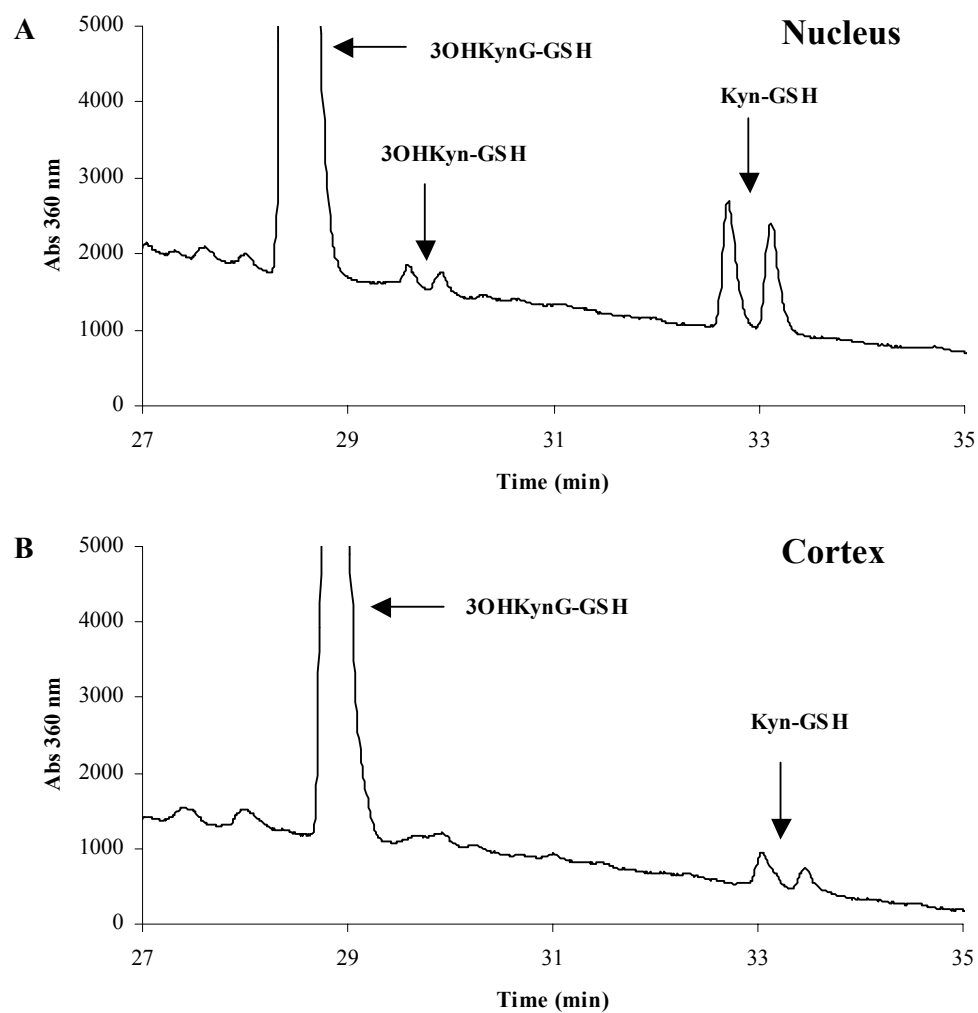


**Figure 3.17** HPLC chromatograms of human lens protein incubated with excess GSH at pH 9.5 for 4 hours. *A*, Normal 79 year old nucleus; *B*, Normal 79 year old cortex.

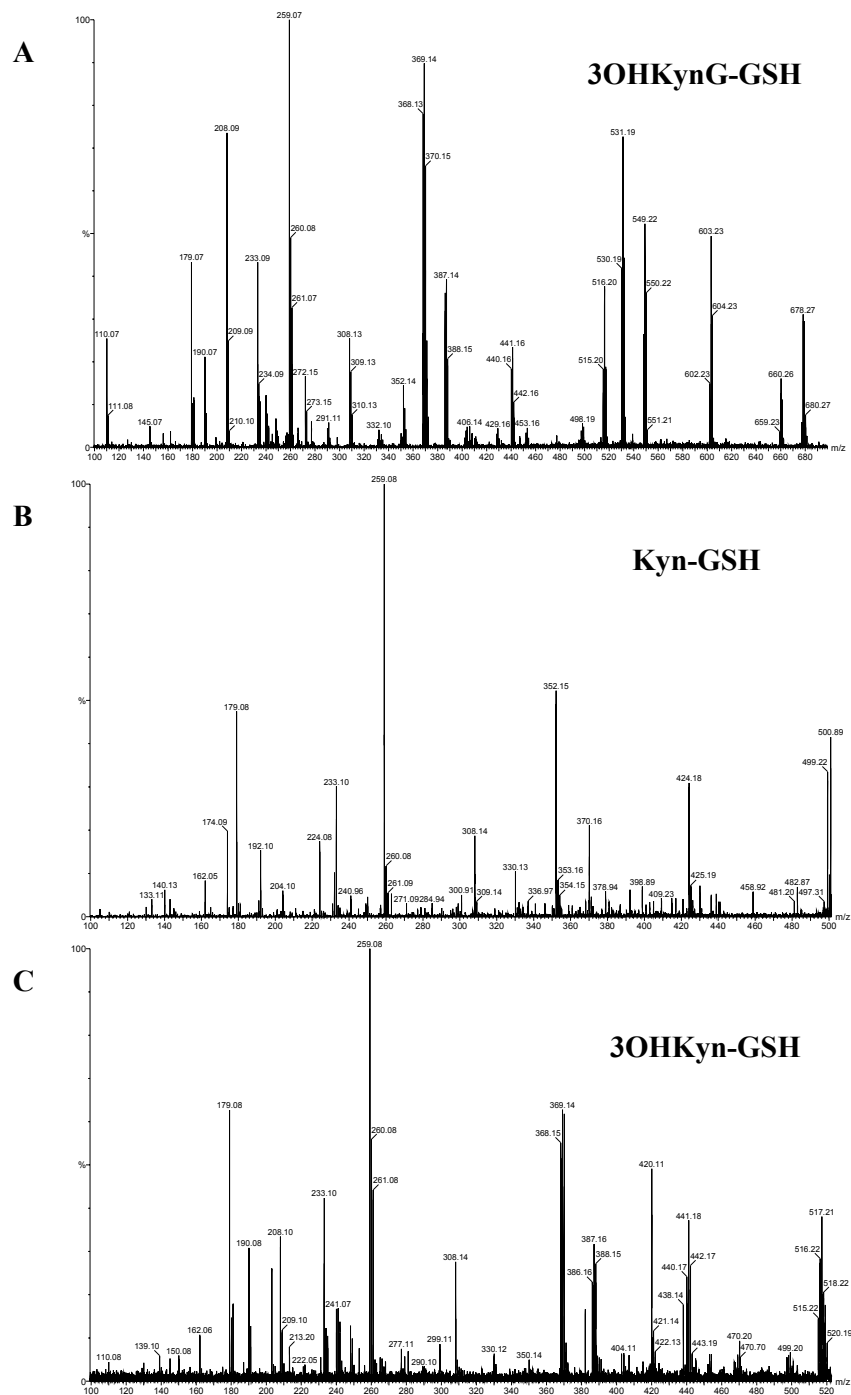


**Figure 3.18** MS/MS spectra of the three kynurenine derived UV filter GSH adducts isolated from a normal human lens nucleus. *A*, Molecular ion  $m/z$  677; *B*, Molecular ion  $m/z$  499; *C*, Molecular ion  $m/z$  515.

Since this new ‘assay’ provides data for all three UV filters, a summary of the levels of free and bound UV filters in the normal and cataract lens nuclei and cortices is shown below.

### *3OHKyn Bound to Lens Proteins*

Twenty-two normal human lenses were analysed and 3OHKyn bound to lens proteins was not detected in the nuclei of lenses 17, 19, 20, 23, 33, 44 and 49 years old. Bound 3OHKyn was detected only in the nuclear proteins of normal lenses aged 50 years and over (Figure 3.19). The average amount of 3OHKyn bound to the nucleus of lenses greater than 50 years old, was 9.21 pmol/mg protein. The cortices of these same lenses were also analysed, however 3OHKyn could not be detected in any of the cortical proteins. 3OHKyn was not bound to any of the cataract lens proteins examined.

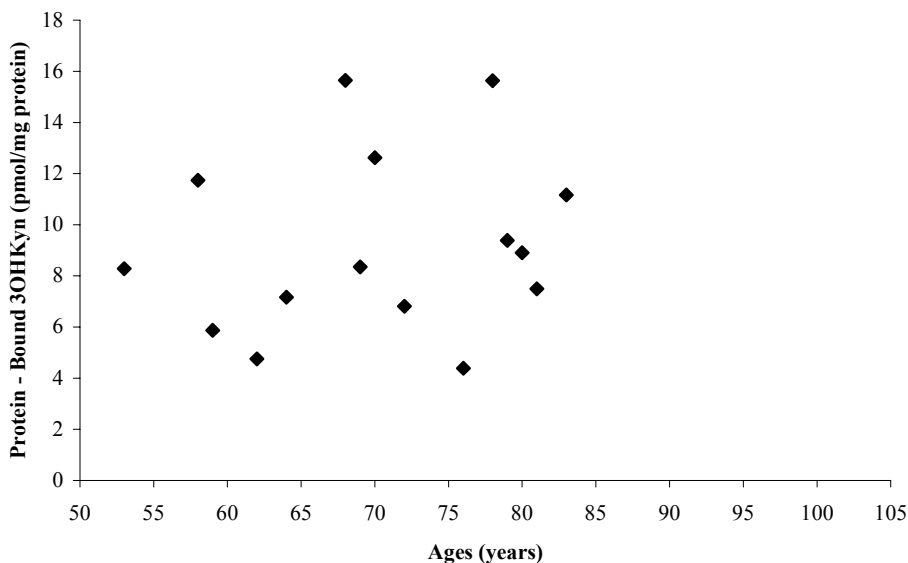


**Figure 3.19** Protein – bound 3OHKyn. The concentration of 3OHKyn bound to the nuclear proteins of normal human lenses as a function of age.

*3OHKyn Free in the Lens*

*Nucleus*

The levels of free 3OHKyn in cataract lenses and some normal lenses were quantified and statistically analysed. The data for free 3OHKyn in the nucleus are shown in Figure 3.20. Only lenses aged greater than 50 were analysed in this study. The average amount of 3OHKyn in the nucleus of normal lenses was 2.61 pmol/mg protein ( $n=5$ ) (Appendix 1). Although only 5 lenses were analysed, these values were comparable to a previous study.<sup>19</sup> The average amount of 3OHKyn in the Dark cataract lenses was 0.068 pmol/mg protein ( $n=10$ ), and the average amount in Light cataract lenses was 0.099 pmol/mg protein ( $n=10$ ) (Appendix 1). Levels in the normal lenses compared to the levels in cataract lenses were statistically significant ( $P < 0.0001$ ). Comparison of the levels between each of the different coloured cataract lenses showed that they were not statistically significant.

*Cortex*

The data for the levels of free 3OHKyn in the cortex are shown in Figure 3.21. The average amount of 3OHKyn in normal lenses was 1.19 pmol/mg protein ( $n=5$ ) (Appendix 1). The average amount of 3OHKyn in the Dark cataract lenses was 0.043 pmol/mg protein ( $n=10$ ), and the average amount in Light cataract lenses was 0.046 pmol/mg protein ( $n=10$ ) (Appendix 1). Levels in the normal lenses compared to the levels in cataract lenses were statistically significantly different ( $P < 0.0001$ ). Comparison of the levels between each of the different coloured cataract lenses showed that they were not statistically significant.

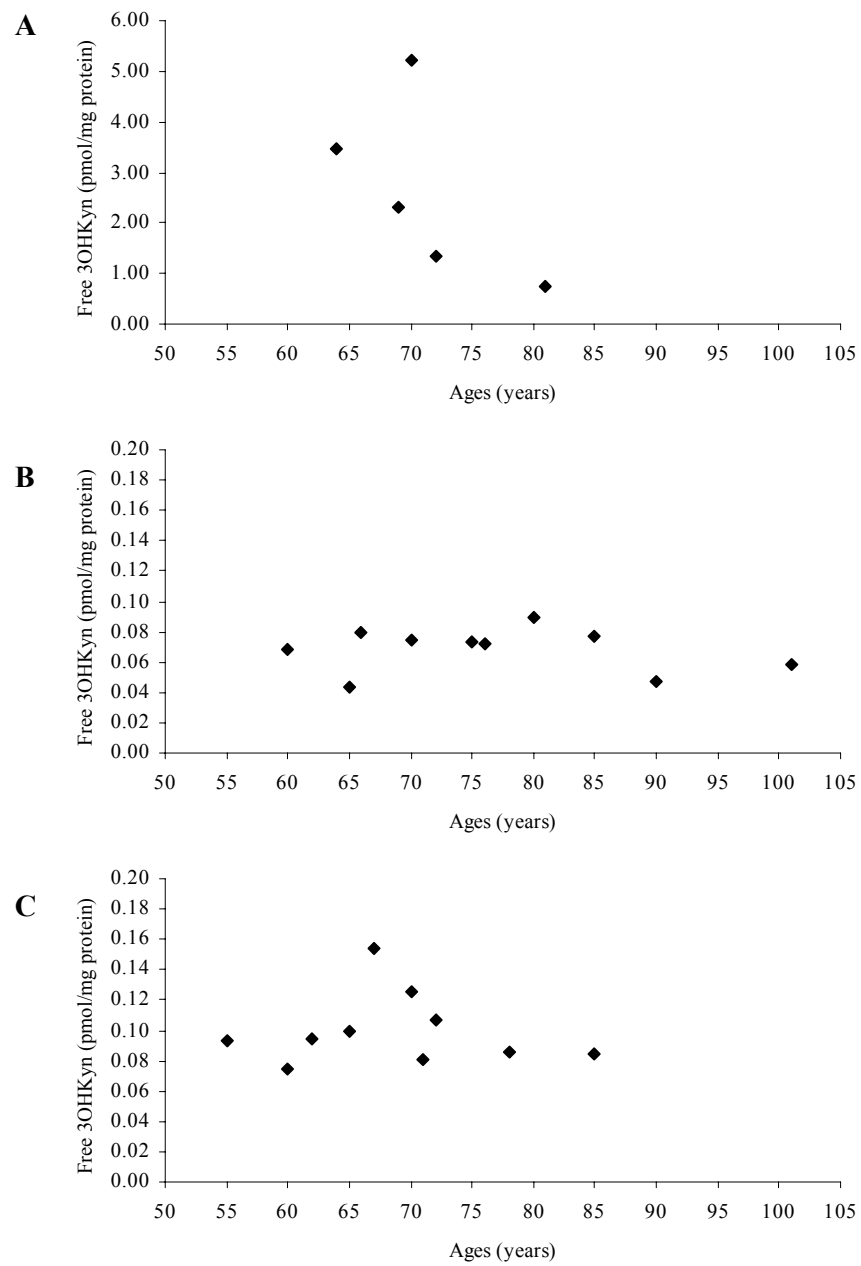


**Figure 3.20** Free 3OHKyn. The concentration of free 3OHKyn in the nucleus. *A*, Normal lenses; *B*, Dark cataract lenses; *C*, Light cataract lenses.

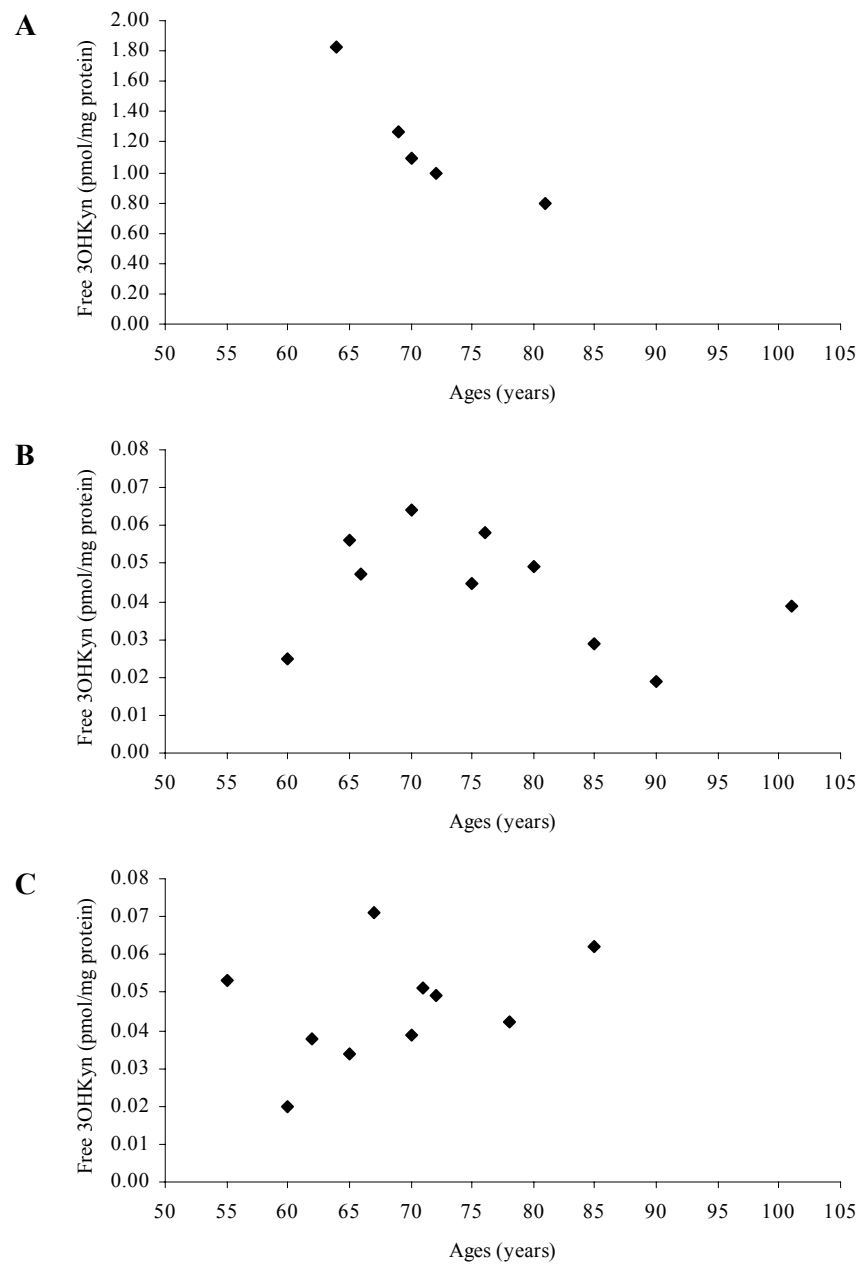


**Figure 3.21** Free 3OHKyn. The concentration of free 3OHKyn in the cortex. *A*, Normal lenses; *B*, Dark cataract lenses; *C*, Light cataract lenses.

*3OHKyn Free vs Bound*

The aim was to determine if there was a relationship between the levels of bound versus the levels of free UV filter in the nucleus and cortex. 3OHKyn was only bound to the nucleus of normal aged lenses (Figure 3.19). Therefore the five normal lenses (aged 64, 69, 70, 72 and 81 years old) that were analysed for bound levels as well as free levels were plotted in Figure 3.22. This is a small sample, and the lens that recorded the highest concentration of bound 3OHKyn, also had the highest concentration of free 3OHKyn. However the other four samples show that although the concentration of free 3OHKyn increases, the concentration of bound 3OHKyn remains steady, therefore there doesn't seem to be a relationship between the levels of free and bound 3OHKyn in the nucleus of normal lenses.

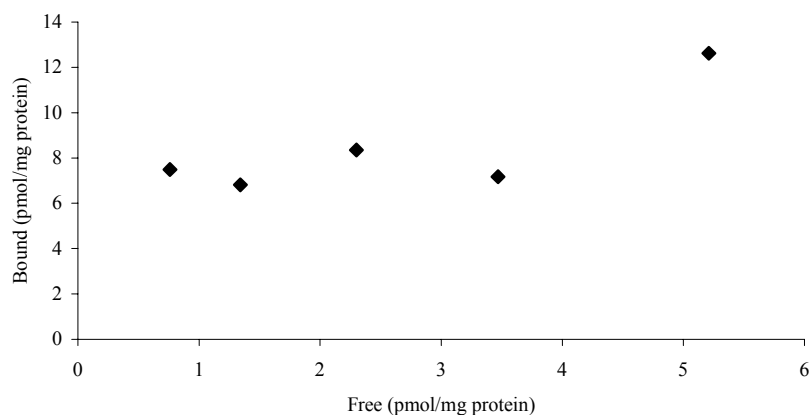


**Figure 3.22** Plot of the concentration of free 3OHKyn in the nucleus versus the concentration of bound 3OHKyn in the nucleus of normal aged lenses.



*3OHKynG Bound to Lens Proteins*

*Nucleus*

3OHKynG was found to be bound to all of the nuclear and cortical proteins that were analysed. The levels of bound 3OHKynG in the nucleus are shown in Figure 3.23. The data for the lenses aged 17, 19, 20, 23, 33, 44 and 49 years old have not been plotted in Figure 3.23A, however the levels of bound 3OHKynG in the nucleus were 98, 156, 47, 153, 106, 241 and 584 pmol/mg protein respectively. The average amount of bound 3OHKynG in the nucleus of normal lenses aged greater than 50 years old was 1307.22 pmol/mg protein ( $n=15$ ) (Appendix 1). The average amount of bound 3OHKynG in Dark cataract lenses was 153.00 pmol/mg protein ( $n=10$ ), and the average amount in Light cataract lenses was 277.02 pmol/mg protein ( $n=10$ ) (Appendix 1). Levels in the normal lenses compared to the levels in cataract lenses were statistically significant ( $P < 0.0001$ ). Comparison of the levels between each of the different coloured cataract lenses showed that they were not statistically significant.

*Cortex*

The levels of bound 3OHKynG in the cortex are shown in Figure 3.24. In the cortex, the data for the lenses aged 17, 19, 20, 23, 33, 44 and 49 years old were not plotted in Figure 3.24A, however the levels of bound 3OHKynG in the cortex are 2.9, 3.3, 4.3, 4.1, 6.7, 7.2 and 14.2 pmol/mg protein respectively. The average amount of bound 3OHKynG in the cortex of normal lenses aged greater than 50 years old was 56.20 pmol/mg protein ( $n=15$ ) (Appendix 1). The average amount of bound 3OHKynG in Dark cataract lenses was 52.82 pmol/mg protein ( $n=10$ ), and the average amount in Light cataract lenses was 45.13 pmol/mg protein ( $n=10$ ) (Appendix 1). Levels in the normal lenses compared to the levels in cataract lenses were not statistically significant ( $P = 0.7659$ ).

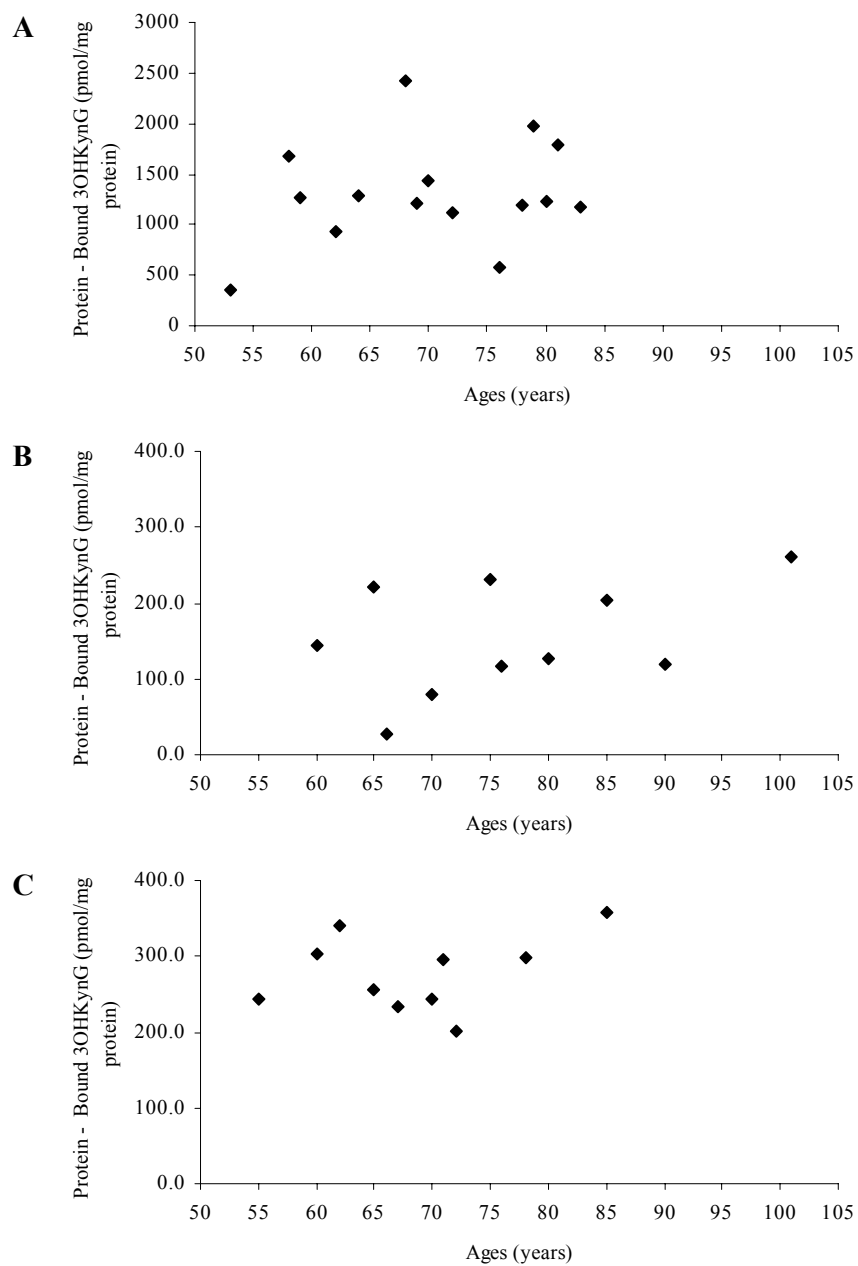


**Figure 3.23** Protein – bound 3OHKynG. The concentration of bound 3OHKynG in the nucleus. *A*, Normal lenses; *B*, Dark cataract lenses; *C*, Light cataract lenses.

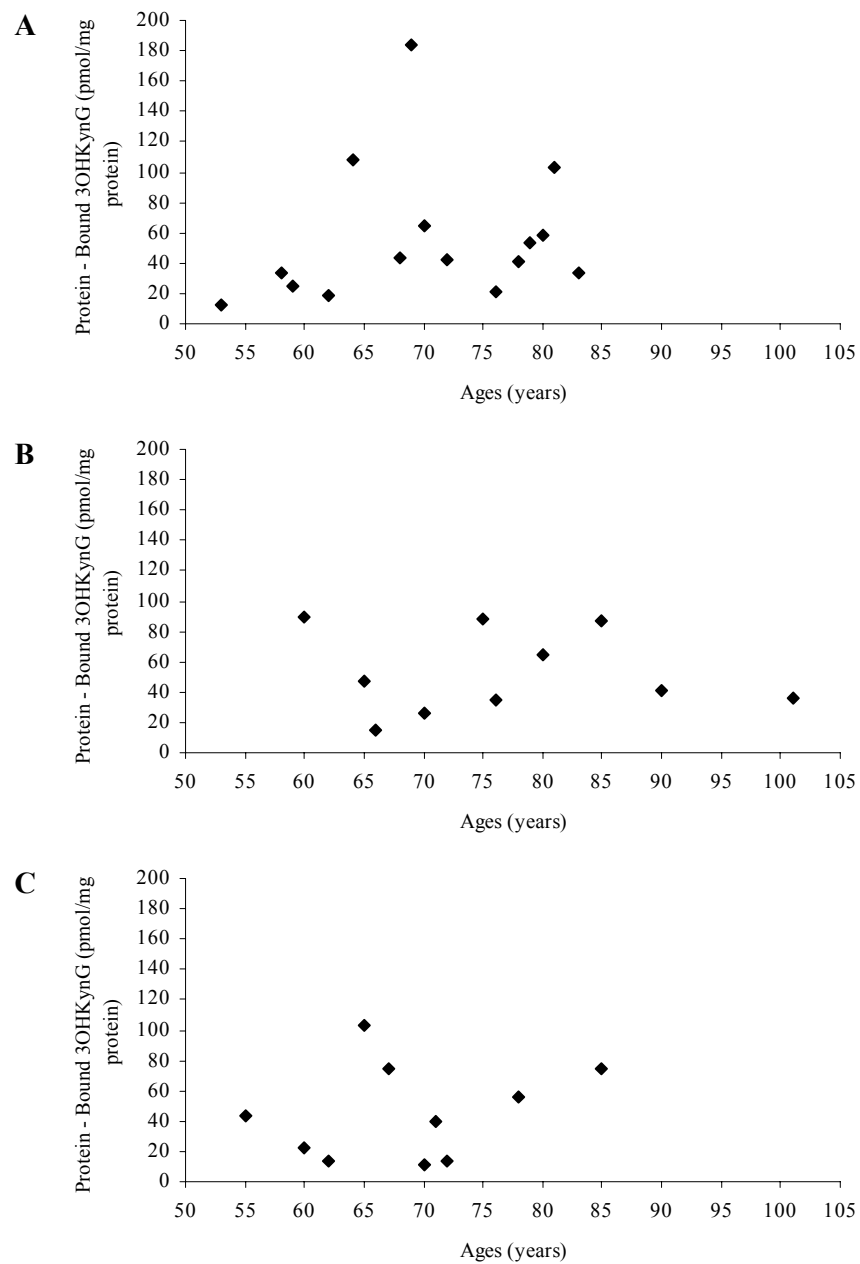


**Figure 3.24** Protein – bound 3OHKynG. The concentration of bound 3OHKynG in the cortex. *A*, Normal lenses; *B*, Dark cataract lenses; *C*, Light cataract lenses.

### *3OHKynG Free in the Lens*

#### *Nucleus*

The levels of free 3OHKynG in the nucleus are shown in Figure 3.25. The average amount of free 3OHKynG in normal lenses aged greater than 50 years old was 533.80 pmol/mg protein ( $n=5$ ) (Appendix 1). Although only 5 lenses were analysed, these values were comparable to those obtained by Bova, *et al.*<sup>19</sup> The average amount of free 3OHKynG in Dark cataract lenses was 30.52 pmol/mg protein ( $n=10$ ), and the average amount in Light cataract lenses was 81.58 pmol/mg protein ( $n=10$ ) (Appendix 1). The levels in normal lenses compared to cataract lenses were statistically significant ( $P < 0.0001$ ). Comparisons of the levels between each of the different coloured cataract lenses showed that they were not statistically significant.

#### *Cortex*

The levels of free 3OHKynG in the cortex are shown in Figure 3.26. The average amount of free 3OHKynG in normal lenses aged greater than 50 years old was 556.80 pmol/mg protein ( $n=5$ ) (Appendix 1). These values were comparable to those obtained by Bova, *et al.*<sup>19</sup> The average amount of free 3OHKynG in Dark cataract lenses was 34.73 pmol/mg protein ( $n=10$ ), and the average amount in Light cataract lenses was 39.55 pmol/mg protein ( $n=10$ ) (Appendix 1). Levels in the normal lenses compared to the levels in cataract lenses were statistically significant ( $P < 0.0001$ ). Comparison of the levels between each of the different coloured cataract lenses showed that they were not statistically significant.

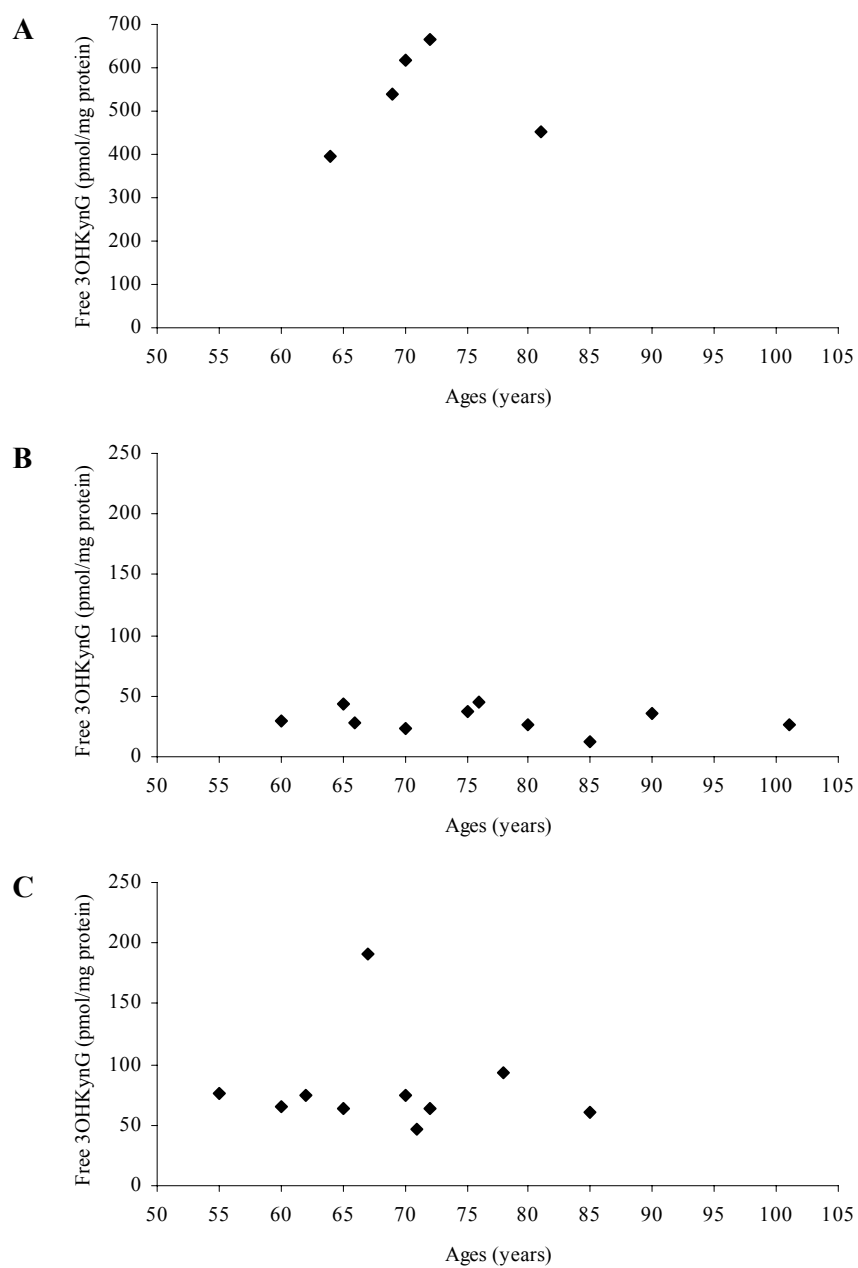


**Figure 3.25** Free 3OHKynG. The concentration of free 3OHKynG in the nucleus. *A*, Normal lenses; *B*, Dark cataract lenses; *C*, Light cataract lenses.

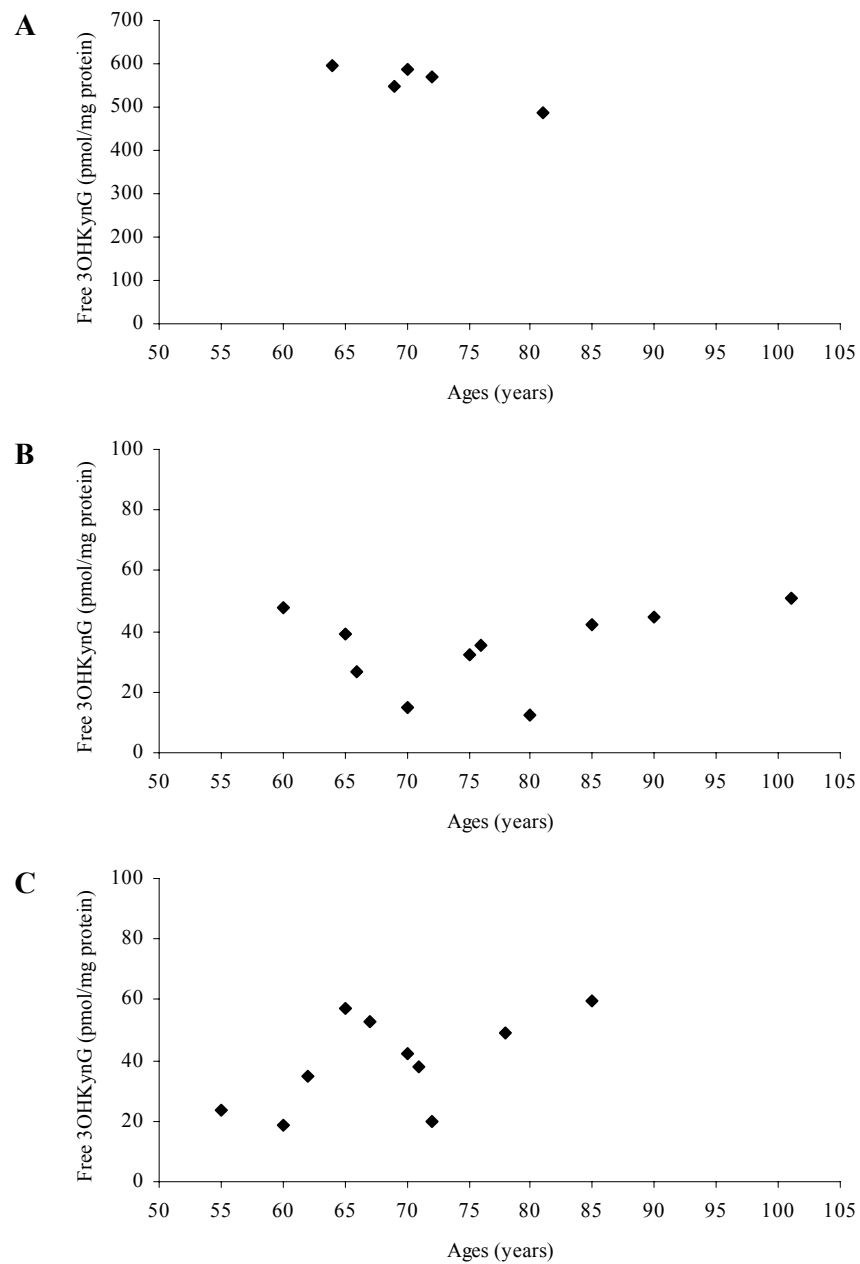


**Figure 3.26** Free 3OHKynG. The concentration of free 3OHKynG in the cortex. *A*, Normal lenses; *B*, Dark cataract lenses; *C*, Light cataract lenses.

*3OHKynG Free vs Bound*

Free and bound levels of 3OHKynG were observed in all of the lenses that were analysed. The concentrations of free 3OHKynG were plotted against the levels of bound 3OHKynG (Figure 3.27). Figure 3.27A shows the plots for the nucleus (Figure 3.27Ai normal lenses, Figure 3.27Aii Dark cataract lenses and Figure 3.27Aiii Light cataract lenses). Figure 3.27B are the plots for the cortex (Figure 3.27Bi normal lenses, Figure 3.27Bii Dark cataract lenses and Figure 3.27Biii Light cataract lenses). Observation of all six plots showed that there is no clear relationship between the free and bound levels of 3OHKynG in any of the different types of lenses.

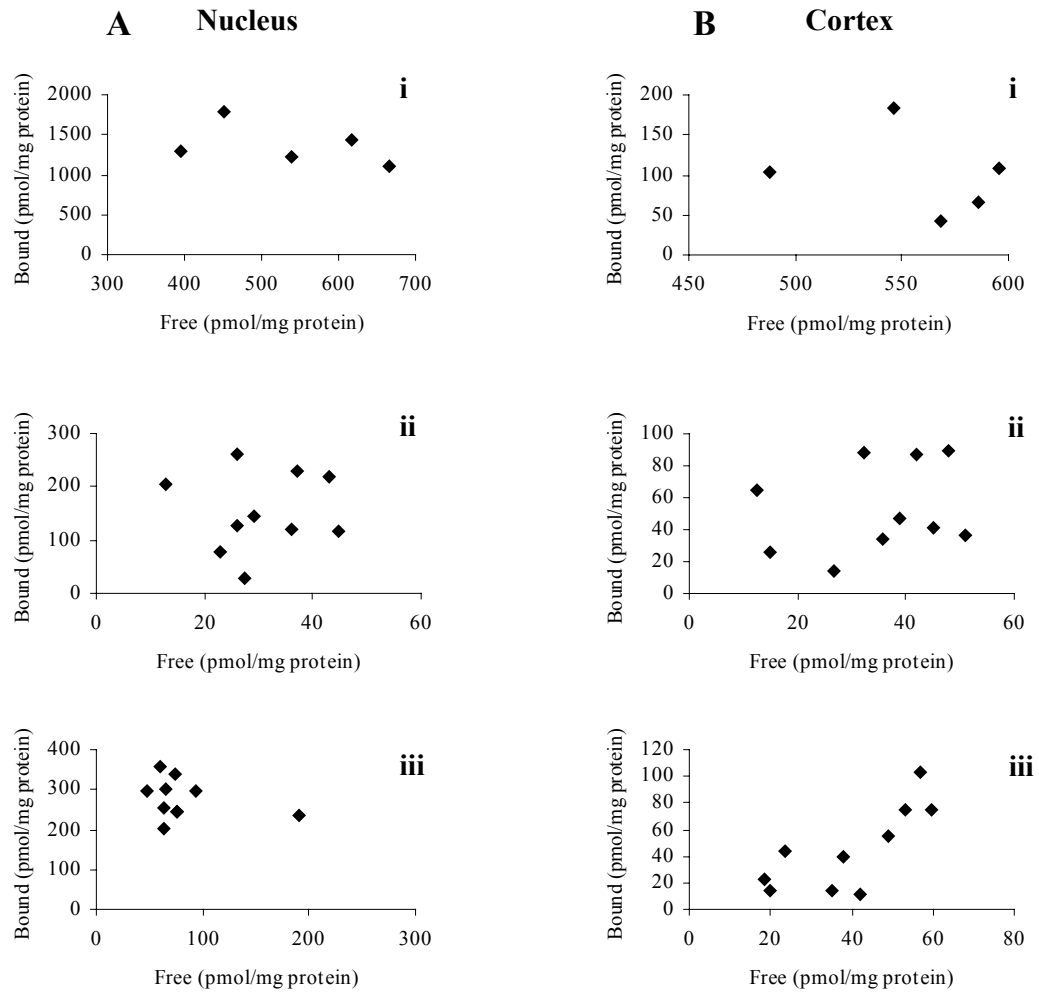


**Figure 3.27** Plot of the concentration of free vs bound 3OHKynG. *A*, Nucleus; *i*, Normal lenses; *ii*, Dark cataract; *iii*, Light cataract lenses; *B*, Cortex; *i*, Normal lenses; *ii*, Dark cataract; *iii*, Light cataract lenses.



*Kyn Bound to Lens Proteins*

*Nucleus*

Kyn was bound to proteins from most of the nuclei and cortices that were analysed. The levels of bound Kyn in the nucleus are shown in Figure 3.28. The data for the lenses aged 17, 19, 20, 23, 33, 44 and 49 years old have not been plotted in Figure 3.28A, however the levels of bound Kyn in the nucleus were 4.7, 6.1, 0, 7.0, 4.1, 5.1 and 15.7 pmol/mg protein respectively. The average amount of bound Kyn in the nucleus of normal lenses aged greater than 50 years old was 37.79 pmol/mg protein ( $n=15$ ) (Appendix 1). The average amount of bound Kyn in Dark cataract lenses was 5.83 pmol/mg protein ( $n=10$ ), and the average amount in Light cataract lenses was 11.41 pmol/mg protein ( $n=10$ ) (Appendix 1). Levels in the normal lenses compared to the levels in cataract lenses were statistically significant ( $P < 0.0001$ ). Comparison of the levels between each of the different coloured cataract lenses showed that they were not statistically significant.

*Cortex*

The levels of bound Kyn in the cortex have been shown in Figure 3.29. In the cortex the data for the lenses aged 17, 19, 20, 23, 33, 44 and 49 years old were not plotted in Figure 3.29A, but bound levels of Kyn could not be detected in the cortices of these lenses. The average amount of bound Kyn in the cortex of normal lenses aged greater than 50 years old was 1.78 pmol/mg protein ( $n=15$ ) (Appendix 1). The average amount of bound Kyn in Dark cataract lenses was 2.18 pmol/mg protein ( $n=10$ ), and the average amount in Light cataract lenses was 3.34 pmol/mg protein ( $n=10$ ) (Appendix 1). Levels in the normal lenses compared to the levels in cataract lenses showed that they were not statistically significant ( $P = 0.1005$ ).

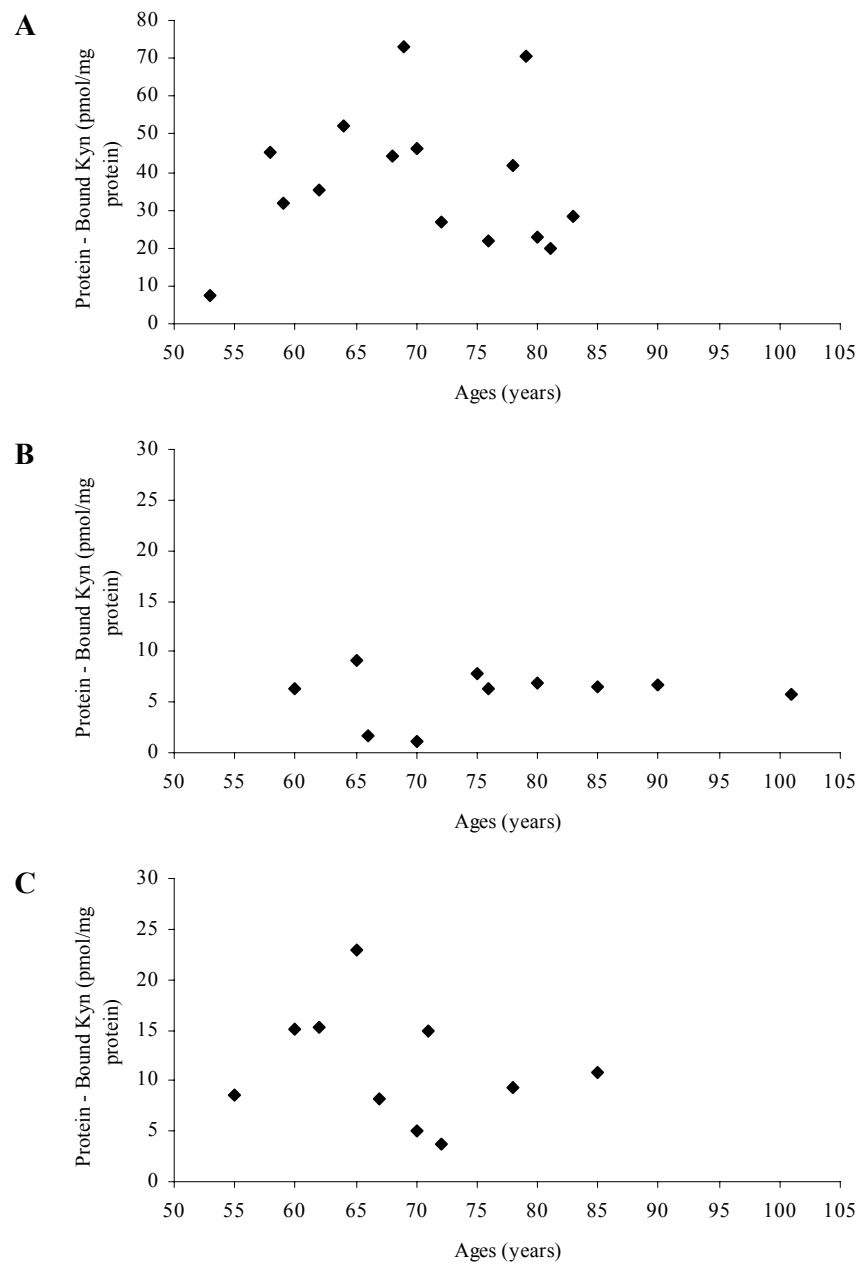


**Figure 3.28** Protein – bound Kyn. The concentration of bound Kyn in the nucleus. *A*, Normal lenses; *B*, Dark cataract lenses; *C*, Light cataract lenses.

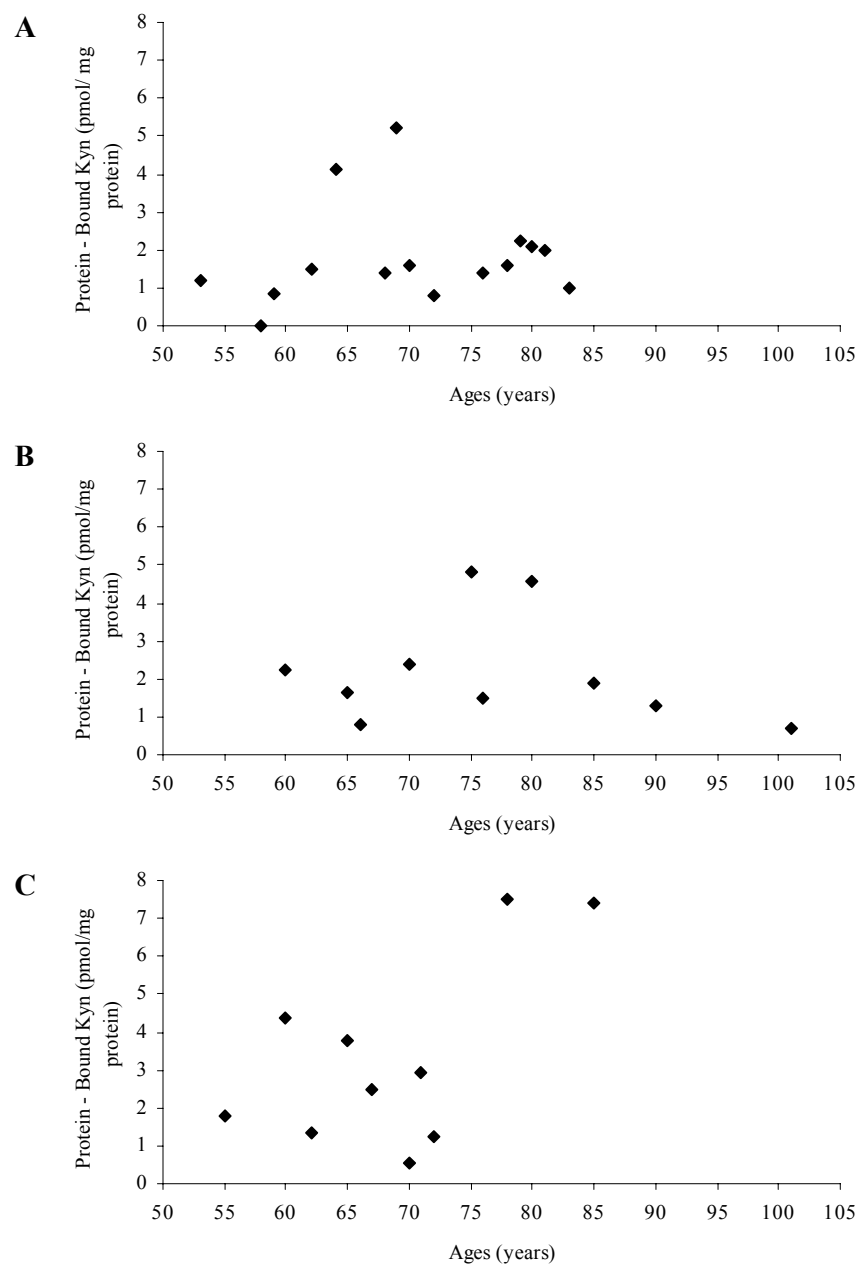


**Figure 3.29** Protein – bound Kyn. The concentration of bound Kyn in the cortex. *A*, Normal lenses; *B*, Dark cataract lenses; *C*, Light cataract lenses.

*Kyn Free in the Lens*

*Nucleus*

The levels of free Kyn in the nucleus are shown in Figure 3.30. The average amount of free Kyn in normal lenses aged greater than 50 years old was 15.40 pmol/mg protein ( $n=5$ ) (Appendix 1). The average amount of free Kyn in Dark cataract lenses was 2.31 pmol/mg protein ( $n=10$ ), and the average amount in Light cataract lenses was 3.93 pmol/mg protein ( $n=10$ ) (Appendix 1). Levels in the normal lenses compared to the levels in cataract lenses were statistically significant ( $P < 0.0001$ ). Comparison of the levels between each of the different coloured cataract lenses showed that they were not statistically significant.

*Cortex*

The levels of free Kyn in the cortex are shown in Figure 3.31. The average amount of free Kyn in normal lenses aged greater than 50 years old was 6.20 pmol/mg protein ( $n=5$ ) (Appendix 1). The average amount of free Kyn in Dark cataract lenses was 1.23 pmol/mg protein ( $n=10$ ), and the average amount in Light cataract lenses was 1.69 pmol/mg protein ( $n=10$ ) (Appendix 1). Levels in the normal lenses compared to the levels in cataract lenses were statistically significant ( $P < 0.0001$ ). Comparison of the levels between each of the different coloured cataract lenses showed that they were not statistically significant.

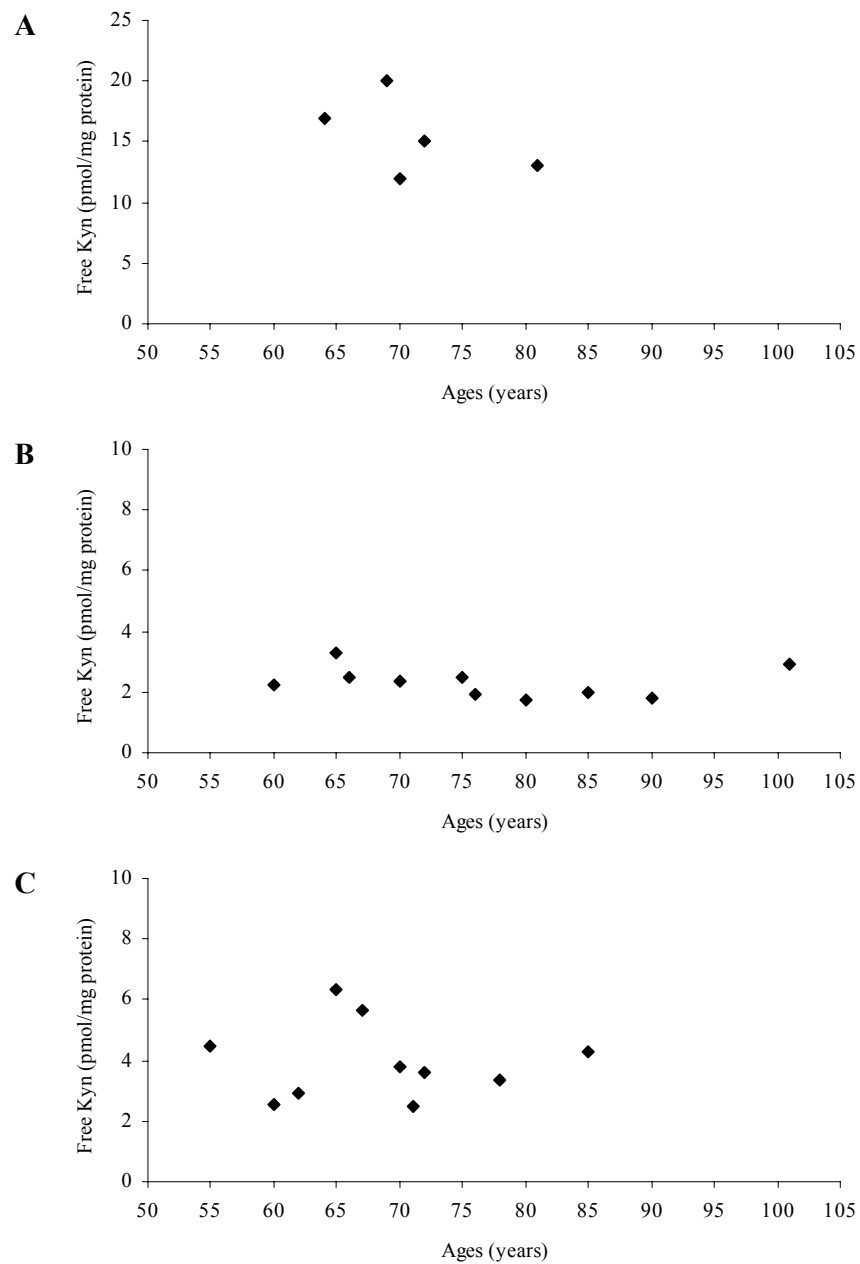


**Figure 3.30** Free Kyn. The concentration of free Kyn in the nucleus. *A*, Normal lenses; *B*, Dark cataract lenses; *C*, Light cataract lenses.

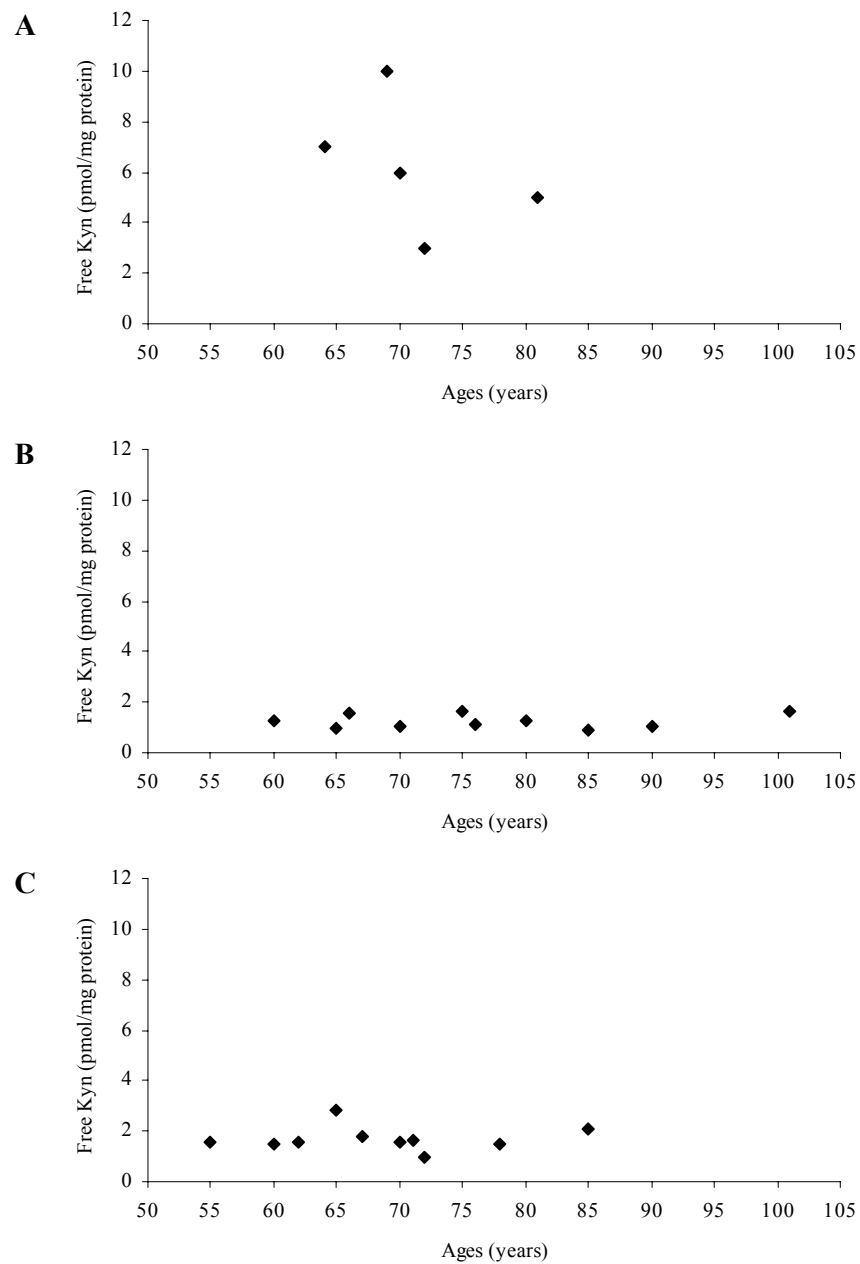


**Figure 3.31** Free Kyn. The concentration of free Kyn in the cortex. *A*, Normal lenses; *B*, Dark cataract lenses; *C*, Light cataract lenses.

*Kyn Free vs Bound*

Free and bound levels of Kyn were observed in all lenses that were analysed. The levels of free Kyn have been plotted against the levels of bound Kyn (Figure 3.32). Figure 3.32A shows the plots for the nucleus (Figure 3.32Ai normal lenses, Figure 3.32Aii Dark cataract lenses and Figure 3.32Aiii Light cataract lenses). Figure 3.32B shows the plots for the cortex (Figure 3.32Bi normal lenses, Figure 3.32Bii Dark cataract lenses and Figure 3.32Biii Light cataract lenses). Observation of the four plots shows no apparent relationship between the free and bound levels of Kyn in the different cataract lenses. The plot for the normal lenses for both the cortex and nucleus does show a linear relationship.

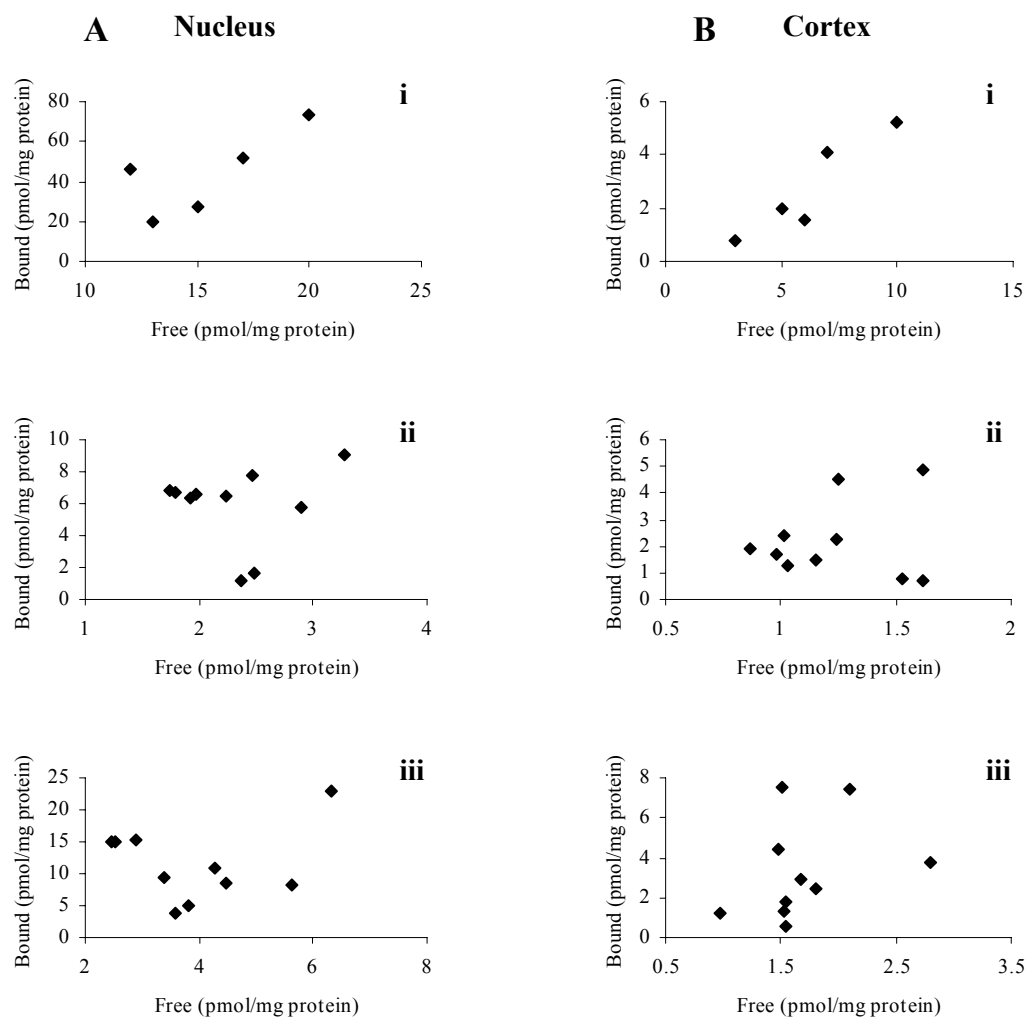


**Figure 3.32** Plot of the concentration of free vs bound Kyn. *A*, Nucleus; *i*, Normal lenses; *ii*, Dark cataract; *iii*, Light cataract lenses; *B*, Cortex; *i*, Normal lenses; *ii*, Dark cataract; *iii*, Light cataract lenses.

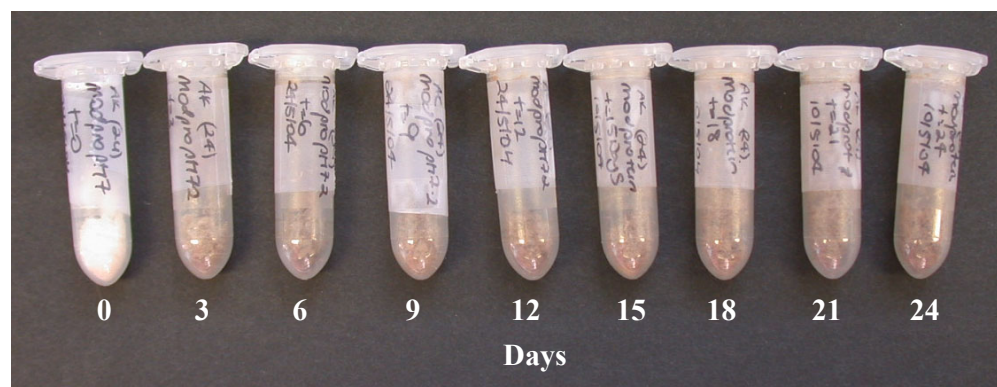


### 3.3.6 CLP Modified with 3OHKyn for 24 Days

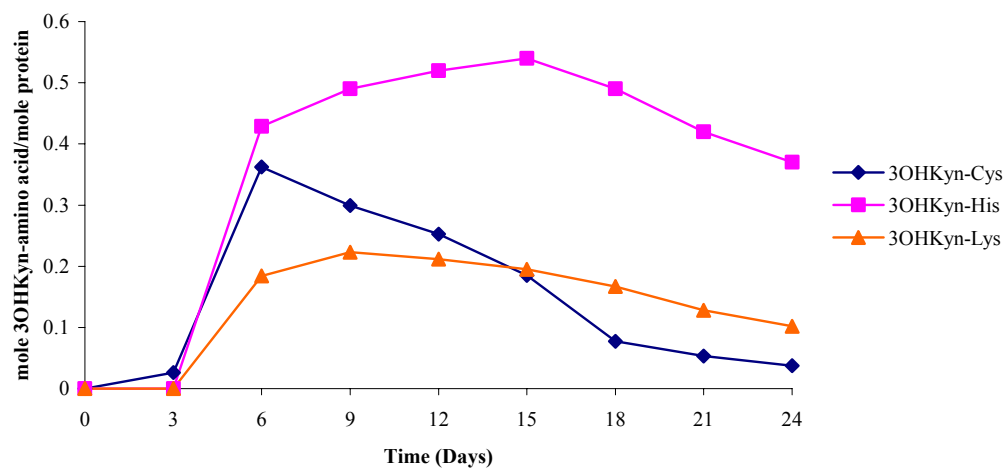
Earlier studies in Section 3.3.3 had shown that when CLP is modified with 3OHKyn at pH 7.2 for 48 hours, Cys residues become modified. His and Lys modifications were only observed when the pH of the incubation was raised to 9.5. Therefore the aim of this study was to modify CLP with 3OHKyn over a long period of time *i.e.* 24 days, at pH 7.2 to observe if modifications to His and Lys would be detected. Aliquots were taken at 0, 3, 6, 9, 12, 15, 18, 21 and 24 days. Each sample was ultra-filtered and the protein freeze dried. A photograph of the dried protein samples is shown in Figure 3.33. The initial protein (0 days) was white, however the modified protein at all the other time points was noticeably brown. The proteins were then hydrolysed with acid in the presence of antioxidants. The relative rate of formation of the 3OHKyn amino acid adducts over 24 days of incubation is shown in Figure 3.34.

Figure 3.34 shows that all three 3OHKyn amino acid adducts were formed when CLP was modified with 3OHKyn at pH 7.2 for 3 weeks. After 3 days of incubation 3OHKyn-Cys was formed (0.026 mole/mole protein). By day 6 the level of 3OHKyn-Cys had increased to 0.36 mole/mole protein, but it then gradually decreased over the following 18 days to a final level of 0.037 mole/mole protein at 24 days of incubation. The formation of 3OHKyn-His was first observed at day 6, with a level of 0.42 mole/mole protein. The level of 3OHKyn-His continued to increase, until a maximum level of 0.78 mole/mole protein was observed on day 15. The level of 3OHKyn-His then slowly declined to 0.60 mole/mole protein on day 24. 3OHKyn-Lys was first observed on day 6. The level of 3OHKyn-Lys increased to 0.23 mole/mole protein on day 9 and then slowly decreased to 0.10 mole/mole protein on day 24.

An assay was undertaken to determine the protein sulfhydryl (PSH) content in the CLP modified with 3OHKyn. PSH was determined for all of the aliquots (Figure 3.35). The initial aliquot at zero time contained 2.5 moles of sulfhydryls (SH) per mole of protein, which is comparable to Berry, *et al.*<sup>198</sup> This value decreased rapidly to 0.34 moles of SH by 3 days of incubation, and then continued to decrease slowly to 0.054 moles of SH per mole of protein by 24 days of incubation.



**Figure 3.33** Photograph of CLP modified with 3OHKyn at pH 7.2 under low oxygen. Aliquots were taken at 0, 3, 6, 9, 12, 15, 18, 21 and 24 days.



**Figure 3.34** Formation of 3OHKyn amino acid adducts in CLP over time. CLP was incubated with 3OHKyn at 37<sup>0</sup>C for a total of 24 days.

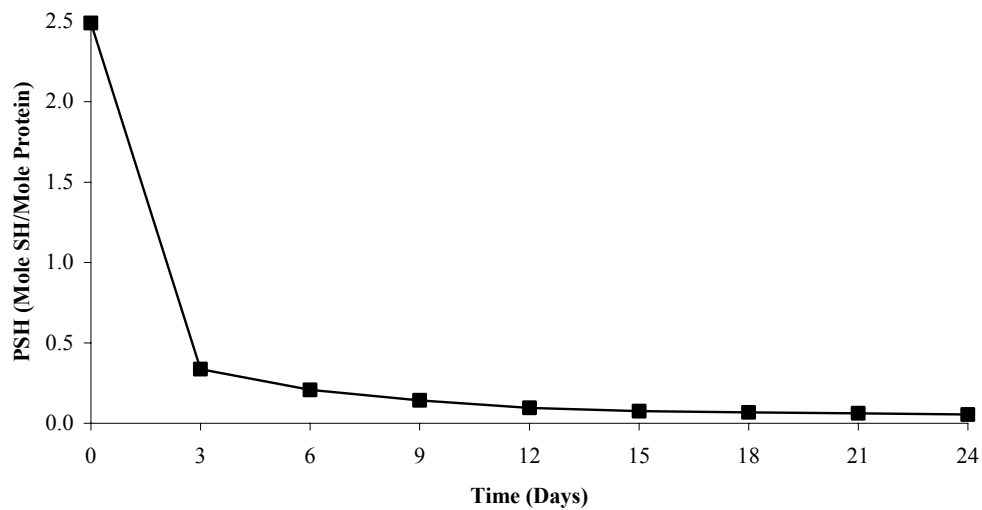


**Figure 3.35** The content of PSH in CLP modified with 3OHKyn at 37<sup>0</sup>C for 24 days.

### 3.3.7 Identification of CLP Peptides Modified with 3OHKyn

The previous Section (3.3.3) demonstrated that 3OHKyn binds to Cys, His and Lys residues. The aim in this section was to identify peptides modified with 3OHKyn. CLP modified with 3OHKyn at pH 7.2 for 12 days (protein aliquot from Section 3.3.6) was digested with trypsin and chromatographed by HPLC (Figure 3.36). Figure 3.36A shows the HPLC chromatogram with absorbance monitored at 360 nm, and Figure 3.36B is the fluorescence chromatogram with fluorescence monitored at Ex 370 nm/Em 520 nm. There were very few peaks that eluted in both spectra. The main peaks eluted at 45.1 min and 50.5 min. These peaks were collected and analysed by mass spectrometry. A database was created by Dr J.A. Aquilina, which lists all of the tryptic peptides for bovine crystallins modified by 3OHKyn at nucleophilic residues.

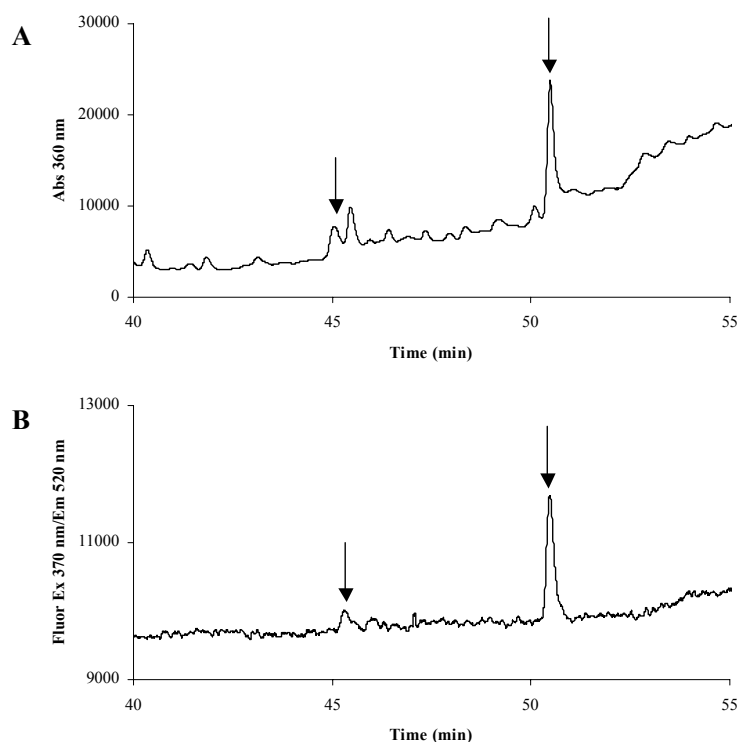


**Figure 3.36** HPLC chromatograms following trypsin digestion of CLP modified with 3OHKyn for 12 days. Arrowed peaks were collected for mass spectral analysis. *A*, UV trace; *B*, Fluorescence trace.

The ESI mass spectrum of the peak eluting at 45.1 min (Figure 3.36) is shown in Figure 3.37. All of the doubly and triply charged ions present in the spectrum were searched for in the database created by Dr J.A. Aquilina. Table 3.1 lists all of the doubly charged  $(M+2H)^{2+}$  ions from the ESI mass spectrum, and Table 3.2 lists all of the triply charged  $(M+3H)^{3+}$  ions. The MS/MS spectra for each ion was examined, however none of the spectra matched the predicted sequences as shown in Table 3.1 and Table 3.2.

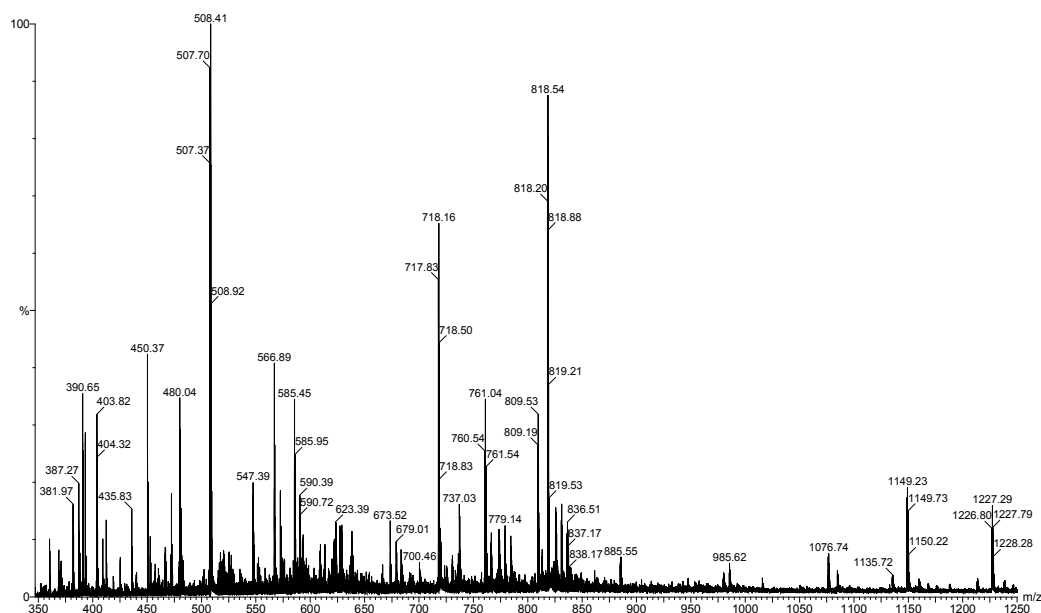


**Figure 3.37** ESI mass spectrum of the peak eluting at 45.1 min in Figure 3.36.

**Table 3.1** Lists all of the doubly charged ions  $(M+2H)^{2+}$  in the ESI mass spectrum (Figure 3.37) detected in the peak eluting at 45.1 min on the HPLC chromatogram (Figure 3.36).

| Ion                                    | Expected Peptide <sup>a</sup> | Bovine Fragment | Residue | Sequence             | Comment  |
|--|-------------------------------|-----------------|---------|----------------------|----------|
| <b><u><math>(M+2H)^{2+}</math></u></b> |                               |                 |         |                      |          |
| 368.8                                  | βA3                           | T14             | 132-137 | ENFIGR               | No match |
| 370.8                                  | No match                      |                 |         |                      |          |
| 403.8                                  | No match                      |                 |         |                      |          |
| 412.3                                  | No match                      |                 |         |                      |          |
| 435.8                                  | 3OHKyn βB2                    | T3              | 42-47   | ETGVEK               | No match |
| 450.3                                  | γS                            | T3              | 7-13    | ITFFEDK              | No match |
| 452.8                                  | No match                      |                 |         |                      |          |
| 508.4                                  | No match                      |                 |         |                      |          |
| 547.3                                  | βA3                           | T12-13          | 123-131 | ESKITIFEK            | No match |
| 566.9                                  | No match                      |                 |         |                      |          |
| 572.4                                  | γD                            | T12-13          | 91-98   | LYEREDYR             | No match |
| 585.4                                  | γA                            | T9              | 80-89   | LIPQHTGTFR           | No match |
|  | γB                            | T9              | 80-89   | LIPQHTGTFR           | No match |
|  | 3OHKyn βB2                    | T16             | 160-167 | GLQYLLEK             | No match |
|  | 3OHKyn βB3                    | T2              | 15-24   | SHGGLGGSYK           | No match |
| 760.5                                  | No match                      |                 |         |                      |          |
| 885.1                                  | No match                      |                 |         |                      |          |
| 1076.2                                 | βB2                           | T17-18          | 168-187 | GDYKDSGDFGAPQPQVQSVR | No match |
| 1084                                   | No match                      |                 |         |                      |          |
| 1148.7                                 | No match                      |                 |         |                      |          |
| 1226.8                                 | No match                      |                 |         |                      |          |

<sup>a</sup>Sequences were obtained from SwissProt, and theoretical tryptic digests were obtained using BioLynx from MassLynx. Unmodified peptides were placed in Excel, and UV filters were added to nucleophilic amino acid residues.

**Table 3.2** Lists all of the triply charged ions  $(M+3H)^{3+}$  in the ESI mass spectrum (Figure 3.37) detected in the peak eluting at 45.1 min on the HPLC chromatogram (Figure 3.36).

| Ion                             | Expected Peptide  | Bovine Fragment | Residue | Sequence              | Comment  |
|---------------------------------|-------------------|-----------------|---------|-----------------------|----------|
| <b><math>(M+3H)^{3+}</math></b> |                   |                 |         |                       |          |
| 360.2                           | 3OHKyn $\alpha$ B | T17-18          | 150-157 | KQASGPER              | No match |
| 381.9                           | $\beta$ B1        | T18             | 151-160 | LCLFEGANFK            | No match |
|                                 | $\gamma$ D        | T12-13          | 91-98   | LYEREDYR              | No match |
| 390.7                           | 3OHKyn $\beta$ B1 | T5              | 52-60   | AELPPGSYK             | No match |
|                                 | 3OHKyn $\beta$ B2 | T16             | 160-167 | GLQYLLEK              | No match |
|                                 | 3OHKyn $\beta$ B3 | T2              | 15-24   | SHGGLGGSYK            | No match |
|                                 | $\gamma$ A        | T19             | 154-163 | YLDWGAMNAK            | No match |
|                                 | $\gamma$ A        | T9              | 80-89   | LIPQHTGTFR            | No match |
|                                 | $\gamma$ B        | T18             | 154-163 | YLDWGAMNAK            | No match |
|                                 | $\gamma$ B        | T9              | 80-89   | LIPQHTGTFR            | No match |
| 466.5                           | $\beta$ B2        | T11             | 108-119 | ITLYENPNFTGK          | No match |
| 480.1                           | $\beta$ B1        | T8              | 74-86   | VEFSGECLNLGDR         | No match |
|                                 | $\beta$ B1        | T2-3            | 7-22    | ASATAAVNPGPDGKGK      | No match |
| 508.3                           | $\beta$ B2        | T11-12          | 108-120 | ITLYENPNFTGKK         | No match |
| 590.4                           | No match          |                 |         |                       |          |
| 718.8                           | No match          |                 |         |                       |          |
| 766.2                           | No match          |                 |         |                       |          |
| 773.4                           | No match          |                 |         |                       |          |
| 778.8                           | No match          |                 |         |                       |          |
| 784.1                           | No match          |                 |         |                       |          |
| 809.1                           | 3OHKyn $\beta$ B1 | T20-21          | 183-202 | VGSVRVSSGTWVGYYQYPGYR | No match |
|                                 | 3OHKyn $\beta$ B2 | T10-11          | 101-119 | VDSQEHKITLYENPNFTGK   | No match |
| 818.2                           | $\alpha$ A        | T10-11          | 79-99   | HFSPEDLTVKVQEDFVEIHGK | No match |
| 825.5                           | No match          |                 |         |                       |          |
| 830.8                           | No match          |                 |         |                       |          |
| 836.1                           | No match          |                 |         |                       |          |

The ESI mass spectrum of the peak eluting at 50.5 min (Figure 3.36) is shown in Figure 3.38. All of the doubly and triply charged ions in the ESI mass spectrum were identified, and listed in Table 3.3. The MS/MS spectrum for each ion was examined and some sequences matched the predicted sequences. However none of the matched sequences contained 3OHKyn modifications.

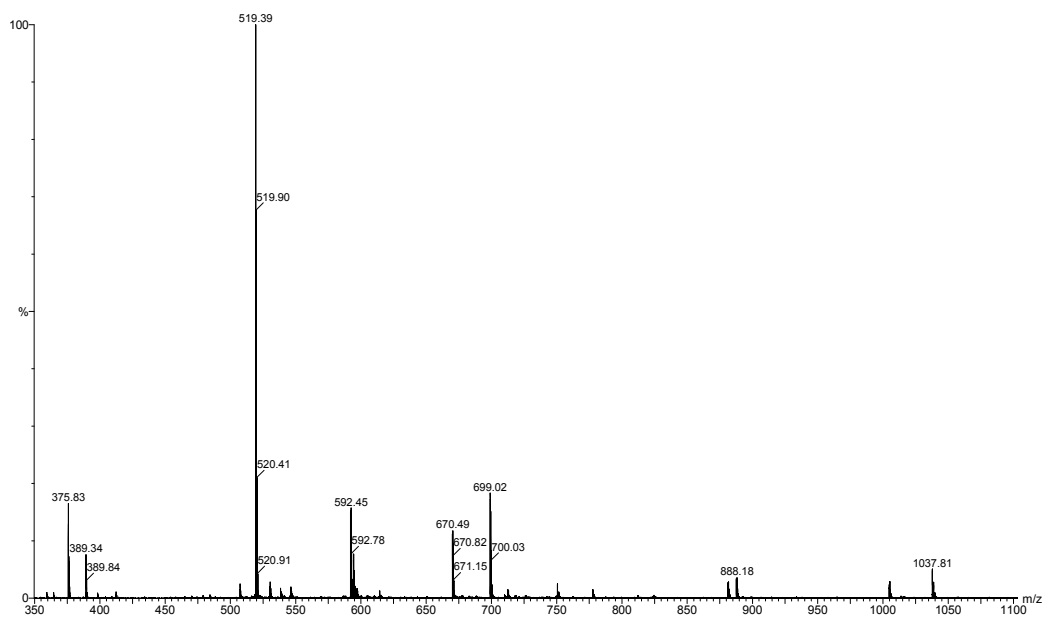


**Figure 3.38** ESI mass spectrum of the peak eluting at 50.5 min (Figure 3.36).



**Table 3.3** Lists all of the charged ions in the ESI mass spectrum (Figure 3.38) for the peak eluting at 50.5 min on the HPLC chromatogram (Figure 3.36).

| Ion                               | Expected Peptide | Bovine Fragment | Residue | Sequence          | Comment        |
|-----------------------------------|------------------|-----------------|---------|-------------------|----------------|
| <b><u>(M+2H)<sup>2+</sup></u></b> |                  |                 |         |                   |                |
| 375.8                             | βA3              | T13             | 126-131 | ITIFEK            | <b>Matched</b> |
| 389.3                             | γS               | T11             | 95-100  | LQIFEK            | <b>Matched</b> |
|                                   | γD               | T21-22          | 168-173 | RVIDIY(-)         | No match       |
|                                   | 3OHKyn αB        | T11             | 104-107 | HEER              | No match       |
| 412.3                             | No match         |                 |         |                   |                |
| 470.4                             | No match         |                 |         |                   |                |
| 507.4                             | No match         |                 |         |                   |                |
| 519.4                             | αA               | T3              | 13-21   | TLGPFYPSR         | <b>Matched</b> |
|                                   | 3OHKyn γA        | T21-22          | 169-174 | RVMDFY(-)         | No match       |
|                                   | 3OHKyn γB        | T20-21          | 169-174 | RVMDFY(-)         | No match       |
| 530.4                             | No match         |                 |         |                   |                |
| 538.4                             | No match         |                 |         |                   |                |
| 546.4                             | βA3              | T6-7            | 59-67   | NFDNVRSLK         | No match       |
| 594.4                             | βB1              | T14             | 124-132 | WDTWSSSYR         | <b>Matched</b> |
|                                   | 3OHKyn αA        | T9              | 71-78   | FVIFLDVK          | No match       |
| 699.0                             | No match         |                 |         |                   |                |
| 712.6                             | 3OHKyn βB2       | T9              | 90-100  | TDSLSSLRPIK       | No match       |
| 881.1                             | 3OHKyn βB1       | T12-13          | 111-123 | GEMFVLEKGEYPR     | No match       |
| 887.7                             | βA4              | T16             | 191-205 | EWGSHAQTFQVQSIR   | No match       |
|                                   | βB3              | T6              | 55-70   | VGSIQVESGPWLA FER | No match       |
| 1004.7                            | βB3              | T20             | 179-194 | HWNEWDANQPQLQSVR  | No match       |
| <b><u>(M+3H)<sup>3+</sup></u></b> |                  |                 |         |                   |                |
| 359.3                             | No match         |                 |         |                   |                |
| 364.6                             | αA               | T13             | 104-112 | QDDHGYISR         | No match       |
|                                   | βA3              | T6-7            | 59-67   | NFDNVRSLK         | No match       |
| 398.3                             | αA               | T2-3            | 12-21   | RTLGPYPSR         | No match       |
|                                   | αB               | T6-7            | 73-82   | DRFSVNLDVK        | <b>Matched</b> |
|                                   | γD               | T19             | 153-162 | YHDWGAMNAK        | No match       |
|                                   | 3OHKyn αB        | T8              | 83-90   | HFSPEELK          | No match       |
|                                   | 3OHKyn γD        | T10             | 80-88   | LIPHAGSHR         | No match       |
| 465.1                             | 3OHKyn βB1       | T14             | 124-132 | WDTWSSSYR         | No match       |
| 479.0                             | No match         |                 |         |                   |                |
| 484.4                             | γA               | T17-18          | 143-153 | QYLLRPGEYRR       | No match       |
|                                   | γB               | T16-17          | 143-153 | QYLLRPGEYRR       | No match       |
| 592.1                             | βB3              | T6              | 55-70   | VGSIQVESGPWLA FER | No match       |
| 670.2                             | No match         |                 |         |                   |                |

The following are examples of peptides that were successfully sequenced using MassLynx from the peak eluting at 50.5 min in the HPLC chromatogram (Figure 3.36). The triply charged ion  $(M+3H)^{3+}$   $m/z$  398.3 was searched for in the database and this  $m/z$  matched the following sequences in bovine crystallin;  $\alpha$ A T2-3 (RTLGPFYPSR),  $\alpha$ B T6-7 (DRFSVNLDVK),  $\gamma$ D T19 (YHDWGAMNAK), 3OHKyn modified  $\alpha$ B T8 (HFSPEELK) and 3OHKyn modified  $\gamma$ D T10 (LIPHAGSHR) (Table 3.3). The MS/MS spectrum of this ion is shown in Figure 3.39 and the fragmentation pattern confirmed that this peptide is  $\alpha$ B T6-7 (DRFSVNLDVK).

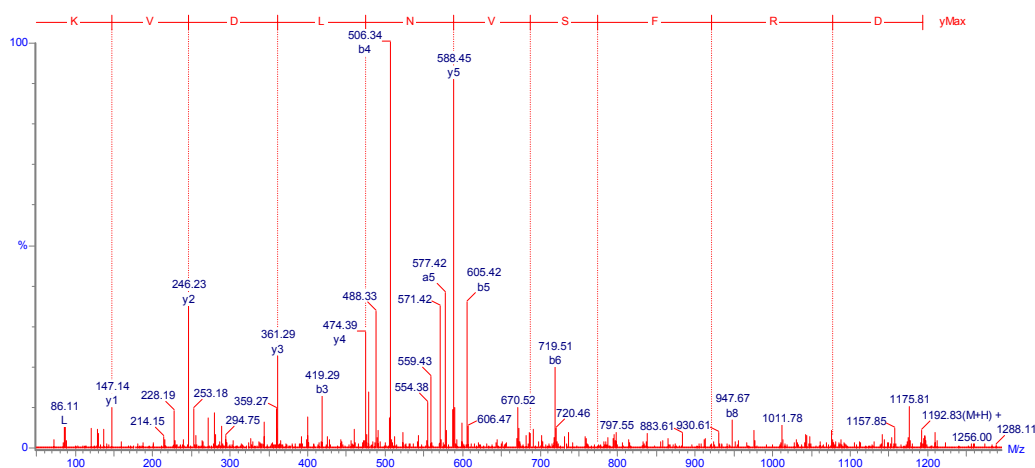


**Figure 3.39** MS/MS spectrum of ion  $(M+3H)^{3+}$   $m/z$  398.3. The sequence confirms that the peptide is  $\alpha$ B T6-7 (DRFSVNLDVK).

Similarly, the doubly charged ion  $(M+2H)^{2+}$   $m/z$  519.4 was searched for in the database and it matched the following sequences in bovine crystallin;  $\alpha$ A T3 (TLGPFYPSR), 3OHKyn modified  $\gamma$ A T21-22 (RVMDFY(-)) and 3OHKyn modified  $\gamma$ B T20-21 (RVMDFY(-)) (Table 3.3) whereby tyrosine (Y) is also a known nucleophilic amino acid. The MS/MS spectrum of this ion is shown in Figure 3.40 and the fragmentation pattern confirmed that this peptide is  $\alpha$ A T3 (TLGPFYPSR).

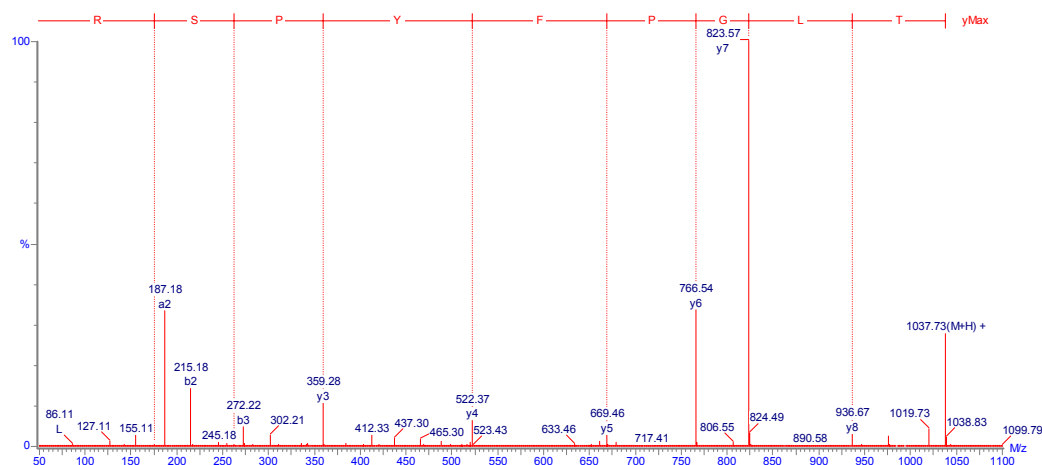


**Figure 3.40** MS/MS spectrum of ion  $(M+2H)^{2+}$   $m/z$  519.4. The sequence confirms that the peptide is  $\alpha$ A T3 (TLGPFYPSR).

Finally, the doubly charged ion  $(M+2H)^{2+}$   $m/z$  594.4 was searched for in the database and it matched the following possible sequences in bovine crystallin;  $\beta$ B1 T14 (WDTWSSSYR) and 3OHKyn modified  $\alpha$ A T9 (FVIFLDVK). The MS/MS spectrum of this ion is shown in Figure 3.41 and the fragmentation pattern confirmed that this peptide is  $\beta$ B1 T14 (WDTWSSSYR).

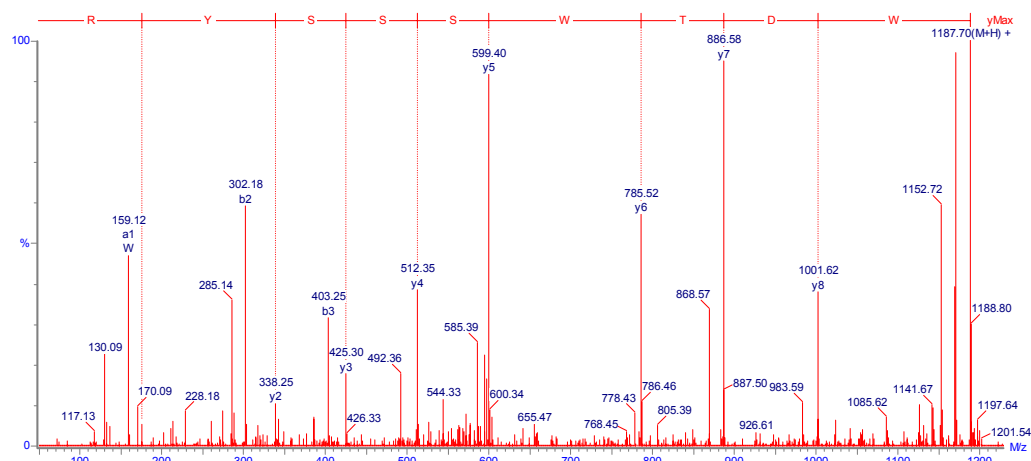


**Figure 3.41** MS/MS spectrum of ion  $(M+2H)^{2+}$   $m/z$  594.4. The sequence confirms that the peptide is  $\beta$ B1 T14 (WDTWSSSYR).

3OHKyn is unstable at pH 7.2, and  $\text{H}_2\text{O}_2$  is produced as a by-product from this reaction.<sup>181,184</sup> This can result in oxidation of the protein. Peptides thought to be modified by 3OHKyn were identified from the database. However the database was not designed to also consider the peptides containing oxidised amino acid residues (for example, methionine and tryptophan). Since there are 3 major types of crystallins in the bovine lens *i.e.*  $\alpha$ ,  $\beta$  and  $\gamma$ , and all with subtypes, the results here established it would be a difficult task to try and identify peptides modified with 3OHKyn from whole CLP, containing all of the crystallins. In order to simplify the task of detecting 3OHKyn modified peptides we decided to look at one crystallin ( $\alpha$ ) modified with 3OHKyn (see Section 3.3.8), and attempt to identify the 3OHKyn-modified peptides.

### 3.3.8 Bovine $\alpha$ -Crystallin Modified with 3OHKyn

Crystallin peptides modified with Kyn and 3OHKynG have been identified previously from *in vitro*<sup>110,111</sup> and *in vivo*<sup>112</sup> studies respectively. The major sites of modification were at Cys, and His amino acid residues. The aim of this present study was to identify 3OHKyn-modified peptides in  $\alpha$ -crystallin. Bovine  $\alpha$ -crystallin was therefore incubated with 3OHKyn at pH 7.2, for 48 hours under low oxygen tension. This was achieved by bubbling the solution with argon for 5 min whereby after this time the oxygen level had fallen to 40 mm Hg (measured with a Strathkelvin electrode). An initial aliquot was taken at time zero for mass spectral analysis, and after 48 hours of incubation the remaining mixture was separated into its component products by HPLC. The HPLC chromatogram (Figure 3.42A) of the sample removed at time zero contained three major peaks. The first peak eluted at 7.5 min and mass spectrometry showed that the molecular ion of this peak was  $m/z$  225, which is the molecular ion for unmodified 3OHKyn. The second peak eluted at 24.8 min and the third peak eluted at 27.3 min. The transformed mass spectrum (Figure 3.43A) of the peak at 24.8 min contained three major species with observed masses of 20,078 Da (native  $\alpha$ B-crystallin), 20,159 Da (phosphorylated  $\alpha$ B-crystallin) and 20,238 Da (doubly phosphorylated  $\alpha$ B-crystallin). The transformed mass spectrum (Figure 3.44A) of the peak eluting at 27.3 min in the HPLC chromatogram gave rise to two peaks with observed masses of 19,831 Da (native  $\alpha$ A-crystallin) and 19,911 Da (phosphorylated  $\alpha$ A-crystallin).

After 48 hours of incubation, the control samples ( $\alpha$ -crystallin without 3OHKyn) showed no change in either their HPLC profiles or in the mass spectra of the separated  $\alpha$ A- and  $\alpha$ B-crystallins (not shown). The HPLC chromatogram (Figure 3.42B) of the  $\alpha$ -crystallin/3OHKyn reaction mixture after 48 hours of incubation, exhibited numerous minor peaks eluting between 7.5 min and ~18 min. The peak at 7.5 min was due to 3OHKyn,<sup>181</sup> and most of the minor peaks were identified as oxidation products of 3OHKyn. Peaks that could not be readily identified were not investigated further.

Two major products also eluted close to the retention times of the unmodified  $\alpha$ A- and  $\alpha$ B-crystallins, however the peaks were broader (Figure 3.42B). The transformed mass spectrum (Figure 3.43B) of the product eluting at 24.4 min contained a number of

species of mass greater than that of native  $\alpha$ B-crystallin. Previous work has shown that, at pH 7, 3OHKyn undergo facile loss of ammonia from the amino acid side chain, yielding deaminated 3OHKyn.<sup>109</sup> The deaminated 3OHKyn contains an  $\alpha,\beta$ -unsaturated moiety that is susceptible to nucleophilic attack. The predicted mass of bovine  $\alpha$ B-crystallin modified with one deaminated 3OHKyn is 20,285 Da. Only a very minor peak among the spectrum noise was observed at this mass, whereas the major species that were observed had masses of 20,110 Da and 20,192 Da (Figure 3.43B). These masses are 32 Da higher than the mass of native and phosphorylated  $\alpha$ B-crystallin respectively. Analysis of the smaller peaks in the spectrum showed that there were further incremental mass increases of 16 Da, with a total of up to 64 Da for both the native and phosphorylated  $\alpha$ B-crystallin. This result suggested that oxidation of methionine (Met) and/or tryptophan (Trp) residues had occurred in the presence of 3OHKyn, whereas no such oxidation was observed in the control experiment.

The transformed mass spectrum (Figure 3.44B) of the product eluting at 27.3 min also exhibited numerous species. The predicted mass of bovine  $\alpha$ A-crystallin modified with deaminated 3OHKyn is 20,038 Da. A peak at this mass can be seen in the transformed mass spectrum, as well as a peak corresponding to the 3OHKyn-modified phosphorylated  $\alpha$ A-crystallin at 20,118 Da. However these were not the major components in the spectrum. The major species that were observed had masses of 19,863 Da and 19,943 Da (Figure 3.44B). These masses correspond to double oxidations (*i.e.* addition of 32 Da) of the native and phosphorylated  $\alpha$ A-crystallin.

The modified  $\alpha$ B-crystallin was freeze dried, similarly the modified  $\alpha$ A-crystallin was also freeze dried. Figure 3.45 shows a photograph of the modified  $\alpha$ A- and  $\alpha$ B-crystallin proteins. The photograph shows that the proteins were pink in colour, which indicates that modification of the proteins had occurred, since native  $\alpha$ -crystallin is white.

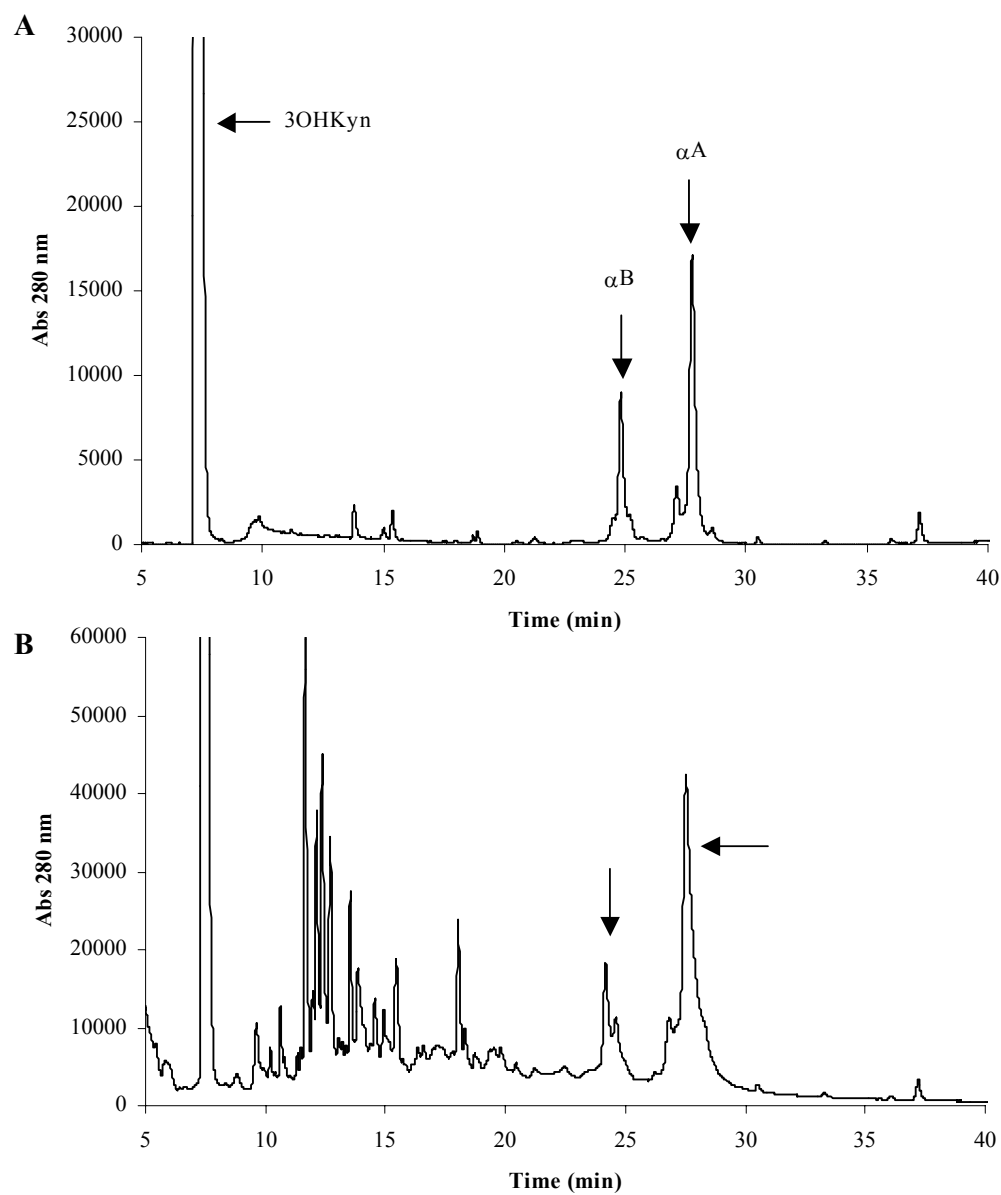


**Figure 3.42**  $\alpha$ -Crystallin was modified with 3OHKyn at 37 °C for 48 hours. *A*, HPLC chromatogram of the initial aliquot of the reaction mixture at time zero; *B*, HPLC chromatogram of the reaction mixture after incubation for 48 hours.

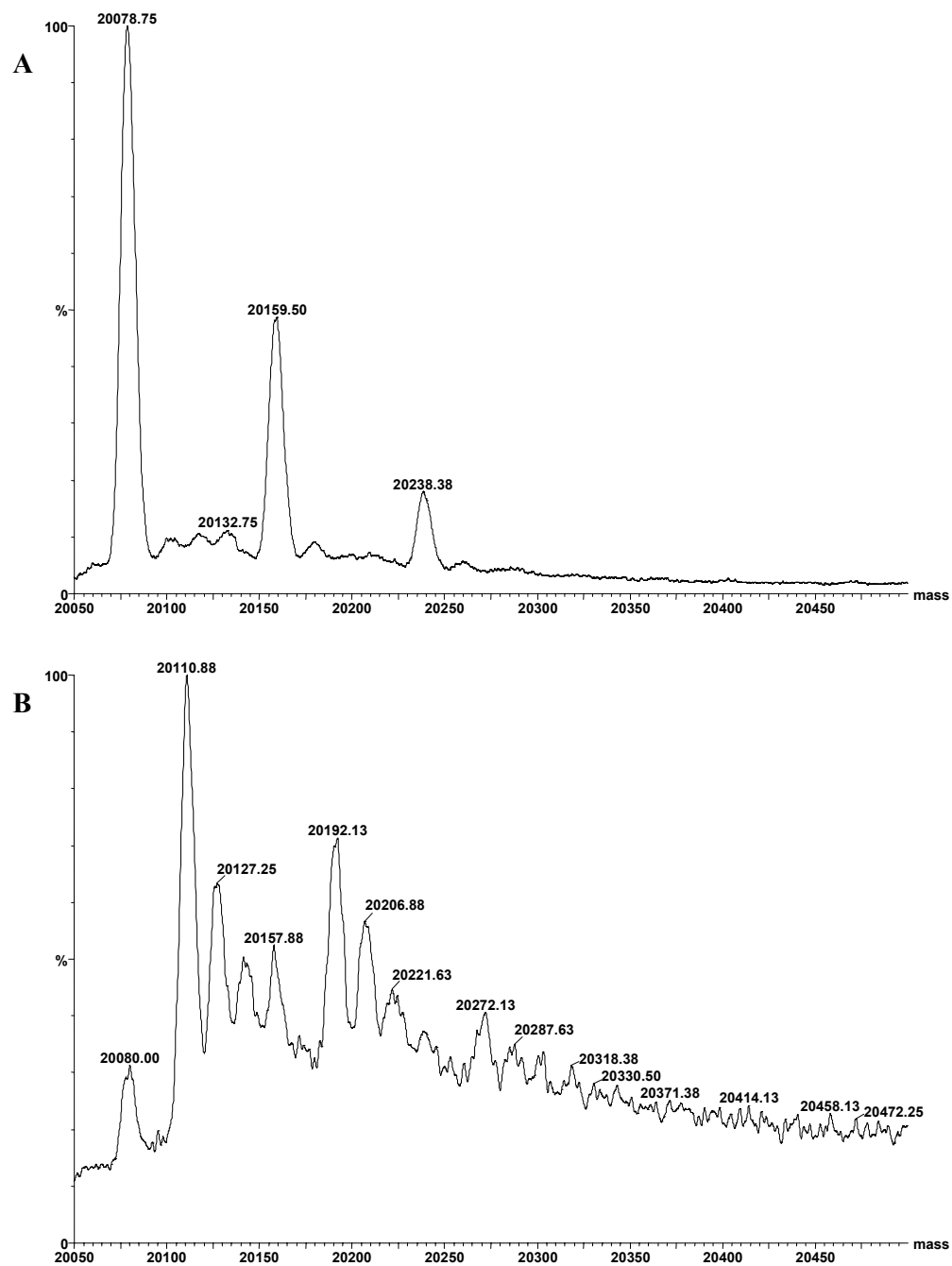


**Figure 3.43** Transformed mass spectra. *A*, Native bovine  $\alpha$ B-crystallin; *B*, Modified bovine  $\alpha$ B-crystallin.



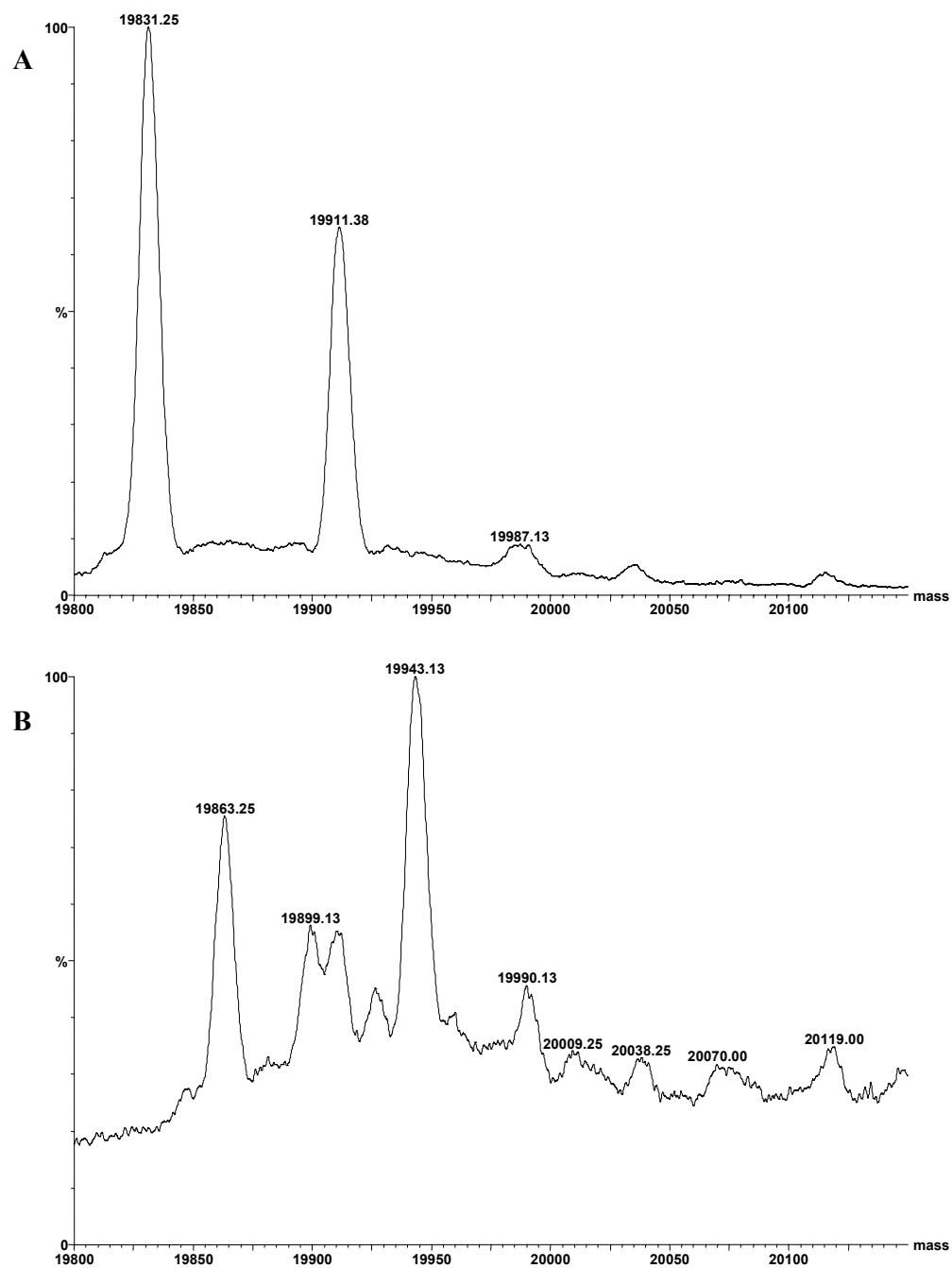


**Figure 3.44** Transformed mass spectra. *A*, Native bovine  $\alpha$ A-crystallin; *B*, Modified bovine  $\alpha$ A-crystallin.

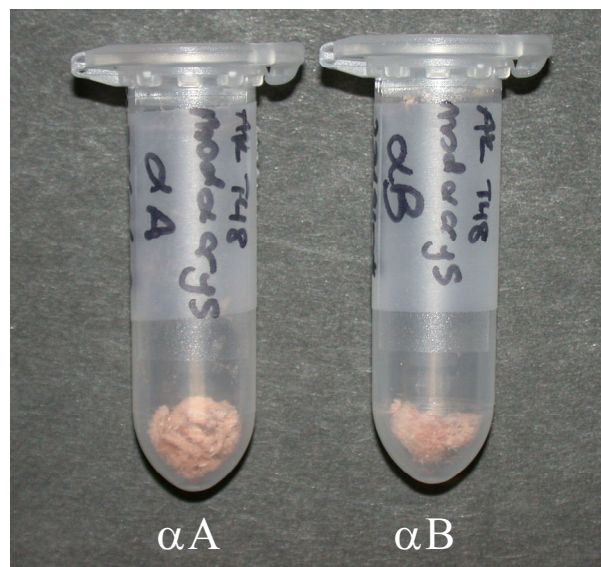


**Figure 3.45** Photograph of modified  $\alpha$ -crystallins. Bovine  $\alpha$ -crystallin was incubated with 3OHKyn at 37°C for 48 hours under low oxygen tension. Native  $\alpha$ -crystallin is white in colour. As shown, the modified  $\alpha A$ - and  $\alpha B$ -crystallins are pink in colour, and were purified by HPLC.

### 3.3.9 Tryptic Digestion of Modified $\alpha$ A-Crystallin

3OHKyn-modified  $\alpha$ A-crystallin purified by HPLC was digested with trypsin in 50 mM ammonium bicarbonate solution, pH 8.0 for three hours. This short time was chosen since 3OHKyn autoxidises quite readily.<sup>181,184</sup> The HPLC chromatogram of the trypsin digest is shown in Figure 3.46 and the peaks were monitored at 229 nm.

The transformed mass spectra (Section 3.3.8) suggested that the modified  $\alpha$ A-crystallin had oxidised possibly at Met residues to form Met sulphoxide ( $M_{ox}$ ). Previous studies have also shown that tryptophan may also oxidise to give oxidised tryptophan ( $W_{ox}$ )<sup>199-204</sup> *i.e.* addition of one oxygen atom anywhere on either ring. Therefore masses of all of the expected possible oxidised and non-oxidised peptides were determined, and the doubly charged molecular ions were calculated, and used as markers when each of the peaks collected from the HPLC were analysed by nanoelectrospray ionisation mass spectrometry (nanoESI-MS).

A major peak eluted at 56.5 min on the HPLC chromatogram (Figure 3.46). NanoESI-MS of this peak showed that there was an abundant  $m/z$  722.5 ion, which was doubly charged ( $M+2H$ )<sup>2+</sup>. This ion corresponded to peptide 1-11 (Ac- $M_{ox}$ DIAIQHPWFK) in which the Met was present as a sulphoxide ( $M_{ox}$ ) and the Trp was intact. The MS/MS spectrum of this peptide is shown in Figure 3.47. The majority of the predicted b and y ions were observed in the spectrum. This N-terminal peptide is acetylated. A characteristic neutral loss of 64 Da ( $CH_3SOH$ ) is observed from  $M_{ox}$ . A close examination of the MS/MS spectrum (Figure 3.47) showed that all of the b ions ( $b_{1-10}$ ) exhibited neutral losses of 64 Da. The abundance of these ions was however much lower than that of the normal b ions.

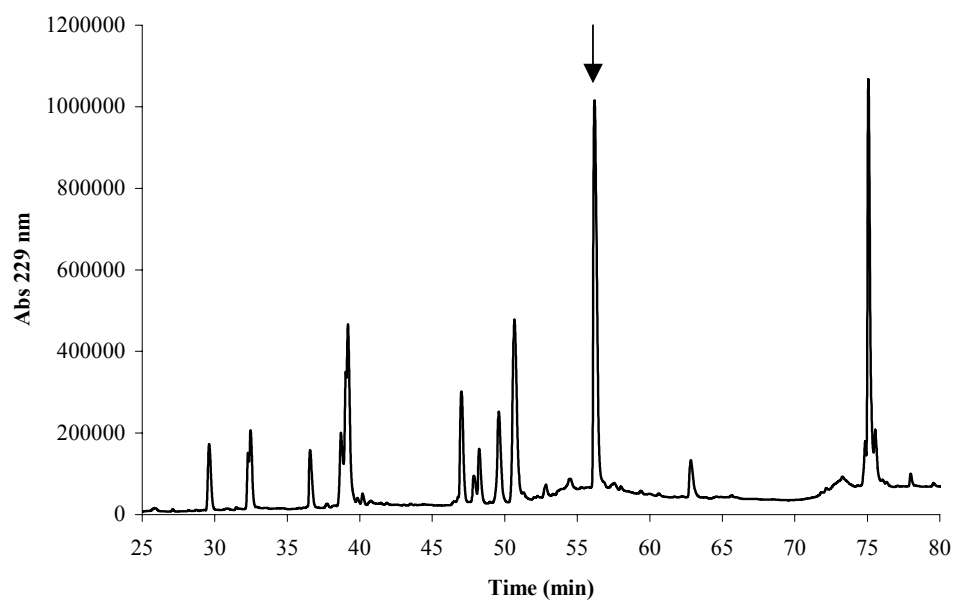


**Figure 3.46** HPLC chromatogram of tryptic digest products of  $\alpha$ A-crystallin following modification with 3OHKyn. Arrow indicates the peak that contained a peptide with an oxidised amino acid residue.

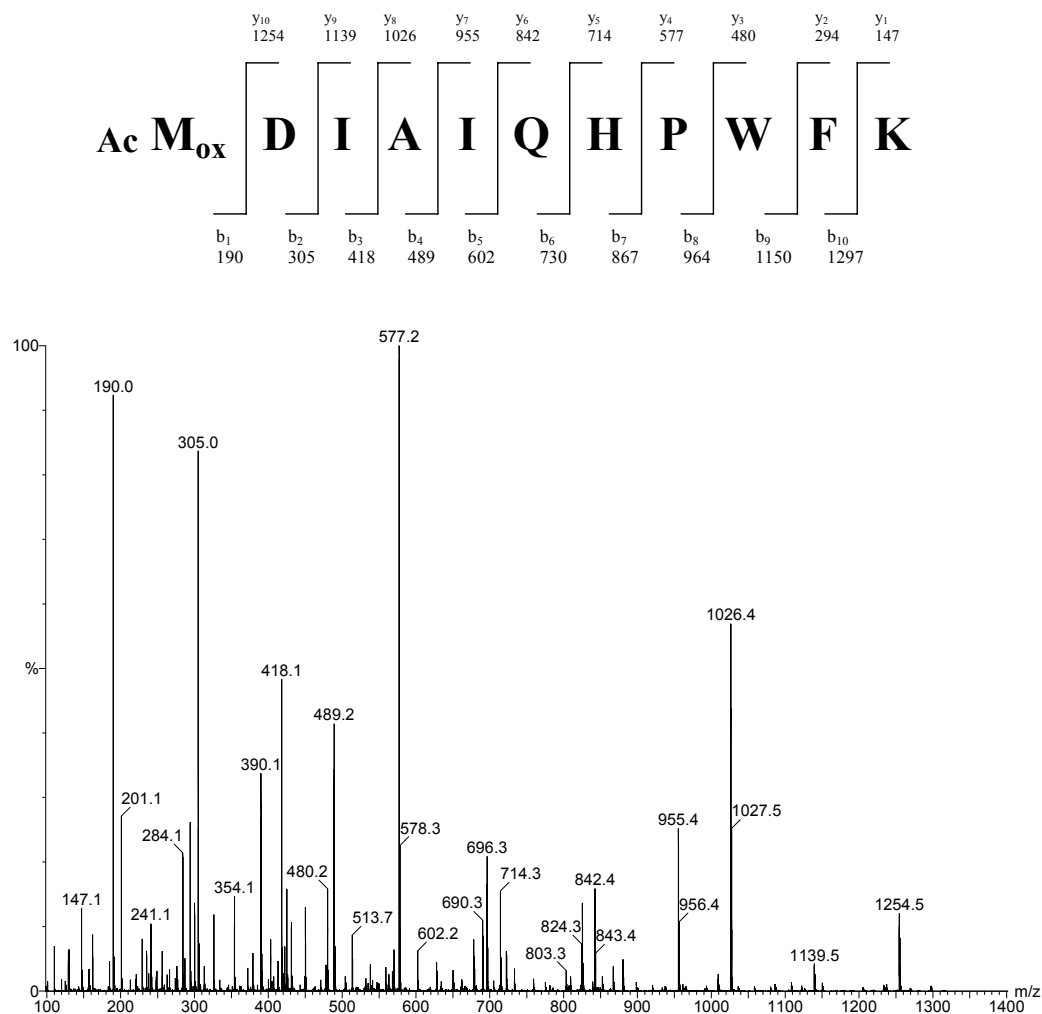


**Figure 3.47** MS/MS spectrum of an oxidised  $\alpha$ A-crystallin peptide, residues 1-11, showing oxidation at Met1. The sequence for this peptide is shown above the spectrum.

Bovine  $\alpha$ A-crystallin has two Met residues. The oxidised N-terminal Met peptide has been observed (Figure 3.47), however the second Met residue belongs to peptide 120-145 (LPSNVDQSALSCSLSadGMLTFSGPK), which also contains a Cys residue (and is therefore a possible site of UV filter modification). The mass of the doubly charged peptide 120-145 including oxidation of Met138 is  $m/z$  1321, and the doubly charged mass of the peptide including oxidation of Met138 and 3OHKyn modification of Cys131 is  $m/z$  1425. Analysis of all HPLC peaks (Figure 3.46) failed to show either of these two masses. Therefore, in order to identify this peptide, the peptide mixture was analysed directly by nanoESI-MS (Figure 3.48). The  $(M+2H)^{2+}$  ion at  $m/z$  722.5 was observed (N-terminal oxidised peptide). A doubly charged ion  $m/z$  1321.9 (Figure 3.48 inset) was observed, corresponding to  $\alpha$ A-crystallin residues 120-145 containing oxidised Met138. The MS/MS spectrum (Figure 3.49) of this peptide confirmed its identity. The mass of  $y_9$  is  $m/z$  953.8, and a neutral loss of 64 Da yields mass  $m/z$  889.7 ( $y_9-64$ ), which shows that Met138 is indeed oxidised.

Close examination of the mass spectral inset in Figure 3.48 revealed that an ion was present at  $m/z$  1425.4, corresponding to peptide 120-145 with both an oxidised Met138, and a covalently attached 3OHKyn. This ion was not sufficiently abundant to obtain useful MS/MS data, thus acid hydrolysis was employed to confirm the site and relative proportion of modification by 3OHKyn.

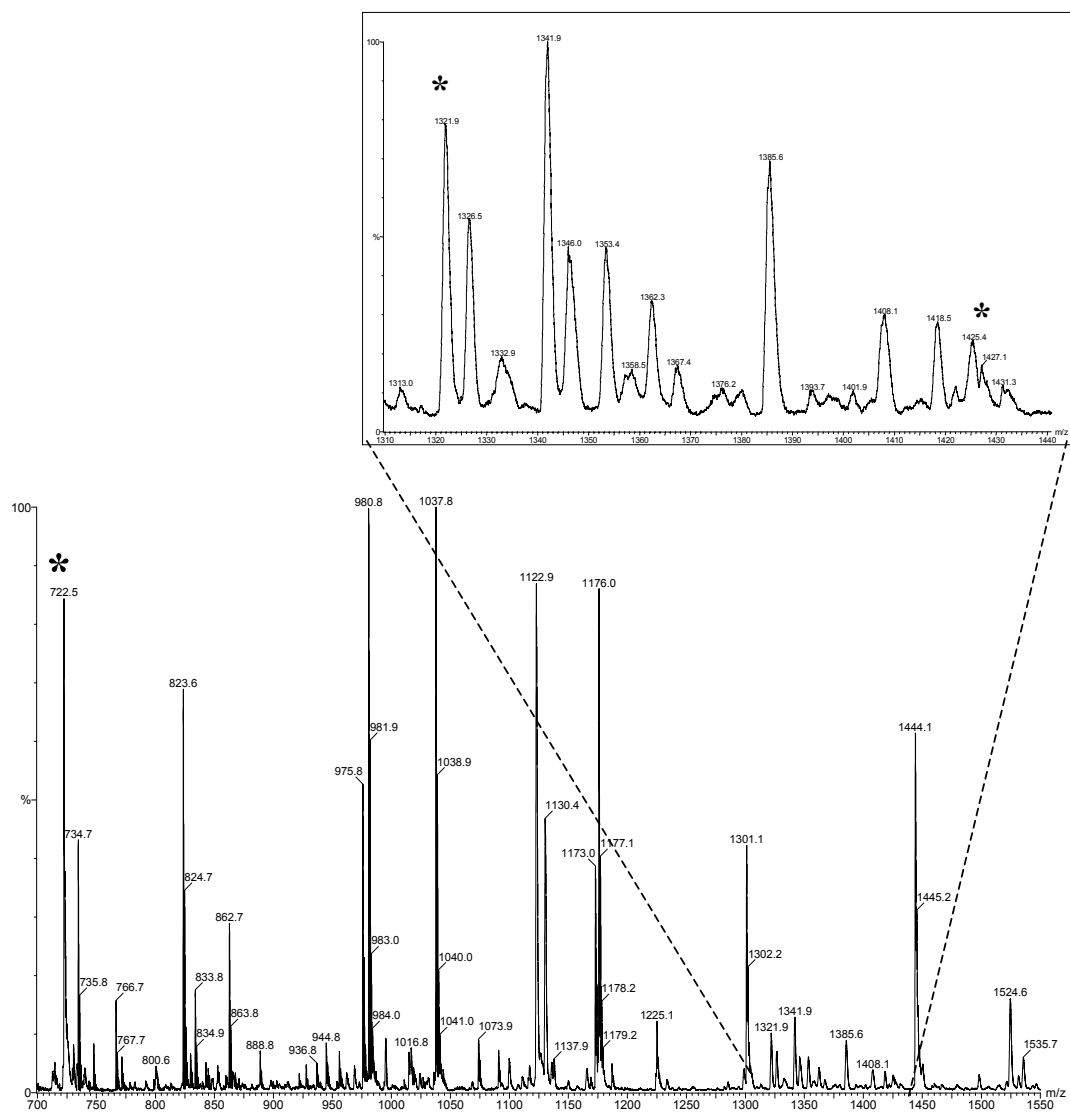


**Figure 3.48** nanoESI-MS spectrum of tryptically digested 3OHKyn-modified  $\alpha$ A-crystallin.

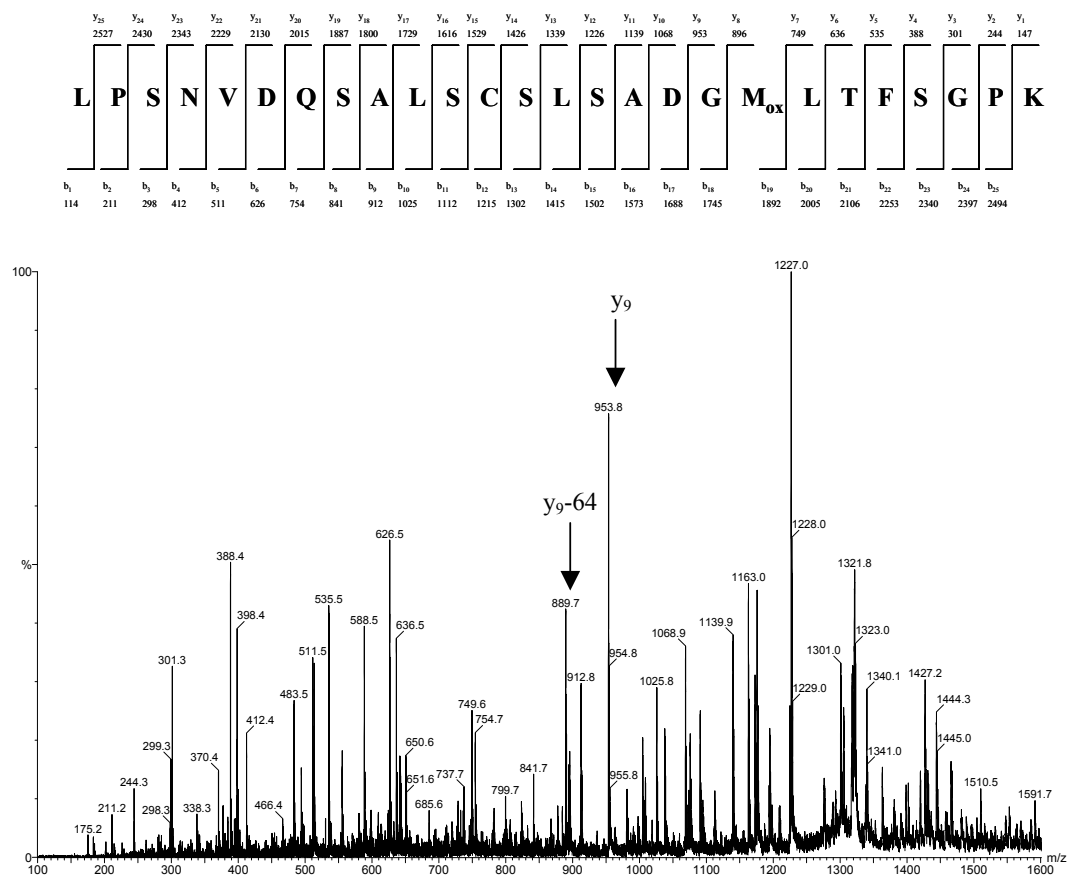


**Figure 3.49** MS/MS spectrum of an oxidised  $\alpha$ A-crystallin peptide, residues 120-145, showing oxidation at Met138.



### 3.3.10 Acid Hydrolysis of Modified $\alpha$ A-Crystallin

$\alpha$ -Crystallin, which had been modified with 3OHKyn and purified by HPLC, was hydrolysed with HCl containing antioxidants. The HPLC chromatogram (Figure 3.50) of the modified  $\alpha$ A-crystallin hydrolysate exhibited a doublet peak eluting at 28.4 min, the retention time corresponding to 3OHKyn-Cys. Mass spectrometry of these two peaks revealed a prominent ion at  $m/z$  329, and MS/MS of this ion confirmed it to be 3OHKyn-Cys. Quantification of material eluting in this doublet showed that there were 0.089 moles of 3OHKyn-Cys per mole of  $\alpha$ A-crystallin, *i.e.* 8.9% of the protein was modified by 3OHKyn. This value corresponds to the relative abundance of the oxidised 3OHKyn-modified and oxidised  $\alpha$ A-crystallin ions observed in the mass spectrum (Figure 3.48 inset) of the tryptic digest (*i.e.* ion  $m/z$  1425.4 is approximately one-tenth the abundance of ion  $m/z$  1321.9).

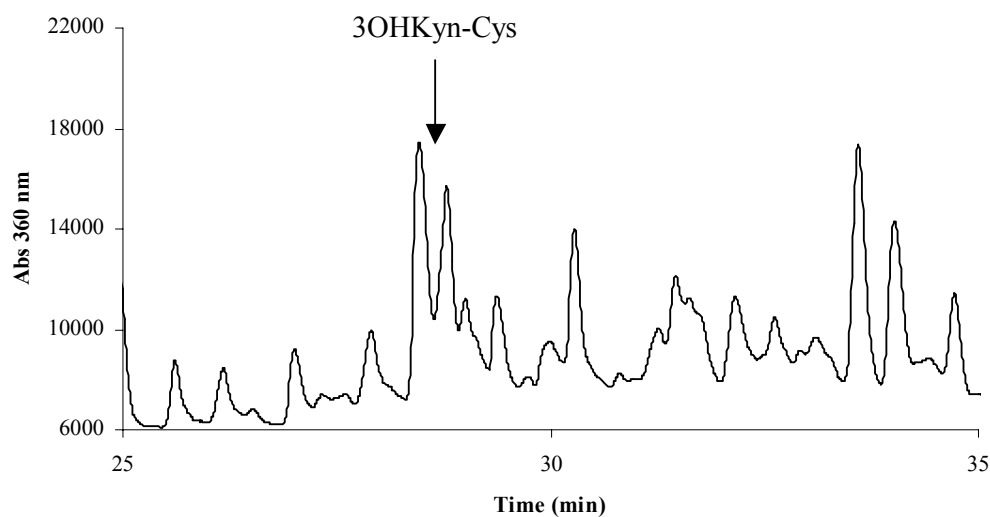


**Figure 3.50** HPLC chromatogram of acid hydrolysed 3OHKyn-modified  $\alpha$ A-crystallin.

### 3.3.11 Tryptic Digestion of Modified $\alpha$ B-Crystallin

In order to confirm that oxidation was responsible for the 16 Da mass increases observed in the transformed mass spectrum, the 3OHKyn-modified  $\alpha$ B-crystallin was also digested with trypsin. The HPLC chromatogram of the tryptic digest is shown in Figure 3.51. The masses of all of the predicted native and modified tryptic peptides were calculated and subsequently used to identify modified species in the HPLC peaks.

A major peak eluted at 52.8 min (Figure 3.51). NanoESI-MS of this peak showed that there was a doubly charged molecular ion  $(M+2H)^{2+}$   $m/z$  723.8, which corresponded to peptide 1-11 (Ac-M<sub>ox</sub>DIAIHHPWIR) whereby the Met had formed a sulfoxide (M<sub>ox</sub>) and Trp was unoxidised. The MS/MS spectrum of this peptide is shown in Figure 3.52. Neutral loss of 64 Da was observed for all of the b ions.

The doubly charged molecular ion  $(M+2H)^{2+}$   $m/z$  731.8 eluted at 51.2 min on the HPLC (Figure 3.51). This ion corresponds to peptide Ac-M<sub>ox</sub>DIAIHHPW<sub>ox</sub>IR in which the Met is present as a sulfoxide (M<sub>ox</sub>) and Trp has the addition of an oxygen atom (W<sub>ox</sub>). The MS/MS spectrum of this peptide is shown in Figure 3.53. A neutral loss of 64 Da was observed for the b ions b<sub>1-8</sub>, however neutral losses for b<sub>9</sub> and b<sub>10</sub> were not observed.

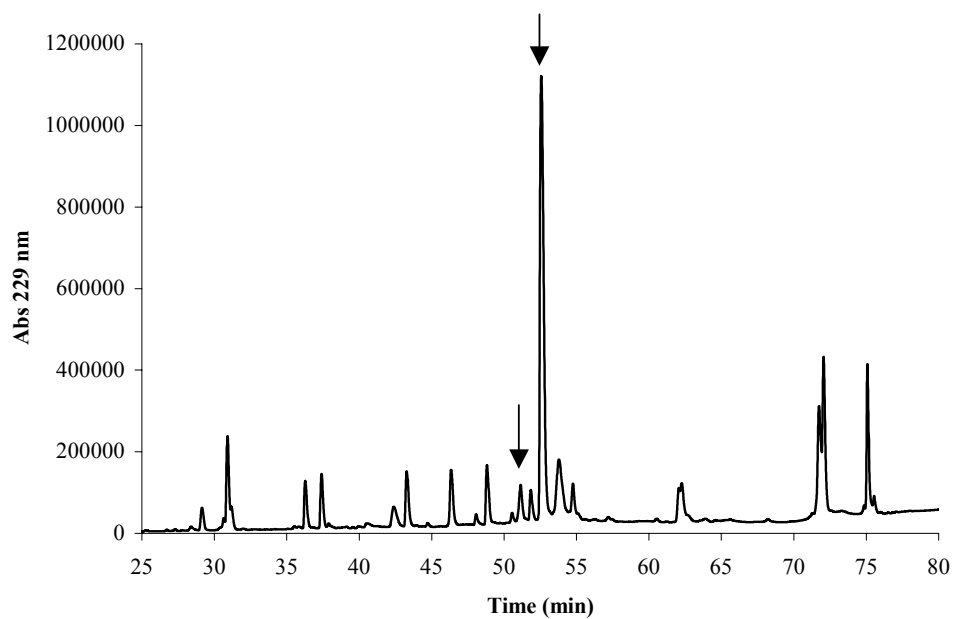


**Figure 3.51** HPLC chromatogram of tryptic digest products of  $\alpha$ B-crystallin after modification with 3OHKyn. Arrows indicate peaks that contained peptides with oxidatively modified amino acid residues.

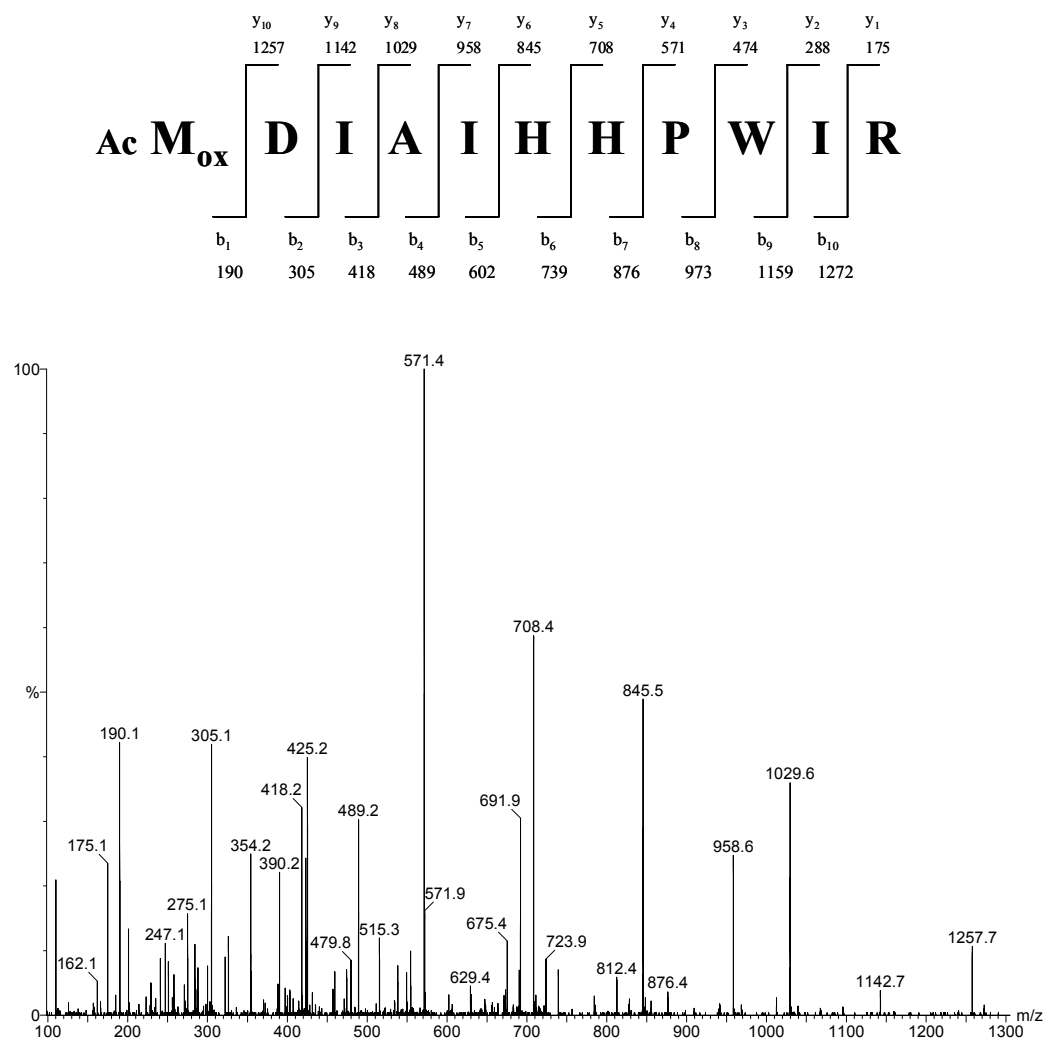


**Figure 3.52** MS/MS spectrum of an oxidised  $\alpha$ B-crystallin peptide, residues 1-11, showing oxidation at Met1.

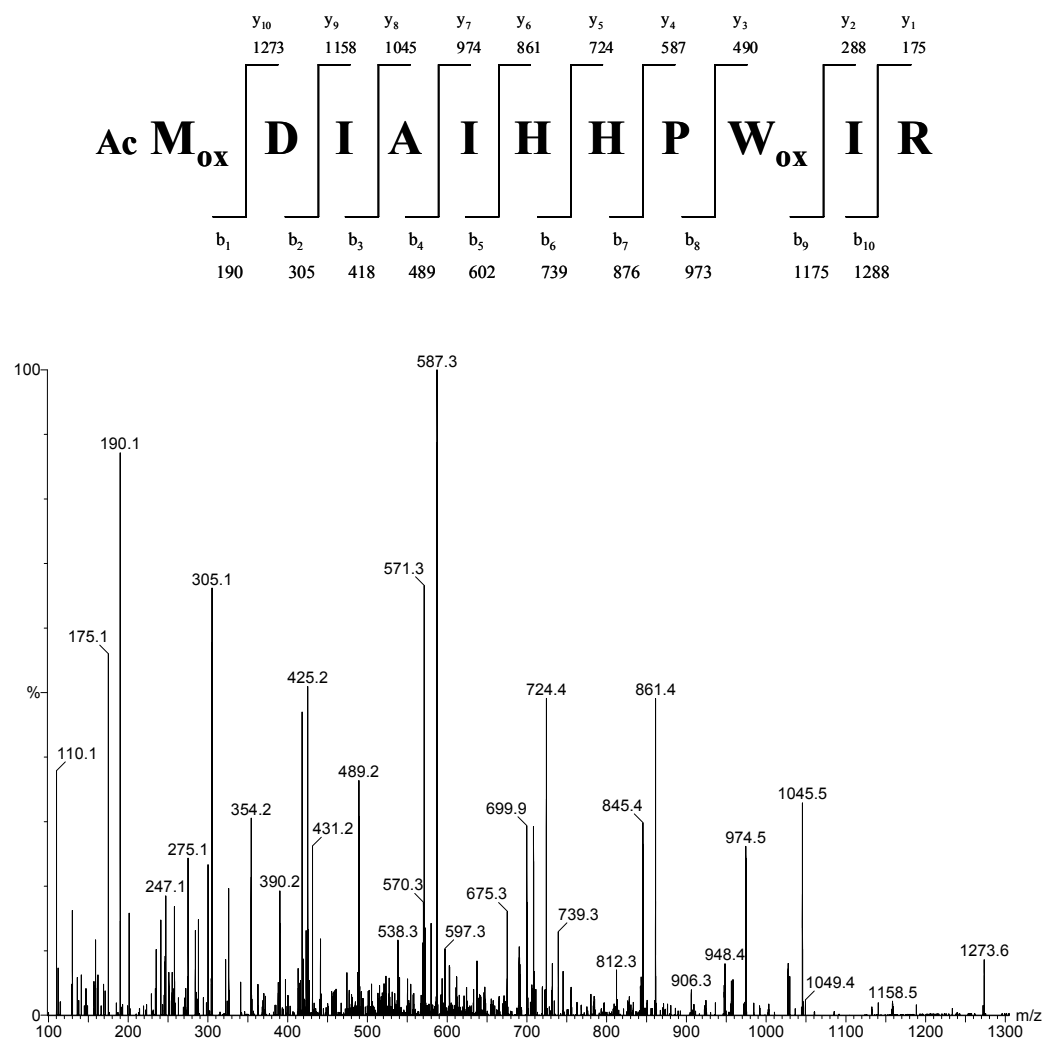


**Figure 3.53** MS/MS spectrum of an oxidised  $\alpha$ B-crystallin peptide, residues 1-11, showing oxidation at Met1 and Trp9.

The second Met residue in bovine  $\alpha$ B-crystallin is Met68 within the tryptic peptide 57-69 (APSWIDTGLSEMR). This peptide also contains a Trp residue at Trp60.

A doubly charged molecular ion  $m/z$  739.8 eluted at 51.2 min on the HPLC chromatogram (Figure 3.51). This ion corresponds to peptide APSWIDTGLSEM<sub>ox</sub>R. The Met has formed a sulphoxide (M<sub>ox</sub>) and Trp is unoxidised. The MS/MS spectrum of this peptide is shown in Figure 3.54. A neutral loss of 64 Da was observed for all of the y ions (y<sub>2-12</sub>) except for y<sub>1</sub>, which is arginine. The neutral loss y ions were very abundant ions in the MS/MS spectrum. The b ions were observed, but were not as abundant as the y ions or the neutral loss y ions.

Co-eluting in the same HPLC peak (51.2 min Figure 3.51) was an (M+2H)<sup>2+</sup> ion of  $m/z$  747.8. This ion corresponds to peptide APSW<sub>ox</sub>IDTGLSEM<sub>ox</sub>R. The Met has formed a sulphoxide (M<sub>ox</sub>) and Trp is oxidised (W<sub>ox</sub>). The MS/MS spectrum of this peptide is shown in Figure 3.55. A neutral loss of 64 Da was also observed for y<sub>2-12</sub>, and these ions were again abundant ions in the MS/MS spectrum. The b ions were approximately the same intensity as the y ions. However only b<sub>1-6</sub> ions (APSW<sub>ox</sub>ID) could be observed, the remaining b ions (b<sub>7-12</sub>) could not be observed.

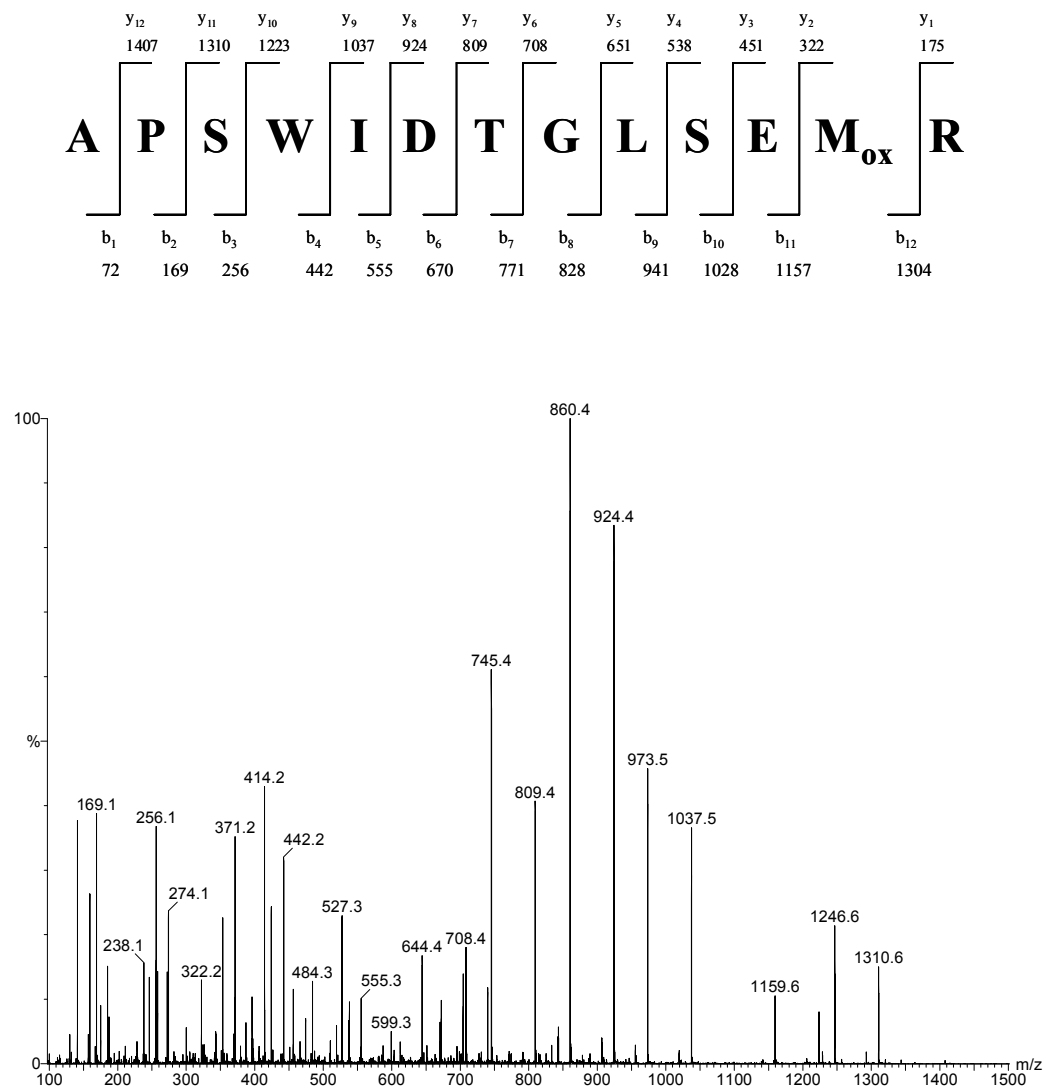


**Figure 3.54** MS/MS spectrum of an oxidised  $\alpha$ B-crystallin peptide, residues 57-69, showing oxidation at Met68.

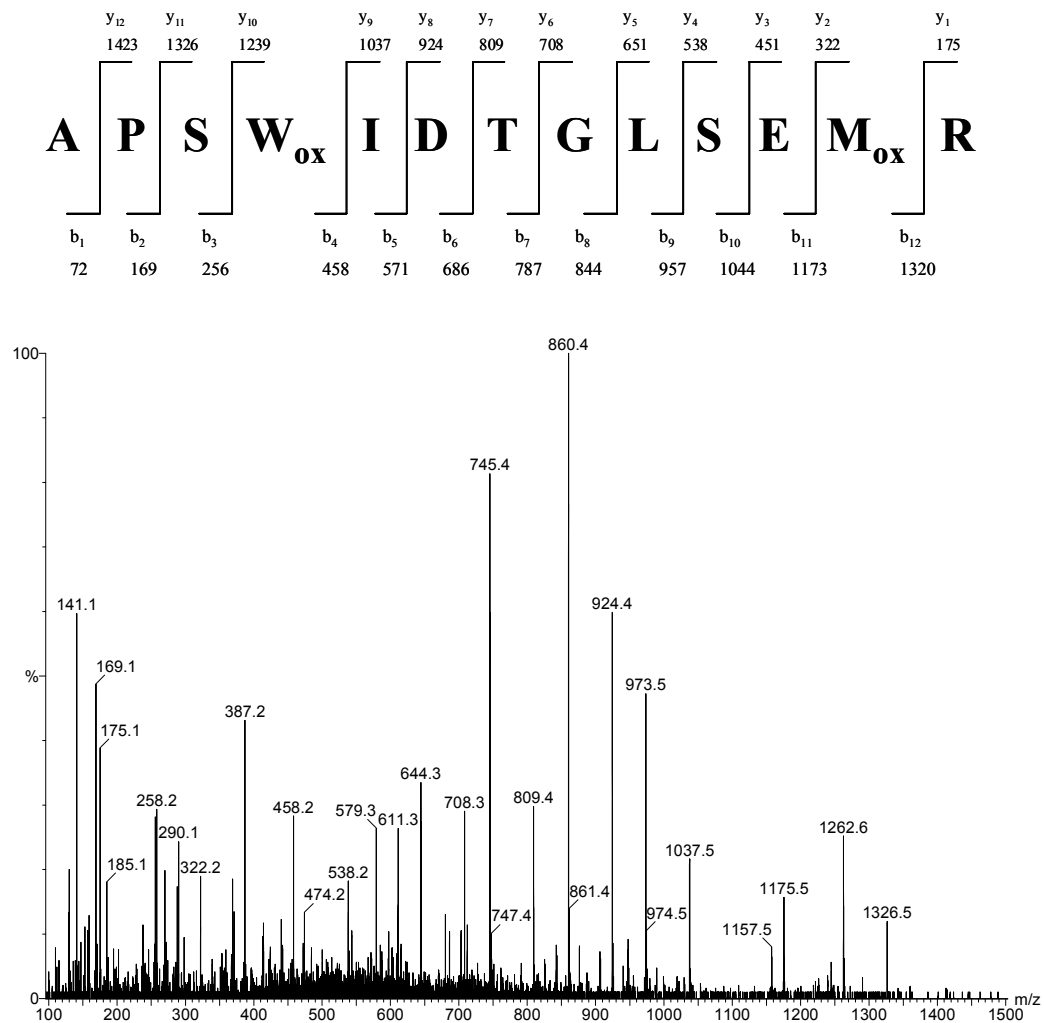


**Figure 3.55** MS/MS spectrum of an oxidised  $\alpha$ B-crystallin peptide, residues 57-69, showing oxidation at Met68 and Trp60.



### 3.4 Discussion

In Chapter 2, 3OHKyn amino acid adducts were synthesised and characterised. It was also demonstrated that the amino acid adducts were relatively unstable under physiological conditions, but that 3OHKyn adducts were recovered in good yields using acid hydrolysis in the presence of antioxidants.

One aim of this chapter was to modify lens proteins with 3OHKyn and identify the sites of attachment using acid hydrolysis and tryptic digestion.

#### *Modification of Proteins*

CLP was modified with 3OHKyn using the method of Vazquez, *et al.*<sup>103</sup> Bovine lens crystallins were used in these studies, since there is a large degree of sequence homology between bovine and human crystallins, and bovine lenses do not metabolise Trp and therefore do not contain UV filters.<sup>73</sup> The protein was initially modified at pH 7.2 for 48 hours. Acid hydrolysis showed that modification had occurred primarily at Cys. The protein was also modified at pH 9.5, since higher pH increases the rate of deamination of the UV filter amino acid side chain.<sup>85,187</sup> Acid hydrolysis showed that modifications had occurred at Cys, His and Lys residues. These findings are analogous to the findings of Vazquez, *et al.* whereby Kyn also modifies CLP at Cys, His and Lys residues at pH 9.5.<sup>103</sup> The colours of the 3OHKyn-modified proteins were of interest. Normal CLP is white in colour, however protein modified by 3OHKyn is brown when modified at pH 9.5. When modifications are done at pH 7.2 the protein was pink (Figure 3.1) but becomes brown (Figure 3.33) when protein aliquots are ultra-filtered in a centrifuge. The proteins modified by 3OHKyn at pH 7.2 and 9.5 were characterised with UV-visible and 3-D fluorescence spectroscopy. Protein modified at pH 7.2 exhibited a broad peak with a maximum absorbance centred at 370 nm. This absorbance was similar to the UV-visible absorbance of each of the 3OHKyn amino acid adducts (Section 2.3.5). The 3-D fluorescence data for protein modified at pH 7.2, is also comparable to the 3-D fluorescence data for each of the 3OHKyn amino acid adducts. The UV-visible spectrum of the protein modified at pH 9.5, exhibited a broad peak with a wavelength maximum centred at 369 nm. The 3-D fluorescence spectrum exhibited a maximal fluorescence intensity at Ex 360 nm/Em 485 nm, which is again comparable to

the data for each the 3OHKyn amino acid adducts. The SDS-PAGE data (Figure 3.2) before and after reduction of the modified proteins showed that the original CLP contained some disulfide-bond linkages, but modification of the protein with 3OHKyn did not result in the formation of non-disulfide crosslinks. It has previously been shown that crosslink formation occurs following incubation of CLP with Kyn.<sup>179</sup>

3OHKyn was incubated with CLP over a total of 24 days at pH 7.2. After three days of incubation, Cys was the major site of modification, and coinciding with this modification, the content of PSH decreased to 0.34 moles SH per mole of protein from the initial 2.5 moles SH per mole protein (Figure 3.35). After six days of incubation, modifications of Lys and His were observed (Figure 3.34). His and Lys modifications occurred when the availability of Cys residues had diminished, due probably to disulfide-bond linkages. The findings (Figure 3.34) of this experiment showed that 3OHKyn-His is the most stable adduct of the three. In addition, the stability studies in Chapter 2 showed that the Lys and Cys adducts were unstable at pH 7.2, however in the presence of protein, these adducts could still be recovered after 24 days of incubation. Over the incubation period the level of these two adducts decreased steadily. It is unknown if these adducts would still be recovered if the incubation were undertaken over a longer period of time, for example, 3 months, and if these adducts are present in the human lens. On the basis of pKa alone, it is anticipated that the order of reactivity of amino acids towards UV filters at pH 7 would be His (pKa 6.5), Cys (pKa 8.5) and Lys (pKa 10.0).<sup>205</sup> However the thiol group is a good nucleophile, due to the presence of high-energy nonbonding lone pairs of electrons.<sup>206</sup> Other systems have also shown that at physiological pH, the relative order of nucleophilicity to be Cys>His>Lys. For example, 4-hydroxynonenal, a lipid aldehyde reacts with proteins at nucleophilic sites via a Michael addition in atherosclerosis and diabetes.<sup>207</sup> Acrolein, an  $\alpha,\beta$ -unsaturated aldehyde, also reacts with proteins, preferentially modifies Cys residues, and modifications at His and Lys have also been observed.<sup>208</sup>

#### *Human Lens Data*

As mentioned, 3OHKyn amino acid adducts can be recovered from acid hydrolysates in good yields provided antioxidants are included. Previously, Vazquez, *et al.* acid

hydrolysed human lens nuclei of various ages, and identified Kyn-His and Kyn-Lys adducts. The concentration of these adducts were found to increase with age.<sup>103</sup> Therefore, acid hydrolysis of human lens nuclei with antioxidants was undertaken. A doublet peak corresponding to 3OHKyn-Cys was observed by HPLC in the hydrolysate of aged human lens protein (Figure 3.6B). Its identity was confirmed by MS/MS. However, this experiment cannot distinguish whether the 3OHKyn-Cys was derived from 3OHKyn attached to Cys residues of proteins, or whether, it was in fact 3OHKynG-Cys; since the glucoside bond, if present, will also be hydrolysed by acid.<sup>209</sup> Previous studies using pH 6.0 tryptic digestion of proteins from older human lenses, revealed that, 3OHKynG is attached to several sites on the crystallins. These include, three Cys residues in  $\gamma$ S-crystallin and one in  $\beta$ B1-crystallin.<sup>112</sup> If 3OHKyn-His, 3OHKyn-Lys or the corresponding glucoside adducts were present in the human lens proteins, the levels were below the limits of detection.

Until now, it has proven difficult to demonstrate covalent binding of 3OHKyn to lens proteins. Principally, this has been due to the low, and possibly transient, levels present, coupled with the known susceptibility to oxidation in the presence of even trace levels of oxygen.<sup>181,184,188</sup> In order, to measure the levels of covalently bound 3OHKyn, some features of the synthetic 3OHKyn amino acid adducts were taken into account. Firstly, the pH dependence of adduct stability. After 12 hours at pH 4.0, approximately 90% of each adduct remained, even in the presence of oxygen (Figure 2.19). Therefore, human lenses were extracted, and the insoluble proteins dialysed overnight at pH 4.0, to ensure complete removal of non-covalently bound compounds.

In the next step, the modified proteins were exposed to basic pH, in the presence of excess GSH. Under these conditions, the synthetic Lys and Cys 3OHKyn adducts were found to decompose rapidly with the formation of the relevant  $\alpha,\beta$ -unsaturated ketone. GSH adducts were recovered from 3OHKyn-Cys and 3OHKyn-*t*-Boc-Lys in good yield (61% and 73% respectively), however under those conditions little (0.5%) 3OHKyn-*t*-Boc-His decomposed. In the case of 3OHKyn, the deaminated molecule is highly labile. Multiple products, including dimers as well as  $\text{H}_2\text{O}_2$ <sup>181,184,188</sup> result when 3OHKyn in incubated at basic pH. To avoid such oxidation, and to prevent other side reactions, such

as dimer formation, the released unsaturated ketones were trapped by incorporating a large excess of GSH in the basic solution that was used for cleavage of the UV filters from the proteins.

HPLC under acidic conditions was able to resolve the diastereoisomeric peaks of the GSH adducts corresponding to 3OHKyn, Kyn and 3OHKynG, in human lens proteins. In this manner, it was shown that 3OHKyn is indeed bound to human lens nuclear proteins and further, that the amounts bound increase with age. Bound 3OHKyn was not detectable in lenses below the age of 50, but all lenses older than 50 contained measurable levels of this UV filter in the nucleus. In a 68 year old lens, the amount bound corresponds to approximately 15.6 pmol/mg of protein (*i.e.* 0.312 mmole/mole of protein) (Figure 3.19). This quantity may be an under estimate because, 3OHKyn-His adducts are not measured using this procedure. Acid hydrolysis of normal aged lenses showed that there was 2.14 nmol of 3OHKyn-Cys/mg of protein. This shows that the majority of the '3OHKyn-Cys' quantified from acid hydrolysis of human lens protein is derived from 3OHKynG because in the lens only 15.6 pmol is due to 3OHKyn.

Peaks corresponding to each of the three UV filters were observed from human lenses treated with base, and in every lens, 3OHKynG was the major UV filter followed by Kyn and 3OHKyn. This is illustrated in Figure 3.17A, and reflects the order of abundance of the free UV filters found in the human lenses.<sup>19</sup> Model studies using the synthesised Kyn amino acid adducts, also showed that GSH adducts were recovered from Kyn-Cys and Kyn-*t*-Boc-Lys in good yield (59% and 80% respectively), however minimum amounts of (3%) Kyn-*t*-Boc-His decomposed. It is anticipated that similar yields would be achieved for the 3OHKynG amino acid adducts, but they were not available. Therefore, this method appears ideal for detecting UV filters bound to Cys and Lys amino acid residues on the protein, but not His. The reason for this is unclear, however, steric hinderance towards the UV filter side chain, may be responsible, since Cys and Lys each have straight chain functional groups binding to the UV filter side chain, whereas His binds via its imidazole ring rendering access more difficult. This assay method may also be useful for determining if Kyn or 3OHKyn are bound to proteins in other tissues,<sup>210</sup> including the brain.<sup>174-176,178</sup>

If oxidation of bound UV filters were responsible for the colouration, and other features associated with ARN cataract, then it would be expected that the levels of 3OHKyn attached to proteins may be decreased in cataract lenses. This appeared to be the case when cataract lenses were analysed. In the case of 3OHKyn, two small peaks were observed in the cataract samples at the position of 3OHKyn-GSH, however, there was insufficient material present in the peaks to allow mass spectral confirmation. Although 3OHKyn showed the largest proportional decrease in amount, the levels of all three UV filters were diminished compared to age-matched normal lenses. This result of decreased UV filter attachment in cataract proteins, agrees with the data published for Kyn using acid hydrolysis, where the authors showed that there is less Kyn bound to cataract lens proteins than normal lens proteins,<sup>195</sup> The reason for this is unclear and more research on this topic is clearly needed.

The findings from this study show that in normal lens nuclei, the ratios of protein-bound 3OHKynG:Kyn:3OHKyn was 145:4:1. 3OHKynG and Kyn were bound to both normal and cataract lens proteins, in both the nucleus and the cortex. The amount attached to the cortical lens proteins was markedly lower than the amounts attached to the nuclear proteins. 3OHKyn was only detected in normal lens nuclear proteins. This finding is consistent with the formation of the barrier. The lack of bound 3OHKyn in nuclear cataract lenses may be due to the presence of redox active metals. In the nucleus, the levels of bound UV filters were significantly different between normal and cataract lenses. Although the Light and Dark cataract lenses displayed different mean values, these were not statistically significant. In the cortex, the levels of bound UV filters were not statistically significant between the normal and cataract lenses. This latter finding provides evidence that, the difference between cataract and normal lens nuclei is not a consequence of the storage/treatment or origin of the cataract lenses. In this study, normal lenses were sourced in Australia and the cataract lenses were from India.

The levels of free UV filters quantified in this study are comparable to those previously published.<sup>19,211</sup> The levels of protein-bound 3OHKynG quantified in the normal lens nuclei of this study are also comparable to the levels previously published using base

hydrolysis, whereby AHAG was released and used as an indirect measure of the levels of 3OHKynG bound to proteins (average, 1307 pmol/mg protein compared to ~1200 pmol/mg<sup>101</sup>). The levels of protein-bound Kyn in this study are however not comparable to the levels previously published.<sup>103</sup> The reason is unknown.

The levels of UV filter protein modification in the aged (average value for greater than 50 years old) human lens nucleus were 1307 pmol/mg protein of 3OHKynG, 37 pmol/mg protein of Kyn and 9 pmol of 3OHKyn per mg protein. The levels of other modifications reported in the normal aged human lenses include MG-H1, 2848 pmol/mg protein, MG-H2, 1504 pmol/mg protein,<sup>130</sup> OP-lysine 150 pmol/mg protein,<sup>106</sup> pentosidine ~ 1 pmol/mg protein,<sup>104</sup> K2P, ~ 400 pmol/mg protein,<sup>107</sup> Vesperlysine A ~ 1 pmol/mg protein,<sup>105</sup> CML ~ 200 pmol/mg protein,<sup>105</sup> histidinoalanine 800 pmol/mg protein<sup>212</sup> and lanthionine ~ 1300 pmol/mg protein.<sup>212</sup> On this basis it appears that 3OHKyn is quantitatively a minor modification in normal older lens proteins. In contrast to the 'AGE'-related modifications (MG-H1 etc), which all increase in cataract, the UV filters all decrease in concentration with the onset of cataract.

This study is the first definitive demonstration that 3OHKyn is bound to human lens proteins, although immunohistochemical evidence was recently published.<sup>193</sup> Also, the finding that 3OHKyn is attached to proteins in normal lenses only after age 50, and that this phenomenon is localised in the nucleus, provides additional evidence for the lens barrier. In normal lenses, the onset of the lens barrier at middle age<sup>88-90</sup> effectively uncouples the metabolically active cortex from the inactive nucleus, and thus, increases the likelihood of PTM by reactive molecules. This is firstly because it limits the rate at which GSH enters the nucleus. Any GSSG formed in the nucleus must return to the cortex in order to be re-reduced. This lessened flux may contribute to a decrease in the concentration of nuclear GSH in older lenses.<sup>19,55</sup> Secondly, in the nucleus there is a decreased general movement of small molecules, including water,<sup>89</sup> therefore small molecules that do enter the lens centre are then located in this region, on average, for a longer time period than in younger lenses. This factor is significant for molecules that are unstable, for example, 3OHKyn.

### *Protein Modification*

The results in this chapter show that 3OHKyn is indeed bound to nuclear proteins in human lenses. Another aim was to identify peptides containing 3OHKyn. CLP incubated with 3OHKyn over a long period (12 days) was tryptically digested, and analysed for 3OHKyn-modified peptides. Ideally, pepsin digestion (at acidic pH) may be more favourable for 3OHKyn, however pepsin does not cleave specifically. Therefore, tryptic digestion at pH 8.0 was employed even though it is not ideal for 3OHKyn-containing compounds. Tryptic digestion would normally be done for at least 16-24 hours, however taking into account the instability of 3OHKyn, digestion was performed for three hours. Numerous peptides were identified from the digest, however, none could be identified as being modified by 3OHKyn. The database (created by Dr J.A. Aquilina) used for this analysis, only took into account peptides containing UV filter modification. The protein was a dark brown colour, which showed that oxidation had occurred. Since there are numerous modifications that can occur in proteins, it was unclear as to the spectrum of modifications 3OHKyn could produce. The database was not designed to consider peptides containing oxidised amino acid residues. Since CLP contains three groups of crystallins each with subtypes, it seemed appropriate to simplify the task by looking at just one crystallin ( $\alpha$ ) and examining the modified peptides in that protein.

### *Bovine $\alpha$ -Crystallin Modified by 3OHKyn*

3OHKyn was incubated with bovine  $\alpha$ -crystallin in an attempt to identify modified peptides.  $\alpha$ A-Crystallin contains one Cys residue, and  $\alpha$ B-crystallin does not have any Cys residues.<sup>213</sup> The mass spectra of the modified intact subunits of  $\alpha$ -crystallin showed that 3OHKyn was bound only to  $\alpha$ A-crystallin. Acid hydrolysis of the modified  $\alpha$ A-crystallin showed that, 3OHKyn was attached to 8.9% of the protein, and the site of modification was the Cys residue, position 131. Similarly, modification at Cys131 has also been identified as the initial and major site of modification by Kyn at physiological pH.<sup>110</sup>  $\alpha$ B-Crystallin does not contain any Cys residues, therefore UV filter attachment was not expected on this protein within the time frame of the reaction. Although modification at His83 on  $\alpha$ B-crystallin by Kyn, has been previously observed,<sup>111</sup> Kyn is

more stable than 3OHKyn, and this modification was observed after a longer period of incubation (14 days compared to 48 hours).

The dominant effect observed as a result of 3OHKyn incubation with bovine  $\alpha$ -crystallin was the oxidation of Met residues to  $M_{ox}$ .  $\alpha$ -Crystallin polypeptides in which both Mets had been oxidised to  $M_{ox}$  were by far the major species observed after 48 hours. Smaller levels of oxidation of Trp to  $W_{ox}$  were also detected. Tryptic digestion and MS/MS sequencing confirmed that, Met1 and Met138 of  $\alpha$ A-crystallin, and Met1, Met68 Trp9, and Trp60 of  $\alpha$ B-crystallin, were oxidised in the presence of 3OHKyn.

The oxidation of Met and Trp residues by 3OHKyn may have important consequences for the aging lens. It is known that  $H_2O_2$  is formed during 3OHKyn oxidation, and that this process occurs rapidly in the absence of a reducing agent.<sup>181</sup> Furthermore, it has been suggested that  $H_2O_2$  is possibly the major oxidant found in the lens, and that the concentration of  $H_2O_2$  increases in cataract lenses.<sup>214</sup> The reasons for this increase are not clear, however, the fact that oxygen is present in the lens,<sup>53,54</sup> as are low levels of 3OHKyn,<sup>19</sup> provides an ideal environment for the generation of  $H_2O_2$ , as the level of the major lens antioxidant, GSH, diminishes with age. In model studies, in which intact bovine lenses (which lack UV filters) were incubated with 3OHKyn, the levels of GSH were found to decrease markedly.<sup>198</sup> This suggests that 3OHKyn can function as an effective pro-oxidant within the environment of the lens.

In the experiment,  $H_2O_2$  measured after 48 hours of incubation of 3OHKyn with  $\alpha$ -crystallin, amounted to 0.83  $\mu$ moles per 0.89  $\mu$ moles of 3OHKyn, corresponding to a  $H_2O_2$  concentration of 200  $\mu$ M. This was sufficient to totally oxidise the Met residues of  $\alpha$ -crystallin. While 3OHKyn readily autoxidises to yield  $H_2O_2$ , other molecules in the lens, such as ascorbate, may also react with oxygen to produce  $H_2O_2$ . Thus, the finding of oxidised residues on crystallins does not necessarily implicate 3OHKyn in this process.

Unlike in the case of ARN cataract lenses where oxidation of Cys or Met residues is progressive and extensive,<sup>159,215</sup> it would appear that there is little significant oxidation



in human lens proteins with age.<sup>91,216</sup> Oxidation of Met and Trp has, however, recently been reported at three sites in  $\alpha$ -crystallin separated from a 25 year old human lens.<sup>204</sup> These oxidised species were present in covalent multimers, suggesting a possible role for such modifications in crosslinking. If such oxidations have not been induced during isolation and digestion, the presence of  $M_{ox}$  in young human lens proteins indicates that Met sulfoxide reductases (Msr) may have limited activity, or are lacking in activity in the lens interior. Msrs are able to reduce  $M_{ox}$  and protect lens cells against oxidative stress, evidenced by the onset of stress-induced cell death upon deletion of their genes.<sup>217</sup> Oxidation of Met has been shown to inactivate the biological function of some proteins,<sup>218</sup> and the observed decrease in  $\alpha$ -crystallin chaperone efficacy upon Met oxidation by  $H_2O_2$  is consistent with this.<sup>219</sup>

Recently, it was reported that a monoclonal antibody raised against 3OHKyn-modified keyhole limpet hemocyanin, reacted with epitopes on proteins associated with the human lens fibre cell plasma membrane.<sup>193</sup> Although the modified membrane-associated protein was not identified,  $\alpha$ -crystallin has long been known to interact with lens plasma membranes, with the suggested involvement of the integral membrane protein aquaporin.<sup>220,221</sup> Furthermore, the levels of  $\alpha$ -crystallin associated with the plasma membrane in cataractous lenses are significantly greater when compared with normals.<sup>222</sup> These observations suggest that  $\alpha$ -crystallin could be one of the 3OHKyn-modified membrane-associated proteins reported by Staniszewska, *et al.*<sup>193</sup>

Approximately half of all Met residues are oxidised in the lenses of advanced nuclear cataract patients,<sup>159</sup> and as much as 60% of the total Met is oxidised in membrane-bound proteins.<sup>215</sup> In this study, 3OHKyn oxidised to produce approximately equimolar amounts of  $H_2O_2$ , that presumably then oxidised the Met residues, and to a lesser extent Trp residues, of  $\alpha$ -crystallin.

In this study, relatively high concentrations of 3OHKyn were used, however, significant oxidation of Met-containing peptides was observed using 50  $\mu M$  3OHKyn, a level approaching that found in the lens (5-10  $\mu M$ ). It is likely that the oxidised Mets found in

nuclear cataract lens proteins are derived from exposure to similarly low  $\text{H}_2\text{O}_2$  levels over long periods of time (*i.e.* months-years).

In the human lens, 3OHKyn may perform a dual role of oxidation and covalent modification of nucleophilic residues. For example, in the centre of nuclear cataractous lenses, where oxidative conditions prevail, both free and protein-bound 3OHKyn may catalyse the formation of  $\text{H}_2\text{O}_2$ , potentially leading to protein oxidation and loss of chaperone activity of  $\alpha$ -crystallin and protein aggregation. Protein-bound 3OHKyn can also undergo further reactions, which result in the formation of intermolecular crosslinks.<sup>185,186,223</sup> Covalent crosslinking of polypeptides is another feature that is characteristic of ARN cataract.

In summary, 3OHKyn covalently binds to lens proteins in the same manner as the other two Kyn UV filters, but the overall role of 3OHKyn in the formation of ARN cataract remains to be elucidated. Model studies with 3OHKyn have clearly shown that this UV filter can produce  $\text{H}_2\text{O}_2$  and can oxidise amino acid residues in lens proteins.

## Chapter 4

### Does 3OHKyn Crosslink Lens Proteins?

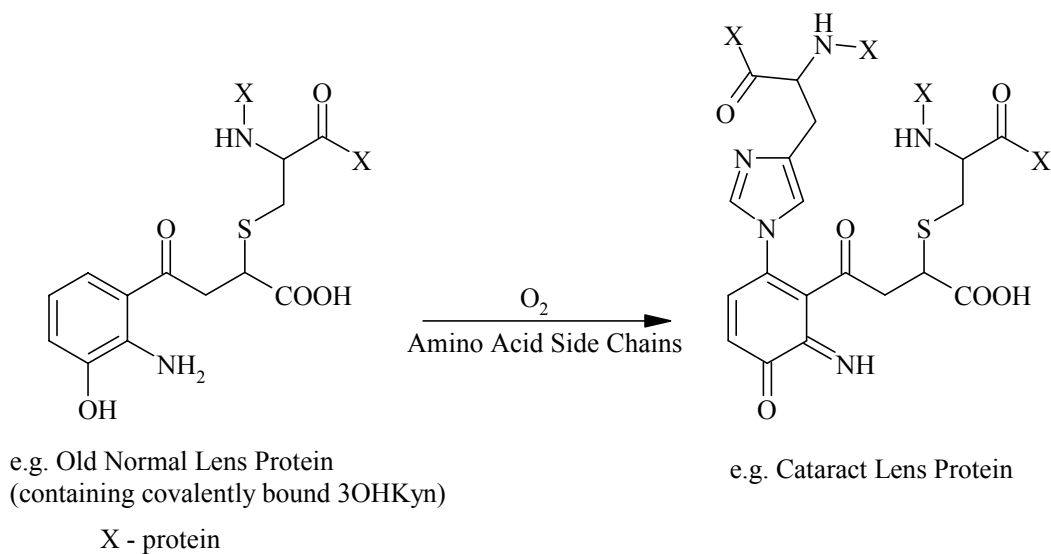
#### 4.1 Introduction

The studies from Chapters 2 and 3 of this thesis have shown that 3OHKyn amino acid adducts are unstable at physiological pH, CLP oxidises when modified with 3OHKyn at pH 7.2, *i.e.* Met and Trp oxidation is observed analogous to the oxidations that occur in human cataractous lenses, and finally small amounts of 3OHKyn are attached to normal aged human lens protein. 3OHKyn is however, undetectable in human cataract lens proteins. These findings demonstrate that 3OHKyn may contribute to the onset of ARN cataract.

Crosslinking of lens polypeptides is also characteristic of ARN cataract.<sup>166</sup> Crosslinking involves disulphide bond linkages as well as various other types of crosslinking of unknown type. One possibility is that 3OHKyn could be involved in these crosslinks.

The hypothesis to be examined in this chapter, is that, 3OHKyn may crosslink proteins in human cataractous lenses. One way in which this could occur is via addition of nucleophilic amino acid residues to 3OHKyn amino acid adducts.

As a first step in testing this theory, 3OHKyn amino acid adducts were incubated in the presence of excess amino acids. The products were analysed by HPLC and mass spectrometry. CLP modified with 3OHKyn at pH 7.2 and pH 9.5 was also examined. An example of the type of crosslinks expected from the above incubations is shown in Scheme 4.1. The aromatic ring of 3OHKyn should oxidise and the quinoneimine be susceptible to nucleophilic attack of another amino acid, *para* to the carbonyl group.



**Scheme 4.1** Possible scheme for formation of 3OHKyn amino acid crosslinks.

## 4.2 Materials and Methods

### 4.2.1 Materials

All organic solvents and acids were HPLC grade (Ajax, Auburn, NSW, Australia). Milli-Q<sup>®</sup> water (purified to 18.2 MΩ/cm<sup>2</sup>) was used in the preparation of all solutions. The amino acids (N- $\alpha$ -*t*-Boc-L-His, and N- $\alpha$ -*t*-Boc-L-Lys), formic acid, HCl (6 M, sequencing grade), 3OHKyn, guanidine HCl, TFA, thioglycolic acid and phenol were obtained from Sigma-Aldrich Chemical Co. (St. Louis, MO, U.S.A.). Vivaspin (6 mL) protein concentrators (MW cut off 10,000 Da) were purchased from Vivascience.

### 4.2.2 Incubations with 3OHKyn-*t*-Boc-His and 3OHKyn-*t*-Boc-Lys

3OHKyn-*t*-Boc-His/3OHKyn-*t*-Boc-Lys (0.2 mg) was dissolved in 0.1 M phosphate buffer, pH 7.2 (4 mL). The  $\alpha$ -amino-blocked amino acid N- $\alpha$ -*t*-Boc-His/N- $\alpha$ -*t*-Boc-Lys was added to the buffer in 20-fold molar excess (see Table 4.1), and chloroform (20  $\mu$ L) was added to inhibit bacterial growth. The solutions were sealed, wrapped in foil and incubated for 12 days at 37<sup>0</sup>C. Aliquots were taken every 3 days, and examined by HPLC.

Control experiments using 3OHKyn-*t*-Boc-His and 3OHKyn-*t*-Boc-Lys, without the addition of excess amino acids (see Table 4.1), were incubated in 0.1 M phosphate buffer as controls.

After the above reaction mixtures were incubated for 12 days, they were acidified with 1% (v/v) aqueous formic acid and purified through a Waters Vac 1cc 100 mg tC18 Sep Pak. The following mobile phase conditions were used: solvent A (aqueous 1% (v/v) formic acid) for 2 mL, then the sample was loaded and washed with 2 mL of solvent A to remove salts, then the sample was eluted with 1 mL solvent B (80% (v/v) ACN/H<sub>2</sub>O, 1% (v/v) formic acid). Samples were then freeze dried and hydrolysed in an evacuated hydrolysis tube with 6 M HCl (1 mL), thioglycolic acid (5% v/v) and phenol (1% w/v) for 24 hours at 110<sup>0</sup>C. Following hydrolysis, the mixture was freeze dried, dissolved in 0.1% (v/v) TFA and purified by HPLC.

**Table 4.1** Combination of incubations undertaken with the 3OHKyn amino acid adducts.

| Crosslink Combination Incubations |  |  |                                  |
|-----------------------------------|--|--|----------------------------------|
| 3OHKyn Adducts                    | Excess Amino Acids                                 |  |                                  |
| <u>3OHKyn-<i>t</i>-Boc-His</u>    | <u>N-<math>\alpha</math>-<i>t</i>-Boc-His</u><br>✓ | <u>N-<math>\alpha</math>-<i>t</i>-Boc-Lys</u><br>✓ | <u>No Amino Acids</u><br>control |
| <u>3OHKyn-<i>t</i>-Boc-Lys</u>    | ✓  | ✓  | control                          |

**4.2.3 Incubation of CLP Modified by 3OHKyn at pH 7.2**

CLP (160 mg) or CLP modified by 3OHKyn at pH 7.2 (160 mg), or CLP modified by 3OHKyn at pH 9.5 (160 mg) was dissolved in 6 M guanidine HCl (5.6 mL) and 0.1 M phosphate buffer, pH 7.2 (2.4 mL), and chloroform (100  $\mu$ L) was added to inhibit bacterial growth. The pH was adjusted to 7.2 with 4 M NaOH if necessary. The solutions were sealed, wrapped in foil and incubated (for 15 or 10 days) at 37°C. Aliquots were taken for 3-D fluorescence analysis, acid hydrolysis and SDS-PAGE analysis.

Aliquots for 3-D fluorescence measurements were ultra-filtered (4°C) in a Vivaspinn concentrator (MW cut off 10,000 Da) to remove non-covalently bound material prior to analysis.

Aliquots for acid hydrolysis were ultra-filtered (4°C) in a Vivaspinn concentrator (MW cut off 10,000 Da) and the protein washed with 1 mL H<sub>2</sub>O (6000 g, 4°C). The protein was freeze dried and hydrolysed in an evacuated hydrolysis tube with 6 M HCl (1 mL), thioglycolic acid (5% v/v) and phenol (1% w/v) for 24 hours at 110°C. Following hydrolysis, the mixture was freeze dried, dissolved in 0.1% (v/v) TFA and purified by HPLC. The filtrate was also examined by HPLC.

#### **4.2.4 SDS-PAGE**

See Section 3.2.18 for details.

#### **4.2.5 HPLC**

See Section 2.2.9 for details.

#### **4.2.6 Mass Spectrometry**

See Section 2.2.10 for details.

#### **4.2.7 Tandem Mass Spectrometry (MS/MS)**

See Section 2.2.11 for details.

#### **4.2.8 Fluorescence and UV-visible Spectroscopy**

See section 2.2.14 for details.

#### **4.2.9 NMR Spectroscopy**

See section 2.2.13 for details.

### 4.3 Results

#### 4.3.1 Incubations with the 3OHKyn-*t*-Boc-His Adduct

##### *Control Experiment with 3OHKyn-t-Boc-His*

In an attempt to synthesise 3OHKyn crosslinked compounds, a control study was first undertaken. 3OHKyn-*t*-Boc-His was incubated at pH 7.2 for 12 days at 37<sup>0</sup>C, in the absence of excess amino acids. Aliquots of the reaction mixture were taken every 3 days and examined by HPLC, and analysed by mass spectrometry. The HPLC chromatogram of the initial reaction mixture is shown in Figure 4.1A. The large peak eluting at 35 min is 3OHKyn-*t*-Boc-His.

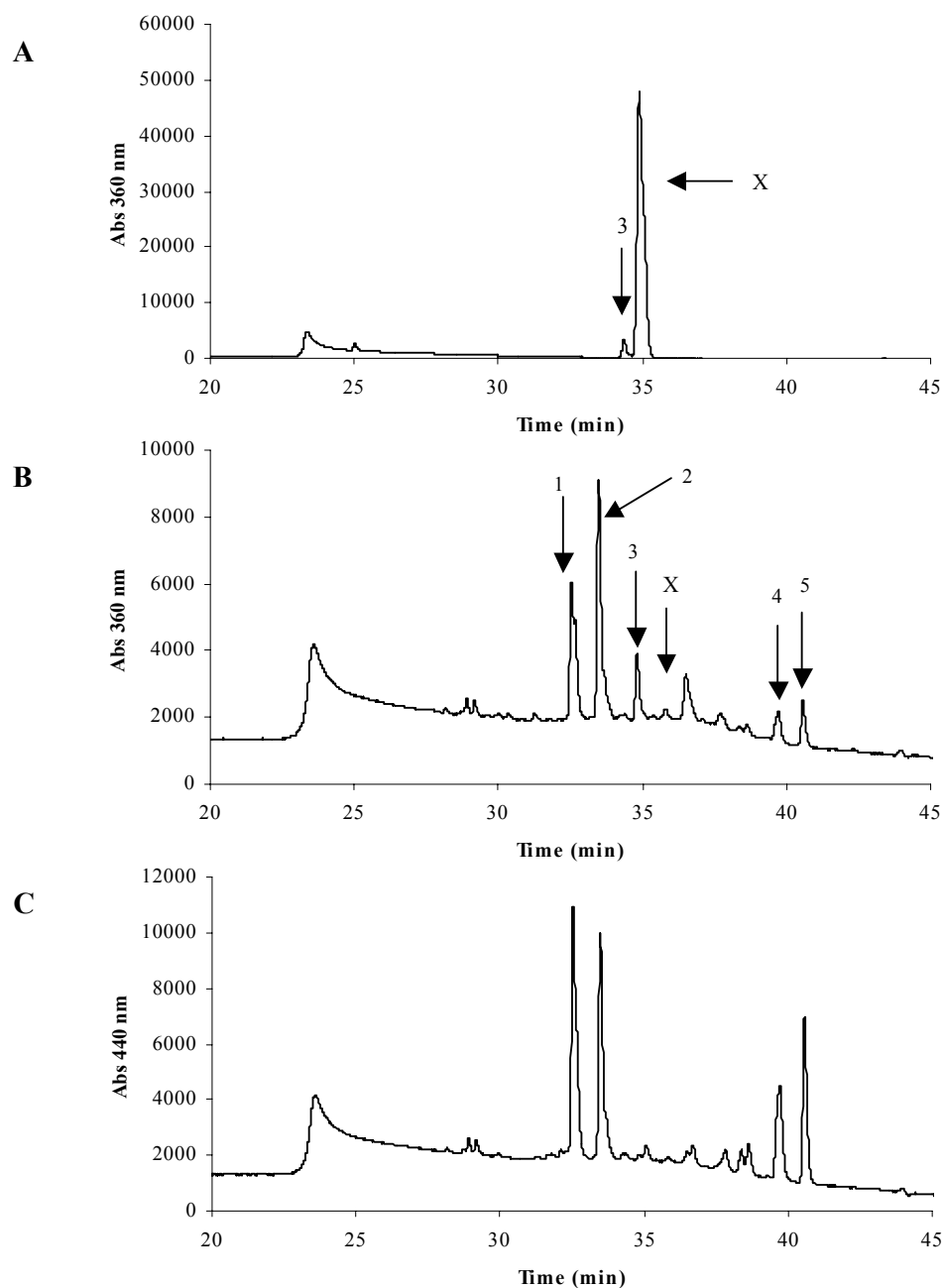
Figure 4.1B is the HPLC profile of the reaction mixture after 12 days of incubation. Numerous peaks were observed. A large peak eluting at 32.5 min (peak 1) revealed a molecular ion of  $m/z$  777 (Figure 4.2A). MS/MS of this ion (spectrum not shown) showed fragment ions at  $m/z$  565, 487, 438, 263, 259, and 135. This compound could not be structurally identified on the basis of mass spectrometry data alone, since none of these fragment ions are typical of 3OHKyn UV filter adducts. The next major peak eluted at 33.5 min (peak 2). The molecular ion appeared to be  $m/z$  650 (Figure 4.2B). The minor peak eluting at 34.9 min (peak 3) could not be identified from the mass spectrum (Figure 4.2C). This peak was also observed in Figure 4.1A, and this minor compound appears to be an impurity from the synthesis of 3OHKyn-*t*-Boc-His, which is also stable to oxidation. A small amount of 3OHKyn-*t*-Boc-His eluted at 35.4 min (labeled X on Figure 4.1B). The peak eluting at 39.7 min (peak 4) exhibited an ion of  $m/z$  664 (Figure 4.2D), (a  $m/z$  664 ion had been observed in Chapter 2 Section 2.3.8) and the MS/MS fragment ions (spectrum not shown) are identical to the compound that has been identified as 1,3,4,5-tetrahydro-11-(2-(*N*- $\alpha$ -*tert*-butyloxycarbonyl-histidyl)-(4-hydroxy-1,4-dioxo-butanyl)-1,5-dioxo-2H-pyrido(3,2-*a*)phenoxazine-3-carboxylic acid (Chapter 2). The peak eluting at 40.6 min (peak 5) also contained a molecular ion  $m/z$  664 (spectrum not shown).

Figure 4.1C is the HPLC profile of the reaction mixture after 12 days of incubation, monitoring absorbance at 440 nm. Phenoxazone compounds absorb highly at 440 nm.<sup>184</sup> Examination of Figure 4.1B and Figure 4.1C shows that peaks 1, 2, 4 and 5 (Figure



4.1B) exhibit absorbances at both 360 and 440 nm. This indicates that these products may contain a phenoxazone within their structure. However, at this stage it is difficult to elucidate a structure for compounds based on mass spectral data alone.

Figure 4.3 shows a graph of the rate of formation of the unknown compounds in peaks 1, 2, 3, 4, and 5 over the 12 day incubation period. Compounds 1 and 2 steadily increase in yield over the 12 days, compound 3 remains constant, and compounds 4 and 5 decrease in yield after 3 days of incubation. 3OHKyn-*t*-Boc-His decreased steadily over time, and at 12 days only a small amount of this compound remained.



**Figure 4.1** HPLC separation of 3OHKyn-*t*-Boc-His incubated at pH 7.2. X is 3OHKyn-*t*-Boc-His. Peak 3 is an impurity stable to oxidation. A, Initial reaction mixture; B, Reaction mixture after 12 days of incubation. Arrowed peaks were collected for mass spectrometry. Absorbance monitored at 360 nm; C, Absorbance monitored at 440 nm.

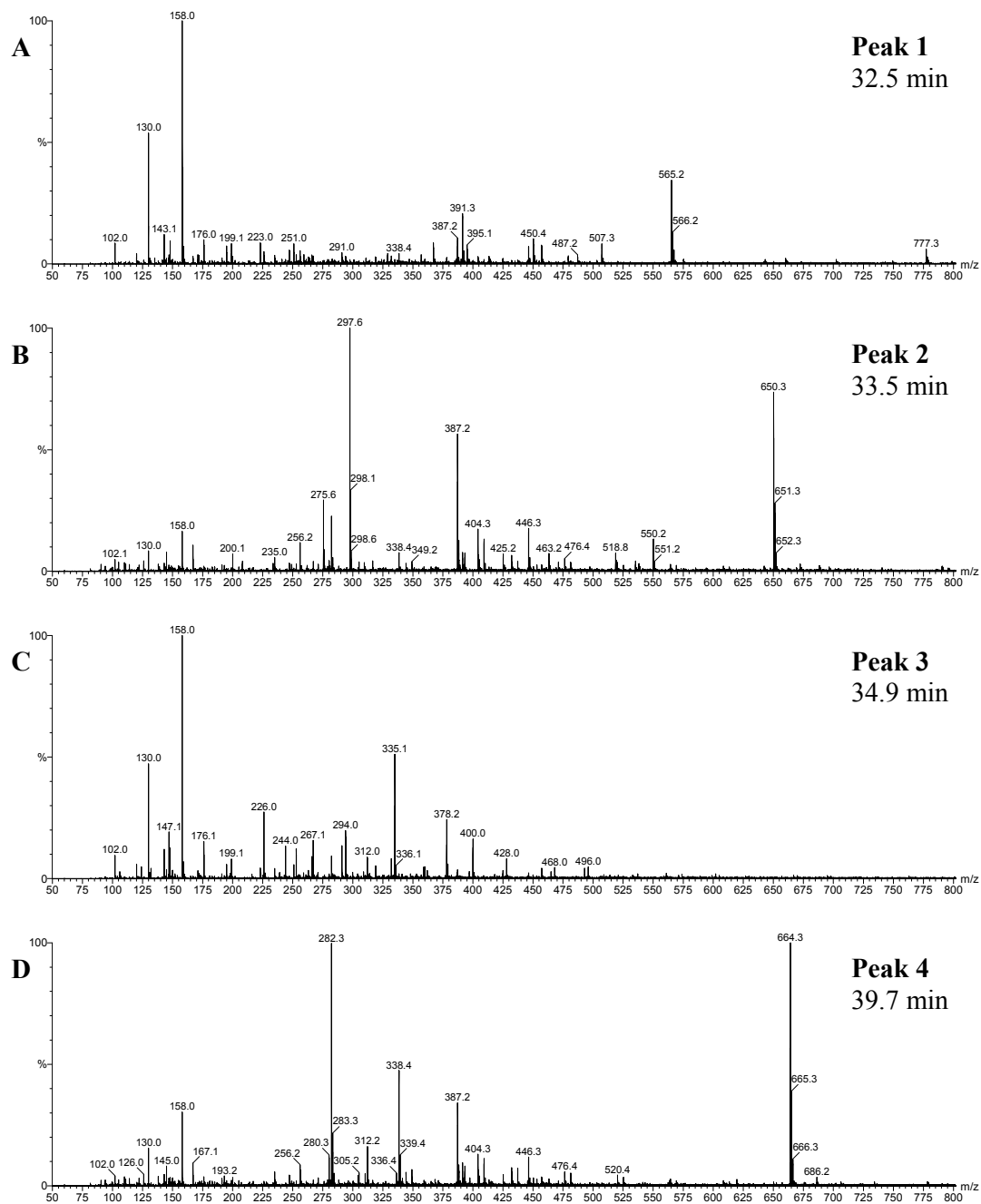


**Figure 4.2** ESI mass spectra of peaks eluting from HPLC chromatogram in Figure 4.1B.

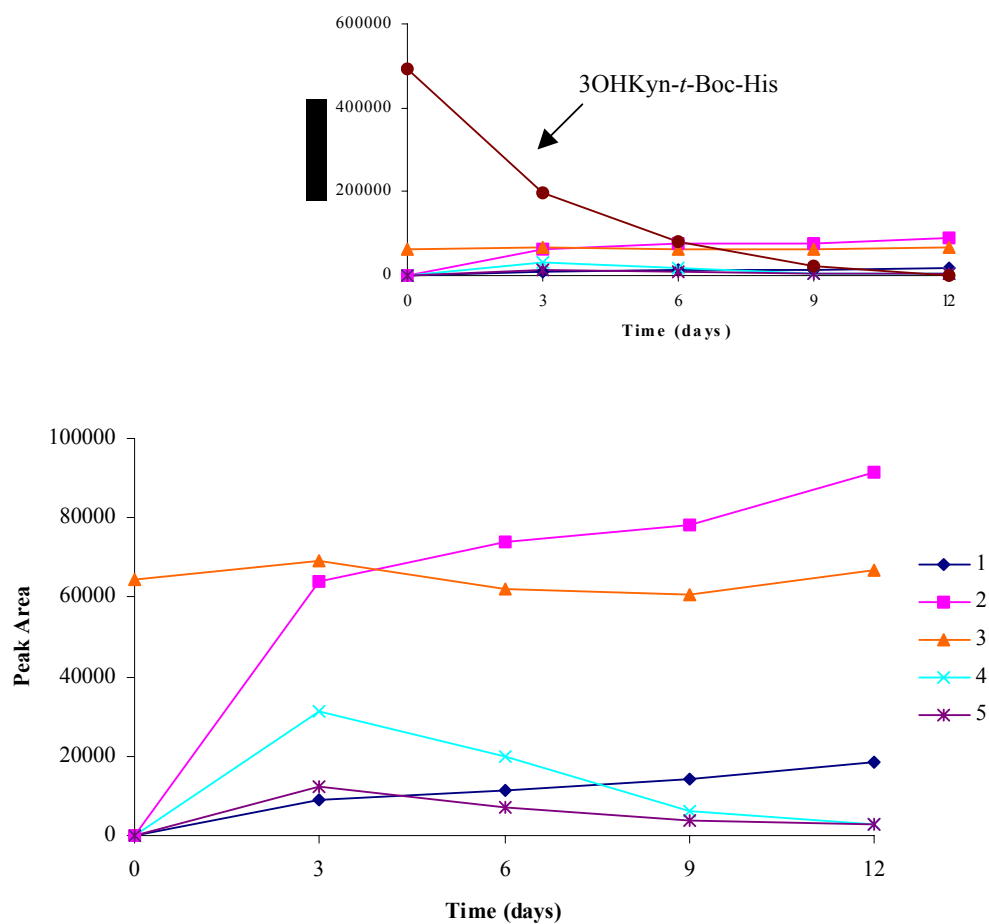


**Figure 4.3** Rate of formation of unknown products in peaks 1, 2, 3, 4, and 5 from Figure 4.1B. The inset shows the rate of loss of 3OHKyn-*t*-Boc-His, in relation to the formation of products. Peak 3 is an impurity from the synthesis of 3OHKyn-*t*-Boc-His, which is stable to oxidation.

Following the 12 day incubation period, the remaining mixture was washed through a Sep Pak to remove the salts from the mixture. The mixture, which eluted from the column, was dried and hydrolysed with acid and antioxidants, since this method could also be used for detecting crosslinked compounds in lens proteins. The hydrolysate was separated by HPLC, and the peaks were monitored at 360 nm and 440 nm, since phenoxazones absorb at 440 nm. The HPLC chromatogram of the hydrolysed reaction mixture of 3OHKyn-*t*-Boc-His following 12 days of incubation is shown in Figure 4.4. Figure 4.4A shows the absorbance monitored at 360 nm, and Figure 4.4B shows the absorbance monitored at 440 nm.

A peak eluting at 24.7 min (peak 1') in Figure 4.4A was identified as 3OHKyn-His, since the ion  $m/z$  363 in Figure 4.5A yielded the fragment ions (spectrum not shown) for authentic 3OHKyn-His. This peak was not observed in Figure 4.4B since 3OHKyn-His does not absorb at 440 nm. A major doublet (peak 2') eluted at 29.0 min, and absorbed highly at 360 and 440 nm, and had a molecular ion of  $m/z$  550 (Figure 4.5B). Peak 3' (32.5 min) also eluted as a doublet, and exhibited an abundant ion at  $m/z$  487 (Figure 4.5C). Finally peak 4' eluted at 34.7 min, and had an observed molecular ion of  $m/z$  764 (Figure 4.5D). The structures of these peaks could not be elucidated from the mass spectral data.

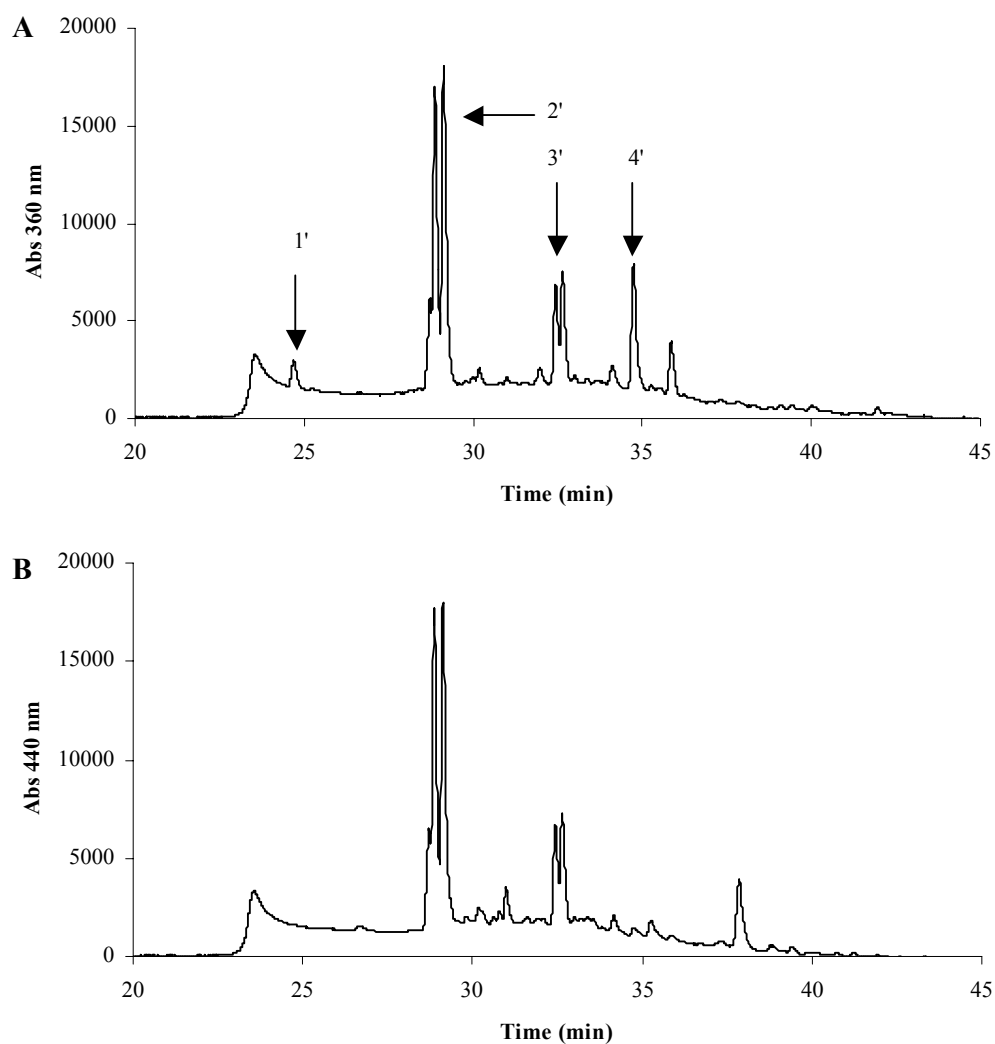


**Figure 4.4** HPLC of the acid digest of 3OHKyn-*t*-Boc-His following incubation for 12 days. HPLC chromatograms of, *A*, Absorbance monitored at 360 nm. Peaks 1, 2, 3, and 4 were collected for mass spectral analysis. *B*, Absorbance monitored at 440 nm.

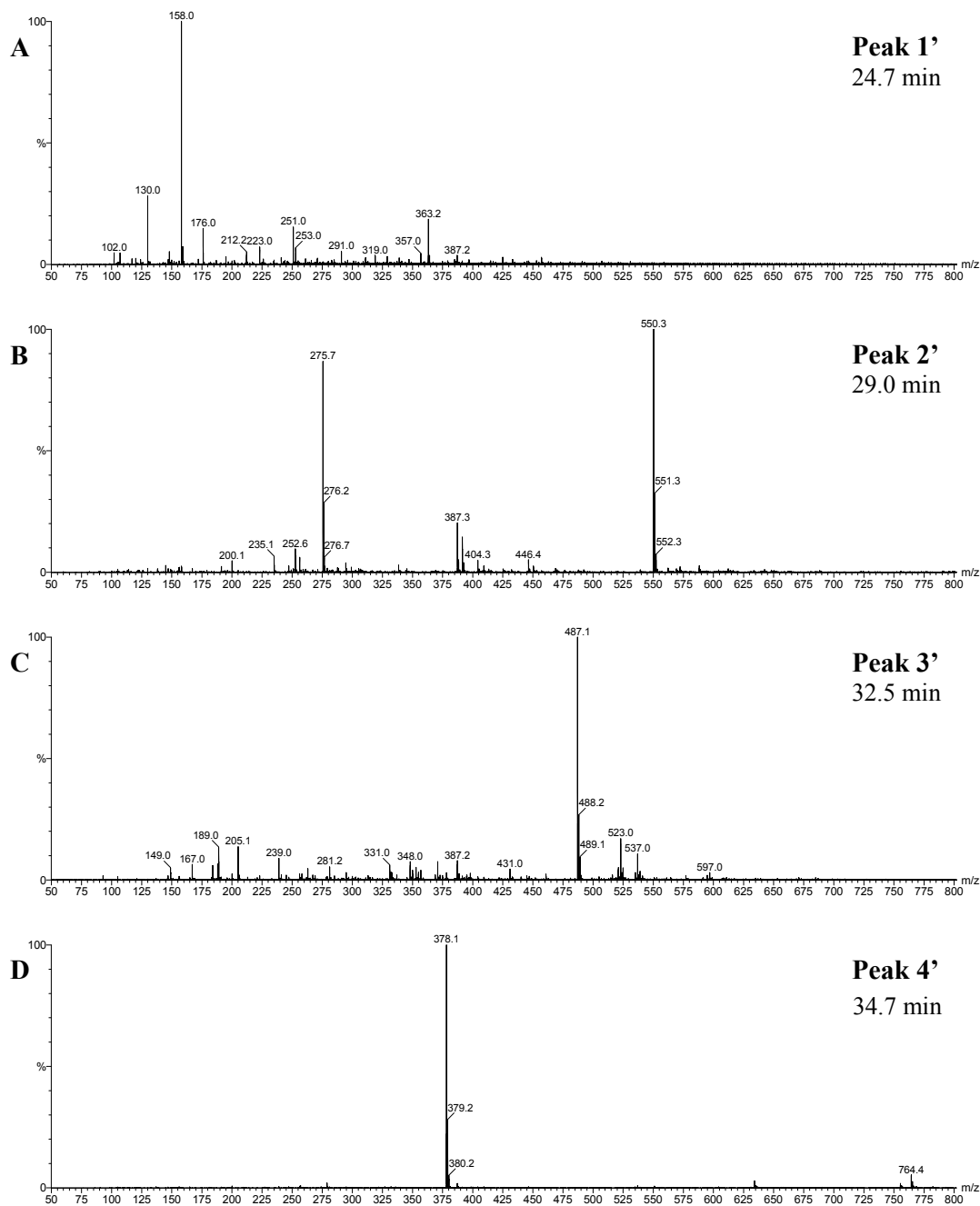


**Figure 4.5** ESI mass spectra of peaks eluting from the HPLC chromatogram in Figure 4.4A.

***Incubation of 3OHKyn-*t*-Boc-His with excess N- $\alpha$ -*t*-Boc-His***

The objective in this section was to form crosslinked compounds, in which, 3OHKyn was crosslinked to other nucleophilic amino acids. Therefore, 3OHKyn-*t*-Boc-His was incubated with a 20-fold molar excess of N- $\alpha$ -*t*-Boc-His at pH 7.2 for 12 days. Aliquots of the reaction mixture were again taken every 3 days, and purified by HPLC, and analysed by mass spectrometry. The HPLC chromatogram of the initial reaction mixture is shown in Figure 4.6A. The large peak eluting at 35.2 min is authentic 3OHKyn-*t*-Boc-His. Figure 4.6B is the HPLC profile of the reaction mixture after 12 days of incubation. This profile was surprisingly, essentially identical to that of Figure 4.1B. In Figure 4.6B peaks eluted at 32.5 min, 33.5 min, 34.9 min, 39.7 min and 40.6 min. Mass spectral analysis of each of these peaks (spectra not shown) showed that they were each, the same as those shown in Figure 4.2.

Similarly, the reaction mixture after 12 days of incubation was applied to a Sep Pak, and the 80% ACN eluate was dried, and acid hydrolysed with antioxidants. Peaks from the HPLC were monitored at 360 nm and 440 nm. The HPLC chromatogram of the hydrolysed reaction mixture of 3OHKyn-*t*-Boc-His incubated with excess N- $\alpha$ -*t*-Boc-His is shown in Figure 4.7. Figure 4.7A exhibits the absorbance monitored at 360 nm, and Figure 4.7B exhibits the absorbance monitored at 440 nm. The HPLC profiles of Figure 4.7 are essentially identical to those of Figure 4.4. In Figure 4.7A peaks eluted at 25.0 min, 28.6 min, 32.5 min and 34.7 min. Mass spectral analysis of each of these peaks (spectra not shown) showed that they were each the same as those shown in Figure 4.5.



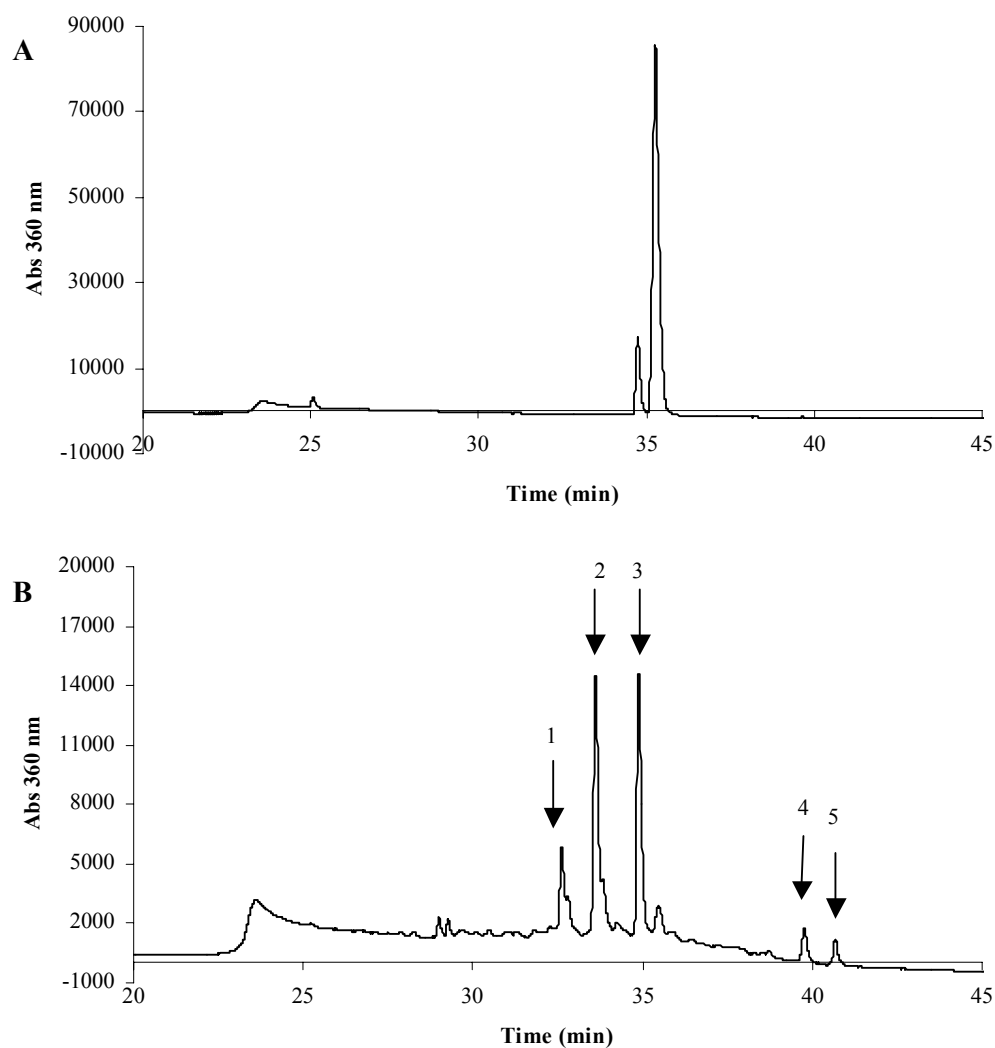


**Figure 4.6** Incubation of 3OHKyn-*t*-Boc-His with a 20-fold molar excess of N- $\alpha$ -*t*-Boc-His for 12 days. HPLC chromatograms of, *A*, Initial reaction mixture; *B*, Reaction mixture after 12 days of incubation. Peak 1 eluted at 32.5 min, peak 2 at 33.5 min, peak 3 at 34.9 min, peak 4 at 39.7 min and peak 5 at 40.6 min (identical to Figure 4.1B).

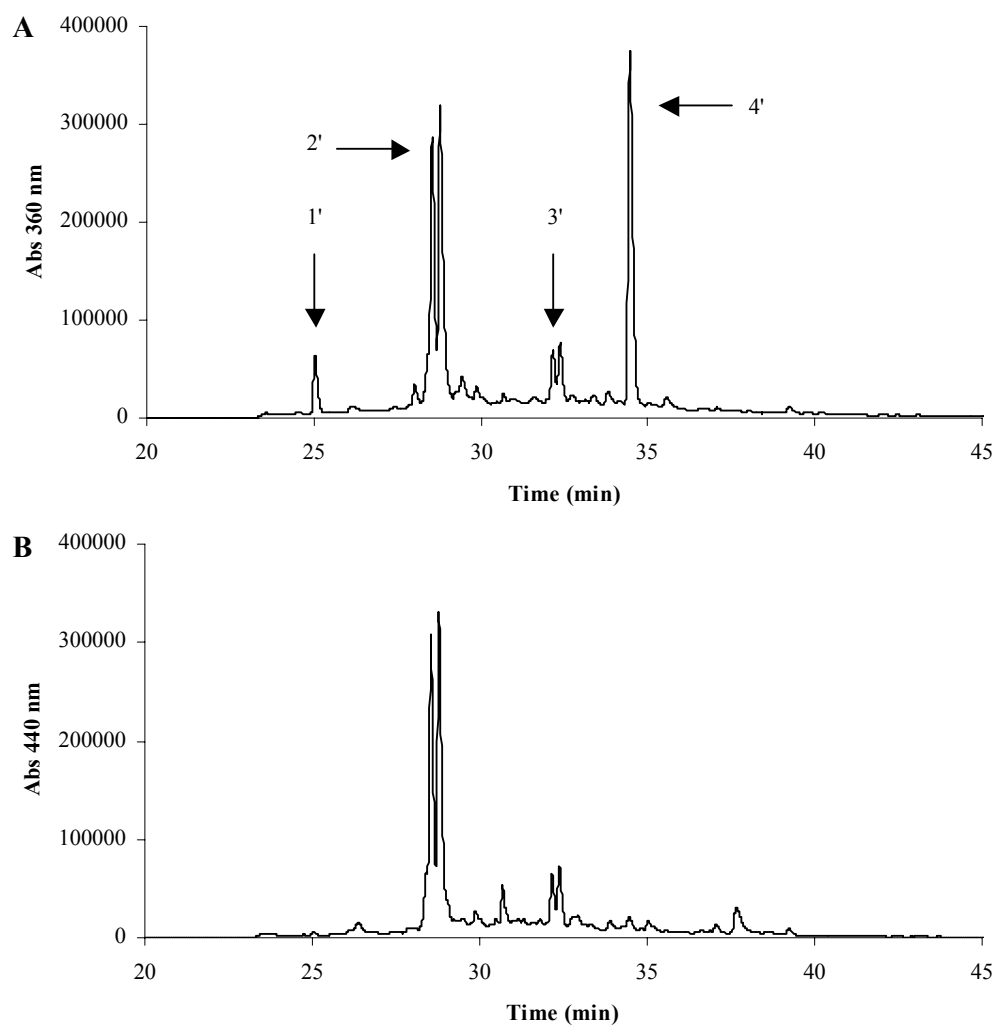


**Figure 4.7** HPLC of the acid digest of 3OHKyn-*t*-Boc-His with a 20-fold molar excess of N- $\alpha$ -*t*-Boc-His following incubation for 12 days. HPLC chromatograms of, *A*, Absorbance monitored at 360 nm. Peak 1 eluted at 25.0 min, peak 2 at 28.6 min, peak 3 at 32.5 min and peak 4 at 34.7 min. *B*, Absorbance monitored at 440 nm.

***Incubation of 3OHKyn-*t*-Boc-His with excess N- $\alpha$ -*t*-Boc-Lys***

3OHKyn-*t*-Boc-His was also incubated with a 20-fold molar excess of N- $\alpha$ -*t*-Boc-Lys at pH 7.2 for 12 days. Aliquots of the reaction mixture were again taken every 3 days, and purified by HPLC, and analysed by mass spectrometry. The HPLC chromatogram of the initial reaction mixture is shown in Figure 4.8A. The large peak eluting at 35.2 min is authentic 3OHKyn-*t*-Boc-His. Figure 4.8B is the HPLC profile of the reaction mixture after 12 days of incubation. This profile is essentially identical to that of Figure 4.1B and 4.6B. In Figure 4.8B, peaks eluted at 32.3 min, 33.2 min, 34.5 min 39.9 min and 40.3 min. Mass spectral analysis of each of these peaks (spectra not shown) showed that each spectrum was the same as the spectra shown in Figure 4.2.

Similarly, the reaction mixture after 12 days of incubation was applied to a Sep Pak, and the 80% ACN eluate was dried and acid hydrolysed with antioxidants. Peaks from the HPLC were again monitored at 360 nm and 440 nm. The HPLC chromatogram of the hydrolysed reaction mixture of 3OHKyn-*t*-Boc-His incubated with excess N- $\alpha$ -*t*-Boc-Lys is shown in Figure 4.9. Figure 4.9A exhibits the absorbance monitored at 360 nm, and Figure 4.9B exhibits the absorbance monitored at 440 nm. The HPLC profiles of Figure 4.9 are essentially identical to those of Figures 4.4 and 4.7. The peak eluting at 25.3 min in Figure 4.9A is 3OHKyn-His. In Figure 4.9A, major peaks also eluted at 28.7 min, 32.5 min and 34.6 min. Mass spectral analysis of each of these peaks (spectra not shown) showed that the spectra were the same as those shown in Figure 4.5.

In summary, these findings suggest that the presence of a 20-fold molar excess of N- $\alpha$ -*t*-Boc-His or N- $\alpha$ -*t*-Boc-Lys, seemed to have no effect on the products that formed on incubation of, 3OHKyn-*t*-Boc-His in the presence of air.

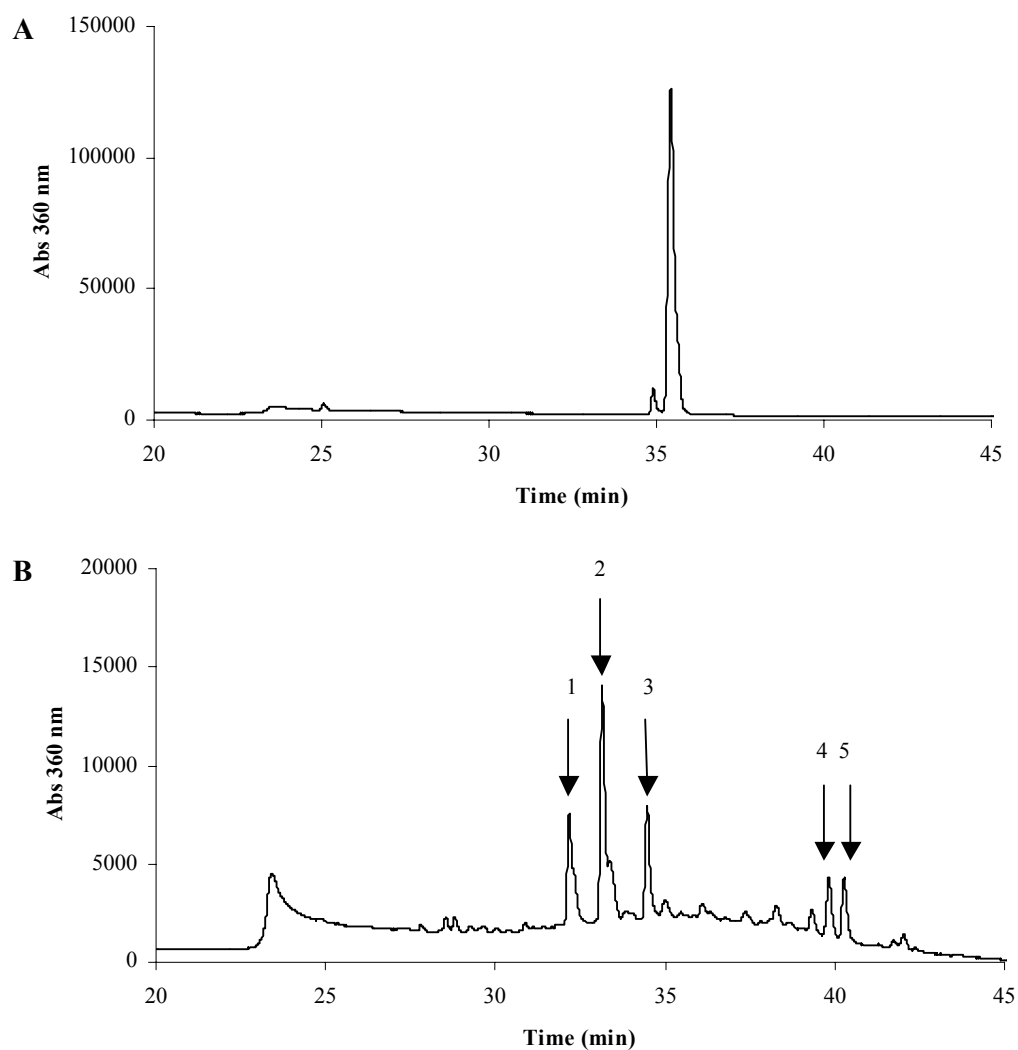


**Figure 4.8** Incubation of 3OHKyn-*t*-Boc-His with a 20-fold molar excess of N- $\alpha$ -*t*-Boc-Lys for 12 days. HPLC chromatograms of, *A*, Initial reaction mixture; *B*, Reaction mixture after 12 days of incubation. Peak 1 eluted at 32.3 min, peak 2 at 33.2 min, peak 3 at 34.5 min, peak 4 at 39.9 min and peak 5 at 40.3 min (~identical to Figure 4.1B).

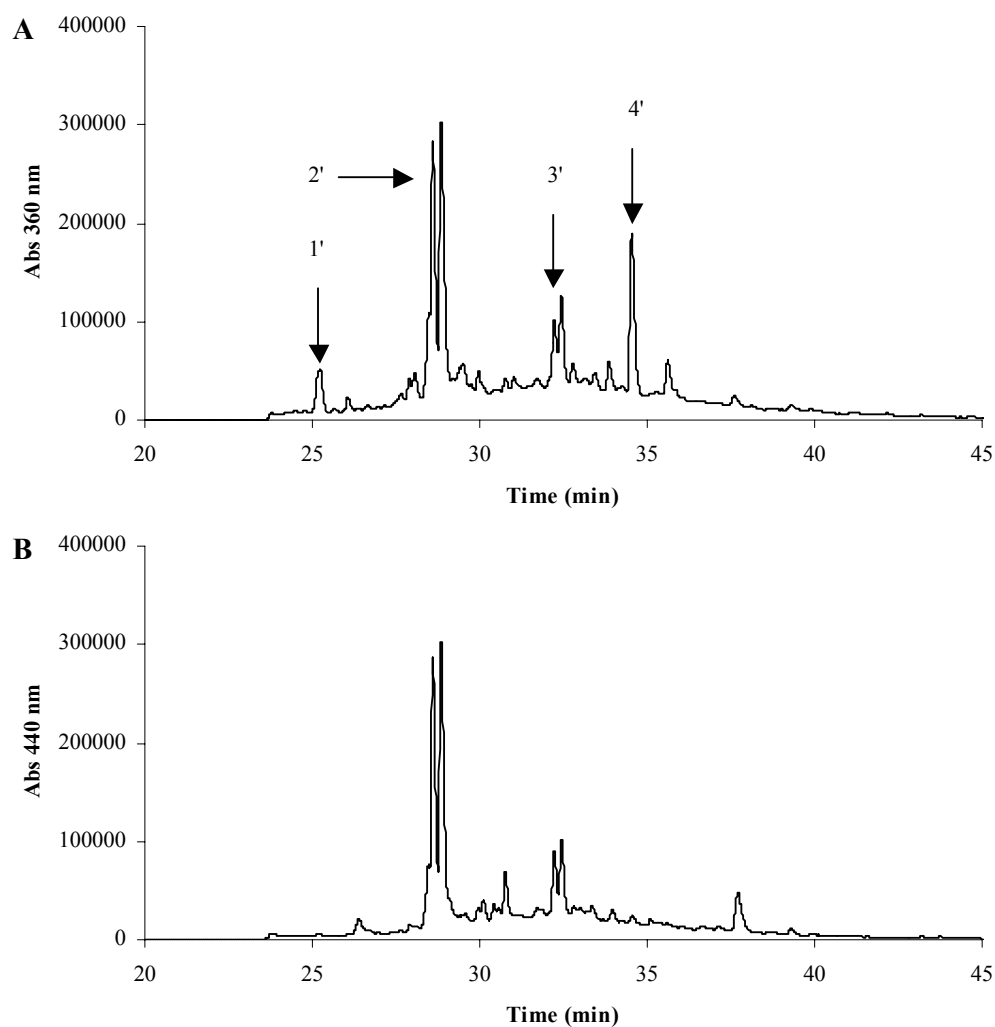


**Figure 4.9** HPLC of the acid digest of 3OHKyn-*t*-Boc-His with a 20-fold molar excess of N- $\alpha$ -*t*-Boc-Lys following incubation for 12 days. HPLC chromatograms of, *A*, Absorbance monitored at 360 nm. Peak 1 eluted at 25.3 min, peak 2 at 28.7 min, peak 3 at 32.5 min and peak 4 at 34.6 min. *B*, Absorbance monitored at 440 nm.

***Analysis of the Peak Eluting as a Doublet (Peak 2') from the HPLC Chromatograms of the Hydrolysed Reaction Mixtures***

Analysis of the reactions involving 3OHKyn-*t*-Boc-His, both in the absence and presence of excess amino acids, all showed that following acid hydrolysis of the final reaction mixture, a prominent doublet (apparently a diastereoisomer) eluted at approximately 29 min, and absorbed at 360 and 440 nm. This compound was investigated further. The molecular ion of the doublet was identified,  $m/z$  550 (Figure 4.5B). MS/MS (Figure 4.10) of this ion yielded fragment ions at  $m/z$  506 (loss of 44 Da), 395 (further loss of 111 Da) and 351 (further loss of 44 Da).

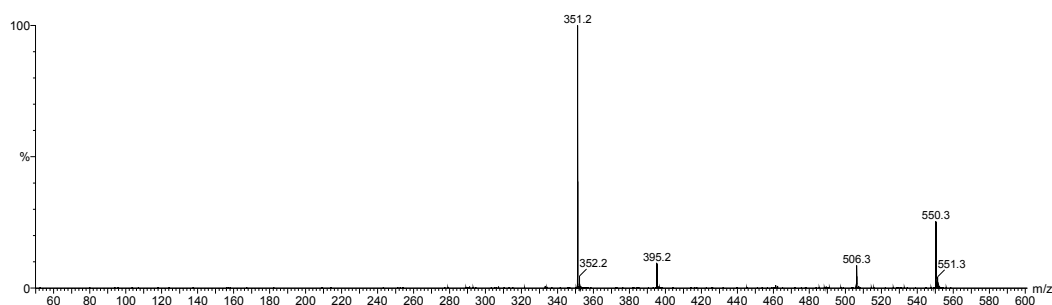


**Figure 4.10** MS/MS spectrum of the molecular ion  $m/z$  550, eluting as a doublet in the hydrolysed HPLC profiles, involving 3OHKyn-*t*-Boc-His incubations.

Following the 12 days of incubation of each reaction, the HPLC profiles (Figure 4.1B, 4.6B and 4.8B) all showed a large peak eluting at approximately 33.4 min (peak 2), with a molecular ion of  $m/z$  650 (Figure 4.2B). Since this is a major peak, and also has a mass difference of 100 Da from the hydrolysed peak ( $m/z$  550), it was assumed that the loss of 100 Da was a result of a *t*-Boc group attached to His, since acid readily cleaves the *t*-Boc group.<sup>209</sup> Therefore, in order to demonstrate that these two peaks were the same compound ( $\pm$  *t*-Boc group), the peak eluting at 33.4 min (peak 2) in Figures 4.1B, 4.6B and 4.8B, was collected, dried down to a minimum volume, and 6 M HCl was added, and the sample was incubated for 20 hours at 37°C (these conditions cleave *t*-Boc groups<sup>209</sup>). Following this short incubation period, the sample was adjusted to pH 4 with NaOH, and examined by HPLC. A doublet eluted at 29 min (Figure 4.11), and mass spectral analysis of this doublet showed that the molecular ion was  $m/z$  550

(spectrum not shown), and MS/MS of this ion yielded fragment ions  $m/z$  506, 395 and 351 (spectrum not shown).

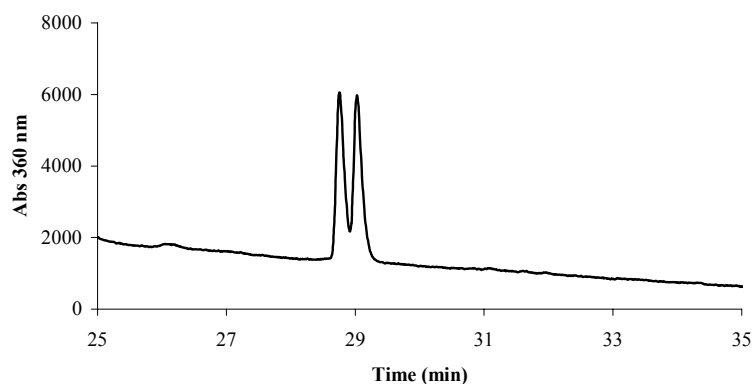


**Figure 4.11** HPLC chromatogram of peak 2 (Figures 4.1B, 4.6B and 4.8B) following deprotection with acid.

As further support that the compound with the molecular ion  $m/z$  650 (peak 2 Figures 4.1B, 4.6B and 4.8B) was indeed the precursor for the doublet with the molecular ion  $m/z$  550 (peak 2' Figures 4.4A, 4.7A and 4.9A), a UV-visible spectrum of each (Figure 4.12) exhibited identical spectra, showing that they contained an identical chromophoric group. The UV-visible spectra also showed that these compounds absorbed most strongly at 408 nm and that 360 and 440 nm, that were used to monitor the peaks from the hydrolysates, were relatively minor wavelengths for the absorption of light.

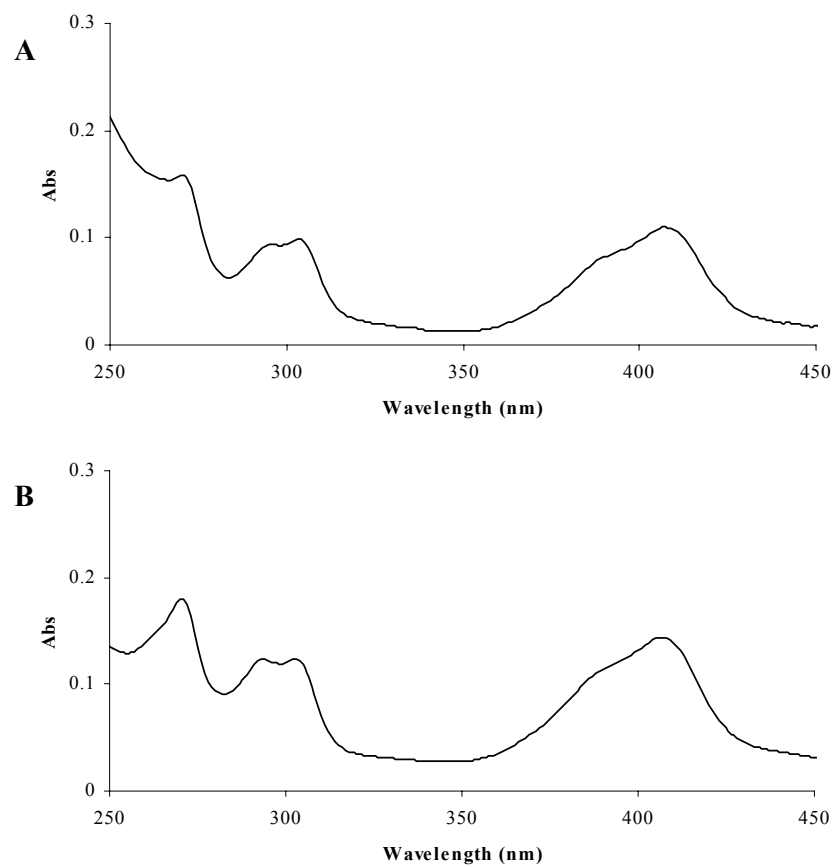


**Figure 4.12** UV-visible spectra. *A*, Peak 2 (Figures 4.1B, 4.6B and 4.8B) ( $m/z$  650); *B*, Peak 2' (Figures 4.4A, 4.7A and 4.9A) ( $m/z$  550).



Phenoxazone compounds absorb at 440 nm on the UV-visible spectrum, however the diastereoisomer (doublet, peak 2') had a maximal absorbance at approximately 408 nm (Figure 4.12B), therefore it was of interest to try to determine the structure of this compound. A large-scale reaction was undertaken, and the product was purified by HPLC, and analysed by nano-NMR spectroscopy. The proton NMR spectrum is shown in Figure 4.13. The compound was analysed by the nano probe, since only 1 mg of sample was obtained after multiple semi-prep HPLC purification. The proton NMR was run for 2 hours, and after this time the spectrum showed the presence of numerous peaks in the aromatic region (*i.e.* 6.8 – 8.8 ppm), and there were various other peaks present. In particular, a large singlet was observed at 3.7 ppm but this was found to be a low molecular weight contaminant in the sample. A gCOSY experiment was undertaken however, after 6 hours of running the experiment there were no peaks present in the spectrum. The unknown compound could not be structurally elucidated from this proton NMR spectrum.

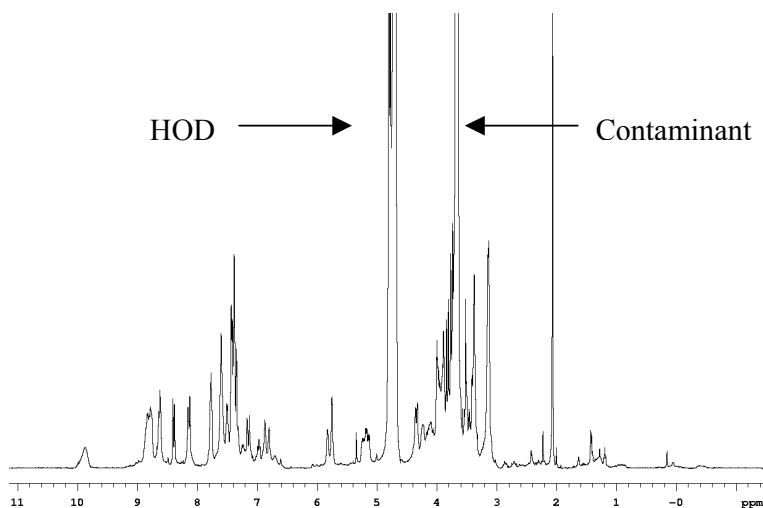


**Figure 4.13** Proton NMR spectrum of peak 2' (Figures 4.4A, 4.7A and 4.9A) ( $m/z$  550).

### 4.3.2 Incubations with the 3OHKyn-*t*-Boc-Lys Adduct

#### *Control Experiment with 3OHKyn-*t*-Boc-Lys*

Incubations were also undertaken with the 3OHKyn-*t*-Boc-Lys adduct, under the same conditions as those for 3OHKyn-*t*-Boc-His. A control experiment involving 3OHKyn-*t*-Boc-Lys was first undertaken. The HPLC chromatograms are shown in Figure 4.14. Figure 4.14A is the HPLC chromatogram of the initial reaction mixture. The peak eluting at 35.7 min is 3OHKyn-*t*-Boc-Lys. Figure 4.14B is the HPLC chromatogram of the reaction mixture after 12 days of incubation. The peaks eluting between 30 and 40 min have a low absorbance. The y-axis of these two chromatograms shows that the compounds eluting in Figure 4.14B are very low absorbing (*i.e.* compounds are all found close to the baseline of the chromatogram) at 360 nm. These compounds could not be identified.

The reaction mixture following 12 days of incubation was acid hydrolysed and the HPLC separation is shown in Figure 4.15. Numerous peaks eluted at 360 nm (Figure 4.15A), and very few low absorbing compounds eluted at 440 nm (Figure 4.14B). Previous studies have shown that 3OHKyn-*t*-Boc-Lys is unstable (Chapter 2), and in agreement with this, the compound was not observed after 12 days of incubation at pH 7.2.

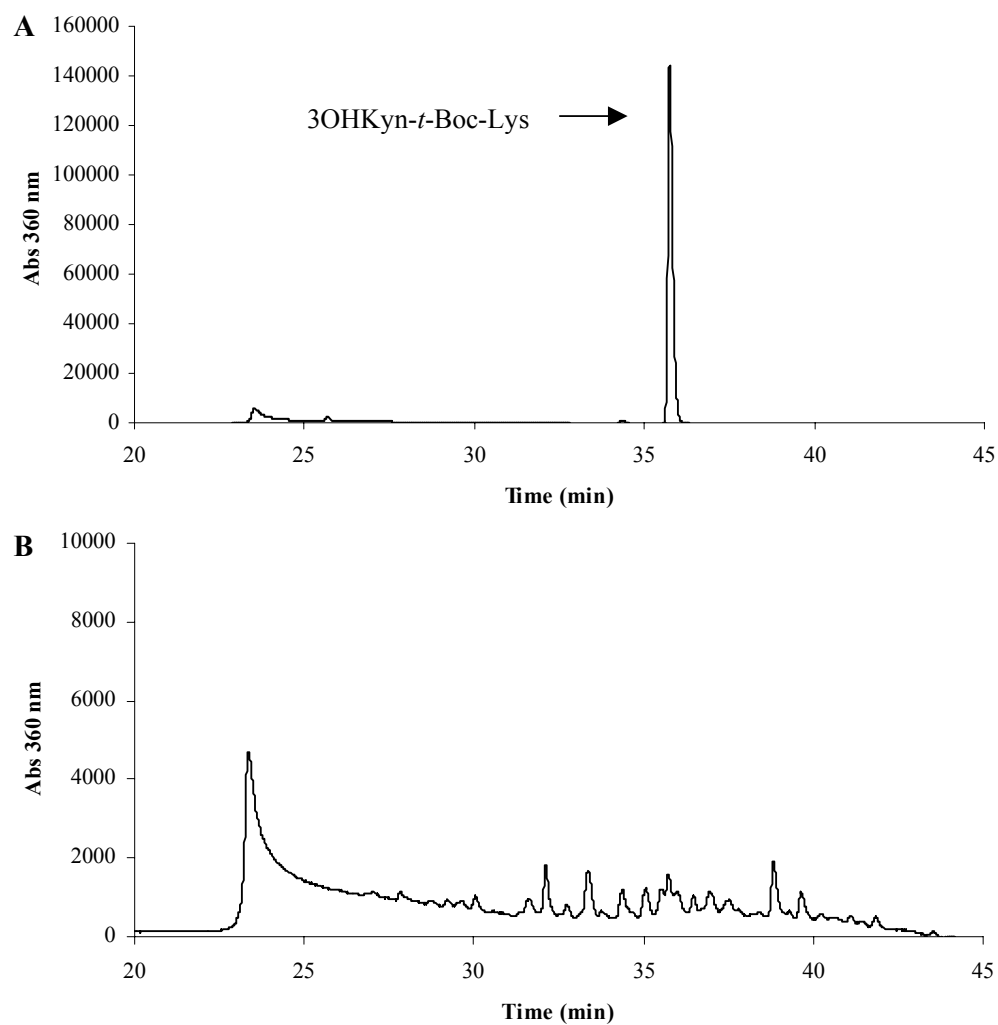


**Figure 4.14** Incubation of 3OHKyn-*t*-Boc-Lys at pH 7.2. HPLC chromatograms, *A*, Initial reaction mixture; *B*, Reaction mixture after 12 days of incubation.

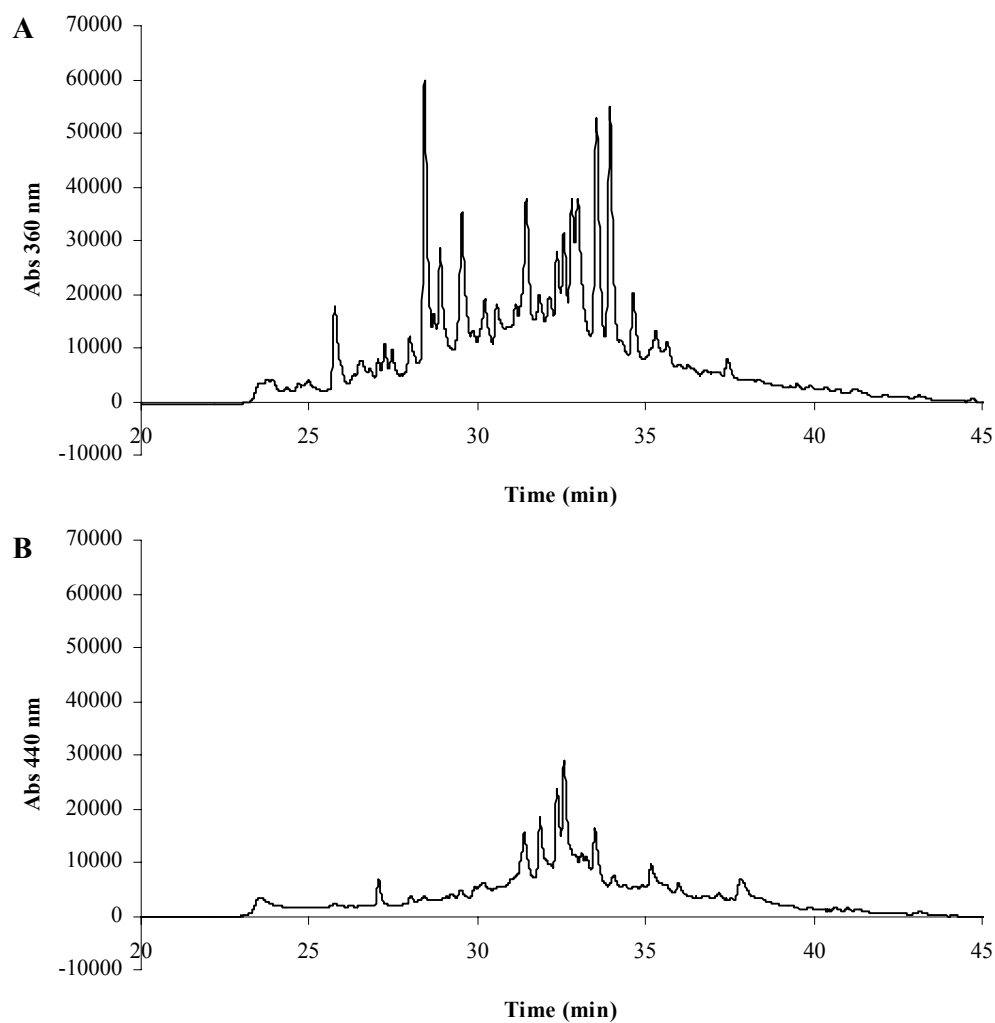


**Figure 4.15** HPLC of the acid digest of 3OHKyn-*t*-Boc-Lys following incubation for 12 days. HPLC chromatograms of, *A*, Absorbance monitored at 360 nm; *B*, Absorbance monitored at 440 nm.

***Incubation of 3OHKyn-*t*-Boc-Lys with excess N- $\alpha$ -*t*-Boc-His***

3OHKyn-*t*-Boc-Lys was also incubated with a 20-fold molar excess of N- $\alpha$ -*t*-Boc-His at pH 7.2 for 12 days. Aliquots of the reaction mixture were again taken every 3 days and purified by HPLC. The HPLC chromatogram of the initial reaction mixture is shown in Figure 4.16A. The peak eluting at 36 min is authentic 3OHKyn-*t*-Boc-Lys. Figure 4.16B is the HPLC profile of the reaction mixture after 12 days of incubation. This profile is essentially identical to that of Figure 4.14B.

Following 12 days of incubation, the reaction mixture was applied to a Sep Pak and the 80% ACN eluate was dried and acid hydrolysed with antioxidants. The HPLC separation is shown in Figure 4.17. Numerous peaks eluted at 360 nm (Figure 4.17A), and very few low absorbing compounds eluted at 440 nm (Figure 4.17B).

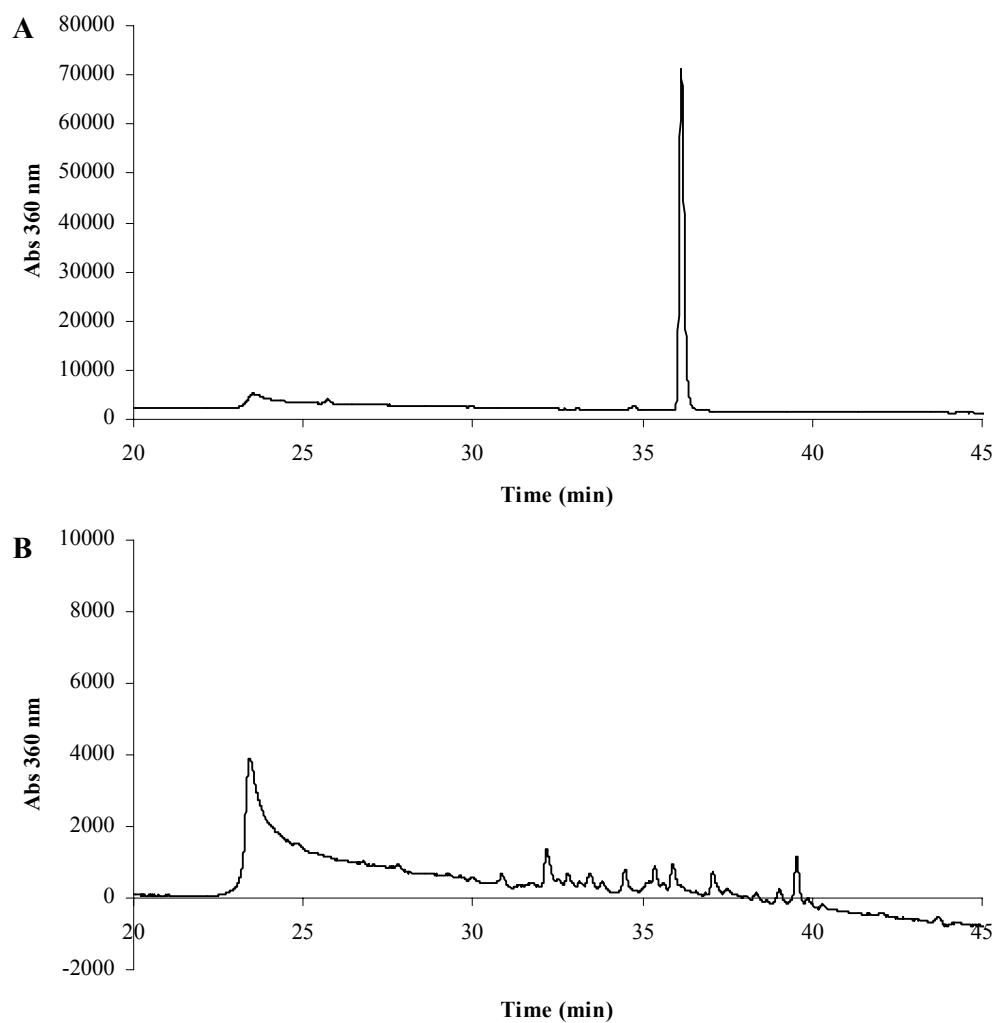


**Figure 4.16** Incubation of 3OHKyn-*t*-Boc-Lys with a 20-fold molar excess of N- $\alpha$ -*t*-Boc-His for 12 days. HPLC chromatograms of, *A*, Initial reaction mixture; *B*, Reaction mixture after 12 days of incubation.

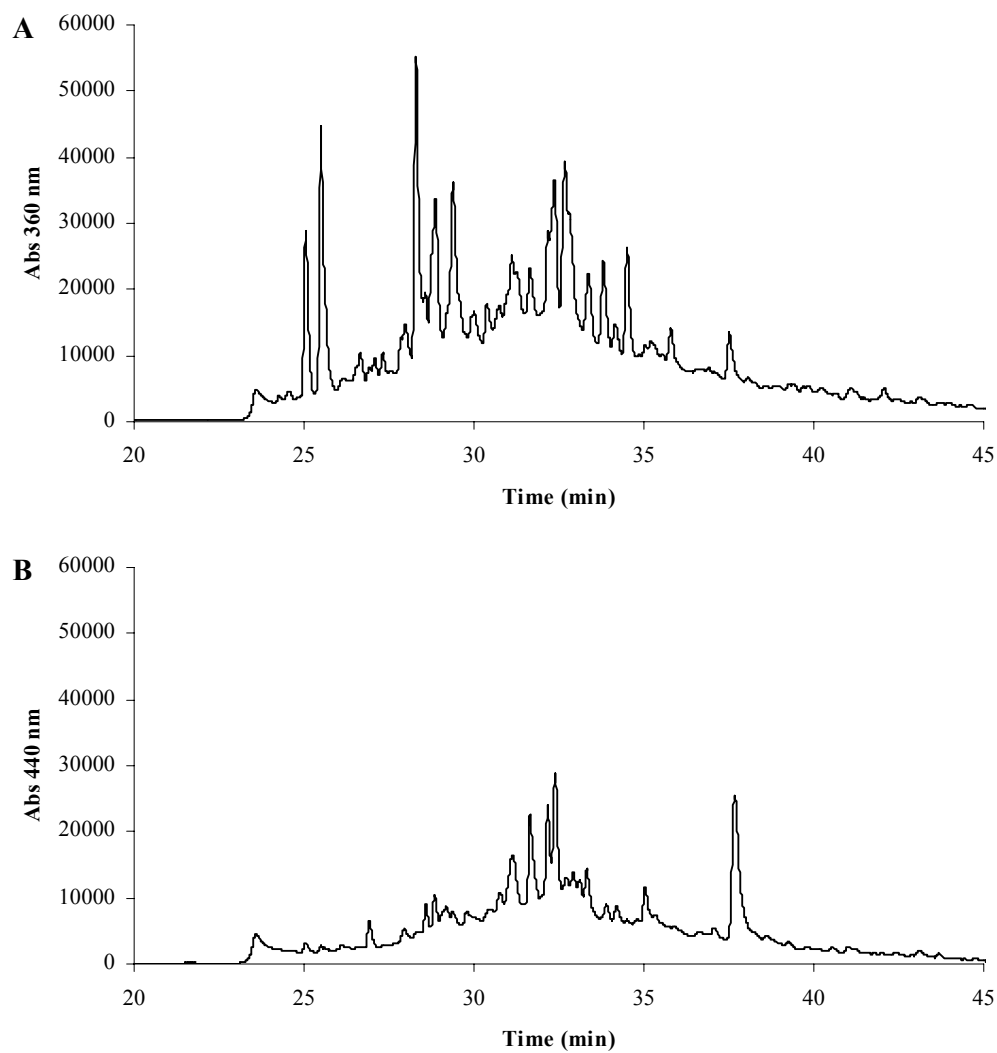


**Figure 4.17** HPLC of the acid digest of 3OHKyn-*t*-Boc-Lys with a 20-fold molar excess of N- $\alpha$ -*t*-Boc-His following incubation for 12 days. HPLC chromatograms of, *A*, Absorbance monitored at 360 nm. *B*, Absorbance monitored at 440 nm.

***Incubation of 3OHKyn-*t*-Boc-Lys with excess N- $\alpha$ -*t*-Boc-Lys***

3OHKyn-*t*-Boc-Lys was incubated with excess N- $\alpha$ -*t*-Boc-Lys at pH 7.2 for 12 days. The HPLC chromatogram of the initial reaction mixture is shown in Figure 4.18A. The peak eluting at 37 min is 3OHKyn-*t*-Boc-Lys. Figure 4.18B is the HPLC profile of the reaction mixture after 12 days of incubation. This profile is essentially identical to that of Figure 4.14B and 4.16B.

Following 12 days of incubation, the reaction mixture was applied to a Sep Pak and the 80% ACN eluate was dried and acid hydrolysed with antioxidants. The HPLC separation is shown in Figure 4.19. Numerous peaks again eluted at 360 nm (Figure 4.19A), and very few compounds eluted at 440 nm (Figure 4.19B).

In summary, the HPLC chromatograms (Figures 4.14 to 4.19, inclusive) from incubations of 3OHKyn-*t*-Boc-Lys in the absence and presence of excess amino acids established that it would be a very difficult task to try and structurally identify these numerous minor compounds eluting in each chromatogram. The chromatograms of the hydrolysates were clearly much more complex than those observed for the 3OHKyn-*t*-Boc-His incubations.



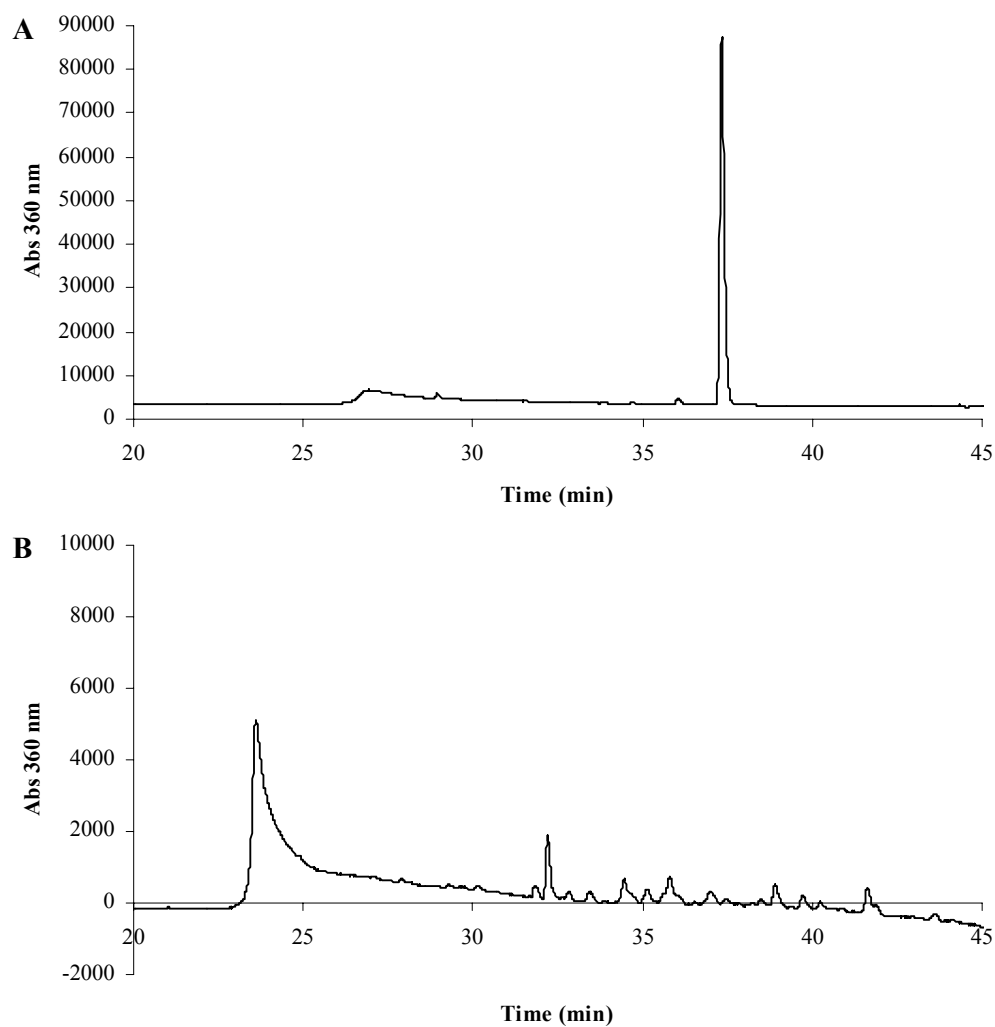


**Figure 4.18** Incubation of 3OHKyn-*t*-Boc-Lys with a 20-fold molar excess of N- $\alpha$ -*t*-Boc-Lys for 12 days. HPLC chromatograms of, *A*, Initial reaction mixture; *B*, Reaction mixture after 12 days of incubation.

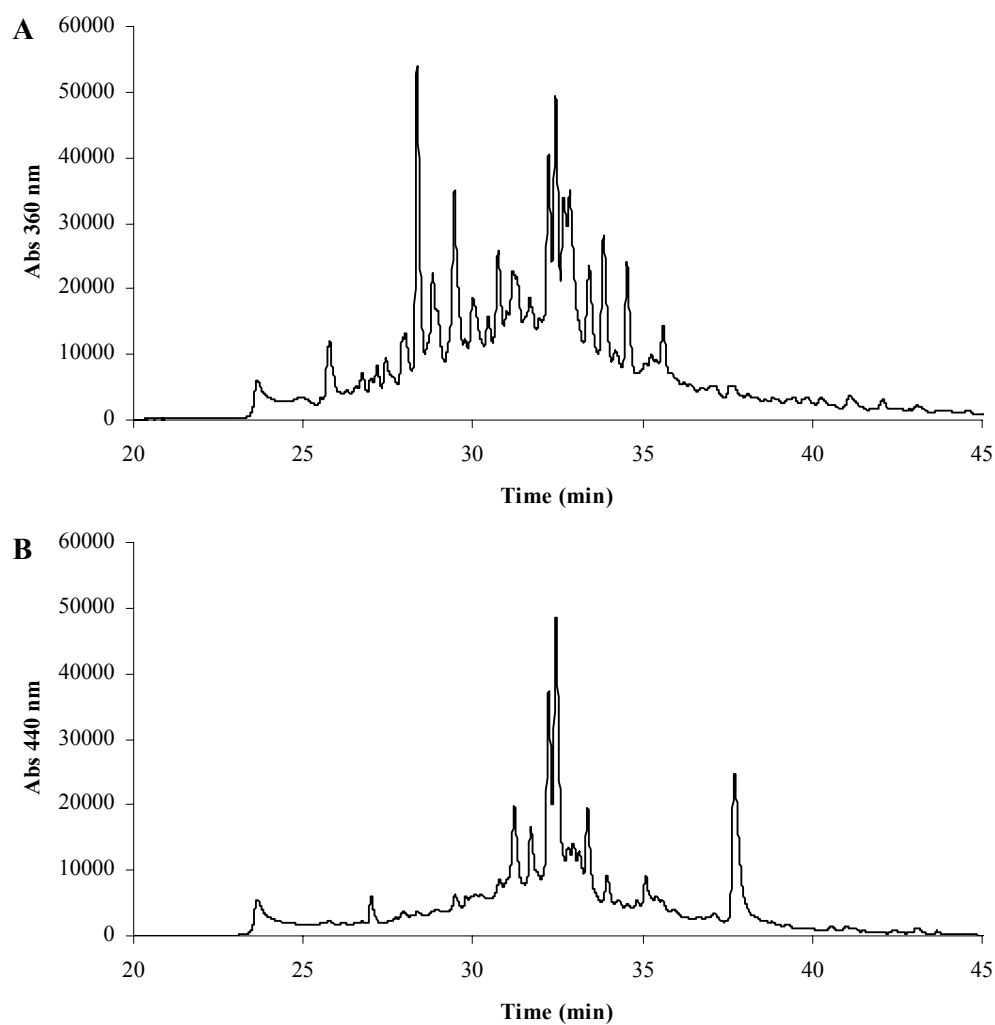


**Figure 4.19** HPLC of the acid digest of 3OHKyn-*t*-Boc-Lys with a 20-fold molar excess of N- $\alpha$ -*t*-Boc-Lys following incubation for 12 days. HPLC chromatograms of, *A*, Absorbance monitored at 360 nm. *B*, Absorbance monitored at 440 nm.

### 4.3.3 Incubation of 3OHKyn-Modified CLP (pH 7.2)

In an attempt to observe the effects of long term exposure of 3OHKyn-modified lens proteins to oxygen, and to hopefully crosslink 3OHKyn in lens proteins, CLP previously modified with 3OHKyn at pH 7.2, (whereby 3OHKyn is only attached to Cys) was incubated for 15 days at pH 7.2. The protein concentration of the solution was 20 mg/mL. Aliquots of the reaction mixture were taken at 0, 1, 2, 3, 6, 9, 12 and at 15 days of incubation, and analysed by, SDS-PAGE, 3-D fluorescence, acid hydrolysis and mass spectrometry.

#### *Analysis by SDS-PAGE*

Aliquots taken during the incubation period were run on an SDS gel to monitor the formation of crosslinks. CLP has a molecular weight of approximately 20 kDa, therefore if a crosslink were to form in the protein during incubation, a band would be visible at approximately 40 kDa. Two gels were performed, one under non-reducing conditions, and the other under reducing condition. Gels are shown in Figure 4.20. The gel in Figure 4.20A was run under non-reducing conditions, and each of the lanes (lanes 2-7) exhibited a visible band between markers 37 and 50 kDa. Aliquots were taken initially, 3, 6, 9, 12 and at 15 days of incubation. A second gel (Figure 4.20B) was undertaken under reducing conditions (*i.e.* DTT was added to reduce disulphide bonds) and, the band between markers 37 and 50 kDa disappeared. This demonstrates that the band present in Figure 4.20A was a result of disulphide bond linkages, and was not a result of any other form of crosslinking in the protein.

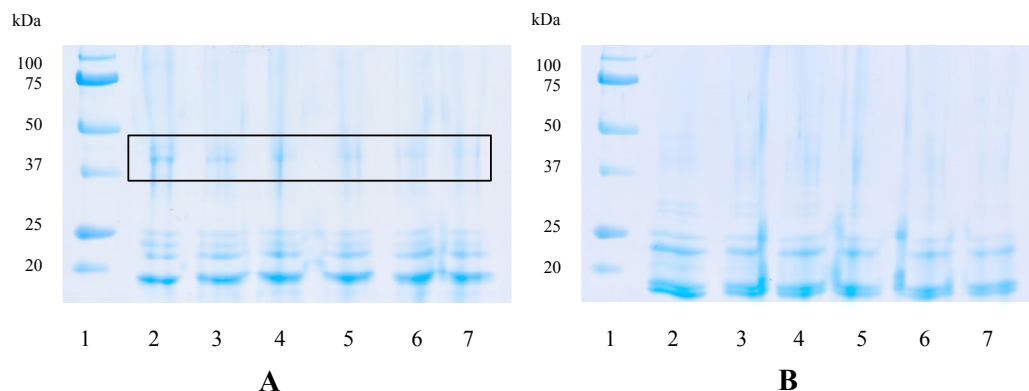


**Figure 4.20** SDS-PAGE of proteins from incubation of 3OHKyn modified CLP. Lane 1: Marker; Lane 2: Aliquot time = 0 days; Lane 3: Aliquot time = 3 days; Lane 4: Aliquot time = 6 days; Lane 5: Aliquot time = 9 days; Lane 6: Aliquot time = 12 days; Lane 7: Aliquot time = 15 days. *A*, Non-reducing conditions; *B*, Reducing conditions.

#### *Analysis by 3-D Fluorescence*

Aliquots taken during the incubation period were monitored by 3-D fluorescence. Each of the aliquots was ultra-filtered with a 10 kDa cut-off membrane, to remove any non-covalently bound material that may have formed during the incubation period. A change in fluorescence was an indication that the protein had altered with respect to its 3OHKyn attachment. Initially the 3OHKyn-modified protein exhibited maximal fluorescence intensity at Ex 370 nm/Em 485 nm (Figure 4.21A). Aliquots taken after 2 days of incubation revealed that the emission of the protein had changed 10 nm from the initial aliquot (see Table 4.2). The fluorescence intensities for all of the protein aliquots are listed in Table 4.2. At the end of the incubation period the maximal fluorescence intensity was observed at Ex 365 nm/Em 470 nm (Figure 4.21B).

**Table 4.2** List of the 3-D fluorescence intensities for each aliquot from the incubation.

| Time (Days) | Ex (nm)/Em (nm) |
|-------------|-----------------|
| 0           | 370/485         |
| 1           | 370/480         |
| 2           | 370/475         |
| 3           | 370/470         |
| 6           | 370/470         |
| 9           | 365/470         |
| 12          | 365/470         |
| 15          | 365/470         |

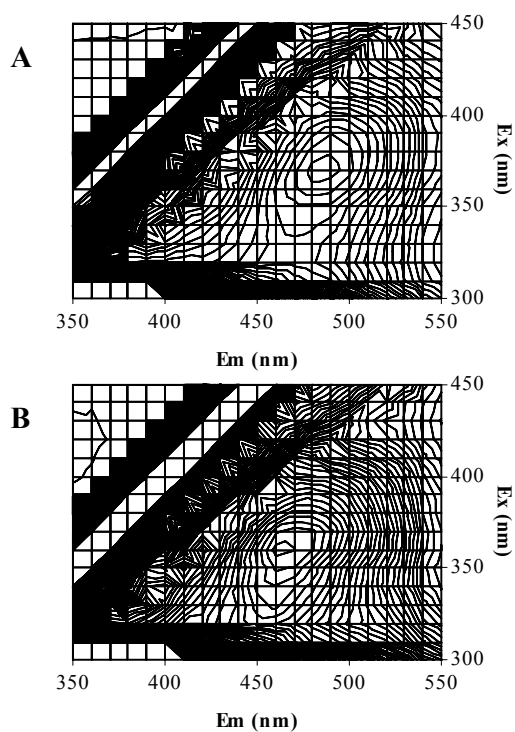


**Figure 4.21** 3-D Fluorescence spectra of aliquots from the protein mixture. *A*, Initial aliquot; *B*, Aliquot after 15 days of incubation.

*Analysis of Filtrate*

Aliquots of the protein at the various time intervals were taken for acid hydrolysis. Each protein aliquot was ultra-filtered to remove non-covalently bound material from the protein. Each filtrate was analysed by HPLC and peaks that eluted were examined by mass spectrometry. Figure 4.22 shows the HPLC chromatogram of the filtrate from the aliquot taken after 1 day of incubation of 3OHKyn-modified protein at pH 7.2.

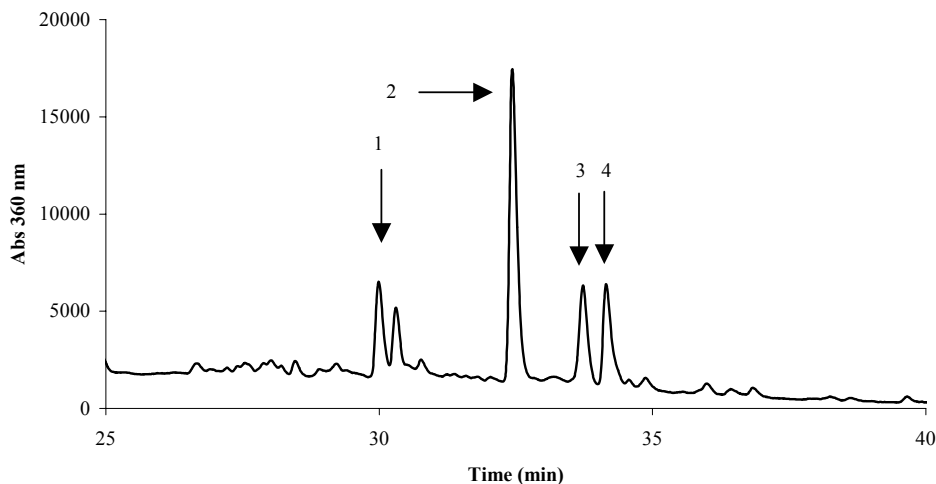


**Figure 4.22** HPLC chromatogram of the filtrate from the protein aliquot after 1 day of incubation at pH 7.2.

Figure 4.22 exhibited 5 peaks eluting between 30 and 35 min, and the arrowed peaks were collected. Peak 1 eluted at 30 min and the ESI mass spectrum (Figure 4.23A) of this peak showed a molecular ion of  $m/z$  206. MS/MS of this ion (spectrum not shown) yielded fragment ions  $m/z$  188 and 160. This compound was identified as xanthurenic acid, since standard xanthurenic acid also yields the same fragment ions (spectrum not shown) and co-eluted with authentic xanthurenic acid. Xanthurenic acid is formed from oxidation of 3OHKyn.<sup>109,191</sup> Peak 2 eluted at 32.4 min on the HPLC chromatogram. The mass spectrum of this peak (Figure 4.23B) showed an ion at  $m/z$  395, MS/MS of this ion (spectrum not shown) resulted in fragment ions  $m/z$  377, 349 and 297. This compound could not be identified, since none of these ions are 3OHKyn fragment ions. Peak 3 eluted at 33.7 min on the HPLC chromatogram. The mass spectrum (Figure 4.23C) showed a prominent ion at  $m/z$  300, and MS/MS of this ion (spectrum not shown) yielded fragment ions  $m/z$  282, 208 and 110. The molecular ion of 3OHKyn-yellow is

$m/z$  208, therefore MS/MS was done on this ion (spectrum not shown) and fragment ions  $m/z$  190, 162 and 110, confirmed that this peak contains 3OHKyn-yellow, which is also attached to a small compound of mass 92 Da. Finally, peak 4 eluted at 34.2 min, and the mass spectrum was identical to that for peak 3 (Figure 4.23C) with a prominent ion at  $m/z$  300. MS/MS (spectrum not shown) yielded the same fragment ions as peak 3. It appears that peak 3 and peak 4 are diastereoisomers.

These findings show that some of the 3OHKyn attached to the CLP has been released from the protein as deaminated 3OHKyn, and due to the instability at pH 7.2 (Chapter 2, stability study at pH 7.2) it has oxidised, to form novel compounds.

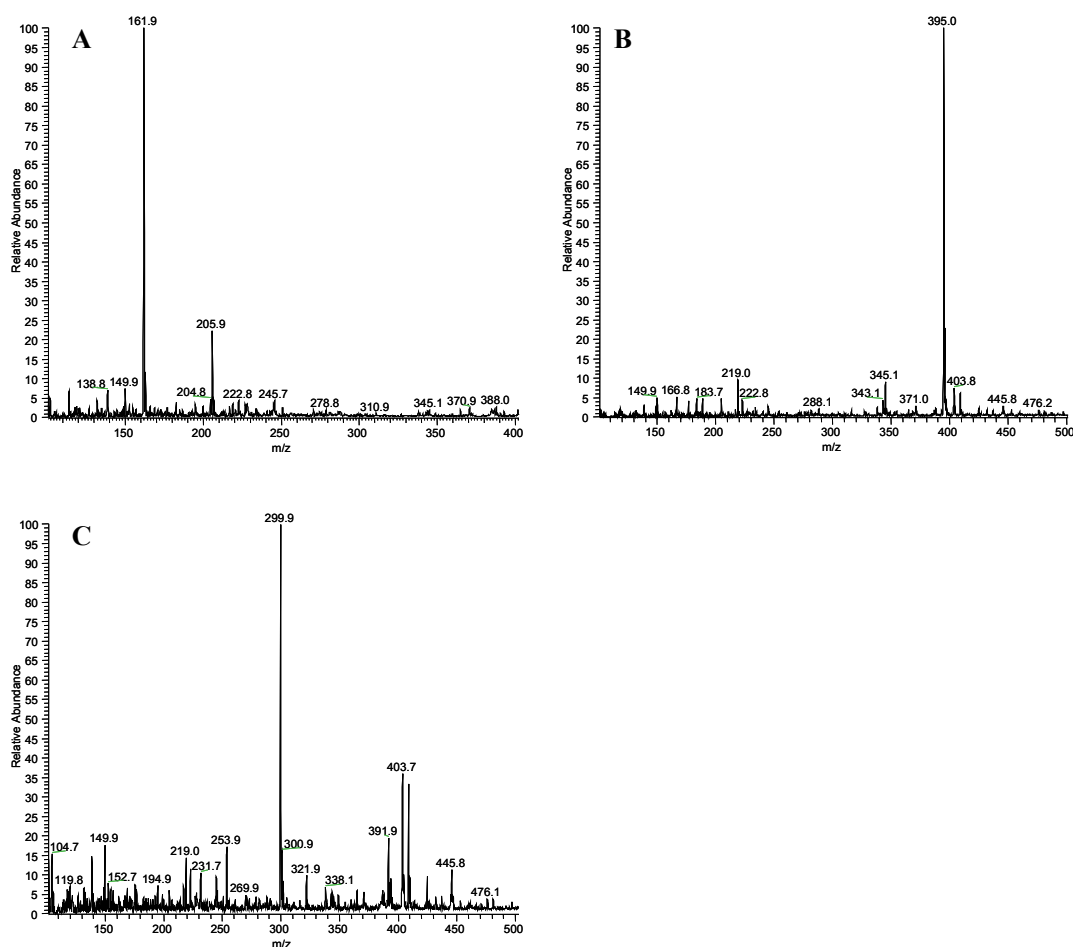


**Figure 4.23** ESI mass spectra of the peaks eluting in Figure 4.22. *A*, Peak 1 eluting at 30 min; *B*, Peak 2 eluting at 32.4 min; *C*, Peak 3 eluting at 33.7 min.

*Acid Hydrolysis of Protein*

Protein aliquots from the reaction mixture were acid hydrolysed after ultra-filtration to remove non-covalently bound compounds. The HPLC chromatogram of the hydrolysate of the initial aliquot is shown in Figure 4.24A. The doublet compound eluting at 28 min was identified as 3OHKyn-Cys. This result was expected since this protein was initially prepared by incubating CLP with 3OHKyn at pH 7.2 for 48 hours (see Chapter 3). The HPLC chromatogram of the hydrolysate of the protein after 15 days of incubation at pH 7.2 is shown in Figure 4.24B. As a result of this incubation period, the chromatogram indicates that the protein had changed in a major way from the initial aliquot. The numbered peaks indicated with an arrow, in Figure 4.24B, were collected and analysed by mass spectrometry for ‘marker’ ions, which were later used to compare with peaks obtained from cataract lens proteins.

In Figure 4.24B, peak 1 eluted at 25 min. The ESI mass spectrum (spectrum not shown) of this peak showed a molecular ion of  $m/z$  363. MS/MS of this ion (spectrum not shown) yielded fragment ions  $m/z$  317, 208, 156 and 110, which are the fragment ions for 3OHKyn-His. Therefore this peak was identified as 3OHKyn-His. Peak 2 eluted at 26.6 min, and the mass spectrum of this peak showed an ion at  $m/z$  518 (Figure 4.25A). MS/MS of this ion (spectrum not shown) resulted in fragment ions  $m/z$  499, 475, 429, 387 and 279. This compound could not be identified. Peak 3 eluted at 28.2 min. The mass spectrum showed many ions (Figure 4.25B) however none could be identified as the molecular ion. Peak 4 eluted at 28.5 min. The mass spectrum exhibited many ions centred between  $m/z$  400 and  $m/z$  600 (Figure 4.25C), MS/MS of  $m/z$  684, exhibited fragment ions  $m/z$  667, 641, 591, 505, 429 and 299 (spectrum not shown). This compound could not be identified. Peak 5 eluted at 29 min. The mass spectrum showed an ion at  $m/z$  528 (Figure 4.25D), MS/MS resulted in fragment ions  $m/z$  511, 484, 423 and 250 (spectrum not shown). Peak 6 eluted at 32.5 min. The mass spectrum exhibited many ions above  $m/z$  400 (Figure 4.25E), however it was difficult to determine the molecular ion for this peak. Peak 7 eluted at 33.5 min. The mass spectrum also showed numerous ions eluting above  $m/z$  400 (Figure 4.25F), making it difficult to determine the molecular ion.



Peak 8 eluted at 33.9 min. The mass spectrum is shown in Figure 4.26A. Ions in this spectrum could not be identified. Peak 9 eluted at 35.3 min and the mass spectrum (Figure 4.26B) failed to show any familiar ions. Peak 10 eluted at 37.8 min, the mass spectrum is shown in Figure 4.26C, ions in the spectrum were not familiar. Peak 11 eluted at 41.2 min and the mass spectrum showed an abundant ion at  $m/z$  542 (Figure 4.26D), MS/MS of this ion yielded fragment ions  $m/z$  497 and 375 (spectrum not shown), this data alone makes it difficult to conclude if this is indeed the molecular ion of this peak. Peak 12 eluted at 42.2 min and the mass spectrum is shown in Figure 4.26E. Finally peak 13 eluted at 46 min and the mass spectrum is shown in Figure 4.26F.

The structures of the majority of these compounds could not be determined from the mass spectrometry data alone and were not pursued further.

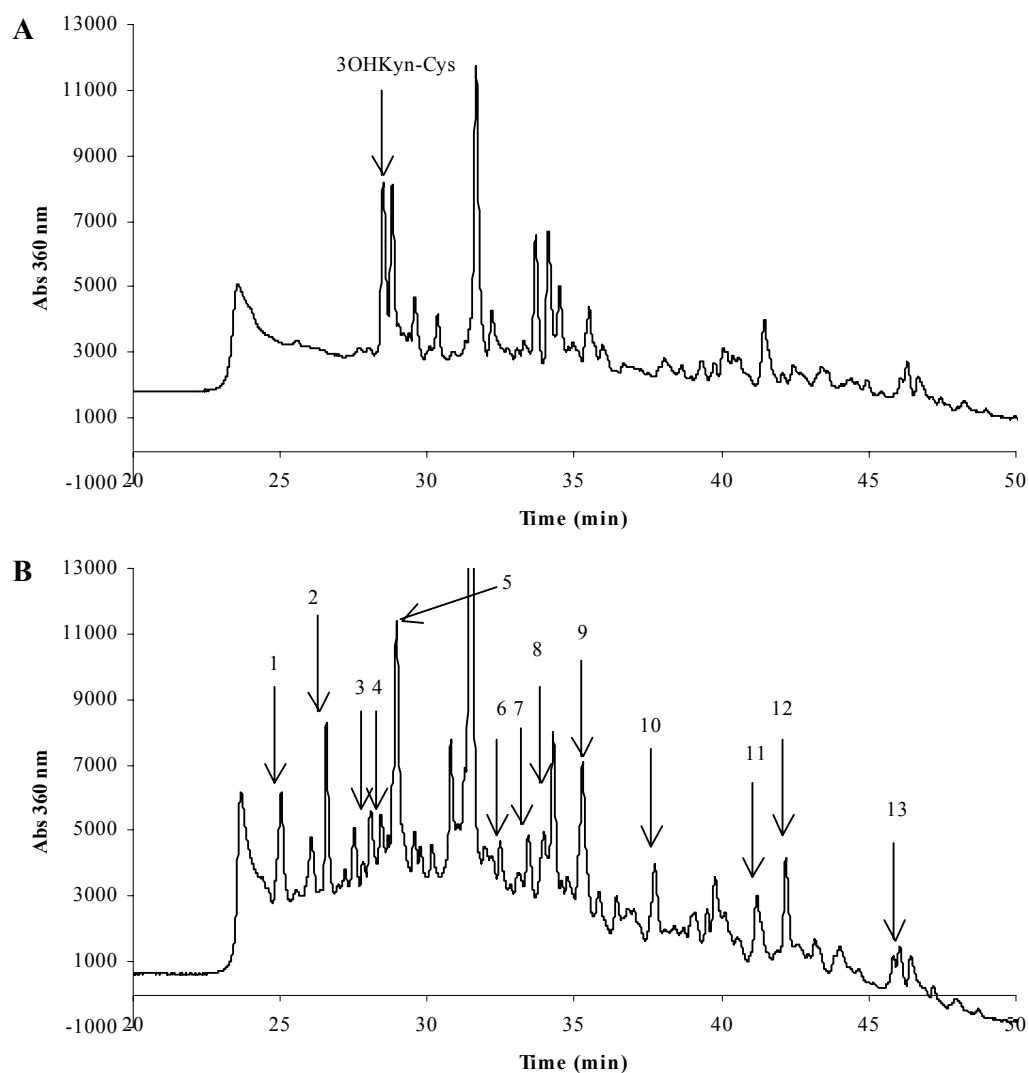


**Figure 4.24** HPLC chromatograms of acid hydrolysed proteins. *A*, Initial aliquot; *B*, Aliquot after 15 days of incubation. Arrowed peaks were collected for mass spectrometry.

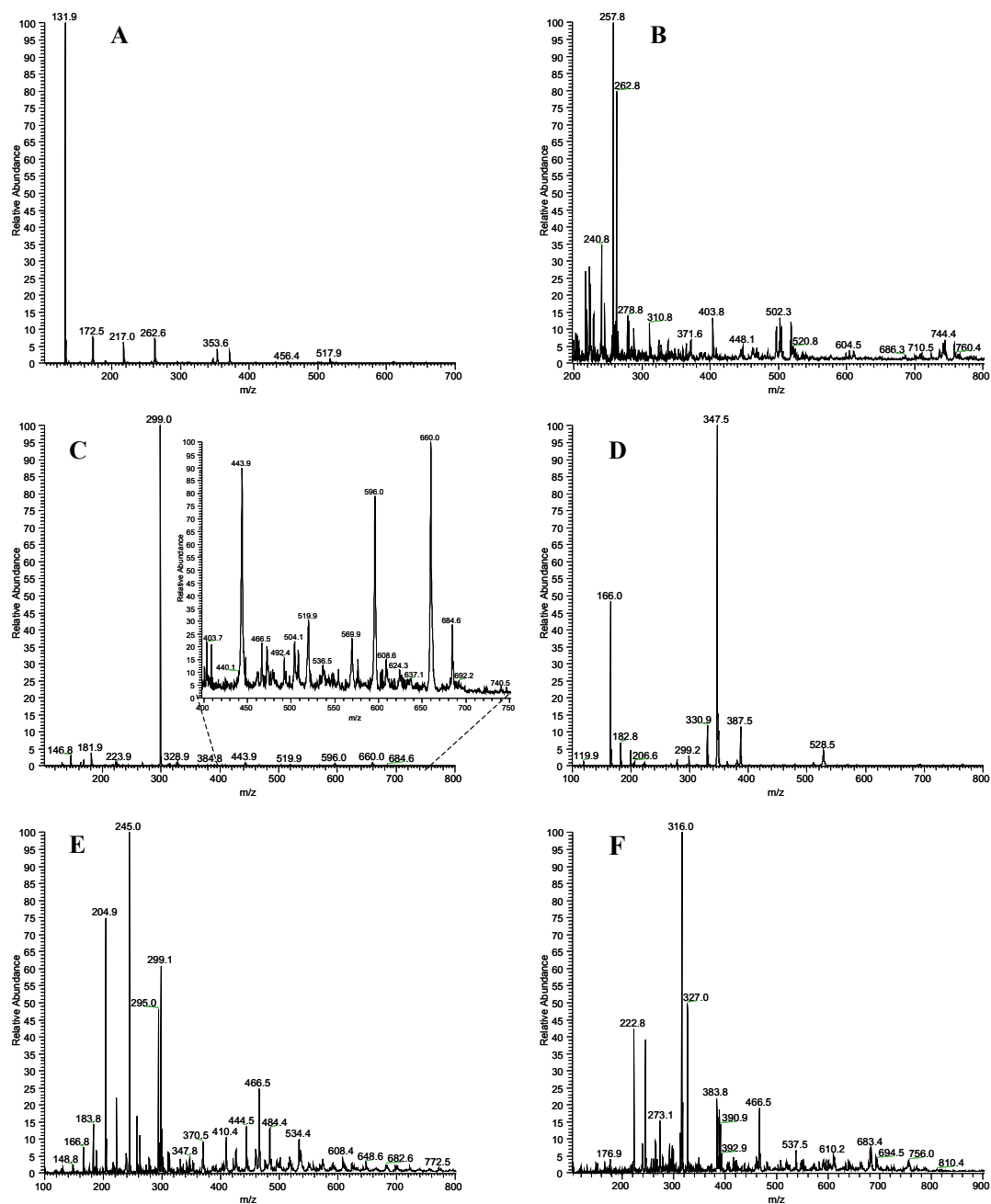


**Figure 4.25** ESI mass spectra of peaks eluting in Figure 4.24B. *A*, Peak 2; *B*, Peak 3; *C*, Peak 4; *D*, Peak 5; *E*, Peak 6; *F*, Peak 7.

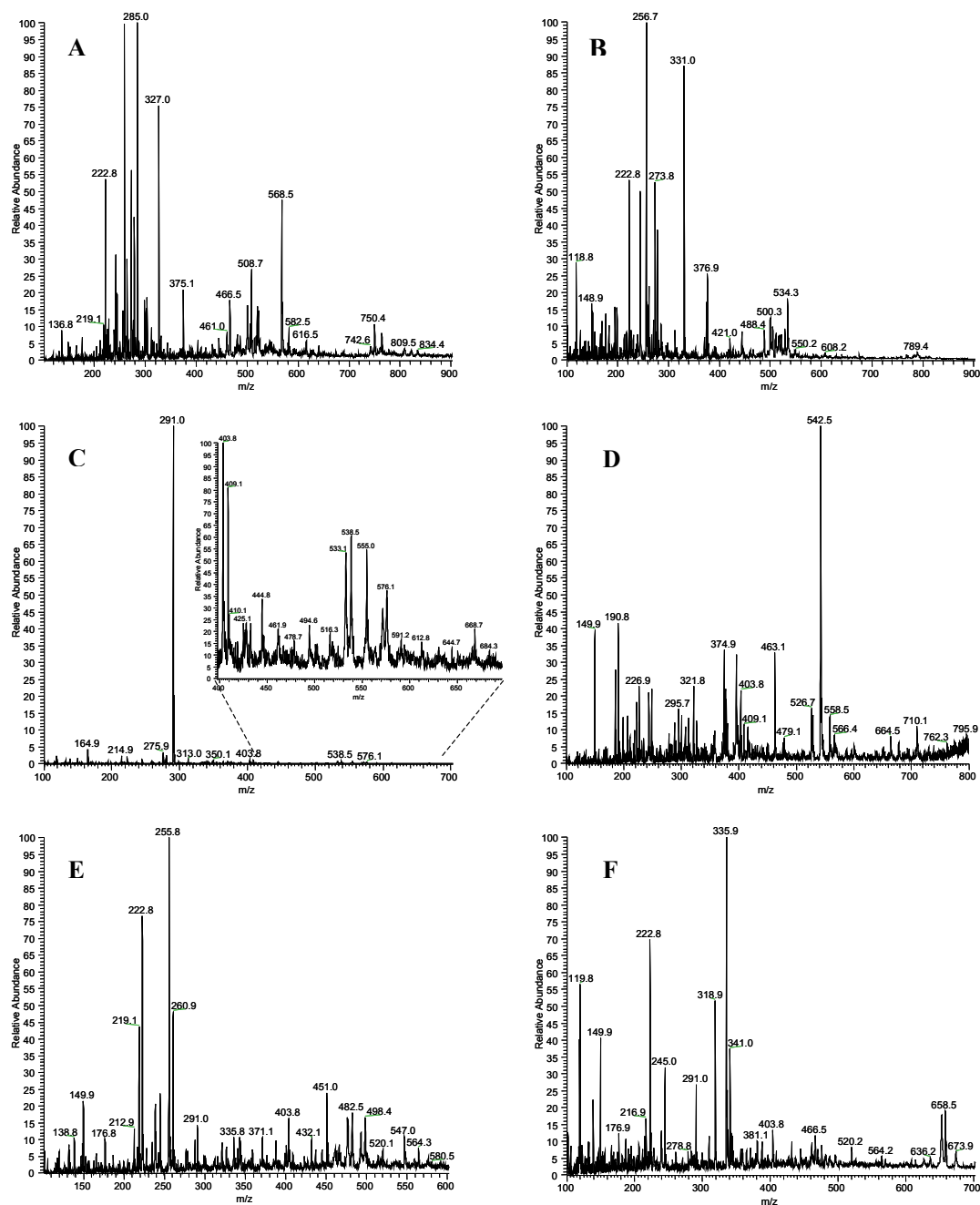


**Figure 4.26** ESI mass spectra of peaks eluting in Figure 4.24B. *A*, Peak 8; *B*, Peak 9; *C*, Peak 10; *D*, Peak 11; *E*, Peak 12; *F*, Peak 13.

The modified CLP used in this study was known to contain modification primarily at Cys. The concentration of 3OHKyn-Cys in the protein aliquots during the incubation at pH 7.2 was quantified and is shown in Figure 4.27. The concentration of 3OHKyn-Cys decreased by 63% after 2 days of incubation and could not be detected after 3 days of incubation. Analysis of the HPLC hydrolysates and mass spectrometry confirmed that 3OHKyn-His was formed after 6 days of incubation. This adduct presumably formed as a result of decomposition of 3OHKyn-Cys with release of deaminated 3OHKyn, which then bound to His residues (see Figure 4.24A and Figure 4.24B).

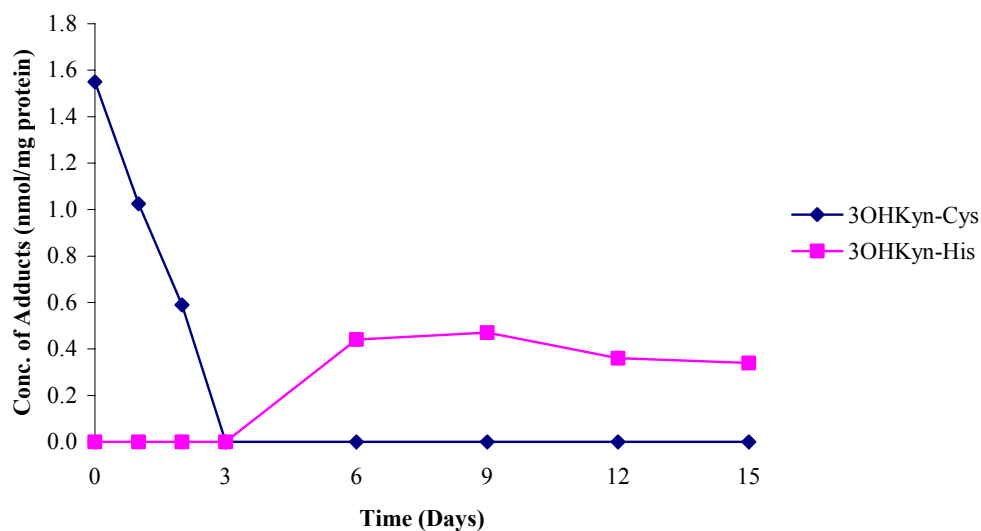


**Figure 4.27** Concentration of 3OHKyn-Cys and 3OHKyn-His in protein samples during incubation of CLP originally modified by 3OHKyn at pH 7.2.

#### 4.3.4 Incubation of 3OHKyn-Modified CLP (pH 9.5)

In this section, another attempt was made to crosslink 3OHKyn-modified lens proteins. The modified protein used in this incubation was CLP modified by 3OHKyn at pH 9.5 which contains modifications at Cys, His and Lys, and a greater degree of modification by 3OHKyn. The protein was incubated for 10 days at pH 7.2 and aliquots were taken at 0, 1, 2, 3, 4, 6, 8 and 10 days. Since this protein was originally modified at a high pH (pH 9.5), the protein reaction mixture at the start of the incubation was a dark brown/black colour (Chapter 3), and this colour was possibly indicative of a high amount of 3OHKyn oxidation in the protein. Each of the aliquots was again analysed by SDS-PAGE, 3-D fluorescence acid hydrolysis and mass spectrometry.

##### *Analysis by SDS-PAGE*

Aliquots of the reaction mixture were again monitored by SDS gels for the formation of crosslinks (*i.e.* band at approximately 40 kDa). Two gels were performed, one under non-reducing conditions and the other under reducing condition. Gels are shown in Figure 4.28. The gel in Figure 4.28A was run under non-reducing conditions, and each of the aliquots exhibited a visible band between markers 37 and 50 kDa. The second gel (Figure 4.28B) was undertaken under reducing conditions (*i.e.* DTT was added to reduce disulphide bonds) and, the band between markers 37 and 50 kDa disappeared. This demonstrates that the band present in Figure 4.28A was a direct result of disulphide bond linkages, and was not the result of any other form of crosslinking in the protein.

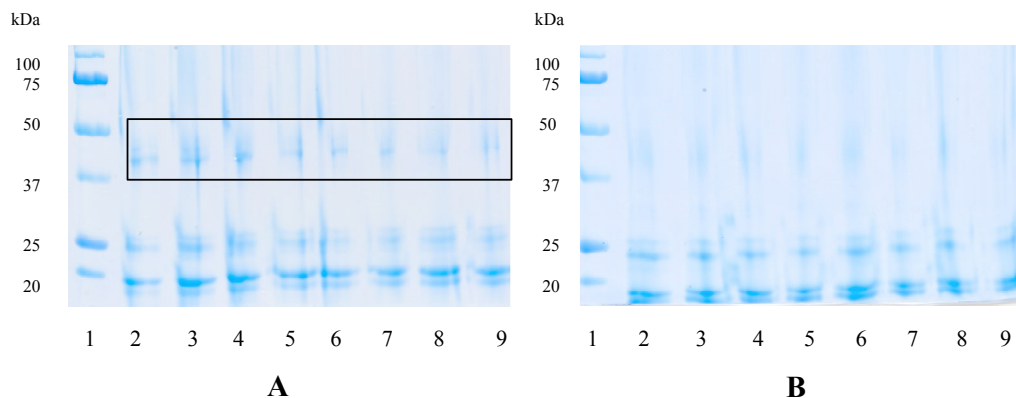


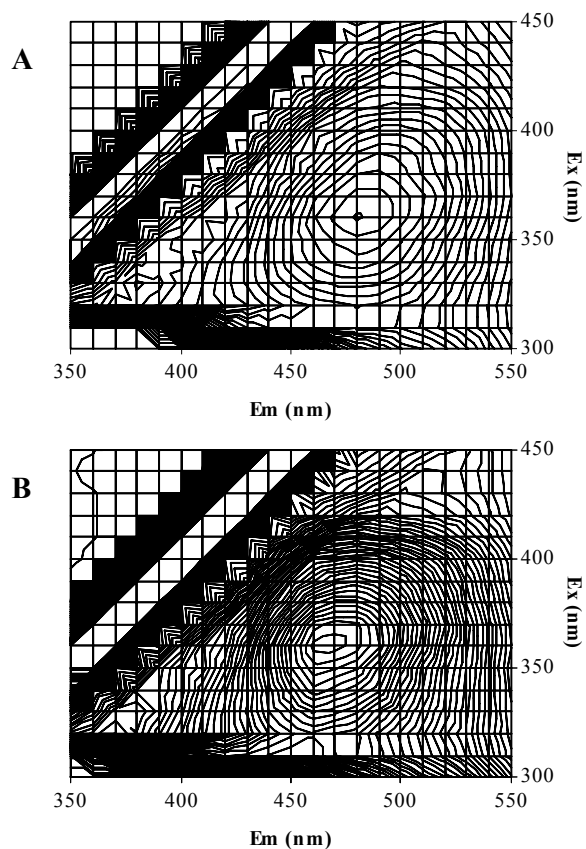
**Figure 4.28** SDS-PAGE of proteins from incubation of 3OHKyn modified CLP. Lane 1: Marker; Lane 2: Aliquot time = 0 days; Lane 3: Aliquot time = 1 days; Lane 4: Aliquot time = 2 days; Lane 5: Aliquot time = 3 days; Lane 6: Aliquot time = 4 days; Lane 7: Aliquot time = 6 days; Lane 8: Aliquot time = 8 days; Lane 9: Aliquot time = 10 days. *A*, Non-reducing conditions; *B*, Reducing conditions.

#### *Analysis by 3-D Fluorescence*

Aliquots of the protein mixture were monitored for modifications by 3-D fluorescence. Each aliquot was first ultra-filtered to remove non-covalently bound compounds. Initially the 3OHKyn-modified protein exhibited maximal fluorescence intensity at Ex 360 nm/Em 480 nm (Figure 4.29A). The fluorescence intensities for all the protein aliquots are listed in Table 4.3. The maximum excitation wavelength for all aliquots remained constant, however the emission gradually decreased by 15 nm over the 10 day incubation period. At the end of the incubation, the protein exhibited maximal fluorescence intensity at Ex 360 nm/Em 465 nm (Figure 4.29B).

**Table 4.3** List of the 3-D fluorescence intensities for each aliquot from the incubation.

| Time (Days) | Ex (nm)/Em (nm) |
|-------------|-----------------|
| 0           | 360/480         |
| 1           | 360/475         |
| 2           | 360/470         |
| 3           | 360/470         |
| 4           | 360/470         |
| 6           | 360/470         |
| 8           | 360/465         |
| 10          | 360/465         |

**Figure 4.29** 3-D Fluorescence spectra of the aliquots from the protein mixture. *A*, Initial aliquot; *B*, Aliquot after 10 days of incubation.



*Analysis of Filtrate*

Aliquots of the incubation mixture were taken for acid hydrolysis of the protein, and were ultra-filtered to remove non-covalently bound material from the protein. Each filtrate was examined by HPLC and peaks that eluted were analysed by mass spectrometry. Figure 4.30 is the HPLC chromatogram of the filtrate from the protein aliquot after 1 day of incubation at pH 7.2.

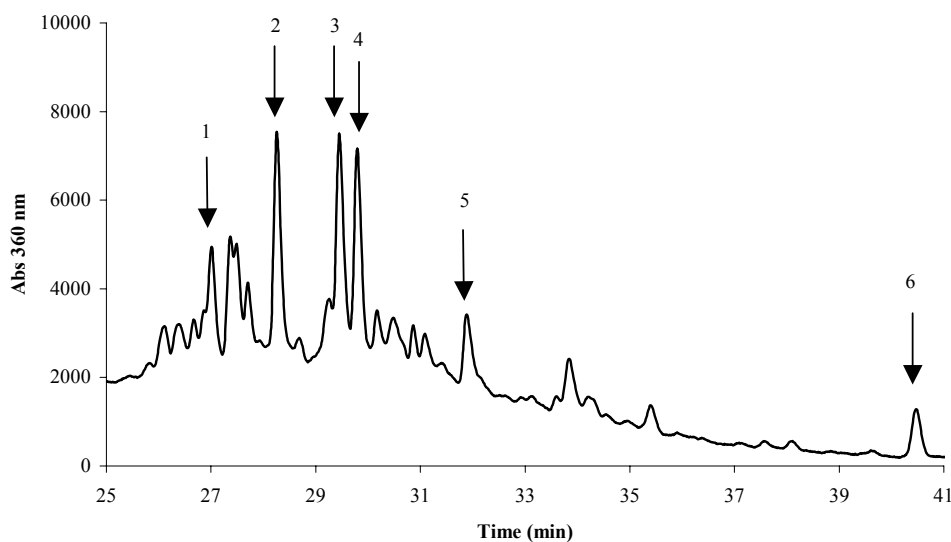


**Figure 4.30** HPLC chromatogram of the filtrate from the protein aliquot after 1 day of incubation.

The HPLC chromatogram exhibited numerous peaks eluting between 26 and 41 min. Six peaks in the HPLC chromatogram were collected and analysed by mass spectrometry (Figure 4.30). Peak 1 eluted at 27 min, and the mass spectrum showed numerous ions (Figure 4.31A). MS/MS of ion  $m/z$  371 (spectrum not shown) yielded fragment ion  $m/z$  268, and MS/MS of ion  $m/z$  343 (spectrum not shown), yielded fragment ion  $m/z$  240. The identity of this peak could not be determined. Peak 2 eluted at 28.3 min on the HPLC chromatogram. The mass spectrum of this peak showed an abundant ion at  $m/z$  305 (Figure 4.31B). MS/MS of this ion yielded fragment ions  $m/z$  286, 261, 212 and 194. This peak was not identified. Peak 3 eluted at 29.4 min on the HPLC chromatogram, and the mass spectrum showed an abundant ion at  $m/z$  206

(Figure 4.31C). MS/MS of this ion resulted in fragment ions  $m/z$  188 and 160 (spectrum not shown), confirming that this peak was indeed xanthurenic acid, since authentic xanthurenic acid co-eluted with this sample. Peak 4 eluted at 29.8 min on the HPLC chromatogram. The mass spectrum of this peak is shown in Figure 4.31D. The mass spectrum shows that there is a small ion at  $m/z$  206, indicating a small amount of xanthurenic acid was present, since this peak eluted so close to peak 3. However this peak did contain an abundant ion at  $m/z$  162, and MS/MS of this ion yielded fragment ions  $m/z$  143, 134, 120 and 105 (spectrum not shown). The ion  $m/z$  162 is a known fragment ion of 3OHKyn (Chapter 2), however the fragment ions ( $m/z$  143, 134, 120 and 105) are not characteristic fragment ions of 3OHKyn. Peak 5 eluted at 31.9 min on the HPLC chromatogram. The mass spectrum showed an abundant ion at  $m/z$  395 (Figure 4.31E). MS/MS of this ion yielded fragment ions  $m/z$  377, 349 and 297. This compound could not be identified, however this compound together with these fragment ions was also seen in the filtrate of Section 4.3.3. Peak 6 eluted at 40.5 min on the HPLC chromatogram, the mass spectrum (Figure 4.31F) showed many ions, however none could be identified. These findings again show that 3OHKyn has deaminated from the protein and formed numerous oxidised compounds which were not structurally elucidated.

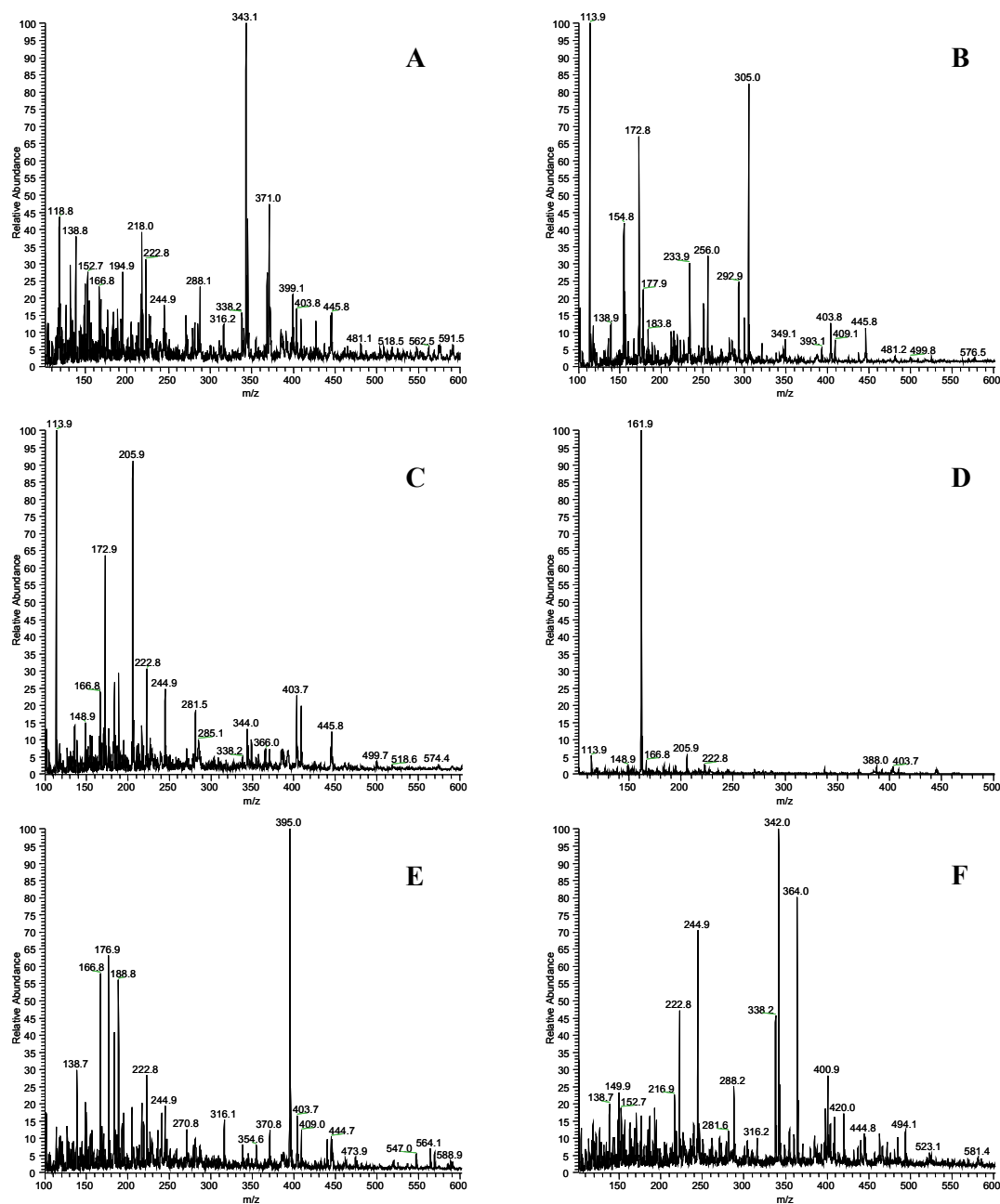


**Figure 4.31** ESI mass spectra of the peaks eluting in Figure 4.30. *A*, Peak 1 eluting at 27 min; *B*, Peak 2 eluting at 28.3 min; *C*, Peak 3 eluting at 29.4 min; *D*, Peak 4 eluting at 29.8 min; *E*, Peak 5 eluting at 31.9 min; *F*, Peak 6 eluting at 40.5 min.

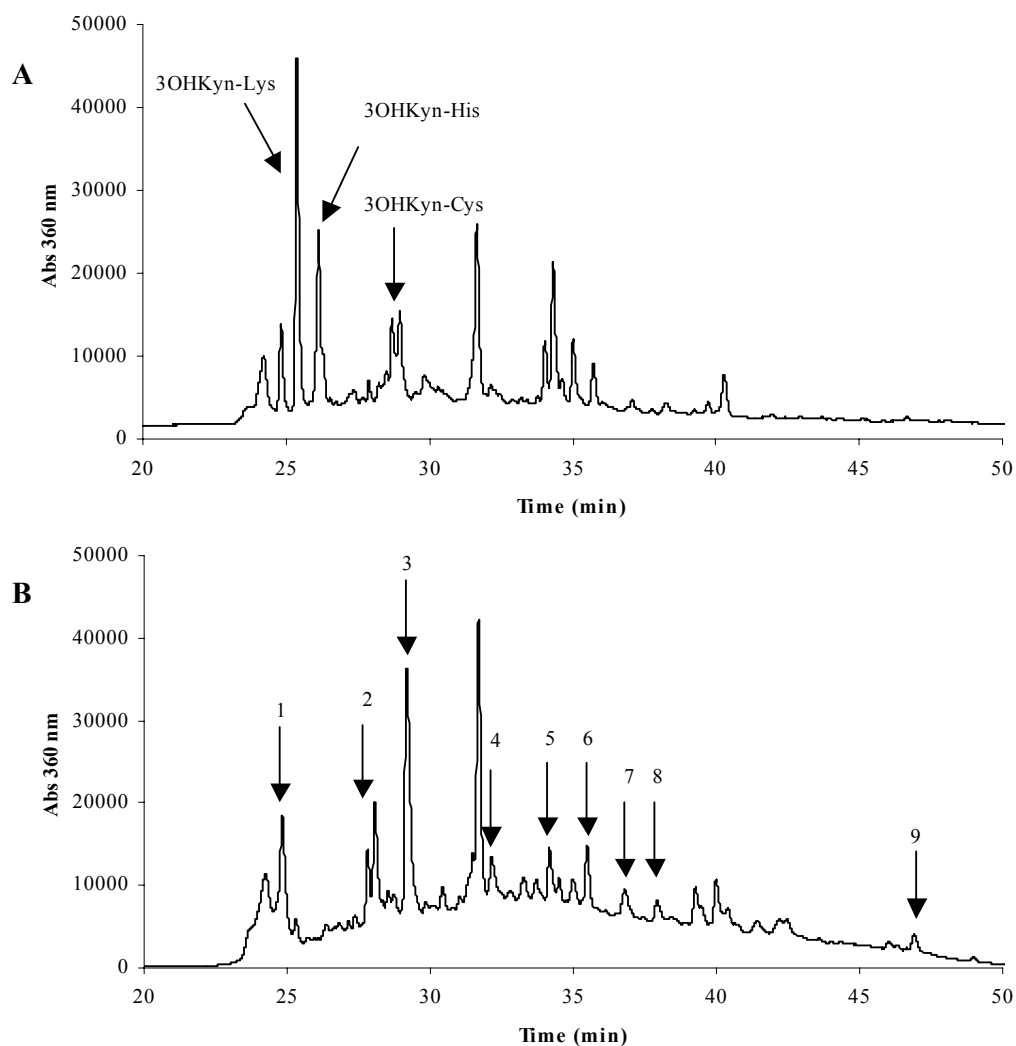
*Acid Hydrolysis of Protein*

Each protein aliquot from the incubation at pH 7.2 was ultra-filtered prior to acid hydrolysis. The HPLC chromatogram of the hydrolysate of the initial aliquot is shown in Figure 4.32A. The peak eluting at 25.3 min was identified as 3OHKyn-Lys, the peak at 26.1 min was identified as 3OHKyn-His and the doublet eluting at 29 min was identified as 3OHKyn-Cys, from MS/MS analysis. These 3OHKyn adducts have been previously observed in Chapter 3, since CLP modified by 3OHKyn at a high pH yields all three adducts.

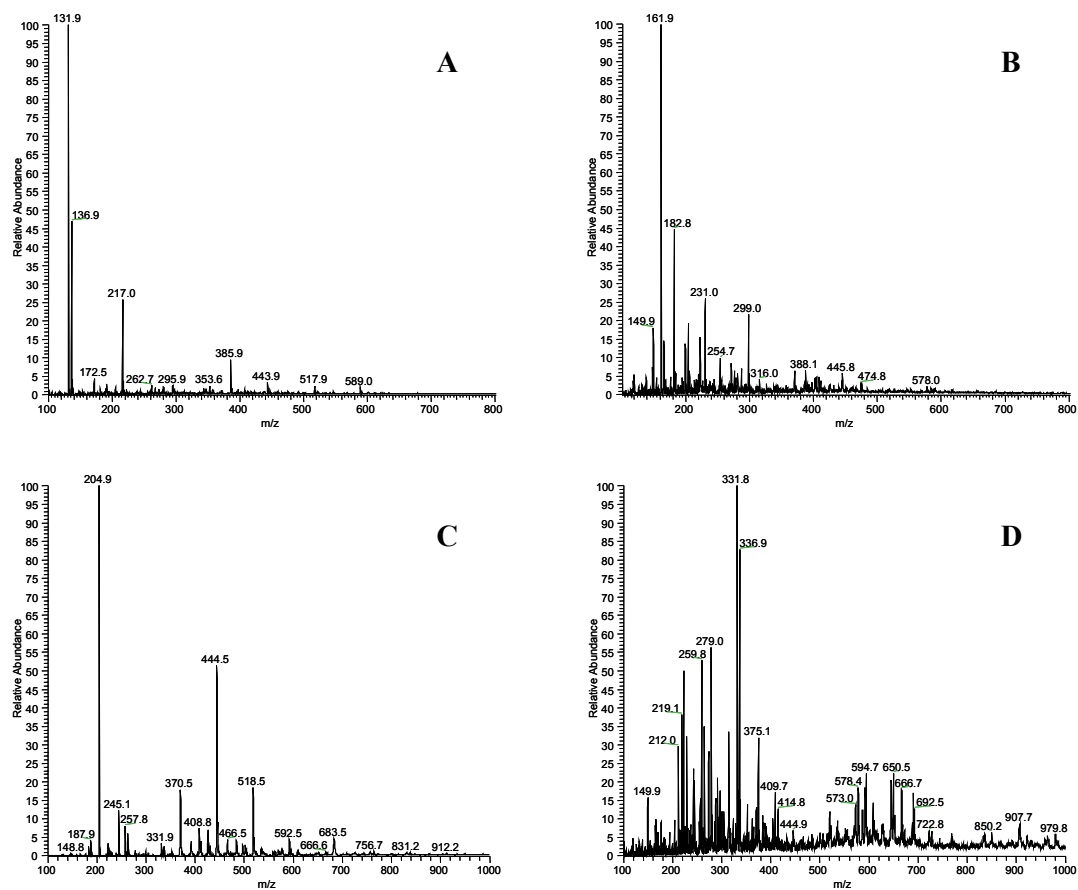
The protein (modified by 3OHKyn at pH 9.5) was incubated at pH 7.2 for 10 days. Figure 4.32B is the HPLC chromatogram of the hydrolysate of that aliquot. Numerous peaks differed from those in Figure 4.32A, however only a few were analysed by mass spectrometry (Figure 4.32B). Peak 1 eluted at 24.9 min, the mass spectrum (spectrum not shown) of this peak showed a molecular ion of  $m/z$  363, MS/MS of this (spectrum not shown) confirmed that this was indeed 3OHKyn-His. Peak 2 eluted at 28 min as what appeared to be a doublet, analysis of this peak by mass spectrometry showed few ions, but none greater than  $m/z$  600 (Figure 4.33A). MS/MS of  $m/z$  589 (spectrum not shown) resulted in fragment ions  $m/z$  571, 460, 442 and 424, of all these ions,  $m/z$  424 is the only familiar ion, since it is also the molecular ion of xanthommatin, however this peak cannot be identified with such little information. Peak 3 eluted at 29.2 min, the mass spectrum (Figure 4.33B) showed numerous ions. MS/MS of  $m/z$  162 (spectrum not shown) showed that it was not a fragment ion of 3OHKyn, since the fragment ions were not characteristic fragment ions of 3OHKyn. Peak 4 eluted at 32.2 min on the HPLC chromatogram. The mass spectrum (Figure 4.33C) exhibited numerous ions, however none were familiar. Peak 5 eluted at 34.2 min on the HPLC chromatogram. The mass of this peak (Figure 4.33D) showed many ions of varying abundance, and thus it was difficult to determine the molecular ion for this peak.

Peak 6 eluted at 35.5 min on the HPLC chromatogram. The mass spectrum of this peak (Figure 4.34A) showed many ions but none could be identified as the molecular ion. Similarly peak 7 eluted at 36.9 min and analysis of the mass spectrum (Figure 4.34B) again showed many ions. MS/MS of  $m/z$  919 resulted in fragment ions  $m/z$  901, 883,

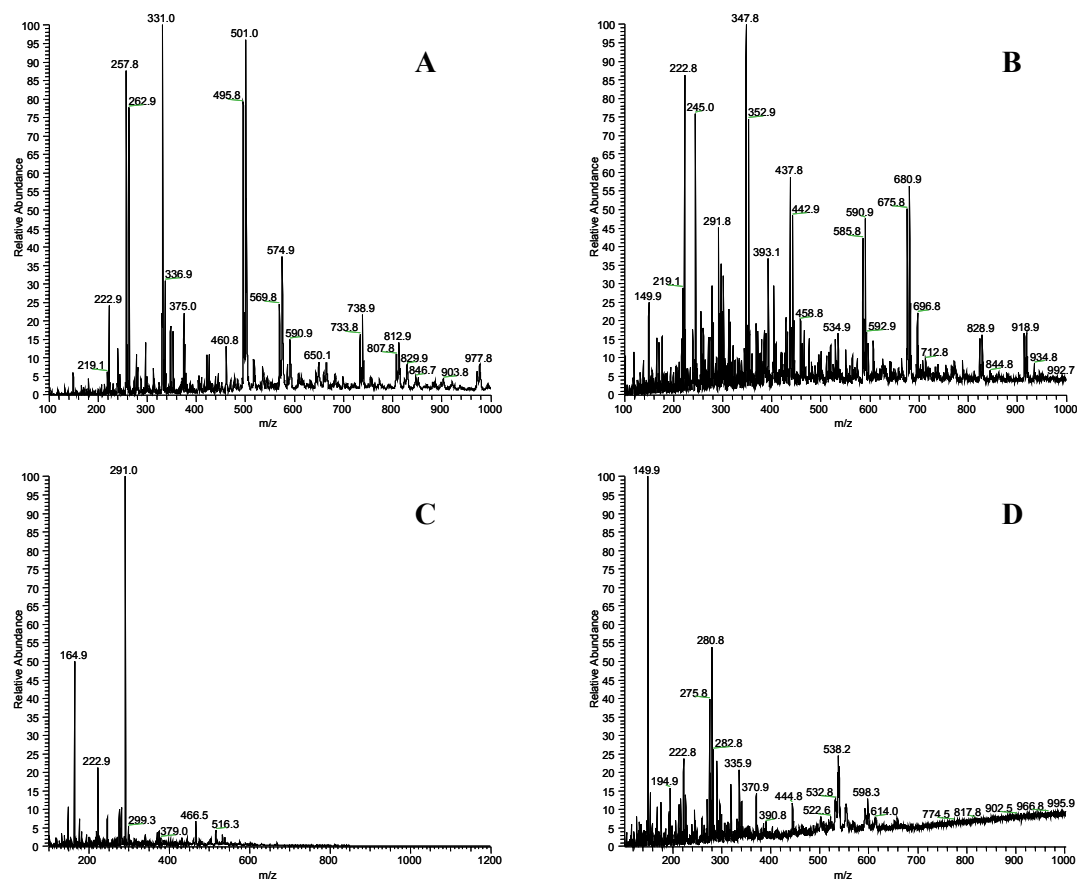
829, 769, 737, 681, 589, 531, 499, 443 and 351. Since many of these fragment ions do appear in the original mass spectrum (Figure 4.34B), it is assumed that  $m/z$  919 is the molecular ion for this peak. Peak 8 eluted at 38 min, the mass spectrum is shown in Figure 4.34C. This peak exhibited very few ions and they were all below  $m/z$  600. Finally peak 9 eluted at 47 min on the HPLC chromatogram. The mass spectrum is shown in Figure 4.34D, and there are numerous ions present, however analysis failed to identify any characteristic ions. Although the HPLC chromatogram of the hydrolysate changed during the incubation of the protein, many peaks could not be identified after mass spectrometry, and the molecular ions in each peak again could not be easily identified.



**Figure 4.32** HPLC chromatograms of acid hydrolysed proteins. *A*, Initial aliquot; *B*, Aliquot after 10 days of incubation. Arrowed peaks were collected for mass spectrometry.



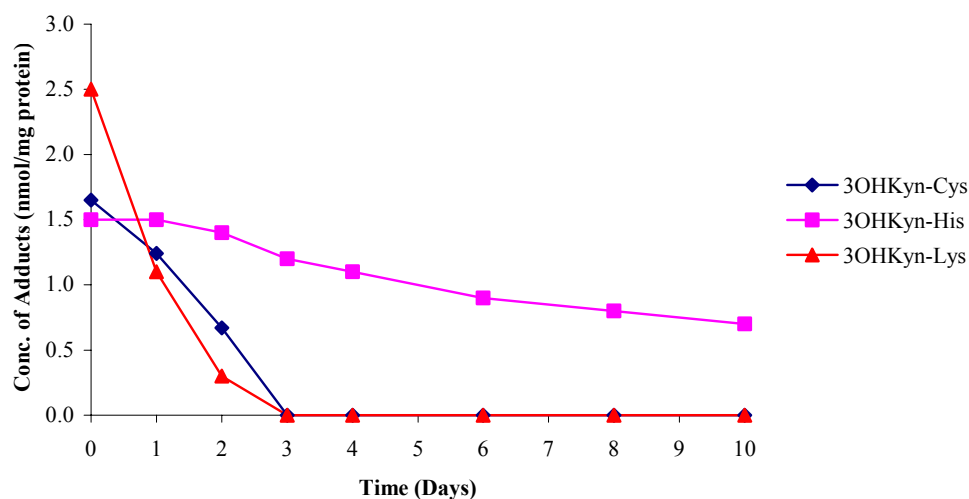
**Figure 4.33** ESI mass spectra of peaks eluting in Figure 4.32B. *A*, Peak 2; *B*, Peak 3; *C*, Peak 4; *D*, Peak 5.



**Figure 4.34** ESI mass spectra of peaks eluting in Figure 4.32B. *A*, Peak 6; *B*, Peak 7; *C*, Peak 8; *D*, Peak 9.



The modified CLP used in this study was known to originally contain modifications at Cys, His and Lys. The concentration of each adduct was quantified and are shown in Figure 4.35. 3OHKyn-Cys was not recovered after 3 days of incubation, and similarly 3OHKyn-Lys was not recovered after 3 days of incubation. 3OHKyn-His was recovered during the whole incubation period. MS/MS was used to identify the adducts in each protein aliquot.

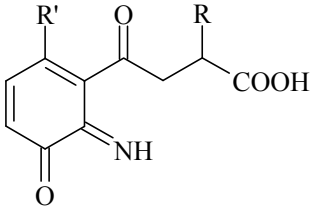


**Figure 4.35** Concentration of 3OHKyn-Cys, 3OHKyn-His and 3OHKyn-Lys in protein samples during incubation of CLP originally modified by 3OHKyn at pH 9.5.

#### 4.4 Discussion

This chapter is a preliminary investigation, examining the potential for 3OHKyn to modify and crosslink lens proteins and to compare the modified proteins with authentic human cataract lens proteins. Crosslinking is characteristic of ARN cataract.<sup>166</sup> Scheme 4.1 showed the expected products from this study. Table 4.4 shows the molecular ions of the expected 3OHKyn crosslink compounds of which none were observed in this study.

**Table 4.4** Expected molecular ions of the 3OHKyn crosslink compounds.

|  |     |                  |               |
|---|-----|------------------|---------------|
| R'  | R   | Molecular Weight | Molecular Ion |
| His   | His | 513.5 Da         | 514.5 Da      |
| Lys   | His | 504.5 Da         | 505.5 Da      |
| Lys   | Lys | 495.5 Da         | 496.5 Da      |
| Cys   | Cys | 445.5 Da         | 446.5 Da      |
| His   | Cys | 479.5 Da         | 480.5 Da      |
| Lys   | Cys | 470.5 Da         | 471.5 Da      |

#### 3OHKyn-*t*-Boc-His

Firstly, the stability of the various 3OHKyn amino acid adducts were examined and the products formed were analysed. The study in Section 4.3.1 demonstrated that the products following incubation of 3OHKyn-*t*-Boc-His in the absence or presence of excess amino acids were essentially identical. In particular one major product (compound with an ion  $m/z$  550) with a high absorbance at both 360 and 440 nm was observed in the acid digest of all reactions. Attempts were made to characterise this compound. Large scale reactions were undertaken with the 3OHKyn-*t*-Boc-His adduct however following HPLC purification, only small yields were observed. Therefore although a relatively large amount of adduct was used, only a small amount of product

was formed for NMR analysis. NMR was performed with the product that was available. NMR could not elucidate the structure of this product. Although the starting material in this experiment was 3OHKyn-*t*-Boc-His, the NMR of 3OHKyn-*t*-Boc-His was distinctly different from that in Figure 4.13. It is likely that the unknown compound contains an impurity that made interpretation of the NMR spectrum difficult. In addition, there was not enough product available to run additional NMR experiments and gain sufficient data for structural elucidation. The HPLC profiles of the acid digests monitored at 440 nm suggested that this product absorbed highly at this wavelength, however the UV-visible spectrum (Figure 4.12) showed that the wavelength maximum of the chromophore was  $\sim 408$  nm, and therefore this data shows that it is unlikely that this compound contains a simple phenoxazine moiety. 3OHKyn yields a phenoxazine when it is oxidised.<sup>184</sup>

The UV-visible spectrum (Figure 4.12) also showed that this unknown product is stable to acid, since Figures 4.12A and 4.12B are identical, and the molecular ion in the mass spectra of Peak 2 and Peak 2' differed by 100 Da, which is equivalent to a *t*-Boc group. The MS/MS spectrum (Figure 4.10) suggest that the imidazole ring of His is linked twice, since there were very few His-related fragment ions resulting from MS/MS of  $m/z$  550. Some possible structures of this unknown compound are shown in Figure 4.36, however the molecular ions of these structures do not equal the mass of the unknown ( $m/z$  550).

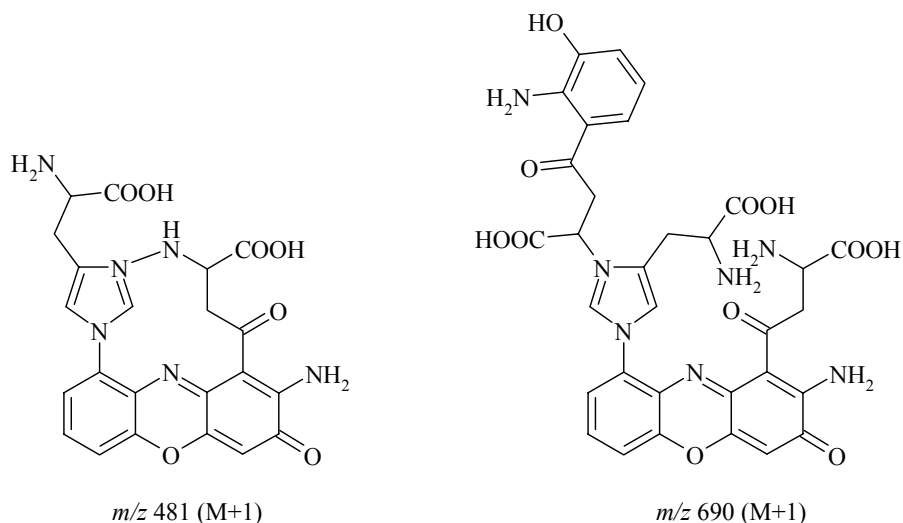


**Figure 4.36** Possible structures of the unknown compound formed from the 3OHKyn-*t*-Boc-His incubations, whereby the imidazole ring is linked twice.

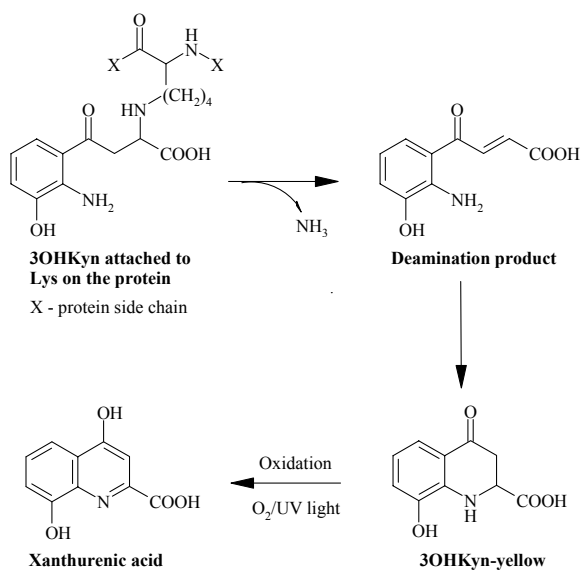
#### 3OHKyn-*t*-Boc-Lys

The incubations with 3OHKyn-*t*-Boc-Lys further demonstrated instability of this 3OHKyn amino acid adduct at pH 7.2. Numerous products were formed as a result of each incubation. However the HPLC profiles of the acid digests were not the same for all three reactions, and therefore, as a result of the inconsistency, it was decided that the products from these incubations would not be further investigated at this time.

#### Protein

A study of proteins modified by 3OHKyn further demonstrated the reactivity of 3OHKyn. For example, protein originally modified at pH 7.2 and then incubated for 15 days, showed that 3OHKyn ‘transferred’ during the incubation period *i.e.* 3OHKyn initially modified Cys on the protein however, after six days of incubation 3OHKyn had become covalently attached to His residues. This further demonstrates the intrinsic instability of the Cys adduct, but it also suggests how bound UV filters may react *in vivo*. The filtrate showed the presence of xanthurenic acid, an oxidation product of 3OHKyn, which is formed when 3OHKyn deaminates at neutral pH.<sup>109</sup> The reactive intermediate cyclises to form 3OHKyn-yellow<sup>191</sup> and is then oxidised in the presence of

UV light or oxygen forming xanthurenic acid (Scheme 4.2). This also shows that in an older lens when 3OHKyn is attached to lens protein at pH 7.2, it may ultimately result in the production of xanthurenic acid if the environment is oxidising (as is the case for cataract lenses).<sup>91,159,163</sup> Xanthurenic acid 8-*O*- $\beta$ -D-glucoside is a compound, which has been reported in brunescant cataracts. It is derived from deamination of 3OHKynG, followed by cyclisation to form 3OHKynG-yellow and then oxidation<sup>224</sup> (similar to Scheme 4.2 for 3OHKyn). Additional studies by Shirao, *et al.* showed that xanthurenic acid 8-*O*- $\beta$ -D-glucoside was not derived artificially through sample preparation since sample preparation conditions were done under acidic conditions at 4<sup>0</sup>C.<sup>224</sup> Similarly, the sample preparation conditions in this thesis were also done at 4<sup>0</sup>C, and at acidic pH, therefore the xanthurenic acid identified in the filtrates was not derived from sample preparation. Rather xanthurenic acid was derived from the intrinsic instability of 3OHKyn at pH 7.2 during the incubation. Bova, *et al.* have shown that 3OHKynG does not deaminate significantly at pH 5.<sup>85</sup>



**Scheme 4.2** Route of formation of xanthurenic acid from autoxidation of protein-bound 3OHKyn.

Similarly the protein originally modified at pH 9.5 and further incubated for 10 days also showed the presence of xanthurenic acid in the filtrate. These modified proteins also showed that 3OHKyn-Cys and 3OHKyn-Lys are both unstable at pH 7.2, but 3OHKyn-His was relatively stable over the incubation period (10 days) (Figure 4.35).

The SDS-PAGE of the protein incubations at 15 days and 10 days did not show evidence of non-disulfide crosslinks forming (*i.e.* a band at ~40 kDa was not observed) in protein modified by 3OHKyn. The fluorescence data did however show that the fluorophore had changed, or that the environment of the fluorophore had changed. Fluorescence measurements were done at pH 5.5 (protein aliquots were added to 6 M guanidine HCl solution). At this pH the protein in Section 4.3.3 had an initial fluorescence at Ex 370 nm/Em 485 nm. These wavelengths are not identical to those of the 3OHKyn amino acid adducts at that pH, but they are close (e.g. 3OHKyn-Cys Ex 340 nm/Em 510 nm, Ex 430 nm/Em 510 nm; 3OHKyn-*t*-Boc-His Ex 350 nm/Em 520 nm; 3OHKyn-*t*-Boc-Lys Ex 350 nm/Em 520 nm, Ex 410 nm/Em 520 nm). The fluorescence at the end of the incubation was measured at Ex 365 nm/Em 470 nm (Table 4.2). Similarly the fluorescence data in Section 4.3.4 was similar to that of Section 4.3.3. Initially the fluorescence was measured at Ex 360 nm/Em 480 nm, and at the end of the incubation the fluorescence of the protein was Ex 360 nm/Em 465 nm (Table 4.3), which is again comparable to the 3OHKyn amino acid adducts. The modified protein may contain other species (*i.e.* oxidised compounds attached to protein), which may be responsible for the observed fluorescence intensities.

The HPLC chromatogram of the hydrolysate of 3OHKyn-modified protein showed observable changes (*i.e.* there were additional peaks eluting in the HPLC chromatograms) at the end of the incubation period compared to the original HPLC profile. Many of the peaks that eluted were collected and examined by mass spectrometry, however the expected crosslink compounds that are listed in Table 4.4 were not observed. The aim of this study was to identify crosslink compounds in proteins modified by 3OHKyn. Chapter 5 is a study of the novel compounds, which are observed in the hydrolysate of cataract lens proteins. The HPLC profiles of cataract lens

proteins will be analysed and compared to those of oxidised 3OHKyn-modified protein and conclusions will be drawn at the end of Chapter 5.

In summary, the findings from this preliminary investigation show that 3OHKyn does not appear to crosslink lens proteins (SDS-PAGE data). However the proteins did undergo changes during the incubation periods, since the fluorescence intensities shifted significantly during the incubation, and the HPLC profiles of the acid digests at the end of the incubation were distinctly different to the initial HPLC profiles. One reason for a lack of observable crosslinking may be that the incubations were done at a protein concentration of 20 mg/mL. The protein concentration in the human lens has been reported as ~450 mg/mL,<sup>21</sup> therefore it would be ideal in the future to attempt incubations at a higher protein concentration.

## Chapter 5

### Isolation of Novel Compounds from Human Cataract Lenses

#### 5.1 Introduction

The aim of this work was to determine if acid hydrolysis of cataract proteins could be a useful technique for isolating novel compounds. If so, their identification would provide information about the changes that result in ARN cataract. In addition, the aim was to determine if there was any evidence for the presence of 3OHKyn or Kyn fragment ions in these novel peaks, that elute in the HPLC of acid digests. The data presented in Chapter 3 of this thesis together with previous data show that all three Kyn UV filters, 3OHKynG, 3OHKyn and Kyn, are attached to normal older lens proteins.<sup>101,103</sup> Table 5.1 lists the characteristic ions of 3OHKyn and Kyn amino acid adducts. In addition, the UV-visible wavelength maxima are also listed for each adduct. The ions highlighted in bold were used as ‘signature’ ions in this study.

**Table 5.1** List of characteristic ions, and absorbance maxima for each of the 3OHKyn and Kyn amino acid adducts.<sup>103</sup>

Previously in Chapter 3, CLP and normal human aged lens protein were hydrolysed with acid in the presence of antioxidants. Figure 5.1A and Figure 5.1B are the HPLC profiles of the hydrolysed CLP and hydrolysed normal aged human lens protein respectively (these HPLC profiles have previously been shown in Figure 3.5A and 3.6B respectively of this thesis). As a comparison, a number of human ARN cataract lens proteins were hydrolysed under the same conditions, and Figure 5.1C shows a



representative HPLC profile of the hydrolysate of human cataractous lens protein. Human cataractous nuclei that appeared very Dark (*i.e.* Types III or IV, Pirie classification<sup>161</sup>) were used for this study. The absorbance was monitored at 360 nm to simplify the profiles, and to assist in identifying UV filter modification sites. The HPLC profile of human cataractous lens protein (Figure 5.1C) was found to exhibit numerous peaks that were not present in calf or normal human lens hydrolysates (Figure 5.1A and Figure 5.1B).

The peaks that were collected and examined were, P1, which eluted at 27.0 min, P2 eluted at 31.1 min, P3 eluted at 32.2 min, and P4, P5 and P6 eluted at 36.0 min, 37.5 min and 45.0 min respectively (Figure 5.1C). Numerous lenses (60) were hydrolysed and individual peaks were pooled in order to obtain sufficient quantities for analysis of each peak by mass spectrometry, UV-visible spectroscopy and NMR spectroscopy. It was found that each peak required a number of purifications by HPLC to ensure purity.

Numerous studies were undertaken to find the best approach for purifying these peaks further. Attempts were made to purify these peaks by HPLC. Various gradients were used and several columns including C8 and C18 columns of various lengths were used. The method that was finally settled upon and gave best separation involved taking the peaks from the first stage of HPLC, where the buffers contained TFA, drying these fractions, and performing HPLC using a different column (Synergi Fusion). A different gradient was used to separate each of P1-P6, and formic acid was used instead of TFA in the buffers. The analysis of P1, P2, P3, P4, P5 and P6 is summarised in Section 5.3.

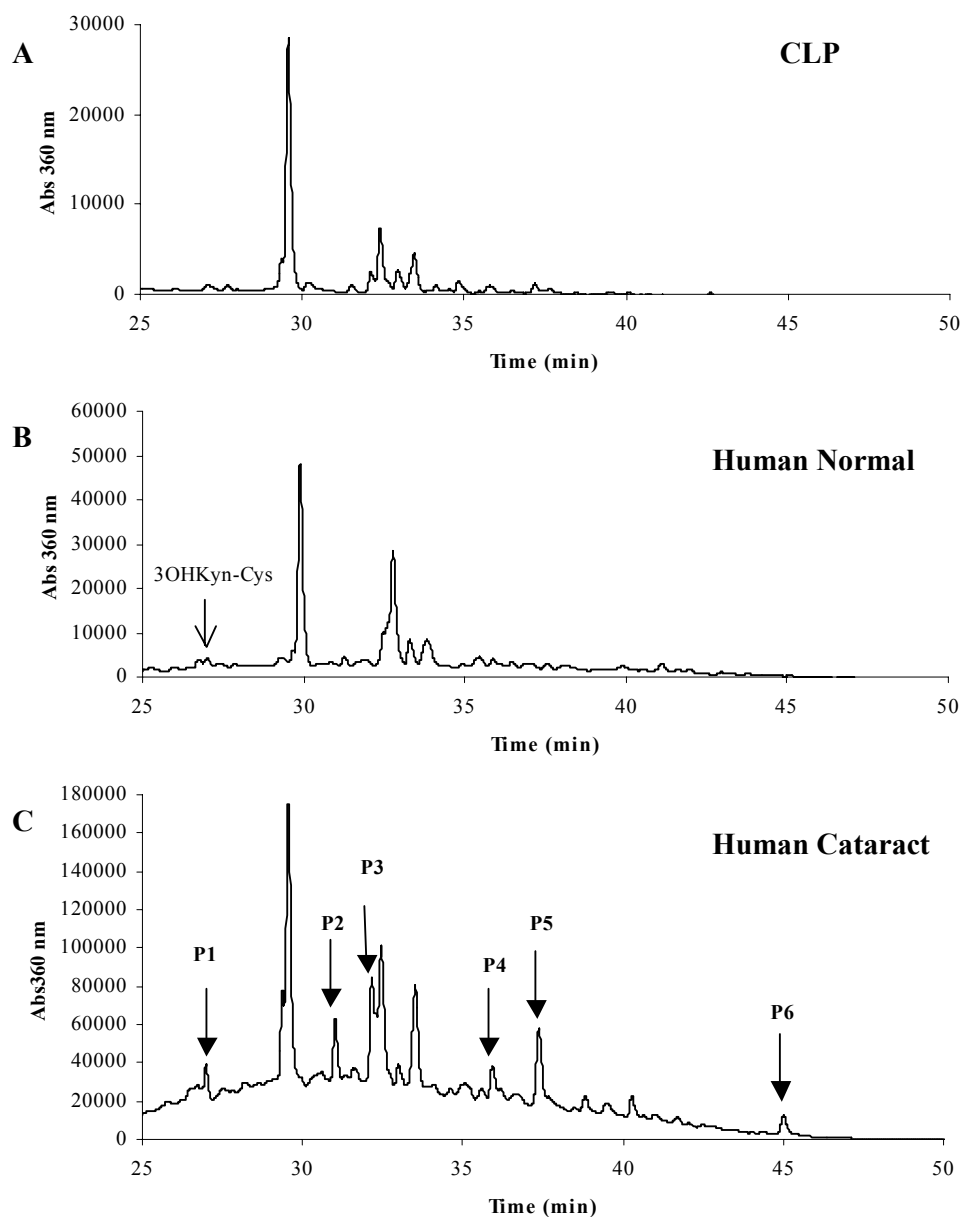


**Figure 5.1** HPLC chromatograms of acid hydrolysed lens protein samples (~ 1 mg hydrolysed protein was injected in each case). *A*, CLP; *B*, Normal human lens nuclear protein, from a 76 year old lens; *C*, Pooled human cataract lens nuclear protein. The HPLC profiles of all human cataract lens protein hydrolysed were consistent.

## **5.2 Materials and Methods**

### **5.2.1 Materials**

All organic solvents and acids were HPLC grade (Ajax, Auburn, NSW, Australia). Milli-Q<sup>®</sup> water (purified to 18.2 M $\Omega$ /cm<sup>2</sup>) was used in the preparation of all solutions. Formic acid, heptafluorobutyric acid, HCl (6 M, sequencing grade), TFA, thioglycolic acid and phenol were obtained from Sigma-Aldrich Chemical Co. (St. Louis, MO, U.S.A.)

### **5.2.2 Preparation of Cataract Lens Protein**

ARN cataract lenses were obtained from K.T. Sheth Eye Hospital, Rajkot, Gujarat, India. Nuclei were obtained using a cork borer (5 mm), and the ends were removed (1 mm). The nuclei were extracted with 80% (v/v) ethanol once, and the insoluble protein was freeze dried and stored at 4<sup>0</sup>C.

### **5.2.3 Hydrolysis of Cataract Lens Protein**

Each extracted nucleus was hydrolysed with 6 M HCl (1 mL), thioglycolic acid (5% v/v) and phenol (1% w/v) in an evacuated hydrolysis tube for 24 hours at 110<sup>0</sup>C. The samples were freeze dried and dissolved in 0.1% (v/v) aqueous TFA and analysed by HPLC. 60 cataract nuclei were hydrolysed for purification.

### **5.2.4 First Stage of HPLC Purification**

RP-HPLC was performed on a Shimadzu HPLC system. For analytical scale separations, a Phenomenex column (Jupiter C18, 300 Å, 5  $\mu$ m, 4.6 x 250 mm) was used with the following mobile phase conditions: solvent A (aqueous 0.1% (v/v) TFA) for 5 minutes followed by linear gradient of 0-50% solvent B (80% (v/v) acetonitrile/H<sub>2</sub>O, 0.1% (v/v) TFA) over 20 minutes followed by a linear gradient of 50-100% B over 15 minutes and re-equilibration in the aqueous phase for 15 minutes. The flow rate was 0.5 mL/min. Six peaks (P1, P2, P3, P4, P5 and P6) were collected. Absorbance was monitored at 360 nm.

### 5.2.5 Second Stage of HPLC Purification

The 6 peaks collected were rerun on the Shimadzu HPLC system. Several test chromatograms were used to determine the best conditions for purification of each of the peaks P1-P6. Analytical separations were with a Phenomenex Synergi Fusion reversed phase column (C18, 80 Å, 4 µm, 3.0 x 150 mm). The flow rate was 0.4 mL/min, and the HPLC solvents were as follows: solvent A (aqueous 0.1% (v/v) formic acid) and solvent B (80% (v/v) acetonitrile/H<sub>2</sub>O, 0.1% (v/v) formic acid). The individual gradients for each of P1, P2, P3, P4, P5 and P6 are listed below. Absorbance was monitored at 360 nm.

#### 5.2.5.1 HPLC Gradient for P1

The following mobile phase conditions were used to purify P1: solvent A for 8 minutes followed by linear gradient of 0-15% B over 12 minutes followed by a linear gradient of 15-60% B over 20 minutes, 60-100% B over 5 minutes and re-equilibration in the aqueous phase for 15 minutes.

#### 5.2.5.2 HPLC Gradient for P2, P3, P4 and P5

The following mobile phase conditions were used to purify P2, P3, P4 and P5: solvent A for 8 minutes followed by linear gradient of 0-45% B over 7 minutes followed by a linear gradient of 45-100% B over 30 minutes, and re-equilibration in the aqueous phase for 15 minutes.

#### 5.2.5.3 HPLC Gradient for P6 (second HPLC purification)

A Phenomenex Luna column (C8, 100 Å, 3 µm, 2.0 x 150 mm) was used. The following mobile phase conditions were used to purify P6: solvent A (aqueous 0.2% (v/v) heptafluorobutyric acid) for 8 minutes followed by linear gradient of 0-30% solvent B (80% (v/v) acetonitrile/H<sub>2</sub>O, 0.2% (v/v) heptafluorobutyric acid) over 7 minutes followed by a linear gradient of 30-70% B over 20 minutes, and a linear gradient of 70-100% B over 10 minutes, and re-equilibration in the aqueous phase for 15 minutes. The flow rate was 0.2 mL/min.

#### **5.2.5.4 HPLC Gradient for P6 (third HPLC purification)**

A Phenomenex Synergi Fusion column (C18, 80 Å, 4 µm, 3.0 x 150 mm) was used. The following mobile phase conditions were used: solvent A (aqueous 0.1% (v/v) formic acid) at 95% for 5 minutes followed by linear gradient of 5-20% solvent B (80% (v/v) acetonitrile/H<sub>2</sub>O, 0.1% (v/v) formic acid) over 10 minutes followed by a linear gradient of 20-80% over 20 minutes, and a linear gradient of 80-100% B over 5 minutes, and re-equilibration in the aqueous phase for 15 minutes. The flow rate was 0.2 mL/min

#### **5.2.6 Mass Spectrometry**

See Section 2.2.10 for details.

#### **5.2.7 Tandem Mass Spectrometry (MS/MS)**

See Section 2.2.11 for details.

#### **5.2.8 High Resolution Mass Spectrometry**

See Section 2.2.12 for details.

#### **5.2.9 NMR Spectroscopy**

See Section 2.2.13 for details.

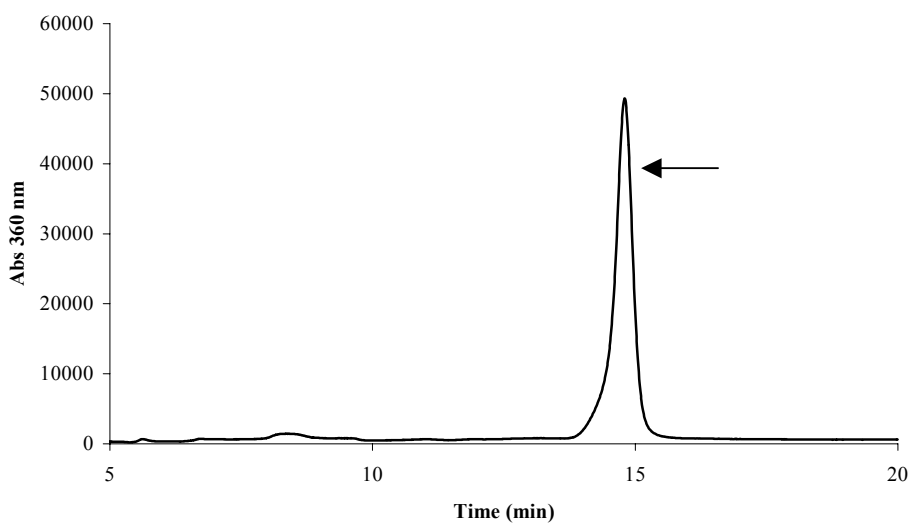
#### **5.2.10 UV-visible Spectroscopy**

See Section 2.2.14 for details.

### 5.3 Results

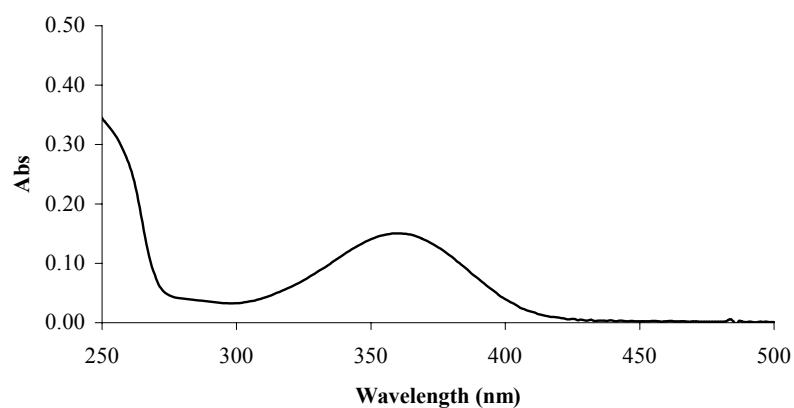
#### 5.3.1 Analysis of P1

Acid hydrolysis of human cataract lenses yielded P1 eluting at 27.0 min (Figure 5.1C). Since it did not elute as a very sharp peak, further purification was necessary. After several trials, P1 was further purified by HPLC using buffers containing 0.1% (v/v) formic acid and a Phenomenex Synergi Fusion column. Figure 5.2 shows the partial HPLC profile of the second phase of HPLC purification. Repurified P1 eluted as a single peak at 14.7 min (Figure 5.2). This peak was collected for UV-visible and mass spectral analysis.



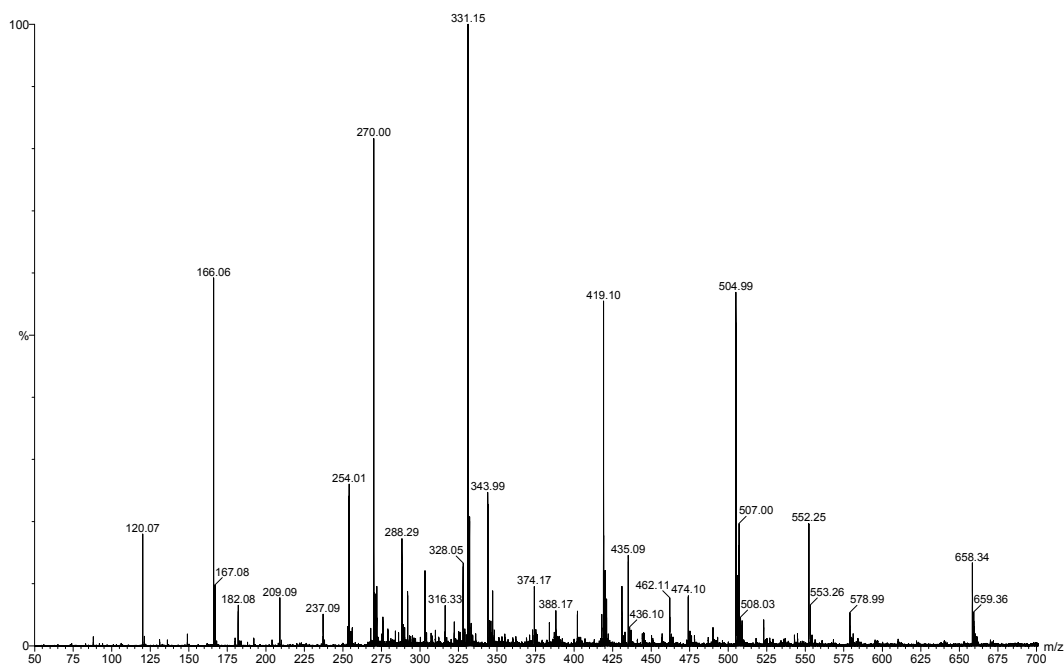
**Figure 5.2** HPLC chromatogram of P1 after a second purification stage using a Phenomenex Synergi Fusion column, and 0.1% (v/v) formic acid HPLC buffers.

A UV-visible spectrum of the peak eluting at 14.7 min in Figure 5.2 shows that this product displays a broad peak with maximum absorbance centred at 360 nm (Figure 5.3). 3OHKyn amino acid adducts and Kyn amino acid adducts all have broad peaks with maximum UV absorbances centred at 365 nm.<sup>103</sup> The UV spectrum (Figure 5.3) indicates that the product could be a UV filter derivative.



**Figure 5.3** UV-visible spectrum of the peak eluting at 14.7 min in Figure 5.2.

The ESI mass spectrum of the peak eluting at 14.7 min in Figure 5.2 is shown in Figure 5.4. There were no ions greater than  $m/z$  700. The largest ion observed was  $m/z$  658, and the most abundant ion at  $m/z$  331. The mass spectrum (Figure 5.4) did not exhibit any of the signature ions listed in Table 5.1, *i.e.* Figure 5.4 does not have ions that correspond to the ions of 3OHKyn and Kyn amino acid adducts. MS/MS was conducted on some of the ions.



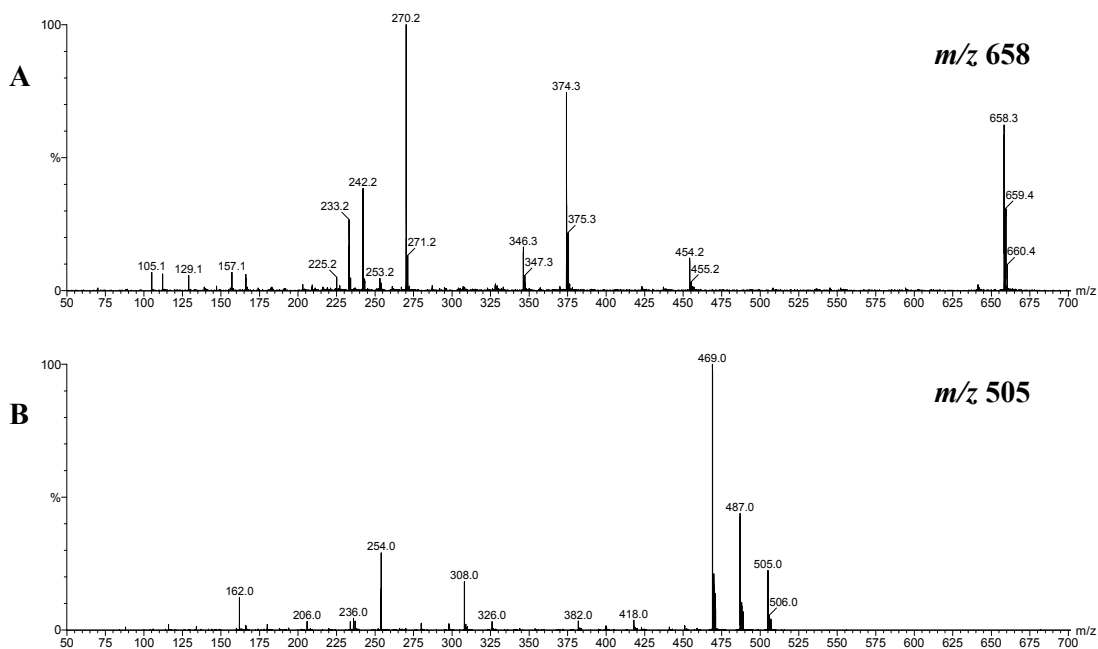
**Figure 5.4** ESI mass spectrum of the peak eluting at 14.7 min in Figure 5.2.

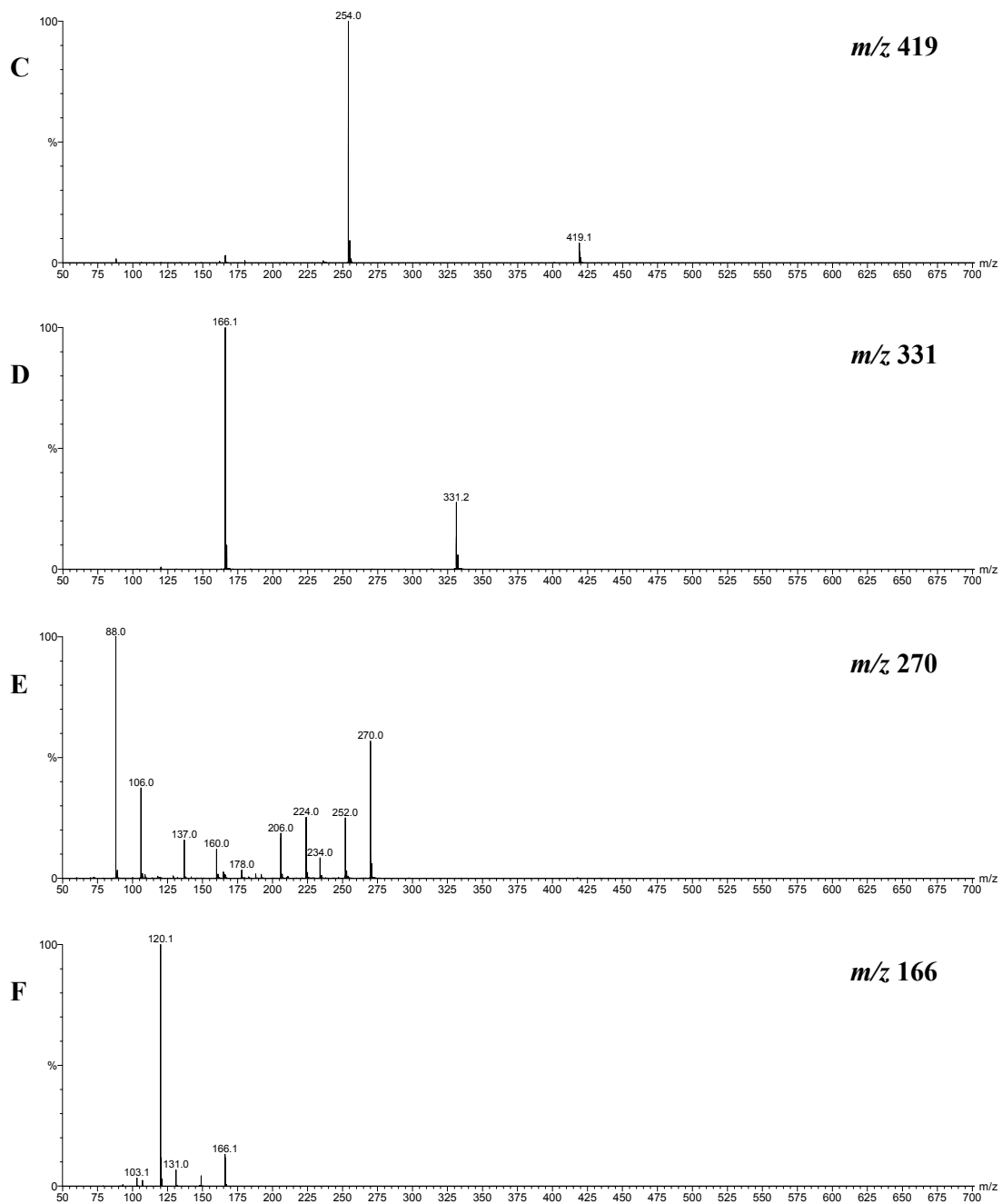


Figure 5.5A shows the MS/MS spectrum of ion  $m/z$  658. The major fragment ions include  $m/z$  641 (loss of  $m/z$  17), 454, 374, 346, 270, 242, and 233. None of these ions correspond to UV filter fragment ions. Figure 5.5B shows the MS/MS spectrum of ion  $m/z$  505. The major fragment ions include  $m/z$  487 (loss of  $m/z$  18), 469 (loss of  $m/z$  18), 418, 382, 326, 308, 254, 236, 206 and 162. Again none of these ions were UV filter fragment ions. A loss of  $m/z$  18 normally is due to the loss of water.<sup>225</sup>

Figure 5.5C shows the MS/MS spectrum of ion  $m/z$  419. The major fragment ions include  $m/z$  254 and 166. Figure 5.5D shows the MS/MS spectrum of ion  $m/z$  331. The fragment ions include  $m/z$  166 and 120. Figure 5.5E shows the MS/MS spectrum of ion  $m/z$  270. Fragment ions include  $m/z$  252, 234, 224, 206, 178, 160, 137, 106 and 88. Finally, Figure 5.5F shows the MS/MS spectrum of ion  $m/z$  166. The fragment ions included  $m/z$  149, 131, 120, 107 and 103.

A summary of the major ions for each of P1-P6, together with the MS/MS data, is shown in Table 5.2.

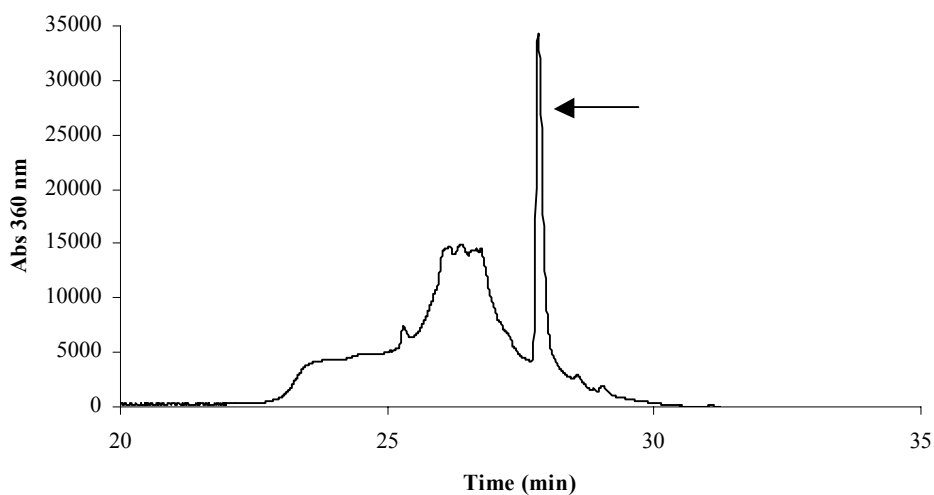




**Figure 5.5** MS/MS spectra. MS/MS of ions that were present in the ESI mass spectrum (Figure 5.4). *A*,  $m/z$  658; *B*,  $m/z$  505; *C*,  $m/z$  419; *D*,  $m/z$  331; *E*,  $m/z$  270; *F*,  $m/z$  166.

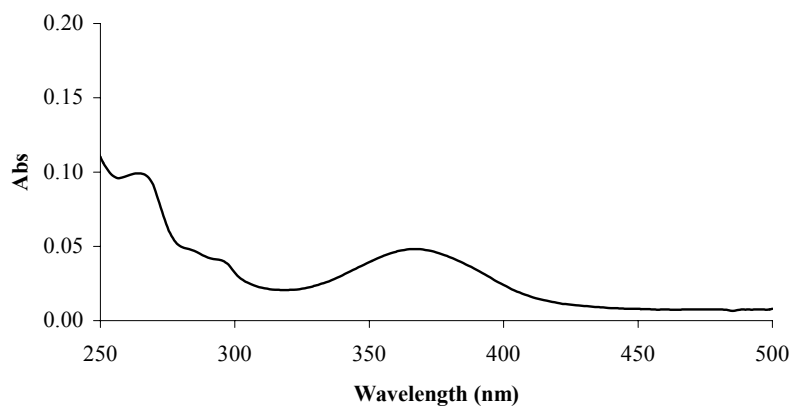
### 5.3.2 Analysis of P2

Acid hydrolysis of human cataract lenses also yielded P2 eluting at 31.1 min (Figure 5.1C). This peak eluted as a medium-sized peak. P2 was further purified under the same conditions as P1 *i.e.* Phenomenex Synergi Fusion, and formic acid HPLC buffers. A different gradient on the HPLC system was used (see Section 5.2.5.2). Figure 5.6 shows the partial HPLC profile of the second phase of HPLC purification. In the second stage of HPLC, P2 eluted as a broad peak followed by a sharp peak eluting at 27.8 min (Figure 5.6). The sharp peak was collected for UV-visible and mass spectral analysis.



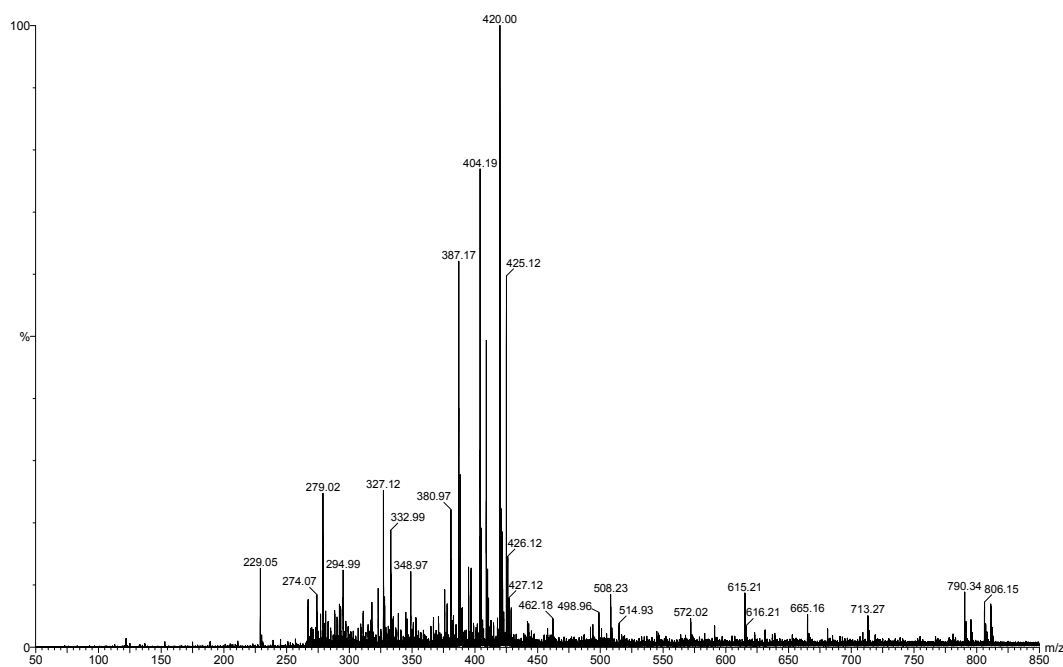
**Figure 5.6** HPLC chromatogram of P2 after a second purification stage using a Phenomenex Synergi Fusion column, and 0.1% (v/v) formic acid HPLC buffers.

A UV-visible spectrum of the peak eluting at 27.8 min in Figure 5.6 shows that this product has a broad peak with a maximum absorbance centred at 368 nm (Figure 5.7). The UV-visible spectrum (Figure 5.7) indicates that the product could be a UV filter derivative, since 3OHKyn and Kyn amino acid adducts have broad peaks with UV absorbances centred at 365 nm.<sup>103</sup>



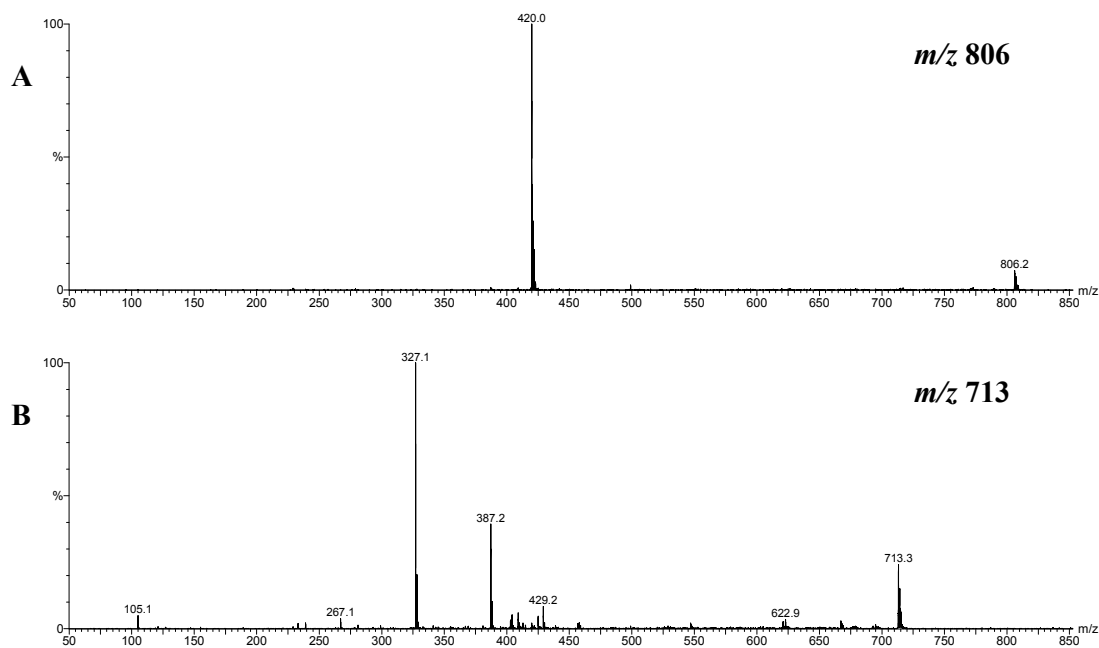
**Figure 5.7** UV-visible spectrum of the peak eluting at 27.8 min in Figure 5.6.

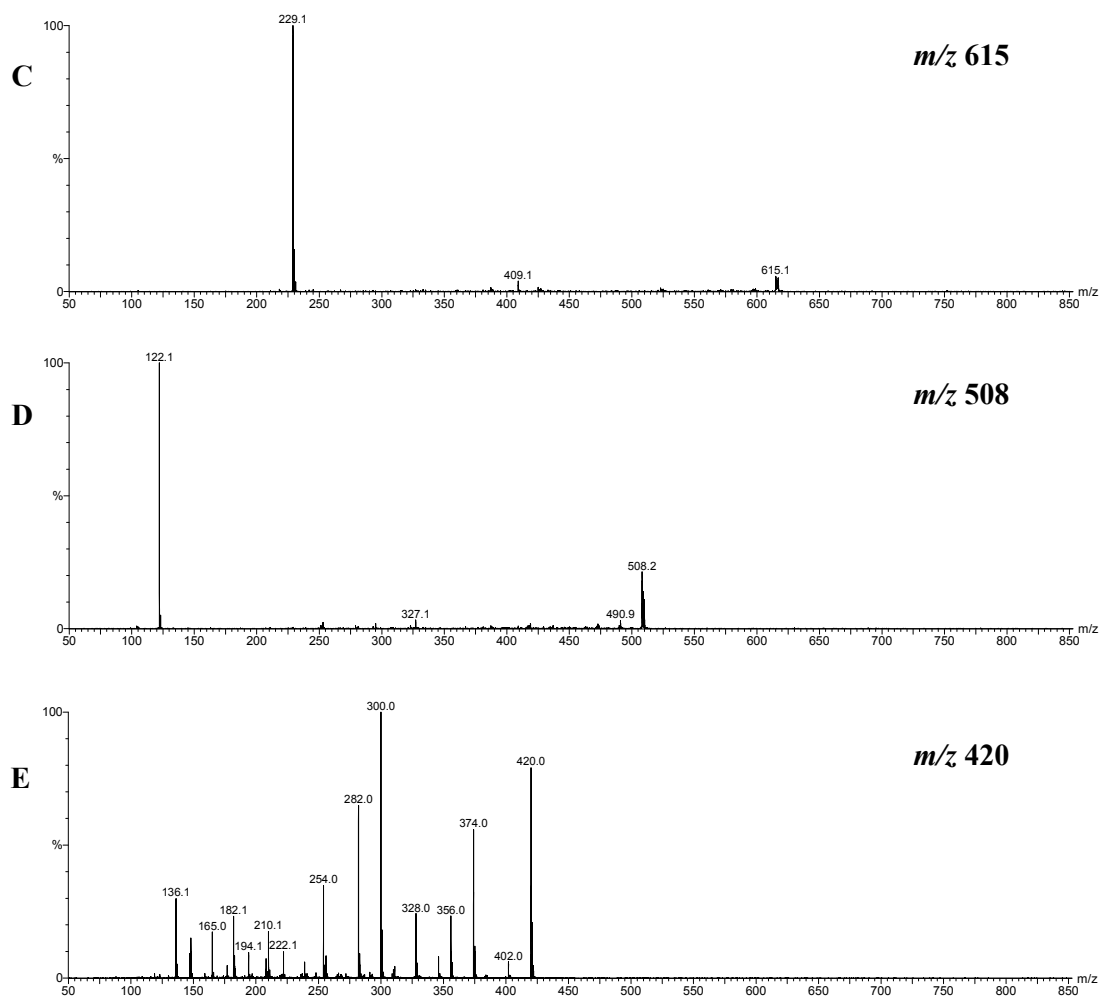
The ESI mass spectrum of the peak eluting at 27.8 min (Figure 5.6) is shown in Figure 5.8. There were no ions greater than  $m/z$  850. The largest ion observed was  $m/z$  811, and the most abundant ion observed was  $m/z$  420. The ions in the mass spectrum (Figure 5.8) had one signature ion,  $m/z$  387, corresponding to the mass of 3OHKynG. However this ion cannot be 3OHKynG, since the lens protein has been acid hydrolysed, and the glucose molecule hydrolyses under those conditions. MS/MS was conducted on some of the other ions.



**Figure 5.8** ESI mass spectrum of the sharp peak eluting at 27.8 min in Figure 5.6.

Figure 5.9A shows the MS/MS spectrum of ion  $m/z$  806. The fragment ion includes  $m/z$  420. Figure 5.9B shows the MS/MS spectrum of ion  $m/z$  713. The major fragment ions include  $m/z$  668, 622, 429, 409, 387, 327, 267 and 105. Figure 5.9C shows the MS/MS spectrum of ion  $m/z$  615. The major fragment ions include  $m/z$  409 and 229. Figure 5.9D shows the MS/MS spectrum of ion  $m/z$  508. The fragment ions include  $m/z$  327 and 122. Finally, Figure 5.9E shows the MS/MS spectrum of ion  $m/z$  420. Fragment ions include  $m/z$  402, 374, 356, 328, 300, 282, 254, 239, 222, 210, 194, 182, 165, 148 and 136.

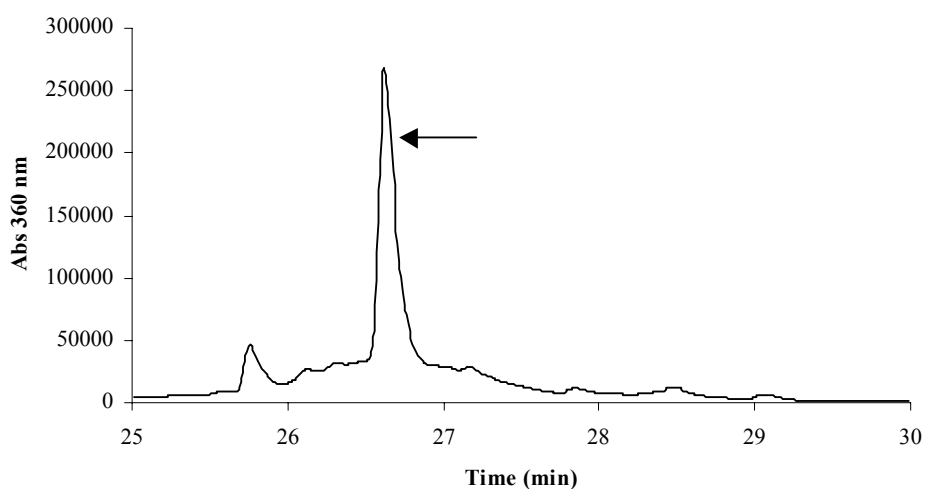




**Figure 5.9** MS/MS spectra. MS/MS of ions that were present in the ESI mass spectrum (Figure 5.8). *A*,  $m/z$  806; *B*,  $m/z$  713; *C*,  $m/z$  615; *D*,  $m/z$  508; *E*,  $m/z$  420.

### 5.3.3 Analysis of P3

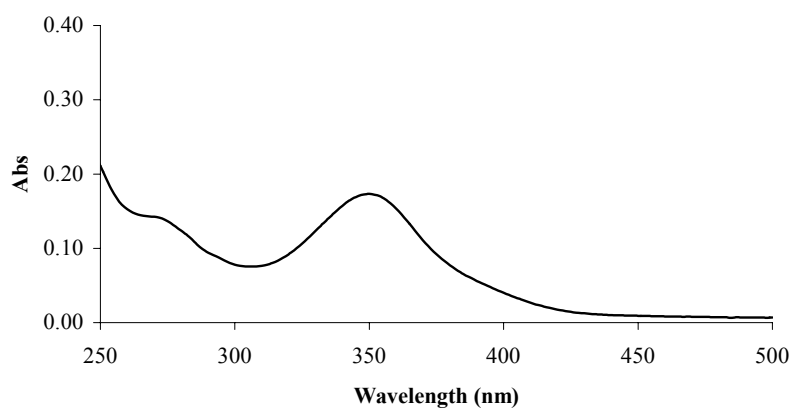
Acid hydrolysis of human cataract lenses also yielded P3 eluting at 32.2 min (Figure 5.1C). This peak eluted as part of a 'doublet' however the left hand peak of the 'doublet' was not present in the HPLC chromatogram of normal human aged lenses or CLP (Figure 5.1B and Figure 5.1A, respectively) hence, it was of interest for further investigation. P3 was further purified see Section 5.2.5 for details. Figure 5.10 shows the partial HPLC profile of the second stage of HPLC purification, where P3 eluted as a sharp peak at 26.6 min (Figure 5.10). The peak was collected for UV-visible and mass spectral analysis.



**Figure 5.10** HPLC chromatogram of P3 after a second purification stage. The single peak eluting at 26.6 min was collected for analysis by UV-visible and mass spectrometry.

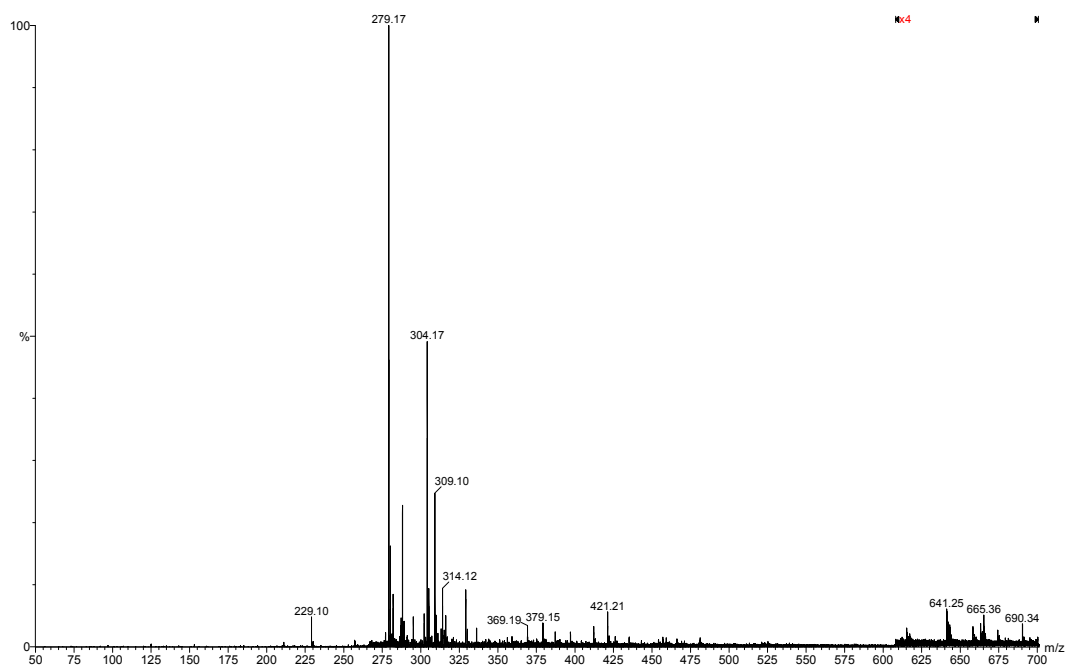


A UV-visible spectrum of the peak eluting at 26.6 min in Figure 5.10 shows that this product had a broad peak with a maximum absorbance centred at 350 nm (Figure 5.11). The UV-visible spectrum (Figure 5.11) indicates that the product could be a UV filter derivative, however UV filter adducts have a broad peak with a maximum absorbance centred at slightly longer wavelengths (365 nm).



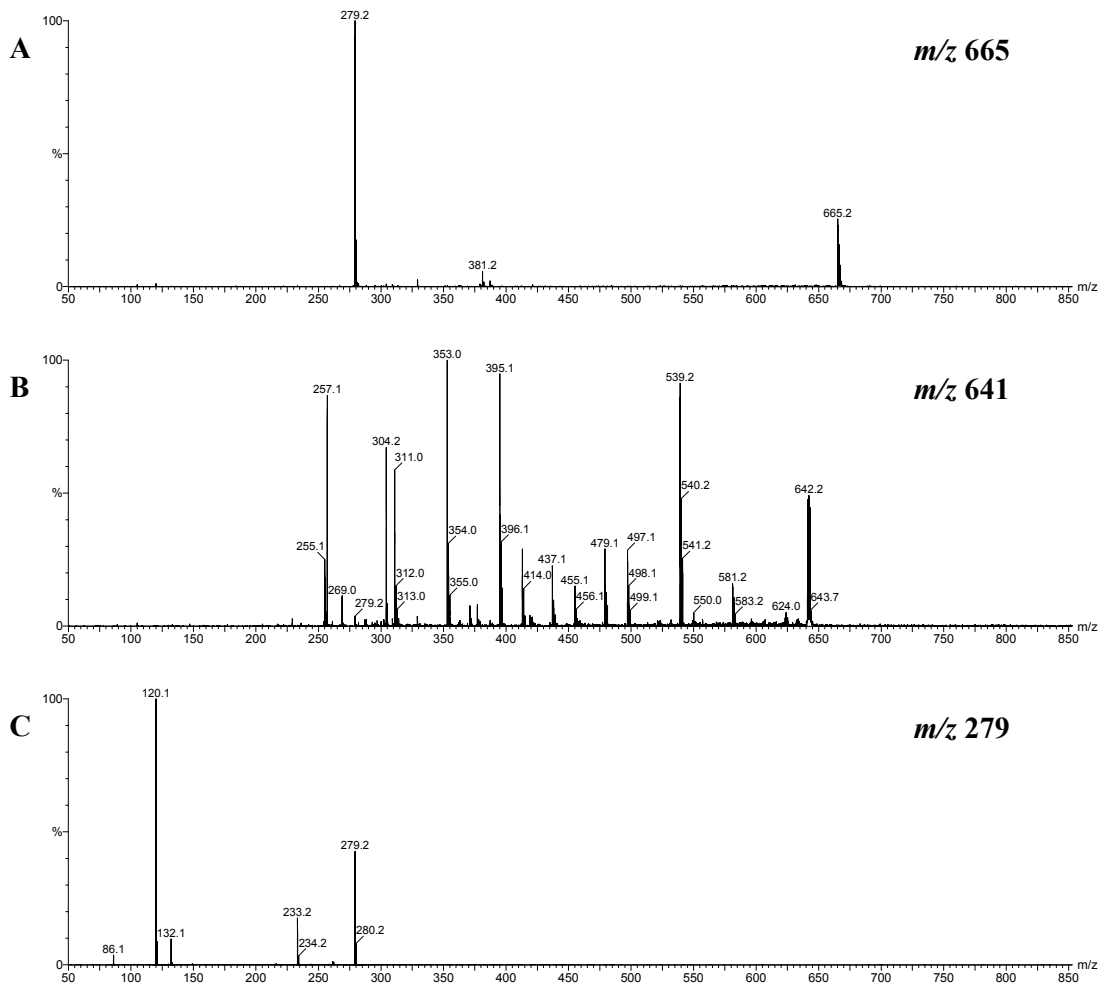
**Figure 5.11** UV-visible spectrum of the peak eluting at 26.6 min in Figure 5.10.

The ESI mass spectrum of the peak eluting at 26.6 min (Figure 5.10) is shown in Figure 5.12. There were no ions greater than  $m/z$  700. The largest ion observed was  $m/z$  690, and the most abundant ion observed was  $m/z$  279. MS/MS was conducted on some of the ions.



**Figure 5.12** ESI mass spectrum of the peak eluting at 26.6 min in Figure 5.10.

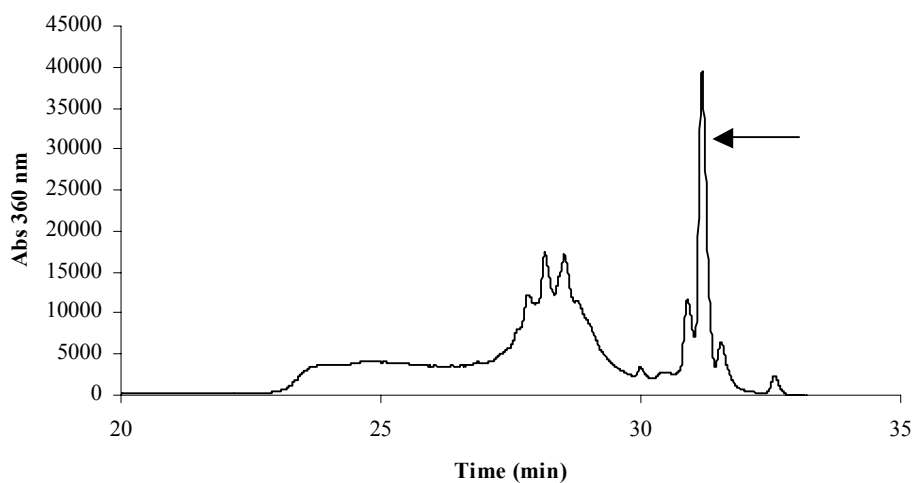
Figure 5.13A shows the MS/MS spectrum of ion  $m/z$  665. The major fragment ions include  $m/z$  381 and 279. Figure 5.13B shows the MS/MS spectrum of ion  $m/z$  641. The major fragment ions include  $m/z$  624, 581, 539, 497, 479, 455, 437, 413, 395, 353, 311, 304 and 257. Figure 5.13C shows the MS/MS spectrum of ion  $m/z$  279. The major fragment ions include  $m/z$  233, 132, 120 and 86.



**Figure 5.13** MS/MS spectra. MS/MS of ions that were present in the ESI mass spectrum (Figure 5.12). *A*,  $m/z$  665; *B*,  $m/z$  641; *C*,  $m/z$  279.

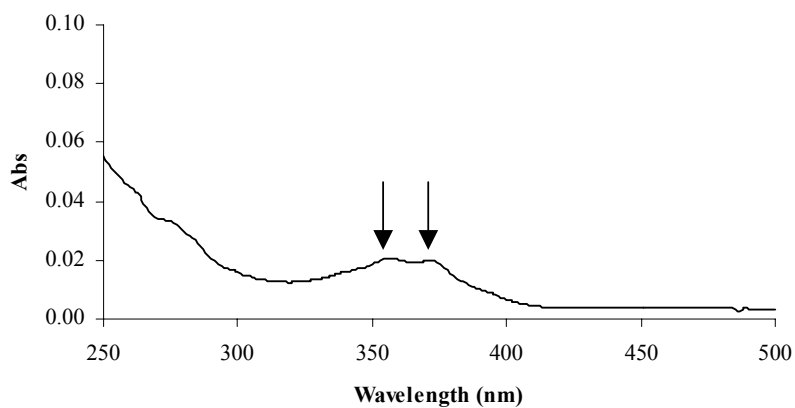
### 5.3.4 Analysis of P4

Acid hydrolysis of human cataract lenses also yielded P4 eluting at 36.0 min (Figure 5.1C). This peak eluted as a small peak in the HPLC chromatogram (Figure 5.1C). P4 was further purified. Figure 5.14 shows the partial HPLC profile of the second phase of HPLC purification. P4 resolved as several minor peaks, but only the major peak eluting at 31.1 min (Figure 5.14) was collected for UV-visible and mass spectral analysis.



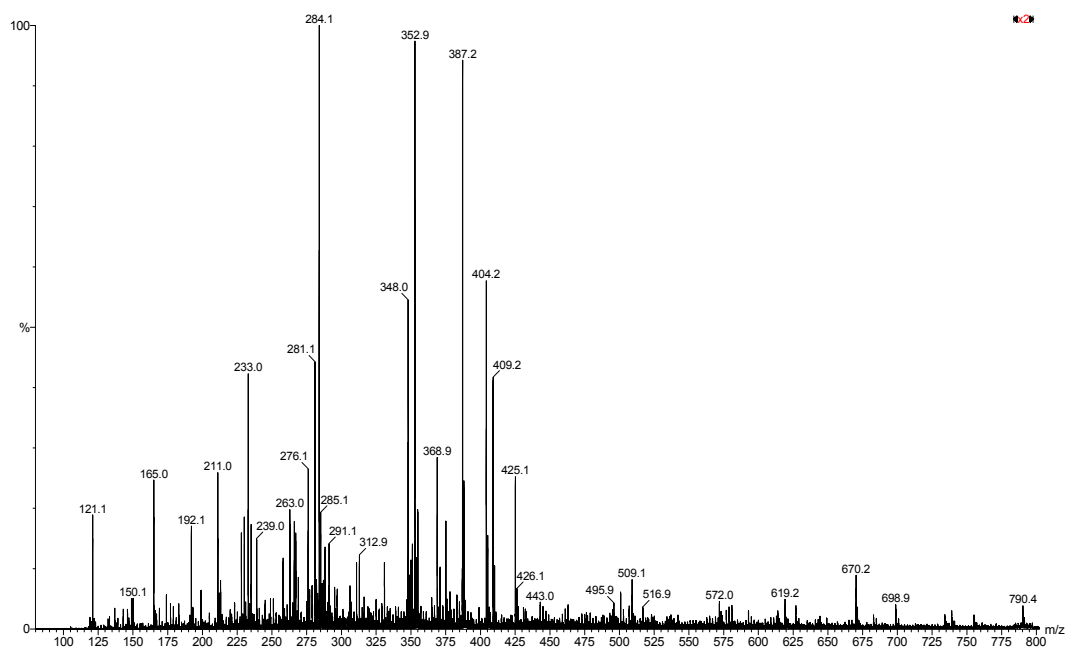
**Figure 5.14** HPLC chromatogram of P4 after a second purification stage. The single peak eluting at 31.1 min was collected for analysis by UV-visible and mass spectrometry.

A UV-visible spectrum of the peak eluting at 31.1 min in Figure 5.14 shows that this product had maximum absorbances centred at 357 and 374 nm (Figure 5.15). The UV-visible spectrum (Figure 5.15) shows that the product could be a UV filter derivative, since UV filter adducts exhibit broad UV absorbances centred at 365 nm.



**Figure 5.15** UV-visible spectrum of the peak eluting at 31.1 min in Figure 5.14.

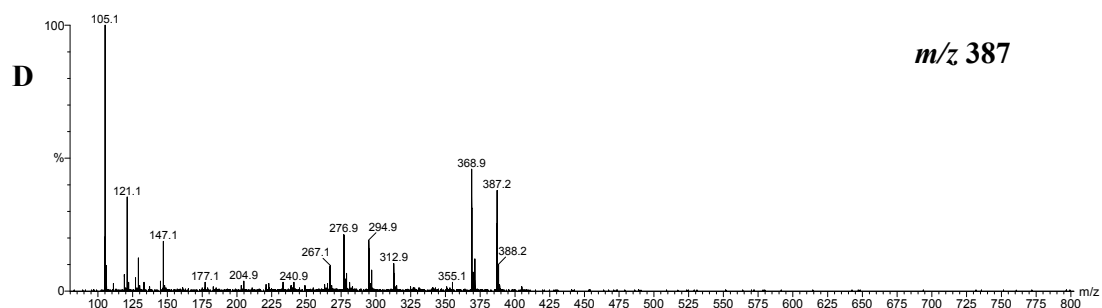
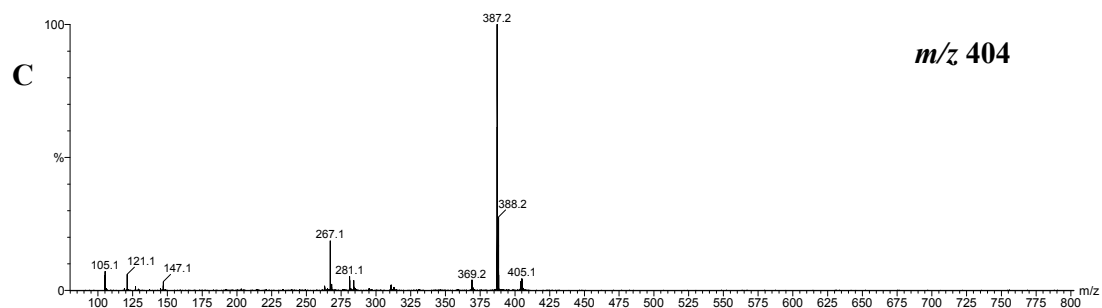
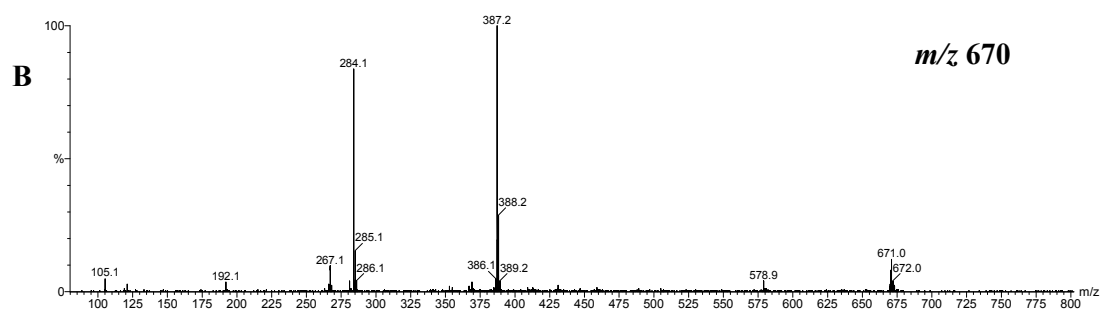
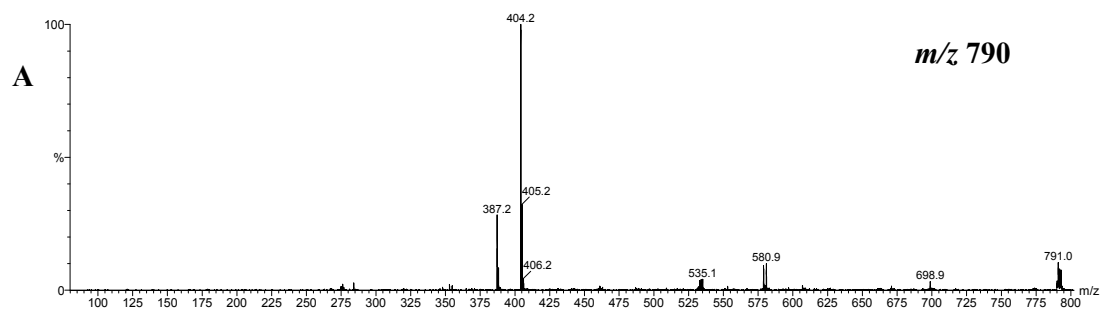
The ESI mass spectrum of the sharp peak eluting at 31.1 min (Figure 5.14) is shown in Figure 5.16. There were no ions greater than  $m/z$  800. The largest ion observed was  $m/z$  790, and the most abundant ion observed was  $m/z$  284. The ESI mass spectrum exhibits one signature UV filter ion,  $m/z$  192, which corresponds to the mass of Kyn-yellow.<sup>109</sup>



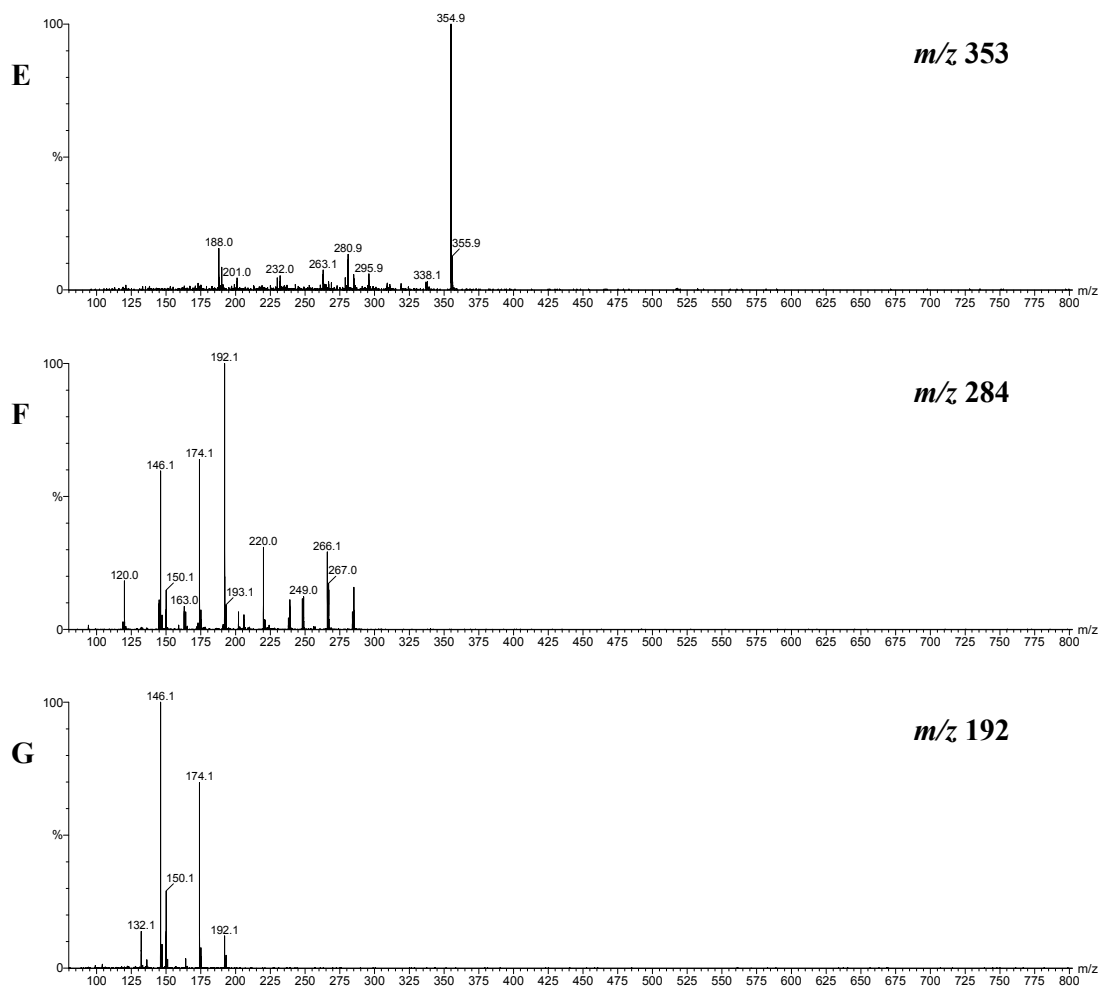
**Figure 5.16** ESI mass spectrum of the peak eluting at 31.1 min in Figure 5.14.

Figure 5.17A shows the MS/MS spectrum of ion  $m/z$  790. MS/MS revealed that the molecule split into two fragments,  $m/z$  404 and 387. Figure 5.17B shows the MS/MS spectrum of ion  $m/z$  670. The major fragment ions include  $m/z$  579, 387, 284, 267, 192 and 105. Figure 5.17C shows the MS/MS spectrum of ion  $m/z$  404. The major fragment ions include  $m/z$  387, 369, 281, 267, 147, 121 and 105. Figure 5.17D shows the MS/MS spectrum of ion  $m/z$  387. The fragment ions include,  $m/z$  369, 313, 295, 277, 267, 147, 121 and 105. Figure 5.17E shows the MS/MS spectrum of ion  $m/z$  353. The fragment ions include,  $m/z$  338, 296, 281, 263, 232, 201 and 188. Figure 5.17F shows the MS/MS spectrum of ion  $m/z$  284. The major fragment ions include  $m/z$  266, 249, 220, 192, 174, 146 and 120. Figure 5.17G shows the MS/MS spectrum of ion  $m/z$  192. The fragment ions include  $m/z$  174, 146 and 132.

The ions  $m/z$  192, 174 and 146 are characteristic fragment ions of Kyn.<sup>103</sup> High resolution mass spectrometric data was obtained for these ions to determine the elemental compositions. Ion  $m/z$  192, 192.0678, calculated for  $C_{10}H_{10}NO_3$ , 192.0661 (mass of Kyn-yellow) and ion  $m/z$  174, 174.0569, calculated for  $C_{10}H_8NO_2$ , 174.0555 (mass of Kyn-yellow minus a water) both correspond to the correct elemental compositions for these fragment compounds of Kyn. Ion  $m/z$  146, 146.0621, calculated for  $C_4H_{10}N_4S$ , did not match that of the expected Kyn fragment. The presence of the ions,  $m/z$  192 and 174 is significant since it shows that P4 could contain a Kyn-derived moiety. As a result of the MS/MS data, it appears that the precursor ion of this Kyn-derived compound is  $m/z$  670, since MS/MS of this ion resulted in two major parts, fragment ions 387 and 284. MS/MS of  $m/z$  284 yielded fragment ions  $m/z$  192 and 174.







**Figure 5.17** MS/MS spectra. MS/MS of ions that were present in the ESI mass spectrum (Figure 5.16). *A*,  $m/z$  790; *B*,  $m/z$  670; *C*,  $m/z$  404; *D*,  $m/z$  387; *E*,  $m/z$  353; *F*,  $m/z$  284; *G*,  $m/z$  192.

### NMR of P4

Since the structure of the product P4 could not be identified from the mass spectral data alone, additional human cataract lenses were acid hydrolysed, purified and analysed by nano-NMR spectroscopy. The product (< 1 mg) was dissolved in 50  $\mu$ L of acidified D<sub>2</sub>O, and the solution appeared very coloured (dark yellow). NMR analysis unfortunately showed that there was insufficient sample to complete even the basic NMR experiments needed for structural analysis.

The proton NMR spectrum is shown in Figure 5.18. The spectrum shows that this isolated compound (Figure 5.18) is still impure, since there are numerous broad peaks on the baseline in the spectrum. The HPLC chromatogram (Figure 5.14) also shows that this compound may still be impure following the second stage of HPLC purification, since there are several peaks that elute close together. The proton NMR experiment was undertaken for 16 hours on a 500 MHz NMR spectrometer. The structure of the Kyn amino acid adducts and their proton NMR assignments are known, therefore, an attempt was made to assign some of the peaks (e.g. aromatic protons) in Figure 5.18 on this basis. The ring for Kyn has 4 aromatic hydrogens (Kyn-Lys,  $\delta$ H 7.72 (doublet of doublets (dd)), 7.31 (doublet of doublet of doublets (ddd)), 6.77 (doublet (d)), 6.70 (dd); Kyn-His,  $\delta$ H 7.71 (dd), 7.27 (ddd), 6.72 (d), 6.67 (dd); Kyn-Cys,  $\delta$ H 8.01 (dd), 7.56 (ddd), 7.27 (d), 7.19 (d)).<sup>103</sup> In Figure 5.18, there are 4 doublets at 7.35, 7.29, 7.22 and 6.92 ppm. However, the peak at 6.92 ppm appears to be overlapping with other protons. Integration of the spectrum showed that the doublets at 7.22 and 6.92 ppm corresponded to the same number of protons. The coupling constants for each of the peaks at 7.22 and 6.92 ppm was 9 Hz, indicating that the protons are *ortho* coupled and part of a *para*-disubstituted aromatic ring. The remaining peaks in the proton NMR spectrum were difficult to assign since the structure of this product is unknown.

A gCOSY experiment was undertaken to show the coupling between the hydrogens in the structure. This experiment was undertaken for 16 hours, and after that time only two peaks were exhibited in the aromatic region of the spectrum (Figure 5.19). The two peaks in Figure 5.19B show that the protons at 7.22 and 6.92 ppm couple to each other.

The NMR spectra (Figure 5.18 and Figure 5.19) demonstrate that there was insufficient material for proper structural elucidation of P4.

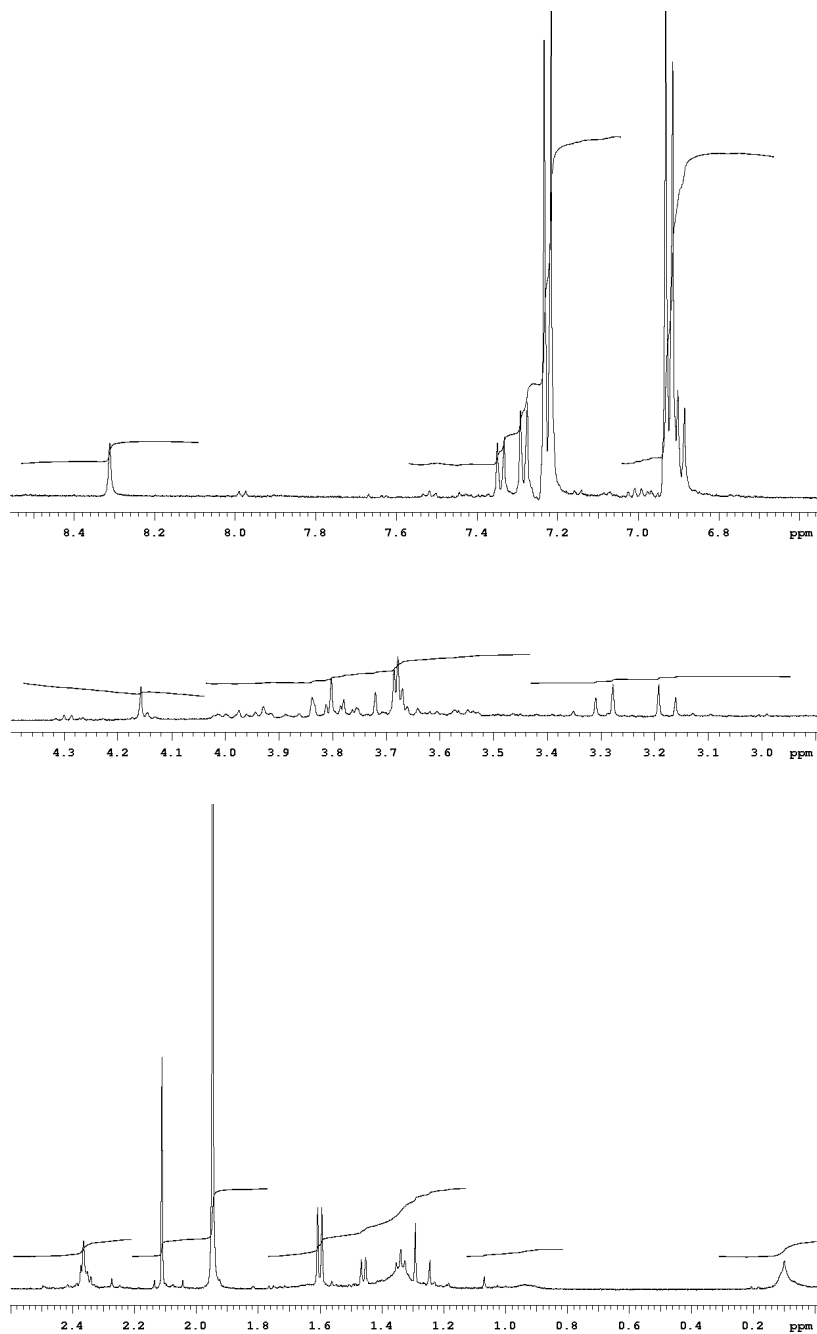


**Figure 5.18** Proton NMR spectrum of the peak eluting at 31.1 min in Figure 5.14.

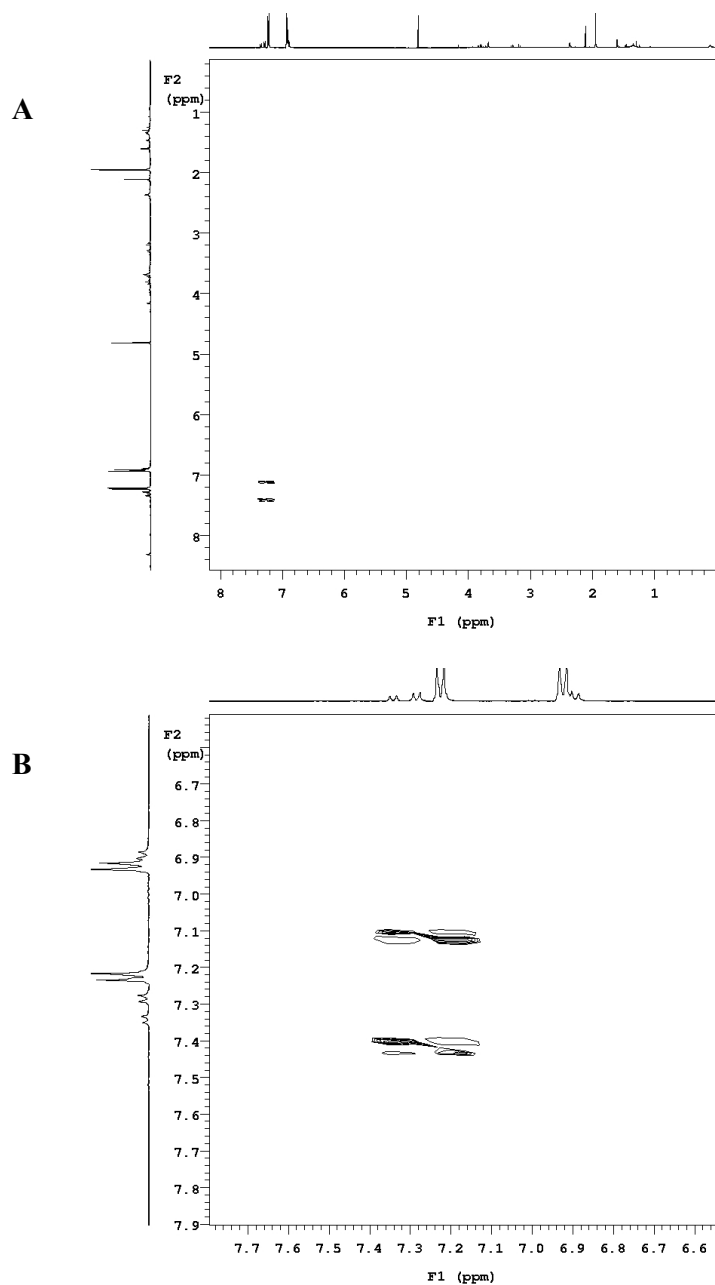


**Figure 5.19** gCOSY spectrum of the peak eluting at 31.1 min in Figure 5.14. *A*, Entire gCOSY spectrum; *B*, Aromatic region of the gCOSY spectrum.

### 5.3.5 Analysis of P5

Acid hydrolysis of human cataract lenses also yielded P5 eluting at 37.5 min (Figure 5.1C). P5 was further purified. Figure 5.20 shows the partial HPLC profile of the second phase of HPLC purification. P5 resolved as many minor peaks, but the major peak eluting at 34.5 min (Figure 5.20) was collected for UV-visible and mass spectral analysis.

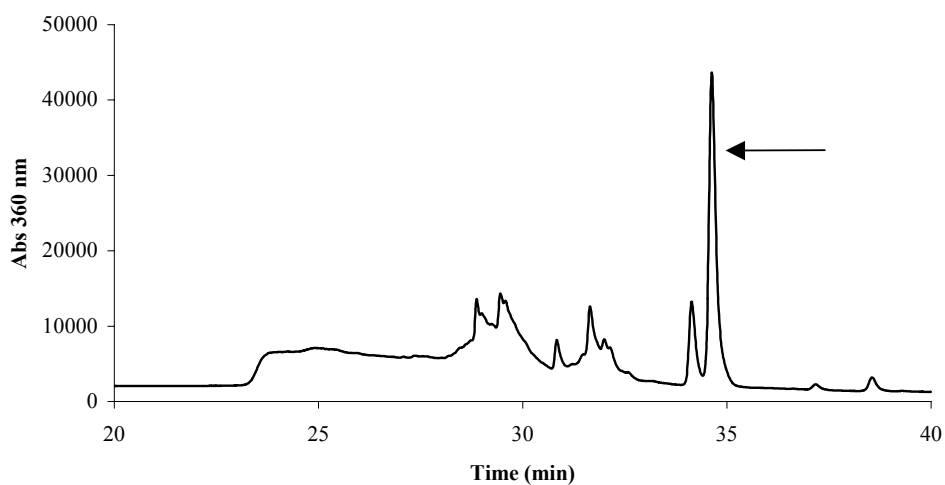


**Figure 5.20** HPLC chromatogram of P5 after a second purification stage. The single peak eluting at 34.5 min was collected for analysis by UV-visible and mass spectrometry.

A UV-visible spectrum of the peak eluting at 34.5 min in Figure 5.20 shows that this product had maximum absorbances centred at 300, 361 and 378 nm (Figure 5.21). The UV-visible spectrum (Figure 5.21) shows that the product may be a UV filter derivative since UV filter adducts exhibit UV absorbances centred at 365 nm.

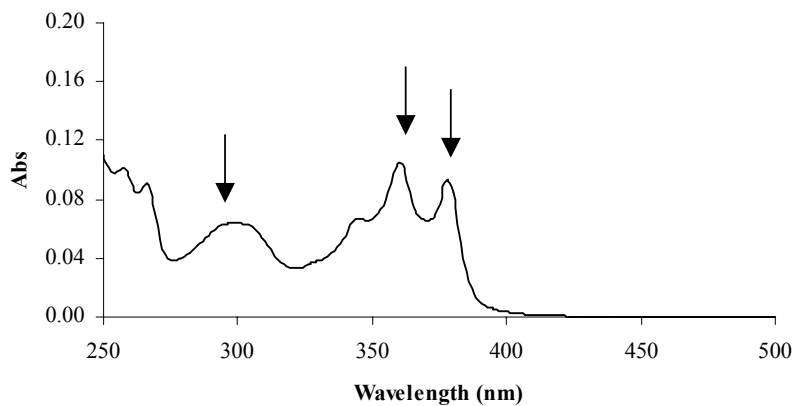


**Figure 5.21** UV-visible spectrum of the peak eluting at 34.5 min in Figure 5.20.

The ESI mass spectrum of the sharp peak eluting at 34.5 min (Figure 5.20) is shown in Figure 5.22. There were no ions greater than  $m/z$  1000. The largest ion observed was  $m/z$  993, and the most abundant ion observed was  $m/z$  607.

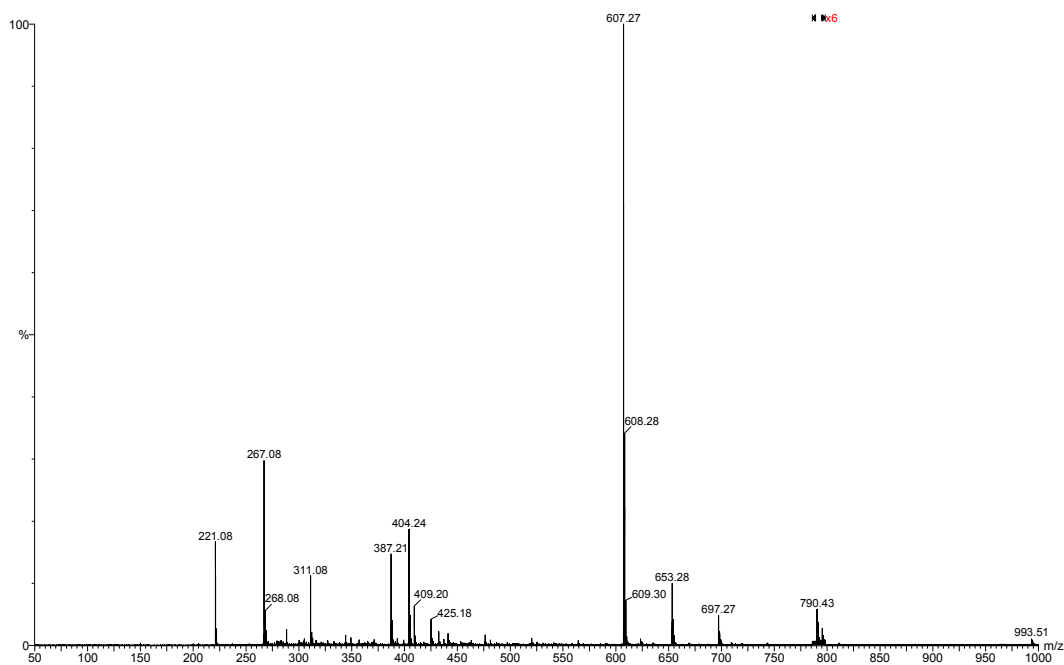


**Figure 5.22** ESI mass spectrum of the peak eluting at 34.5 min in Figure 5.20.

Figure 5.23A shows the MS/MS spectrum of ion  $m/z$  993. The major fragment ions include  $m/z$  607 and 221. Figure 5.23B shows the MS/MS spectrum of ion  $m/z$  790. The major fragment ions include  $m/z$  404, 387 and 221. Figure 5.23C shows the MS/MS spectrum of ion  $m/z$  697. The major fragment ion observed was  $m/z$  311. Figure 5.23D shows the MS/MS spectrum of ion  $m/z$  607. The fragment ions include  $m/z$  387 and 221.

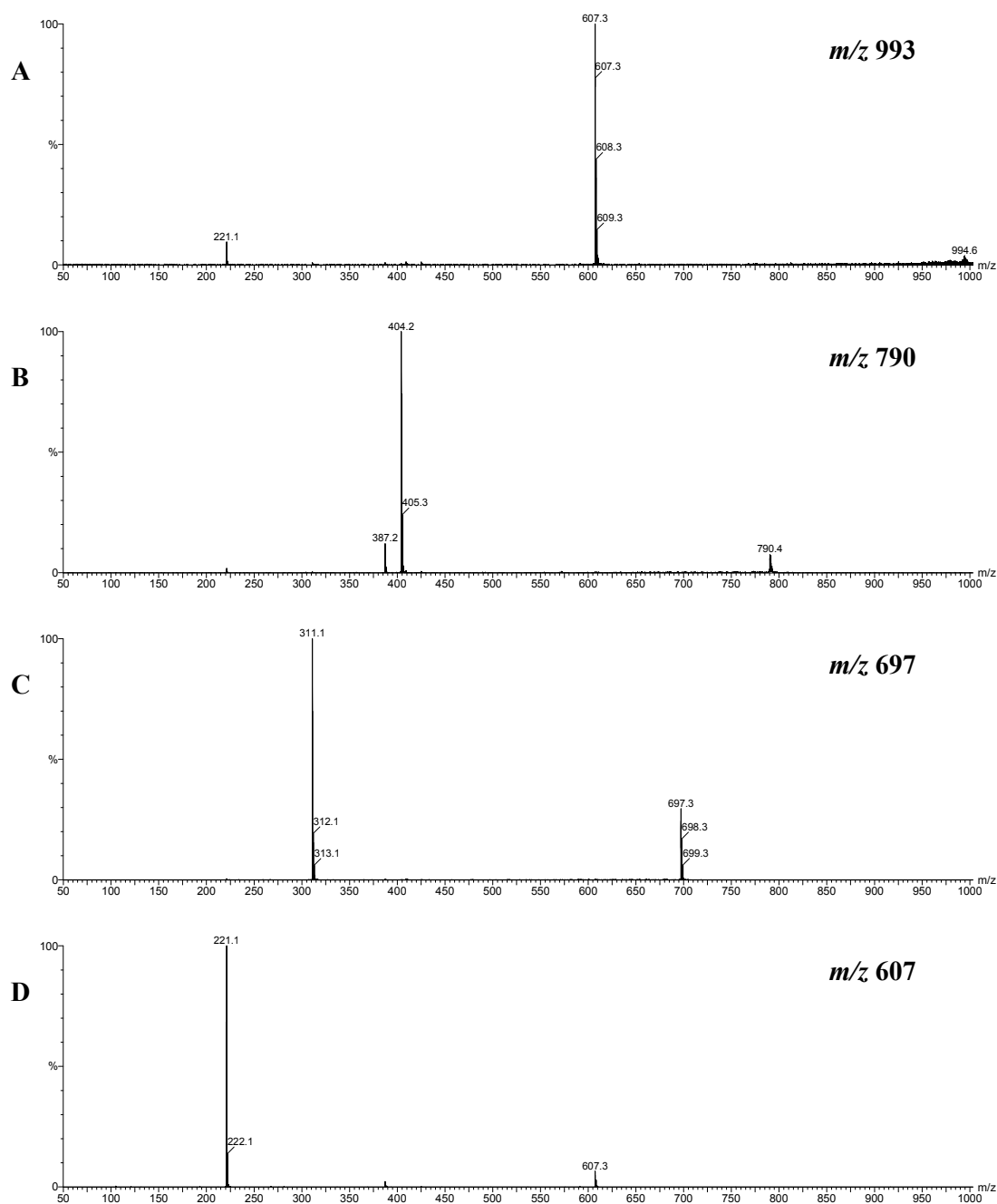


**Figure 5.23** MS/MS spectra. MS/MS of ions that were present in the ESI mass spectrum (Figure 5.22). *A*,  $m/z$  993; *B*,  $m/z$  790; *C*,  $m/z$  697; *D*,  $m/z$  607.



### 5.3.6 Analysis of P6

P6 was purified by Dr Peter Hains, and he provided the HPLC chromatogram of the second and third stage of HPLC purification, and the mass spectrum of the compound. P6 eluted at 45.0 min on the HPLC chromatogram in Figure 5.1C. P6 was purified twice after the initial HPLC purification, see Sections 5.2.5.3 and 5.2.5.4 for details. The HPLC chromatogram of the second phase of HPLC purification is shown in Figure 5.24A. The HPLC buffers contained heptafluorobutyric acid instead of TFA. The large peak eluting at 42.5 min (Figure 5.24A) was collected and purified further. The HPLC chromatogram of the third phase of HPLC purification is shown in Figure 5.24B. The HPLC buffers contained formic acid at this final stage of HPLC purification. The two large peaks eluting as a doublet at 28 min (Figure 5.24B) were collected, and the mass spectrum of these two peaks are shown in Figure 5.24C. The mass spectrum shows an abundant ion at  $m/z$  367, and the largest ion observed is  $m/z$  734. The mass spectrum did not exhibit any characteristic UV filter ions.

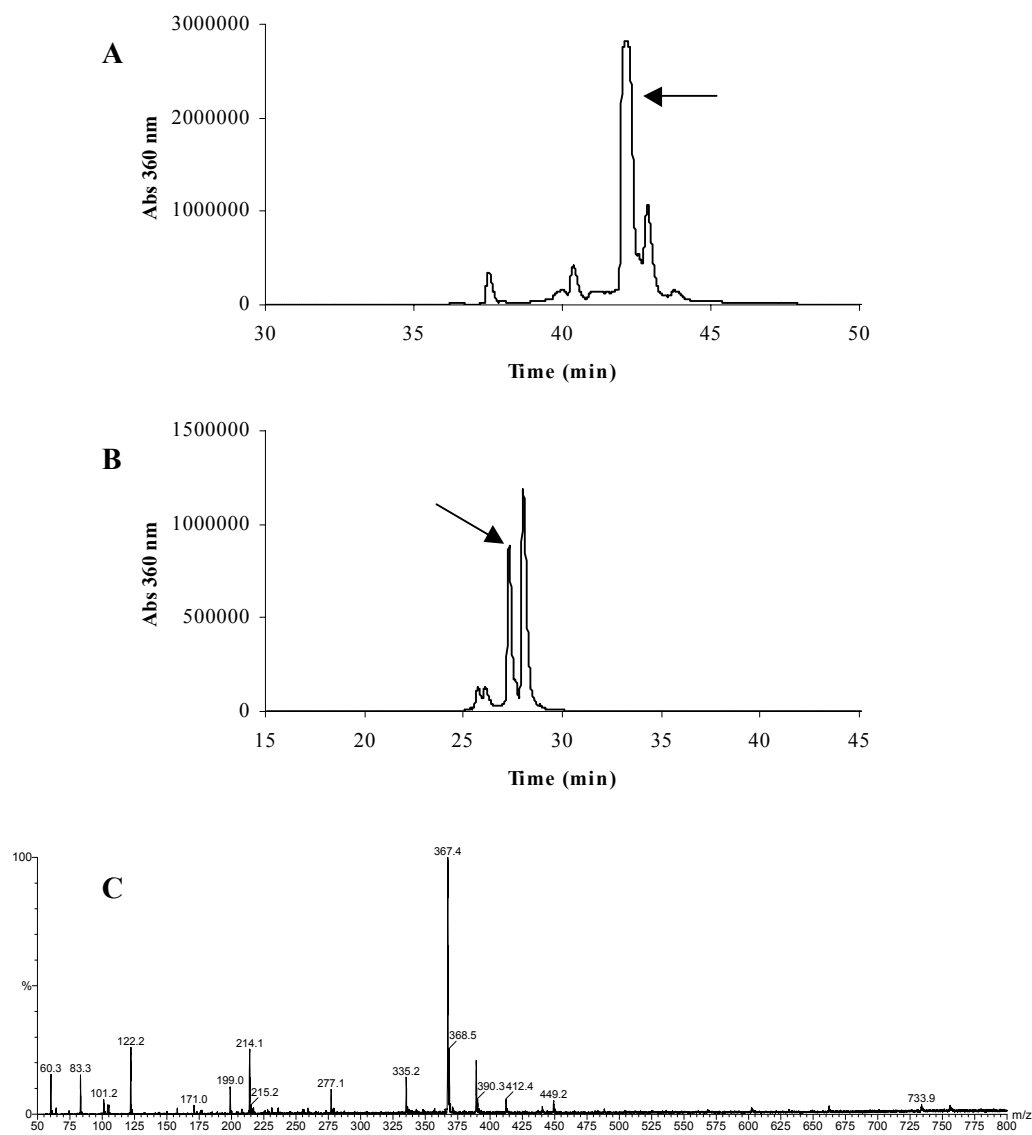


**Figure 5.24** Purification of P6. *A*, HPLC chromatogram of second purification (see Section 5.2.5.3 for details); *B*, HPLC chromatogram of third purification (see Section 5.2.5.4 for details); *C*, ESI mass spectrum of the peaks eluting as a doublet at 28 min in Figure 5.24B.

## 5.4 Discussion

The aim of this study was to see if unusual peaks could be observed in acid digests of cataract lens proteins. If so, this may enable us to draw conclusions as to the species involved in protein modifications in cataract. Another key aim was to obtain structural information on these species, and see, if they may be related to the 3OHKyn or Kyn amino acid adducts. Previous studies, together with the results presented in Chapter 3 of this thesis, show that the three Kyn UV filters, 3OHKynG, 3OHKyn and Kyn, are all attached to the proteins of normal aged human lenses.<sup>101,103</sup> ARN cataract is characterised by oxidation, colouration, insolubilisation and crosslinking of the proteins in the lens.<sup>14,157-160</sup> Cataract lenses differ from normal lenses, which, for example, do not contain oxidised amino acid residues, and normal lenses, whilst yellow, are not as colourised as cataract lenses. It has been proposed that oxidation of protein-bound UV filters may be an important factor in the formation of ARN cataract.

In this study, the HPLC profile of the hydrolysate of human cataract protein was found to differ greatly from the HPLC profiles of acid hydrolysed CLP and acid hydrolysed normal human aged lens protein (Figure 5.1). It was of particular interest to examine the properties of the novel peaks in the HPLC profile of acid hydrolysed cataract lenses that eluted at 360 nm wavelength. This wavelength was chosen since Kyn UV filters exhibit maximum UV-visible absorbances centred at 365 nm.<sup>102</sup> Breakdown products of UV filters, which absorb at other wavelengths would not be not detected. HCl is known to cause Trp to breakdown to Kyn.<sup>209</sup> This is an important consideration, however controls were incorporated into this study, *i.e.* the cataract hydrolysates were compared to the hydrolysates of CLP and normal aged human lens protein. In addition antioxidants, phenol and thioglycolic acid, were added to the acid during hydrolysis. However, antioxidants do not entirely prevent Trp breakdown.

Hydrolysis of cataract lens nuclear proteins resulted in the elution of six significant peaks (P1, P2, P3, P4, P5, and P6) in the HPLC chromatogram (Figure 5.1C), that were not present in the hydrolysate of normal aged lens proteins (Figure 5.1B). These were observed consistently in different batches of cataract lenses. Each peak was collected, and rerun on HPLC for purity. UV-visible spectroscopy was used to detect if peaks

resembled UV filters. Mass spectrometry was employed to identify UV filter ions, and NMR spectroscopy was employed for structural elucidation of P4.

The UV-visible spectra for each of the peaks, P1, P2, P3, P4 and P5, showed that the product in each of the peaks was possibly a UV filter derivative, since absorbance was broad and centred at 360-370 nm in each of the UV-visible spectra. The UV-visible spectrum of P1 (Figure 5.3) and P2 (Figure 5.7) were fairly similar *i.e.* broad peaks with maximum absorbances centred at 360 nm. These two UV-visible spectra are comparable to the UV-visible spectra for each of the 3OHKyn amino acid adducts at acidic and neutral pH (Chapter 2 of this thesis). The UV-visible spectra of P1 and P2 are also comparable to the UV spectra of the Kyn amino acid adducts.<sup>103</sup> Therefore, P1 and P2 may be derived from UV filters. The UV-visible spectrum of P3 varied slightly to that of P1 and P2. The maximum absorbance of P3 was centred at 350 nm (Figure 5.11), although the absorbance is lower in wavelength than that expected for UV filters (360-370 nm), the shape of the curve in the UV-visible spectrum suggests that P3 could also be a UV filter derivative. The UV-visible spectra of P4 (Figure 5.15) and P5 (Figure 5.21) were distinctly different to those of P1, P2 and P3. Maximal absorbance was still centred in the 360-370 nm range, however, two maximal absorbances were observed in that wavelength region. Therefore, the chromophore of P4 and P5 could be very similar to each other, but different to the chromophores of P1, P2 and P3. P4 and P5 may still be UV filter derivatives since such ‘double peak’ absorbances are characteristic of phenoxazone compounds, for example, xanthommatin<sup>184</sup> that are formed by oxidation of 3OHKyn or 3-hydroxyanthranilic acid. No UV-visible data was available for P6. In summary, the UV-visible spectra showed that the novel peaks isolated from the cataract lenses could all be UV filter derived compounds.

Mass spectrometry was employed to identify ‘signature’ UV filter ions in each of the novel peaks. Since the protein was acid hydrolysed, ions related to Kyn (Kyn-His,  $m/z$  347; Kyn-Lys,  $m/z$  338; Kyn-Cys,  $m/z$  313<sup>103</sup>) or 3OHKyn adduct ions (3OHKyn-His,  $m/z$  363; 3OHKyn-Lys,  $m/z$  354; 3OHKyn-Cys,  $m/z$  329) were expected, but not fragment ions from 3OHKynG, since acid hydrolysis cleaves the glucose from 3OHKynG. Table 5.1 lists the Kyn and 3OHKyn amino acid adduct ‘signature’ ions

and, Table 5.2 is a summary of all of the ions and fragment ions that were identified in each of P1, P2, P3, P4, P5 and P6. Ions in Table 5.1 were generally not observed in Table 5.2 *i.e.* the characteristic ions of the UV filters adducts were not present in any of the ESI mass spectra of the novel compounds, except for the ESI mass spectrum of P4 (Figure 5.16), which had a low abundance  $m/z$  313 ion (theoretical mass of Kyn-Cys<sup>103</sup>).

The ESI and MS/MS mass spectra of P1, P2 and P3 did not show any familiar ‘signature’ ions, and structural elucidation was not possible from mass spectral data alone. The ESI mass spectrum of P6 again did not show any UV filter ‘signature’ ions.

Kyn ‘signature’ ions were identified in the ESI and MS/MS spectra of P4. Apart from the  $m/z$  313 ion in the ESI spectrum,  $m/z$  192 was also present (Kyn fragment ion). MS/MS of the higher molecular weight ions in the ESI spectrum showed that, MS/MS of  $m/z$  670 yielded fragment ions  $m/z$  579, 387, 284, 267, 192 and 105. MS/MS of  $m/z$  192 yielded  $m/z$  174 and 146 which are both fragment ions of Kyn.<sup>103</sup> MS/MS of  $m/z$  387, resulted in fragment ions,  $m/z$  369, 313, 295, 277, 267, 147, 121 and 105. If ion  $m/z$  313 were that of Kyn-Cys (theoretical molecular ion), then MS/MS of  $m/z$  387 should yield fragment ions of Kyn-Cys which include  $m/z$  295, 224, 202, 192, 174, 146 and 122.<sup>103</sup> Since these fragment ions were not present, Kyn-Cys is not a component of P4, but P4 very likely consists of a Kyn derivative, since high resolution mass spectrometric data of ions,  $m/z$  192 and 174 resulted in the expected elemental compositions for these two characteristic Kyn fragment ions. In summary, the source for the unknown Kyn derivative in P4 appears to be  $m/z$  670. NMR analysis of P4 showed that there was insufficient sample for structural elucidation but showed that P4 was an aromatic molecule.

The ESI mass spectrum of P5 showed that there was an ion  $m/z$  790, which was also present in the ESI mass spectrum of P4. MS/MS of  $m/z$  790 (in P5) resulted in fragment ions 404 and 387 (Figure 5.23B), and MS/MS of  $m/z$  790 (in P4) also resulted in the same two fragment ions (Figure 5.17A), and both ions appeared in the similar ratio as that observed in P5 *i.e.*  $m/z$  404 was the most abundant (100%), and  $m/z$  387 was at 15-

25% the abundance of the  $m/z$  404 ion. Therefore, it is very likely that a component of P4 and P5 are closely related in structure.

Because it is likely that oxidation of UV filters has taken place during ARN cataract formation, it may not be surprising that ions characteristic of unoxidised UV filters were absent. The ions of the expected 3OHKyn crosslink compounds in Chapter 4, Table 4.4, were also not observed in any of the ESI or MS/MS spectra of P1-P6. In addition, the HPLC profile of hydrolysed cataract lens protein (Figure 5.1C) was not comparable to the HPLC profiles of oxidised 3OHKyn-modified protein (Figure 4.24B and Figure 4.32B), *i.e.* there was no similarity in the pattern of the peaks that eluted in the hydrolysate of cataract protein and 3OHKyn-modified protein.

In this study, the aim was to hydrolyse cataract lens proteins and identify novel compounds. With age, the concentration of the major lens antioxidant, GSH, decreases significantly, especially in the nucleus of the lens.<sup>19,55</sup> The nucleus of a cataract lens is an oxidising environment, and maintenance of adequate GSH levels in the nucleus of the lens is crucial<sup>91,226,227</sup> for minimising polypeptide modifications. Although the isolated compounds could not be structurally characterised, the approach undertaken in this study was shown to be feasible, since in the past, acid hydrolysis of normal aged lens protein has revealed UV filter modifications.<sup>103</sup>

There have been a number of novel modifications reported in the literature. The majority of the studies used acid hydrolysis to isolate the novel compounds from the hydrolysates. Table 5.3 lists the modifications that have been identified in cataract lenses, and the quantitations are also listed (see Figures 1.4 and 1.6 for the structures of the modifications). The absorbance of the UV detector used in the HPLC purification has also been listed. Of all the modifications listed, two studies used enzymatic digestion. Cheng, *et al.* identified K2P,<sup>107</sup> and Ahmed, *et al.* identified MG-H1 and MG-H2<sup>130</sup> using enzymatic digestion of cataractous lens proteins. Although enzymatic digestion is a ‘gentler’ method, a disadvantage of enzymatic digestion is insufficient digestion of the proteins.

A future aim is to identify oxidised UV filter compounds that survive acid hydrolysis of modified protein, and to compare it with authentic cataract lens digests.

**Table 5.2** Summary of the ions and fragment ions identified in the peaks, P1, P2, P3, P4, P5 and P6, which were isolated and purified from hydrolysed human cataract lens proteins.

| <b>Peak</b> | <b>Ions</b> | <b>Fragment Ions</b>  |
|-------------|-------------|---|
| <b>P1</b>   | - $m/z$ 658 | - $m/z$ 641, 454, 374, 346, 270, 242, 233   |
|             | - $m/z$ 505 | - $m/z$ 487, 469, 418, 382, 326, 308, 254, 236, 206, 162                          |
|             | - $m/z$ 419 | - $m/z$ 254, 166  |
|             | - $m/z$ 331 | - $m/z$ 166, 120  |
|             | - $m/z$ 270 | - $m/z$ 252, 234, 224, 206, 178, 160, 137, 106, 88                                |
|             | - $m/z$ 166 | - $m/z$ 149, 131, 120, 107, 103   |
| <b>P2</b>   | - $m/z$ 806 | - $m/z$ 420   |
|             | - $m/z$ 713 | - $m/z$ 668, 622, 429, 409, 387, 327, 267, 105                                    |
|             | - $m/z$ 615 | - $m/z$ 409, 229  |
|             | - $m/z$ 508 | - $m/z$ 327, 122  |
|             | - $m/z$ 420 | - $m/z$ 402, 374, 356, 328, 300, 282, 254, 239, 222, 210, 194, 182, 165, 148, 136 |
| <b>P3</b>   | - $m/z$ 665 | - $m/z$ 381, 279  |
|             | - $m/z$ 641 | - $m/z$ 624, 581, 539, 497, 479, 455, 437, 413, 395, 353, 311, 304, 257           |
|             | - $m/z$ 279 | - $m/z$ 233, 132, 120, 86   |
| <b>P4</b>   | - $m/z$ 790 | - $m/z$ 404, 387  |
|             | - $m/z$ 670 | - $m/z$ 579, 387, 284, 267, 192, 105  |
|             | - $m/z$ 404 | - $m/z$ 387, 369, 281, 267, 147, 121, 105   |
|             | - $m/z$ 387 | - $m/z$ 369, 313, 295, 277, 267, 147, 121, 105                                    |
|             | - $m/z$ 353 | - $m/z$ 338, 296, 281, 263, 232, 201, 188   |
|             | - $m/z$ 284 | - $m/z$ 266, 249, 220, 192, 174, 146, 120   |
|             | - $m/z$ 192 | - $m/z$ 174, 146, 132   |
| <b>P5</b>   | - $m/z$ 993 | - $m/z$ 607, 221  |
|             | - $m/z$ 790 | - $m/z$ 404, 387, 221   |
|             | - $m/z$ 697 | - $m/z$ 311   |
|             | - $m/z$ 607 | - $m/z$ 387, 221  |
| <b>P6</b>   | - $m/z$ 734 |   |
|             | - $m/z$ 449 |   |
|             | - $m/z$ 389 |   |
|             | - $m/z$ 367 |   |
|             | - $m/z$ 335 |   |
|             | - $m/z$ 277 |   |
|             | - $m/z$ 214 |   |
|             | - $m/z$ 122 |   |

**Table 5.3** List of modifications in human cataract lens proteins.<sup>104-107,130,212</sup>

See Figures 1.4 and 1.6 for the structures of the modifications



## Chapter 6

### **Conclusions and Future Directions**

The aim of this thesis was to examine the role of 3OHKyn in the human lens and in particular its interaction with proteins. Initially model studies were undertaken to mimic the role of 3OHKyn in the normal lens. 3OHKyn amino acid adducts were synthesised and characterised. Like 3OHKyn, the 3OHKyn amino acid adducts were found to be unstable at pH 7.2. The fragment ions identified for each adduct will be important in future studies, since they can be used as markers in protein digests. In addition a novel oxidation product of 3OHKyn-*t*-Boc-His was also identified.

Hydrolysis has previously been used to show Kyn and 3OHKynG bound covalently to lens proteins. However, acid hydrolysis was not an appropriate method for determining the levels of 3OHKyn bound to proteins. A new and simple method was developed to determine the levels of protein-bound kynurenines. 3OHKynG was found to be present at the highest amounts followed by Kyn with 3OHKyn being attached in the lowest amount. The ratio was approximately 145:4:1 (3OHKynG:Kyn:3OHKyn). This is in agreement with the finding that 3OHKynG is the most abundant free UV filter in the lens followed by Kyn and 3OHKyn. The findings from this study also showed that there was no relationship between the levels of bound and free UV filters, suggesting that the binding of UV filters to proteins reflects not so much the concentration of available UV filter, but more probably the degree of lens barrier formation. This study also showed that all of the UV filters are bound to normal human lens nuclear proteins after middle age. The levels in the nucleus were found to be much higher than in the cortex. In addition the levels of bound UV filters in normal lens proteins was much higher than in cataract lens proteins. Bound 3OHKyn could not be detected in cataract lens proteins, indicating that once bound to normal lens proteins, 3OHKyn may possibly oxidise and play a role in the progression of cataract.

Since 3OHKyn is indeed bound to human lens nuclear proteins, another key objective was to characterise the properties of such 3OHKyn-modified proteins. The level of bound 3OHKyn in the nuclear proteins is extremely low, and 3OHKyn is reactive. Therefore, it was unlikely that a peptide could be readily isolated and analysed from

human protein. A model study with CLP modified by 3OHKyn at pH 7.2 failed to identify 3OHKyn modified peptides, since CLP contains several crystallin subgroups, and many modifications may result from a reaction involving 3OHKyn. A peptide modified at Cys was however identified when purified  $\alpha$ -crystallin was incubated with 3OHKyn. In this same study, major Met and minor Trp oxidation were also observed. Oxidation of Met is a characteristic feature of cataract lens proteins. The findings from this study suggest that 3OHKyn may contribute to the formation of cataract, since oxidation of 3OHKyn results in the formation of  $H_2O_2$ , and  $H_2O_2$  readily induces protein oxidation. However, there are other sources of  $H_2O_2$  in the lens, and 3OHKyn may not be the sole agent responsible for the protein oxidation that occurs in cataract.

Crosslinking is another feature of ARN cataract. The theory that 3OHKyn may crosslink lens proteins was examined in preliminary experiments. Model studies with the 3OHKyn amino acid adducts were first undertaken. Incubation of 3OHKyn-*t*-Boc-His yielded a compound with a molecular ion of  $m/z$  550, which eluted as a doublet on the HPLC, and had a wavelength maximum centred at 408 nm. This product was produced in the absence and presence of excess amino acids, and its molecular weight suggests that crosslinking may have occurred, but unfortunately, structural characterisation of this compound was not achieved. Model studies with CLP modified with 3OHKyn at pH 7.2 and 9.5 also failed to show any evidence of crosslinking when the protein was allowed to incubate over an extended period of time. 3-D Fluorescence profiles showed a shift in fluorescence over the incubation period, however the SDS-PAGE data did not show crosslink formation. Acid hydrolysis of the modified proteins following the incubation showed numerous fractions eluting on the HPLC, but none could be conclusively identified by mass spectrometry, as crosslinked compounds. The study did however show that during the incubation, bound 3OHKyn cleaved and formed xanthurenic acid via oxidation. This demonstrates that in cataract lenses when 3OHKyn is attached to lens proteins at pH 7, it may ultimately result in the formation of xanthurenic acid.

3OHKyn was found to be facilely transferred between amino acid residues during the incubation. For example, the protein originally modified at pH 7.2, was modified

predominantly at Cys. However following incubation over 15 days, the recovery of 3OHKyn-Cys diminished, and His modification was observed after 6 days. This demonstrates the intrinsic instability of 3OHKyn adducts in proteins, and also suggests how the UV filter may react *in vivo*.

In future studies it would be ideal if the product,  $m/z$  550, resulting from 3OHKyn-*t*-Boc-His incubations could be structurally characterised, since 3OHKyn-*t*-Boc-His is the most stable of the three 3OHKyn amino acid adducts. It is possible that this stable product may be present in aged normal or cataract lens proteins, but this was not examined.

Acid hydrolysis of human cataract lens proteins showed that 6 novel peaks eluted in the HPLC chromatogram of the hydrolysate. These peaks were not observed in the hydrolysate of CLP or normal aged lens protein. Isolation and examination of each peak by UV-visible spectroscopy and mass spectrometry showed that several of the 5 peaks, P1-P5, may be UV filter derived compounds based on the UV-visible data. However, the mass spectral data alone was insufficient to identify characteristic UV filter ions except for P4. P4 contained a Kyn fragment ion and extensive mass spectral analysis showed that the unknown Kyn derivative in P4, appears to have a molecular ion of  $m/z$  670. Unfortunately at this stage NMR characterisation was unsuccessful due to a lack of sufficient material.

In summary, in the normal human lens, 3OHKyn binds to lens proteins after middle age, and in this sense behaves like the other two UV filters. The reason for the development of ARN cataract is not known, but, since it is now known that 3OHKyn is bound to proteins, 3OHKyn may have a role in cataract formation, and this requires further investigation. The model studies outlined in Chapter 4 provided the means to investigate the problem. Initial investigation suggest it may be fruitful to isolate, and to structurally characterise fractions from acid hydrolysed cataract lenses, since this may reveal the identity of the major species that modifies lens proteins in cataract.

## References

- (1) [www.v2020.org/right\\_to\\_sight/index.asp](http://www.v2020.org/right_to_sight/index.asp) (Cited 20/02/06).
- (2) McCarty, C. A.; Taylor, H. R. Recent developments in vision research. *Invest. Ophthalmol. Vis. Sci.* **1996**, *37*, 1720-1723.
- (3) Neale, R. E.; Purdie, J. L.; Hirst, L. W.; Green, A. C. Sun exposure as a risk factor for nuclear cataract. *Epidemiology* **2003**, *14*, 707-712.
- (4) Bron, A. J.; Vrensen, G. F.; Koretz, J.; Maraini, G.; Harding, J. J. The ageing lens. *Ophthalmologica* **2000**, *214*, 86-104.
- (5) Evans, J.; Minassian, D. Epidemiology of age-related cataract. *Community Eye Health* **1992**, *9*, 2-6.
- (6) [www.v2020.org/Eye\\_disease/cataract.asp](http://www.v2020.org/Eye_disease/cataract.asp) (Cited 20/02/06).
- (7) Pitts, D. G.; Bergmanson, J. P. G. The UV problem: Have the rules changed? *J. Am. Optom. Assoc.* **1989**, *60*, 420-442.
- (8) Sherwood, L. *Human physiology from cells to systems (3rd Ed.)*; Wadsworth Publishing Company: Albany, New York, 1997.
- (9) Berman, E. R. *Biochemistry of the eye*; Plenum Press: New York, 1991.
- (10) Gordon, S. *The aging eye*; Simon & Schuster Inc.: New York, 2001.
- (11) Delaye, M.; Tardieu, A. Short-range packing of crystallins proteins accounts for eye lens transparency. *Nature* **1983**, *302*, 415-417.
- (12) Pierscionek, B.; Smith, G.; Augusteyn, R. C. The refractive increments of bovine alpha, beta and gamma crystallins. *Vis. Res.* **1987**, *27*, 1539-1541.
- (13) Harding, J. J.; Dilley, K. J. Structural proteins of the mammalian lens: A review with emphasis on changes in development, aging and cataract. *Exp. Eye Res.* **1976**, *22*, 1-73.
- (14) Harding, J. J. *Cataract. Biochemistry, epidemiology and pharmacology*; Chapman and Hall: London, U.K., 1991.
- (15) Zigler, J. S. J.; Goosey, J. Aging of protein molecules: Lens crystallins as a model system. *Trend Biol. Sci.* **1981**, *6*, 133-136.
- (16) Davson, H. *The eye*; Academic Press: New York, 1969.
- (17) Davson, H. *Physiology of the eye*; Churchill Livingstone: Edinburgh, 1980.
- (18) Harding, J. J.; Crabbe, M. J. C. *The Lens: Development, proteins, metabolism and cataract*; Academic Press: Orlando, 1984.
- (19) Bova, L. M.; Sweeney, M. H. J.; Jamie, J. F.; Truscott, R. J. W. Major changes in human ocular UV protection with age. *Invest. Ophthalmol. Vis. Sci.* **2001**, *42*, 200-205.
- (20) Sen, A. C.; Ueno, N.; Chakrabarti, B. Studies on human lens: I. Origin and development of fluorescent pigments. *Photochem. Photobiol.* **1992**, *55*, 753-764.
- (21) Fagerholm, P. P.; Philipson, B. T.; Lindstrom, B. Normal human lens - the distribution of proteins. *Exp. Eye Res.* **1981**, *33*, 615-620.
- (22) Horwitz, J. The function of alpha-crystallin. *Invest. Ophthalmol. Vis. Sci.* **1993**, *34*, 10-22.
- (23) Bloemendal, H. *Molecular and Cellular Biology of the Eye Lens*; Wiley: New York, 1981.
- (24) Wistow, G. J.; Piatigorsky, J. Lens crystallins: the evolution and expression of proteins for a highly specialized tissue. *Annu. Rev. Biochem.* **1988**, *57*, 479-504.

- (25) Bloemendal, H.; de Jong, W. W. *Lens Proteins and their Genes*; Academic Press: San Diego, 1991; 259-281.
- (26) Piatigorsky, J. Lens crystallins: innovation associated with changes in gene regulation. *J. Biol. Chem.* **1992**, *267*, 4277-4280.
- (27) Basaglia, F.; Di Luca, D. A comparative study of vertebrate eye lens crystallins using isoelectric focusing and densitometry. *Comp. Biochem. Physiol. B: Comp. Biochem.* **1993**, *106*, 575-586.
- (28) Huang, Q.-L.; Russell, P.; Stone, S. H.; Zigler, J. S. J. Zeta-crystallin, a novel lens protein from the guinea pig. *Curr. Eye Res.* **1987**, *6*, 725-732.
- (29) Horwitz, J. Alpha-crystallin. *Exp. Eye Res.* **2003**, *76*, 145-153.
- (30) Horwitz, J. Alpha-crystallin can function as a molecular chaperone. *Proc. Natl. Acad. Sci. U.S.A.* **1992**, *89*, 10449-10453.
- (31) Carver, J. A.; Aquilina, J. A.; Truscott, R. J. W. A possible chaperone-like quaternary structure for alpha-crystallin [letter]. *Exp. Eye Res.* **1994**, *59*, 231-234.
- (32) Nicholl, I.; Quinlan, R. Chaperone activity of alpha-crystallins modulates intermediate filament assembly. *EMBO Journal* **1994**, *13*, 945-953.
- (33) Rao, P. V.; Huang, Q.; Horwitz, J.; Zigler, J. S. J. Evidence that  $\alpha$ -crystallin prevents non-specific protein aggregation in the intact eye lens. *Biochim. Biophys. Acta* **1995**, *1245*, 439-447.
- (34) Aarts, H. J.; Lubsen, N. H.; J.G.G., S. Crystallin gene expression during rat lens development. *Eur. J. Biochem.* **1989**, *183*, 31-36.
- (35) Voorter, C. E.; Haard-Hoekman, W. A.; Hermans, M. M.; Bloemendal, H.; de Jong, W. W. Differential synthesis of crystallins in the developing rat eye lens. *Exp. Eye Res.* **1990**, *50*, 429-437.
- (36) Lampi, K. J.; Ma, Z.; Hanson, S. R.; Azuma, M.; Shih, M.; Shearer, T. R.; Smith, D. L.; Smith, J. B.; David, L. L. Age-related changes in human lens crystallins identified by two-dimensional electrophoresis and mass spectrometry. *Exp. Eye Res.* **1998**, *67*, 31-43.
- (37) Ueda, Y.; Duncan, M. K.; David, L. L. Lens proteomics: the accumulation of crystallin modifications in the mouse lens with age. *Invest. Ophthalmol. Vis. Sci.* **2002**, *43*, 205-215.
- (38) McAvoy, J. W. Cell division, cell elongation and distribution of alpha-, beta- and gamma-crystallins in the rat lens. *J. Embryol. Exp. Morphol.* **1978**, *44*, 149-165.
- (39) van Leen, R. W.; Breuer, M. L.; Lubsen, N. H.; Schoenmakers, J. G. G. Developmental expression of crystallin genes: in situ hybridization reveals a differential localization of specific mRNAs. *Dev. Biol.* **1987**, *123*, 338-345.
- (40) Bhat, S. P.; Nagineni, C. N. Alpha B subunit of lens specific protein alpha-crystallin is present in other ocular and non-ocular tissues. *Biochem. Biophys. Res. Comm.* **1989**, *158*, 319-325.
- (41) Dubin, R. A.; Wawrousek, E. F.; Piatigorsky, J. Expression of the murine alpha B-crystallin is not restricted to the lens. *Mol. Cell Biol.* **1989**, *9*, 1083-1091.
- (42) Iwaki, T.; Kume-Iwaki, A.; Goldman, J. E. Cellular distribution of alpha B-crystallin in non-lenticular tissues. *J. Histochem. Cytochem.* **1990**, *38*, 31-39.
- (43) Iwaki, T.; Kume-Iwaki, A.; Liem, R. K.; Goldman, J. E. Alpha B-crystallin is expressed in non-lenticular tissues and accumulates in Alexander's disease brain. *Cell* **1989**, *57*, 71-78.

## References

- (44) Iwaki, T.; Wisniewski, T.; Akiko, I.; Corbin, E.; Tomokane, N.; Tateishi, J.; Goldman, J. E. Accumulation of alpha B-crystallin in central nervous system glia and neurons in pathologic conditions. *Am. J. Pathol.* **1992**, *140*, 345-356.
- (45) Renkawek, K.; de Jong, W. W.; Merk, K. B.; Frenken, C. W. G. M.; van Workum, F. P. A.; Bosman, G. J. C. G. M. Alpha B-crystallin is present in reactive glia in Creutzfeldt-Jakob disease. *Acta. Neuropathol.* **1992**, *83*, 324-327.
- (46) Lowe, J.; McDermott, H.; Pike, I.; Speudlove, I.; Landon, M.; Mayer, R. Alpha B-crystallin expression in non-lenticular tissues and selective presence in ubiquitinated inclusion bodies in human disease. *J. Pathol.* **1992**, *166*, 61-68.
- (47) Bloemendal, H.; de Jong, W. W.; Jaenicke, R.; Lubsen, N. H.; Slingsby, C.; Tardieu, A. Ageing and vision: structure, stability and function of lens crystallins. *Prog. Biophys. Mol. Biol.* **2004**, *86*, 407-485.
- (48) Herbrink, P.; van Westreenen, H.; Bloemendal, H. Further studies on the polypeptide chains of beta-crystallin. *Exp. Eye Res.* **1975**, *20*, 541-548.
- (49) Berbers, G. A.; Hoekman, W. A.; Bloemendal, H.; de Jong, W. W.; Kleinschmidt, T.; Braunitzer, G. Homology between the primary structures of the major bovine beta-crystallin chains. *Eur. J. Biochem.* **1984**, *139*, 467-479.
- (50) Lampi, K. J.; Ma, Z.; Shih, M.; Shearer, T. R.; Smith, J. B.; Smith, D. L.; David, L. L. Sequence analysis of  $\beta$ A3,  $\beta$ B3, and  $\beta$ A4 crystallins completes the identification of the major proteins in young human lens. *J. Biol. Chem.* **1997**, *272*, 2268-2275.
- (51) den Dunnen, J. T.; Moormann, R. J.; Lubsen, N. H.; Schoenmakers, J. G. G. Concerted and divergent evolution within the rat gamma-crystallin gene family. *J. Mol. Biol.* **1986**, *189*, 37-46.
- (52) Peek, R.; McAvoy, J. W.; Lubsen, N. H.; Schoenmakers, J. G. G. Rise and fall of crystallin gene messenger levels during fibroblast growth factor induced terminal differentiation of lens cells. *Dev. Biol.* **1992**, *152*, 152-160.
- (53) Barbazetto, I. A.; Liang, J.; Chang, S.; Zheng, L.; Spector, A.; Dillon, J. P. Oxygen tension in the rabbit lens and vitreous before and after vitrectomy. *Exp. Eye Res.* **2004**, *78*, 917-924.
- (54) McNulty, R.; Wang, H.; Mathias, R. T.; Ortwerth, B. J.; Truscott, R. J. W.; Bassnett, S. Regulation of tissue oxygen levels in the mammalian lens. *J Physiol* **2004**, *559*, 883-898.
- (55) Dickerson Jr., J. E.; Lou, M. F. Free cysteine levels in normal human lenses. *Exp. Eye Res.* **1997**, *65*, 451-454.
- (56) Heath, H. The distribution and possible functions of ascorbic acid in the eye. *Exp. Eye Res.* **1962**, *1*, 362-367.
- (57) Wolff, S. P.; Wang, G.-M.; Spector, A. Pro-oxidant activation of ocular reductants. 1. Copper and riboflavin stimulate ascorbate oxidation causing lens epithelial cytotoxicity in vitro. *Exp. Eye Res.* **1987**, *45*, 777-789.
- (58) Garland, D. L.; Zigler, J. S. J.; Kinoshita, J. H. Structural changes in bovine lens crystallins induced by ascorbate, metal and oxygen. *Arch. Biochem. Biophys.* **1986**, *251*, 771-776.
- (59) Lohmann, W.; Schmehl, W.; Strobel, J. Nuclear cataract: oxidative damage to the lens. *Exp. Eye Res.* **1986**, *43*, 859-862.
- (60) Ortwerth, B. J.; Olesen, P. R. Glutathione inhibits the glycation and crosslinking of lens proteins by ascorbic acid. *Exp. Eye Res.* **1988**, *47*, 737-750.

## References

- (61) Ortwerth, B. J.; Feather, M. S.; Olesen, P. R. The precipitation and cross-linking of lens crystallins by ascorbic acid. *Exp. Eye Res.* **1988**, *47*, 155-168.
- (62) Ortwerth, B. J.; Olesen, P. R. Ascorbic acid-induced crosslinking of lens proteins: evidence supporting a Maillard reaction. *Biochim. Biophys. Acta* **1988**, *956*, 10-22.
- (63) Giblin, F. J.; McCready, J. P.; Reddan, J. R.; Dziedzic, D. C.; Reddy, V. N. Detoxification of hydrogen peroxide by cultured rabbit lens epithelial cells: Participation of the glutathione redox cycle. *Exp. Eye Res.* **1985**, *40*, 827-840.
- (64) Lou, M. F. Redox regulation in the lens. *Prog. Retin. Eye Res* **2003**, *22*, 657-682.
- (65) Harding, J. Free and protein bound glutathione in normal and cataractous human lenses. *Biochem. J.* **1970**, *117*, 957-960.
- (66) Reddy, V. N. Metabolism of glutathione in the lens. *Exp. Eye Res.* **1971**, *11*, 310-328.
- (67) Reddy, V. N.; Giblin, F. J.; Matsuda, H. *Defense system of the lens against oxidative damage*; Elsevier: New York, 1980.
- (68) Kinsey, V. E.; Merriam, F. C. Studies on the crystalline lens. II. Synthesis of glutathione in the normal and cataractous rabbit lens. *Arch. Ophthalmol.* **1950**, *44*, 370-380.
- (69) McMillan, P. J.; Ryerson, S. J.; Mortensen, R. A. The metabolism of lens glutathione studied with glycine <sup>14</sup>C. *Arch. Biochem. Biophys.* **1959**, *81*, 119-123.
- (70) Cliffe, E. E.; Waley, S. G. Acidic peptides of the lens. 4. The biosynthesis of ophthalmic acid. *Biochem. J.* **1958**, *69*, 649-655.
- (71) Rathbun, W. B. *Glutathione biosynthesis in the lens and erythrocyte*; Elsevier: New York, 1980.
- (72) Reddy, V. N. Glutathione and its function in the lens - an overview. *Exp. Eye Res.* **1990**, *50*, 771-778.
- (73) van Heyningen, R. The glucoside of 3-hydroxykynurenine and other fluorescent compounds in the human lens. *Ciba Found. Symp.* **1973**, *19*, 151-171.
- (74) Zigman, S.; Paxhia, T. The nature and properties of squirrel lens yellow pigment. *Exp. Eye Res.* **1988**, *47*, 819-824.
- (75) van Heyningen, R. Fluorescent glucoside in the human lens. *Nature* **1971**, *230*, 393-394.
- (76) van Heyningen, R. Photo-oxidation of lens proteins by sunlight in the presence of fluorescent derivatives of kynureine, isolated from the human lens. *Exp. Eye Res.* **1973**, *17*, 137-147.
- (77) van Heyningen, R. Assay of fluorescent glucosides in the human lens. *Exp. Eye Res.* **1973**, *15*, 121-126.
- (78) Wood, A. M.; Truscott, R. J. W. UV filters in human lenses: tryptophan catabolism. *Exp. Eye Res.* **1993**, *56*, 317-325.
- (79) Wood, A. M.; Truscott, R. J. W. Ultraviolet filter compounds in human lenses: 3-hydroxykynurenine glucoside formation. *Vis. Res.* **1994**, *34*, 1369-1374.
- (80) Taylor, L. M.; Aquilina, J. A.; Willis, R. H.; Jamie, J. F.; Truscott, R. J. W. Identification of a new human lens UV filter compound. *FEBS Lett.* **2001**, *509*, 6-10.

## References

- (81) Truscott, R. J. W.; Wood, A. M.; Carver, J. A.; Sheil, M. M.; Stutchbury, G. M.; Zhu, J.; Kilby, G. W. A new UV-filter compound in human lenses. *FEBS Lett.* **1994**, *348*, 173-176.
- (82) Garner, B.; Vazquez, S.; Griffith, R.; Lindner, R. A.; Carver, J. A.; Truscott, R. J. W. Identification of glutathionyl-3-hydroxykynurenine glucoside as a novel fluorophore associated with aging of the human lens. *J. Biol. Chem.* **1999**, *274*, 20847-20854.
- (83) Takikawa, O.; Littlejohn, T. K.; Truscott, R. J. W. Indoleamine 2,3-dioxygenase in the human lens, the first enzyme in the synthesis of UV filters. *Exp. Eye Res.* **2001**, *72*, 271-277.
- (84) Moroni, F. Tryptophan metabolism and brain function: focus on kynurenine and other indole metabolites. *Eur. J. Pharmacol.* **1999**, *375*, 87-100.
- (85) Bova, L. M.; Wood, A. M.; Jamie, J. F.; Truscott, R. J. W. UV filter compounds in human lenses: The origin of 4-(2-amino-3-hydroxyphenyl)-4-oxobutanoic acid O- $\beta$ -D-glucoside. *Invest. Ophthalmol. Vis. Sci.* **1999**, *40*, 3237-3244.
- (86) Malina, H. Z.; Martin, X. D. Deamination of 3-hydroxykynurenine in bovine lenses: A possible mechanism of cataract formation in general. *Graefe's Arch. Clin. Exp. Ophthalmol.* **1995**, *233*, 38-44.
- (87) Hains, P. G.; Gao, L.; Truscott, R. J. W. The photosensitizer xanthurenic acid is not present in normal human lenses. *Exp. Eye Res.* **2003**, *77*, 547-553.
- (88) Sweeney, M. H. J.; Truscott, R. J. W. An impediment to glutathione diffusion in older normal human lenses: a possible precondition for nuclear cataract. *Exp. Eye Res.* **1998**, *67*, 587-595.
- (89) Moffat, B. A.; Landman, K. A.; Truscott, R. J. W.; Sweeney, M. H. J.; Pope, J. M. Age-related changes in the kinetics of water transport in normal human lenses. *Exp. Eye Res.* **1999**, *69*, 663-669.
- (90) Truscott, R. J. W. Age-related nuclear cataract: a lens transport problem. *Ophthalmic Res.* **2000**, *32*, 185-194.
- (91) Truscott, R. J. W. Age-related nuclear cataract - oxidation is the key. *Exp. Eye Res.* **2005**, *80*, 709-725.
- (92) Weale, R. A. The aging eye. *Sci. Basis Med. Annu. Rev.* **1971**.
- (93) Lerman, S.; Borkman, R. Spectroscopic evaluation and classification of the normal, aging, and cataractous lens. *Ophthalmic Res.* **1976**, *8*, 335-353.
- (94) Bessems, G. J. H.; Keizer, E.; Wollensak, J.; Hoenders, H. J. Non-tryptophan fluorescence of crystallins from normal and cataractous human lenses. *Invest. Ophthalmol. Vis. Sci.* **1987**, *28*, 1157-1163.
- (95) Weale, R. A. Age and the transmittance of the human crystalline lens. *J Physiol* **1988**, *395*, 577-587.
- (96) Garcia-Castineiras, S.; Dillon, J.; Spector, A. Effects of reduction on absorption and fluorescence of human lens protein. *Exp. Eye Res.* **1979**, *29*, 573-575.
- (97) Yu, N. T.; Barron, B. C.; Kuck, J. F. R. J. Distribution of two metabolically related fluorophores in human lens measured by laser microprobe. *Exp. Eye Res.* **1989**, *49*, 189-194.
- (98) Yappert, M. C.; Lal, S.; Borchman, D. Age dependence and distribution of green and blue fluorophores in human lens homogenates. *Invest. Ophthalmol. Vis. Sci.* **1992**, *33*, 3555-3560.



- (99) Bando, M.; Mikuni, I.; Obazawa, H. Calcium-induced lens protein aggregation accelerated by reactive oxygen species photosensitized in the presence of hydroxykynurenines. *Exp. Eye Res.* **1985**, *40*, 813-818.
- (100) Stutchbury, G. M.; Truscott, R. J. W. The modification of proteins by 3-hydroxykynurenine. *Exp. Eye Res.* **1993**, *57*, 149-155.
- (101) Hood, B. D.; Garner, B.; Truscott, R. J. W. Human lens coloration and aging evidence for crystallin modification by the major ultraviolet filter, 3-hydroxykynurenine *O*- $\beta$ -D-glucoside. *J. Biol. Chem.* **1999**, *274*, 32547-32550.
- (102) Dillon, J.; Skonieczna, M.; Mandal, K.; Paik, D. The photochemical attachment of the *o*-glucoside of 3-hydroxykynurenine to  $\alpha$ -crystallin: a model for lenticular aging. *Photochem. Photobiol.* **1999**, *69*, 248-253.
- (103) Vazquez, S.; Aquilina, J. A.; Jamie, J. F.; Sheil, M. M.; Truscott, R. J. W. Novel protein modification by kynurenine in human lenses. *J. Biol. Chem.* **2002**, *277*, 4867-4873.
- (104) Nagaraj, R. H.; D.R., S.; Prabhakaram, M.; Ortwerth, B. J.; Monnier, V. M. High correlation between pentosidine protein crosslinks and pigmentation implicates ascorbate oxidation in human lens senescence and cataractogenesis. *Proc. Natl. Acad. Sci. U.S.A.* **1991**, *88*, 10257-10261.
- (105) Tessier, F.; Obrenovich, M.; Monnier, V. M. Structure and mechanism of formation of human lens fluorophore LM-1 relationship to vesperlysine a and the advanced maillard reaction in aging, diabetes, and cataractogenesis. *J. Biol. Chem.* **1999**, *274*, 20796-20804.
- (106) Argirov, O. K.; Lin, B.; Ortwerth, B. J. 2-Ammonio-6-(3-oxidopyridinium-1-yl)hexanoate (OP-lysine) is a newly identified advanced glycation end product in catarctous and aged human lenses. *J. Biol. Chem.* **2004**, *279*, 6487-6495.
- (107) Cheng, R.; Feng, Q.; Argirov, O. K.; Ortwerth, B. J. Structure elucidation of a novel yellow chromophore from human lens proteins. *J. Biol. Chem.* **2004**, *279*, 45441-45449.
- (108) Heys, K. R.; Cram, S. L.; Truscott, R. J. W. Massive increase in the stiffness of the human lens nucleus with age: the basis for presbyopia? *Mol. Vis.* **2004**, *10*, 956-963.
- (109) Taylor, L. M.; Aquilina, J. A.; Jamie, J. F.; Truscott, R. J. W. UV filter instability: consequences for the human lens. *Exp. Eye Res.* **2002**, *75*, 165-175.
- (110) Aquilina, J. A.; Truscott, R. J. W. Cysteine is the initial site of modification of  $\alpha$ -crystallin by kynurenine. *Biochem. Biophys. Res. Comm.* **2000**, *276*, 216-223.
- (111) Aquilina, J. A.; Truscott, R. J. W. Kynurenine binds to the peptide binding region of the chaperone  $\alpha$ B-crystallin. *Biochem. Biophys. Res. Comm.* **2001**, *285*, 1107-1113.
- (112) Aquilina, J. A.; Truscott, R. J. W. Identifying sites of attachment of UV filters to proteins in older human lenses. *Biochim. Biophys. Acta* **2002**, *1596*, 6-15.
- (113) Hanson, S. R. A.; Smith, D. L.; Smith, J. B. Deamidation and disulfide bonding in human lens  $\gamma$ -crystallins. *Exp. Eye Res.* **1998**, *67*, 301-312.
- (114) Srivastava, O. P.; Srivastava, K. Existence of deamidated  $\alpha$ B-crystallin fragments in normal and cataractous human lenses. *Mol. Vis.* **2003**, *9*, 110-118.
- (115) Takemoto, L.; Boyle, D. Deamidation of specific glutamine residues from alpha-A crystallin during aging of the human lens. *Biochemistry* **1998**, *37*, 13681-13685.

- (116) Takemoto, L. Increased deamidation of asparagine-101 from alpha-A crystallin in the high molecular weight aggregate of the normal human lens. *Exp. Eye Res.* **1999**, *68*, 641-645.
- (117) Monnier, V. M.; Cerami, A. Nonenzymatic browning in vivo: possible process for aging of long-lived proteins. *Science* **1981**, *211*, 491-493.
- (118) Monnier, Y. M.; Cerami, A. Detection of nonenzymatic browning products in the human lens. *Biochim. Biophys. Acta* **1983**, *760*, 97-103.
- (119) Pongor, S.; Ulrich, P. C.; Bencsath, F. A.; Cerami, A. Aging of proteins: isolation and identification of a fluorescent chromophore from the reaction of polypeptides with glucose. *Proc. Natl. Acad. Sci. U.S.A.* **1984**, *81*, 2684-2688.
- (120) Garlick, R. L.; Mazer, J. S.; Chylack, L. T. J.; Tung, W. H.; Bunn, H. F. Nonenzymatic glycation of human lens crystallins. Effect of aging and diabetes mellitus. *J. Clin. Invest.* **1984**, *74*, 1742-1749.
- (121) Nagaraj, R. H.; Monnier, V. M. Isolation and characterization of a blue fluorophore from human eye lens crystallins: In vitro formation from maillard reaction with ascorbate and ribose. *Biochim. Biophys. Acta* **1992**, *1116*, 34-42.
- (122) Biemel, K. M.; Friedl, D. A.; Lederer, M. O. Identification and quantification of major maillard cross-links in human serum albumin and lens protein evidence for glucosepane as the dominant compound. *J. Biol. Chem.* **2002**, *277*, 24907-24915.
- (123) Thorpe, S. R.; Baynes, J. W. *Drugs Aging* **1996**, *9*, 69-77.
- (124) Wells-Knecht, K. J.; Zyzak, D. V.; Litchfield, L. E.; Thorpe, S. R.; Baynes, J. W. Mechanism of autoxidative glycosylation: identification of glyoxal and arabinose as intermediates in the autoxidative modification of proteins by glucose. *Biochemistry* **1995**, *34*, 3702-3709.
- (125) Wells-Knecht, K. J.; Brinkman, E.; Thorpe, S. R.; Baynes, J. W. Characterization of an imidazolium salt formed from glyoxal and *N* $\alpha$ -hippuryllysine: A model for Maillard reaction crosslinks in proteins. *J. Org. Chem.* **1995**, *60*, 6246-6247.
- (126) Brinkman, E.; Wells-Knecht, K. J.; Thorpe, S. R.; Baynes, J. W. Characterization of an imidazolium compound formed by reaction of methylglyoxal and *N* $\alpha$ -hippuryllysine. *J. Chem. Soc. Perkin Trans. 1* **1995**, *22*, 2817-2818.
- (127) Ahmed, M. U.; Thorpe, S. R.; Baynes, J. W. Identification of *N*<sup>E</sup>-carboxymethyllysine as a degradation product of fructoselysine in glycated protein. *J. Biol. Chem.* **1986**, *261*, 4889-4894.
- (128) Ahmed, M. U.; Brinkman Frye, E.; Degenhardt, T. P.; Thorpe, S. R.; Baynes, J. W. *N*<sup>E</sup>-(Carboxyethyl)lysine, a product of the chemical modification of proteins by methylglyoxal, increases with age in human lens proteins. *Biochem. J.* **1997**, *324*, 565-570.
- (129) Nakamura, K.; Nakzawa, Y.; Ienaga, K. Acid-stable fluorescent advanced glycation end products: Vesperlysines A, B, and C are formed as crosslinked products in the Maillard reaction between lysine or proteins with glucose. *Biochem. Biophys. Res. Comm.* **1997**, *232*, 227-230.
- (130) Ahmed, N.; Thornalley, P. J.; Dawczynski, J.; Franke, S.; Strobel, J.; Stein, G.; Haik, G. M. Methylglyoxal-derived hydroimidazolone advanced glycation end-products of human lens proteins. *Invest. Ophthalmol. Vis. Sci.* **2003**, *44*, 5287-5292.

- (131) Brinkman Frye, E.; Degenhardt, T. P.; Thorpe, S. R.; Baynes, J. W. Role of the Maillard reaction in aging of tissue proteins advanced glycation end product-depended increase in imidazolium cross-links in human lens proteins. *J. Biol. Chem.* **1998**, *273*, 18714-18719.
- (132) Miesbauer, L.; Zhou, S.; Yang, Z. C.; Yang, Z. Y.; Sun, Y.; Smith, D. L.; Smith, J. B. Posttranslational modifications of water soluble human lens crystallins from young adults. *J. Biol. Chem.* **1994**, *269*, 12494-12502.
- (133) Kamei, A.; Hamaguchi, T.; Matsuura, N.; Iwase, H.; Masuda, K. Post-translational modification of  $\alpha$ B-crystallin of normal human lens. *Biol. Pharm. Bull.* **2000**, *23*, 226-230.
- (134) Masters, P. M.; Bada, J. L.; Zigler, J. S. J. Aspartic acid racemisation in the human lens during ageing and in cataract formation. *Nature* **1977**, *268*, 71-73.
- (135) Masters, P. M.; Bada, J. L.; Zigler, J. S. J. Aspartic acid racemization in heavy molecular weight crystallins and water-insoluble protein from normal human lenses and cataracts. *Proc. Natl. Acad. Sci. U.S.A.* **1978**, *75*, 1204-1208.
- (136) Fujii, N.; Satoh, K.; Harada, K.; Ishibashi, Y. *J. Biol. Chem.* **1994**, *116*, 663-669.
- (137) Momose, Y.; Fujii, N.; Kodama, M. Racemization and isomerization at Asp-105 and Asp-106 in human  $\alpha$ A-crystallin. *Viva Origino* **2000**, *27*, 219-230.
- (138) Fujii, N.; Ishibashi, Y.; Satoh, K.; Fujino, M.; Harada, K. *Biochim. Biophys. Acta* **1994**, *1204*, 157-163.
- (139) Kamei, A.; Iwase, H.; Masuda, K. Cleavage of amino acid residue(s) from the N-terminal region of  $\alpha$ A- and  $\alpha$ B-crystallins in human crystalline lens during aging. *Biochem. Biophys. Res. Comm.* **1997**, *231*, 273-278.
- (140) Srivastava, O. P.; Srivastava, K. Degradation of  $\gamma$ D- and  $\gamma$ S-crystallins in human lenses. *Biochem. Biophys. Res. Comm.* **1998**, *253*, 288-294.
- (141) Ma, Z.; Hanson, S. R.; Lampi, K. J.; David, L. L.; Smith, D. L.; Smith, J. B. Age-related changes in human lens crystallins identified by HPLC and mass spectrometry. *Exp. Eye Res.* **1998**, *67*, 21-30.
- (142) Srivastava, O. P.; Srivastava, K.  $\beta$ B2-crystallin undergoes extensive truncation during aging in human lenses. *Biochem. Biophys. Res. Comm.* **2003**, *301*, 44-49.
- (143) Clark, R.; Zigman, S.; Lerman, S. Studies on the structural proteins of the human lens. *Exp. Eye Res.* **1969**, *8*, 172-182.
- (144) Coghlan, S. D.; Augusteyn, R. C. Changes in the distribution of proteins in the aging human lens. *Exp. Eye Res.* **1977**, *25*, 603-611.
- (145) McFall-Ngai, M. J.; Ding, L. L.; Takemoto, L.; Horwitz, J. Spatial and temporal mapping of the age-related changes in human lens crystallins. *Exp. Eye Res.* **1985**, *41*, 745-758.
- (146) McCarty, C. A.; Mukesh, B. N.; Fu, C.; Taylor, H. The epidemiology of cataract in Australia. *Am. J. Ophthalmol.* **1999**, *128*, 446-465.
- (147) Taylor, H. R. Eye care for the future the Weisenfeld lecture. *Invest. Ophthalmol. Vis. Sci.* **2003**, *44*, 1413-1414.
- (148) Klein, B. E.; Klein, R. Cataracts and macular degeneration in older Americans. *Arch. Ophthalmol.* **1982**, *100*, 571-573.
- (149) Clayton, R. M.; Cuthbert, J.; Seth, J.; Phillips, C. I.; Bartholomew, R. S.; Reid, J. M. Epidemiological and other studies in the assessment of factors contributing to cataractogenesis. *Ciba Found. Symp.* **1984**, *106*, 25-47.

## References

- (150) Harding, J.; van Heyningen, R. Drugs, including alcohol, that act as risk factors for cataract, and possible protection against cataract by aspirin-like analgesics and cyclopentiazide. *Br. J. Ophthalmol.* **1988**, *72*, 809-814.
- (151) Das, B. N.; Thompson, J. R.; Patel, R.; Rosenthal, A. R. The prevalence of age related cataract in the Asian community of Leicester: A community based study. *Eye* **1990**, *4*, 723-726.
- (152) Sarma, U.; Brunner, E.; Evans, J.; Wormald, R. Nutrition and the epidemiology of cataract and age-related maculopathy. *Eur. J. Clin. Nutr.* **1994**, *48*, 1-8.
- (153) Livingston, P. M.; Carson, C. A.; Taylor, H. The epidemiology of cataract: A review of the literature. *Ophthalmic Epidemiol.* **1995**, *2*, 151-164.
- (154) Johnson, G. J. Limitations of epidemiology in understanding pathogenesis of cataracts. *Lancet* **1998**, *351*, 925-926.
- (155) Verges, C.; Llevat, E. Laser cataract surgery: technique and clinical results. *J. Cataract Refract. Surg* **2003**, *29*, 1339-1345.
- (156) Duran, S.; Zato, M. Erbium:YAG laser emulsification of the cataractous lens. *J. Cataract Refract. Surg* **2001**, *27*, 1025-1032.
- (157) Dilley, K. J.; Pirie, A. Changes to the proteins of the human lens nucleus in cataract. *Exp. Eye Res.* **1974**, *19*, 59-72.
- (158) Truscott, R. J. W.; Augusteyn, R. C. Changes in human lens proteins during nuclear cataract formation. *Exp. Eye Res.* **1977**, *24*, 159-170.
- (159) Truscott, R. J. W.; Augusteyn, R. C. Oxidative changes in human lens proteins during senile nuclear cataract formation. *Biochim. Biophys. Acta* **1977**, *492*, 43-52.
- (160) Spector, A. Oxidation and cataract. *Ciba Found. Symp.* **1984**, *106*, 48-64.
- (161) Pirie, A. Color and solubility of the proteins of human cataracts. *Invest. Ophthalmol.* **1968**, *7*, 634-650.
- (162) Maraini, G.; Mangili, R. *The human lens in relation to cataract*; Elsevier: Amsterdam, 1973.
- (163) Truscott, R. J. W.; Augusteyn, R. C. The state of sulphydryl groups in normal and cataractous human lenses. *Exp. Eye Res.* **1977**, *25*, 139-148.
- (164) Marcantonio, J. M.; Duncan, G.; Davies, P. D.; Bushell, A. R. Classification of human senile cataracts by nuclear colour and sodium content. *Exp. Eye Res.* **1980**, *31*, 227-237.
- (165) Fu, S.; Dean, R.; Southan, M.; Truscott, R. J. W. The hydroxyl radical in lens nuclear cataractogenesis. *J. Biol. Chem.* **1998**, *273*, 28603-28609.
- (166) Buckingham, R. H. The behaviour of reduced proteins from normal and catarctous lenses in highly dissociating media: cross-linked protein in catarctous lenses. *Exp. Eye Res.* **1972**, *14*, 123-129.
- (167) Harding, J. J. Disulphide cross-linked protein of high molecular weight in human cataractous lenses. *Exp. Eye Res.* **1973**, *17*, 377-383.
- (168) Fujimoto, D. Aging of human connective tissue: increase in the content of a cross-linking amino acid histidinoalanine. *Biochem. Int.* **1982**, *5*, 743-746.
- (169) Kanayama, T.; Miyanaga, Y.; Horiuchi, K.; Fujimoto, D. Detection of the cross-linking amino acid, histidinoalanine, in human brown cataractous lens protein. *Exp. Eye Res.* **1987**, *44*, 165-169.
- (170) Fujimoto, D. Formation of histidinoalanine cross-links in heated proteins. *Experientia* **1984**, *40*, 832-833.

## References

- (171) Fujimoto, D. Aging and cross-links in human aorta. *Biochem. Biophys. Res. Comm.* **1982**, *109*, 1264-1269.
- (172) Bessems, G. J. H.; Rennen, H. J. J. M.; Hoenders, H. J. Lanthionine, a protein cross-link in cataractous human lenses. *Exp. Eye Res.* **1987**, *44*, 691-695.
- (173) Snow, J. T.; Finley, J. W.; Friedman, M. Relative reactivities of sulfhydryl groups with N-acetyl dehydroalanine and N-acetyl dehydroalanine methyl ester. *Int. J. Pept. Protein Res.* **1976**, *7*, 460-466.
- (174) Reynolds, G. P.; Pearson, S. J. Increased brain 3-hydroxykynurenine in Huntington's disease. *Lancet* **1989**, *2*, 979-980.
- (175) Pearson, S. J.; Reynolds, G. P. Increased brain concentrations of a neurotoxin, 3-hydroxykynurenine, in Huntington's disease. *Neurosci. Lett.* **1992**, *144*, 199-201.
- (176) Ogawa, T.; Matson, W. R.; Beal, M. F.; Myers, R. H.; Bird, E. D.; Milbury, P.; Saso, S. Kynurenine pathway abnormalities in Parkinson's disease. *Neurology* **1992**, *42*, 1702-1706.
- (177) Okuda, S.; Nishiyama, N.; Saito, H.; Katsuki, H. Hydrogen peroxide-mediated neuronal cell death induced by an endogenous neurotoxin, 3-hydroxykynurenine. *Proc. Natl. Acad. Sci. U.S.A.* **1996**, *93*, 12553-12558.
- (178) Chiarugi, A.; Meli, E.; Moroni, F. Similarities and differences in the neuronal death processes activated by 3OH-kynurenine and quinolinic acid. *J. Neurochem.* **2001**, *77*, 1310-1318.
- (179) Goldstein, L. E.; Leopold, M. C.; Huang, X.; Atwood, C. S.; Saunders, A. J.; Hartshorn, M.; Lim, J. T.; Faget, K. Y.; Muffat, J. A.; Scarpa, R. C.; Chylack, L. T. J.; Bowden, E. F.; Tanzi, R. E.; Bush, A. I. 3-Hydroxykynurenine and 3-hydroxyanthranilic acid generate hydrogen peroxide and promote  $\alpha$ -crystallin cross-linking by metal ion reduction. *Biochemistry* **2000**, *39*, 7266-7275.
- (180) van Reyk, D. M.; Brown, A. J.; Jessup, W.; Dean, R. T. Batch-to batch variation of Chelix-100 confounds metal-catalyzed oxidation. Leaching of inhibitory compounds from a batch of Chelix-100 and their removal by a pre-washing procedure. *Free Rad. Res.* **1995**, *23*, 533-535.
- (181) Vazquez, S.; Garner, B.; Sheil, M. M.; Truscott, R. J. W. Characterisation of the major autoxidation products of 3-hydroxykynurenine under physiological conditions. *Free Rad. Res.* **2000**, *32*, 11-23.
- (182) Atherton, S. J.; Dillon, J.; Gaillard, E. R. A pulse radiolysis study of the reactions of 3-hydroxykynurenine and kynurenine with oxidizing and reducing radicals. *Biochim. Biophys. Acta* **1993**, *1158*, 75-82.
- (183) Becker, E. Z. *Vererbungslehre* **1942**, *80*, 157.
- (184) Butenandt, A.; Schafer, W. *Ommochromes*. In *Chemistry of natural and synthetic colouring matter*; Academic Press: New York, 1962; (pp. 13-33).
- (185) Aquilina, J. A.; Carver, J. A.; Truscott, R. J. W. Oxidation products of 3-hydroxykynurenine bind to lens proteins: relevance for nuclear cataract. *Exp. Eye Res.* **1997**, *64*, 727-735.
- (186) Aquilina, J. A.; Carver, J. A.; Truscott, R. J. W. Elucidation of a novel polypeptide cross-link involving 3-hydroxykynurenine. *Biochemistry* **1999**, *38*, 11455-11464.
- (187) Garner, B.; Shaw, D. C.; Lindner, R. A.; Carver, J. A.; Truscott, R. J. W. Non-oxidative modification of lens crystallins by kynurenine: a novel post-translational protein modification with possible relevance to ageing and cataract. *Biochimica et Biophysica Acta* **2000**, *1476*, 265-278.

## References

- (188) Butenandt, A.; Schiedt, U.; Bickert, E. Uber ommochrome. III. Mitteilung: synthese des xanthommatins. *Liebigs Ann.* **1954**, *588*, 106-116.
- (189) Tomoda, A.; Yoneyama, Y.; Yamaguchi, T.; Shirao, E.; Kawasaki, K. Mechanism of coloration of human lenses induced by near-ultraviolet-photo-oxidized 3-hydroxykynurenine. *Ophthalmic Res.* **1990**, *22*, 152-159.
- (190) Ellozy, A. R.; Wang, R. H.; Dillon, J. Photolysis of intact young human, baboon and rhesus monkey lenses. *Photochem. Photobiol.* **1994**, *59*, 474-478.
- (191) Tokuyama, T.; Senoh, S.; Sakan, T.; Brown, K. S. J.; Witkop, B. The photoreduction of kynurenine acid to kynurenine yellow and the occurrence of 3-hydroxy-L-kynurenine in butterflies. *J. Am. Chem. Soc.* **1967**, *89*, 1017-1021.
- (192) Vazquez, S. Human lens protein modification: the role of kynurenine and 3-hydroxykynurenine. In *Chemistry*; University of Wollongong: Wollongong, 2001.
- (193) Staniszewska, M. M.; Nagaraj, R. H. 3-Hydroxykynurenine-mediated modification of human lens proteins structure determination of a major modification using a monoclonal antibody. *J. Biol. Chem.* **2005**, *280*, 22154-22164.
- (194) Parker, N. R. The role of kynurenine and UV light in lens protein modification. In *Chemistry*; University of Wollongong: Wollongong, 2005.
- (195) Vazquez, S.; Parker, N. R.; Sheil, M. M.; Truscott, R. J. W. Protein-bound kynurenine decreases with the progression of age-related nuclear cataract. *Invest. Ophthalmol. Vis. Sci.* **2004**, *45*, 879-883.
- (196) Taylor, L. M.; Aquilina, J. A.; Jamie, J. F.; Truscott, R. J. W. Glutathione and NADH, but not ascorbate, protect the lens proteins from modification by UV filters. *Exp. Eye Res.* **2002**, *74*, 503-511.
- (197) Taylor, L. M. Human lens UV filters. In *Chemistry*; University of Wollongong: Wollongong, 2002.
- (198) Berry, Y.; Truscott, R. J. W. The presence of a human UV filter within the lens represents an oxidative stress. *Exp. Eye Res.* **2001**, *72*, 411-421.
- (199) Takemoto, L.; Horwitz, J.; Emmons, T. Oxidation of the N-terminal methionine of lens  $\alpha$ A-crystallin. *Curr. Eye Res.* **1992**, *11*, 651-655.
- (200) Lund, A. L.; Smith, J. B.; Smith, D. L. Modifications of the water-insoluble human lens a-crystallins. *Exp. Eye Res.* **1996**, *63*, 661-672.
- (201) Hanson, S. R.; Hasan, A.; Smith, D. L.; Smith, J. B. The major in vivo modifications of the human water-insoluble lens crystallins are disulfide bonds, deamidation, methionine oxidation and backbone cleavage. *Exp. Eye Res.* **2000**, *71*, 195-207.
- (202) Schey, K. L.; Finley, E. L. Identification of peptide oxidation by tandem mass spectrometry. *Acc. Chem. Res.* **2000**, *33*, 299-306.
- (203) Searle, B. C.; Dasari, S.; Turner, M.; Reddy, A. P.; Choi, D.; Wilmarth, P. A.; McCormack, A. L.; David, L. L.; Nagalla, S. R. High-throughput identification of proteins and unanticipated sequence modifications using a mass-based alignment algorithm for MS/MS de novo sequencing results. *Anal. Chem.* **2004**, *76*, 2220-2230.
- (204) Srivastava, O. P.; Kirk, M. C.; Srivastava, K. Characterization of covalent multimers of crystallins in aging human lenses. *J. Biol. Chem.* **2004**, *279*, 10901-10909.
- (205) Stryer, L. *Biochemistry 4th Ed.*; W.H. Freeman and Company: New York, 1995.

- (206) Clayden; Greeves; Warren *Wothers Organo-main-group chemistry 1: Sulfur. Organic chemistry*; Oxford University Press: New York, 2001; 1247-1269.
- (207) Doorn, J. A.; Petersen, D. R. Covalent adduction of nucleophilic amino acids by 4-hydroxynonenal and 4-oxononenal. *Chem-Biol. Interact* **2003**, *143-144*, 93-100.
- (208) Burcham, P. C.; Fontaine, F. R.; Petersen, D. R.; Pyke, S. M. Reactivity with tris(hydroxymethyl)aminomethane confounds immunodetection of acrolein-adducted proteins. *Chem. Res. Toxicol.* **2003**, *16*, 1196-1201.
- (209) Ege, S. *Organic chemistry structure and reactivity*; D.C. Heath and Company: Lexington, 1994.
- (210) Sala, A.; Campagnoli, M.; Perani, E.; Romano, A.; Labo, S.; Monzani, E.; Minchiotti, L.; Galliano, M. Human  $\alpha$ -1-microglobulin is covalently bound to kynurenine-derived chromophores. *J. Biol. Chem.* **2004**, *279*, 51033-51041.
- (211) Streete, I. M.; Jamie, J. F.; Truscott, R. J. W. Lenticular levels of amino acids and free UV filters differ significantly between normals and cataract patients. *Invest. Ophthalmol. Vis. Sci.* **2004**, *45*, 4091-4098.
- (212) Linetsky, M.; Hill, J. M. W.; LeGrand, R. D.; Hu, F. Dehydroalanine crosslinks in human lens. *Exp. Eye Res.* **2004**, *79*, 499-512.
- (213) Andley, U. P.; Clark, B. A. Accessibilities of the sulfhydryl groups of native and photooxidized lens crystallins: A fluorescence lifetime and quenching study. *Biochemistry* **1988**, *27*, 810-820.
- (214) Spector, A.; Zhou, W.; Ma, W.; Chignell, C. F.; Reszka, K. J. Investigation of the mechanism of action of microperoxidase-11, (MP11), a potential anti-cataract agent, with hydrogen peroxide and ascorbate. *Exp. Eye Res.* **2000**, *71*, 183-194.
- (215) Garner, M. H.; Spector, A. Selective oxidation of cysteine and methionine in normal and cataractous lenses. *Proc. Natl. Acad. Sci. U.S.A.* **1980**, *77*, 1274-1277.
- (216) Baynes, J. W. The role of AGEs in aging: Causation or correlation. *Exp. Gerontol.* **2001**, *36*, 1527-1537.
- (217) Marchetti, M. A.; Pizarro, G. O.; Sagher, D.; Deamicis, C.; Brot, N.; Hejtmancik, J. F.; Weissbach, H.; Kantorow, M. Methionine sulfoxide reductases B1, B2, and B3 are present in human lens and confer oxidative stress resistance to lens cells. *Invest. Ophthalmol. Vis. Sci.* **2005**, *46*, 2107-2112.
- (218) Brot, N.; Weissbach, H. Peptide methionine sulfoxide reductase: Biochemistry and physiological role. *Biopolymers* **2000**, *55*, 288-296.
- (219) Cherian, M.; Abraham, E. C. Decreased molecular chaperone property of  $\alpha$ -crystallin due to posttranslational modifications. *Biochem. Biophys. Res. Comm.* **1995**, *208*, 675-679.
- (220) Mulders, J. W.; Stokkermans, J.; Leunissen, J. A.; Benedetti, E. L.; Bloemendal, H.; de Jong, W. W. Interaction of  $\alpha$ -crystallin with lens plasma membranes. Affinity for MP26. *Eur. J. Biochem.* **1985**, *152*, 721-728.
- (221) Cobb, B. A.; Petrash, J. M. Characterization of  $\alpha$ -crystallin-plasma membrane binding. *J. Biol. Chem.* **2000**, *275*, 6664-6672.
- (222) Boyle, D.; Takemoto, L. EM immunolocalization of  $\alpha$ -crystallins: Association with the plasma membrane from normal and cataractous human lenses. *Curr. Eye Res.* **1996**, *15*, 577-582.

## References

- (223) Aquilina, J. A.; Carver, J. A.; Truscott, R. J. W. Polypeptide modification and cross-linking by oxidized 3-hydroxykynurenine. *Biochemistry* **2000**, *39*, 16176-16184.
- (224) Shirao, E.; Ando, K.; Inoue, A.; Shirao, Y.; Balasubramanian, D. Identification of a novel fluorophore, xanthurenic acid 8-*O*- $\beta$ -D-glucoside in human brunescent cataract. *Exp. Eye Res.* **2001**, *73*, 421-431.
- (225) Pavia, D. L.; Lampman, G. M.; Kriz, G. S. *Introduction to spectroscopy a guide for students of organic chemistry*; Harcourt Brace College Publishers: Philadelphia, 1996.
- (226) Reddy, V. N.; Giblin, F. J. Metabolism and function of glutathione in the lens. *Ciba Found. Symp.* **1984**, *106*, 65-87.
- (227) Giblin, F. J. Glutathione: a vital lens antioxidant. *J. Ocular Pharmacol. Ther.* **2000**, *16*, 121-135.



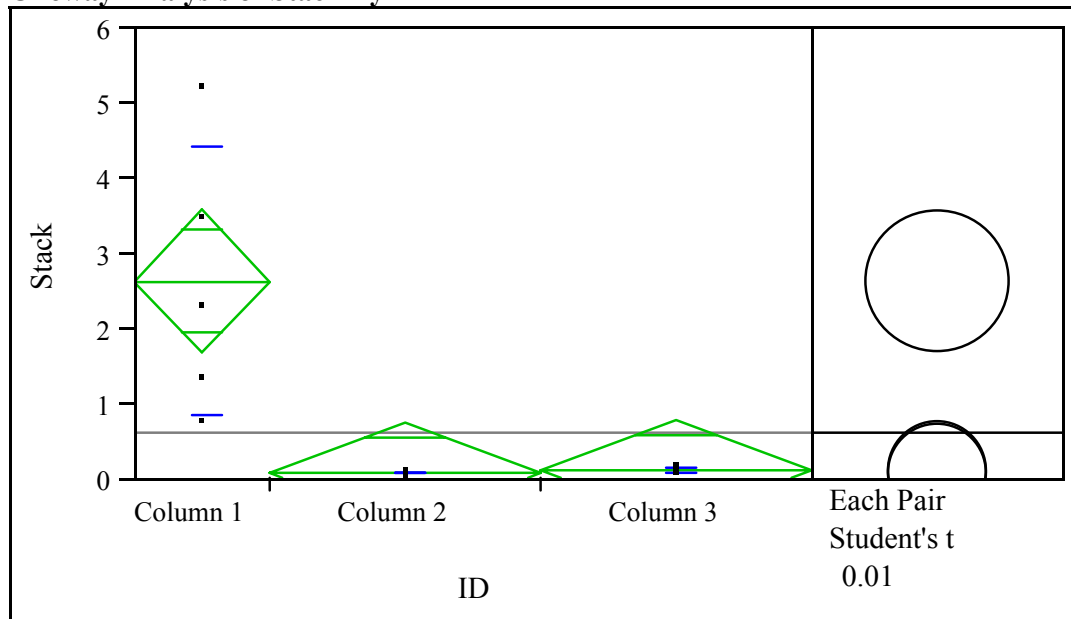
## **Appendix 1**

Statistical analysis was performed using JMP 5.1 software. An ANOVA one-way analysis was done to determine statistical significance between the sample data (*i.e.* comparisons between the normal lenses and each of the cataract lenses). P values less than 0.01 were considered significant. In addition, Wilcoxon/Kruskal-Wallis Tests, Tests that the Variances are Equal and, a Means Comparison for each pair using a Student's t –test (also called least significant difference) was done to further confirm whether the samples were statistically significant. Attached are the printouts of each statistical analysis. Levels in lenses aged 50 years and over were statistically analysed.

Column 1 – Normal lens data

Column 2 – Dark cataract lens data

Column 3 – Light cataract lens data

**3OHKyn free in lens nucleus****Oneway Analysis of Stack By ID****Oneway Anova  
Summary of Fit**

Rsquare 0.669899  
 Adj Rsquare 0.63989  
 Root Mean Square Error 0.757926  
 Mean of Response 0.590476  
 Observations (or Sum Wgts) 25  
 Analysis of Variance

| Source   | DF | Sum of Squares | Mean Square | F Ratio | Prob > F |
|----------|----|----------------|-------------|---------|----------|
| ID       | 2  | 25.647161      | 12.8236     | 22.3231 | <.0001   |
| Error    | 22 | 12.637948      | 0.5745      |         |          |
| C. Total | 24 | 38.285109      |             |         |          |

**Means for Oneway Anova**

| Level    | Number | Mean    | Std Error | Lower 99% | Upper 99% |
|----------|--------|---------|-----------|-----------|-----------|
| Column 1 | 5      | 2.61600 | 0.33895   | 1.661     | 3.5714    |
| Column 2 | 10     | 0.06830 | 0.23968   | -0.607    | 0.7439    |
| Column 3 | 10     | 0.09989 | 0.23968   | -0.576    | 0.7755    |

Std Error uses a pooled estimate of error variance

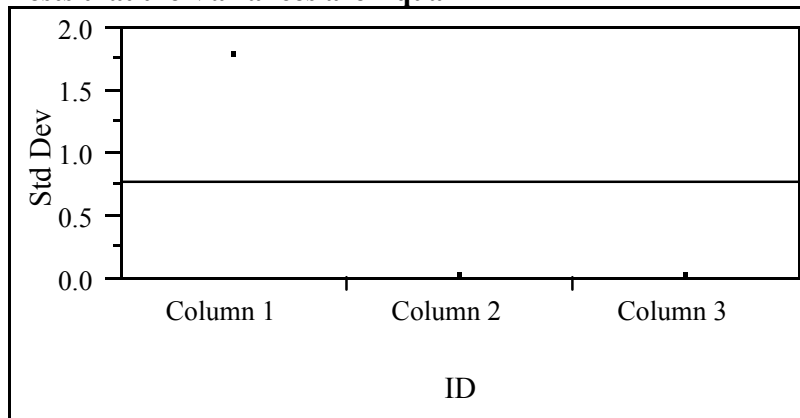
**Wilcoxon / Kruskal-Wallis Tests (Rank Sums)**

| Level    | Count | Score Sum | Score Mean | (Mean-Mean0)/Std0 |
|----------|-------|-----------|------------|-------------------|
| Column 1 | 5     | 115       | 23.0000    | 3.363             |
| Column 2 | 10    | 62        | 6.2000     | -3.744            |
| Column 3 | 10    | 148       | 14.8000    | 0.971             |

**1-way Test, ChiSquare Approximation**

| ChiSquare | DF | Prob>ChiSq |
|-----------|----|------------|
|-----------|----|------------|

**ChiSquare**      **DF**      **Prob>ChiSq**  
 18.3655          2          0.0001

**Tests that the Variances are Equal**

| Level    | Count | Std Dev  | MeanAbsDif to Mean | MeanAbsDif to Median |
|----------|-------|----------|--------------------|----------------------|
| Column 1 | 5     | 1.777000 | 1.379200           | 1.508000             |
| Column 2 | 10    | 0.014538 | 0.011240           | 0.010500             |
| Column 3 | 10    | 0.023865 | 0.017266           | 0.016110             |

| Test           | F Ratio | DFNum | DFDen | Prob > F |
|----------------|---------|-------|-------|----------|
| O'Brien(.5)    | 7.2549  | 2     | 22    | 0.0038   |
| Brown-Forsythe | 36.6073 | 2     | 22    | <.0001   |
| Levene         | 26.2518 | 2     | 22    | <.0001   |
| Bartlett       | 59.0963 | 2     | .     | <.0001   |

Warning: Small sample sizes. Use Caution.

Welch Anova testing Means Equal, allowing Std Devs Not Equal

**F Ratio**      **DFNum**      **DFDen**      **Prob > F**  
 10.6494          2          8.406          0.0050

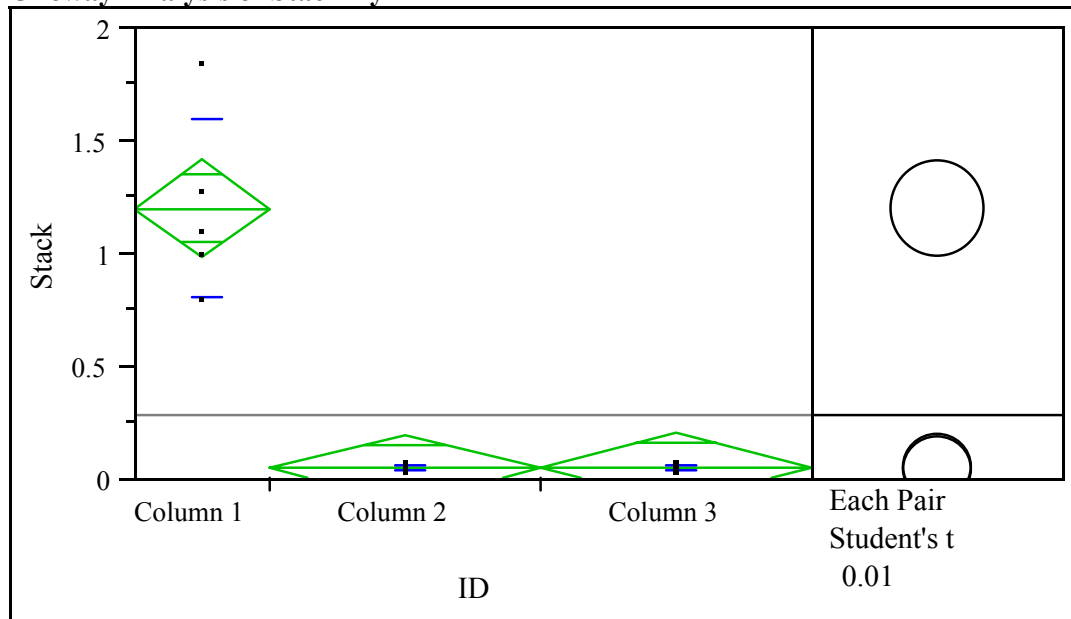
**Means Comparisons****Comparisons for each pair using Student's t**

|              | <b>t</b>        | <b>Alpha</b>    |                 |
|--------------|-----------------|-----------------|-----------------|
|              | 2.81876         | 0.01            |                 |
| Abs(Dif)-LSD |                 |                 |                 |
|              | <b>Column 1</b> | <b>Column 3</b> | <b>Column 2</b> |
| Column 1     | -1.3512         | 1.3460          | 1.3775          |
| Column 3     | 1.3460          | -0.9554         | -0.9238         |
| Column 2     | 1.3775          | -0.9238         | -0.9554         |

| Level         | Mean      |
|---------------|-----------|
| Column 1    A | 2.6160000 |
| Column 3    B | 0.0998900 |
| Column 2    B | 0.0683000 |

Levels not connected by same letter are significantly different

| Level    | - Level  | Difference | Lower CL | Upper CL | p-Value   |
|----------|----------|------------|----------|----------|-----------|
| Column 1 | Column 2 | 2.547700   | 1.37754  | 3.717859 | 0.0000035 |
| Column 1 | Column 3 | 2.516110   | 1.34595  | 3.686269 | 0.0000042 |
| Column 3 | Column 2 | 0.031590   | -0.92384 | 0.987021 | 0.9265896 |

3OHKyn free in lens cortex**Oneway Analysis of Stack By ID****Oneway Anova  
Summary of Fit**

Rsquare 0.893527  
 Adj Rsquare 0.883847  
 Root Mean Square Error 0.169201  
 Mean of Response 0.274388  
 Observations (or Sum Wgts) 25

**Analysis of Variance**

| Source   | DF | Sum of Squares | Mean Square | F Ratio | Prob > F |
|----------|----|----------------|-------------|---------|----------|
| ID       | 2  | 5.2855790      | 2.64279     | 92.3121 | <.0001   |
| Error    | 22 | 0.6298347      | 0.02863     |         |          |
| C. Total | 24 | 5.9154137      |             |         |          |

**Means for Oneway Anova**

| Level    | Number | Mean    | Std Error | Lower 99% | Upper 99% |
|----------|--------|---------|-----------|-----------|-----------|
| Column 1 | 5      | 1.19400 | 0.07567   | 0.981     | 1.4073    |
| Column 2 | 10     | 0.04307 | 0.05351   | -0.108    | 0.1939    |
| Column 3 | 10     | 0.04590 | 0.05351   | -0.105    | 0.1967    |

Std Error uses a pooled estimate of error variance

**Wilcoxon / Kruskal-Wallis Tests (Rank Sums)**

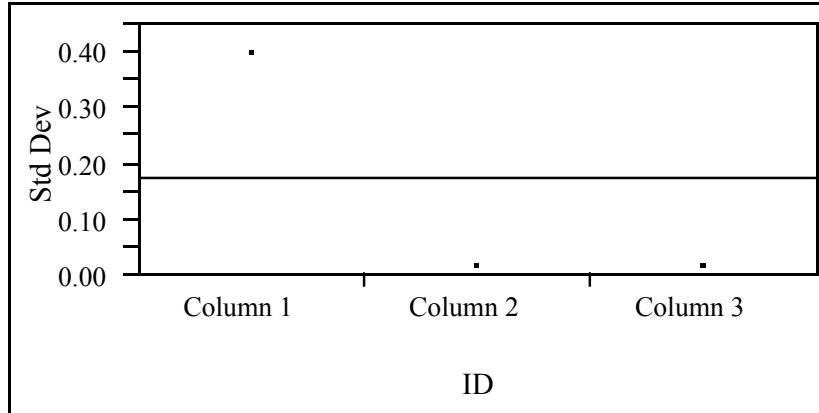
| Level    | Count | Score Sum | Score Mean | (Mean-Mean0)/Std0 |
|----------|-------|-----------|------------|-------------------|
| Column 1 | 5     | 115       | 23.0000    | 3.364             |
| Column 2 | 10    | 101       | 10.1000    | -1.582            |
| Column 3 | 10    | 109       | 10.9000    | -1.138            |

**1-way Test, ChiSquare Approximation**

| ChiSquare | DF | Prob>ChiSq |
|-----------|----|------------|
| 11.6065   | 2  | 0.0030     |

## Appendix 1

Tests that the Variances are Equal



| Level          | Count | Std Dev   | MeanAbsDif to Mean | MeanAbsDif to Median |          |
|----------------|-------|-----------|--------------------|----------------------|----------|
| Column 1       | 5     | 0.3955755 | 0.2848000          | 0.2840000            |          |
| Column 2       | 10    | 0.0149140 | 0.0120560          | 0.0117300            |          |
| Column 3       | 10    | 0.0145789 | 0.0113000          | 0.0113000            |          |
| Test           |       | F Ratio   | DFNum              | DFDen                | Prob > F |
| O'Brien(.5)    |       | 4.4398    | 2                  | 22                   | 0.0240   |
| Brown-Forsythe |       | 11.3411   | 2                  | 22                   | 0.0004   |
| Levene         |       | 14.8149   | 2                  | 22                   | <.0001   |
| Bartlett       |       | 37.8345   | 2                  | .                    | <.0001   |

Warning: Small sample sizes. Use Caution.

Welch Anova testing Means Equal, allowing Std Devs Not Equal

| F Ratio | DFNum | DFDen  | Prob > F |
|---------|-------|--------|----------|
| 19.6910 | 2     | 8.7303 | 0.0006   |

## Means Comparisons

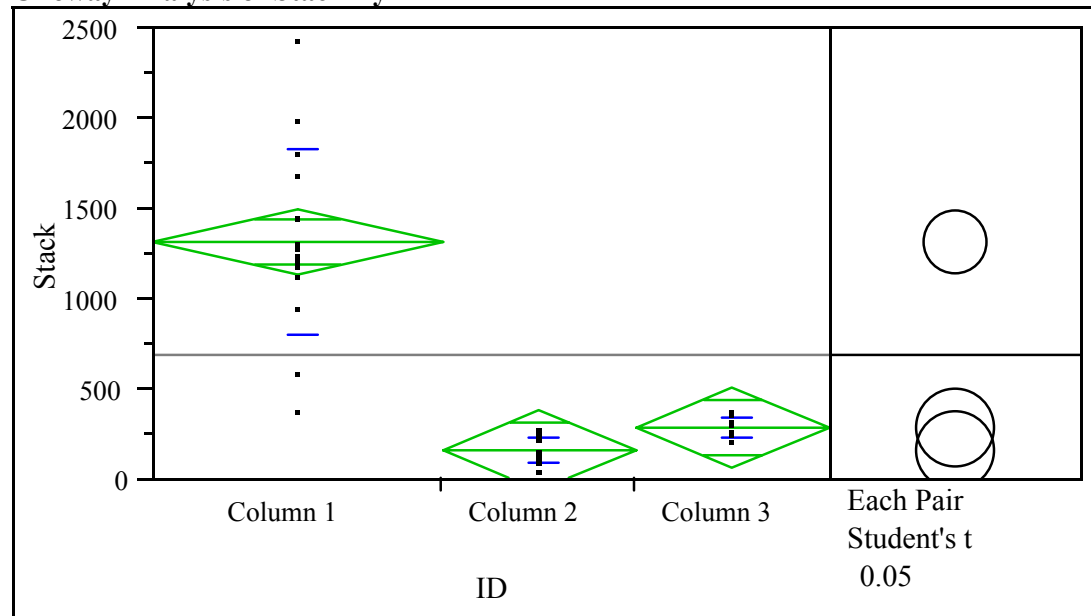
Comparisons for each pair using Student's t

| t            | Alpha    |          |          |
|--------------|----------|----------|----------|
| 2.81876      | 0.01     |          |          |
| Abs(Dif)-LSD | Column 1 | Column 3 | Column 2 |
| Column 1     | -0.30164 | 0.88687  | 0.88970  |
| Column 3     | 0.88687  | -0.21329 | -0.21046 |
| Column 2     | 0.88970  | -0.21046 | -0.21329 |

| Level      | Mean      |
|------------|-----------|
| Column 1 A | 1.1940000 |
| Column 3 B | 0.0459000 |
| Column 2 B | 0.0430700 |

Levels not connected by same letter are significantly different

| Level    | - Level  | Difference | Lower CL  | Upper CL | p-Value   |
|----------|----------|------------|-----------|----------|-----------|
| Column 1 | Column 2 | 1.150930   | 0.889702  | 1.412158 | 2.1e-11   |
| Column 1 | Column 3 | 1.148100   | 0.886872  | 1.409328 | 2.2e-11   |
| Column 3 | Column 2 | 0.002830   | -0.210462 | 0.216122 | 0.9705035 |

**3OHKynG bound to nucleus proteins****Oneway Analysis of Stack By ID****Oneway Anova  
Summary of Fit**

Rsquare 0.731479  
 Adj Rsquare 0.714696  
 Root Mean Square Error 343.7734  
 Mean of Response 683.1005  
 Observations (or Sum Wgts) 35  
 Analysis of Variance

| Source   | DF | Sum of Squares | Mean Square | F Ratio | Prob > F |
|----------|----|----------------|-------------|---------|----------|
| ID       | 2  | 10301898       | 5150949     | 43.5856 | <.0001   |
| Error    | 32 | 3781766        | 118180      |         |          |
| C. Total | 34 | 14083664       |             |         |          |

**Means for Oneway Anova**

| Level    | Number | Mean    | Std Error | Lower 95% | Upper 95% |
|----------|--------|---------|-----------|-----------|-----------|
| Column 1 | 15     | 1307.22 | 88.76     | 1126      | 1488.0    |
| Column 2 | 10     | 153.00  | 108.71    | -68       | 374.4     |
| Column 3 | 10     | 277.02  | 108.71    | 56        | 498.5     |

Std Error uses a pooled estimate of error variance

**Wilcoxon / Kruskal-Wallis Tests (Rank Sums)**

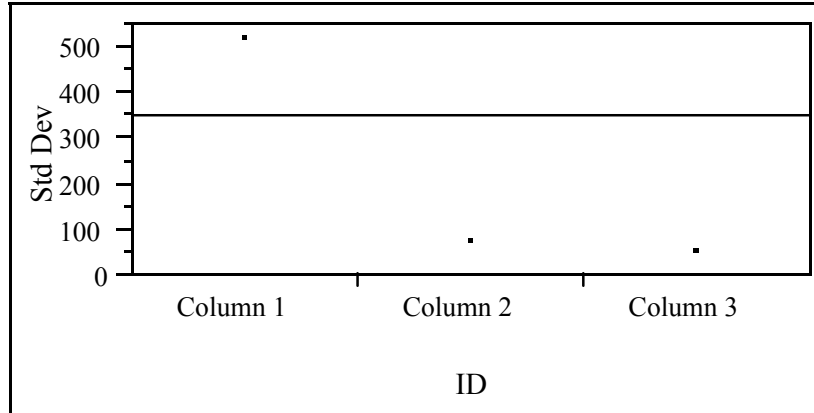
| Level    | Count | Score Sum | Score Mean | (Mean-Mean0)/Std0 |
|----------|-------|-----------|------------|-------------------|
| Column 1 | 15    | 420       | 28.0000    | 4.983             |
| Column 2 | 10    | 63        | 6.3000     | -4.254            |
| Column 3 | 10    | 147       | 14.7000    | -1.187            |

**1-way Test, ChiSquare Approximation**

| ChiSquare | DF | Prob>ChiSq |
|-----------|----|------------|
| 28.3600   | 2  | <.0001     |

## Appendix 1

Tests that the Variances are Equal



| Level    | Count | Std Dev  | MeanAbsDif to Mean | MeanAbsDif to Median |
|----------|-------|----------|--------------------|----------------------|
| Column 1 | 15    | 514.8460 | 364.5582           | 352.1253             |
| Column 2 | 10    | 73.5205  | 60.3872            | 58.7870              |
| Column 3 | 10    | 49.6524  | 41.5788            | 41.5788              |

| Test           | F Ratio | DFNum | DFDen | Prob > F |
|----------------|---------|-------|-------|----------|
| O'Brien(.5)    | 3.8255  | 2     | 32    | 0.0324   |
| Brown-Forsythe | 6.3736  | 2     | 32    | 0.0047   |
| Levene         | 7.7911  | 2     | 32    | 0.0018   |
| Bartlett       | 24.5674 | 2     | .     | <.0001   |

Welch Anova testing Means Equal, allowing Std Devs Not Equal

| F Ratio | DFNum | DFDen  | Prob > F |
|---------|-------|--------|----------|
| 40.4435 | 2     | 19.856 | <.0001   |

### Means Comparisons

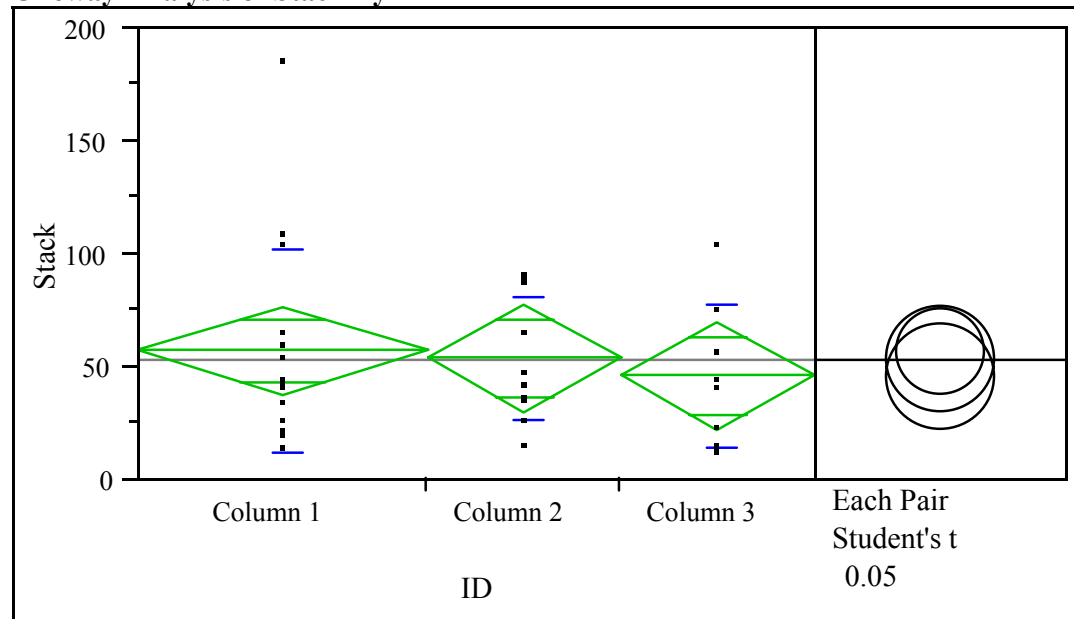
Comparisons for each pair using Student's t

| t            | Alpha    |          |          |
|--------------|----------|----------|----------|
| 2.03693      | 0.05     |          |          |
| Abs(Dif)-LSD | Column 1 | Column 3 | Column 2 |
| Column 1     | -255.69  | 744.32   | 868.34   |
| Column 3     | 744.32   | -313.16  | -189.14  |
| Column 2     | 868.34   | -189.14  | -313.16  |

| Level      | Mean      |
|------------|-----------|
| Column 1 A | 1307.2187 |
| Column 3 B | 277.0228  |
| Column 2 B | 153.0010  |

Levels not connected by same letter are significantly different

| Level    | - Level  | Difference | Lower CL | Upper CL | p-Value   |
|----------|----------|------------|----------|----------|-----------|
| Column 1 | Column 2 | 1154.218   | 868.344  | 1440.091 | 2.15e-9   |
| Column 1 | Column 3 | 1030.196   | 744.323  | 1316.069 | 2.4e-8    |
| Column 3 | Column 2 | 124.022    | -189.137 | 437.180  | 0.4257960 |

**3OHKynG bound to cortex proteins****Oneway Analysis of Stack By ID****Oneway Anova  
Summary of Fit**

|                            |          |
|----------------------------|----------|
| Rsquare                    | 0.01653  |
| Adj Rsquare                | -0.04494 |
| Root Mean Square Error     | 37.1686  |
| Mean of Response           | 52.07629 |
| Observations (or Sum Wgts) | 35       |

**Analysis of Variance**

| Source   | DF | Sum of Squares | Mean Square | F Ratio | Prob > F |
|----------|----|----------------|-------------|---------|----------|
| ID       | 2  | 743.055        | 371.53      | 0.2689  | 0.7659   |
| Error    | 32 | 44208.144      | 1381.50     |         |          |
| C. Total | 34 | 44951.198      |             |         |          |

**Means for Oneway Anova**

| Level    | Number | Mean    | Std Error | Lower 95% | Upper 95% |
|----------|--------|---------|-----------|-----------|-----------|
| Column 1 | 15     | 56.2060 | 9.597     | 36.658    | 75.754    |
| Column 2 | 10     | 52.8220 | 11.754    | 28.880    | 76.764    |
| Column 3 | 10     | 45.1360 | 11.754    | 21.194    | 69.078    |

Std Error uses a pooled estimate of error variance

**Wilcoxon / Kruskal-Wallis Tests (Rank Sums)**

| Level    | Count | Score Sum | Score Mean | (Mean-Mean0)/Std0 |
|----------|-------|-----------|------------|-------------------|
| Column 1 | 15    | 274.5     | 18.3000    | 0.133             |
| Column 2 | 10    | 195       | 19.5000    | 0.530             |
| Column 3 | 10    | 160.5     | 16.0500    | -0.694            |

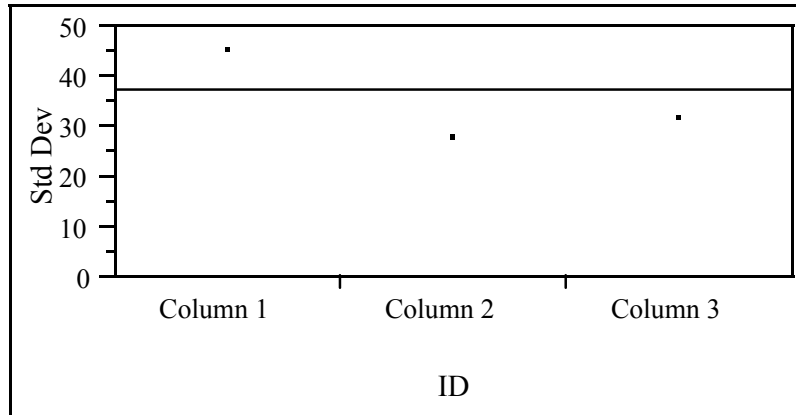
**1-way Test, ChiSquare Approximation**

| ChiSquare | DF | Prob>ChiSq |
|-----------|----|------------|
| 0.5894    | 2  | 0.7448     |



## Appendix 1

Tests that the Variances are Equal



| Level    | Count | Std Dev  | MeanAbsDif to Mean | MeanAbsDif to Median |
|----------|-------|----------|--------------------|----------------------|
| Column 1 | 15    | 45.02404 | 31.69320           | 28.71653             |
| Column 2 | 10    | 27.70627 | 23.62840           | 22.46400             |
| Column 3 | 10    | 31.48034 | 25.46320           | 25.06000             |

| Test           | F Ratio | DFNum | DFDen | Prob > F |
|----------------|---------|-------|-------|----------|
| O'Brien(.5)    | 0.6058  | 2     | 32    | 0.5518   |
| Brown-Forsythe | 0.1598  | 2     | 32    | 0.8530   |
| Levene         | 0.4261  | 2     | 32    | 0.6567   |
| Bartlett       | 1.3939  | 2     | .     | 0.2481   |

Welch Anova testing Means Equal, allowing Std Devs Not Equal

| F Ratio | DFNum | DFDen  | Prob > F |
|---------|-------|--------|----------|
| 0.2861  | 2     | 20.953 | 0.7541   |

### Means Comparisons

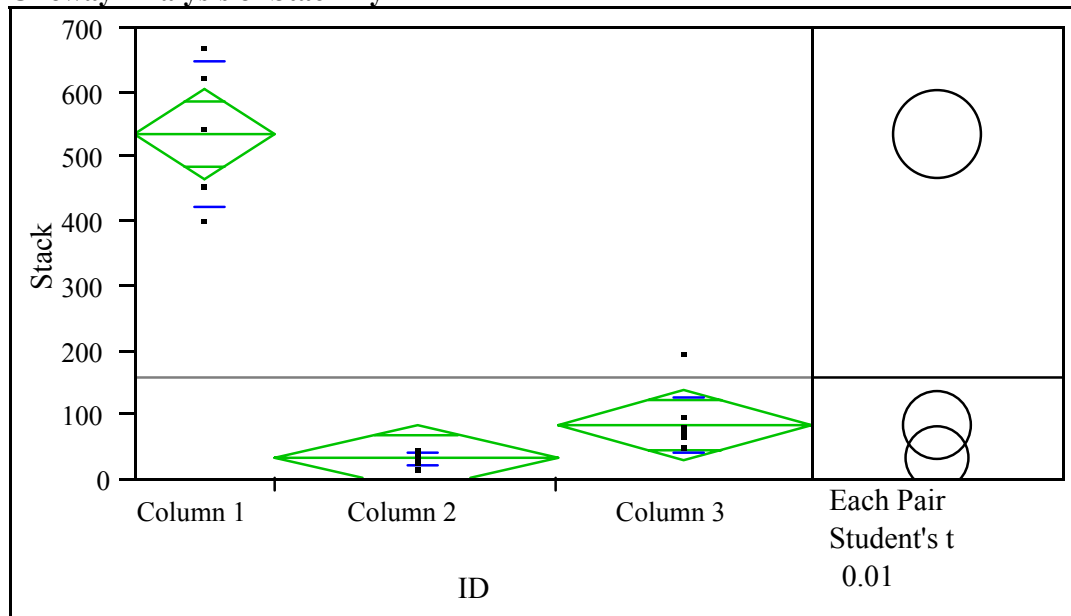
Comparisons for each pair using Student's t

| t            | Alpha    |          |          |
|--------------|----------|----------|----------|
| 2.03693      | 0.05     |          |          |
| Abs(Dif)-LSD | Column 1 | Column 2 | Column 3 |
| Column 1     | -27.645  | -27.524  | -19.838  |
| Column 2     | -27.524  | -33.859  | -26.173  |
| Column 3     | -19.838  | -26.173  | -33.859  |

| Level      | Mean      |
|------------|-----------|
| Column 1 A | 56.206000 |
| Column 2 A | 52.822000 |
| Column 3 A | 45.136000 |

Levels not connected by same letter are significantly different

| Level    | - Level  | Difference | Lower CL | Upper CL | p-Value   |
|----------|----------|------------|----------|----------|-----------|
| Column 1 | Column 3 | 11.07000   | -19.8385 | 41.97846 | 0.4709802 |
| Column 2 | Column 3 | 7.68600    | -26.1725 | 41.54452 | 0.6469298 |
| Column 1 | Column 2 | 3.38400    | -27.5245 | 34.29246 | 0.8249430 |

**3OHKynG free in lens nucleus****Oneway Analysis of Stack By ID****Oneway Anova  
Summary of Fit**

Rsquare 0.933349  
 Adj Rsquare 0.927002  
 Root Mean Square Error 55.95952  
 Mean of Response 154.5217  
 Observations (or Sum Wgts) 24

**Analysis of Variance**

| Source   | DF | Sum of Squares | Mean Square | F Ratio  | Prob > F |
|----------|----|----------------|-------------|----------|----------|
| ID       | 2  | 920888.07      | 460444      | 147.0378 | <.0001   |
| Error    | 21 | 65760.82       | 3131        |          |          |
| C. Total | 23 | 986648.89      |             |          |          |

**Means for Oneway Anova**

| Level    | Number | Mean    | Std Error | Lower 99% | Upper 99% |
|----------|--------|---------|-----------|-----------|-----------|
| Column 1 | 5      | 533.800 | 25.026    | 462.9     | 604.66    |
| Column 2 | 10     | 30.526  | 17.696    | -19.6     | 80.63     |
| Column 3 | 9      | 81.584  | 18.653    | 28.8      | 134.40    |

Std Error uses a pooled estimate of error variance

**Wilcoxon / Kruskal-Wallis Tests (Rank Sums)**

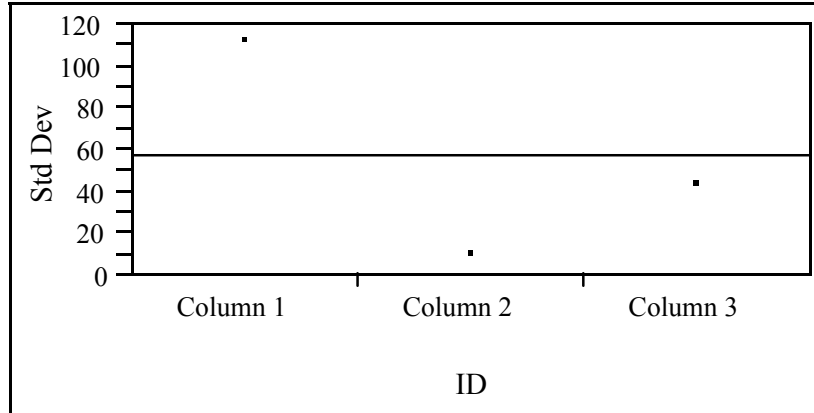
| Level    | Count | Score Sum | Score Mean | (Mean-Mean0)/Std0 |
|----------|-------|-----------|------------|-------------------|
| Column 1 | 5     | 110       | 22.0000    | 3.341             |
| Column 2 | 10    | 55        | 5.5000     | -4.070            |
| Column 3 | 9     | 135       | 15.0000    | 1.312             |

**1-way Test, ChiSquare Approximation**

| ChiSquare | DF | Prob>ChiSq |
|-----------|----|------------|
| 19.9500   | 2  | <.0001     |

## Appendix 1

Tests that the Variances are Equal



| Level    | Count | Std Dev  | MeanAbsDif to Mean | MeanAbsDif to Median |
|----------|-------|----------|--------------------|----------------------|
| Column 1 | 5     | 111.9495 | 88.24000           | 102.4000             |
| Column 2 | 10    | 9.6876   | 7.73920            | 7.4340               |
| Column 3 | 9     | 42.9904  | 27.02247           | 22.4044              |

| Test           | F Ratio | DFNum | DFDen | Prob > F |
|----------------|---------|-------|-------|----------|
| O'Brien(.5)    | 7.9508  | 2     | 21    | 0.0027   |
| Brown-Forsythe | 19.6279 | 2     | 21    | <.0001   |
| Levene         | 11.7090 | 2     | 21    | 0.0004   |
| Bartlett       | 14.0899 | 2     | .     | <.0001   |

Warning: Small sample sizes. Use Caution.

Welch Anova testing Means Equal, allowing Std Devs Not Equal

| F Ratio | DFNum | DFDen  | Prob > F |
|---------|-------|--------|----------|
| 51.3147 | 2     | 7.3499 | <.0001   |

### Means Comparisons

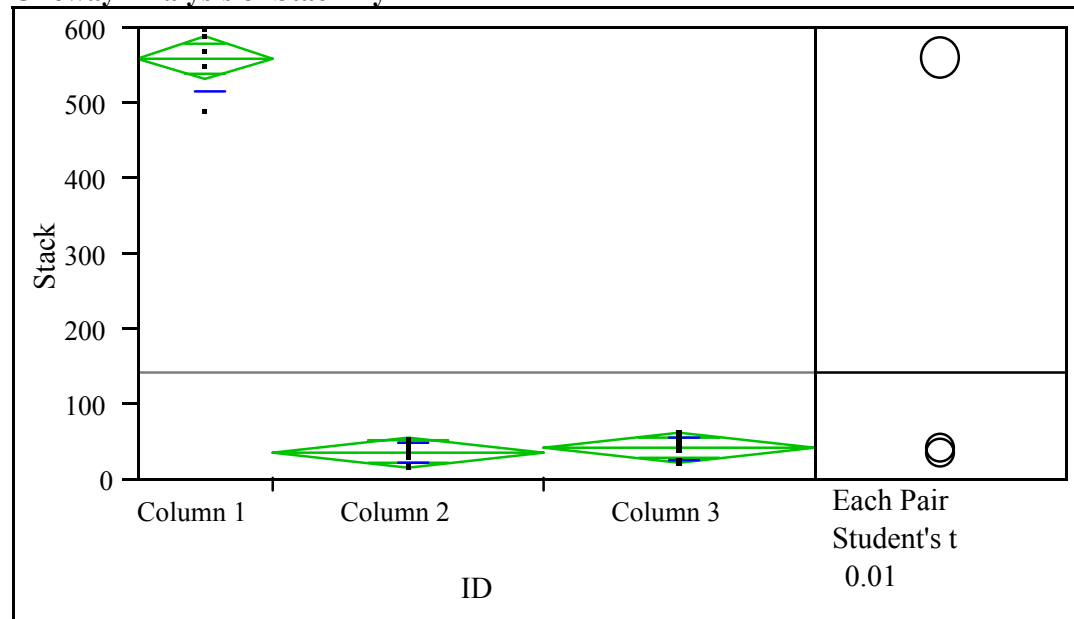
Comparisons for each pair using Student's t

| t            | Alpha    |          |          |
|--------------|----------|----------|----------|
| 2.83136      | 0.01     |          |          |
| Abs(Dif)-LSD | Column 1 | Column 3 | Column 2 |
| Column 1     | -100.21  | 363.84   | 416.49   |
| Column 3     | 363.84   | -74.69   | -21.74   |
| Column 2     | 416.49   | -21.74   | -70.86   |

| Level      | Mean      |
|------------|-----------|
| Column 1 A | 533.80000 |
| Column 3 B | 81.58444  |
| Column 2 B | 30.52600  |

Levels not connected by same letter are significantly different

| Level    | - Level  | Difference | Lower CL | Upper CL | p-Value   |
|----------|----------|------------|----------|----------|-----------|
| Column 1 | Column 2 | 503.2740   | 416.492  | 590.0560 | 1.9e-13   |
| Column 1 | Column 3 | 452.2156   | 363.841  | 540.5900 | 2.1e-12   |
| Column 3 | Column 2 | 51.0584    | -21.740  | 123.8573 | 0.0602642 |

**3OHKynG free in lens cortex****Oneway Analysis of Stack By ID****Oneway Anova  
Summary of Fit**

Rsquare 0.989901  
 Adj Rsquare 0.988983  
 Root Mean Square Error 22.38229  
 Mean of Response 141.0744  
 Observations (or Sum Wgts) 25  
 Analysis of Variance

| Source   | DF | Sum of Squares | Mean Square | F Ratio  | Prob > F |
|----------|----|----------------|-------------|----------|----------|
| ID       | 2  | 1080289.8      | 540145      | 1078.205 | <.0001   |
| Error    | 22 | 11021.3        | 501         |          |          |
| C. Total | 24 | 1091311.0      |             |          |          |

**Means for Oneway Anova**

| Level    | Number | Mean    | Std Error | Lower 99% | Upper 99% |
|----------|--------|---------|-----------|-----------|-----------|
| Column 1 | 5      | 556.800 | 10.010    | 528.59    | 585.01    |
| Column 2 | 10     | 34.733  | 7.078     | 14.78     | 54.68     |
| Column 3 | 10     | 39.553  | 7.078     | 19.60     | 59.50     |

Std Error uses a pooled estimate of error variance

**Wilcoxon / Kruskal-Wallis Tests (Rank Sums)**

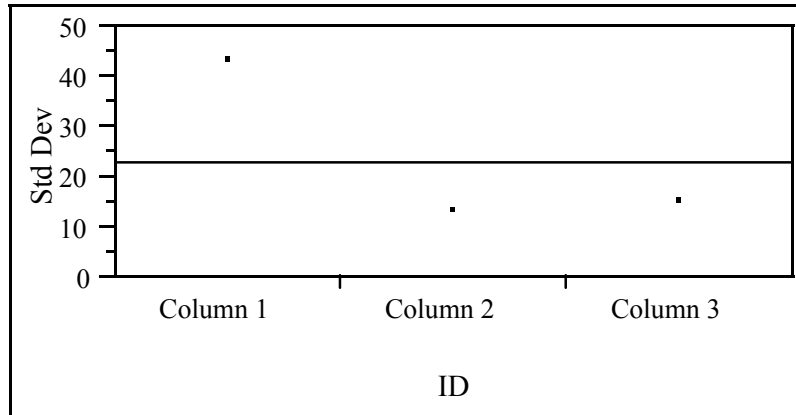
| Level    | Count | Score Sum | Score Mean | (Mean-Mean0)/Std0 |
|----------|-------|-----------|------------|-------------------|
| Column 1 | 5     | 115       | 23.0000    | 3.364             |
| Column 2 | 10    | 94.5      | 9.4500     | -1.942            |
| Column 3 | 10    | 115.5     | 11.5500    | -0.777            |

**1-way Test, ChiSquare Approximation**

| ChiSquare | DF | Prob>ChiSq |
|-----------|----|------------|
| 11.9501   | 2  | 0.0025     |

## Appendix 1

Tests that the Variances are Equal



| Level    | Count | Std Dev  | MeanAbsDif to Mean | MeanAbsDif to Median |
|----------|-------|----------|--------------------|----------------------|
| Column 1 | 5     | 42.90921 | 31.84000           | 33.20000             |
| Column 2 | 10    | 13.21324 | 10.46040           | 10.26700             |
| Column 3 | 10    | 15.22119 | 12.54900           | 12.54900             |

| Test           | F Ratio | DFNum | DFDen | Prob > F |
|----------------|---------|-------|-------|----------|
| O'Brien(.5)    | 3.7002  | 2     | 22    | 0.0412   |
| Brown-Forsythe | 5.4272  | 2     | 22    | 0.0121   |
| Levene         | 5.6147  | 2     | 22    | 0.0107   |
| Bartlett       | 5.2379  | 2     | .     | 0.0053   |

Warning: Small sample sizes. Use Caution.

Welch Anova testing Means Equal, allowing Std Devs Not Equal

| F Ratio  | DFNum | DFDen  | Prob > F |
|----------|-------|--------|----------|
| 333.0716 | 2     | 8.9917 | <.0001   |

### Means Comparisons

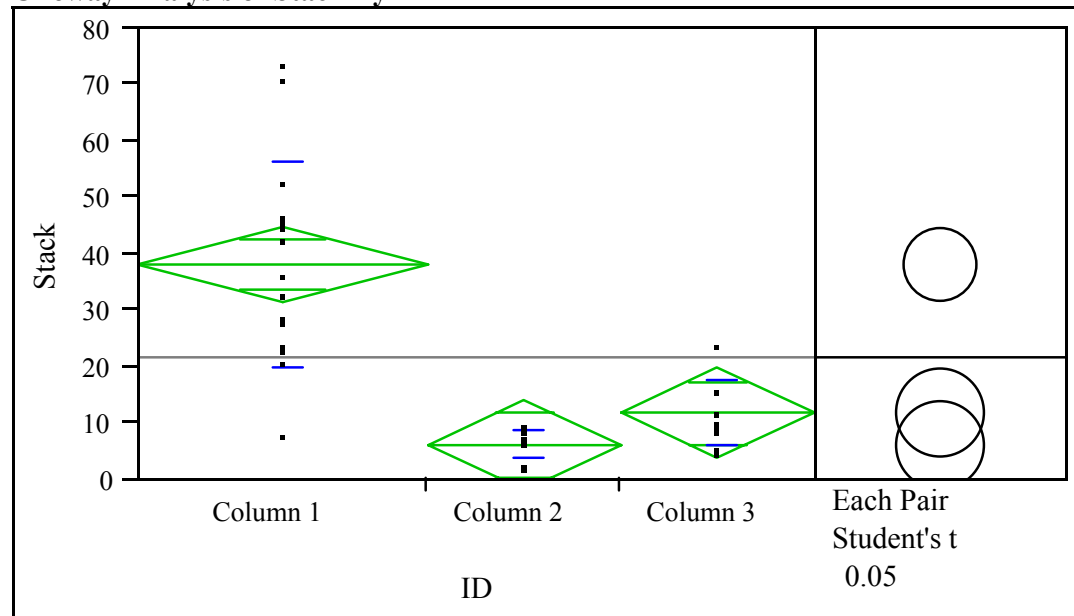
Comparisons for each pair using Student's t

| t            | Alpha    |          |          |
|--------------|----------|----------|----------|
| 2.81876      | 0.01     |          |          |
| Abs(Dif)-LSD | Column 1 | Column 3 | Column 2 |
| Column 1     | -39.90   | 482.69   | 487.51   |
| Column 3     | 482.69   | -28.21   | -23.39   |
| Column 2     | 487.51   | -23.39   | -28.21   |

| Level      | Mean      |
|------------|-----------|
| Column 1 A | 556.80000 |
| Column 3 B | 39.55300  |
| Column 2 B | 34.73300  |

Levels not connected by same letter are significantly different

| Level    | - Level  | Difference | Lower CL | Upper CL | p-Value   |
|----------|----------|------------|----------|----------|-----------|
| Column 1 | Column 2 | 522.0670   | 487.511  | 556.6229 | 1.2e-22   |
| Column 1 | Column 3 | 517.2470   | 482.691  | 551.8029 | 1.5e-22   |
| Column 3 | Column 2 | 4.8200     | -23.395  | 33.0348  | 0.6348918 |

**Kyn bound to nucleus proteins****Oneway Analysis of Stack By ID****Oneway Anova  
Summary of Fit**

Rsquare 0.598532  
 Adj Rsquare 0.57344  
 Root Mean Square Error 12.49607  
 Mean of Response 21.1272  
 Observations (or Sum Wgts) 35

**Analysis of Variance**

| Source   | DF | Sum of Squares | Mean Square | F Ratio | Prob > F |
|----------|----|----------------|-------------|---------|----------|
| ID       | 2  | 7449.607       | 3724.80     | 23.8537 | <.0001   |
| Error    | 32 | 4996.856       | 156.15      |         |          |
| C. Total | 34 | 12446.462      |             |         |          |

**Means for Oneway Anova**

| Level    | Number | Mean    | Std Error | Lower 95% | Upper 95% |
|----------|--------|---------|-----------|-----------|-----------|
| Column 1 | 15     | 37.7968 | 3.2265    | 31.22     | 44.369    |
| Column 2 | 10     | 5.8378  | 3.9516    | -2.21     | 13.887    |
| Column 3 | 10     | 11.4122 | 3.9516    | 3.36      | 19.461    |

Std Error uses a pooled estimate of error variance

**Wilcoxon / Kruskal-Wallis Tests (Rank Sums)**

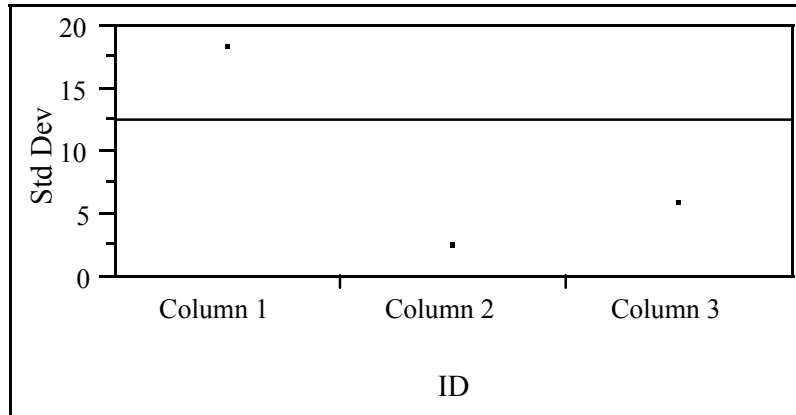
| Level    | Count | Score Sum | Score Mean | (Mean-Mean0)/Std0 |
|----------|-------|-----------|------------|-------------------|
| Column 1 | 15    | 407       | 27.1333    | 4.550             |
| Column 2 | 10    | 75        | 7.5000     | -3.816            |
| Column 3 | 10    | 148       | 14.8000    | -1.150            |

**1-way Test, ChiSquare Approximation**

| ChiSquare | DF | Prob>ChiSq |
|-----------|----|------------|
| 23.3921   | 2  | <.0001     |

## Appendix 1

Tests that the Variances are Equal



| Level          | Count | Std Dev  | MeanAbsDif to Mean | MeanAbsDif to Median |          |
|----------------|-------|----------|--------------------|----------------------|----------|
| Column 1       | 15    | 18.21449 | 14.36298           | 14.44549             |          |
| Column 2       | 10    | 2.48977  | 1.76908            | 1.55020              |          |
| Column 3       | 10    | 5.73797  | 4.52824            | 4.42580              |          |
| Test           |       | F Ratio  | DFNum              | DFDen                | Prob > F |
| O'Brien(.5)    |       | 4.5357   | 2                  | 32                   | 0.0184   |
| Brown-Forsythe |       | 10.5662  | 2                  | 32                   | 0.0003   |
| Levene         |       | 10.7175  | 2                  | 32                   | 0.0003   |
| Bartlett       |       | 15.5677  | 2                  | .                    | <.0001   |

Welch Anova testing Means Equal, allowing Std Devs Not Equal

| F Ratio | DFNum | DFDen  | Prob > F |
|---------|-------|--------|----------|
| 24.3784 | 2     | 17.653 | <.0001   |

### Means Comparisons

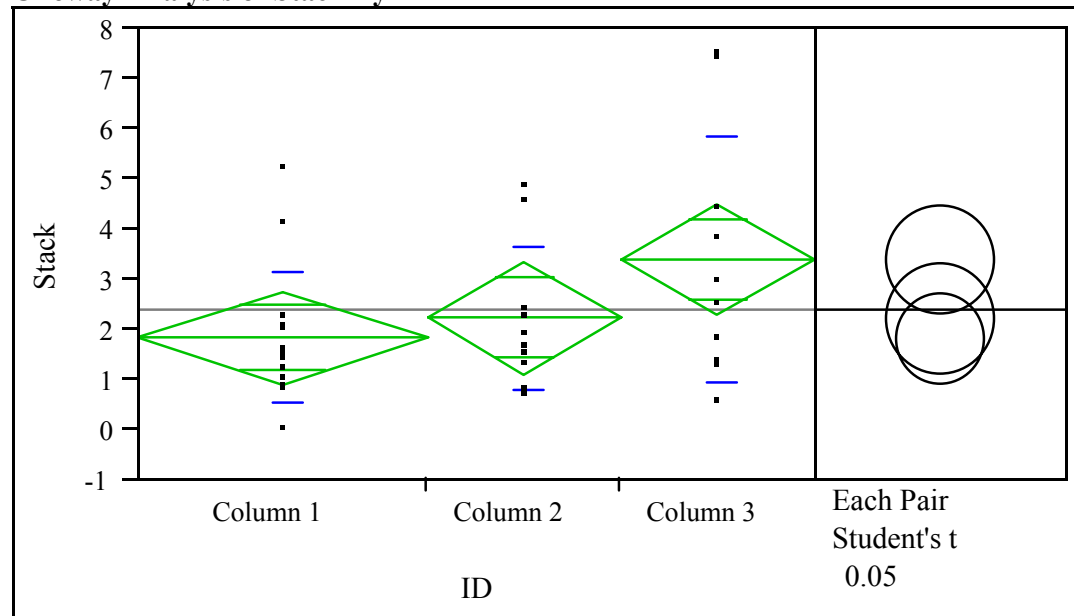
Comparisons for each pair using Student's t

| t            | Alpha    |          |          |
|--------------|----------|----------|----------|
| 2.03693      | 0.05     |          |          |
| Abs(Dif)-LSD | Column 1 | Column 3 | Column 2 |
| Column 1     | -9.294   | 15.993   | 21.568   |
| Column 3     | 15.993   | -11.383  | -5.809   |
| Column 2     | 21.568   | -5.809   | -11.383  |

| Level      | Mean      |
|------------|-----------|
| Column 1 A | 37.796807 |
| Column 3 B | 11.412200 |
| Column 2 B | 5.837800  |

Levels not connected by same letter are significantly different

| Level    | - Level  | Difference | Lower CL | Upper CL | p-Value   |
|----------|----------|------------|----------|----------|-----------|
| Column 1 | Column 2 | 31.95901   | 21.5676  | 42.35042 | 5.06e-7   |
| Column 1 | Column 3 | 26.38461   | 15.9932  | 36.77602 | 0.0000121 |
| Column 3 | Column 2 | 5.57440    | -5.8088  | 16.95762 | 0.3260089 |

**Kyn bound to cortex proteins****Oneway Analysis of Stack By ID****Oneway Anova  
Summary of Fit**

Rsquare 0.133787  
 Adj Rsquare 0.079649  
 Root Mean Square Error 1.738443  
 Mean of Response 2.347611  
 Observations (or Sum Wgts) 35  
 Analysis of Variance

| Source   | DF | Sum of Squares | Mean Square | F Ratio | Prob > F |
|----------|----|----------------|-------------|---------|----------|
| ID       | 2  | 14.93688       | 7.46844     | 2.4712  | 0.1005   |
| Error    | 32 | 96.70994       | 3.02219     |         |          |
| C. Total | 34 | 111.64682      |             |         |          |

**Means for Oneway Anova**

| Level    | Number | Mean    | Std Error | Lower 95% | Upper 95% |
|----------|--------|---------|-----------|-----------|-----------|
| Column 1 | 15     | 1.78720 | 0.44886   | 0.8729    | 2.7015    |
| Column 2 | 10     | 2.18944 | 0.54974   | 1.0696    | 3.3092    |
| Column 3 | 10     | 3.34640 | 0.54974   | 2.2266    | 4.4662    |

Std Error uses a pooled estimate of error variance

**Wilcoxon / Kruskal-Wallis Tests (Rank Sums)**

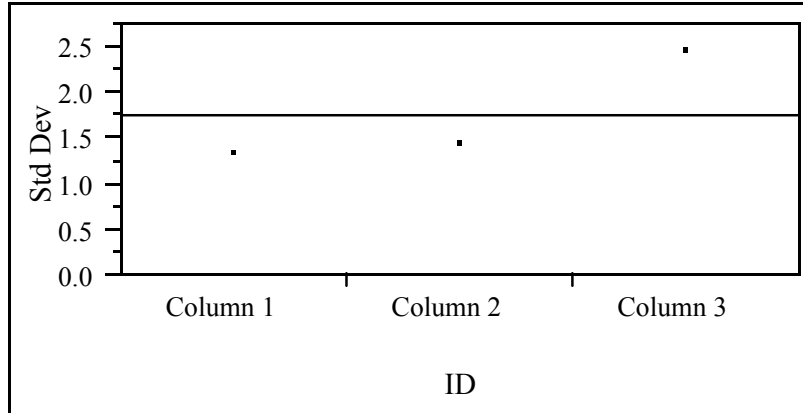
| Level    | Count | Score Sum | Score Mean | (Mean-Mean0)/Std0 |
|----------|-------|-----------|------------|-------------------|
| Column 1 | 15    | 226       | 15.0667    | -1.450            |
| Column 2 | 10    | 183       | 18.3000    | 0.091             |
| Column 3 | 10    | 221       | 22.1000    | 1.479             |

**1-way Test, ChiSquare Approximation**

| ChiSquare | DF | Prob>ChiSq |
|-----------|----|------------|
| 2.8387    | 2  | 0.2419     |



Tests that the Variances are Equal



| Level    | Count | Std Dev  | MeanAbsDif to Mean | MeanAbsDif to Median |
|----------|-------|----------|--------------------|----------------------|
| Column 1 | 15    | 1.306394 | 0.888133           | 0.816000             |
| Column 2 | 10    | 1.429431 | 1.054448           | 0.996560             |
| Column 3 | 10    | 2.459159 | 1.938080           | 1.856800             |

| Test           | F Ratio | DFNum | DFDen | Prob > F |
|----------------|---------|-------|-------|----------|
| O'Brien(.5)    | 2.6293  | 2     | 32    | 0.0877   |
| Brown-Forsythe | 2.2290  | 2     | 32    | 0.1241   |
| Levene         | 3.1268  | 2     | 32    | 0.0575   |
| Bartlett       | 2.5294  | 2     | .     | 0.0797   |

Welch Anova testing Means Equal, allowing Std Devs Not Equal

| F Ratio | DFNum | DFDen  | Prob > F |
|---------|-------|--------|----------|
| 1.6681  | 2     | 17.432 | 0.2173   |

**Means Comparisons**

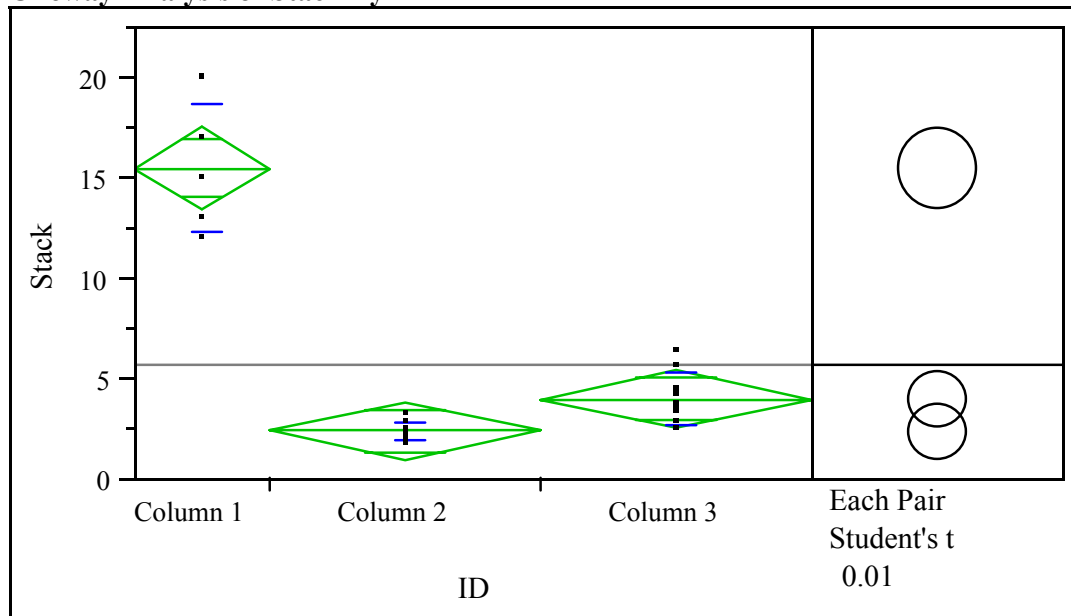
Comparisons for each pair using Student's t

| t            | Alpha    |          |          |
|--------------|----------|----------|----------|
| 2.03693      | 0.05     |          |          |
| Abs(Dif)-LSD | Column 3 | Column 2 | Column 1 |
| Column 3     | -1.5836  | -0.4267  | 0.1136   |
| Column 2     | -0.4267  | -1.5836  | -1.0434  |
| Column 1     | 0.1136   | -1.0434  | -1.2930  |

| Level        | Mean      |
|--------------|-----------|
| Column 3 A   | 3.3464000 |
| Column 2 A B | 2.1894400 |
| Column 1 B   | 1.7872000 |

Levels not connected by same letter are significantly different

| Level    | - Level  | Difference | Lower CL | Upper CL | p-Value   |
|----------|----------|------------|----------|----------|-----------|
| Column 3 | Column 1 | 1.559200   | 0.11355  | 3.004845 | 0.0353836 |
| Column 3 | Column 2 | 1.156960   | -0.42667 | 2.740585 | 0.1465041 |
| Column 2 | Column 1 | 0.402240   | -1.04341 | 1.847885 | 0.5748305 |

Kyn free in lens nucleus**Oneway Analysis of Stack By ID****Oneway Anova  
Summary of Fit**

Rsquare 0.913912  
 Adj Rsquare 0.906086  
 Root Mean Square Error 1.623639  
 Mean of Response 5.5812  
 Observations (or Sum Wgts) 25

**Analysis of Variance**

| Source   | DF | Sum of Squares | Mean Square | F Ratio  | Prob > F |
|----------|----|----------------|-------------|----------|----------|
| ID       | 2  | 615.69341      | 307.847     | 116.7766 | <.0001   |
| Error    | 22 | 57.99645       | 2.636       |          |          |
| C. Total | 24 | 673.68986      |             |          |          |

**Means for Oneway Anova**

| Level    | Number | Mean    | Std Error | Lower 99% | Upper 99% |
|----------|--------|---------|-----------|-----------|-----------|
| Column 1 | 5      | 15.4000 | 0.72611   | 13.353    | 17.447    |
| Column 2 | 10     | 2.3160  | 0.51344   | 0.869     | 3.763     |
| Column 3 | 10     | 3.9370  | 0.51344   | 2.490     | 5.384     |

Std Error uses a pooled estimate of error variance

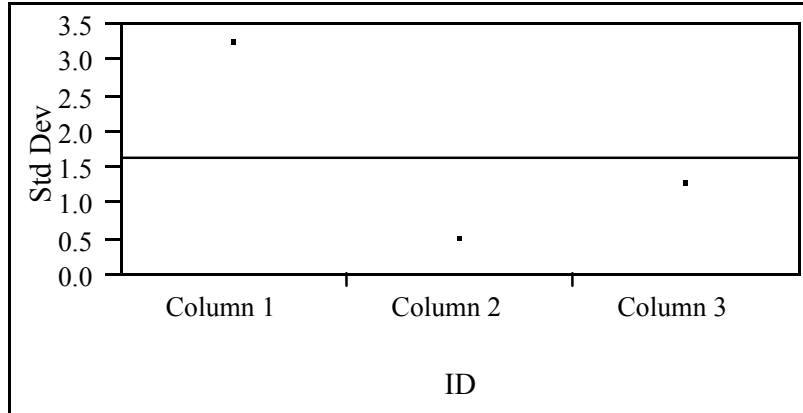
**Wilcoxon / Kruskal-Wallis Tests (Rank Sums)**

| Level    | Count | Score Sum | Score Mean | (Mean-Mean0)/Std0 |
|----------|-------|-----------|------------|-------------------|
| Column 1 | 5     | 115       | 23.0000    | 3.364             |
| Column 2 | 10    | 61.5      | 6.1500     | -3.773            |
| Column 3 | 10    | 148.5     | 14.8500    | 0.999             |

**1-way Test, ChiSquare Approximation**

| ChiSquare | DF | Prob>ChiSq |
|-----------|----|------------|
| 18.5324   | 2  | <.0001     |

Tests that the Variances are Equal



| Level    | Count | Std Dev  | MeanAbsDif to Mean | MeanAbsDif to Median |
|----------|-------|----------|--------------------|----------------------|
| Column 1 | 5     | 3.209361 | 2.480000           | 2.800000             |
| Column 2 | 10    | 0.493563 | 0.382000           | 0.382000             |
| Column 3 | 10    | 1.273840 | 0.990400           | 0.965000             |

| Test           | F Ratio | DFNum | DFDen | Prob > F |
|----------------|---------|-------|-------|----------|
| O'Brien(.5)    | 6.1909  | 2     | 22    | 0.0074   |
| Brown-Forsythe | 16.2253 | 2     | 22    | <.0001   |
| Levene         | 10.1361 | 2     | 22    | 0.0008   |
| Bartlett       | 9.4994  | 2     | .     | <.0001   |

Warning: Small sample sizes. Use Caution.

Welch Anova testing Means Equal, allowing Std Devs Not Equal

| F Ratio | DFNum | DFDen  | Prob > F |
|---------|-------|--------|----------|
| 43.2648 | 2     | 8.0479 | <.0001   |

**Means Comparisons**

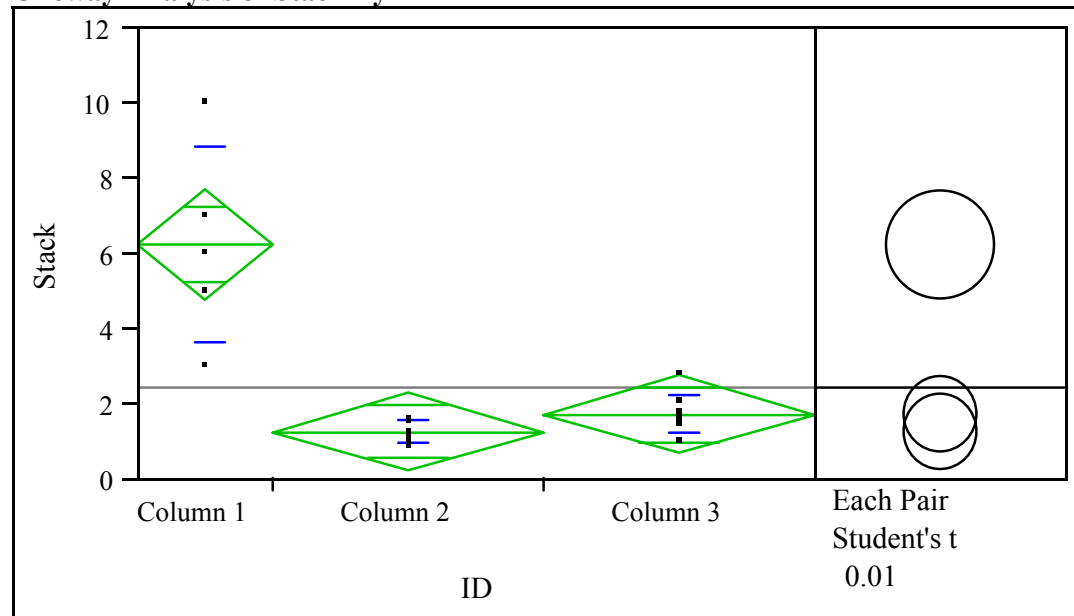
Comparisons for each pair using Student's t

| t            | Alpha    |          |          |
|--------------|----------|----------|----------|
| 2.81876      | 0.01     |          |          |
| Abs(Dif)-LSD | Column 1 | Column 3 | Column 2 |
| Column 1     | -2.895   | 8.956    | 10.577   |
| Column 3     | 8.956    | -2.047   | -0.426   |
| Column 2     | 10.577   | -0.426   | -2.047   |

| Level      | Mean      |
|------------|-----------|
| Column 1 A | 15.400000 |
| Column 3 B | 3.937000  |
| Column 2 B | 2.316000  |

Levels not connected by same letter are significantly different

| Level    | - Level  | Difference | Lower CL | Upper CL | p-Value   |
|----------|----------|------------|----------|----------|-----------|
| Column 1 | Column 2 | 13.08400   | 10.5773  | 15.59073 | 7.2e-13   |
| Column 1 | Column 3 | 11.46300   | 8.9563   | 13.96973 | 9.9e-12   |
| Column 3 | Column 2 | 1.62100    | -0.4257  | 3.66774  | 0.0360854 |

Kyn free in lens cortex**Oneway Analysis of Stack By ID****Oneway Anova  
Summary of Fit**

Rsquare 0.754597  
 Adj Rsquare 0.732288  
 Root Mean Square Error 1.158805  
 Mean of Response 2.41028  
 Observations (or Sum Wgts) 25

**Analysis of Variance**

| Source   | DF | Sum of Squares | Mean Square | F Ratio | Prob > F |
|----------|----|----------------|-------------|---------|----------|
| ID       | 2  | 90.84023       | 45.4201     | 33.8242 | <.0001   |
| Error    | 22 | 29.54221       | 1.3428      |         |          |
| C. Total | 24 | 120.38245      |             |         |          |

**Means for Oneway Anova**

| Level    | Number | Mean    | Std Error | Lower 99% | Upper 99% |
|----------|--------|---------|-----------|-----------|-----------|
| Column 1 | 5      | 6.20000 | 0.51823   | 4.7392    | 7.6608    |
| Column 2 | 10     | 1.23070 | 0.36645   | 0.1978    | 2.2636    |
| Column 3 | 10     | 1.69500 | 0.36645   | 0.6621    | 2.7279    |

Std Error uses a pooled estimate of error variance

**Wilcoxon / Kruskal-Wallis Tests (Rank Sums)**

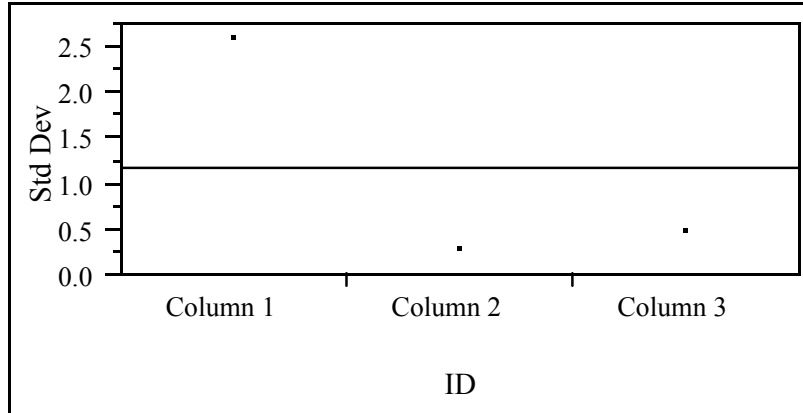
| Level    | Count | Score Sum | Score Mean | (Mean-Mean0)/Std0 |
|----------|-------|-----------|------------|-------------------|
| Column 1 | 5     | 115       | 23.0000    | 3.365             |
| Column 2 | 10    | 76        | 7.6000     | -2.970            |
| Column 3 | 10    | 134       | 13.4000    | 0.194             |

**1-way Test, ChiSquare Approximation**

| ChiSquare | DF | Prob>ChiSq |
|-----------|----|------------|
| 14.6663   | 2  | 0.0007     |

## Appendix 1

Tests that the Variances are Equal



| Level    | Count | Std Dev  | MeanAbsDif to Mean | MeanAbsDif to Median |
|----------|-------|----------|--------------------|----------------------|
| Column 1 | 5     | 2.588436 | 1.840000           | 2.000000             |
| Column 2 | 10    | 0.274583 | 0.221300           | 0.221300             |
| Column 3 | 10    | 0.478847 | 0.323000           | 0.287000             |

| Test           | F Ratio | DFNum | DFDen | Prob > F |
|----------------|---------|-------|-------|----------|
| O'Brien(.5)    | 5.1270  | 2     | 22    | 0.0149   |
| Brown-Forsythe | 13.8765 | 2     | 22    | 0.0001   |
| Levene         | 9.8119  | 2     | 22    | 0.0009   |
| Bartlett       | 16.5230 | 2     | .     | <.0001   |

Warning: Small sample sizes. Use Caution.

Welch Anova testing Means Equal, allowing Std Devs Not Equal

| F Ratio | DFNum | DFDen  | Prob > F |
|---------|-------|--------|----------|
| 11.3882 | 2     | 8.3864 | 0.0041   |

### Means Comparisons

Comparisons for each pair using Student's t

| t            | Alpha    |          |          |
|--------------|----------|----------|----------|
| 2.81876      | 0.01     |          |          |
| Abs(Dif)-LSD | Column 1 | Column 3 | Column 2 |
| Column 1     | -2.0658  | 2.7159   | 3.1802   |
| Column 3     | 2.7159   | -1.4608  | -0.9965  |
| Column 2     | 3.1802   | -0.9965  | -1.4608  |

| Level      | Mean      |
|------------|-----------|
| Column 1 A | 6.2000000 |
| Column 3 B | 1.6950000 |
| Column 2 B | 1.2307000 |

Levels not connected by same letter are significantly different

| Level    | - Level  | Difference | Lower CL | Upper CL | p-Value   |
|----------|----------|------------|----------|----------|-----------|
| Column 1 | Column 2 | 4.969300   | 3.18023  | 6.758374 | 8.43e-8   |
| Column 1 | Column 3 | 4.505000   | 2.71593  | 6.294074 | 4.05e-7   |
| Column 3 | Column 2 | 0.464300   | -0.99647 | 1.925073 | 0.3799897 |